Imperial College London

Structural and Catalytic Studies on Novel Copper Complexes

PhD Thesis

Benjamin Sylvester Zelenay

September 1st, 2017

Advisor: Dr. Silvia Díez-González

Department of Chemistry

Imperial College London

Abstract

Transition metal complexes and their chemistry are providing synthetic chemists and the chemical industry with simpler and less tedious synthetic procedures but also opened endless doors to new synthetic transformations that had been thought impossible. The main advantage of transition metal chemistry is that these complexes are often used in sub-stoichiometric amounts to perform the desired reaction. Other benefits such as high atom efficiency or fewer amount of by-products are often observed as well. Despite all these advantages, the commonly utilised transition metals are either expensive, toxic, and/or prospected from politically unstable regions. Copper, a less toxic and economical transition metal, circumvents these downsides.

The first Chapter outlines a brief overview of Schiff bases and their utilisation in transition metal chemistry including a discussion on diazabutadiene (DAB) and iminopyridine (ImPy) ligands, their complexes, and their reported applications. Furthermore, it includes the accounts for the preparation of DAB and ImPy ligands and their novel copper(I) complexes. The characterisation and X-ray structures of these complexes and in depth studies into the solution behaviour of [Cu(DAB)] complexes are discussed as well.

The second Chapter outlines an introduction to the chemistry of amines. It gives a brief overview over their importance in chemistry and their preparation, and a focus on the synthesis of primary amines from azide precursors. Furthermore, the utilisation of amines in the hydroamination reaction is reviewed and the application of copper(I) complexes in the literature is examined.

In Chapter 3, results of our successful attempts to exploit [Cu(DAB)] in the reduction of aryl azides are presented. In addition, computational studies are included to introduce the proposed reaction mechanism.

The fourth Chapter includes our efforts to apply the prepared copper(I) complexes in the intra- and intermolecular hydroamination reaction of primary and secondary amines to a variety of carbon–carbon unsaturated bonds. The preparation for the various starting materials and the isolation of their corresponding products is discussed.

The fifth Chapter provides a summary and the general conclusions of our studies and the final Chapter contains all experimental procedures and characterisation data for all compounds synthesised during this project.

Acknowledgements

First and foremost, I would like to thank my supervisor Dr. Silvia Díez-González for all the guidance and support she provided during this project. With her knowledge and exceptional enthusiasm for chemistry, she was always able to point me to the silver lining on every passing cloud. Ultimately, it was her vision and advices that lead to the success of this endeavour.

Further, I would like to express my gratitude to Prof. Feliu Maseras for his encouragement and counsel during my research visit in his group as well as Dr. Maria Besora for her guidance and tremendous patience that allowed for the computational investigations to succeed.

I would also like to thank Prof. King Kuok (Mimi) Hii for the many helpful and prolific discussions but also for sharing her laboratory equipment and chemicals.

I had the opportunity to meet and work with truly amazing people in the Barton Laboratory and with whom I spent many joyful moments. In particular, I would like to mention Dr. John Brazier, a man with many tales to tell, and Dr. Benjamin Deadman who selflessly helped me on many occasion but also Benedict Barron and Chris Mulligan for enduring my company and my mislead English idioms from the first day on. I am also obliged to Zaira Monasterio-Peiteado, David Ventura-Espinosa, Tian (Steffi) Xiaojie, Jamie Pimblett-Speck, Stephanie Pong, and Shuang He for their effort and contributions to the various chapters of this work.

Furthermore, I am indebted to Dr. Andrew White for solving our X-ray structures and Mr Peter Haycock for the excellent service at the Cross Faculty NMR Facility. This project would have been impossible without the financial support from Imperial College, the Engineering and Physical Sciences Research Council (EPSRC), and the Swiss National Science Foundation (SNF).

An exceptional thanks to my parents for their love and benevolence towards my ambitions but also for their constant supply of Swiss cheese to me. Moreover ,I would like to mention my sisters Veronika and Viviane who comforted me with their own PhD experiences and helped me to add this thesis into a larger picture. I am grateful to my brother Dominik for being my social anchor outside of chemistry and who visited me on many occasions in London.

Further I would like to thank Davide, Ilan, Markéta, Lucy, Marie, and Silvia for being there for me.

Finally, I would like to express my dearest appreciation to Llanberis Mountain Rescue: if it was not for them, this thesis would not have been submitted.

Declarations

Originality

I hereby declare that I am the sole author of the work presented in this thesis and that all contributions from other persons are appropriately referenced.

Copyright

Contents

List of Figures

List of Tables

List of Schemes

Acronyms and Abbreviations

a^{-1}	*Per annum*
Ac	Acetyl
Ad	Adamantyl (Tricyclo[3.3.1.1^{3,7}]decane)
Anis	Anisyl (4-Methoxyphenyl)
aq.	Aqueous
asymm	Asymmetric
ATRP	Atom-transfer radical-polymerisation
BIAN	Bis(arylimino)acenaphthene
BINAP	2,2′-Bis(diphenylphosphino)-1,1′-binaphthyl
bipy	Bipyridine
Bn	Benzyl
Boc	1,1-Dimethylethyloxycarbonyl
Bu	Butyl
t-Bu	1,1-Dimethylethyl
Bz	Benzoyl
calcd	Calculated
Cbz	Benzyloxycarbonyl
COD	1,5-Cyclooctadiene
corr.	Corrected
Cy	Cyclohexyl
d	Day
DAB	1,3-Diazabutadiene
DAB^{Ad}	*N*,*N*′-Diadamantyl-1,4-diazabuta-1,3-diene
DAB^{Anis}	*N*,*N*′-Bis(4-methoxyphenyl)-1,4-diaza-1,3-butadiene
DAB^{Cy}	*N*,*N*′-Dicyclohexyl-1,4-diazabuta-1,3-diene
DAB^{DIPh}	*N*,*N*′-Bis(2,6-bis(diphenylmethyl)-4-methylphenyl)-1,4-diaza-1,3-butadiene
DAB^{DIPP}	*N*,*N*′-Bis(2,6-diisopropylphenyl)-1,4-diaza-1,3-butadiene

DAB^{DMA}	*N,N'*-Bis(4-*N,N*-dimethylaminophenyl)-1,4-diaza-1,3-butadiene
DAB^{Mes}	*N,N'*-Bis(2,4,6-trimethylphenyl)-1,4-diazabuta-1,3-diene
DAB^{PhOMe3}	*N,N'*-Bis(3,4,5-trimethoxyphenyl)-1,4-diazabuta-1,3-diene
DAB^{tBu}	*N,N'*-Bis(1,1-dimethylethyl)-1,4-diaza-1,3-butadiene
DAB^{tBu3Ph}	*N,N'*-Bis(2,4,6-tris(1,1-dimethylethyl)phenyl)-1,4-diazabuta-1,3-diene
^{Me}DAB^{DMA}	*N,N'*-Bis(4-*N,N*-dimethylaminophenyl)-1,4-diaza-2,3-dimethyl-1,3-butadiene
DCM	Dichloromethane
DIPh	2,6-Bis(diphenylmethyl)-4-methylphenyl
DIPP	2,6-Diisopropylphenyl
DFT	Density functional theory
DMA	Dimethylaniline
DMF	Dimethylformamide
DOSY	Diffusion-ordered spectroscopy
DMSO	Dimethylsulfoxide
E_h	Hartree energy
EDG	Electron donating group
EDTA	Ethylenediaminetetraacetic acid
e.g.	*Exempli gratia*
EI	Electron ionisation
energ.	Energy
equiv	Equivalent
EPR	Electron paramagnetic resonance
ESI	Electron spray ionisation
Et	Ethyl
EWG	Electron withdrawing group
exp.	Experimental
g	Gram
h	Hour
HMDST	Hexamethyldisilathiane
HRMS	High-resolution mass spectrometry
Hz	Hertz
i.e.	*Id est*
i-	*Iso-*
IAd	1,3-Diadamantylimidazol-2-ylidene
IMes	1,3-Bis(2,4,6-trimethylphenyl)imidazol-2-ylidene
ImPy	Iminopyridine
ImPy^{Ad}	2-(Adamantyliminomethyl)pyridine
ImPy^{Anis}	2-(4-Methoxyphenyliminomethyl)pyridine
ImPy^{Cumene}	2-(2-isopropylphenyliminomethyl)pyridine
ImPy^{DIPP}	2-(2,6-diisopropylphenyliminomethyl)pyridine

ImPy^{DMA}	2-(4-(N,N-dimethylamino)phenyliminomethyl)pyridine
ImPy^{Mes}	2-(2,4,6-Trimethylphenyliminomethyl)pyridine
ImPy^{Ph}	2-(Phenyliminomethyl)pyridine
IPr	1,3-Bis(2,6-diisopropylphenyl)imidazol-2-ylidene
IR	Infrared
J	Coupling constant
K	Equilibrium constant
м	Molar
m	*Meta*
max	Maximum
Me	Methyl (1,3,5-Trimethylphenyl)
MECP	Minimum energy conversion point
Mes	Mesityl
m	Milli
m/z	Mass per charge number
min	Minute
MLCT	Metal-to-ligand-charge-transfer
MMA	Methyl methacrylate
MMAO	Modified methylaluminoxane
Mp	Melting point
MS	Molecular sieves
Ms	Methansulfonyl
n-	*Normal*
NHC	N-Heterocyclic carbene
NMP	N-Methyl-2-pyrrolidone
NMR	Nuclear Magnetic Resonance
o	*Ortho*
p	*Para*
PCM	Polarizable continuum model
PDI	Polydispersity index
PE	Petroleum ether
Ph	Phenyl
phen	1,10-Phenanthroline
PhOMe3	3,4,5-Trismethoxyphenyl
pot.	Potential
Pr	Propyl
ppm	Parts Per Million
PSP	Pyrrole-2-carbohydrazide
R	Boltzmann constant
rel.	Relative
r.t.	Room temperature
s	Second
S$_N$2	Bimolecular nucleophilic substitution

S.M.	Starting material
SIPr	1,3-Bis(2,6-diisopropylphenyl)-imidazolin-2-ylidene
st	Stretch
sym	Symmetric
t	*Tert-*
t	Ton
T	Temperature
TBAB	Tetrabutylammonium bromide
TBAF	Tetrabutylammonium fluoride
tBu3Ph	2,4,6-tris-(*tert*-butylphenyl)
Tf	Trifluoromethanesulfonyl
TFA	Trifluoroacetamide
THF	Tetrahydrofuran
THP	Tetrahydropyridine
TLC	Thin Layer Chromatography
TMS	Trimethylsilyl
Tol	Toluene
TON	Turn-over-number
Tos	*p*-Toluenesulfonyl
UV	Ultraviolet
Vis	Visible
w/w	Weight per unit weight
Xantphos	4,5-Bis(diphenylphosphino)-9,9-dimethylxanthene
δ	Chemical shift
$\%V_{\mathrm{B}}$	Percentage buried volume

Chapter 1

Diazabutadiene and Iminopyridine Copper(I) Complexes

1.1 Introduction

Schiff bases are widespread in the field of transition metal chemistry, and have heavily helped the development of not only coordination chemistry but also of catalytic[1] and biochemical[2,3] uses of transition metals.

Copper(I) coordination complexes with aromatic diimines with their outstanding potential for chemical and material applications still attract the interest of the scientific community and indeed, compounds with either 1,10-phenanthroline (phen) or 2,2'-bipyridine (bipy) derivatives have shown great promise in the preparation of supramolecular assemblies,[4] as catalysts in organic reactions,[5–9] or as luminescent materials (Figure 1.1).[10–12] Ligands with rigid backbones around the C–C bond such as phen or bis(arylimino)-acenaphthene (BIAN) are usually preferred for copper(I) centres due to the low configurational stability of the resulting complexes even in non-coordinating solvents.[13] Furthermore, complexes bearing more flexible bipy ligands often require additional ancillary ligands to prevent a disproportionation of the copper(I) centre.[14] Therefore, it is not surprising that despite intensive efforts, reports on the use of even more flexible iminopyridine (ImPy) and diazabutadiene (DAB) ligands in copper(I) chemistry are still scarce even though they hold very promising features.[15–18]
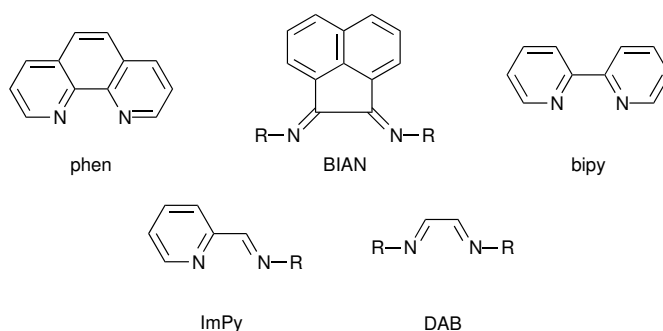
Figure 1.1: Structures of bidentate N-ligands.

1,3-Diazabutadiene (DAB) complexes have been studied since the 1950's, when Krumholz prepared a ferrous–DAB complex [Fe(DAB^{Me})$_3$]I$_2$.[19] DAB ligands are easily prepared *via* a condensation reaction of glyoxal derivatives and primary amines (Scheme 1.1), since the R group on the DAB^R ligand can be easily modified by using different primary amines.

DAB ligands are good σ donors and strong π-acceptors due to the diimine system and this ability has been shown on [M(CO)$_4$(DAB)] complexes (M = Cr, Mo, W), where after a one-electron reduction the oxidation state of the metal remained unchanged as the additional electron was actually accommodated by the DAB ligand.[20] Therefore, these ligands might stabilise
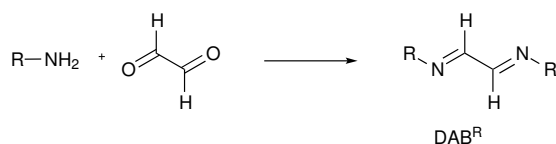
Scheme 1.1: Synthesis of DAB^R from glyoxal and primary amines.

metal low oxidation-states and give access to low valent metal complexes. DAB ligands have attracted steady attention from the scientific community over the years since they not only show exceptional electron accepting effects, but also display a versatile coordination behaviour.[21] These ligands can coordinate to a single metal centre in a monodentate (σ-N, **2e**)[22] or bidentate (σ-N, σ-N′, **4e**)[21] fashion (Figure 1.2). Between two metal centres, the DAB ligand can act as a two sigma donor bridge (σ-N, σ-N′, **2e** + **2e**)[23] or by chelation to the first metal centre using two sigma interaction and its π system to coordinate to the second metal centre (σ-N, σ-N′, η^2-C=N, η^2-C=N′, **8e**).[24] A last reported coordination mode (Figure 1.2) displays a sigma coordinated nitrogen, whereas the other one bridges two metal centres and its carbon–nitrogen double bond is coordinated as well (σ-N, μ-C=N′, η^2-C=N′, **6e**).[25] Even if the π-coordination of DAB ligands has been reported for metal carbonyl clusters of Groups 7 and 8, the most common coordination mode for all other transition metal complexes remains the bidentate one (σ-N, σ-N′, **4e**).
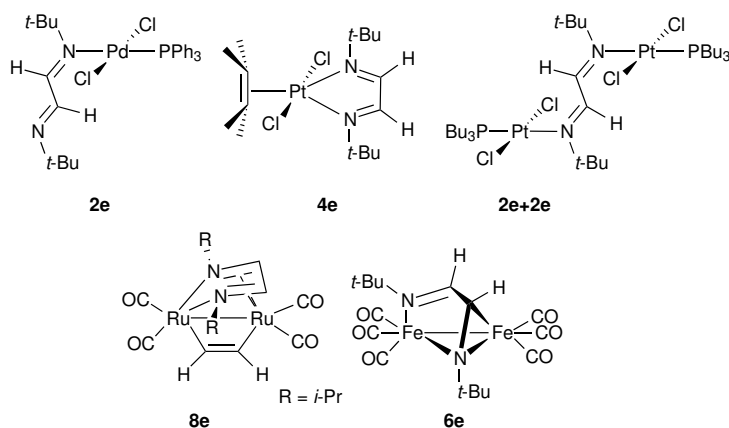
Figure 1.2: Different coordination modes reported for DAB ligands.

Several applications in catalysis have been reported for DAB-containing complexes. For example, [Pt(DAB)] complexes have been shown to be active in the C–H activation of methane, however, only stoichiometrically so far.[26] Nonetheless, catalytic C–H activation of benzene with [Pt(DAB)] and acetic acid has been reported with turn-over-numbers (TON) of 1500 (Scheme 1.2).[27]

4
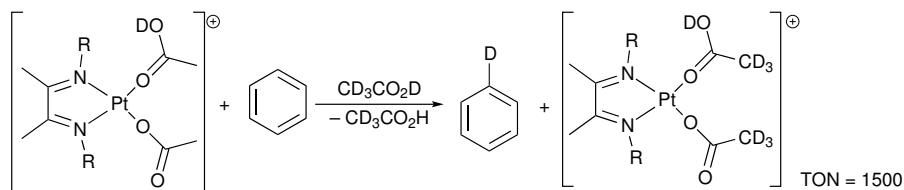
Scheme 1.2: Catalytic C–H activation of benzene with [Pt(DAB)].

Nickel(II) and palladium(II) based systems with DAB have been intensively studied as polymerisation catalysts of ethylene and *α*-olefins in the presence of modified methylaluminoxane (MMAO) and they have been shown to give high molecular weight polymers with a high catalytic activity comparable to well-established early transition metal polymerisation catalysts (Scheme 1.3).[28–31]
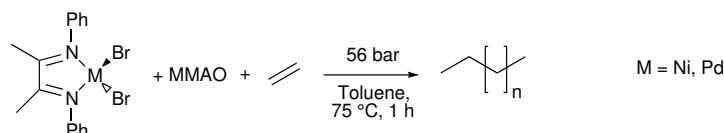
Scheme 1.3: Nickel– and palladium–DAB-based ethylene polymerisation reactions.

Also, [Pd(DAB)] complexes have been successfully applied to Mizoroki-Heck cross-coupling[32] and alkynes/alkenes hydrogenation reactions.[33] Furthermore, titanium based DAB complexes have been studied in hydrosilylation reactions.[34]

Surprisingly, [Cu(DAB)] complexes have received little attention in the literature despite both copper and DAB being very promising ingredients for a successful catalyst. [Cu(DAB)] complexes were first reported by tom Dieck and co-workers, who prepared different neutral [CuX(DAB^R)] and cationic [Cu(DAB^R)$_2$](CuCl$_2$), [Cu(DAB^R)$_2$](ClO$_4$) complexes.[15,17] The crystal structure for both complex types showed a bidentate coordinated DAB ligand to a single copper(I) centre. Additionally, coordination polymers were observed where the DAB ligand was bridging between two copper centres ([Cu$_5$Cl$_5$(DAB^R)$_2$]) (Figure 1.3).

[CuX(DAB^R)]

X = Cl, Br, I, CN, SCN

[Cu(DAB^R)$_2$]Y

Y = ClO$_4$, CuCl$_2$

[Cu$_5$Cl$_5$(DAB^R)$_2$]
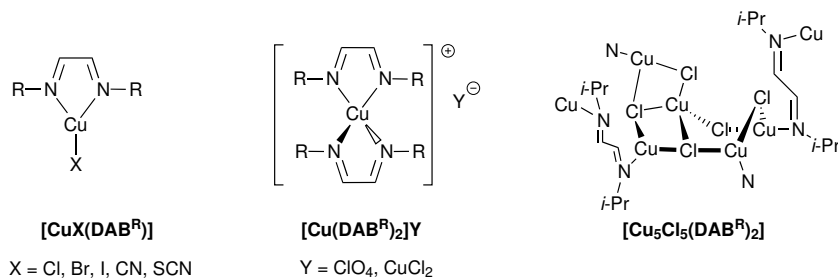
Figure 1.3: Reported [Cu(DAB)] structures in the literature.

Accordingly, the catalytic applications of copper(I)–DAB complexes remain scarce. Anga *et al.* reported the carbon–carbon cross-coupling followed by an intramolecular hydroalkoxylation of phenylacetylene and 2-iodophenol to 2-phenylbenzo[b]furan using $10\,mol\%$ [Cu(DAB^{biPh})(NCMe)$_2$](PF$_6$) (Scheme 1.4).[35]
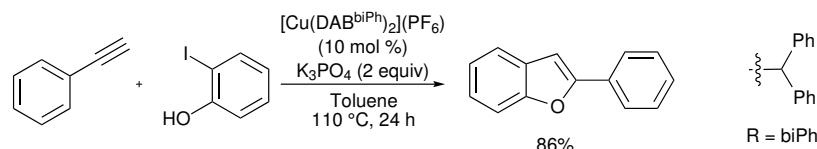
Scheme 1.4: Synthesis of 2-phenylbenzo[b]furan mediated by [Cu(DAB^{biPh})$_2$](PF$_6$).

On the other hand, a recent report by Liu and Yang showed the application of [CuCl (DAB^{Xyl})] in the Ullmann coupling of iodobenzene and *N,N*-diphenylamine to give triphenylamine in 90% yield (Scheme 1.5).[36] Despite only a small number of reported applications, copper(I) DAB complexes still hold great potential to be explored.
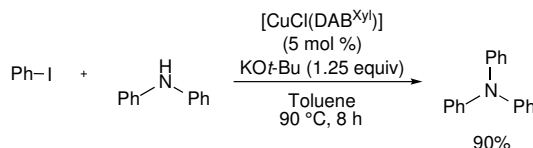
Scheme 1.5: Ullmann reaction between iodophenyl and diphenylamine.

Iminopyridine (ImPy) ligands are structurally related to DABs where one coordination site of the ligand is embedded in a pyridyl moiety. This allows for a ligand with similar electronic properties found in DAB systems, such as good σ-donor and π-acceptor and eventually act as redox non-innocent ligand.[37,38] Additionally, iminopyridine ligands are sterically less demanding than DAB ligands. However, they share a similar facile synthesis procedure as DAB ligands and are readily prepared by a condensation reaction of a primary amine or aniline source with 2-formylpyridine (Scheme 1.6).
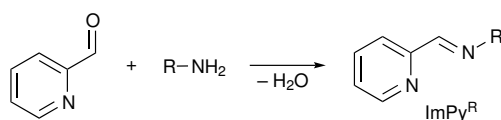
Scheme 1.6: Typical preparation of ImPy^R ligands.

A wide range of iminopyridine complexes bearing different metal centres have been disclosed in literature for diverse applications. For example, iron iminopyridine complexes were reported to catalyse the 1,4-addition of α-olefins to dienes (Scheme 1.7).[39]
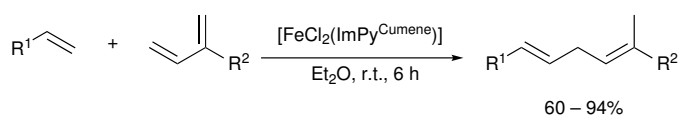
Scheme 1.7: [Fe(ImPy)]-catalysed 1,4-addition of α-olefins to dienes.

Furthermore, iron and cobalt iminopyridine complexes were found to be active in the oxidation of water to dihydrogen and dioxygen, and in the oxidation of activated methylene groups or secondary alcohols to ketones.[38,40,41]

Undoubtedly, the area in which iminopyridine based complexes have been most studied is polymer chemistry. Iron-, cobalt-, nickel-, and palladium-based iminopyridine complexes have been successfully applied in the polymerisation of ethylene.[42,43]

To the best of our knowledge, there has been only a few reports on copper(I) centred iminopyridine complexes. A variety of different cycloalkyl and phenyl substituted copper(I) iminopyridines were prepared, their quasi-reversible redox behaviour studied and a correlation between the tetrahedral distortion of the complex and its redox potential was found (Figure 1.4).[44,45]
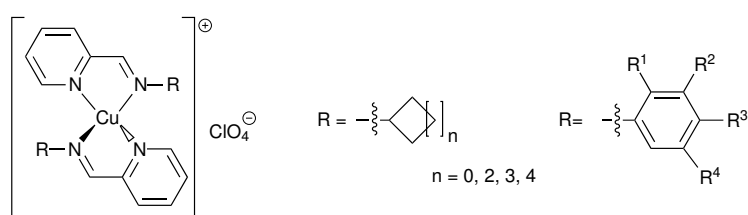
Figure 1.4: Reported [Cu(ImPy^R)] structures in the literature.

Another study described the application of branched and unbranched alkyl substituted copper(I) iminopyridine complexes in the atom-transfer radical-polymerisation (ATRP) (Scheme 1.8).[46] These complexes were identified as effective polymerisation catalysts of methyl methacrylate (MMA) to give polymers with good molecular weights and PDIs of up to 1.2.[46]
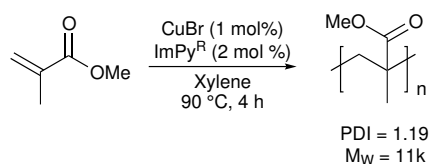
Scheme 1.8: Application of [Cu(ImPy^R)] complex as polymerisation catalyst.

1.2 Aims and Objectives

The aim of this work is to expand the current, reported library of [Cu(DAB^R)] and [Cu(ImPy^R)] complexes and possibly identify new families of [Cu(DAB)] complexes with different binding modes of the DAB ligand.

In order to achieve our goal, we will prepare DAB and ImPy ligands with different electronic and steric properties and their corresponding copper(I) complexes. All prepared complexes will be fully characterised by spectroscopic methods (*i.e.* NMR, IR, UV/Vis). Specifically, we will investigate their behaviour in solution since they are known to be coordinatively labile complexes even in non-coordinating solvents.[13,16] In view of prospective catalytic applications, we will prepare and characterise iminopyridine ligands and their copper(I) complexes with similar substituents as on the [Cu(DAB)] systems. Some of our results presented in this Chapter have been reported in a peer-reviewed journal.[47]

1.3 Preparation of DAB and ImPy Ligands

In a first step, DAB and ImPy ligands were prepared following reported synthetic procedures. DAB^R ligands were synthesised *via* condensation of different primary amines with aqueous glyoxal whereby pure ligands (R = Anis, Cy, DIPP, DMA, Mes, and *t*-Bu) were obtained in good to excellent yields after a simple filtration at the end of the reaction (Scheme 1.9).[15,48–50] Due to solubility issues, the preparation of DAB^{Ad} and DAB^{DIPh} was carried out in a mixture of acetone/H$_2$O and DCM, respectively.[51]

For 2,3-propandione or more sterically demanding amine substrates, the reaction had to be stirred under reflux in either EtOH or DCM, respectively, to obtain DAB^{tBu3Ph} and ^{Me}DAB^{DMA} in moderate yields (Scheme 1.10).

Bis(3,4,5-trimethoxyphenyl)diazabutadiene DAB^{PhOMe3} was prepared through a multi-step procedure as the direct formation by a condensation of the trimethoxyaniline and glyoxal led to the recovery of the starting materials. The aniline was first transformed into the corresponding azide, reduced to the phosphanimine by PPh$_3$ and then heated with glyoxal trimer dihy-
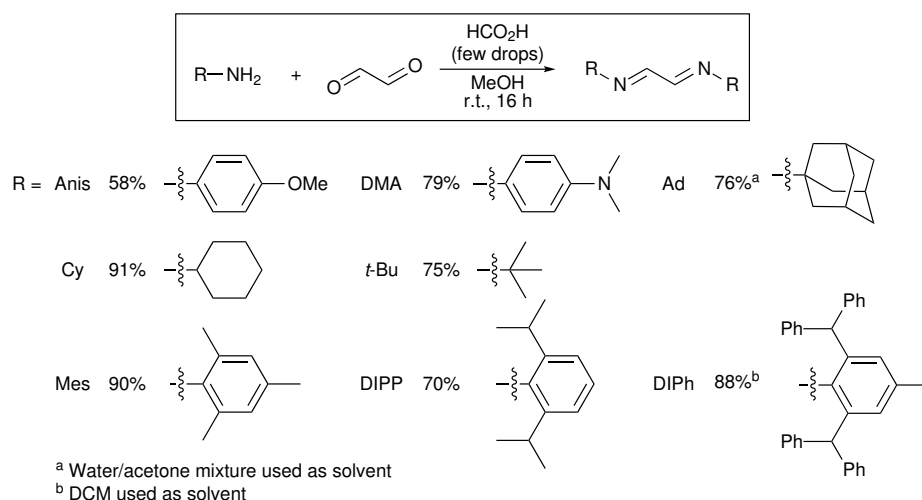
Scheme 1.9: Synthesis of readily prepared DAB^R ligands.
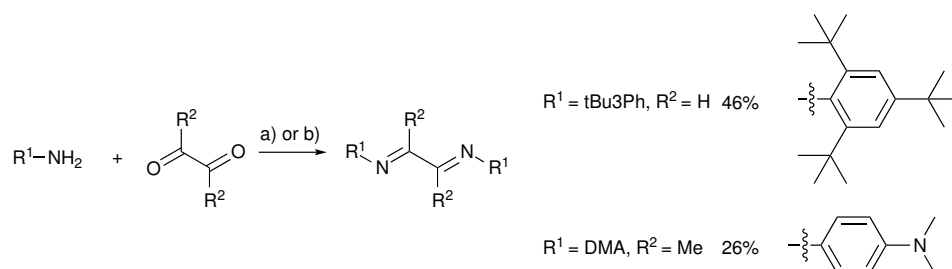
Scheme 1.10: Synthesis of DAB^{tBu3Ph} and ^{Me}DAB^{DMA}. a) Amine (2.0 equiv), glyoxal (1.0 equiv), MeOH, room temperature, 16 h; b) Amine (2.0 equiv), 2,3-butadione (1.0 equiv), HCO$_2$H (few drops), DCM, reflux, 16 h.

drate in THF under reflux to yield DAB^{PhOMe3} in comparable yields with the ones in literature (Scheme 1.11).[52]

Furthermore, DAB ligands with electron neutral or withdrawing aryl rings were intended to be studied as ligands for copper(I) complexes. In a first attempt, phenyl substituted DAB^{Ph} was prepared following a reported procedure.[15] The formed beige precipitate was collected and dissolved in CDCl$_3$ or acetone-d6 but in both cases the colour of the solution changed from colourless to deep red immediately and the ^{1}H NMR spectrum showed a plethora of signals none of which belonged to the reported compound. Lowering the reaction temperature to 0 °C as reported by Nourmohamma-dian and Gholami for the same reaction did lead to a similar outcome (Scheme 1.12).[53] On the other hand, the reaction of methyl 4-aminobenzoate or 4-nitroaniline with glyoxal led to the recovery of the starting materials

9
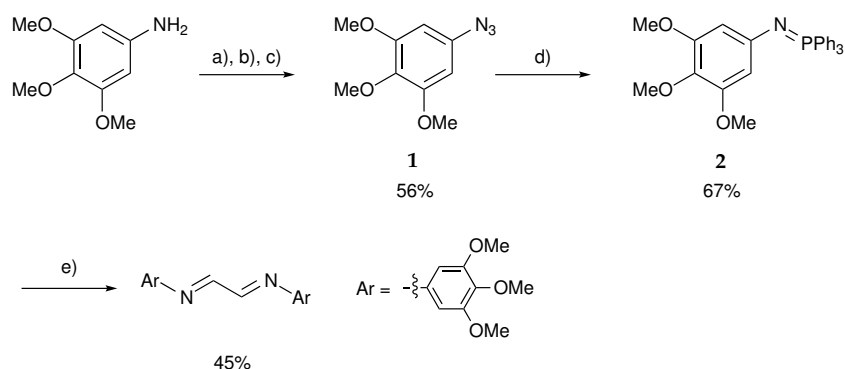
Scheme 1.11: Synthesis of DAB^{PhOMe3}. a) Aniline (1.0 equiv), conc. aq. HCl (4.2 equiv), 0 °C, 10 min; b) NaNO$_2$ (1.0 equiv), H$_2$O, 0 °C, 10 min; c) NaN$_3$ (1.0 equiv), H$_2$O, room temperature, 2 h; d) PPh$_3$ (1.0 equiv), Et$_2$O, 0 °C, 30 min; e) Glyoxal trimer dihydrate (0.5 equiv), 4 Å molecular sieves, THF, reflux, 16 h.

without any DAB formation even under reflux conditions. Even though none of these compounds are known in the literature, such reaction outcomes were surprising, since a DAB^R has been reported with a benzoic acid moiety (R = 4-CO$_2$H-C$_6$H$_4$).[54]
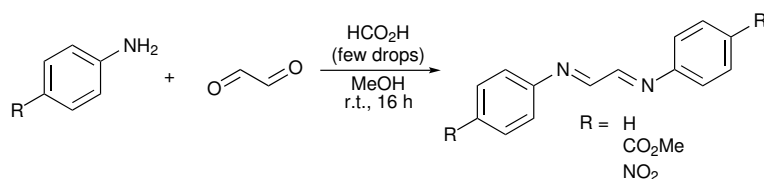
Scheme 1.12: Attempted synthesis of DAB^R.

Finally, ImPy ligands were synthesised following reported procedures for the condensation of 2-formylpyridine and different primary amines.[55–57] Anis, DIPP, and Ph substituted ImPy^R ligands were formed in dry toluene in the presence of molecular sieves at room temperature after 16 h. On the other hand, Ad, DMA, and Mes substituted ImPy^R ligands were synthesised in refluxing EtOH within 2 h. In all cases, pure ligands were obtained after removal of the unreacted starting materials by Kugelrohr distillation in moderate to good yields (Scheme 1.13).

R =	Ad	65%	DMA	89%
	Anis	66%	Mes	84%
	DIPP	47%	Ph	61%
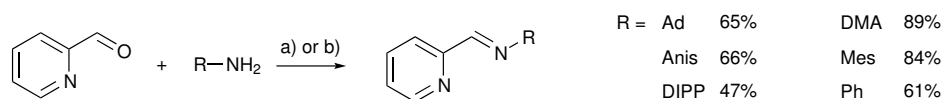
Scheme 1.13: Synthesis of ImPy^R ligands. a) Formylpyridine (1.0 equiv), aniline (1.0 equiv), 4 Å molecular sieves, room temperature, 16 h; b) Formylpyridine (1.0 equiv), aniline (1.0 equiv), 70 °C, 2 h.

1.4 Synthesis and Characterisation of [Cu(DAB)] Complexes

In the first experiments to form [Cu(DAB)] complexes, [Cu(NCMe)$_4$](BF$_4$) was used as copper(I) source and stirred with two equivalents of DAB^R in DCM at room temperature for 16 h. Homoleptic, cationic complexes [Cu(DAB^R)$_2$](BF$_4$) (R = Ad, Anis, Cy, DMA, Mes, PhOMe3, and *t*-Bu) with two DAB^R ligands *per* copper centre were isolated in good yields after recrystallisation (Scheme 1.14). The dimethyl-substituted homologous [Cu(^{Me}DAB^{DMA})$_2$](BF$_4$) was prepared in a similar way as the other homoleptic, cationic complexes and was isolated in a moderate yield.
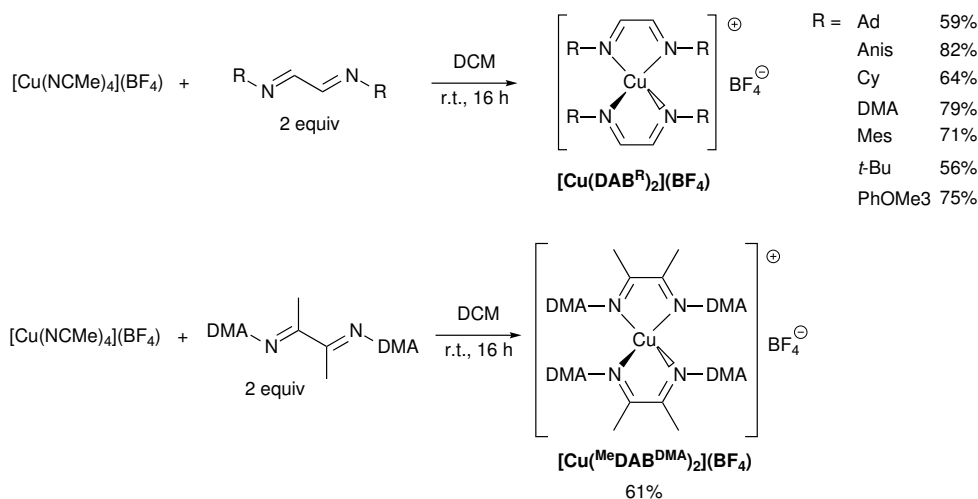
Scheme 1.14: Preparation of homoleptic, cationic complexes [Cu(DAB^R)](BF$_4$) and [Cu(^{Me}DAB^R)](BF$_4$).

No mono-DAB copper(I) complexes could be isolated when a 1:1 Cu/DAB^R stoichiometry was used in different solvents (DCM, acetone, or MeCN) and only homoleptic, cationic complexes were isolated in all cases. Despite being reported in literature, no spectroscopic data or yield was provided for [Cu(DAB^{Mes})$_2$](BF$_4$) and thus it will be discussed here as well.[58]

On the other hand, a different reactivity was observed when DAB^{DIPP} or DAB^{DIPh} were reacted with [Cu(NCMe)$_4$](BF$_4$) and only heteroleptic, cationic [Cu(DAB^R)(NCMe)$_2$](BF$_4$) complexes were formed (Scheme 1.15). The outcome of the reaction remained unchanged even when different stoichiometries or reaction conditions were employed. Additionally, no [Cu(DAB)] complexes could be formed with DAB^{tBu3Ph} and only starting materials were recovered.

On the other hand, the reaction of equimolar amounts of DAB and CuCl af-
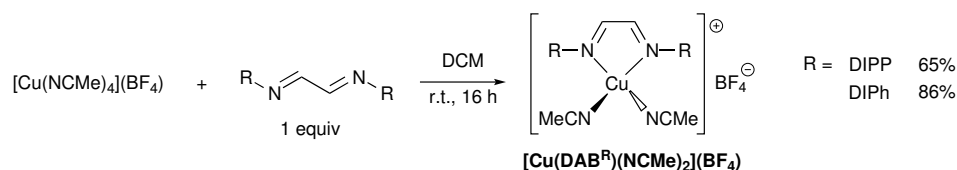
Scheme 1.15: Preparation of heteroleptic, cationic [Cu(DAB^R)(NCMe)$_2$](BF$_4$) complexes.

forded the heteroleptic, neutral [CuCl(DAB^R)] complexes (R = Ad, Anis, Cy, DMA, and *t*-Bu) bearing one DAB^R ligand *per* copper centre (Scheme 1.16). They were isolated in fair to excellent yields after recrystallisation. Nonetheless, no neutral complexes could be isolated for DAB^R ligands bearing Mes or DIPP groups and only starting materials were recovered even with increased reaction temperatures.
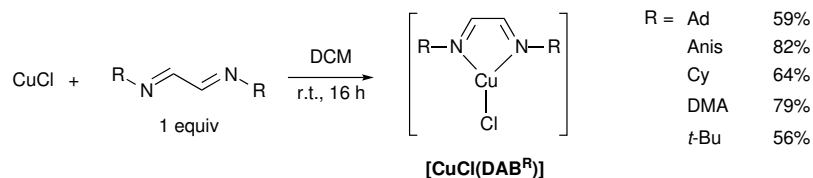
Scheme 1.16: Preparation of heteroleptic, neutral [CuCl(DAB^R)] complexes.

All isolated complexes were indefinitely stable towards oxygen and moisture in the solid state without any particular need for precautions. The only exceptions were heteroleptic, cationic complexes [Cu(DAB^R)(NCMe)$_2$](BF$_4$), which slowly decomposed over the course of three months if not stored under an inert atmosphere. A similar reactivity has been disclosed in the literature for DAB ligands with triphenylmethyl substituents.[35] Also, after three days, all complexes dissolved in CD$_2$Cl$_2$ started showing significant broadening of the signals in the ^{1}H NMR spectra, indicating an oxidation to paramagnetic copper(II) species. It is also important to note that all these complexes were strongly coloured and ranged throughout the whole visible spectrum from red to violet. Red colour was observed for alkyl substituted ligands DAB^R (R = Ad, Cy, and *t*-Bu) and purple for DAB^{DMA}.

All complexes were fully characterised by spectroscopic methods as well as elemental analysis, mass and for several complexes single-crystal were obtained for X-ray diffraction. In the ^{1}H NMR spectra, the resonances of the imino protons on the backbone of the ligands appear considerably shifted to lower field after metal coordination, consistent with the expected electron donation from the diimine ligands to the copper centre.

This effect is particularly strong in complexes bearing DAB^R ligands with alkyl substituents (*i.e.* δ = 8.51 ppm for [Cu(DAB^{Ad})$_2$](BF$_4$), compared to

δ = 7.95 ppm in the free ligand) or with a *para*-anisyl group (*i.e.* δ = 8.99 ppm for [Cu(DAB^{Anis})$_2$](BF$_4$), compared to δ = 8.45 ppm in the free ligand). In stark contrast to the general downfield shift of the imine proton upon complexation, [Cu(DAB^{DIPh})(NCMe)$_2$](BF$_4$) protons displayed an upfield shift of 0.55 ppm.

Interestingly, no downfield shift was observed for all complexes in the ^{13}C$\{^1H\}$ spectra, instead, all signals were slightly shifted upfield. The degree of shift depended on the substituent on the DAB ligand where similar shifts were observed for homoleptic and heteroleptic complexes. Small upfield shifts in the ^{13}C$\{^1H\}$ NMR of 0–1.5 ppm were observed for alkyl-, medium shifts of 1.5–3.5 ppm for aromatic substituents and the highest upfield shift of 21.9 ppm was displayed by [Cu(DAB^{DIPh})(NCMe)$_2$](BF$_4$). The special characteristics of the [Cu(DAB^{DIPh})(NCMe)$_2$](BF$_4$) in the NMR spectra might be due to shielding effects of the eight phenyl rings present on the side arms of the ligand.

The IR spectra of these complexes displayed medium absorption bands between 1557–1644 cm^{-1} for the asymmetric and between 1358–1569 cm^{-1} for the symmetric C=N stretches. Alkyl substituted complexes showed higher energies for both symmetric and asymmetric stretches, whereas aryl substituted ones exposed lower energies. The energies for the asymmetric stretches are within the typical region for C=N vibrations. Also, these values are shifted to lower wavenumbers with respect to those of the free diimine ligands, which agrees with the coordination of both nitrogen atoms of the DAB ligands to the copper centre as d electrons are located within the π* orbital of the N=C–C=N, system weakening these bonds. Additionally, all cationic complexes displayed a single stretching band at ~1050 cm^{-1} for the B–F bonds, as expected for complexes with a counterion without significant interaction with the metal centre. Mass spectra of all cationic complexes showed peaks for the expected metal cation, [Cu(DAB^R)$_2$]$^+$, [Cu(DAB^{DIPP})]$^+$, or [Cu(DAB^{DIPh})]$^+$. No molecular peaks were obtained for neutral complexes and values of m/z consistent with [Cu(DAB^R)(NCMe)]$^+$ species were systematically observed instead.

Suitable crystals for single-crystal X-ray diffraction were obtained for several complexes by slow diffusion of hexane into DCM solutions, except for [Cu(DAB^{Ad})$_2$](BF$_4$), where an acetone/pentane combination was used instead. A summary of the crystallographic data for these compounds is provided Table 1.1.

Ball-and-stick representations of the obtained structures are given in Figures 1.5–1.8, 1.10, 1.12, 1.13, 1.15, and 1.16 and selected bond lengths are provided in the captions of these figures.

In the lattice of [Cu(DAB^{Cy})$_2$](BF$_4$) and [CuCl(DAB^{Anis})] four independent units (A–D) were disclosed (Figure 1.9 and Figure 1.17) and the correspond-

Table 1.1: Summary of the crystallographic data for [Cu(DAB)] complexes. Data were collected using Oxford Diffraction Xcalibur PX Ultra ([Cu(DAB^{Mes})$_2$](BF$_4$), [Cu(DAB^{Anis})$_2$](BF$_4$), [Cu(DAB^{Cy})$_2$](BF$_4$), [CuCl(DAB^{Anis})] and [CuCl(DAB^{Cy})]) and Xcalibur 3 ([Cu(DAB^{Ad})$_2$](BF$_4$), [Cu(DAB^{DIPP})(NCMe)$_2$](BF$_4$), and [Cu(DAB^{DIPPh})(NCMe)$_2$](BF$_4$))) diffractometers, and the structures were refined using the SHELXTL, SHELX-97, and SHELX-2013 program systems.[59] The absolute structure of [Cu(DAB^{Mes})$_2$](BF$_4$) was determined by a combination of R-factor tests [R_1^+ = 0.0315, R_1^- = 0.0393] and by use of the Flack parameter [x^+ = 0.000(17), x^- = 1.030(17)]. CDC 1409952 to 1409958.

	[Cu(DAB^{Mes})$_2$](BF$_4$)	[Cu(DAB^{Anis})$_2$](BF$_4$)	[Cu(DAB^{Cy})$_2$](BF$_4$)	[Cu(DAB^{Ad})$_2$](BF$_4$)	[Cu(DAB^{DIPP})(NCMe)$_2$](BF$_4$)	[Cu(DAB^{DIPPh})(NCMe)$_2$](BF$_4$)	[CuCl(DAB^{Anis})]	[CuCl(DAB^{Cy})]
formula	[C$_{40}$H$_{48}$CuN$_4$](BF$_4$)	[C$_{52}$H$_{52}$CuN$_4$O$_4$](BF$_4$)	[C$_{28}$H$_{48}$CuN$_4$](BF$_4$)	[C$_{44}$H$_{64}$CuN$_4$](BF$_4$)	[C$_{30}$H$_{42}$CuN$_4$](BF$_4$)	[C$_{77}$H$_{62}$CuN$_4$](BF$_4$)	C$_{32}$H$_{32}$Cl$_2$Cu$_2$N$_4$O$_4$	C$_{28}$H$_{48}$Cl$_2$Cu$_2$N$_4$
solvent	–	½ CH$_2$Cl$_2$	–	½ C$_3$H$_6$O	CH$_2$Cl$_2$	CH$_2$Cl$_2$	–	–
Fw	735.17	694.04	591.05	828.38	693.95	1133.67	734.60	638.68
T (°C)	-100	-100	-100	-100	-100	-100	-100	-100
space group	$P2_12_12_1$ (no. 19)	$P\bar{3}c1$ (no. 165)	$P\bar{1}$ (no. 2)	$P\bar{1}$ (no. 2)	$P2_1/c$ (no. 14)	$Pbca$ (no. 61)	$P2_1/c$ (no. 14)	$P2_1/c$ (no. 14)
a (Å)	14.12849(8)	20.91645(12)	14.4357(4)	11.1511(3)	12.10209(18)	12.10209(18)	31.6929(5)	13.812(4)
b (Å)	15.61579(8)	20.91645(12)	21.4133(7)	11.2689(3)	16.7871(2)	22.3064(5)	11.59389(16)	13.1498(2)
c (Å)	16.64347(9)	25.50567(18)	21.8614(7)	18.2683(7)	18.9558(3)	24.4072(6)	34.2062(4)	8.32834(18)
α (deg)	90	90	116.132(3)	83.625(3)	90	90	90	90
β (deg)	90	90	95.076(2)	81.121(3)	107.9455(17)	90	95.2904(13)	102.693(2)
γ (deg)	90	120	93.921(2)	70.353(3)	90	90	90	90
V (Å^3)	3672.01(3)	9663.70(10)	5999.5(4)	2131.73(12)	3663.69(10)	12022.8(5)	12515.3(3)	1475.75(6)
Z	4	12	8^c	2	4	8	16^c	2^d
ρ_{calcd} (g cm^{-3})	1.330	1.431	1.309	1.291	1.258	1.257	1.559	1.437
λ (Å)	1.54184	1.54184	1.54184	0.71073	0.71073	0.71073	1.54184	1.54184
μ (mm^{-1})	1.288	1.659	1.433	0.568	0.787	0.426	3.608	3.613
no. of unique ref measured	7215	6387	40463	13887	11585	12099	24208	5365
observed |F$_0$| > 4σ(|F$_0$|)	6773	5737	29178	11121	9073	8480	16663	4647
R$_1$ (obs)^a	0.0315	0.0417	0.0599	0.0413	0.0412	0.0513	0.0370	0.0405
wR$_2$ (all)^b	0.0823	0.1204	0.1864	0.1083	0.1149	0.1494	0.1118	0.1189

a) $R_1 = \frac{\Sigma||F_0|-|F_c||}{\Sigma|F_0|}$; b) $wR_2 = \left[\frac{\Sigma[w(F_0^2-F_c^2)^2]}{\Sigma[w(F_0^2)^2]}\right]^{0.5}$ where $w^{-1} = \sigma^2(F_0^2) + (aP)^2 + bP$; c) There are four crystallographically independent molecules in the asymmetric unit; d) The molecule has crystallographic C_i symmetry.
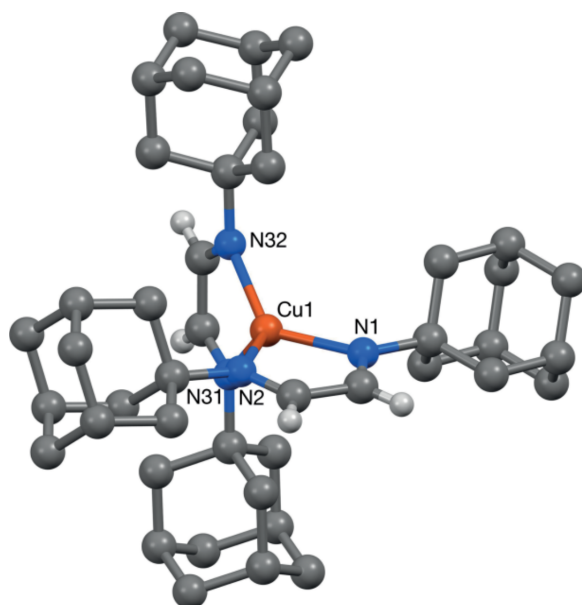
Figure 1.5: Structure of the cation present in the crystal of $[Cu(DAB^{Ad})_2](BF_4)$. Most hydrogen atoms are omitted for clarity. Selected bond lengths [Å] and angles [°]: Cu(1)–N(1) 2.0374(11), Cu(1)–N(2) 2.0389(11), Cu(1)–N(31) 2.0559(12), Cu(1)–N(32) 2.0267(11); N(1)–Cu(1)–N(2) 81.95(5), N(1)–Cu(1)–N(31) 120.12(5), N(1)–Cu(1)–N(32) 129.81(5), N(2)–Cu(1)–N(31) 119.50(5), N(2)–Cu(1)–N(32) 128.66(5), N(31)–Cu(1)–N(32) 81.91(5).
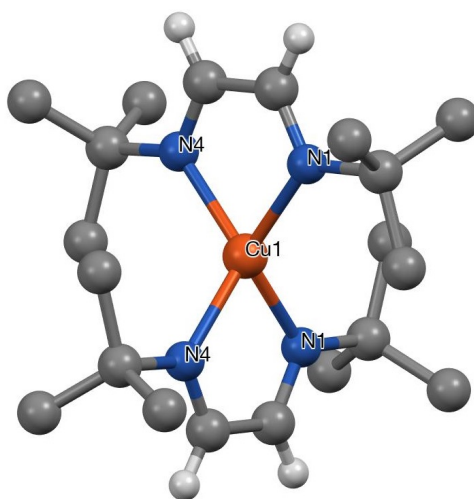
Figure 1.6: Structure of the cation present in the crystal of $[Cu(DAB^{tBu})_2](BF_4)$. Most hydrogen atoms are omitted for clarity. Selected bond lengths [Å] and angles [°]: Cu(1)–N(1) 2.010, Cu(1)–N(4) 2.026; N(1)–Cu(1)–N(4) 82.15(3), N(1)–Cu(1)–N(1) 124.77(4), N(4)–Cu(1)–N(4) 122.40(2), N(1)–Cu(1)–N(4) 126.49(8).
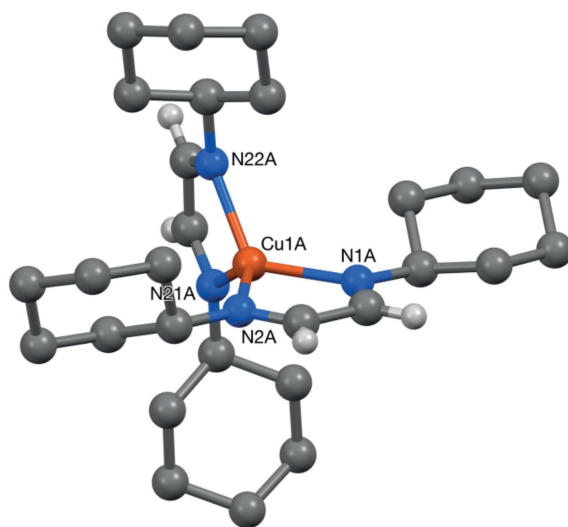
Figure 1.7: Structure of the cation present in the crystal of [Cu(DAB^Cy^)₂](BF₄). Most hydrogen atoms are omitted for clarity. Selected bond lengths [Å] and angles [°]: Cu(1)–N(1) 2.041(3), Cu(1)–N(2) 2.011(3), Cu(1)–N(21) 2.020(3), Cu(1)–N(22) 2.031(3); N(1)–Cu(1)–N(2) 82.31(12), N(1)–Cu(1)–N(21) 117.44(12), N(1)–Cu(1)–N(22) 121.20(11), N(2)–Cu(1)–N(21) 135.45(12), N(2)–Cu(1)–N(22) 124.09(12), N(21)–Cu(1)–N(22) 81.47(11)
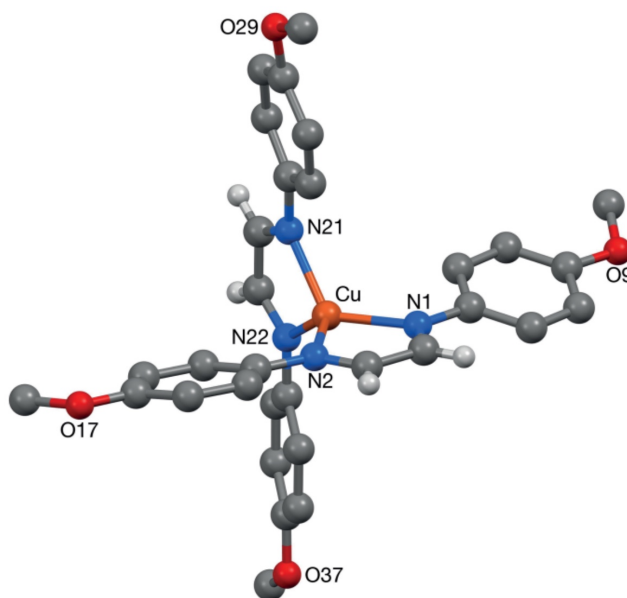
Figure 1.8: Structure of the cation present in the crystal of [Cu(DAB^Anis^)₂](BF₄). Most hydrogen atoms are omitted for clarity. Selected bond lengths [Å] and angles [°]: Cu–N(1) 2.0099(17), Cu–N(2) 2.0095(17), Cu–N(21) 2.0292(18), Cu–N(22) 2.0027(17), N(1)–Cu–N(2) 82.35(7), N(1)–Cu–N(21) 121.46(7), N(1)–Cu–N(22) 126.91(7); N(2)–Cu–N(21) 120.85(7), N(2)–Cu–N(22) 128.18(7), N(21)–Cu–N(22) 82.41(6), 145.46(7), N(2)–Cu–N(21) 145.49(7), N(2)–Cu–N(22) 107.64(7), N(21)–Cu–N(22) 82.41(6).

ing bond lengths and angles for the structures (B–D) are given in Table 1.2 and Table 1.3.
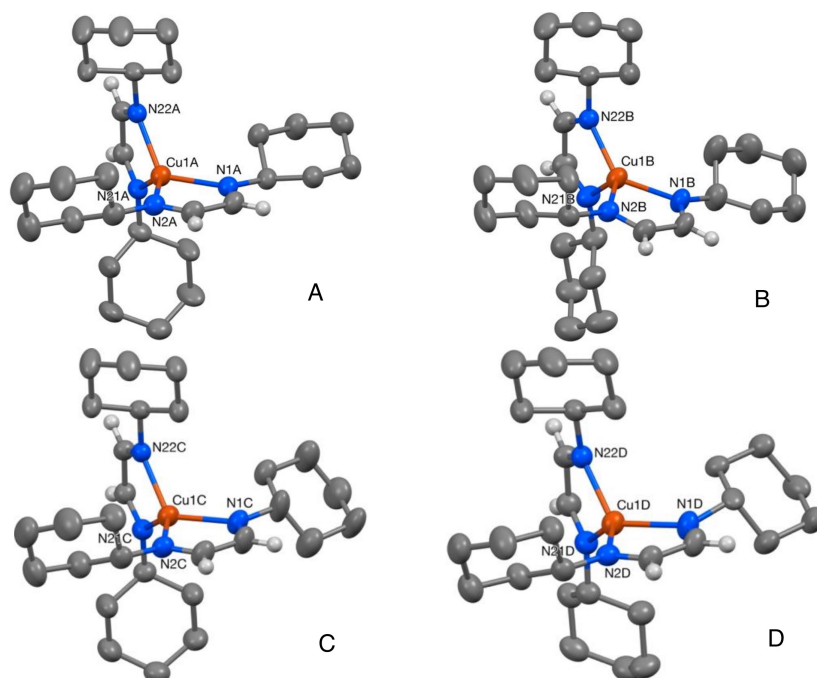
Figure 1.9: Structures A–D of the four cations present in the crystal of [Cu(DAB^{Cy})$_2$](BF$_4$).

Table 1.2: Selected bond lengths (Å) and angles (°) for the four independent cations (A to D) present in the crystal of [Cu(DAB^{Cy})$_2$](BF$_4$).

		A	**B**	**C**	**D**
1	Cu(1)–N(1)	2.041(3)	2.023(3)	2.043(3)	2.050(3)
2	Cu(1)–N(2)	2.011(3)	2.016(3)	2.007(3)	2.007(3)
3	Cu(1)–N(21)	2.020(3)	2.033(3)	2.021(3)	2.022(3)
4	Cu(1)–N(22)	2.031(3)	2.014(3)	2.030(3)	2.016(3)
5	N(1)-Cu(1)-N(2)	82.31(12)	81.75(13)	81.99(12)	81.68(12)
6	N(1)-Cu(1)-N(21)	117.44(12)	114.25(13)	121.22(13)	122.44(13)
7	N(1)-Cu(1)-N(22)	121.20(11)	135.08(13)	118.96(12)	118.90(12)
8	N(2)-Cu(1)-N(21)	135.45(12)	124.22(13)	134.36(12)	132.88(12)
9	N(2)-Cu(1)-N(22)	124.09(12)	125.03(12)	123.18(12)	124.04(12)
10	N(21)-Cu(1)-N(22)	81.47(11)	81.96(12)	82.01(12)	82.01(12)

17

All copper centres in the obtained structures are tetracoordinated. To properly quantify their distortion from the ideal tetrahedral geometry, the τ_4 index, introduced by Yang *et al.*, was calculated.[60] This index is based on the formula $\tau_4 = \frac{360° - (\alpha + \beta)}{141°}$, α and β are the two largest θ angles in the four-coordinate species where an index of 1.0 represents an ideal tetrahedral and an index of 0.0 an ideal square-planar geometry. The calculated τ_4 values for all complexes ranged between 0.88 for $[Cu(DAB^{Ad})_2](BF_4)$ and $[Cu(DAB^{DIPP})(NCMe)_2](BF_4)$ and 0.74 for $[Cu(DAB^{Anis})_2](BF_4)$, which agrees with distorted tetrahedral arrangements. Nonetheless, the calculated τ_4 value for $[Cu(DAB^{Mes})_2](BF_4)$ was considerably lower (0.49) indicating that this geometry might be described as distorted square-planar. The difference can be seen with the bare eye when comparing cationic complexes (Figures 1.5–1.10, 1.12, and 1.13). Indeed, for the homoleptic, cationic complexes $[Cu(DAB^R)_2](BF_4)$ and $[Cu(DAB^R)(NCMe)_2](BF_4)$ the angles between the N–C–N chelate planes vary, being ca. 90, 89, 84, 81, 87, 88, 86, and 54° for R = Ad, Anis, Cy-A, Cy-B, Cy-C, Cy-D, *t*-Bu, and Mes. These planes are almost orthogonal except for $[Cu(DAB^{Mes})_2](BF_4)$. The significantly smaller angle seen in this complex is associated with a pair of intramolecular $\pi - \pi$ interaction between the adjacent mesityl rings on the two coordinated ligands (Figure 1.10).
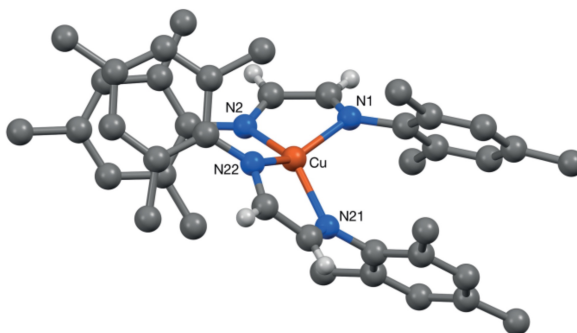
Figure 1.10: Structure of the cation present in the crystal of $[Cu(DAB^{Mes})_2](BF_4)$. Most hydrogen atoms are omitted for clarity. Selected bond lengths [Å] and angles [°]: Cu–N(1) 2.0239(16), Cu–N(2) 2.0256(17), Cu–N(21) 2.0268(15), Cu–N(22) 2.0334(17); N(1)–Cu–N(2) 82.24(7), N(1)–Cu–N(21) 108.44(7), N(1)–Cu–N(22) 145.46(7), N(2)–Cu–N(21) 145.49(7), N(2)–Cu–N(22) 107.64(7), N(21)–Cu–N(22) 82.41(6).

In this complex, the N(1)-bound ring overlays the N(21)-bound ring with centroid⋯centroid and mean interplanar separations of ca. 3.63 and 3.53 Å, the two rings being inclined by ca. 5°, whilst the N(2)- and N(22)-bound rings overlap in a similar fashion (centroid⋯centroid and mean interplanar separations of ca. 3.51 and 3.46 Å, rings inclined by ca. 1°). Overall, the τ_4 index clearly accounts for the intramolecular π-stacking with the mesityl rings in $[Cu(DAB^{Mes})_2](BF_4)$. No such interaction was evidenced

in [Cu(DAB^{Anis})$_2$](BF$_4$), the other homoleptic complex bearing aromatic sub-stituents in this study. However, through DFT calculations the energy differ-ence between the observed unfolded structure of [Cu(DAB^{Anis})$_2$](BF$_4$), and a folded structure similar to [Cu(DAB^{Mes})$_2$](BF$_4$), was determined to be only 1.9 kcal mol^{-1} (Figure 1.11). The most likely reason why the slightly more stable folded version is not observed in the solid state is a different crystal packing favouring the unfolded structure.
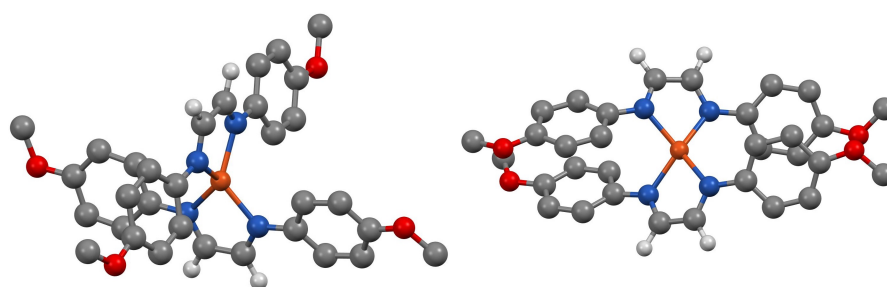
Figure 1.11: Calculated structures for unfolded (right) and unfolded (left) DAB ligands on [Cu(DAB^{Anis})$_2$]$^+$.

For heteroleptic, cationic complex [Cu(DAB^{DIPP})(NCMe)$_2$](BF$_4$), the diiso-propylphenyl groups adopt an almost perpendicular orientation relative to the chelate plane with torsion angles about the N(1)–C(Ar) and N(2)–C(Ar) bonds of ca. 78 and 79°, respectively. This arrangement effectively shields the copper(I) centre above and below the coordination plane, which make accommodating a second DAB ligand difficult (Figure 1.12).
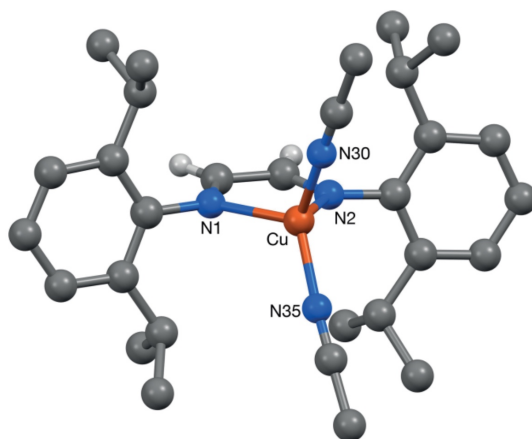
Figure 1.12: Structure of the cation present in the crystal of [Cu(DAB^{DIPP})(NCMe)$_2$](BF$_4$). Most hydrogen atoms are omitted for clarity. Selected bond lengths [Å] and angles [°]: Cu(1)–N(1) 2.0821(12), Cu–N(2) 2.0798(12), Cu–N(30) 1.9424(15), Cu–N(35) 1.9391(14); N(1)–Cu–N(2) 78.82(5), N(1)–Cu–N(30) 112.60(6), N(1)–Cu–N(35) 117.91(5), N(2)–Cu–N(30) 110.21(6), N(2)–Cu–N(35) 117.88(5), N(30)–Cu–N(35) 114.52(6).

Similar torsion angles are observed for [Cu(DAB^{DIPh})(NCMe)$_2$](BF$_4$) with values of 77 and 80° (Figure 1.13). Additionally, the obtained structure for [Cu(DAB^{DIPh})(NCMe)$_2$](BF$_4$) shows how the imine protons and carbons C(1) and C(2) are interlaid in-between four phenyl rings explaining their upfield shift in the ^{1}H and ^{13}C NMR spectra upon complexation (Figure 1.14).
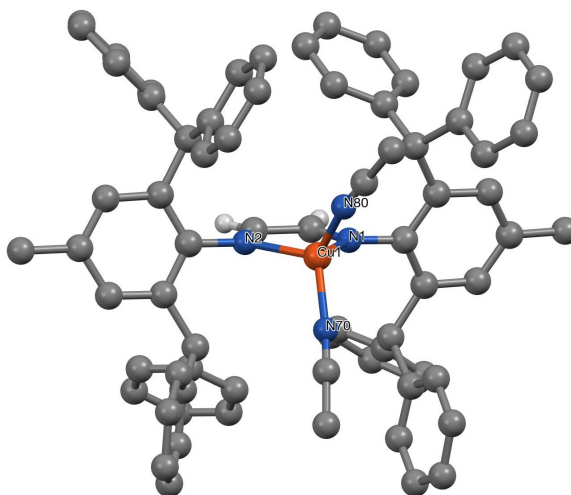
Figure 1.13:   Structure of the cation present in the crystal of [Cu(DAB^{DIPh})(NCMe)$_2$](BF$_4$). Most hydrogen atoms are omitted for clarity. Selected bond lengths [Å] and angles [°]: Cu(1)–N(1) 2.100(2), Cu(1)–N(2) 2.087(2), Cu(1)–N(70) 1.951(3), Cu(1)–N(80) 1.949(3); N(1)–Cu(1)–N(2) 79.91, N(1)–Cu(1)–N(70) 118.78, N(1)–Cu(1)–N(80) 114.34, N(2)–Cu(1)–N(70) 115.46, N(2)–Cu(1)–N(80) 122.21, N(70)–Cu(1)–N(80) 105.38.
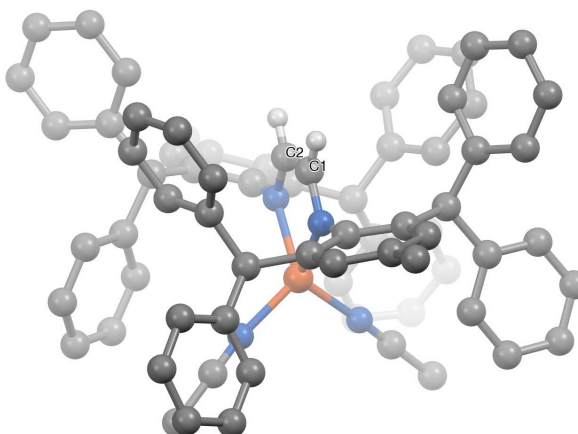
Figure 1.14:   Interlaid DAB backbone in the solid state structure of [Cu(DAB^{DIPh})(NCMe)$_2$](BF$_4$). Most hydrogen atoms are omitted for clarity.

Heteroleptic, neutral complexes [CuCl(DAB^R)] (R = Anis and Cy) both present central Cu_2Cl_2 rings in which the copper(I) and the chlorine ions each occupy opposite corners. This ring is perfectly flat in [CuCl(DAB^{Cy})] as a consequence of the centre of symmetry in the middle of the ring (Figure 1.15), but distinct folds of ca. 21, 13, 16 and 26°, respectively, are seen between the two CuCl$_2$ planes for the four independent complexes of [CuCl(DAB^{Anis})] (Figure 1.16).
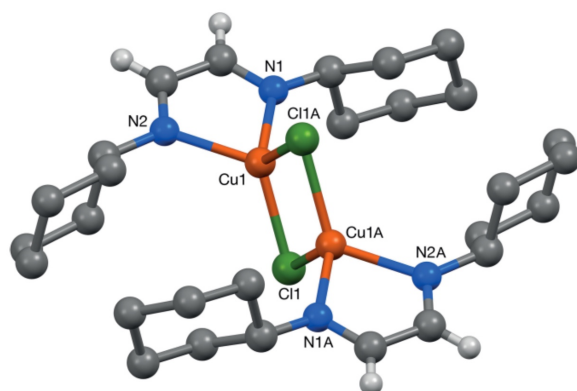
Figure 1.15: Structure of the cation present in the crystal of [CuCl(DAB^{Cy})]. Most hydrogen atoms are omitted for clarity. Selected bond lengths [Å] and angles [°]: Cu(1)–Cl(1) 2.3625(5), Cu(1)–N(1) 2.0875(15), Cu(1)–N(2) 2.1025(15), Cu(1)–Cl(1A) 2.2909(5); Cl(1)–Cu(1)–N(1) 114.93(4), Cl(1)–Cu(1)–N(2) 112.57(4), Cl(1)–Cu(1)–Cl(1A) 101.846(17), N(1)–Cu(1)–N(2) 79.94(6), N(1)–Cu(1)–Cl(1A) 125.28(5), N(2)–Cu(1)–Cl(1A) 122.07(5), Cu(1)–Cl(1)–Cu(1A) 78.154(17).
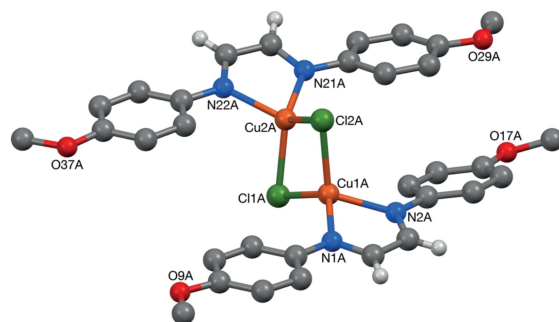
Figure 1.16: Structure of the cation present in the crystal of [CuCl(DAB^{Anis})]. Most hydrogen atoms are omitted for clarity. Selected bond lengths [Å] and angles [°]: Cu(1A)–Cl(1A) 2.2773(7), Cu(1A)–N(1A) 2.073(2), Cu(1A)–N(2A) 2.0641(19), Cu(1A)–Cl(2A) 2.3534(7); Cl(1A)–Cu(1A)–N(1A) 125.29(6), Cl(1A)–Cu(1A)–N(2A) 123.56(6), Cl(1A)–Cu(1A)–Cl(2A) 105.29(2), N(1A)–Cu(1A)–N(2A) 80.53(8), N(1A)–Cu(1A)–Cl(2A) 109.85(6), N(2A)–Cu(1A)–Cl(2A) 110.54(6), Cu(1A)–Cl(1A)–Cu(2A) 73.58(2).
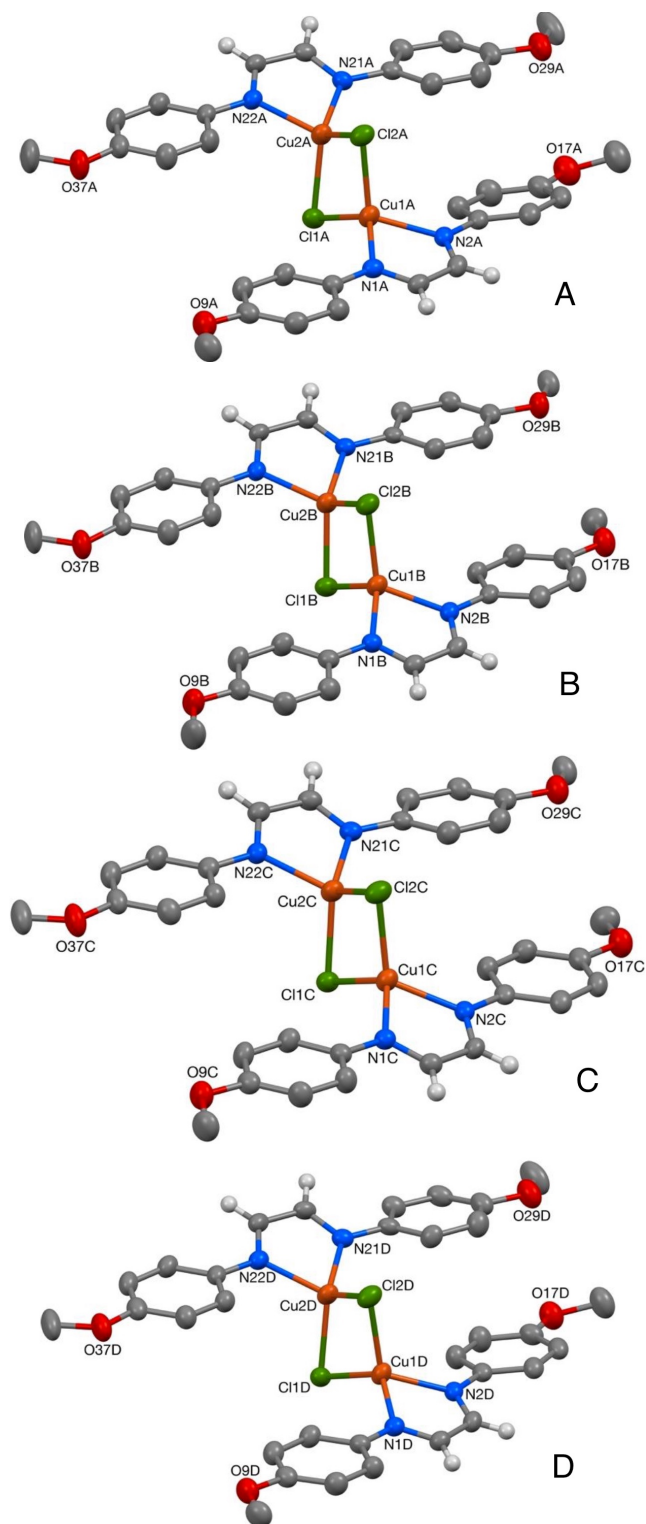
Figure 1.17: Structures A–D of the four cations present in the crystal of [CuCl(DAB^{Anis})]. Most hydrogen atoms are omitted for clarity.

Table 1.3: Selected bond lengths (Å) and angles (°) for the four independent cations (A to D) present in the crystal of [CuCl(DAB^{Anis})].

		A	B	C	D
1	Cu(1)–Cl(1)	2.2773(7)	2.2884(7)	2.3042(6)	2.2984(6)
2	Cu(1)–Cl(2)	2.3534(7)	2.3339(7)	2.3317(7)	2.3408(7)
3	Cu(1)–N(1)	2.073(2)	2.0853(19)	2.0788(19)	2.074(2)
4	Cu(1)–N(2)	2.0641(19)	2.0576(19)	2.0670(18)	2.0648(19)
5	Cu(2)–Cl(1)	2.3396(7)	2.3338(7)	2.3363(6)	2.3342(7)
6	Cu(2)–Cl(2)	2.2913(7)	2.2906(6)	2.2726(6)	2.2711(7)
7	Cu(2)–N(21)	2.0522(19)	2.0564(19)	2.0447(19)	2.038(2)
8	Cu(2)–N(22)	2.0772(19)	2.0793(18)	2.0788(19)	2.0793(19)
9	Cl(1)–Cu(1)–Cl(2)	105.29(2)	103.92(2)	103.54(2)	104.35(2)
10	Cl(1)–Cu(1)–N(1)	125.29(6)	119.67(6)	121.52(6)	125.99(6)
11	Cl(1)–Cu(1)–N(2)	123.56(6)	121.50(6)	119.52(6)	120.53(6)
12	Cl(2)–Cu(1)–N(1)	109.85(6)	115.47(6)	113.47(6)	108.72(6)
13	Cl(2)–Cu(1)–N(2)	110.54(6)	115.43(6)	118.03(6)	115.76(6)
14	N(1)–Cu(1)–N(2)	80.53(8)	80.49(8)	80.60(7)	80.65(8)
15	Cl(1)–Cu(2)–Cl(2)	105.30(2)	103.85(2)	104.39(2)	105.44(2)
16	Cl(1)–Cu(2)–N(21)	121.77(6)	120.62(6)	121.38(5)	122.61(6)
17	Cl(1)–Cu(2)–N(22)	108.41(6)	110.46(6)	111.78(6)	110.30(6)
18	Cl(2)–Cu(2)–N(21)	117.49(6)	117.72(6)	118.15(6)	118.41(6)
19	Cl(2)–Cu(2)–N(22)	122.74(6)	123.77(6)	119.96(6)	118.01(6)
20	N(21)–Cu(2)–N(22)	80.37(8)	80.31(7)	80.67(8)	80.72(8)
21	Cu(1)–Cl(1)–Cu(2)	73.58(2)	73.07(2)	75.57(2)	75.53(2)
22	Cu(1)–Cl(2)–Cu(2)	74.87(2)	75.55(2)	72.61(2)	72.97(2)

The observed Cu···Cu distances in each independent unit (2.74–2.83 Å) are just around the sum of their van der Waals radii (2.80 Å),[61] which might be indicative of a weak attractive interaction between the two closed-shell d10 metal ions. No such interaction can be postulated in [CuCl(DAB^{Cy})] as the observed Cu···Cu separation of 2.934 Å is too long.

The sp^2 character of the C and N atoms in the chelate ring of all complexes is confirmed by imine bond lengths of 1.269(2)–1.275(3) Å for cationic [Cu(DAB^{Cy})$_2$](BF$_4$), or 1.280(3) Å for neutral [CuCl(DAB^{Cy})], for instance, and both are very similar to standard sp^2 C=N double bonds.[62]

In an attempt to better understand the steric environment imposed by these diimine ligands in the solid state, and maybe also the specific stoichiometries obtained for the prepared complexes, we quantified such effect of DAB^R using the percent buried volume (%V_B) method, originally developed by Cavallo and co-workers as a steric probe of N-heterocyclic carbene ligands.[63,64] A simple on-line tool calculates the percentage of the volume of a metal-centred sphere of defined radius that is occupied by a given ligand.[65]

For these calculations we used the crystallographic data obtained for cationic complexes [Cu(DAB^R)] (R = Ad, Anis, DIPP, DIPh, Mes, *t*-Bu), and according to the obtained %V_B values (41.4–50.1), the steric demand of the diimine ligands used in this study follows the sequence: DAB^{Anis}~DAB^{Cy}<DAB^{Ad} ~ DAB^{tBu}<DAB^{DIPP}<DAB^{Mes}<DAB^{DIPh}. It was not surprising to find that the most sterically hindered ligand was DAB^{DIPh}. However, it was surprising that DAB^{Mes} and not DAB^{DIPP} was second in this list as the isolation of heteroleptic [Cu(DAB^{DIPP})(NCMe)$_2$](BF$_4$) would suggest. These values clearly show both steric and electronic factors determine the nature of the accessible complexes for these ligands.

1.5 Investigation into Solution Behaviour of [Cu(DAB)]

As mentioned before, all prepared and isolated complexes were coloured, with shades ranging from pink to violet. UV/Vis studies were carried out to understand the behaviour in solution as there have been accounts on ligand dissociation in related complexes.[13] The main focus laid on homoleptic cationic complexes as there is some precedent in the literature for [CuCl(DAB^R)] complexes,[15] and also the low solubility of CuCl in organic solvents would impede any titration experiments.

In a first step, the absorption spectrum of [Cu(DAB^{Anis})$_2$](BF$_4$) was recorded in DCM (15 μM) and it revealed an intense broad band between 420 and 452 nm (ε = 35280±697 L mol^{-1} cm^{-1}) and a smaller band at a higher wavelength (593 nm, 5100±70 L mol^{-1} cm^{-1}). Both bands were assigned to d$\pi - \pi^*$ metal-to-ligand charge transfer (MLCT) absorptions since the free ligand, DAB^{Anis}, in DCM displayed a band at 375 nm (24810±293 L mol^{-1} cm^{-1}).

The initial measurements were followed by titration experiments carried out with $[Cu(NCMe)_4](BF_4)$ solutions in degassed DCM (15 µм) and increasing amounts of free ligand DAB^{Anis} (0.2–3 equiv). A constant increase of both bands was observed between 0.2 and 1.6 equivalents of ligand (Figure 1.18). With higher equivalents of added ligand, a band at 425 nm appeared and progressively red-shifted towards the absorption band of DAB^{Anis}.
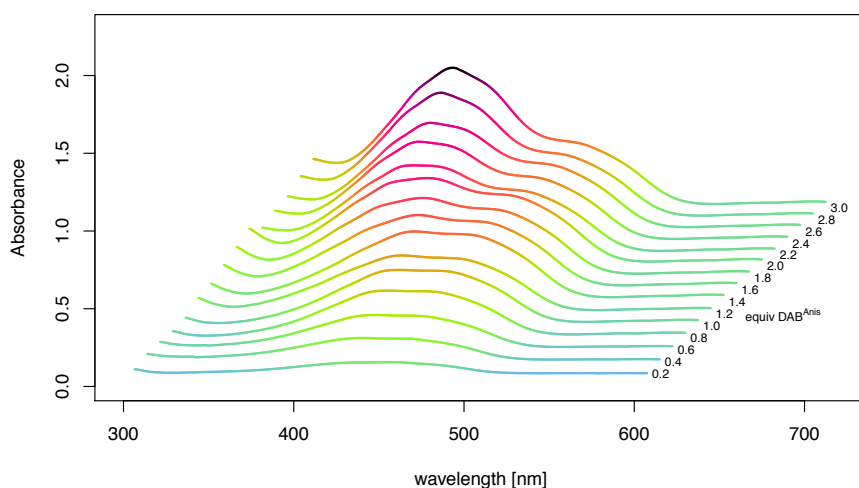
Figure 1.18: UV/Vis spectra for the titration experiments with $[Cu(NCMe)_4](BF_4)$ (15 µм) and different equivalents of DAB^{Anis} in DCM.

Plotting the absorption intensity against the equivalents of ligand showed that the intensity of both bands increased continuously up to 1.5 equivalents of ligand, and remained constant above that (Figure 1.19, a and b). Furthermore, Job plots for these two bands indicate a mol fraction of 0.64 and 0.62 for DAB^{Anis}, with both values very close to a 2:3 Cu/L ratio for the species in solution (Figure 1.19, c and d).

(a) 452 nm   (b) 593 nm   (c) 452 nm   (d) 593 nm
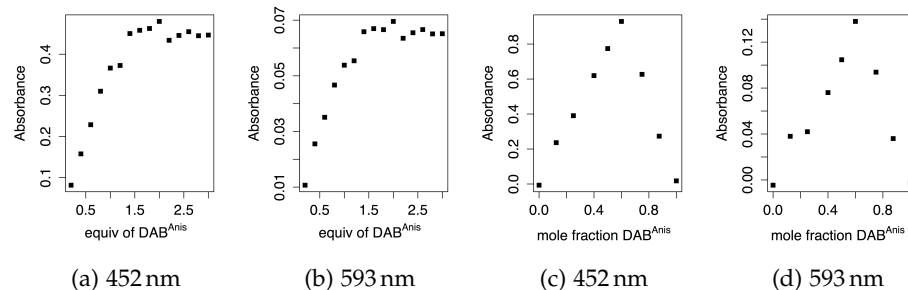
Figure 1.19: Absorption intensities *versus* ligand equivalents and Job plot for the titration experiments with DAB^{Anis} in DCM.

These results suggest a different stoichiometry of the species in solution when compared to isolated $[\mathrm{Cu(DAB^{Anis})_2}](\mathrm{BF_4})$. It is important to point out that the UV/Vis spectrum obtained for $[\mathrm{Cu(DAB^{Anis})_2}](\mathrm{BF_4})$ was virtually identical to that from a titration experiment with a 2:3 and not a 1:2 Cu/L ratio as it could have been expected (Figure 1.20).
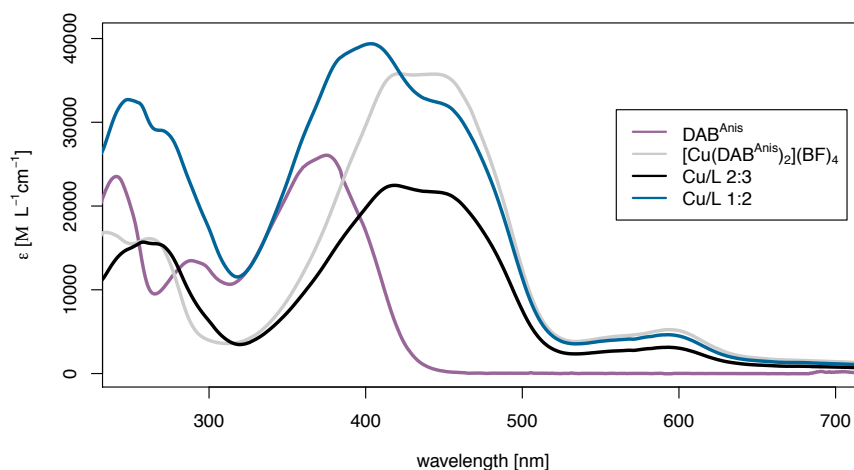
Figure 1.20: Comparison of UV/Vis spectra in DCM for the Cu/DAB$^{\text{Anis}}$ system ([Cu] = 15 μм).

These observations were further investigated using NMR spectroscopy and a ^{1}H NMR spectrum of a 15 μм solution of $[\mathrm{Cu(DAB^{Anis})_2}](\mathrm{BF_4})$ in $\mathrm{CD_2Cl_2}$ was recorded. As suspected, no signals corresponding to $[\mathrm{Cu(DAB^{Anis})_2}](\mathrm{BF_4})$ were found at this low concentration. Instead, the signals corresponding to free DAB$^{\text{Anis}}$ were observed, together with those corresponding to a new ligated species with a single chemical environment for all diimine hydrogen atoms present (Figure 1.21).
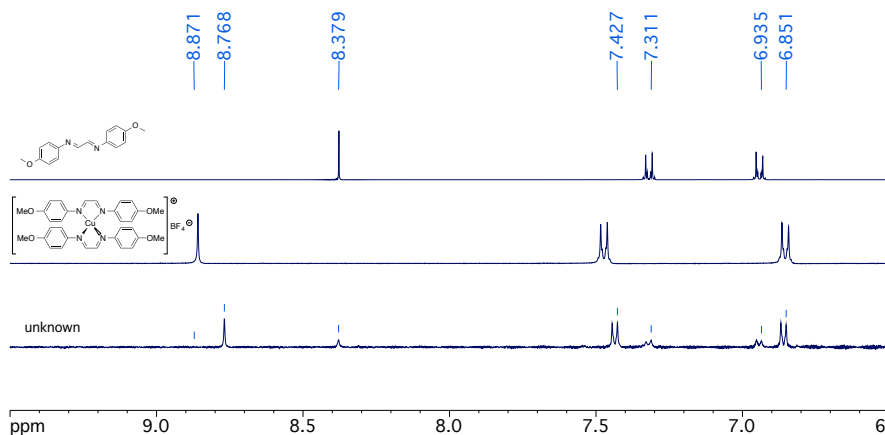
Figure 1.21: Comparison of ^{1}H NMR spectra for the Cu/DAB$^{\text{Anis}}$ system in $\mathrm{CD_2Cl_2}$.

Unfortunately, the low concentration prevented the acquisition of a DOSY spectrum within reasonable time. Taking these results into account, a structure featuring a dinuclear copper complexes with three bridging DAB[Anis] is proposed for the copper complex formed in the titration experiments, featuring a dicopper complex with three bridging diimine ligands (Figure 1.22).[21]
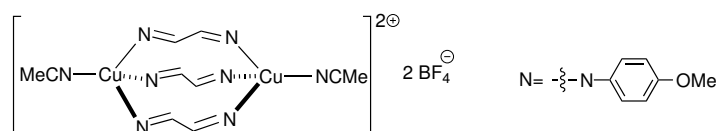
Figure 1.22: Plausible structure for the species formed by the Cu/DAB[Anis] system in DCM.

$[Cu(DAB^{Ad})_2](BF_4)$ was investigated next in order to obtain more information about these homoleptic complexes. DAB^{Ad} does not absorb in the visible region and the only absorption observed in DCM is at 228 nm ($14450 \pm 503 \, L \, mol^{-1} \, cm^{-1}$), which is useful in this context. The measurements for $[Cu(DAB^{Ad})_2](BF_4)$ were carried out at a higher concentration (typically 300 μM) as both the complex and the ligand are significantly less absorbent than in the previous case. Nonetheless, it should be noted that identical UV/Vis bands were recorded at lower concentrations, down to 40 μM. Two absorption bands were observed in the spectrum of $[Cu(DAB^{Ad})_2](BF_4)$, the first, a small one at 430 nm and a second one, much stronger, at 530 nm and both were attributed to $d\pi - \pi^*$ MLCT absorptions.

Again, titration experiments were performed in degassed DCM with a constant concentration of $[Cu(NCMe)_4](BF_4)$ (300 μM) and an increasing concentration of DAB^{Ad} (60–900 μM, 0.2–5 equiv, Figure 1.23). Between 0.2 and 1
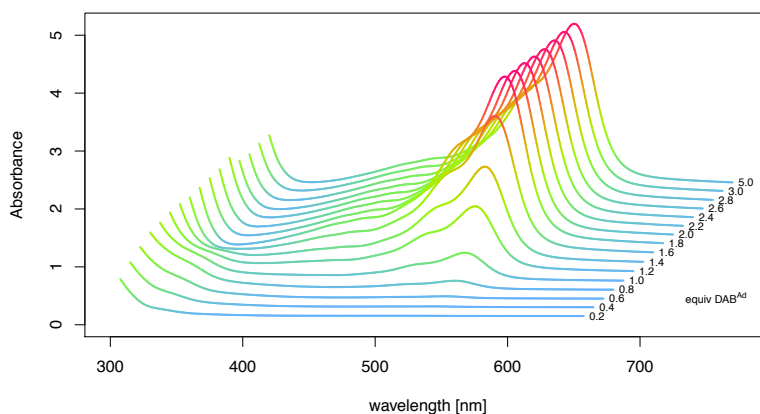
Figure 1.23: UV/Vis spectra for the titration experiments with $[Cu(NCMe)_4](BF_4)$ (300 μM) and different equivalents of DAB^{Ad} in DCM.

27

equiv of ligand an absorption band at 530 nm was observed together with a very small band at 326 nm. From 1 to 2 equivalents of ligand, the intensity of the band at 326 nm decreased, whereas the absorption band at 430 and 530 nm steadily increased. Further addition of DAB^{Ad} (up to 5 equivalents) did not alter the absorption spectrum. Plotting the absorption intensity against the equivalents of ligand showed that the intensity at 326 nm increased up to 1 equivalent of DAB^{Ad} and then dropped, whereas the intensity at 430 and 530 nm steadily increased up to 2 equivalents and then levelled off (Figure 1.24). Additionally, the UV/Vis spectrum of [Cu(DAB^{Ad})$_2$] (BF$_4$) and the one obtained from the titration experiment with a Cu/L ratio of 1:2 are identical. Therefore, it was assumed that the band at 326 nm belonged to a heteroleptic complex [Cu(DAB^{Ad})(NCMe)$_2$](BF$_4$).

(a) 326 nm   (b) ▲ 430 nm ■ 530 nm
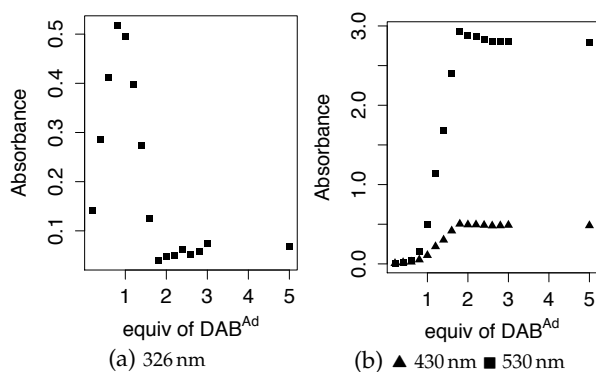
Figure 1.24: Absorption intensities plotted *versus* ligand equivalents for the titration experiments with DAB^{Ad} in DCM.

In order to gather additional evidence, we next carried out UV/Vis studies in MeCN, a coordinating solvent and two bands were observed again in the spectrum of [Cu(DAB^{Ad})$_2$](BF$_4$), one at 398 nm and a more intense one at 525 nm. When this spectrum was recorded at different concentrations (0.15–1.2 mM), it became clear that as the concentration was reduced, the band at 525 nm decreased in intensity at a faster rate than the band at 398 nm (Figure 1.25). When intensities of these bands were plotted against
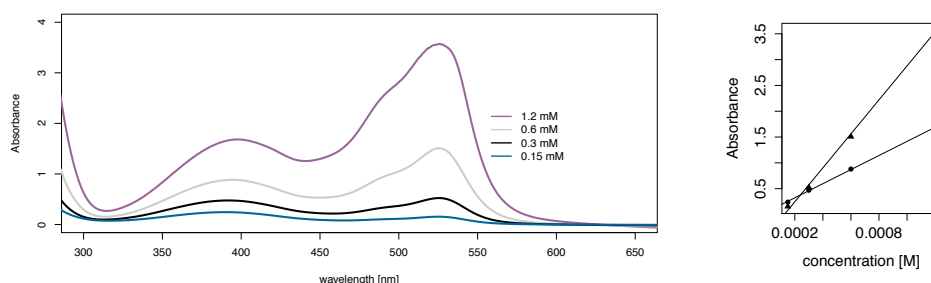
Figure 1.25: UV/Vis spectra for the titration experiments with [Cu(NCMe)$_4$](BF$_4$) (300 μM) and different equivalents of DAB^{Ad} in MeCN.

concentration, both lines eventually cross each other, giving evidence that these two bands do not belong to the same species in solution. Further evidence comes from a vastly different shape of normalised spectra recorded at different concentrations. The absorption intensities were divided by the concentration (Figure 1.26). If both bands had belonged to the same species, they would have shown identical band intensities. It is also evident that the band at 398 nm has the same extinction coefficient throughout all measurements, whereas the band at 525 nm varies and thus gave evidence for the presence of an alternate species at different concentrations. These results indicate that MeCN can indeed displace the DAB^{Ad} ligand at low concentrations, possibly forming [Cu(DAB^{Ad})(NCMe)$_2$](BF$_4$) *in situ*.
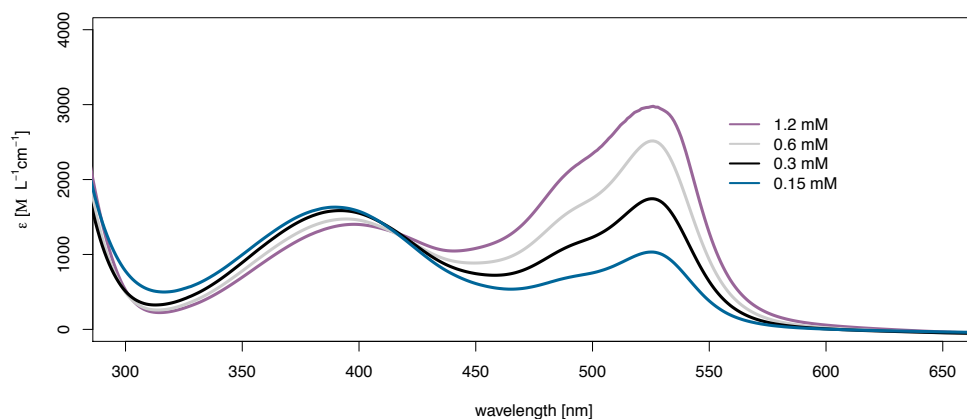
Figure 1.26: Absorption spectra of [Cu(DAB^{Ad})$_2$](BF$_4$) at different dilutions normalised by their concentrations.

Furthermore, titration experiments in degassed MeCN with a constant concentration of [Cu(NCMe)$_4$](BF$_4$) (0.2 mM) and a variable amount of DAB^{Ad} led to additional information compared to titration experiments obtained in DCM. For 0.1, 0.13, and 0.2 equivalents of ligand, only an absorption band at 398 nm was observed. The band at 525 nm started appearing after 0.6 equivalents of ligand were added and persisted throughout the end of the titration experiment (Figure 1.27).

When the absorption intensities for each band were plotted against the equivalent of ligand added, it showed that the intensity of the band at 398 nm increased linearly until about 2 equivalents of ligand after which the intensity levelled off. On the other hand, the intensity of this band at 525 nm steadily increased throughout the titration experiment (Figure 1.28, a, b). The Job plot derived from this data showed that the maximum for the 398 nm band laid within 0.5 mol fraction of the ligand, pointing towards a 1:1 Cu/L ratio (Figure 1.28, c, d). For the band at 525 nm, the maximum
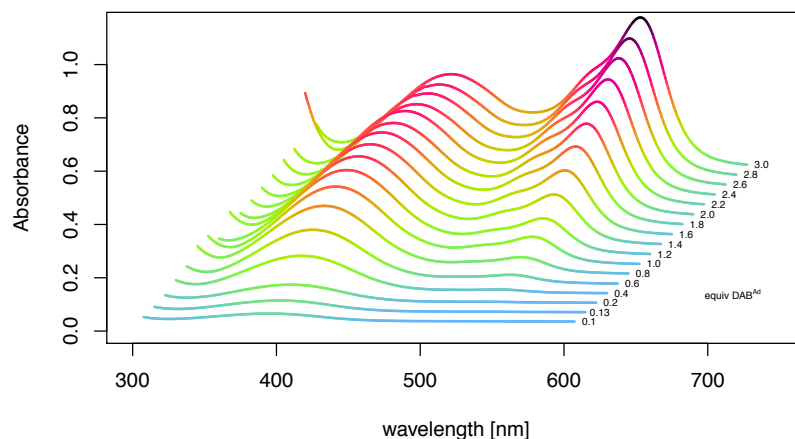
Figure 1.27: UV/Vis spectra for the titration experiments with $[Cu(NCMe)_4](BF_4)$ (200 μM) and different equivalents of DAB^{Ad} in MeCN.

absorbance was between 0.6 and 0.7, which could be attributed to a 1:2 or a 2:3 copper/ligand ratio. Considering the bulky adamantyl groups on the ligand, a 1:2 stoichiometry for the copper complex was favoured.

| (a) 398 nm | (b) 525 nm | (c) 398 nm | (d) 525 nm |
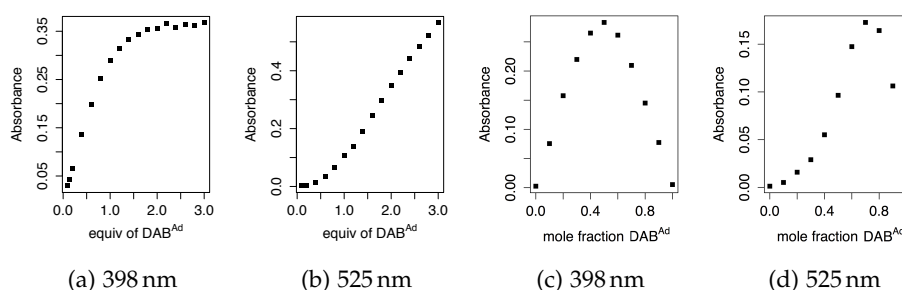
Figure 1.28: Absorption intensities *versus* ligand equivalents and Job plot for the titration experiments with DAB^{Ad} in MeCN.

The extinction coefficient for the absorption band at 398 nm, attributed to heteroleptic $[Cu(DAB^{Ad})(NCMe)_2](BF_4)$, could be calculated from titration experiments with a large excess of $[Cu(NCMe)_4](BF_4)$ (up to 1000 equiv) to prevent the formation of the homoleptic complex. Under these conditions, no band at 525 nm was observed and an extinction coefficient of $2191 \pm 22\,L\,mol^{-1}\,cm^{-1}$ was obtained (Figure 1.29).

On the other hand, the dilution of $[Cu(DAB^{Ad})_2](BF_4)$ (0.06–0.6 mM) in solutions of acetonitrile saturated with DAB^{Ad} led to UV/Vis spectra with only
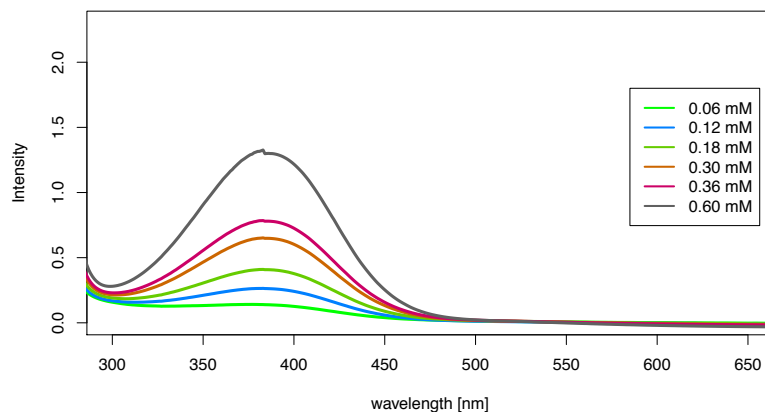
Figure 1.29: Absorbance of $[Cu(DAB^{Ad})(NCMe)_2](BF_4)$ in different concentrations in MeCN.

the band at 525 nm, and the extinction coefficient found for this species was $7448\pm255\,L\,mol^{-1}\,cm^{-1}$ (Figure 1.30).
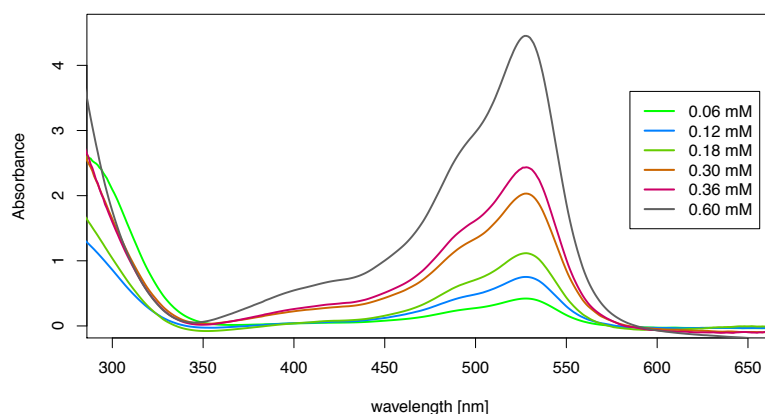
Figure 1.30: Absorbance of $[Cu(DAB^{Ad})_2]^+$ in different concentrations in MeCN.

With this data in hand, the equilibrium constant for the reaction depicted in Scheme 1.17 was found to be 5.02×10^3. It is important to note that only data obtained at copper concentrations between 0.04 and 0.3 mM could be used in these calculations, since at higher concentrations the Beer-Lambert law is not fulfilled any more, most probably because of additional equilibria present in the system. Using the thermodynamic principle $\Delta G = -RT \ln K$ where ΔG is the free energy, R the Boltzmann constant, T the temperature in Kelvin, and K the equilibrium constant, the free energy for this equilibrium was determined to be $4.1\,kcal\,mol^{-1}$. The initial energy differences calculated by
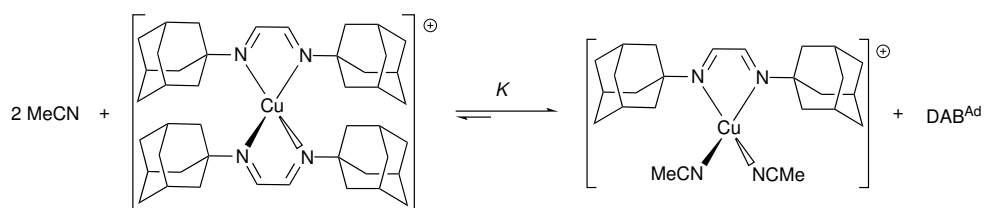
Scheme 1.17: Equilibrium between homo and heteroleptic species of [Cu(DAB^{Ad})$_2$](BF$_4$).

DFT methods between homo- and heteroleptic complex were too high and a different structure was proposed with an interaction between the BF$_4^-$ anion and the copper centre, which lowered the energy difference significantly to 7.6 kcal mol^{-1} between the two species. (The computational experiment was calculated with M06-X2, 6-31g, sdd(Cu), and in MeCN with PCM as solvation model Figure 1.31). Despite being slightly different in energy the experimental and theoretical results support the idea of a heteroleptic type complex [Cu(DAB^{Ad})(NCMe)$_2$]$^+$.
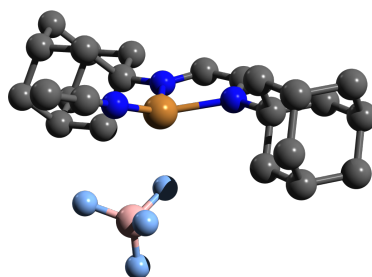
Figure 1.31: Calculated, lowest energy structure for the heteroleptic species [Cu(DAB^{Ad})(NCMe)$_2$]$^+$ for the equilibrium of [Cu(DAB^{Ad})$_2$](BF$_4$).

All attempts to isolate the proposed heteroleptic [Cu(DAB^{Ad})(NCMe)$_2$](BF$_4$) failed and no crystals suitable for X-ray analysis could be grown. Upon concentration, only homoleptic [Cu(DAB^{Ad})$_2$](BF$_4$) was observed by NMR spectroscopy. However, further evidence could be obtained by ^{1}H NMR analysis. Several spectra of [Cu(DAB^{Ad})$_2$](BF$_4$) were recorded in CD$_3$CN at different concentrations (Figure 1.32). When the concentration was lowered from 12 to 0.3 mM, an upfield shift of the signal of the imine hydrogen in the copper complex was observed from 8.3 to 8.0 ppm and the signal also became very broad indicating a rapid exchange process of the DAB^{Ad} on the NMR scale (Figure 1.32, a, b, and c). When the same spectrum was recorded at −40 °C, three imine environments were observed, homoleptic complex (δ = 8.3 ppm), free DAB^{Ad} (δ = 7.8 ppm), and a new signal (δ = 8.0 ppm). Furthermore, as a mixture of [Cu(NCMe)$_4$](BF$_4$) and DAB^{Ad} in a 1:0.2 ratio showed only the band at 398 nm in the UV/Vis spectrum, these conditions

were studied by ^{1}H NMR (Figure 1.32, d) and only a single resonance at $\delta =$ 8.0 ppm was obtained at room temperature.
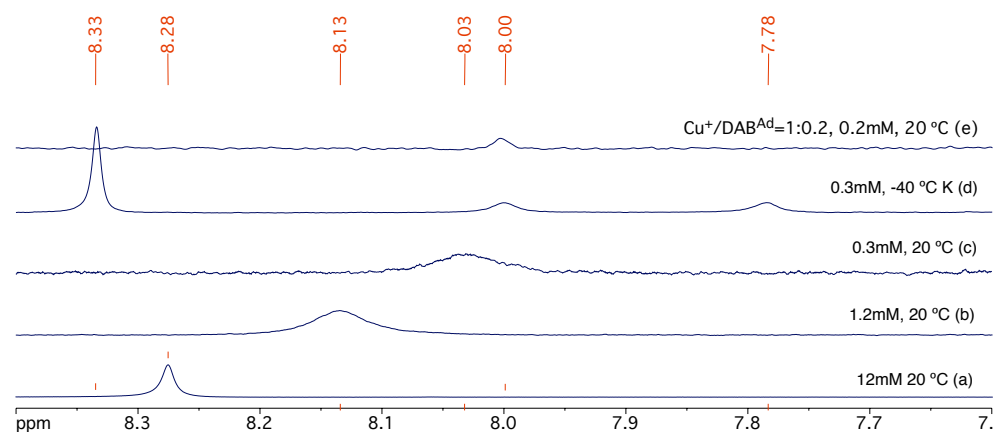
Figure 1.32: Comparison of ^{1}H NMR spectra for the Cu/DAB^{Ad} system in CD$_3$CN.

Overall, these results show that even if they might not be isolable, [Cu(DAB^R)(NCMe)$_2$](BF$_4$) complexes can be formed as diluted solutions either by dilution of pre-isolated [Cu(DAB^R)$_2$](BF$_4$) complexes or by the reaction of the ligand with a large excess (*e.g.* 5 equiv) of the copper source. Notably, the heteroleptic [Cu(DAB^{Ad})(NCMe)$_2$]$^+$ showed a similar UV/Vis spectrum as the isolable, cationic, heteroleptic complexes [Cu(DAB^{DIPP})(NCMe)$_2$](BF$_4$) and its lowest energy band appeared at 353 nm (1709 ± 4 L mol^{-1} cm^{-1}) in MeCN. Quite surprisingly, this particular compound is almost as stable as the rest of the complexes reported in this work.

Since similar complexes had been shown to be fluorescent,[66] the fluorescence of [CuCl(DAB^{Anis})], [Cu(DAB^{Anis})$_2$](BF$_4$), [CuCl(DAB^{Ad})], and [Cu(DAB^{Ad})$_2$](BF$_4$) was investigated. In a first step, [CuCl(DAB^{Anis})] was measured and showed fluorescence at three distinct wavelengths (350, 410, and 450 nm) in DCM. However, the fluorescence was very weak and superimposed by the fluorescent signal of the photospectroscopic grade solvent. The signal from the solvent could not be lowered by distillation and thus, the fluorescence spectrum of complex was calculated by subtraction of a blank DCM sample (Figure 1.33). Additionally, the fluorescence of DAB^{Anis} was measured as well as [Ru(bipy)$_3$]Cl$_2$, which was used as reference sample. Figure 1.33 shows that in presence of CuCl the fluorescence of DAB^{Anis} is quenched. In comparison to [Ru(bipy)$_3$]Cl$_2$ and even DAB^{Anis}, the quantum yield of the copper complex is very low. Furthermore, [Cu(DAB^{Anis})$_2$](BF$_4$), [CuCl(DAB^{Ad})], and [Cu(DAB^{Ad})$_2$](BF$_4$) did not show any fluorescence un-

der any excitation wavelength.
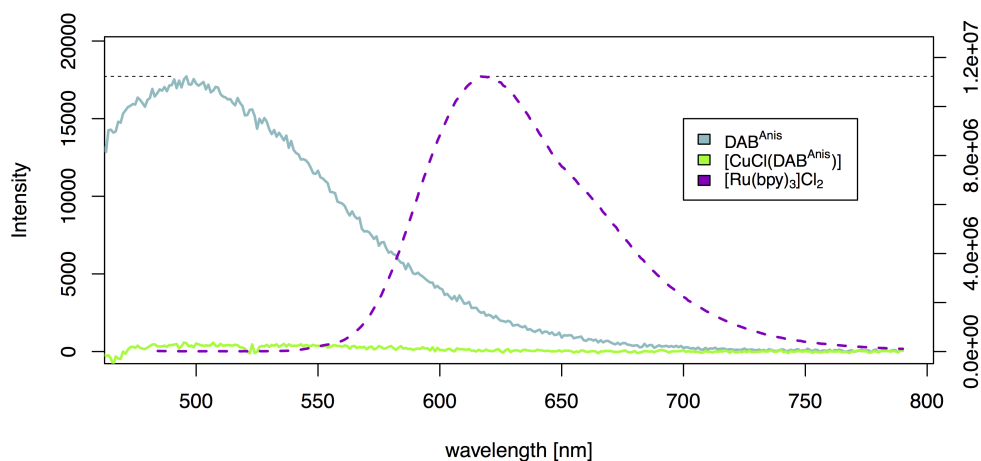
Figure 1.33: Fluorescence measurements of DAB^{Anis}, [CuCl(DAB^{Anis})], and [Ru(bipy)$_3$]Cl$_2$ at an excitation wavelength of 450 nm in DCM.

1.6 Synthesis and Characterisation of [Cu(ImPy)] Complexes

Initially, to synthesise [Cu(ImPy^R)$_2$](BF$_4$) complexes successful reported procedures for similar copper(I) complexes were followed (Scheme 1.18). [44–46] Unfortunately, reaction of ImPy^{Anis} with [Cu(NCMe)$_4$](BF$_4$) in MeOH or MeCN did not lead to the formation of the desired complex and the obtained solids turned readily green in air, which indicated an oxidation to copper(II) and indeed, the ^{1}H NMR spectrum showed only very broad signals as expected for paramagnetic copper(II) species.
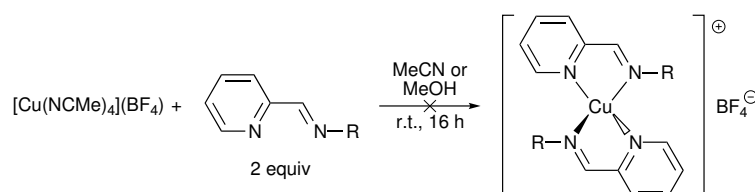
Scheme 1.18: Reported procedures for the synthesis of homoleptic, cationic [Cu(ImPy^R)] (BF$_4$) complexes.

In a further attempt to synthesise a [Cu(ImPy)] complex, a method reported by van Stein *et al.* from $Cu(OTf) \cdot (C_6H_6)_{0.5}$ was used.[67] Indeed, we could then obtain [Cu (ImPy^{DIPP})$_2$](OTf) from ImPy^{DIPP} and $Cu(OTf) \cdot (C_7H_8)_{0.5}$ in excellent yield (Scheme 1.19). Related [Cu(ImPy^R)$_2$](OTf) complexes (R = Ad, Anis, and Mes) were then prepared using the same method in similar good yields (45–95%).
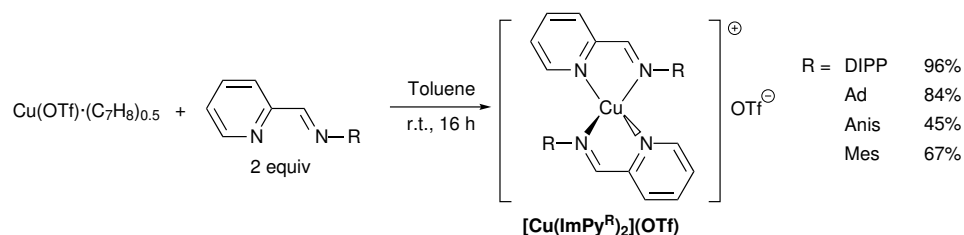
Scheme 1.19: Adopted procedure for the formation of [Cu(ImPy^R)](OTf).

All isolated complexes were indefinitely stable towards oxygen and moisture in the solid state without any particular need for precautions. Also, all complexes showed the same brown colour in the solid state and these properties matched the reports on similar copper(I) ImPy complexes.[44–46,67] These complexes were then fully characterised by spectroscopic methods and single-crystal X-ray diffraction.

Similar to [Cu(DAB)] complexes, in the ^{1}H NMR spectra the resonances of the imino proton on the backbone of the ligand appeared to be shifted to a lower field after metal coordination agreeing with the expected electron donation from the ImPy ligand to the copper centre. In contrast to [Cu(DAB)], the magnitude of the downfield shift seemed to depend greatly on the substituent on the ImPy^R. The imino proton on [Cu(ImPy^{Ad})$_2$](OTf) showed only a shift by 0.07 ppm compared to the free ligand, whereas [Cu(ImPy^{Anis})$_2$](OTf) displayed a shift of 0.80 ppm. In the ^{13}C NMR spectra no significant downfield shift was observed for the imino carbon (*i.e.* δ = 156.2 ppm for [Cu(ImPy^{Ad})$_2$](OTf), compared to δ = 156.2 ppm in the free ligand or δ = 164.6 ppm for [Cu(ImPy^{DIPP})$_2$](OTf), compared to δ = 168.8 ppm in the free ligand).

The IR spectra of the obtained [Cu(ImPy^R)$_2$](OTf) complexes revealed medium absorption bands for the asymmetric C=N stretches between 1596–1647 cm^{-1} and for the symmetric C=N stretches between 1506–1593 cm^{-1}, with the electron rich ligand ImPy^{Anis} showing the lowest wavenumber for all [Cu(ImPy^R)] complexes. The energies for both symmetric and asymmetric stretches were within the typical region for C=N vibrations. The wavenumbers for the C=N stretches shifted towards lower energies upon complexation to the copper(I) centre by about 75 cm^{-1}. Additionally, for all

complexes a band around $1270\,\mathrm{cm^{-1}}$ was evident, which is associated with the presence of the OTf$^-$ counterion.[68] Furthermore, the mass spectra for all prepared [Cu(ImPy)] complexes displayed *m/z* signals for the expected metal cation [Cu(ImPy^R)$_2$]$^+$.

Suitable crystals for single-crystal X-ray diffraction for [Cu(ImPy^{Ad})$_2$](OTf) and [Cu(ImPy^{DIPP})$_2$](OTf) were grown by slow diffusion of petroleum ether into DCM solutions. Ball-and-stick representation are given in Figure 1.34 and 1.35 with selected bond lengths and angles provided in the captions of these figures. The summary for the crystallographic data is provided in Table 1.4.
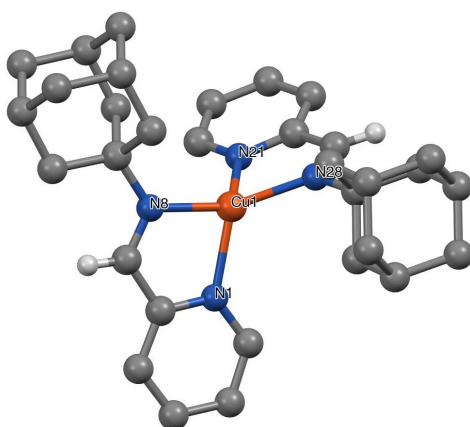
Figure 1.34: Structure of the cation present in the crystal of [Cu(ImPy^{Ad})$_2$](OTf). Most hydrogen atoms are omitted for clarity. Selected bond lengths [Å] and angles [°]: Cu(1)–N(1) 2.077(2), Cu(1)–N(8) 2.026(2), Cu(1)–N(21) 2.080(2), Cu(1)–N(28) 2.020(2); N(1)–Cu(1)–N(8) 81.25(7), N(1)–Cu(1)–N(21) 119.79(7), N(1)–Cu(1)–N(28) 119.99(7), N(8)–Cu(1)–N(21) 116.67(7), N(8)–Cu(1)–N(28) 142.27(7), N(21)–Cu(1)–N(28) 81.42(7).
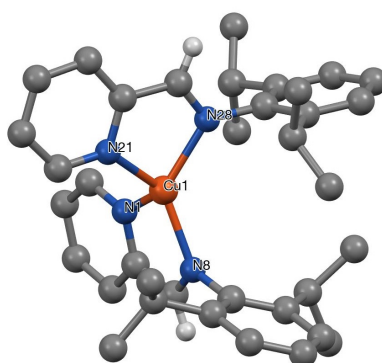
Figure 1.35: Structure of the cation present in the crystal of [Cu(ImPy^{DIPP})$_2$](OTf). Most hydrogen atoms are omitted for clarity. Selected bond lengths [Å] and angles [°]: Cu(1)–N(1) 2.051(2), Cu(1)–N(8) 2.026(2), Cu(1)–N(21) 2.057(2), Cu(1)–N(28) 2.021(2); N(1)–Cu(1)–N(8) 80.98(9), N(1)–Cu(1)–N(21) 110.45(9), N(1)–Cu(1)–N(28) 127.33(9), N(8)–Cu(1)–N(21) 134.01(9), N(8)–Cu(1)–N(28) 128.58(8), N(21)–Cu(1)–N(28) 80.76(9).

Table 1.4: Summary of the crystallographic data for [Cu(ImPy)] complexes. Data were collected using Oxford Diffraction Xcalibur PX Ultra ([Cu(ImPy^{Ad})$_2$](OTf)) and Xcalibur 3 ([Cu(ImPy^{DIPP})$_2$](OTf) and [Cu(ImPy^{DIPP})$_2$(OH$_2$)](OTf)$_2$) diffractometers, and the structures were refined using the SHELXTL, SHELX-97, and SHELX-2013 program systems.[59]

	[Cu(ImPy^{Ad})$_2$](OTf)	**[Cu(ImPy^{DIPP})$_2$](OTf)**	**[Cu(ImPy^{DIPP})$_2$(OH$_2$)](OTf)$_2$**
formulea	[C$_{32}$H$_{40}$CuN$_4$](CF$_3$O$_3$S)	[C$_{36}$H$_{44}$CuN$_4$](CF$_3$O$_3$S)	[C$_{36}$H$_{46}$CuN$_4$O]$_2$(CF$_3$O$_3$S)
solvent	½ CH$_2$Cl$_2$	–	3 H$_2$O
Fw	735.75	745.36	966.49
T (°C)	-100	-100	-100
space group	P2$_1$/n (no. 14)	P-1 (no. 2)	Fdd2 (no. 43)
a (Å)	12.3905(3)	9.1002(5)	21.033(3)
b (Å)	19.0233(5)	10.9858(6)	21.3226(13)
c (Å)	14.4810(3)	19.3481(7)	39.427(2)
α (deg)	90	89.693(4)	90
β (deg)	102.996(2)	79.192(4)	90
γ (deg)	90	82.793(4)	90
V (Å^3)	3325.85(14)	1884.64(16)	17682(3)
Z	4	2	16
ρ_{calcd} (g cm^{-3})	1.469	1.313	1.452
λ (Å)	1.54184	0.71073	0.71073
μ (mm^{-1})	2.744	0.689	0.689
no. of unique ref measured	6376	7408	4983
observed $|F_o| > 4\sigma(|F_o|)$	4921	5713	4177
R$_1$ (obs)[a]	0.0397	0.0504	0.0391
wR$_2$ (all)[b]	0.1092	0.1271	0.0905

a) $R_1 = \frac{\sum ||F_o| - |F_c||}{\sum |F_o|}$; b) wR$_2$ = $\frac{\sum [w(F_o^2 - F_c^2)^2]^{0.5}}{\sum [w(F_o^2)^2])}$ where $w^{-1} = \sigma^2(F_o^2) + (aP)^2 + bP$.

Both structures showed tetracoordinated copper centres with τ_4 values[60] of 0.69 for both structures indicating a distorted tetrahedral coordination sphere. The obtained values were within the range of 0.69–0.72 for similar reported [Cu(ImPy)] complexes.[44] Furthermore, no interaction between the counterion and the imine hydrogen or any other atom was evident in either structures. The sp^2 character of the C and N atoms in the chelate ring was confirmed with bond lengths of 1.284(2) and 1.272(4) respectively.[62] Due to the pyridyl moiety on the ImPy ligand a lower buried volume was expected for ImPy^{Ad} and ImPy^{DIPP}. In fact, with buried volumes of 39.0 and 41.2%, both were lower than any found for the DAB ligands.

During the preparation of X-ray suitable samples of [Cu(ImPy^{DIPP})$_2$](OTf) a turquoise crystalline-solid formed along the brown crystals of [Cu(Im-Py^{DIPP})$_2$](OTf). Due to the turquoise colour, it was assumed that the copper(I) centre oxidised to copper(II) which was confirmed by X-ray diffraction of the sample (Figure 1.36). This complex displayed a penta coordi-
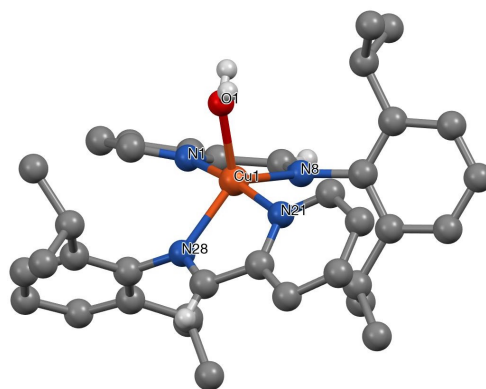
Figure 1.36: Structure of the cation present in the crystal of [Cu(ImPy^{DIPP})$_2$(OH$_2$)](OTf)$_2$. Most hydrogen atoms are omitted for clarity. Selected bond lengths [Å] and angles [°]: Cu(1)–N(1) 1.977(5), Cu(1)–N(8) 2.100(6), Cu(1)–N(21) 2.000(5), Cu(1)–N(28) 2.091(6), Cu(1)–O(1) 2.015(4); N(1)–Cu(1)–N(8) 80.1(2), N(1)–Cu(1)–N(21) 172.1(2), N(1)–Cu(1)–N(28) 94.4(2), N(1)–Cu(1)–O(1) 93.1(2), N(8)–Cu(1)–N(21) 98.1(2), N(8)–Cu(1)–N(28) 128.6(2), N(8)–Cu(1)–O(1) 110.2(2), N(21)–Cu(1)–N(28) 80.7(2), N(21)–Cu(1)–O(1) 94.8(2), N(28)–Cu(1)–O(1) 121.2(2).

nated copper(II) centre with two ImPy^{DIPP} ligands and a H$_2$O molecule. To assign the correct geometry between the possible trigonal bipyramidal and a square pyramidal one the τ_5 value was calculated using the formula $\tau_5 = \frac{\beta - \alpha}{60°}$ where α and β are the greatest valance angles of the coordination centre and $\beta > \alpha$.[69] An index of 1.0 represents an ideal trigonal bipyramidal and an index of 0.0 an ideal square pyramidal geometry. For the [Cu(ImPy^{DIPP})$_2$ (OH$_2$)](OTf)$_2$ complex a τ_5 value of 0.73 was obtained characterising it as a predominantly trigonal bipyramidal geometry. To the best of our knowl-

edge, there are only reports on two similar structures based on pyridyl ben-zothiozoles and 2-phenyleth-1-yl iminomethylpyridine with calculated τ_5 values of 0.72 and 0.92 (Figure 1.37).[70,71] Additionally, the observed copper–nitrogen and copper–oxygen bond lengths in $[Cu(ImPy^{DIPP})_2(OH_2)](OTf)_2$ related well with the reported distances. The copper(I) complex might be oxidised by dioxygen or H_2O under formation of hydroxide to give the cor-responding copper(II) complex.
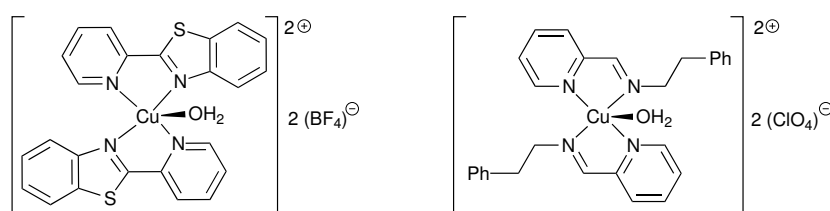
Figure 1.37: Related structures to $[Cu(ImPy^{DIPP})_2(OH_2)](OTf)_2$ based on benzothiozoles and phenylethyliminopyridines.

1.7 Conclusions

Three related families of copper(I) complexes bearing diazabutadiene lig-ands have been prepared and fully characterised: homoleptic $[Cu(DAB^R)_2]$ (BF_4), heteroleptic $[Cu(DAB^R)(NCMe)_2](BF_4)$ and neutral $[CuCl(DAB^R)]$ com-plexes. Surprisingly, the ratio between copper and ligand is not dictated by the stoichiometry of the reaction but rather by the chosen copper source and the type of ligand. All these complexes are indefinitely stable in the solid state and do not require any particular precautions to exclude oxygen or moisture, except for $[Cu(DAB^R)(NCMe)_2](BF_4)$. The prepared complexes displayed a tetracoordinated copper centre in the solid state, with different degrees of distortion from the expected tetrahedral geometry. Unfortunately, no fluorescence was observed for $[Cu(DAB)]$ complexes.

The solution behaviour of $[Cu(DAB)]$ complexes was investigated by UV/Vis and NMR spectroscopy and the obtained results showed that even if they might only be stable under diluted conditions, heteroleptic cations $[Cu(DAB^R)(NCMe)_2]^+$ appear to be intermediates in the formation of the iso-lated homoleptic $[Cu(DAB^R)_2](BF_4)$ complexes. Furthermore, a diimine lig-and in the homoleptic complex might be displaced by a coordinating solvent in diluted solutions or the initial complex might even rearrange into a bin-uclear species, which is in agreement with the known lability of copper di-imine complexes. While this feature is often regarded as a drawback for the exploitation of the photochemical properties of these compounds, it can also

be regarded as a very easy activation mode for catalytic applications. Therefore, addition of a sub-stoichiometric amount of such copper complexes to a solution will give rise to a new coordinatively unsaturated species prone to act as a catalyst. In fact, we recently reported that these complexes are competent catalysts for the copper(I)-catalysed Click azide-alkyne cycloaddition reaction,[72] with $[Cu(DAB^{Cy})_2](BF_4)$ as the best performing catalyst and in the aryl azide reduction reaction with toluene and water as reductants.

Moreover, a series of novel copper(I) iminopyridine complexes was prepared and fully characterised. The two complexes characterised by X-ray diffraction, $[Cu(ImPy^{Ad})_2](OTf)$ and $[Cu(ImPy^{DIPP})_2](OTf)$, displayed a slightly distorted tetrahedral coordinated copper(I) centre. All isolated complexes showed to be moisture and oxygen insensitive in the solid state whereas oxidation in solution was observed and the oxidised copper(II) complex of $[Cu(ImPy^{DIPP})_2(OH_2)](OTf)_2$ was characterised by X-ray diffraction.

Preparation of Amines and Application in Hydroamination Reactions

2.1 Introduction

Amines are one of the main building blocks in synthetic chemistry as well as in biochemistry.[73] They play an important role in life itself as amino acids are linked through their amino group and carbonic acid ends to form proteins necessary for any form of life on earth.[74] The importance of amines is also given by their ability to interact on a supramolecular level through hydrogen bonding. This may be through the lone pair on the nitrogen interacting with carbonyls or through hydrogen bonding with other protic molecules. This is apparent since drug molecules such as Morphine (analgesic), Ritalin (central nervous system stimulant), or Afloqualone (sedative) contain amines as functional groups (Figure 2.1). It is therefore not surprising that since the discovery of amines by Wurtz, chemists have developed many methods for their preparation.[75]
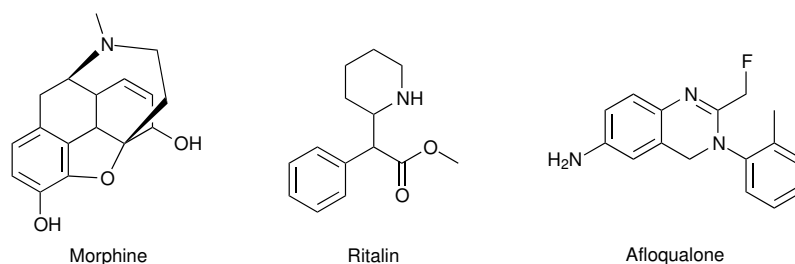
Figure 2.1: Examples of drug molecules containing amine groups.

2.2 Preparation of Primary Amines

A straight forward method to access primary amines is the Gabriel synthesis.[76] An alkyl halide is transformed into the corresponding alkyl phthalamide and consecutively deprotected to give the primary amine. However, it is clear that this procedure generates a large amount of by-products in the form halogen salts and phthalic acid or phthalhydrazide (Scheme 2.1). Additionally, this method is not very useful when the amino functionality needs to be introduced at a later stage of a multi-step synthesis since carbon–halogen bonds react readily with most nucleophiles.
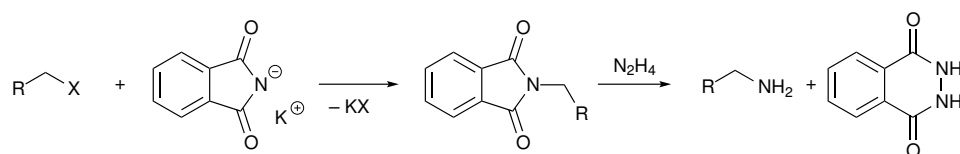
Scheme 2.1: Gabriel synthesis.

43

On the other hand, nitro and azido groups can be used as amino synthons as well and additionally, they are stable towards most reaction conditions. Amines can be accessed from nitro groups by reduction and the most commonly one is in the presence of palladium on charcoal under either hydrogen or CO atmosphere.[77] Particularly, the use of CO allows for a broader functional group tolerance since alkenes, nitriles, or acetophenone are not reduced under these conditions.[78]

Nonetheless, the most utilised synthon for amines are azides, which upon rearrangement or reduction give access to their corresponding primary amines.[79]

Azides are a versatile functional group and have been utilised in various reactions and among them are cyclisation, ring expansions but also ring contractions.[80] Another innovative reaction involving azides is the 1,3-dipolar azide-alkyne Huisgen reaction, which gives rise to a mixture of regioisomeric 1,2,3-triazoles.[81] This reaction was further developed and the copper(I)-catalysed azide-alkyne cycloaddition (CuAAC) allows for the exclusive formation of a 1,4-disubstituted 1,2,3-triazoles (Scheme 2.2).

$$R^1\text{---}\!\!\equiv\quad+\quad R^2\text{---}N_3\quad\xrightarrow{[Cu(I)]}\quad \underset{R^1}{\overset{R^2\text{-}N\text{-}N\text{-}N}{\diagdown}}$$
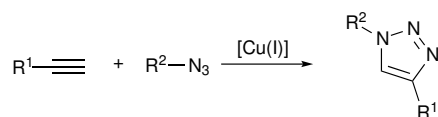
Scheme 2.2: Copper(I)-catalysed azide-alkyne cycloaddition.

Also, CuAAC generated a lot of interest towards Click chemistry, a term defined by Sharpless, and describes reactions, which are high yielding, stereospecific, can be conducted in easily removable or benign solvents, and create only by-products that are easily removed without chromatography.[82] Ultimately, this allowed for a rapid development in the medicinal chemistry due to a simpler method of labelling of biological molecules (*i.e.* DNA and proteins).[83]

Azides have also found application in the Curtius rearrangement, which forms primary amines upon thermal decomposition of acyl azide into an acyl nitrene, which rearranges into the corresponding isocyanate. A consequent hydrolysis gives access upon release of CO_2 to the primary amine (Scheme 2.3).[84] However, this methodology suffers from the harsh reaction conditions to access acyl azides, which are formed by the reaction of the corresponding carbonic acid with $SOCl_2$ followed by NaN_3 or hydrazine, then by nitric acid. These reagents are well known to react with many other functional groups, which need to be protected before accessing the amine

through the Curtius rearrangement. Additionally, the heat sensitivity of acyl azide does not allow for high reaction temperatures preceding the rearrangement.
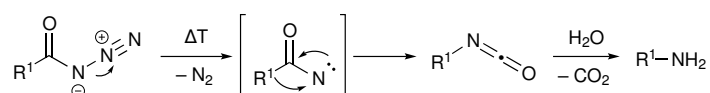
Scheme 2.3: The Curtius rearrangement.

Furthermore, the Schmidt reaction allows the preparation of primary amines directly from carbonic acids.[76] These are dehydrated by a Brønsted acid to give the corresponding oxonium ions, which react with hydrazoic acid to form protonated acyl azides. Ultimately, these rearrange to isocyanates and upon hydrolysis and release of CO_2, the corresponding primary amines are formed (Scheme 2.4). Unfortunately, this method does not allow for ketones or alkenes to be present as side-reactions are observed giving rise to their corresponding amides or imines.[85]
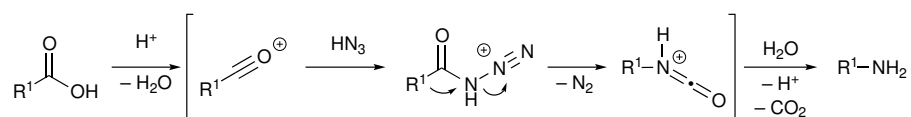
Scheme 2.4: The Schmidt reaction.

Additionally, various methods have been reported to access amines directly by the reduction of azides.[79] This is being widely used in the synthesis of aminoglycosides, highly potent, broad-spectrum antibiotics, containing multiple amino groups on an oligosaccharide core.[86] During their synthesis, the azide group has been employed as protecting group for amines and has allowed for a rapid development in this field. In comparison to other protecting groups, azides can be introduced orthogonally on aminoglycosides in three different positions. Additionally, azides allow for an easier interpretation of NMR spectra compared to carbamates due to the absence of slowly interconverting E/Z rotamers, which lead to multiple sets of signals.[87]

Azides need to be reduced to access the amine functionality, which can be achieved by main group metal hydrides[79,88] or by H_2 methods utilising transition metals.[88] However, these methodologies do not allow for functional groups such as alcohols, acids, or unsaturated groups such as alkenes, alkynes, nitriles or carbonyls on the substrate. Nonetheless, a catalytic methodology was developed by Kotsuki *et al.*, which reduced aliphatic and

aryl azides in good yields with a high functional group tolerance in the presence of palladium (Scheme 2.5).[89] HSiEt$_3$ was necessary as reducing agent, generating a substantial high molecular weight by-products compared to hydrogenation by H$_2$.
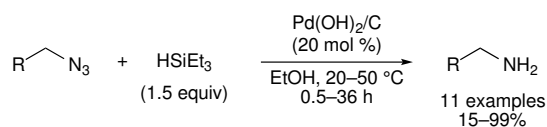
Scheme 2.5: Palladium-catalysed reduction of aliphatic and aryl azides with HSiEt$_3$.

The most popular methodology, especially in carbohydrate chemistry, is the Staudinger reduction, which transforms the azide in the presence of triaryl- or trialkylphosphines to iminophosphoranes, which upon hydrolysis form the primary amines and the corresponding phosphine oxides.[90] The reaction mechanism is believed to proceed *via* a four-membered phosphazide transition state, which subsequently loses N$_2$ and forms the iminophosphorane.[91] The Staudinger reduction allows for mild reaction conditions and reduces the azide selectively in the presence of esters or benzyl esters, which are frequently used as alcohol-protecting groups. However, this method's disadvantage is the generation of a stoichiometric, high molecular weight by-product.
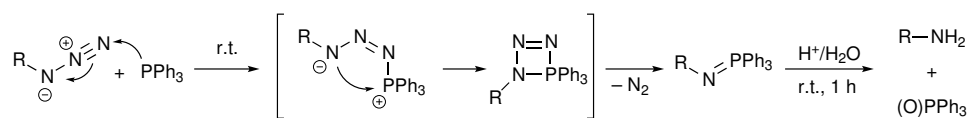
Scheme 2.6: Staudinger reduction.

Another metal-free reduction has been reported in the presence of dithiol and stoichiometric amounts of triethylamine (Scheme 2.7).[92] The reaction proceeds under mild conditions, however, it requires an oxygen-free environment and 2–5 equiv of dithiol and NEt$_3$. Nonetheless, excellent yields were achieved within minutes for electron poor aryl azides, whereas aliphatic ones required much longer reaction times of up to 20 h. A very good yield for the reduction of 1-adamantylazide was obtained after 120 h.
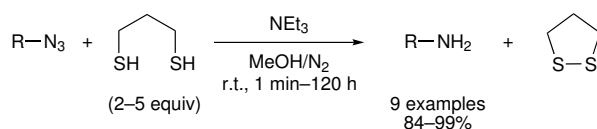
Scheme 2.7: Azide reduction with propan-1,3-dithiol.

Additionally, the reduction of heterocyclic- and electron poor aryl-azides with hexamethyldisilathiane (HMDST) under mild reaction conditions was disclosed and moderate to very good yields were obtained (Scheme 2.8).[93] However, this reaction generates stoichiometric amounts of elemental sulfur and two equivalents of methoxytrimethylsilane as by-products, lowering the atom efficiency significantly.
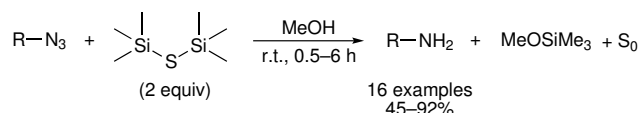
Scheme 2.8: Azide reduction with hexamethyldisilathiane.

Several methods have been reported for metal salt assisted catalytic reduction in the presence of $NaBH_4$. Notably, a procedure was disclosed exploiting $CuSO_4$ and $NaBH_4$ for the formation of amines from aryl azides (Scheme 2.9).[94] Unfortunately, this methodology did not seem to tolerate other functional groups prone to reduction, which was possibly due to the four-fold excess of H^- present in the reaction.
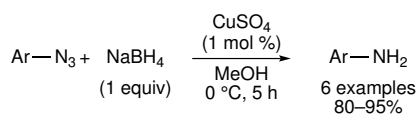
Scheme 2.9: Copper(II) assisted reduction of aryl azides in the presence of $NaBH_4$.

On the other hand, a similar reaction based on $CuSO_4$ was reported but with sodium ascorbate as reducing agent instead (Scheme 2.10).[95] This procedure seemed to work only with very electron-poor aryl azides, however, allowed for carbonic acids or esters to be present in the reaction. Nonetheless, longer reaction times were required and much lower yields were obtained.
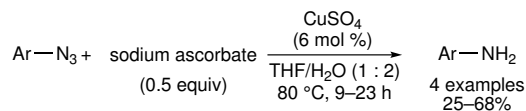
Scheme 2.10: Copper(II) assisted reduction of aryl azides in the presence of sodium ascorbate.

A rather unusual reduction was disclosed by Peng *et al.*, where the transformation of 4-azido-7-nitrobenzo[*c*][1,2,5]oxadiazole to the corresponding amine was observed in the presence of CuCl in a 3:1 mixture of $DMSO/H_2O$ at 80 °C (Scheme 2.11).[96] Unfortunately, no other substrates were investi-

47

gated and the mechanism of this reaction and the involved reducing agent remained unclear. However, a copper(II) hyperfine splitting was observed during the reaction by Electron Paramagnetic Resonance (EPR), which indicated the formation of a copper(II)–nitrene species.
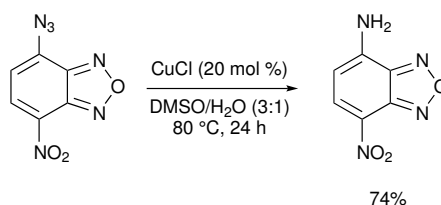
Scheme 2.11: Copper(I)-catalysed reduction of aryl azides in DMSO/H_2O.

2.3 Preparation of Secondary Amines

Secondary amines may be formed using a variety of reactions that generally require a primary amine as a reactant.[97] The most common route is direct *N*-alkylation by treating the primary amine with an alkyl halide (Scheme 2.12).[97] Alkyl halides can be replaced by alcohols in this direct alkylation as long as they are first transformed into sulfate or sulfonate esters. This method seems deceptively simple, however, it suffers from several drawbacks, such as over-alkylation of the amine to tertiary ammonium salts.[98] This may be prevented by using a large excess of amine, which can be a very expensive workaround, especially if chiral amines are used. Additionally, this reaction generates at least a stoichiometric amount of waste product.
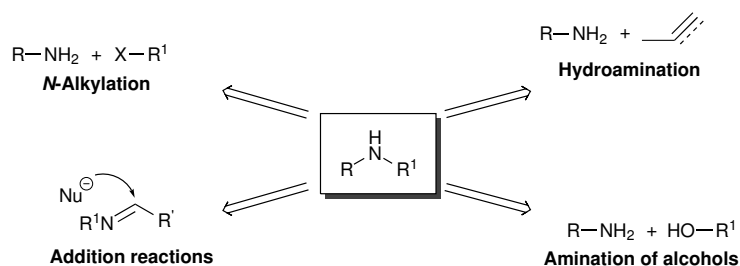
Scheme 2.12: Overview of the different methods to synthesise secondary amines.

A second method involves the nucleophilic attack on an imine or iminium salt to form the corresponding secondary amine. A notable example of this approach is the Mannich reaction (Scheme 2.13), whereby an imine is formed from a primary amine and formaldehyde, which undergoes a nu-
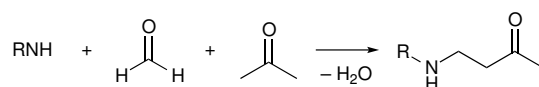
Scheme 2.13: The Mannich reaction.

cleophilic attack by an enolate, formed by the reaction between the acetyl group and the amine. This well-established methodology has been used in the synthesis of many natural products (*e.g.* Febrifugine[99] and Nikkomycine B,[100] Figure 2.2).
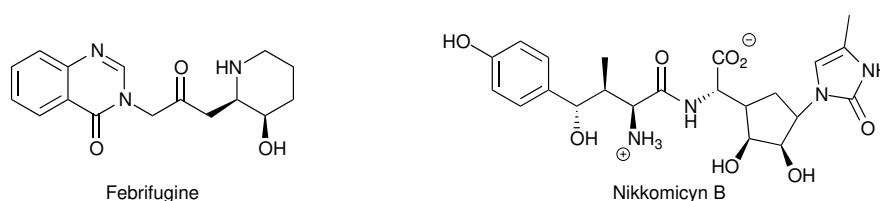
Figure 2.2: Natural products synthesised *via* a Mannich reaction.

The direct catalytic amination of alcohols has recently gained a lot of (Scheme 2.14).[101] In a first step, the alcohol undergoes a two electron oxidation in the presence of the transition metal to give the corresponding aldehyde and metal hydride. Through a condensation reaction with the primary amine, an imine is formed, which is then reduced by the previously formed metal hydride to form the secondary amine. As appealing and powerful this one-pot reaction is, its main obstacle is the use of expensive metals such as iridium or ruthenium as low conversions are achieved with other metals.[101]
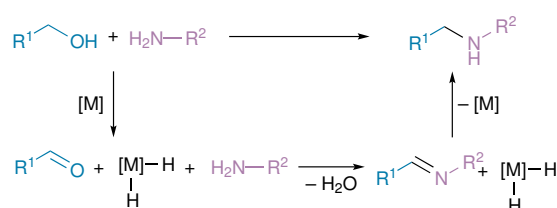
Scheme 2.14: Direct catalytic amination of alcohols in a one-pot reaction.

2.4 Hydroamination Reactions

Currently one of the most popular strategies for the formation of C−N bonds is the hydroamination reaction, which adds a secondary or primary amine to

a C=C or C≡C bond in the presence of a catalyst (Scheme 2.15). Hydroamination has benefited from the recent advances on catalyst design and availability of inexpensive, small molecules containing unsaturated carbon–carbon bonds and amine groups. [102]
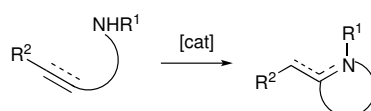
Scheme 2.15: Intramolecular hydroamination of different unsaturated carbon–carbon bonds.

The required catalyst can be either a Brønsted acid or base, early or late transition metal, or Group 1 and 2 complexes. [103] This is an attractive and 100% atom efficient approach that has been utilised in the synthesis of several different natural products the first one being Monomorine, a trail pheromone isolated from the Pharaoh ant (Figure 2.3). [104] Crispine A, active component to treat colds isolated from a herb in the daisy family, was prepared *via* a sequence containing the intramolecular hydramination of a homopropargylic amine to form 5,6-dihydro-8,9-dimethoxypyrrolo[2,1-a]-isoquinoline, which was then hydrogenated. [105] For tricyclic Porantheridine, which was isolated from *Porenthera Cyrombosa* (Figure 2.3), a key intermediate oxazolidine was prepared from an allene using a silver-catalysed intramolecular hydroamination reaction. [106]

Monomorine   Crispine A   Porantheridine
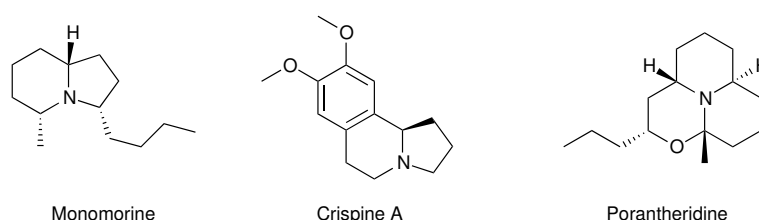
Figure 2.3: Natural products for which the hydroamination reaction was utilised.

Inherently, the addition of an amine to an unsaturated carbon–carbon bond might lead to Markovnikov or anti-Markovnikov products (Scheme 2.16). A similar regioselectivity problem is observed for internal carbon–carbon unsaturated bonds and *E*- or *Z*-alkenes can be formed as products when alkynes are used. Both selectivity issues can be addressed with an appropriate catalytic system. However important, these are not relevant for the presented work and the Reader is advised to refer to the excellent reviews available in literature. [102,103]
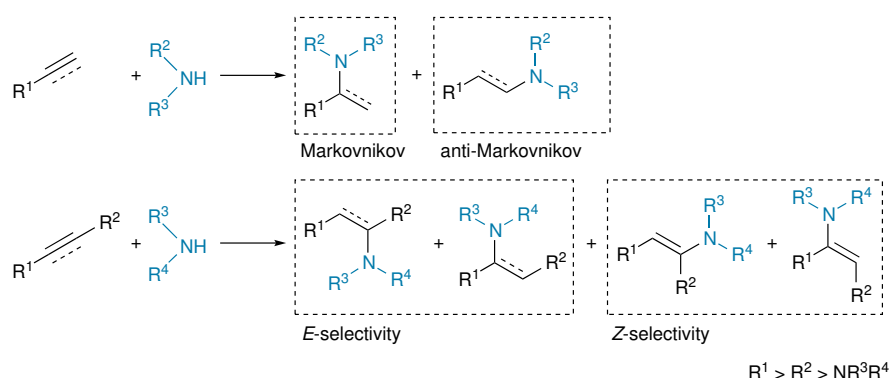
Scheme 2.16: Different regioselectivity in the hydroamination gives rise to different products.

Hydroamination reactions do not only give rise to secondary or tertiary amines but allow for the synthesis of imines and enamines as well. Enamines usually originate from the addition of secondary amines to alkynes and allenes, whereas imines usually require primary amines (Scheme 2.17).
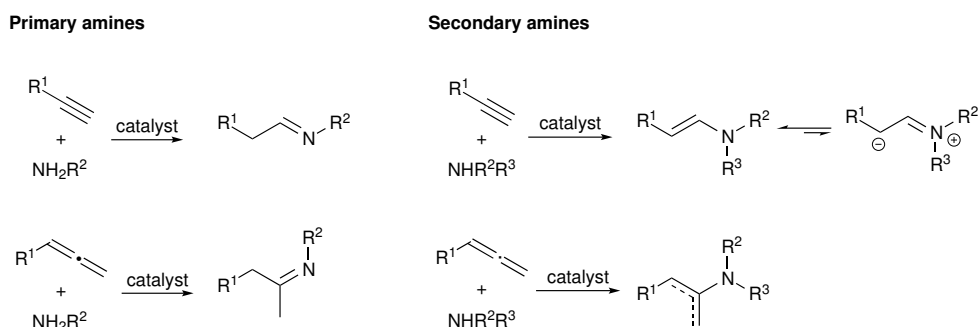
Scheme 2.17: Formation of imines and enamines in hydroamination reactions.

The formation of imines over enamines is thermodynamically favoured by $18.6\,\mathrm{kcal\,mol^{-1}}$.[107] However, only secondary enamines can rearrange to imines, since tertiary enamines would form zwitterionic iminium species (Scheme 2.17). Apart from their relevance in naturally occuring bioactive substrates,[74] imines and enamines are important building blocks in chemistry as well (Scheme 2.18).[102]

Enamides (R^4 or $R^5 = CO_2R$) have found application in polymer research and industry.[108,109] A prominent example is N-vinylpyrrolidone (NVP), which is prepared from pyrrolidone and ethylene under high pressure on a $31\,000\,\mathrm{t\,a^{-1}}$ scale worldwide. The polymer is usually prepared by radical polymerisation and offers remarkable physical properties such as being bio compatible and stable within a wide pH range.[110,111]

Scheme 2.18: Different uses for imine and enamine building blocks.
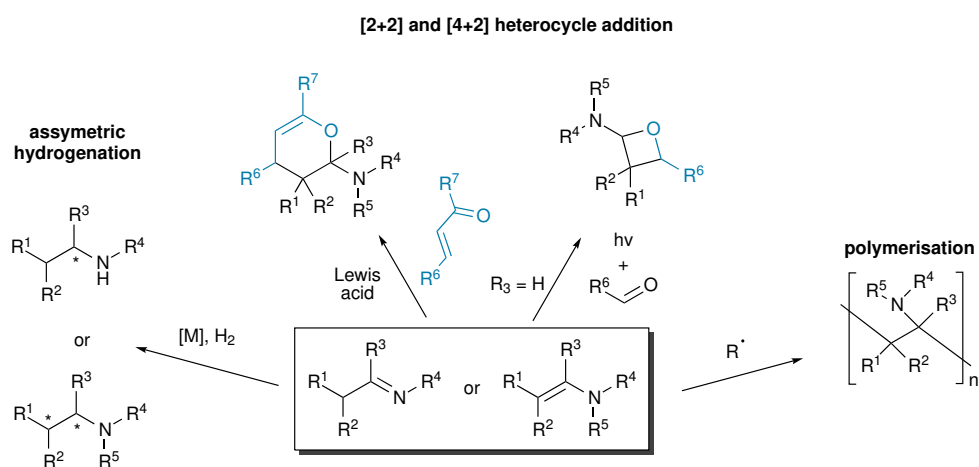
Imines and enamines are often prepared to be used in asymmetric hydrogenation to form the corresponding amines. The hydroamination of alkynes to form imines and consecutive asymmetric hydrogenation is much easier to achieve than a direct asymmetric hydroamination of alkenes.[102] Indeed, only in 2010 did Buchwald *et al.* report a rhodium-catalysed intramolecular asymmetric hydroamination of alkenes.[112] Two years later, Shibata *et al.* disclosed the first intermolecular enantioselective version utilising a ruthenium catalyst.[113]

Additionally, imines and enamines can be used as dienophiles in the [2+2] and [4+2] heterocycloaddition.[114,115] Several groups reported these reactions with high regio- and enantioselectivity to form highly functionalised heterocycles.[116,117]

On the other hand, intramolecular hydroamination reactions allow the direct, expedient construction of different nitrogen-containing heterocycles.[118] A wide range of differently substituted pyrrolines, tetrahydropyridines, azepanes, pyrrolidines, piperidines[119] and indoles[120] have been prepared using a hydroamination protocol, as well as 1,4-oxazines, 1,4-oxazepines,[121] and cyclic guanidines[122] (Scheme 2.19).

Scheme 2.19: Different N-heterocycles prepared *via* hydroamination.
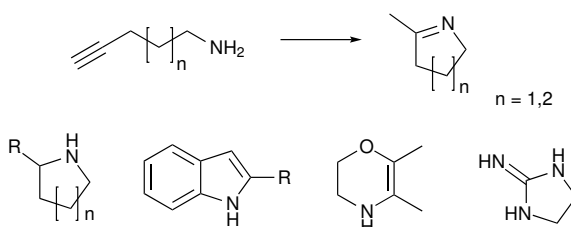
Hydroamination reactions have also found application in industry. The most prominent example is probably the Takasago process, which produces (−)-menthol on a $1500 \, t \, a^{-1}$ scale.[123] A hydroamination reaction is the first step in this process, transforming myrcene with lithium dibutylamide into geranyl amine. After four additional reaction steps, (−)menthol is obtained (Scheme 2.20). Geranyl amine is further used as starting material for accessing a variety of terpenoids, such as geraniol, nerol, citral, or (+)-citronellal, or (+)-citronellol.[124]

myrcene   geranyl amine   (−)-menthol
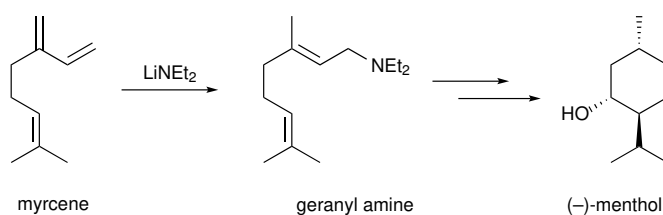
Scheme 2.20: Overview of the Takasago process.

The first reported example of a hydroamination reactions dates back to 1936 and was described by Kozlov.[125] The reaction involved the addition of aniline to acetylene in the presence of $HgCl_2$ (Scheme 2.21). This reaction was later modified to use internal alkynes and, instead of $HgCl_2$, HgO with BF_3 was used to give the desired hydroamination products.[126] Despite its toxicity, mercury was commonly used until the 1990.[127]

17%
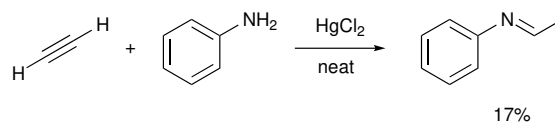
Scheme 2.21: The first reported catalytic hydroamination reaction.

The first account on the hydroamination of alkenes was reported in 1954 for the addition of ammonia to ethene in the presence of metallic lithium or sodium under high pressures of 1000 bar and temperatures around 200 °C.[128] The first transition metal-catalysed hydroamination reaction was reported by Coulson in 1971 for the addition of secondary aliphatic amines to ethene with rhodium(I–III) and iridium(III) complexes.[129]

Early transition metals received an increasing attention in this context after Bergman and Livinghouse reported the application of zirconocenes and titanocenes in the hydroamination of alkenes and alkynes in 1992,[130,131] and a broad area of research has evolved since.[102,103]

Thermodynamically, the addition of ammonia or amines to olefins is a vi-

able reaction with a free enthalpy for the addition of ammonia to ethylene of $_\Delta G° \approx -4.1\,\text{kcal}\,\text{mol}^{-1}$.[132] Free enthalpies for the hydroamination of higher alkenes are between -6.9 and $-16.0\,\text{kcal}\,\text{mol}^{-1}$. Nevertheless, the addition of N–H is characterised by a high activation barrier, preventing the reactions to occur under ambient conditions. This is due to electron repulsion between the lone pair on the nitrogen and the π-electrons on the unsaturated carbon–carbon bond.[133] Additionally, an increased temperature to overcome the high activation energy would only favour the formation of starting materials as the entropy of the reaction is highly negative. Hence, the use of a catalyst to lower the activation barrier is essential.

The reaction mechanism for the hydroamination reaction is mainly dominated by the nature of the catalyst and can be divided into five distinct categories: Brønsted acids, Brønsted bases and alkali and earth alkali metals, early transition metals (Group 4), and late transition metals with a differentiation between Group 9 and Groups 10–11.

Brønsted acid catalysts would react by protonation of the carbon–carbon unsaturated bond and formation of a carbenium ion, to which the amine group would add (Scheme 2.22). Upon proton transfer from the formed ammonium product to the carbon–carbon unsaturated bond on the next molecule of starting material, the catalytic cycle would be closed. It is clear from the last step, that due to the more basic character of the nitrogen the protonation of the π system should be less favourable. However, good yields were reported for this reaction with $[PhNH_3][B(C_6F_5)_4]$ as catalyst.[134]
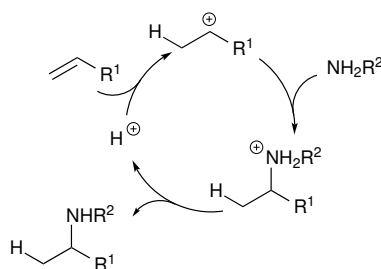
Scheme 2.22: Proposed reaction mechanism for Brønsted acid-catalysed hydroamination.

Brønsted bases and Group 1 and 2 metals would initially form a metal–amido species under formation of H_2 or by deprotonation of the free amine by a metal ligand. The metal-amido bond would consecutively insert into the unsaturated carbon–carbon bond forming the carbon–nitrogen and a carbon–metal bond (Scheme 2.23). In the final step, the carbon–metal bond would be protonated by a second free amine forming the product and a metal–amido species to close the reaction cycle.[133] Due to the inherent instability of Group 1 and 2 metals, the reactions need to be run under oxygen-

and moisture-free conditions. Additionally, these catalysts suffer from a limited functional group tolerance.
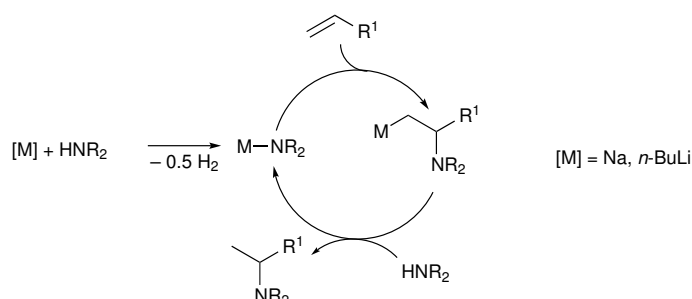
Scheme 2.23: Proposed reaction mechanism for Brønsted base and Group 1 and 2 catalysed hydroamination with sodium and *n*-BuLi as example catalysts.

Early transition metals in Group 4 differentiate themselves from Group 1 and 2 as their key intermediate would be a metal–imido species (Scheme 2.24). This would be formed by coordination of the free amine and its double deprotonation by two metal ligands, often methyl ligands, to give the metal–imido intermediate. The metal–imido species would then undergo a [2+2] addition with the unsaturated carbon–carbon bond to form a metalocycle. This would then be protonated and opened by a free amine to form a bis-amido species, which would release the reaction product and form the metal–imido species *via* proton transfer.[135] Overall, Group 4 catalysts suffer from the same inherent disadvantages as Group 1 and 2 metals.
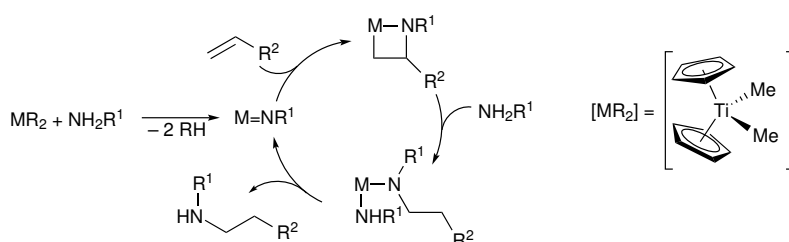
Scheme 2.24: Proposed reaction mechanism for Group 4-catalysed hydroamination with with [TiCp$_2$Me$_2$] as example catalyst.

On the other hand, Group 9 metals would undergo an oxidative addition with the amine to form a metal–hydride and metal–amido bond, followed by an insertion of the unsaturated carbon–carbon bond into the latter to form a new nitrogen–carbon and metal–carbon bonds (Scheme 2.25).[136,137] Alternatively, the unsaturated carbon–carbon bond might insert into the metal–hydride bond.[138] In a last step, the product would be formed by a reductive

elimination to close the reaction cycle and to regenerate the catalyst.
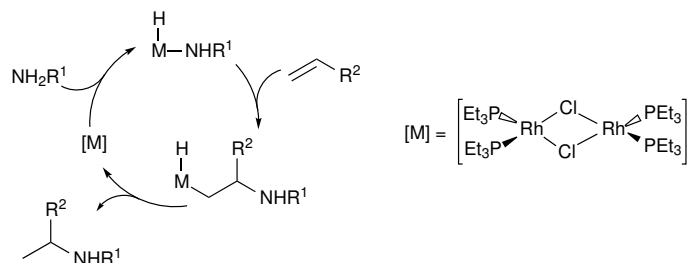
Scheme 2.25: Proposed reaction mechanism for Group 9 catalysed hydroamination with $[RhCl(PPh_3)_2]_2$ as example catalyst.

The mechanism for late transition metals in Groups 10 and 11 would involve the activation of the unsaturated carbon–carbon bond by coordination of a Lewis acidic metal centre to reduce the electron density on the carbon–carbon bond and making it more prone to nucleophilic attack by the lone pair on the amine (Scheme 2.26). After protonation of the carbon–metal bond by the present ammonia, the product would be formed and removed from the active catalyst to close the reaction cycle.[139]
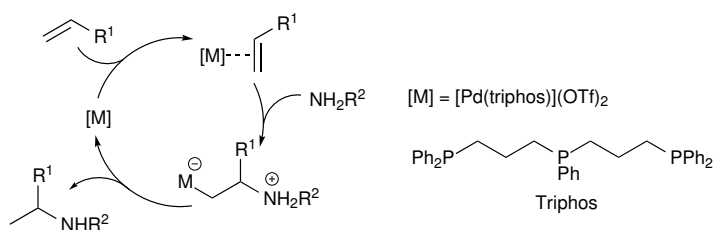
Scheme 2.26: Proposed reaction mechanism for Group 10 and 11 catalysed hydroamination with [Pd(triphos)](OTf) as example catalyst.

Late transition metals of Groups 9–11 are very versatile catalysts as they tolerate a much broader range of functional groups and are mostly oxygen and moisture insensitive. Nonetheless, their application is overshadowed by a high environmental toxicity (Ni, Pd, Co) and/or high economical cost (Au, Ag, Pt, Pd, Ir). On the other hand, copper does not bare any of these disadvantages. However, despite being in Group 11, the reactivity and the scope of copper complexes have not been thoroughly studied in the literature.[102,103]

Hence, only a handful of reports targeted the addition of amines to alkynes with copper complexes. A recent report disclosed the hydroamination of trifluoromethyl substituted alkyne with anilines and secondary, aliphatic amines. The reaction occurred in the presence of the strong Lewis acid

$Cu(OTf)_2$ and molecular sieves and the products were isolated in good yields after reduction with $NaBH_3CN$ to their corresponding amines (Scheme 2.27).[140]
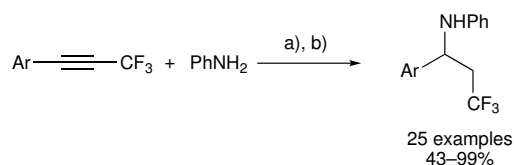
Scheme 2.27: Reported hydroamination of CF_3 substituted alkynes. a) $Cu(OTf)_2$ (10 mol %), 4 Å MS, THF, 40 °C, 12 h; b) $NaBH_3CN$, AcOH, room temperature, 5 min.

Recently, a reductive hydroamination of alkynes with *N,N*-dibenzyl-*O*-benzoylhydroxylamine in the presence of $Cu(OTf)_2$ and $HSiMe(OEt)_2$ was reported to give the corresponding enamines or amines.[141] It was proposed that an intermediate copper(I)–hydride would attack the alkyne to give a vinyl–copper(I) species, to which the nitrogen–oxygen bond would insert to give access to the enamine and benzylalcohol as by-product (Scheme 2.28).
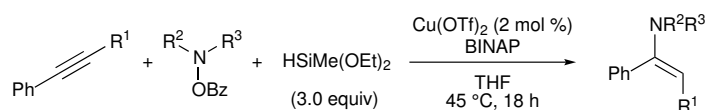
Scheme 2.28: Reductive hydroamination.

The intermolecular hydroamination of terminal allenes with piperidine and morpholine derivatives in the presence of $Cu(OTf)_2$ and 4 Å molecular sieves was reported (Scheme 2.29).[142] However, elevated temperatures and an increased catalyst loading were necessary for the reaction to proceed.
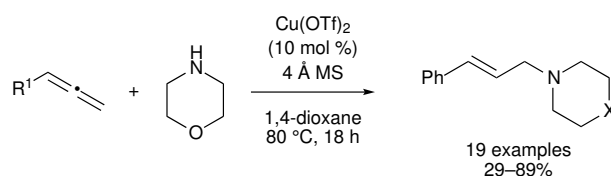
Scheme 2.29: Reported intermolecular hydroamination of allenes.

The intermolecular addition of tosylamide to styrene derivatives with a $Cu(OTf)_2$ BINAP system to access the corresponding amines in moderate to excellent yields (Scheme 2.30) was disclosed by Taylor *et al.*[143]

Similarly, reports on copper(I)-catalysed hydroamination reaction are scarce
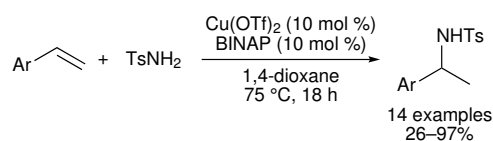
Scheme 2.30: Reported intermolecular hydroamination of alkenes with tosylamide.

as well. A first report mentioned the hydroamination of 6-hexynylamine with [Cu(NCMe)$_4$](PF$_6$) (Scheme 2.31).[144] However, this reaction was only run as part of a screening to identify an optimal catalyst among different metal complexes.
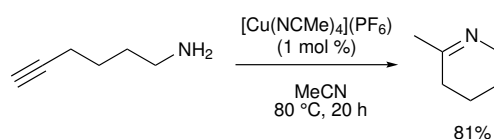
Scheme 2.31: Reported copper-catalysed hydroamination of 6-hexynylamine.

Alternatively, 5 mol % of [CuMe(IMes)] led to full conversion at 120 °C within 9 h in nitrobenzene.[145] Unlike in the first report, the sensitivity of the copper complex required moisture- and oxygen-free conditions. Interestingly, this substrate was also studied with a zeolite based, heterogeneous copper(I) catalyst in MeCN, which displayed an excellent activity.[146]

Furthermore, the intramolecular hydroamination of terminal allenes in the presence of a variety of copper(I) and copper(II) salts has been reported at room temperature in DCM (Scheme 2.32).[147]
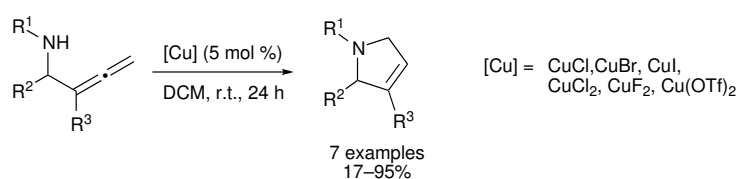
Scheme 2.32: Reported intramolecular hydroamination of allenes.

Challenging alkenes have also been studied with copper catalysis. The intramolecular addition of secondary amines to terminal alkenes was reported in the presence of [Cu(Ot-Bu)] and Xantphos (Scheme 2.33).[148] Elevated temperatures, prolonged reaction times and oxygen- and moisture-free conditions were required to obtain the pyrrolidines in excellent yields.

To conclude this chapter, it was shown that azides are easily prepared and are used in many important reactions in organic chemistry. Among which,
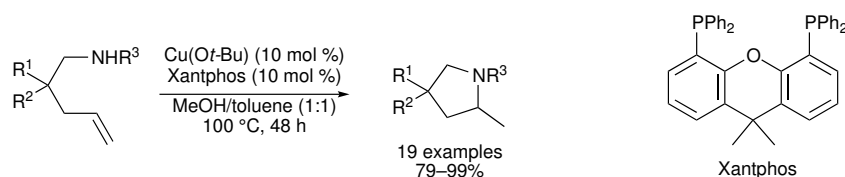
Scheme 2.33: Reported intramolecular hydroamination of alkenes.

they are used as synthon or protecting group for primary amines, since they allow access to primary amines under mild reducing conditions. This renders azides very useful, since the amine group can be introduce in a late stage of a multistep synthesis.

A plethora of different methodologies for the reduction of azides to amines have been developed, amidst the Staudinger reduction is the most utilised one, since it allows for very benign reaction conditions and does not interfere with other functional groups and protecting groups. However, this reduction generates stoichiometric amounts of waste product and it is desirable to develop a method, which circumvents this issue and catalysis might offer this solution.

Additionally, the importance of the hydroamination reaction was disclosed due to its ability to access secondary amines, imines, enamines, and heterocyclic compounds, which are important building blocks in chemistry and industry. This reaction offers a 100% atomic efficiency generating no by-products. However, due to a large activation barrier the reaction requires the use of a catalyst, which can be in the form of a Brønsted acid or base, alkali, earth alkali metals, or transition metal complexes. Unfortunately, most of these catalysts require oxygen- and/or moisture-free conditions, are incompatible with a variety of functional groups, or are toxic, expensive or their economic availability is influenced by politics. It is therefore desirable to study copper(I) complexes as catalysts in the hydroamination reaction, since they do not display most of the afore mentioned downsides or at least to a lower extend.

Chapter 3

Aryl Azide Reduction by [Cu(DAB)] Complexes

3.1 Aims and Objectives

Azides are an important functional group in organic chemistry, and are particularly used as synthon or protecting group for primary amines. The amine functionality is accessed by the reduction of the azide and a plethora of methodologies have been developed with various reducing agents.

Our group has recently discovered the reduction of azides in the presence of [Cu(DAB)] complexes in a mixture of toluene and water without any obvious reducing agent.

The aim of this work is to investigate this reduction catalysed by [Cu(DAB)] complexes and to develop optimised reaction conditions by screening different copper(I) complexes bearing DAB, ImPy, or NHC ligands, solvents, and temperatures. Moreover, a variety of different aryl and heterocyclic azides will be prepared and tested to investigate the substrate scope. Since no obvious reducing agent is present in this reaction, we will find a possible oxidation product and the corresponding reaction mechanism by computational methods. An optimal method and basis set will be looked for and the calculation will be run with a solvation model.

3.2 Optimisation of the [Cu(DAB)]-Catalysed Aryl Azide Reduction

While studying the formation of aziridine **5**, our group discovered the catalytic reduction of aryl azides to anilines by [Cu(DAB)] complexes.[149] At 70 °C and over the course of three days, the reaction of phenylazide **3a** in the presence of [Cu(DAB^{Cy})$_2$](BF$_4$) gave aniline **4a** in high yields (Scheme 3.1).
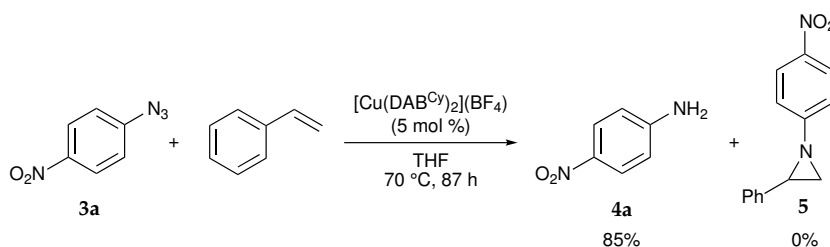
Scheme 3.1: Aryl azide reaction previously observed in our group.

An initial optimisation of the reaction conditions was undertaken and solvents such as EtOAc, MeOH, and MeCN led to very little conversion into aniline **4a** after 87 h (Table 3.1, entries 1–3). Surprisingly, in absence of styrene the conversion into aniline in THF dropped to 5% (Table 3.1, entry 4). This

might indicate a non-innocent role of the styrene when the reaction is run in THF. Additionally, no other by-products were observed. Propan-2-ol and toluene led to slightly better but still unsatisfactory results after 87 h (Table 3.1, entries 5 and 6). On the other hand, H_2O and 1,4-dioxane displayed very good conversion of 72 and 87% (Table 3.1, entries 7 and 8). Following these results, different mixtures of water and organic solvents were tested and excellent conversion of >95% was obtained in a 1:1 water/toluene mixture (Table 3.1, entry 9).

Table 3.1: Solvent screening for the aryl azide reduction reaction.

	solvent	T (°C)	conv. (%)[a]
1	EtOAc	70	<5
2	MeOH	60	<5
3	MeCN	80	6
4	THF	70	5
5	propan-2-ol	80	16
6	toluene	110	19
7	H_2O	100	72
8	dioxane	100	87
9	toluene/H_2O	100	>95

[a] ^{1}H NMR conversions were calculated with respect to 1,3,5-trimethoxybenzene as an internal standard as an average of at least two independent reactions.

In a next step, different [Cu(DAB)] catalysts were screened with model substrate **3a** in a 1:1 mixture of toluene/H_2O. Homoleptic complexes with DAB^R bearing aliphatic substituents (R = Cy, *t*-Bu) led to conversions of 24 and 5% into aniline **4a** (Table 3.2, entries 1 and 2). Moreover, [Cu(DAB^{Anis})$_2$] (BF$_4$) led to a conversion of 48%. However, not all DAB systems with aromatic substituents showed an increased reactivity and with [Cu(DAB^{Mes})$_2$] (BF$_4$) only 7% of aniline **4a** was formed (Table 3.2, entries 3 and 4). Nonetheless, total conversion into aniline was achieved with [Cu(DAB^{DMA})$_2$](BF$_4$) (Table 3.2, entry 5). Neutral, heteroleptic complex [CuCl(DAB^{DMA})] and heteroleptic, cationic complex [Cu(DAB^{DIPP})(NCMe)$_2$](BF$_4$) showed a lower reactivity with a conversion of 28 and 10%, respectively, which led to the conclusion that these two types of complexes held a lower reactivity for this reaction (Table 3.2, entries 6 and 7). For neutral complexes, their low reactivity might be linked to their general low solubility.

Table 3.2: Catalyst screening for the aryl azide reduction reaction.

	catalyst	conv. (%)[a]
1	$[Cu(DAB^{Cy})_2](BF_4)$	24
2	$[Cu(DAB^{tBu})_2](BF_4)$	5
3	$[Cu(DAB^{Anis})_2](BF_4)$	48
4	$[Cu(DAB^{Mes})_2](BF_4)$	7
5	$[Cu(DAB^{DMA})_2](BF_4)$	>95
6	$[CuCl(DAB^{DMA})]$	28
7	$[Cu(DAB^{DIPP})(NCMe)_2](BF_4)$	10

[a] ^{1}H NMR conversions were calculated with respect to 1,3,5-trimethoxybenzene as an internal standard as an average of at least two independent reactions.

While studying $[Cu(DAB^{DMA})_2](BF_4)$, we observed that the conversion into 4-nitroaniline **4a** fluctuated between 80 and >95%, whereas a 1:2 mixture of toluene/water gave persistently excellent conversions of >95%. This solvent ratio was then used for all further studies.

Next, copper(I) complexes based on $^{Me}DAB^R$, NHC, and ImPy ligands were tested with varying results. $[Cu(^{Me}DAB^{DMA})_2](BF_4)$ showed the same reactivity as $[Cu(DAB^{DMA})_2](BF_4)$ with either 10 or 5 mol% and both complexes were considered to have equal activity and due to convenience $[Cu(^{Me}DAB^{DMA})_2](BF_4)$ was chosen (Table 3.3, entries 1 and 2).

ImPy based complexes did not reach the same conversion as $[Cu(DAB^{DMA})_2](BF_4)$ (Table 3.3, entries 3 and 4). On the other hand, neutral NHC complexes [CuX(NHC)] displayed improved conversions compared to homoleptic NHC complexes $[Cu(NHC)_2](BF_4)$ (Table 3.3, entries 5–9). Additionally, higher conversions were observed for unsaturated NHC ligand complexes and IPr excelled the most (Table 3.3, entries 5 and 9). Furthermore, iodine based [CuI(IPr)] led to a better conversion than [CuBr(IPr)] (Table 3.3, entries 6 and 7). However, only 24% of aniline **4a** was formed in the presence of 5 mol% of [CuI(IPr)]. Furthermore, only small or no conversion was observed for CuI and $[Cu(NCMe)_4](BF_4)$ (Table 3.3, entries 10 and 11). Overall, $[Cu(DAB^{DMA})_2](BF_4)$ remained the catalyst of choice for this transformation.

Organic azides are generally prone to decomposition at elevated temperature and their stability depends on their substituents.[150] This instability was confirmed by heating 1-azido-4-nitrobenzene **3a** in a 1:2 toluene/wa-

Table 3.3: DAD, ImPy, and NHC based catalyst screening.
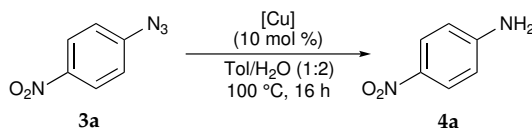
	catalyst	conv. (%)[a] (10 mol % [Cu])	conv. (%)[a] (5 mol % [Cu])
1	[Cu(DAB^{DMA})$_2$](BF$_4$)	>95	>95
2	[Cu(^{Me}DAB^{DMA})$_2$](BF$_4$)	>95	>95
3	[Cu(ImPy^{DMA})$_2$](OTf)	88	–
4	[Cu(ImPy^{DIPP})$_2$](OTf)	57	–
5	[CuI(IAd)]	84	–
6	[CuI(IPr)]	>95	24
7	[CuBr(IPr)]	75	–
8	[CuI(SIPr)]	84	–
9	[Cu(IPr)$_2$](BF$_4$)	19	–
10	CuI	9	–
11	[Cu(NCMe)$_4$](BF$_4$)	0	–

[a] ^{1}H NMR conversions were calculated with respect to 1,3,5-trimethoxybenzene as an internal standard.
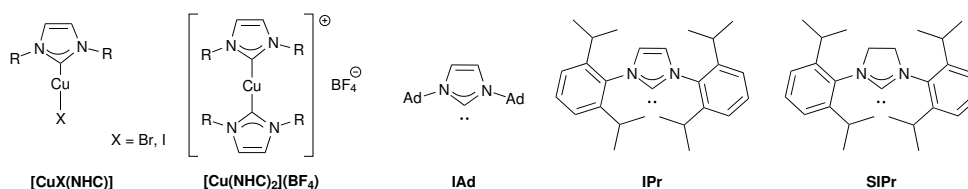
ter mixture at 100 °C for 16 h, which led to the decomposition of 15% of the substrate according to the ^{1}H NMR spectrum. In an attempt to avoid decomposition to unknown products, the model catalytic reaction was carried out at 80 °C, however, only a disappointing 15% conversion into **4a** was obtained. Consequently, the temperature for further reaction remained at 100 °C.

Overall, the optimal reaction conditions were identified with [Cu(DAB^{DMA})$_2$] (BF$_4$) as catalyst with a loading of 10 mol % in a mixture of toluene/H$_2$O (1:2) at 100 °C.
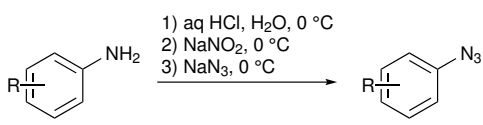
3.3 Preparation of Aryl Azides
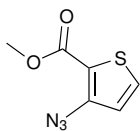
As a second step in this study, a range of aryl and heterocyclic azides was prepared following literature procedures. These consisted on addition of

sodium nitrate to a solution of aniline in aqueous hydrochloric acid to form an arenediazonium intermediate, which was then treated with sodium azide to give the corresponding aryl azide substrate in good to excellent yield (Table 3.4).

Table 3.4: Preparation of aryl azides.

entry	R		yield (%)
1	4-NO$_2$	**3a**	74
2	3-NO$_2$	**3b**	69
3	2-NO$_2$	**3c**	91
4	4-CN	**3d**	71
5	4-C(O)CH$_3$	**3e**	96
6	4-C(O)OCH$_3$	**3f**	94
7	3,5-(CF$_3$)$_2$	**3g**	73
8	4-CF$_3$	**3h**	79
9	4-Cl	**3i**	68
10	4-Br	**3j**	72
11	4-I	**3k**	49
12	4-CH$_3$	**3l**	79
13	4-OCH$_3$	**3m**	74
14		**3n**	99

4-Azidopyridine **3o** and furazan **3p** were prepared by simple aromatic substitutions. The corresponding chloroarene precursors were treated with sodium azide in ethanol or water/acetone mixture to give azides **3o** and **3p** in average to excellent yields (Scheme 3.2).

3.4 Substrate Scope of [Cu(DAB)] Catalysed Aryl Azide Reduction

With an optimised catalytic system in hand, the substrate scope was next investigated. It is important to note that the work-up procedure greatly influenced the final, isolated yields. Several work-up procedures were tested and
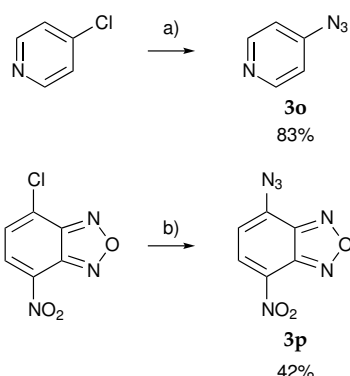
Scheme 3.2: Preparation procedure for pyridine and furazane based azides **3o** and **3p**. a) NaN$_3$ (2 equiv), EtOH, 75 °C, 4 h; b) NaN$_3$ (3.0 equiv), acetone/H$_2$O, room temperature, 15 min.

the optimal one consisted of dissolving the reaction mixture in EtOAc and filtration through celite to remove solids. The solids and reaction residue needed to be washed several times (~10) with EtOAc. The organic solution was then washed with a saturated aqueous solution of Na$_4$EDTA, dried over Na$_2$SO$_4$, filtered, and concentrated under high vacuum to remove toluene (<0.1 mbar). The obtained residue was then purified by column chromatography using basified silica as stationary phase.

3- and 4-Nitro-substituted phenylazides gave the corresponding nitroanilines **4a** in very good yields (Table 3.5, entries 1 and 2). Despite having similar electronic properties, **3d** was obtained with a substantially lower yield (Table 3.5, entry 3). This effect might be due to decomposition of the starting azide **3d** during the reaction.

For methyl 4-azidobenzoate **3f** the obtained yield was very good compared to homologous 4-acetylphenylazide **3e** for which only 35% were isolated (Table 3.5, entries 4 and 5). A comparable observation was made for 3,5-bis-(trifluoromethyl)phenyl azide **3g** as the yield was half of 4-trifluoromethyl-phenylazide **3h** (Table 3.5, entries 6 and 7).

Also, different heterocyclic azides were investigated and thiophene, pyridine, and furazan containing substrates led to yields around 50% (Table 3.5, entries, 8–10).

Curiously, while 3- and 4-nitrophenylazides **3a** and **3b** gave access to excellent yields 2-nitrophenyl azide decomposed completely (Table 3.6, entry 1). Complete decomposition was also observed for 4-chloro and 4-iodophenyl-azides (Table 3.6, entries 2 and 3), whereas electronic neutral or rich phenyl azides showed no reactivity whatsoever and the starting materials were recovered (Table 3.6, entries 4–6).

Table 3.5: Substrate scope for the aryl azide reduction reaction.

entry	azide	amine	yield (%)
1	3a	4a	89
2	3b	4b	91
3	3d	4d	65
4	3f	4f	85
5	3e	4e	35
6	3h	4h	64
7	3g	4g	23
8	3n	4n	45
9	3o	4o	45
10	3p	4p	55

[a] Isolated yields are the average of two independent reactions.

Table 3.6: Substrates that did not undergo reduction.
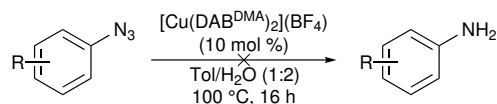
entry	R	reactivity
1	2-NO$_2$	decomposition
2	4-Cl	decomposition
3	4-I	decomposition
4	4-H	S.M. recovered
5	4-CH$_3$	S.M. recovered
6	4-OCH$_3$	S.M. recovered

3.5 Mechanistic Studies

A similar reaction with azido-furazan **3p** to amino-furazan **4p** in the presence of copper(I) and copper(II) in a DMSO/H$_2$O mixture had been reported, and it also occurred in the absence of any obvious reducing agent.[96] Even though no full reaction mechanism was disclosed, the reaction was studied with electron paramagnetic resonance (EPR) and a hyperfine splitting for the copper(II) centre was observed, which suggested the presence of a copper–nitrene intermediate. Following this finding, it was suggested that the nitrene species would be formed by thermal extrusion of dinitrogen, which then would coordinate to the copper centre. Based on these findings, we were interested in investigating this intriguing reaction further with computational methods to eventually provide a mechanistic rationale.

To evaluate the optimal method and basis set for this DFT study, the C=N stretching frequencies for model complex [Cu(DAB^{Me})$_2$]$^+$ were calculated with different methods and basis sets (Table 3.7). The obtained results were then compared to the measured frequencies of [Cu(DAB^R)] complexes (R = aliphatic Table 3.8). Methyl substitution on the DAB ligand was chosen to allow for a short computational time and a fast screening.

All methods provided frequencies that were too high in energy compared to the experimental results but BP86. Among the different basis sets investigated, all disclosed too low energies for both symmetric and asymmetric stretches, except for 6-31g(d), which was then chosen.

Next, the stretching frequencies of [Cu(DAB^{tBu})$_2$](BF$_4$) were calculated with

Table 3.7: Calculated frequencies for C=N stretches for [Cu(DAB^{Me})$_2$]$^+$ using different methods and basis sets. All values are given in cm^{-1}.

Method	M06	wb97xD	b3lyp-D3	BP86-D3	BP86-D3	BP86-D3	BP86-D3
Basis Set	*6-31g(d)*	*6-31g(d)*	*6-31g(d)*	*6-31g(d)*	*ccpVTZ*	*ccpVQZ*	*sdd ccpVTZ*
sym C=N	1677	1706	1643	1551	1528	1527	1531
	1679	1707	1644	1555	1533	1532	1536
asymm C=N	1747	1774	1725	1630	1610	1609	1613
	1748	1774	1725	1630	1610	1609	1613

Table 3.8: Measured IR frequencies for [Cu(DAB^R)]. All values are given in cm^{-1}.

	[Cu(DAB^{Cy})$_2$](BF$_4$)	[Cu(DAB^{Ad})$_2$](BF$_4$)	[Cu(DAB^{tBu})$_2$](BF$_4$)
sym C=N	1541	1531 1558	1542
asymm C=N	1627	1634	1627

the chosen method and basis set. However, the calculated frequencies did not match the experimental values and a reported correction term was introduced (Table 3.9).[151] For comparison purposes, the stretching frequencies including the correction term were also computed with other methods and basis sets, but the best match remained BP86-D3 and 6-31g(d).

Table 3.9: Calculated stretching frequencies including correction term for [Cu(DAB^{tBu})$_2$](BF$_4$). All values are given in cm^{-1} and the basis set is given for copper.

Experimental	BP86-D3 sdd (corrected)	BP86 ccpVTZ (corrected)	b3lyp sdd (corrected)	b3lyp ccpVTZ (corrected)
corr. value[151]	1.021	1.028	0.991	0.999
1541	1505 (1537)	1526 (1484)	1592 (1606)	1590 (1591)
	1515 (1547)	1539 (1497)	1593 (1607)	1599 (1601)
1627	1600 (1634)	1628 (1584)	1689 (1704)	1692 (1693)
	1601 (1634)	1628 (1584)	1689 (1705)	1695 (1696)

In a final step, the solid state structures of [Cu(DAB^R)$_2$](BF$_4$) (R = Ad, Cy, Mes) and [CuCl(DAB^{Cy})] were geometrically optimised and their C=N stretching frequencies were calculated with the BP86 method. Pleasantly, all of the calculated frequencies were in strong agreement with the experimental values (Table 3.10).

After having found an optimal method and basis set, a possible reductant needed to be identified through computational methods as no oxidation product could be observed experimentally. Since no oxidation of the complex or ligand was evident, only toluene and/or H$_2$O could act as reductant.

Table 3.10: Comparison of experimental and calculated C=N stretching frequencies for various [Cu(DAB)]. All values are given in cm^{-1} and method BP86-D3 with basis sets sdd and 6-31g(d) was utilised.

	$[Cu(DAB^{Ad})_2](BF_4)$		$[CuCl(DAB^{Cy})]$		$[Cu(DAB^{Cy})_2](BF_4)$		$[Cu(DAB^{Mes})_2](BF_4)$	
	exp.	calcd	exp.	calcd	exp.	calcd	exp.	calcd
symm C=N	1531	1532	1569	1558	1541	1543	1439	1442
	1557	1557				1556	1475	1473
asymm C=N	1634	1634	1644	1641	1627	1637	1571	1572

Relevant oxidation products of toluene and/or H_2O and their energies are shown in Figure 3.1. The energies were calculated by comparing the reaction products ($PhNH_2$, N_2, and oxidation product) to the starting materials (PhN_3, toluene, and H_2O) and all shown oxidation products disclosed feasible energies.
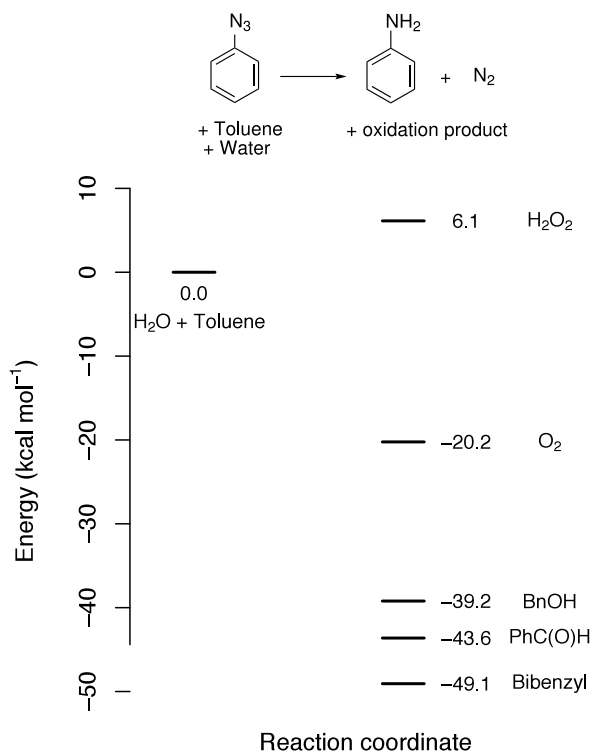
Figure 3.1: Overview of the energies of different oxidation products.

The formation of H_2O_2 would be possible, however, oxidation of the formed anilines to hydroxylanilines would have been expected.[152] Additionally, oxidation of toluene with H_2O_2 to benzyl alcohol by copper complexes has been reported in literature.[153,154]

The formation of O_2 as oxidation product from H_2O was very intriguing and

would have allowed the catalytic system to be exploited in the field of water splitting.[155] However, this reaction requires a binuclear copper species[156] and preliminary calculations on such a system led to energies much higher than the eventually proposed mononuclear pathway (Scheme 3.3).
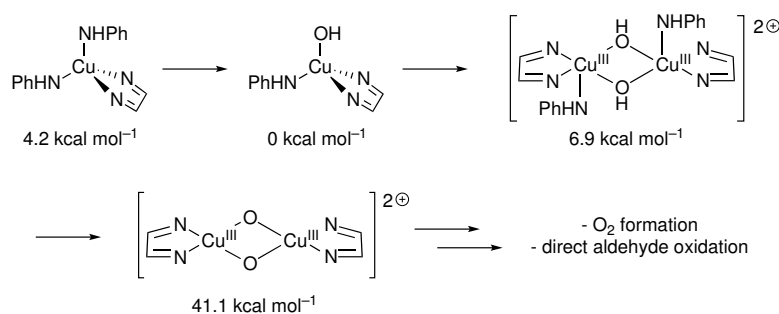
Scheme 3.3: Calculated energies for dinuclear copper–DAB species

On the other hand, the energies of oxidation products based on toluene showed to be more thermodynamical viable and promised a lower activation energy compared to H_2O_2 or O_2. Despite their low reaction enthalpy, the formation of bibenzyl was ruled out as it was not observed experimentally. The direct oxidation of toluene with water to benzaldehyde can only be achieved by a dinuclear copper complex under the formation of two equivalents of anilines or oxidation of benzyl alcohol by a mononuclear complex. Since the energies for DAB based dinuclear copper complexes were $30\,\text{kcal}\,\text{mol}^{-1}$ higher in energy the direct formation of benzaldehyde from toluene was dismissed as well.

Therefore, toluene was studied as hydride source with benzyl alcohol as oxidation product. Phenylazide and homoleptic $[\text{Cu(DAB}^{\text{Me}})_2]^+$ were chosen for the model reaction (Scheme 3.4).
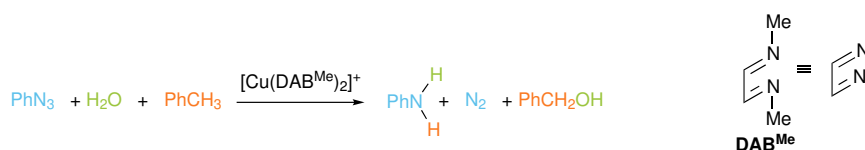
Scheme 3.4: Model reaction for computational studies.

Systematic conformation analyses were carried out for all steps and therefore only results with the most stable conformers will be discussed herein. The complete reaction cycle was computed and an overview with selected intermediates is shown in Scheme 3.5 and their corresponding energies in Figure 3.2. The full reaction cycle is depicted in Scheme 3.6.
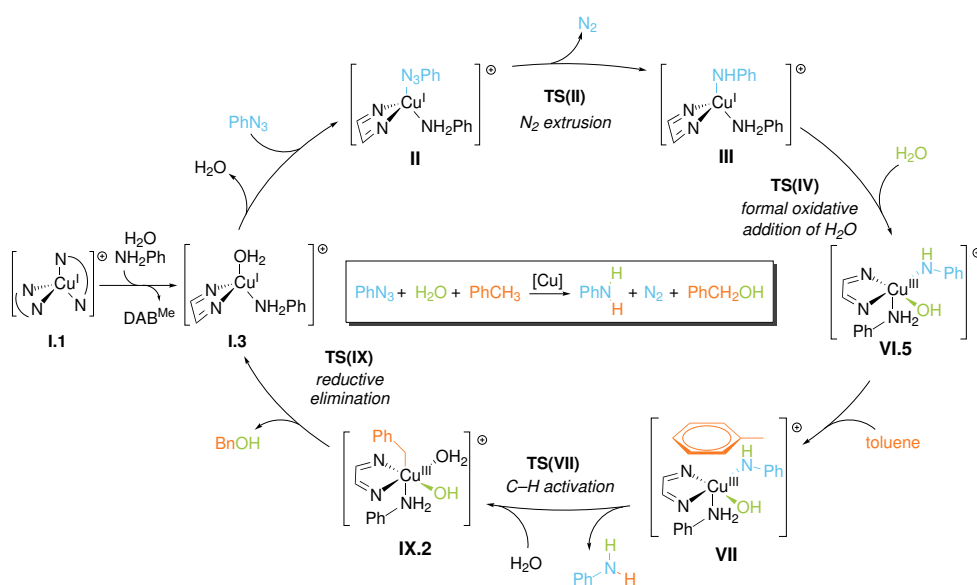
Scheme 3.5: Overview of the proposed catalytic cycle with selected intermediates.
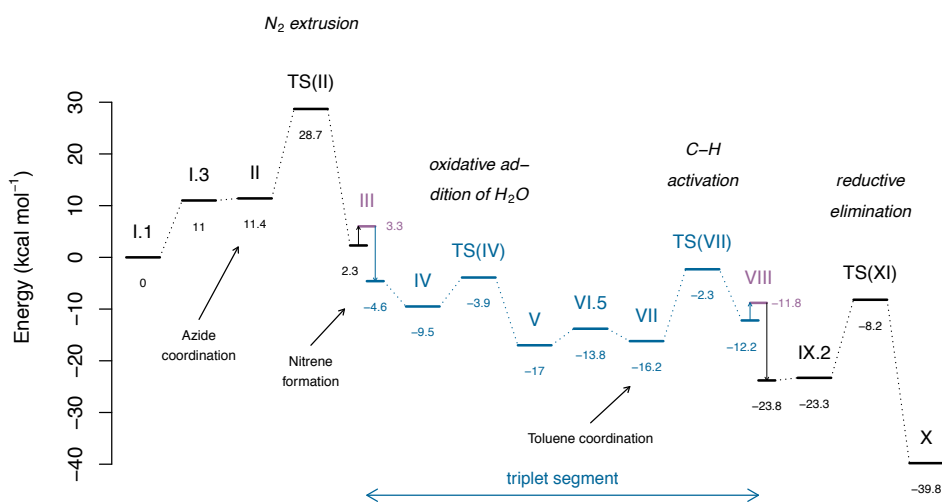
Figure 3.2: Energy diagram for the proposed catalytic cycle with selected intermediates.

In a first step, the catalyst would be activated by displacement of one DAB^{Me} ligand with H$_2$O and aniline to form tetracoordinated copper intermediate **I.3**. Such displacement is expected to be straightforward under catalytic conditions (Chapter 1.4). Aniline for this step would originate from the hydrolysis of the DAB ligand. From DAB^{Me} methylamine would be formed instead, however, aniline would mimic better the behaviour of 4-dimethylaminoaniline that is formed experimentally, which would be present in the reaction mixture upon hydrolysis of DAB^{DMA}. Phenyl azide could
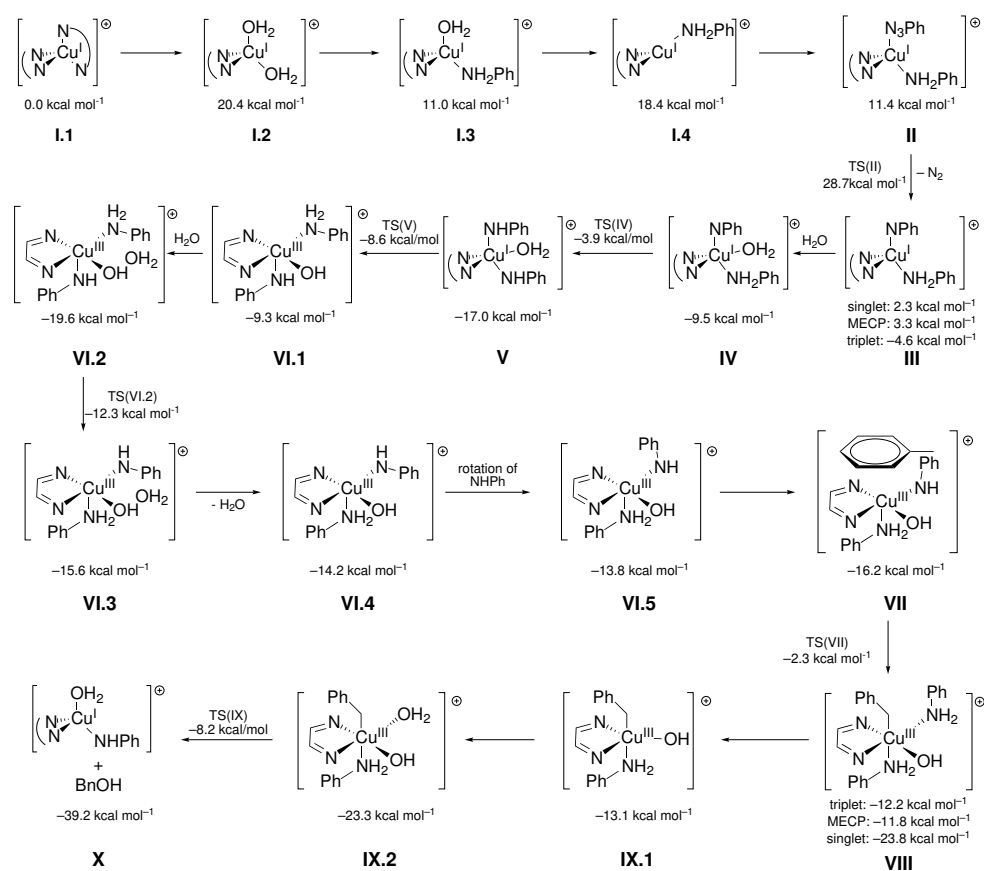
Scheme 3.6: Full proposed mechanism.

then coordinate the copper(I) centre by displacing H_2O to give intermediate **II**, which has a very close energy to **I.3** (Scheme 3.6). Dinitrogen would then be extruded in **TS(II)** with an activation energy of 28.7 kcal mol^{-1} (Figure 3.3). This high energy correlates with the required high reaction temperature and the irreversibility of this step contributes further to its feasibility. Also, this extrusion of dinitrogen would represent the rate limiting step in the proposed reaction mechanism.
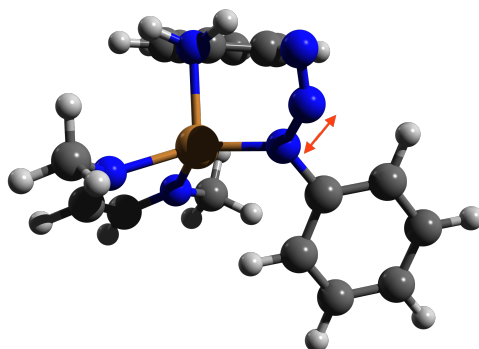
Figure 3.3: Calculated transition state for dinitrogen extrusion **TS(II)**.

It is noteworthy that the uncatalysed extrusion of N_2 from phenyl azide was calculated to proceed through a transition state above $45\,\mathrm{kcal\,mol^{-1}}$. From **TS(II)** singlet nitrene intermediate **III** (Scheme 3.6) would be formed and undergo a spin-cross over to form the more stable triplet species of **III**. The minimum energy conversion point (MECP) for the spin-crossover was located at $3.3\,\mathrm{kcal\,mol^{-1}}$, close to the singlet species with **III** at $2.3\,\mathrm{kcal\,mol^{-1}}$. Therefore the spin-crossover would readily take place to form the triplet species with an energy of $-4.6\,\mathrm{kcal\,mol^{-1}}$. An intersection between the energy surfaces of the singlet and triplet species was sought close to the transition state **TS(II)** but none was found as the energy surface of the triplet species was too high compared to the transition state. This finding would support the idea that the triplet species of **III** is formed after the formation of the singlet intermediate of **III**.

From triplet intermediate **III**, coordination of a H_2O molecule would form **IV** (Scheme 3.6), in which H_2O would act as a proton shuttle to form a diamido intermediate **V** stabilising it by $12.4\,\mathrm{kcal\,mol^{-1}}$ compared to **III**. This water molecule would then undergo an oxidative addition during **TS(V)** forming a copper(III) hydroxyl amido aniline complex **VI.1** (Figure 3.4).
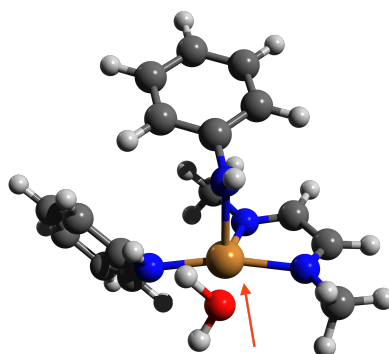
Figure 3.4: Calculated transition state for the formal oxidative addition of water **TS(V)**.

Penta coordinated copper(III) **VI.1** would already allow for a toluene molecule to bind through dispersion interaction. However, for the reaction to proceed the amido group needs to be in equatorial position to allow for a hydrogen transfer from the bound toluene to the amido group. Therefore, intermediates **VI.1** to **VI.5** describe the required rearrangement to bring the amido group to an equatorial position and the aniline group into an axial one (Scheme 3.6). This process would take place *via* an additional water molecule that would be present in the second coordination sphere of the copper centre and act as a proton shuttle between the amido and aniline to lead to intermediate **VI.5**, which is $4.5\,\mathrm{kcal\,mol^{-1}}$ lower in energy than **VI.1**. Following this rearrangement, toluene would bind through dispersion

interaction to copper(III) complex **VII**, where an sp³ hydrogen from toluene would then be transferred to the amido moiety with a reasonable activation barrier of 13.9 kcal mol⁻¹. The corresponding transition state is shown in Figure 3.5. This transfer seems to be a radical process rather than a deprotonation as a spin-density of 0.55, indicating the presence of an unpaired electron, was observed on the nitrogen before the transfer.
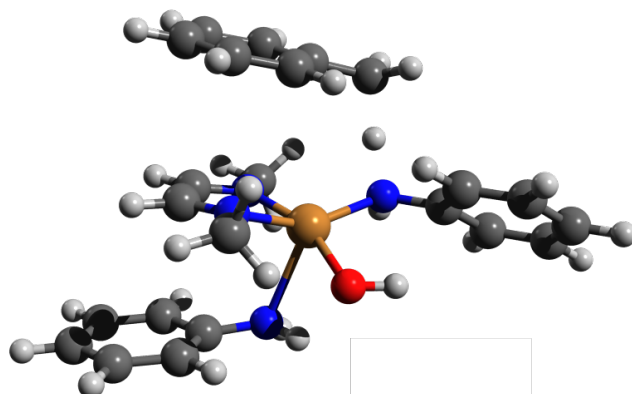
Figure 3.5: Calculated transition state for the hydrogen abstraction **TS(VII)**.

Following this hydrogen abstraction, copper(III)–benzyl intermediate **VIII** would readily undergo a spin-crossover to form a much more stable singlet species (−23.8 kcal mol⁻¹ compared to −12.2 kcal mol⁻¹, Scheme 3.6). Again, no intersection between the triplet and the singlet energy surfaces could be found around the transition state. Aniline, the reaction product, would then be displaced by a water molecule without a significant increase in free energy, after which benzyl alcohol is reductively eliminated and the active catalytic species **I.3** would be regenerated (Figure 3.6).
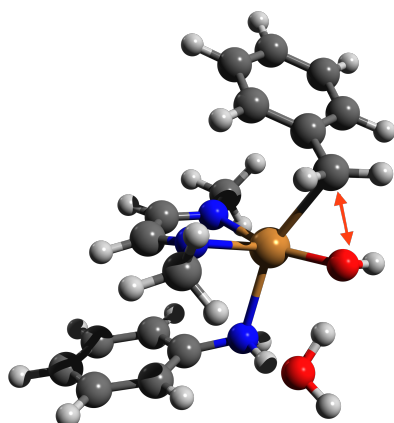
Figure 3.6: Calculated transition state for the reductive elimination of benzylalcohol **TS(IX)**.

The experimental confirmation of benzyl alcohol in this reaction has been not achieved either by ^{1}H NMR or mass spectroscopy. This might be because benzyl alcohol reacts further eventually decomposing and further studies on this are required.

In an initial attempt to understand the kinetics of this azide reduction catalysed by [Cu(DAB)], the reaction order of the catalyst was investigated. 4-Cyanophenylazide **3d** was used as model substrate and reactions with 5 and 10 mol % catalyst loadings were performed and the conversions were measured every two hours for 16 h. The amounts of starting azide and resulting aniline were calculated against an internal standard and plotted in Figure 3.7. Azide **3d** was fully consumed after 8 h and a 65% conversion was reached with a 10 mol % [Cu(DAB)]. As no other products were detected by ^{1}H NMR in this reaction, the thermal decomposition of **3d** was estimated to be 35%, which is higher than the observed 15% for 4-nitrophenylazide **3a**. A similar observation was made for the reactions with a catalyst loading of 5 mol %. However, in this case the decomposition was about 10% higher than with 10 mol % catalyst, as expected for slower reactions with lower catalytic loadings. Most important though, was the fact, that with 10 mol % the amount of product **4d** observed over the course of the reaction was twice the product with 5 mol % indicating that in fact the reaction order of catalyst $[Cu(DAB^{DMA})_2](BF_4)$ was 1, which is in accordance with the proposed reaction mechanism. This result matched the obtained yield for this substrate (Table 3.5, entry 3).
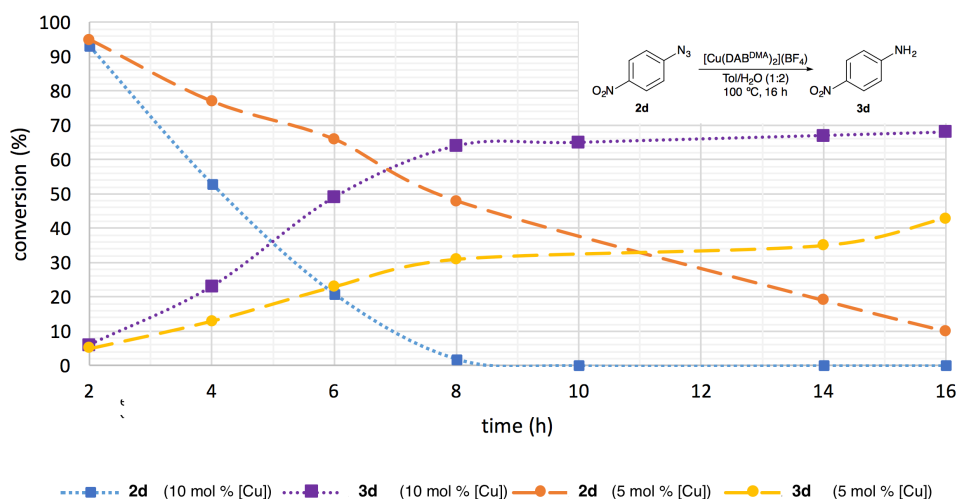
Figure 3.7: Reaction profile with 4-cyanophenylazide **3d**.

3.6 Conclusions

The [Cu(DAB)]-catalysed reduction of aryl azide was optimised and a privileged reaction conditions were disclosed with 10 mol % [Cu(DAB^{DMA})$_2$](BF$_4$) in a mixture of toluene/H$_2$O (1:2) at 100 °C. Different copper(I) complexes based on DAB, NHC, and ImPy ligands were tested for this reaction. Overall, [Cu(DAB^{DMA})$_2$](BF$_4$) was the best performing catalyst.

Different aryl and heteroaryl azides were prepared and average to excellent yields were obtained for electron poor substrates in the reduction reaction, whereas electron neutral or rich compounds showed no reactivity. The lower yield for some substrates might have been due to a possible substrate decomposition during the reaction. Lower temperatures were investigated as well but since the conversion dropped from <95% at 100 °C to 15% at 80 °C for 4-nitroazide **3a** the temperature was left unchanged. Also, an optimised work-up procedure was developed since the work-up procedure greatly influenced the isolated yields.

With the help of DFT methods several oxidation products based on water and toluene were identified and benzyl alcohol was chosen as the most probable one. From there, a reaction mechanism was suggested utilising DFT methods at the BP86 level in the gas phase.

The key intermediates and transition states showed the extrusion of N$_2$ would take place while the aryl azide is coordinated to the copper(I) centre. Additionally, this N$_2$ extrusion would be the rate limiting step with an activation energy of 28.7 kcal mol^{-1}. After the N$_2$ extrusion, the resulting singlet copper(I) nitrene would undergo a spin-crossover to give a triplet copper(I) nitrene intermediate, which would agree with a similar reported reaction intermediate.[96] The next key step would be a formal oxidative addition of water resulting in a copper(III) amido hydroxyl species. Unfortunately, to the best of our knowledge the structure of a comparable copper(III) hydroxyl species remains unknown. However, a reported copper(III)–bipy complex showed a square pyramidal geometry similar to our suggested intermediate.[157]

After coordination of toluene through dispersion interaction, a hydrogen would be abstracted by the amido moiety to give a copper(III) benzyl hydroxyl species from which benzyl alcohol would be reductively eliminated closing the reaction cycle. Benzyl alcohol was not directly identified in the reaction mixture it, which might suggest its decomposition in the presence of [Cu(DAB)].

Readily Available Copper(I) Catalysts in the Hydroamination Reaction

4.1 Aims and Objectives

The hydroamination reaction is an exceptional tool for the formation of carbon–nitrogen bonds from primary and secondary amines and unsaturated carbon–carbon bonds. This catalysed reaction offers a 100% atom efficiency, however, the utilised transition metals for this reaction are often expensive, hazardous to the environment, and often prospected in politically unstable region. Copper does not posses any of these disadvantages and is an ideal candidate as hydroamination catalyst, especially when compared to precious metal complexes.

The aim of this work is to explore the reactivity of readily available and economical copper(I) complexes as catalysts for the homogeneous hydroamination reaction and to develop this reaction to be as user-friendly as possible and to avoid high purity solvents, or oxygen- or moisture-free conditions.

Additionally, the focus lays on the addition of primary amines as they are more challenging substrates compared to secondary amines due to their electron pair on the nitrogen binding stronger to the copper and thus inhibiting the forward reactions (Scheme 4.1).
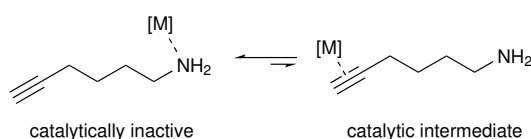
Scheme 4.1: Inhibition of forward reaction in the hydroamination reaction due to substrate binding to the catalyst.

First, optimal reaction conditions will be sought by screening different copper(I) complexes, solvents, and temperatures. Next, we intend to prepare a large library of substrates with primary or secondary amines and alkynyl, 1,2- and 1,3-dienyl, or alkenyl moieties to develop the scope for the optimised reaction. This will be followed by the study of intermolecular hydroamination reactions. Additionally, we will find isolation methods for the obtained hydroamination products, since such purification procedures are scarce in literature.

4.2 Synthesis of Hydroamination Substrates

Several substrates with primary and secondary amines and different carbon–carbon unsaturated bonds were prepared for the investigation of copper complexes in the hydroamination reaction. The substrates contained terminal or internal alkynes, as well as 1,2- 1,3-dienes, or alkenes (Figure 4.1).
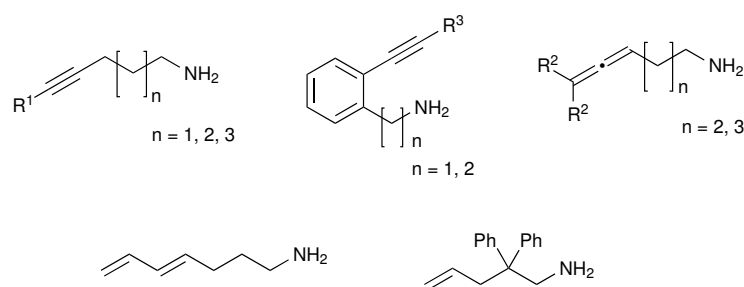
Figure 4.1: Overview of the different hydroamination substrates.

A model substrate, pent-4-yn-1-amine **8a**, was synthesised from commercially available chloropentyne **6a** *via* the Gabriel amine synthesis and subsequent deprotection to the primary amine following a reported procedure (Scheme 4.2).[119,158] Crude **7a** was purified by column chromatography (SiO$_2$, DCM) to remove excess phthalamide. However, this purification step is not necessary as long as the remaining phthalamide in crude **7a** is taken into account in the subsequent deprotection step. An alternative procedure using sodium phthalimide, K$_2$CO$_3$, and KI yielded pure **7a** without any further purification but in lower yield (47%). Phthalamide pentyne **7a** was then reacted with hydrazine in hot methanol, and crude **8a** was purified by Kugelrohr distillation (85 °C/200 mbar), using dry ice for condensing the distilled product. However, small, unknown impurities were still present after distillation (>5%). Unfortunately, purification of **8a** by column chromatography with different solvent mixtures was not possible as it adhered strongly to either basic or neutral aluminium oxide, or silica.
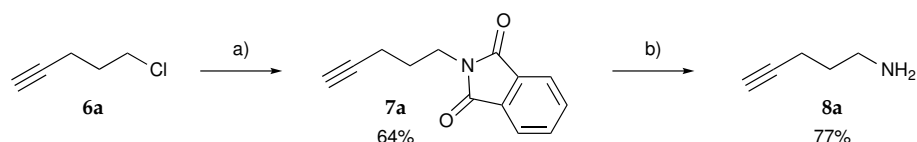
Scheme 4.2: Synthesis of pent-4-ynamine **8a** using the Gabriel amine procedure. a) Phthalamide (1.2 equiv), K$_2$CO$_3$ (1.0 equiv), KI (1 mol %), DMF, 70 °C, 16 h; b) NH$_2$H$_4$·H$_2$O (1.1 equiv), EtOH, 70 °C, 2 h.

A different synthetic approach was then used to prepare pent-4-yne-1-amine **8a** to overcome the issues encountered in the Gabriel amination protocol (Scheme 4.3).[159] 4-Pentynol **9** was mesylated in diethyl ether to provide **10**, which was then subjected to a S$_N$2 reaction with sodium azide to form 4-pentynazide **11**. In an attempt to improve the yield, this reaction was also carried out in DMSO, since sodium azide is more soluble in this solvent. Nevertheless, only a similar yield of 65 % was achieved under these conditions. In the last step, **11** was reduced with PPh$_3$ to the corresponding

phosphine imine followed by an acidic hydrolysis to form **8a**. The formed (O)PPh$_3$ precipitated out of the reaction mixture leaving **8a** in solution. After work-up, **8a** was isolated with still small traces of (O)PPh$_3$ (~ 5%) according to the ^{1}H and ^{31}P NMR spectra. As the remaining phosphine oxide could not be removed by repeating the work-up, the crude product was then distilled to yield pure **8a**. It is important to note that this was the only purification step required in this synthetic sequence.
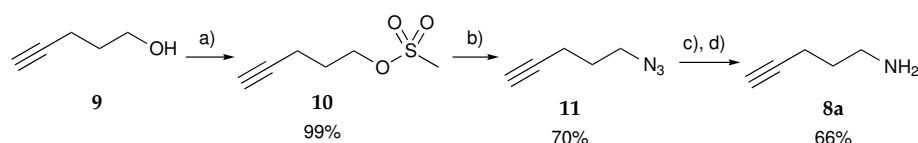
Scheme 4.3: Synthesis of **8a** *via* the Staudinger phosphine imine reduction procedure. a) NEt$_3$ (1.1 equiv), MsCl (1.1 equiv), Et$_2$O, 0 °C, 15 min; b) NaN$_3$ (1.1 equiv), DMF, 70 °C, 3 h; c) PPh$_3$ (1.0 equiv), Et$_2$O, 0 °C, 16 h; d) HCl/H$_2$O, room temperature, 16 h.

Next, the Gabriel synthesis was used for preparing hex-5-ynylamine **8b**. [119,158] 6-Chlorohex-1-yne **6b** was transformed into **7b** using phthalimide under basic conditions and purified by column chromatography. **7b** was then deprotected by hydrazine in hot ethanol to isolate pure **8b** after distillation (Scheme 4.4). An alternative route using the Staudinger reduction from the corresponding azide was also attempted, however the yield for the preparation of the azide from 5-cholorohexyne **6b** was very low (<10 %).
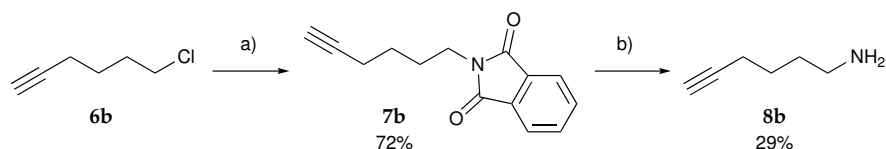
Scheme 4.4: Synthesis of **8b** *via* the Gabriel procedure. a) Phthalamide (1.2 equiv), K$_2$CO$_3$ (1.0 equiv), KI (1 mol %), DMF, 70 °C, 16 h; b) NH$_2$H$_4$ · H$_2$O (1.1 equiv), EtOH, 70 °C, 2 h.

Preparation of heptynylamine **8c** followed a reported procedure where alkyne chloride **6b** was transformed into the corresponding nitrile using NaCN to then be reduced with LiAlH$_4$ to the corresponding primary amine **8c**. [160] Pleasantly, the obtained yields in both steps were very high (95 and 94%) without any purification required (Scheme 4.5).
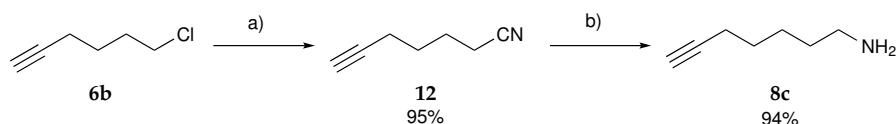
Scheme 4.5: Synthesis of **8c**. a) NaCN (1.2 equiv), DMSO, 80 °C, 16 h; b) LiAlH$_4$ (1.1 equiv), Et$_2$O, 0 °C, 1 h.

Methyl substituted alkynes were prepared from chloroalkynes **6a,b**. These were lithiated with *n*-butyllithium and treated with methyl iodide (Scheme 4.6). **13a,b** were then reacted with NaN_3 and consecutively reduced to the final primary amine *via* the Staudinger reduction. For the formation of **15c**, chloro alkyne **13b** was first treated with NaCN and then reduced by $LiAlH_4$. All reductions afforded good to excellent yields in the desired amines (74–84%).
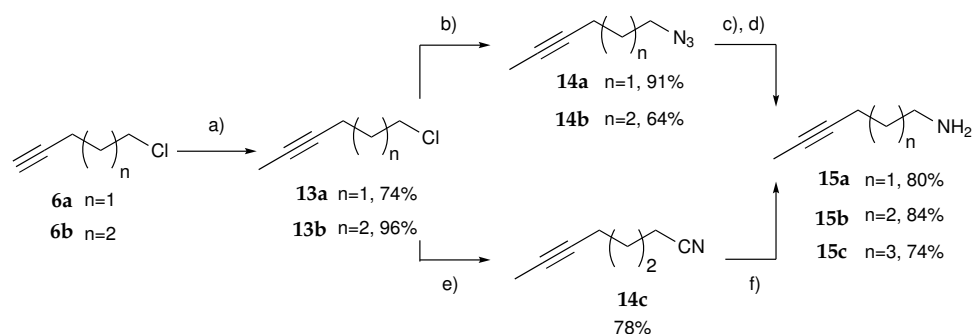
Scheme 4.6: Synthesis of methyl-substituted alkynes **15a–c**. a) *n*-BuLi (1.05 equiv), MeI (1.15 equiv), THF, –78 °C, 10 min; b) NaN_3 (1.2 equiv), DMSO, 70 °C, 16 h; c) PPh_3 (1.0 equiv), Et_2O, 0 °C, 2 h; d) HCl/H_2O, room temperature, 16 h; e) NaCN (1.2 equiv), DMSO, 80 °C, 16 h; f) $LiAlH_4$ (2.0 equiv), Et_2O, 0 °C, 30 min.

Commercially available TMS-chloroalkyne **16a** was used for the preparation of trimethylsilane substituted alkyne **18a** following a reported Gabriel amination procedure (Scheme 4.7).[119] TMS-heptynylamine **16b** had to be prepared from the terminal alkyne **6b**, which was first lithiated and treated with TMSCl. This was then converted to the corresponding amine following an identical procedure.
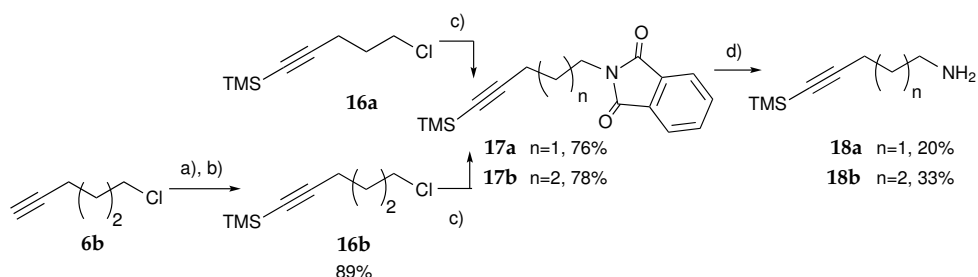
Scheme 4.7: Synthesis of trimethylsilyl-substituted alkynes **18a,b**. a) *n*-BuLi (1.1 equiv), THF, –78 °C; b) TMSCl (1.2 equiv), 0 °C; c) Phthalamide (1.2 equiv), K_2CO_3 (1.0 equiv), KI (1 mol %), DMF, 70 °C, 16 h; d) $N_2H_4 \cdot H_2O$ (1.2 equiv), EtOH, 70 °C, 2 h.

Phenyl substituted alkyl amines **21a–c** were synthesised following an adapted literature procedure (Scheme 4.8).[119] Lithium phenyl acetylide in THF was prepared by addition of *n*-buthyllithium to a solution of phenylacetylene and then added to a solution of a (bromo)(chloro)alkane to form **19a,b**. It is important to note that for the synthesis of lithium phenylacetylide the reaction concentration should not exceed 0.3 M and the reaction should not be stirred longer than 15 min at –78 °C as formation of a precipitate and a consequent lower yield were observed otherwise.
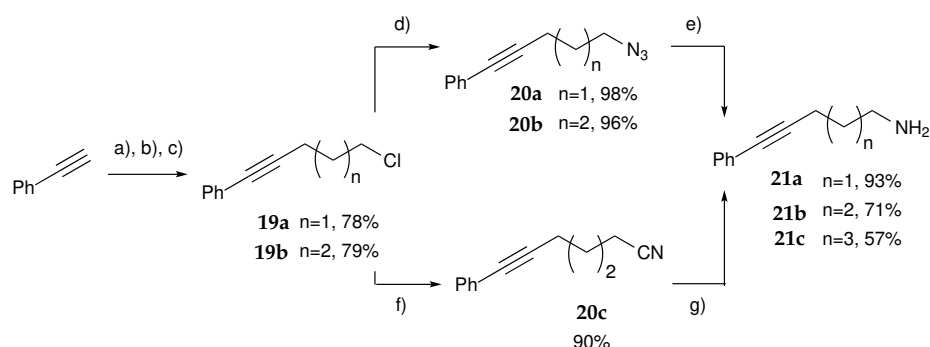
Scheme 4.8: Synthesis of phenyl substituted alkynes **21a–c**. a) *n*-BuLi (1.1 equiv), THF, –78 °C, 15 min; b) Br(CH$_2$)$_n$Cl (n=3,4) (1.0 equiv), THF, 0 °C, 2 h; c) reflux, 3 h; d) NaN$_3$ (1.1 equiv), DMSO, 70 °C, 16 h; e) LiAlH$_4$ (1.1 equiv), Et$_2$O, 0 °C, 1 h; f) NaCN (1.2 equiv), DMSO, 80 °C, 16 h; g) LiAlH$_4$ (1.1 equiv), Et$_2$O, 0 °C.

The crude products were distilled at 95 °C *in vacuo* to give pure **19a,b** in good yields. These were subsequently treated with NaN$_3$ in hot DMSO to form the corresponding azides **20a,b** in excellent yields. In the homologation reaction to form phenylheptyne amine **21c**, **19b** was reacted with NaCN to form nitrile **20c**. **20a–c** were then reduced with LiAlH$_4$ in Et$_2$O to give corresponding amines **21a–c** in fair to excellent yields. No purification was required for the final products, except for **21a**.

Phenylethynyl aniline **23b** was prepared from 2-iodoaniline and phenylacetylene *via* a Sonogashira cross-coupling in a mixture of THF and NEt$_3$ at room temperature (Scheme 4.9).[161] After purification by column chromatography, **23b** was obtained in a yield comparable to the reported one.
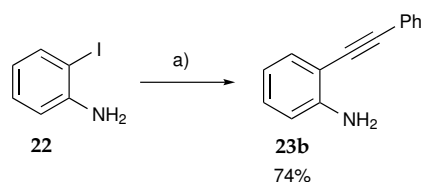
Scheme 4.9: Preparation of 2-(phenylethynyl)aniline **23b** *via* Sonogashira coupling. a) Phenyl acetylene (1.5 equiv), [PdCl$_2$(PPh$_3$)$_2$] (1 mol %), CuI (3 mol %), THF/NEt$_3$ = 3:1, room temperature, 16 h.

For the preparation of amino ethynyl benzenes **26a–c** a modified, reported procedure was followed.[120] Starting from iodobenzonitrile **24**, the ethynyl group was introduced *via* a Sonogashira cross coupling (Scheme 4.10). After purification by column chromatography, **25a–c** were reduced with LiAlH$_4$ to access the corresponding amino ethynyl benzenes **26a–c** as black oils without further purification. The obtained yields were very close to those previously reported.[120] 2-Ethynylbenzylamine **26a** is unstable and decomposes over several days into unknown fragments even when stored at –18 °C. In contrast, phenyl- and hexyl-substituted ethynylbenzylamines **25b,c** did not show any signs of decomposition over time.
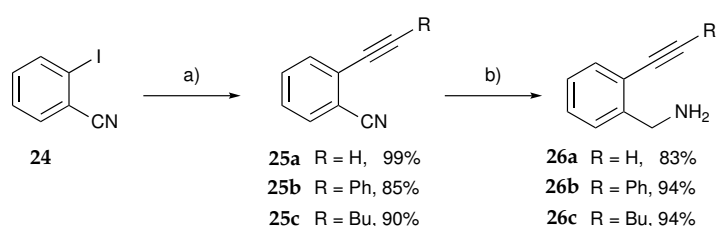
Scheme 4.10: Preparation of substituted ethynyl benzyl amines **26a–c** *via* Sonogashira coupling. a) Alkyne (1.5 equiv), [PdCl$_2$(PPh$_3$)$_2$] (1 mol %), CuI (3 mol %), THF/NEt$_3$ = 3:1, room temperature, 16 h; b) LiAlH$_4$ (1.1 equiv), Et$_2$O, 0 °C, 1 h.

A number of secondary amines was also synthesised to compare their reactivity to that of primary amines. **27a,b** were prepared from the primary alkylamines **8a** and **21a** upon stirring with TosCl and K$_2$CO$_3$ in acetonitrile to give the corresponding tosyl amides in good yields (Scheme 4.11).[162] Acetyl pentynamines **28a,b** were synthesised from the corresponding primary amines using acetylchloride and NEt$_3$ and were isolated in good yields without any purification required.
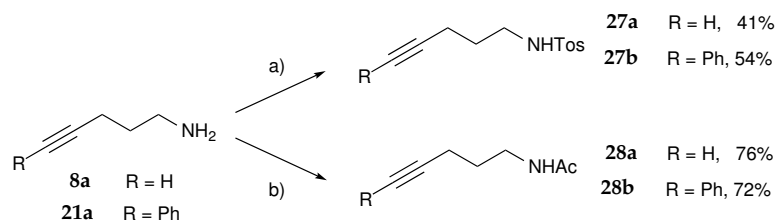
Scheme 4.11: Preparation *N*-tosyl and *N*-acetyl substituted pentynamine **27a,b** and **28a,b**. a) Tosylchloride (1.0 equiv), K$_2$CO$_3$ (2.0 equiv), MeCN, 80 °C, 16 h; b) Acetylchloride (1.0 equiv), NEt$_3$ (1.0 equiv), Et$_2$O, room temperature, 16 h.

Benzyl and *t*-butyl pentynyl amines **29a,b** and **30** were prepared by reacting the corresponding pentynylchloride with a six-fold excess of benzyl or *t*-butyl amine at room temperature (Scheme 4.12). After 16 h, pure products

were isolated in good yields after a simple aqueous work-up.
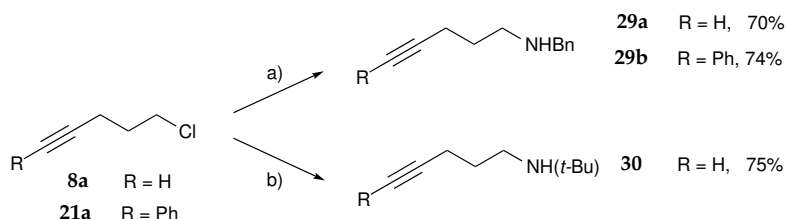
Scheme 4.12: Preparation *N*-benzyl and *N*-*t*-butyl substituted pentynamines **29a,b** and **30**. a) Benzylamine (6.0 equiv), room temperature, 16 h; b) *t*-Butylamine (6.0 equiv), room temperature, 16 h.

Alternatively, *N*-propylpentynamine **32** was formed by a condensation reaction of pentynal **31** and propylamine, followed by the reduction of the resulting imine to secondary amine **32** (Scheme 4.13). The final product was purified by column chromatography on basic alumina. A large fraction of the initial mass remained on the column, which was later washed down with a methanol/EtOAc mixture. However, the washed down residue showed decomposition in the ^{1}H NMR and only a yield of 15% of **32** was eventually obtained.
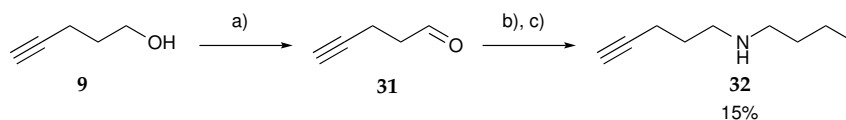
Scheme 4.13: Preparation of propyl pent-4-ynyl amine **32**. a) Oxalyl chloride (1.0 equiv), DMSO (1.0 equiv), pent-4-ynol **9** (1.0 equiv), –78 °C, 1 h; b) Propylamine (2.0 equiv), room temperature, 16 h; c) NaBH$_4$ (0.5 equiv), 0 °C, 30 min.

Boc substituted secondary amine **33** was prepared from the primary amine using Boc$_2$O in diethyl ether and was isolated in good yield (Scheme 4.14).
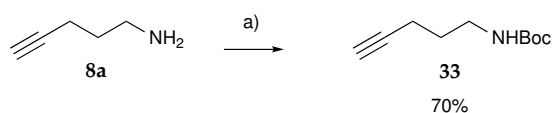
Scheme 4.14: Preparation *N*-Boc substituted pentynamine **33**. a) NEt$_3$ (1.5 equiv), Boc$_2$O (1.0 equiv), 0 °C, 16 h.

On the other hand, *N*-tosyl and *N*-trifluoroacetamide phenylethynylanilines were synthesised following a standard protection procedure.[120,163] Aniline **23b** was treated with pyridine and tosylchloride or trifluoroacetanhydride in

DCM giving the corresponding amide in very good yield after purification by column chromatography (Scheme 4.15).
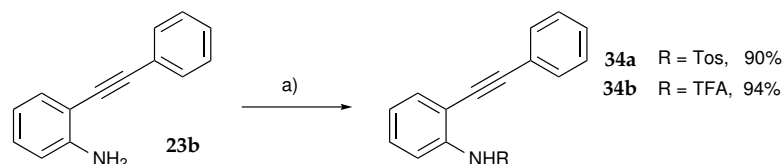
Scheme 4.15: Preparation of *N*-tosyl and *N*-trifluoroacetyl substituted phenylethynylanilines **34a,b**. a) Pyridine (2.0 equiv), tosylchloride or trifluoroacetanhydride (1.2 equiv), DCM, 0 °C, 16 h.

To explore further hydroamidation reactions with our catalytic system, *ortho*-ethynylbenzamide **36a** was prepared by a Sonogashira cross-coupling of 2-bromobenzamide **35a** and trimethylsilylacetylene followed by deprotection of the TMS group by KOH in methanol/water (Scheme 4.16). The obtained yield was higher than the reported one (65 % compared to 14 % overall yield[120]), which might be attributed to the use of degassed solvents in our laboratory. Additionally, *para*-substituted ethynyl benzamides were prepared following a similar procedure. However, for 4-bromobenzamides, it was crucial to use diethylamine as base/solvent as reactions in different solvent mixtures (*e.g.* NEt$_3$, toluene/NEt$_3$, or THF/NEt$_3$) did not yield any product.[164]
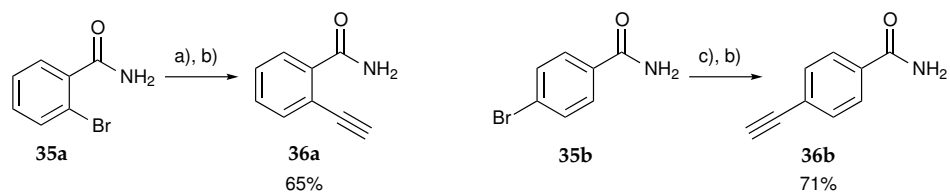
Scheme 4.16: Synthesis of 2- and 4-ethynyl benzamide **36** *via* Sonogashira coupling. a) Trimethylsilylacetylene (1.5 equiv), [PdCl$_2$(PPh$_3$)$_2$] (5 mol %), CuI (5 mol %), PPh$_3$ (20 mol %), NEt$_3$, 80 °C, 16 h; b) KOH (2.0 equiv), MeOH/H$_2$O, room temperature, 5 min; c) Trimethylsilylacetylene (3 equiv), [PdCl$_2$(PPh$_3$)$_2$] (4 mol %), CuI (8 mol %), NHEt$_2$, 80 °C, 16 h.

Several allenes were also prepared since they give rise to enamines, a highly versatile compound that can be used as reactant a variety of different reactions. Following a reported procedure propargylic alcohols were heated in triethyl orthoacetate with substoichiometric amounts of propionic acid to form allene esters **37a** and **41** *via* an *ortho*-Claisen rearrangement (Scheme 4.17).[165,166] For the synthesis of terminal allene **37a** it was crucial to remove ethanol formed during the reaction by distillation. In a first stage, **37a** and **41** were purified by column chromatography, but only 25% of the expected

mass was recovered for either of these esters. Due to the large mass loss during the purification step all intermediates were then used without purification. Allene esters were first reduced to the corresponding alcohols and then mesylated. The mesyl group was next displaced by NaCN, which was then reduced in a final step to obtain pure primary amines **40a** and **44**. Most of the obtained yields are comparable to the ones reported in the literature.[165,166]
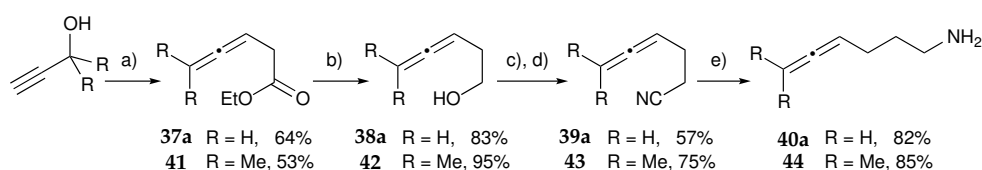
Scheme 4.17: Synthesis of allene amines **40a** and **44** an *ortho*-Claisen rearrangement. a) MeC(OEt)$_3$ (3.0 equiv), propionic acid (0.05 equiv), 130 °C, 4 h; b) LiAlH$_4$ (2.3 equiv), Et$_2$O, 0 °C, 1 h; c) MsCl (1.2 equiv), NEt$_3$ (1.0 equiv), Et$_2$O, room temperature, 30 min; d) NaCN (1.2 equiv), DMSO, 70 °C, 16 h; e) LiAlH$_4$ (2.0 equiv), Et$_2$O, 0 °C, 1 h.

For the preparation of the homologous amino allene **40b**, a reported Crabbé-type reaction was used (Scheme 4.18).[167] Propargyl phthalamide **7b** was heated with CuBr, paraformaldehyde and diisopropylamine in dioxane to form allene **45**, which was then deprotected using hydrazine in ethanol with a similar yield as the reported one.[167]
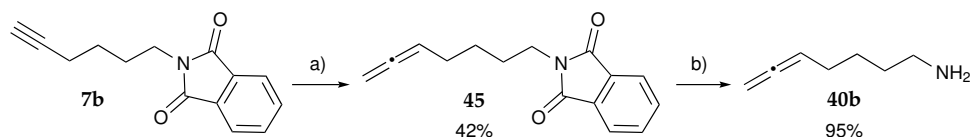
Scheme 4.18: Synthesis of hept-5,6-dieneamine **40b** *via* a Crabbé type reaction. a) (H$_2$CO)$_n$ (2.0 equiv), (*i*-Pr)$_2$NH (2.0 equiv), CuBr (0.35 equiv), 1,4-dioxane, 120 °C, 5 h; b) N$_2$H$_4 \cdot$ H$_2$O (2.0 equiv), EtOH, 70 °C, 2 h.

To study the less reactive 1,3-dienes that would eventually give rise to products containing allylamines, hepta-4,6-dienamine was prepared in a three-step synthesis (Scheme 4.19).[168,169] First, ester **46** was obtained from 1,4-penten-3-ol *via* an *ortho*-Claisen rearrangement using triethylorthoacetate with a yield of 72%.[168] In a second step, the ester group was reacted with [AlCl(Me)(NH$_2$)] in toluene to obtain 1,3-dieneamide **47** in excellent yield. This amide was consecutively reduced with LiAlH$_4$ to give (*E*)-hepta-4,6-dien-1-amine **48** in 35% yield, which is similar to the reported one.[169]

Alkenes were chosen as the final substrate class to be investigated. Since alkenes are challenging substrates for copper catalysts,[103] amino-diphenyl-
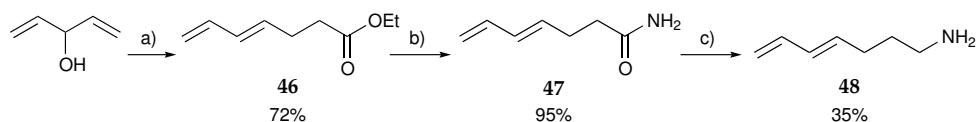
Scheme 4.19: Preparation of (*E*)-hepta-4,6-dien-1-amine **48**. a) MeC(OEt)$_3$ (6.0 equiv), propionic acid (0.05 equiv), 130 °C, 3 h; b) [AlCl(Me)(NH$_2$)] (3.0 equiv), toluene, 55 °C, 2 d; c) LiAlH$_4$ (1.4 equiv), THF, 0 °C, 4 h.

pentene **50** was chosen as first substrate. Due to their steric effect, the two phenyl rings force the alkyne and amine group in 1,3 position closer together and thus lowering the entropic penalty of the hydroamination reaction making it more likely to react. Following a reported literature procedure, diphenylacetonitrile was added to a cooled solution of lithium diisopropylamide followed by allylbromide.[170] After purification by column chromatography, nitrile **49** was reduced by LiAlH$_4$ to give amino-diphenylpentene **50** in good yield (Scheme 4.20).[170]
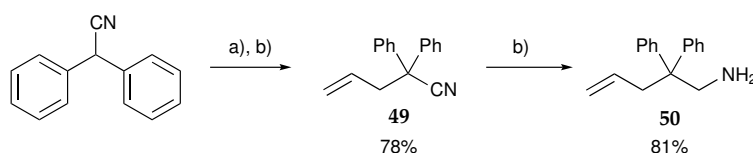
Scheme 4.20: Synthesis of amino-diphenylpentene **50**. a) (*i*-Pr)$_2$NH (1.07 equiv), *n*-BuLi (1.05 equiv), nitrile (1.0 equiv), allylbromide (1.0 equiv), THF, –78 °C, 3 h; b) Room temperature, 16 h; c) LiAlH$_4$ (3.9 equiv), Et$_2$O, room temperature, 16 h.

4.3 Optimisation Studies

The primary aims of this study was to develop a more sustainable method using copper(I) complexes in hydroamination reactions. In the previous Chapter, we showed the preparation of [Cu(DAB)] complexes, which are readily prepared in a two-step synthesis from commercially available materials and are genuinely easy to handle as they are not air or moisture sensitive.[47] As [Cu(DAB)] complexes were promising candidates, the initial optimisation studies started with [CuCl(DAB^{Anis})] and pent-4-ynamine **8a** as the model reaction. Different technical, deuterated solvents were first tested at 80 °C with a substrate concentration of 0.44 M. This concentration is significantly higher than to other reported copper(I)-catalysed hydroamination reactions.[171] However, concentrations between 0.1 and 1.0 M have been reported for other transition metals.[172,173] After 2 h, a conversion of around 50 % was measured both in chloroform-d1 and benzene-d6 (Table 4.1, entries 1 and 2). The conversion observed in toluene-d8 was lower than in benzene, which was somewhat surprising (37 %, Table 4.1, entry 3). Overall, the best

reactivity was observed in acetonitrile-d3 (Table 4.1, entry 4). Background reactions were also carried out in the absence of copper at 80 °C over 16 h and no conversion was observed in any solvent (Table 4.1). Additionally, no oligomerisation or other by-products were evident by ^{1}H NMR spectroscopy.

Table 4.1: Solvent screening for the intramolecular hydroamination of **8a**.

entry	solvent	conv. (%)[a]
1	CDCl$_3$	48
2	C$_6$D$_6$	50
3	toluene-d8	37
4	CD$_3$CN	64
5	acetone-d6	19[b]

[a] ^{1}H NMR conversions were calculated with respect to 1,3,5-trimethoxybenzene as an internal standard.
[b] Partially deuterated pyrroline **52** was observed as only product.

Among all the tested solvents, acetone-d6 led to the lowest conversion and partially deuterated pyrroline-d5 **52** was observed instead of pyrroline **51a**. The partial deuteration of cyclic imines is well known and had been reported with hexynylamine **8b** and a variety of late transition metal catalysts.[161] This reaction outcome had been rationalised by a proton induced equilibrium of the pyrroline in protic solvents (Scheme 4.21). The equilibrium consists of the *endo*-enamine, the *exo*-enamine, and the imine. Due to the large excess of deuterons, the original protons are replaced and the partially deuterated pyrroline forms. It is believed that the metal allows for a faster exchange of protons as partial deuteration had been observed in absence of metal as well but at a slower rate.[161]
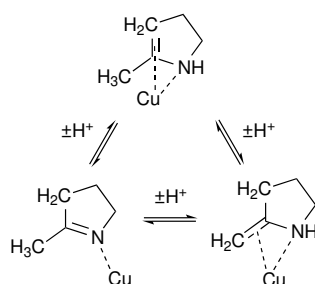
Scheme 4.21: Proton induced equilibrium for pyrrolines.

93

Next, a differentiation between homoleptic and heteroleptic [Cu(DAB)] complexes was sought after. Indeed, a significantly higher conversion was observed with homoleptic [Cu(DAB^{Anis})$_2$](BF$_4$) compared to heteroleptic [CuCl(DAB^{Anis})] (Table 4.2, entries 1 and 3).

Table 4.2: Hydroamination catalyst screening in CD$_3$CN.
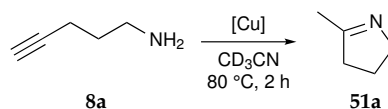
entry	catalyst	[Cu] (mol %)	conv. (%)^a
1	[CuCl(DAB^{Anis})]	2.0	64
2	CuCl	2.0	74^b
3	[Cu(DAB^{Anis})$_2$](BF$_4$)	2.0	>95
4	[Cu(DAB^{Anis})$_2$](BF$_4$)	0.5	65
5	[Cu(NCMe)$_4$](BF$_4$)	0.5	70

^{a} ^{1}H NMR conversions were calculated with respect to 1,3,5-trimethoxybenzene as an internal standard.

^{b} >95% conversion was observed after 10 h.
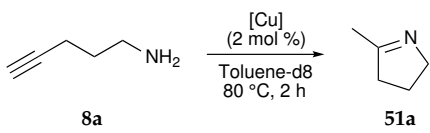
Significantly, the black colour of the solution changed to a light green upon addition of the substrate to either the homoleptic or heteroleptic complex. This colour change might imply a displacement of the DAB ligand and its subsequent decomposition to glyoxal and aniline. This hypothesis was substantiated by the recorded ^{1}H spectrum, which showed no signals for either coordinated or free DAB^{Anis} between 8.4 and 9.0 ppm but signals corresponding to *p*-anisidine, the ligand precursor instead. Therefore, control experiments were carried out with the corresponding copper(I) salts, CuCl and [Cu(NCMe)$_4$](BF$_4$). These showed a similar or slightly better reactivity than their corresponding DAB^{Anis} complexes (Table 4.2, entries 2 and 5).

Further experiments were then carried out in toluene-d8 to study whether the issue with ligand displacement encountered in acetonitrile-d3 would persist in a non-coordinative solvent. Indeed, again both copper salts showed comparable activity to their corresponding [Cu(DAB^{Anis})] complexes (Table 4.3). Additionally, the model reaction was performed in the presence of HBF$_4$ and no conversion into pyrroline was observed, ruling out a possible Brønsted acid-catalysed reaction (Table 4.3, entry 5).[103]

Due to the increased solubility of [Cu(NCMe)$_4$](BF$_4$) in H$_2$O and methanol compared to [Cu(DAB)] complexes, these two solvents were studied as well. Conversions of 70% for methanol and 86% for deuterium oxide were observed (Scheme 4.22). However, no pyrroline **51a** was observed but deuter-

Table 4.3: Hydroamination catalyst screening in toluene-d8.

entry	catalyst	conv. (%)[a]
1	[CuCl(DAB^{Anis})]	37
2	CuCl	32
3	[Cu(DAB^{Anis})$_2$](BF$_4$)	92
4	[Cu(NCMe)$_4$](BF$_4$)	86
5	HBF$_4$	0

[a] ^{1}H NMR conversions were calculated with respect to 1,3,5-trimethoxybenzene as an internal standard.

ated pyrroline-d5 **52** instead. Additionally, background reactions were carried out in both solvents and for deuterium oxide a conversion of 17% into deuterated pyrroline **52** was observed. In methanol-d4 no formation of pyrroline or partially deuterated pyrroline was evidenced by ^{1}H and ^{2}H NMR. However, deuteration at the acetylenic position of the starting material was observed (17%).
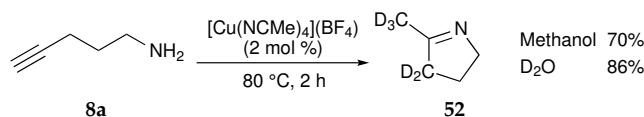
Scheme 4.22: Partially deuterated pyrroline in deuteric solvents.

Overall, these optimisation studies provided a catalytic system for the hydroamination reaction with a readily prepared and commercially available copper(I) catalyst, a relatively green solvent, a reasonable temperature of 80 °C, and a fast reaction time of 2 h for pentynamine **8a**.

4.4 Substrate Scope of [Cu(NCMe)$_4$](BF$_4$)-Catalysed Hydroamination Reactions

Building on the promising results obtained for **8a**, several substrates were tested with [Cu(NCMe)$_4$](BF$_4$). All reactions were run in air and in technical acetonitrile with a concentration of 0.44 м. Temperature was set at 80 °C and the catalyst loadings varied between 2–20 mol % with reaction times between

2–16 h. NMR scale reactions were run with 0.22 mmol of substrate, whereas for isolation purposes, the scale was increased to 2.2 mmol. The isolation of the hydroamination products was generally challenging, especially with molecules with low molecular weight as separation from the solvent was difficult due to their high volatility. Furthermore, lower yields were sometimes obtained due to the high solubility in water of certain products. On the other hand, purification by column chromatography was often difficult as the reaction products tended to adhere strongly to silica and even to basic aluminium oxide. Unfortunately, no generally applicable isolation and purification method could be produced. Nonetheless, a work-up with aqueous, saturated Na_4EDTA generally improved the isolated yield, especially for products with higher molecular weight.

4.4.1 Alkyne Substrates

Alkyne substrates homologous to **8a** are depicted in Table 4.4. Terminal alkynes reacted within 2–3 h while phenyl and trimethylsilyl ones required longer reaction times. Methyl substituted alkynes also required significantly increased catalyst loadings (5–20 mol %). In general, pyrrolines were formed more readily than tetrahydropyridines (THPs) while all attempts to prepare tetrahydroazepines were unsuccessful, even with increased catalyst loadings and reaction times. Due to their volatility, pyrrolines **51a** and **54a** were isolated after methylation with methyl iodide (Table 4.4, entries 1 and 4). In these reactions, separation of the remaining starting amines was not possible by column chromatography, and therefore it was necessary that the starting material was fully converted before treating the reaction mixture with methyl iodide. The hydroamination of **51a** was also performed on a larger scale of 18 mmol with an excellent isolated yield (3.68 g, 91%, Table 4.4, entry 1). Indeed, the isolated yield of **51a** did not change significantly when run on a 2.2 mmol scale (89%). THP **51b** and **54b** were isolated in moderate to good yields after column chromatography (Table 4.4, entries 2 and 5). Silica was used as stationary phase with a mixture of EtOAc, MeOH, and saturated aqueous NH_4OH as mobile phase. TMS-substituted pyrrolines **56a,b** were formed in good conversions of 83 and 75% with increased catalyst loadings (3 and 10 mol %) after 16 h (Table 4.4, entries 6 and 7). Purification by column chromatography was attempted although no product could be isolated and the crude mass was not recovered even after washing the column multiple times. This might have been due to the presence of NH_4OH in the mobile phase that led to the removal of the TMS group and the formation of pyrrolines **51a** and **51b** of which trace amounts were obtained. This is in agreement with previous purification attempts on **51a,b**, where it was observed that these pyrrolines adhered strongly to the stationary phase and were difficult to remove from the silica. Nonetheless, formation of TMS-methylpyrroline **56a** (Table 4.4, entry 7) could be confirmed by

Table 4.4: Substrate scope of primary alkynyl amines for intramolecular hydroamination with [Cu(NCMe)$_4$](BF$_4$).
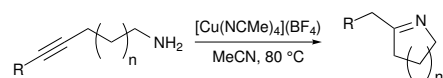
entry	substrate	product	[Cu] (mol %)	time (h)	conv.[a] (%)	yield (%)
1	**8a**	**51a** **53a**	2	2	>95	91
2	**8b**	**51b**	2	4	>95	83
3	**8c**	**51c**	10	16	0	–
4	**15a**	**54a** **55a**	5	16	69	65
5	**15b**	**54b**	20	16	75	41
7	**18a**	**56a**	3	16	83	–
8	**18b**	**56b**	10	16	75	–
9	**21a**	**57a**	2	16	82	68
10	**21b**	**57b**	5	16	79	73

[a] ^{1}H NMR conversions were calculated with respect to 1,3,5-trimethoxybenzene as an internal standard.

mass spectrometry. Benzyl substituted pyrrolines **57a** and **57b** led to high conversions of 84 and 79% with low catalyst loadings between 2 and 5 mol % and were isolated in good yields of 68 and 73% (Table 4.4, entries 9 and 10).

The only side-products were observed for **15a** and **21a** and along hydroamination products **15a** and **57a** 23 and 16% of oxidised acetyl- and benzoyl-pyrroline **58** and **59** were observed (Scheme 4.23). On the other hand, formation of benzoyl tetrahydropyridine from phenylhexynamine **21b** was observed only in trace amounts (<5%).
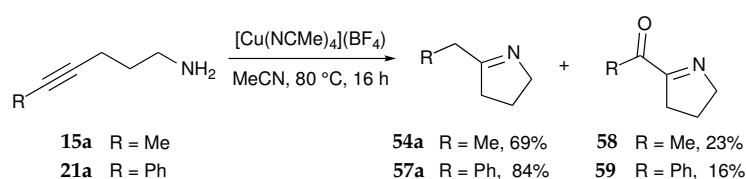
Scheme 4.23: Product distribution observed in the intramolecular hydroamination of methyl- and phenyl-substituted pentynamines **15a** and **21a**.

To determine whether water was involved in the formation of these oxidation products, one equivalent of water was added to the hydroamination reaction. However, a similar conversion of 11% into benzoyl pyrroline **59** was obtained under these conditions. When the reaction was performed under anhydrous conditions (solvent and substrate were dried prior use over CaH$_2$), only 4% of benzoylpyrroline was formed. No benzoylpyrroline was observed at all if the reaction was run under exclusion of O$_2$ and anhydrous conditions. Nevertheless, it was observed that after isolation benzylpyrroline **21a** converted into benzoylpyrroline **59** when stored neat at room temperature (30 % within two days). A similar observation was reported by Xu *et al.* where during an alcohol protection reaction with NH(TMS)$_2$ in air, the benzylic carbon on (4-aminophenyl)methylpyrroline **60** was oxidised to (4-aminophenyl)methanonpyrroline **61** (Scheme 4.24).[174] However, no yield, reaction conditions, or explanation were provided for this outcome and to the best of our knowledge, there are no other reports in literature on this type of oxidation.
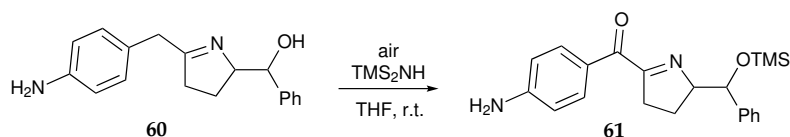
Scheme 4.24: Precedent for the oxidation of benzyl pyrrolines.

Next, *ortho*-ethynyl substituted anilines were screened in the hydroamination reaction with [Cu(NCMe)$_4$](BF$_4$). Under our optimised conditions, the conversion of ethynyl substituted anilines **23a** never exceeded the mole percentage of catalyst, indicating a turn-over number of 1 (Table 4.5, entry 1). Phenylethynyl **23b** showed with one and two equivalents of [Cu(NCMe)$_4$] (BF$_4$) only conversions of 27 and 47% after 16 h (Table 4.5, entry 2). Using one equivalent of [Cu(NCMe)$_4$](BF$_4$) in DMF increased the conversion to 100% and further allowed to reduce the reaction time to 2 from 16 h at an increased temperature of 100 °C. Phenylindole **62a** was then isolated pure without further purification required after work-up. These reaction conditions were originally reported for CuI.[175] However, the reaction with substoichiometric amounts of [Cu(NCMe)$_4$](BF$_4$) did not lead to full conversion of the starting material.

Table 4.5: Ethynyl anilines and benzylamines substrate screening.

entry	substrate	product	[Cu] (mol %)	time (h)	conv. (%)	yield (%)
1	**23a**	**62b**	10	16	10	-
2	**23b**		200	16	47	-
3[b]		**62a**	100	2	>95	99
4	**26a**	**63a**	10	16	0	-
5	**26b**	**63b**	20	16	5	-
6	**26c**	**63c**	5	16	51	49

[a] ^{1}H NMR conversions were calculated with respect to 1,3,5-trimethoxybenzene as an internal standard.
[b] Reaction carried out in DMF at 100 °C.

Reaction of **26a** only led to the formation of decomposition products. This is in agreement with a previous report on the hydroamination of this substrate in the presence of ruthenium.[120] Phenylethynyl benzylamine **26b** also decomposed over the course of the reaction and 3-phenyldihydroisoquinoline was not observed at all (Table 4.5, entry 4). To prevent decomposition, lower reaction temperatures were studied with **26b**. However, no reaction of the benzylamine was observed at room temperature and at already 40 °C decomposition was observed again.

On the other hand, while *n*-butylethynyl benzylamine **26c** led to less decomposition, no dihydroisoquinoline product was identified by ^{1}H NMR either. Instead, its oxidised homologue 3-butyl isoquinoline **63c** was observed with a conversion of 51% (Table 4.5, entry 5). In addition to the signals of isoquinoline **63c** (7.5–9.2 ppm) other signals were observed, notably multiplets at 6.84 and 6.71 ppm. After work-up with a saturated aqueous Na_4EDTA solution, all other signals disappeared with only isoquinoline **63c** remaining, which was then isolated by column chromatography in 49% yield (Table 4.5 entry 5). The residue on the column was washed down and constituted of unknown decomposition products.

The reaction temperature was then lowered in an attempt to avoid undesired decomposition. **26c** was stirred at room temperature for 4 h, during which a colour change from colourless to dark red was observed. However, the ^{1}H NMR looked similar to the starting material, with the exception that the two doublets and the triplet between 7.4 and 7.3 ppm merged into two triplets. Additionally, the signal for the hydrogen atoms vicinal to the amine group at 4.0 ppm broadened (Figure 4.2; 4 h; r.t.), possibly due the coordination of the substrate to the copper centre. After heating at 40 °C for 4 h, numerous new signals appeared that were present in the previous reaction (Figure 4.2;
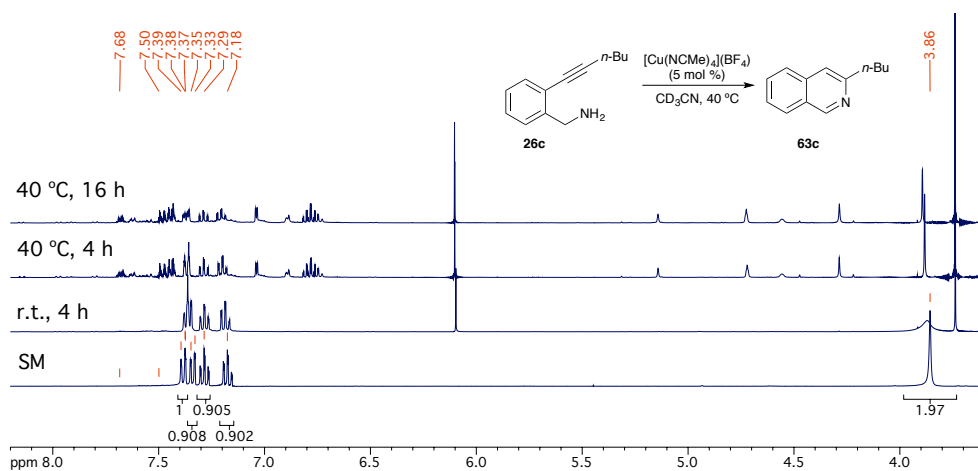
Figure 4.2: Reaction of hexynylbenzylamine **26** and [Cu(NCMe)$_4$](BF$_4$) in CD$_3$CN.

40 °C, 4 h) but no isoquinoline **63c** and no starting material were observed. The ^{1}H NMR spectrum did not change significantly after heating the sample for 12 more hours (Figure 4.2; 40 °C, 12 h).

In an attempt to isolate any newly formed compound, the solvent was removed *in vacuo* and the residue was directly purified without the usual work-up with aqueous, saturated Na$_4$EDTA, since in the original preparation of isoquinoline **63c** similar signals were observed but disappeared after such treatment. After purification by column chromatography, the mass of all collected fractions accounted for only a tenth of the initial crude weight and their ^{1}H NMR spectra did not allow an identification as they showed signs of both polymerisation and decomposition that had been observed before.

Secondary, linear alkynyl amines, amides, and carbamates were also investigated, however, no reaction was observed with any of them in the presence of [Cu(NCMe)$_4$](BF$_4$) or [CuCl(DAB^{Anis})] (Scheme 4.25). [Cu(DAB)] complexes were tested here again, since no decomposition of the complexes was observed in the presence of secondary amines. However, in all cases no reaction was observed for tosyl- or acetyl-amides or carbamates in the presence of any of the copper complexes and the starting material was recovered. For butyl, phenyl, and *t*-butyl substituted substrates **29a,b**, **30** and **32** decomposition was observed giving rise to a multitude of unidentified signals in the ^{1}H NMR spectra.

SM recovered			decomposition		
R^1	R^2		R^1	R^2	
H	Tos	**27a**	H	Bn	**29a**
Ph	Tos	**27b**	Ph	Bn	**29b**
H	Ac	**28a**	H	*t*-Bu	**30**
Ph	Ac	**28b**	H	*n*-Bu	**32**
H	Boc	**33**			

[Cu] = [Cu(NCMe)$_4$](BF$_4$) or [CuCl(DAB^{Anis})]
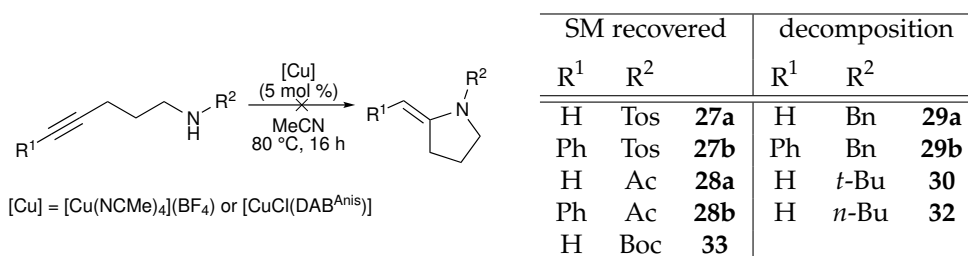
Scheme 4.25: Attempted hydroamination and hydroamidation of secondary amines and amides **27a,b**, **28a,b**, **29a,b**, **30**, **32** and **33**.

On the other hand, it had been showed in the literature that the hydroamidation of *N*-tosyl phenylethynylaniline **34a** could be performed using 5 mol % CuI, 10 mol % tetrabuthylammonium bromide (TBAB) and polystyrene-supported pyrrole-2-carbohydrazide (PSP) as catalyst support in H$_2$O at 80 °C in 99% yield (Scheme 4.26).[176]

This reaction was repeated under the same conditions but without PSP and [Cu(NCMe)$_4$](BF$_4$) instead of CuI and the same high isolated yield of 99% was obtained. Full conversion into indole **64** was actually observed after only 5 min. Since such a rapid conversion was observed, the reaction was attempted at 40 °C, however the obtained conversions were not reproducible
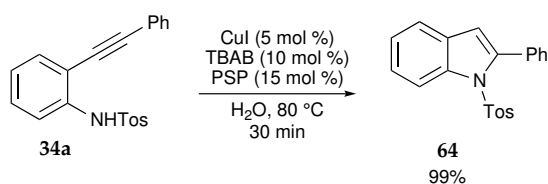
Scheme 4.26: Reported intramolecular hydroamination of *N*-tosyl-2-(2-phenylethynyl)aniline **34a**.

(Table 4.6). Reactions for 1 and 2 h (Table 4.6, entry 1) were run three times and high standard deviations of 22 and 18% were obtained. At a higher temperature (60 °C) the conversion after 2 h was lower than after 1 h, which might imply a solubility issue with the substrate at lower temperatures (Table 4.6, entry 2). On the other hand, reactions at room temperature did not reach full conversion even after 40 h (Table 4.6, entry 3). Taking these results into account, a reaction temperature of 80 °C offered the best conversion and reproducibility.

Table 4.6: Investigation of the reaction of *N*-tosyl-2-(2-phenylethynyl)aniline **34a**.
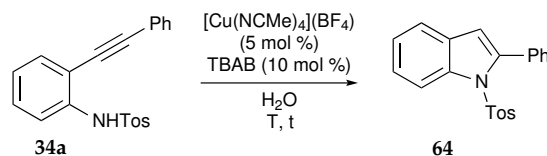
entry	temperature	conv. (%)[a] 0.5 h	conv. (%)[a] 1 h	conv. (%)[a] 2 h	conv. (%)[a] 16 h
1	40 °C	38	$77 \pm 22\%$	80 ± 18	-
2	60 °C	-	64	47	-
3	r.t.	-	-	-	51

[a] ^{1}H NMR conversions were calculated with respect to 1,3,5-trimethoxybenzene as an internal standard.

In a next step, it was investigated whether the combination of TBAB and water could be replaced by an organic, water miscible solvent (MeCN, MeOH, or acetone). The reaction was therefore repeated without TBAB and with 1:1 and 1:9 solvent mixtures of water and different organic solvents. However, no conversion was observed after 0.5 h for any of the solvent mixtures (Table 4.7, entries 1–3). After prolonged reaction times conversions of 41 and 69% were observed in a 1:1 water/MeCN mixture after 16 and 40 h. However, these results are not competitive with the reaction in presence of TBAB (5 and 30 min instead). In a final step it was investigated whether the bromide in TBAB had any substantial role and the reaction was run in

Table 4.7: Solvent screening for the reaction of *N*-tosyl-2-(2-phenylethynyl)aniline **34a**.

entry	solvent	conv. (%, 0.5 h)[a]		conv. (%, 16 h)[a]	conv. (%, 40 h)[a]
		1:1	1:9	1:1	1:1
1	MeCN/H$_2$O	0	0	41	69
2	MeOH/H$_2$O	0	0	-	-
3	Acetone/H$_2$O	0	0	-	-
4[b]	MeCN/H$_2$O	0	0	-	-
5[b]	H$_2$O	0	-	0	-
6	MeCN	0	-	0	-

[a] ^{1}H NMR conversions were calculated with respect to 1,3,5-trimethoxybenzene as an internal standard.
[b] 10 mol % NaBr was used.

the presence of NaBr instead of TBAB but again, no reaction was observed leaving the role of TBAB undisputed in this reaction (Table 4.7, entries 4 and 5).

The optimised reaction conditions were then applied to *N*-tosylated pentynyl substrates **27a** and **27b** as these did not display any reactivity with [Cu(NCMe)$_4$](BF$_4$) in acetonitrile (Scheme 4.27). However, no reaction was observed for these substrates in the presence of TBAB in H$_2$O either.
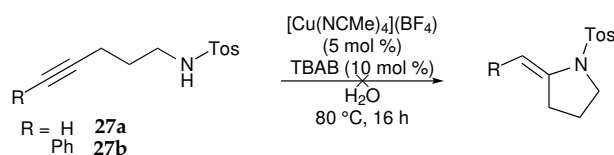
Scheme 4.27: Attempted intramolecular hydroamination of tosyl substituted pentynyl amines **27a,b**.

On the other hand, the hydroamidation of phenylethynyl trifluoroacetanilide **34b** to indole **62b** had been reported in the presence of 10 mol % [Cu(phen)(PPh$_3$)$_2$]NO$_3$ and K$_3$PO$_4$ in toluene at 110 °C (Scheme 4.28).[163] The trifluoroacetamide group is known to be readily removed under mild conditions using K$_2$CO$_3$ in MeOH and H$_2$O.[177] It is therefore not surprising that the TFA group was cleaved in this reaction. However, since the reaction of ethynylaniline **23b** required stoichiometric amounts of copper, it can be as-

sumed that the cleavage of the TFA group might occur after the cyclisation.
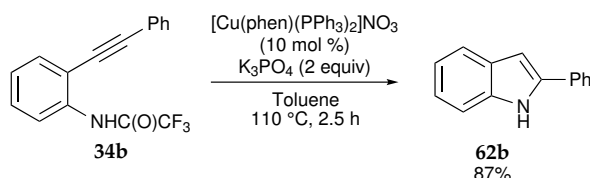
Scheme 4.28: Reported intramolecular hydroamidation of trifluoroacetamide **34b**.

This reaction was repeated with $[Cu(NCMe)_4](BF_4)$ as catalyst and a ^1H NMR yield of 64% was obtained under otherwise identical conditions (Table 4.8, entry 1). Gratifyingly, changing the solvent from toluene to acetonitrile while lowering the catalyst loading to 5 mol % afforded an isolated yield of 99% (Table 4.8, entry 2). Control reactions without base or $[Cu(NCMe)_4](BF_4)$ showed no conversion of the starting material (Table 4.8, entries 3 and 4), whereas stoichiometric and substoichiometric amounts of base (10 mol %) led to reduced conversions of 27 and 48%, respectively (Table 4.8, entries 5 and 6).

Table 4.8: Investigation of 2-(2-phenylethynyl)phenyl trifluoroacetamide **34b** in the intramolecular hydroamidation.
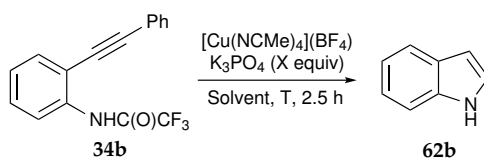
entry	[Cu] (mol %)	solvent	T (°C)	equiv base	conv. (%)[a]
1	10	Toluene	110	2.0	64
2	5	MeCN	80	2.0	99[b]
3	5	MeCN	80	-	0
4	0	MeCN	80	2.0	0
5	5	MeCN	80	0.1	27
6	5	MeCN	80	1.0	48

[a] ^1H NMR conversions were calculated with respect to 1,3,5-trimethoxybenzene as an internal standard.
[b] Isolated yield.

An unexpected observation was made for ethynyl benzamide **36a**. Instead of the desired hydroamidation product,[120] a dehydration of the amide and concomitant hydration of the alkyne group to 2-acetylbenzonitrile **65** was

observed with >95% conversion (Scheme 4.29). The reaction is likely to undergo a copper(I)-catalysed intramolecular hydrogen and oxygen shift between the amide and the ethynyl group. This might be supported by the fact that no such reaction was observed for 4-ethynylbenzamide or between benzamide and phenylethynyl. To the best of our knowledge, there is not any precedent for this in literature.

>95% conv, 41% yield
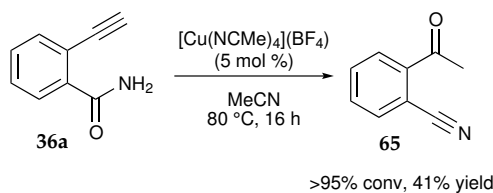
Scheme 4.29: Intramolecular dehydration/hydration tandem reaction of 2-ethynylbenzamide **36a**.

To show the orthogonality of our developed catalytic system, competition reactions between primary amines and secondary amines or alcohols[178] were investigated next (Scheme 4.30). Under optimised reaction conditions, primary amine **8a** was completely converted after 2 h, whereas secondary amine **33** did not react. The reaction was repeated with pentynol **9** and while full conversion of the pentynamine **8a** was again observed with no traces of the hydroalkoxylation product.
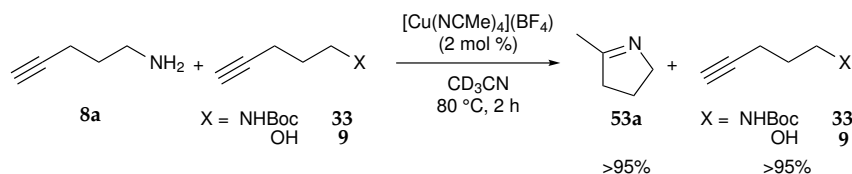
Scheme 4.30: Competition reactions.

We also investigated our catalytic system in the intermolecular hydroamination reaction of secondary amines and alkynes. The addition of morpholine to phenylacetylene in the presence of CuCl in *N*-methyl-2-pyrrolidone (NMP) was reported to give a variety of different hydroamination products.[179] This reaction was then studied with 10 mol % [Cu(NCMe)$_4$](BF$_4$) in MeCN. As reported, four different products were observed in the crude ^{1}H NMR spectrum (Scheme 4.31). This reactivity is particularly interesting, since no reactivity had been observed in the intramolecular hydroamination of alkynes with secondary amines (Scheme 4.25). The major product was acetophenone **67** along Markovnikov and anti-Markovnikov hydroamination products **66** and **68** and dieneamine **69** (Scheme 4.31).
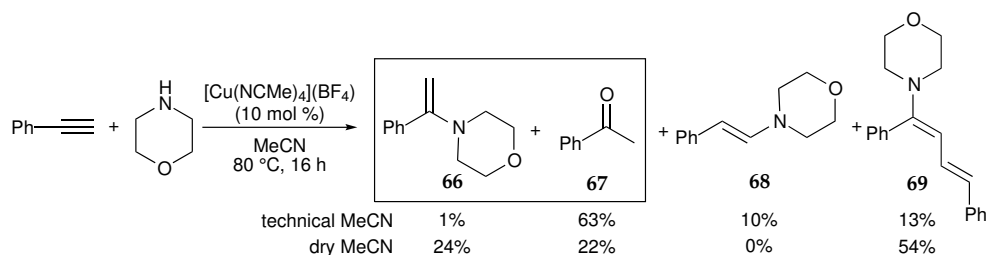
Scheme 4.31: Intermolecular hydroamination of phenylacetylene and morpholine using [Cu(NCMe)$_4$](BF$_4$).

The formation of acetophenone originated in the hydrolysis of the Markovnikov product **66** as no acetophenone formation due to the hydration of ethynylbenzene was observed in the absence of morpholine. The experiment was repeated in dry acetonitrile to avoid hydrolysis of **66**. Phenylacetylene was consumed fully, no anti-Markovnikov product **68** was formed and the amount of dieneamine **69** increased to 54%. Also, the total amount of products due to a Markovnikov-hydroamination dropped from 64 to 46%. However, the observed hydrolysis of the Markovnikov product **66** indicated that the reaction was not completely moisture free and might have been introduced by the undried morpholine and phenylacetylene. Overall, our results are similar from the reported, optimised reaction conditions where under strict anhydrous and oxygen-free conditions dieneamine **69** was the major product with 75% conversion and Markovnikov products added up to 21%. However, if moisture free conditions are applied to our catalytic system a similar good performance might be achieved with a much more benign solvent at lower temperatures compared to the reported conditions.

Similarly, the reaction of phenyl acetylene and *p*-toluidine with 10 mol % [Cu(NCMe)$_4$](BF$_4$) at 80 °C showed formation of three products after 16 h (Scheme 4.32). The major product was the Markovnikov product **70**, together with small amounts of its hydrolysis product acetophenone **67**.
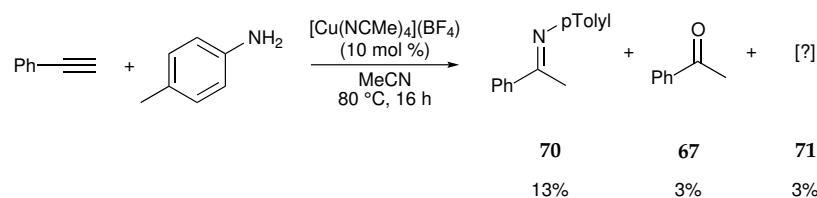
Scheme 4.32: Intermolecular hydroamination of phenylacetylene and *p*-toluidine.

A third, unknown product **71** was isolated by column chromatography (silica, EtOAc:PE = 20:1) and characterised by NMR, IR, and mass spectrometry. However, the identification of the unknown product was not possible. From

the recorded NMRs it can be concluded, that the molecule contains a CH$_3$ group (2.42 ppm), an aromatic AB system, and an internal carbon carbon triple bond (81.7 and 74.1 ppm).[180]

Ethynylbenzene was replaced by 2-ethynylpyridine in the hope of an increased reactivity, due to the ability of the pyridine to coordinate to the copper(I) centre and thus increasing the probability of interaction of the triple bond with the copper centre. The reaction was performed with *p*-toluidine and 10 mol % of [Cu(NCMe)$_4$](BF$_4$) in MeCN. However, after the work-up only the starting materials and small, very broad signals that could not be assigned were observed by ^{1}H NMR (Figure 4.3).
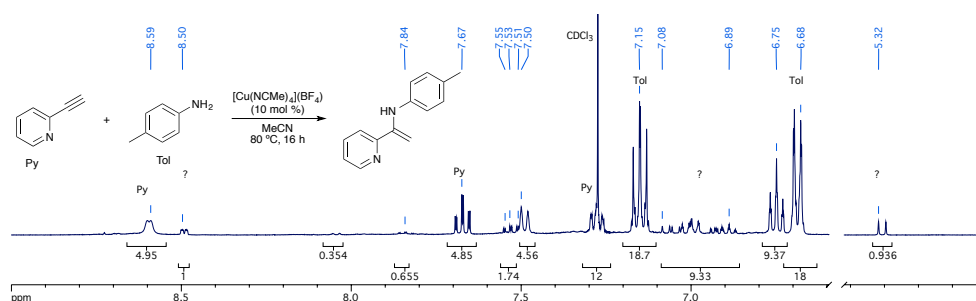
Figure 4.3: ^{1}H NMR spectrum for the reaction of ethynylpyridine and aniline in chloroform-d1 after work-up.

Furthermore, following reported results the intramolecular hydroamination of pentynyl benzylamine **29b** followed by an addition of phenylacetylene to the imine bond was performed (Scheme 4.33). The reaction was carried out with 5 mol % [Cu(NCMe)$_4$](BF$_4$) in acetonitrile at 80 °C and after 16 h a 78% conversion of pentynyl benzylamine was observed, which is substantially lower than to the reported yield of 99% with 5 mol % CuBr in dioxane at 100 °C over the course of 12 h.[181] Nonetheless, our simple catalytic system showed under technical and more benign conditions a comparable performance to literature.
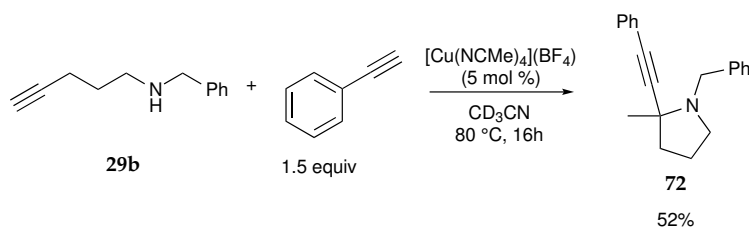
Scheme 4.33: Intramolecular hydroamination reaction of phenylacetylene and benzylpentynylamine **29b**.

4.4.2 Diene Substrates

Next, our focus moved to allenes and gratifyingly, they showed good reactivity, even if vinyl pyrrolidines were formed more readily than vinyl piperidines and, as expected, internal allenes showed a lower reactivity than terminal ones (Table 4.9). Of note, in all reactions using allenes a copper mir-

Table 4.9: Substrate screening of allenes **40a,b** and **44** for the intramolecular hydroamination reaction.

entry	substrate	product	loading (mol %)	time (h)	conv.[a]
1	**40a**	**73a**	5	16	>95
2	**40b**	**73b**	5	16	45
3	**44**	**74**	10	16	62

[a] ^{1}H NMR conversions were calculated with respect to 1,3,5-trimethoxybenzene as an internal standard.

ror formed on the wall of the vials, which has not been observed with other substrates. Vinylpyrrolidine **73a** was obtained in quantitative NMR yield. Due to its volatility it was attempted to isolated **73a** directly from the reaction solution as hydrochloric salt as reported.[182] However, after addition of HCl to the reaction solution the ^{1}H spectrum showed a plethora of signals not corresponding to the desired product. The conversion into vinylpiperidine **73b** could not be raised higher than 45 % (Table 4.9, entry 2) even with catalytic loadings up to 20 mol %.

Due to the partial conversion, **73b** could not be isolated as its hydrochloric salt and the separation from unreacted **40b** failed due to the volatility and basicity of both compounds. On the other hand, the conversion of internal allene **44** never exceeded 62% even with catalyst loadings above 10 mol % (Table 4.9, entry 3). Purification by column chromatography was attempted as the product was not expected to be as volatile as vinyl pyrroline **73a**. Yet, none of the ^{1}H NMR spectra obtained from the fractions corresponded

to either starting material **44**, pyrrolidine **74**, or any other signals observed before in the crude. The only reported purification for **44** was achieved by distillation though no further details were disclosed.[183]

Finally, a 1,3-diene, heptadienamine **48**, was studied. Unfortunately, even with 20 mol % of [Cu(NCMe)$_4$](BF$_4$) and a prolonged reaction time of 16 h no conversion was observed by ^{1}H NMR (Scheme 4.34).
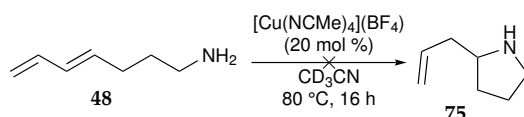
Scheme 4.34: Attempted intramolecular hydroamination of heptadienamine **48**.

4.4.3 Alkene Substrates

Even though no reactivity was observed for 1,3-diene **48**, the intramolecular hydroamination of alkenes was investigated with diphenylpentenamine **50**, due to its Thorpe-Ingold effect. However, no reaction was observed for **50** even with high catalyst loading and thus no other unactivated alkene substrates were tested (Scheme 4.35).
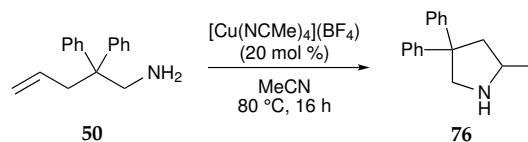
Scheme 4.35: Attempted intramolecular hydroamination of alkene **50**.

Finally, [Cu(NCMe)$_4$](BF$_4$) was tested as catalyst in the addition of different Michael acceptors with morpholine (Table 4.10). Since significant background reactions were expected,[184,185] the temperature was not raised above room temperature. First acrylonitrile was investigated and a conversion of 66 % was reached after 2 and full conversion after 3 h (Table 4.10, entry 1). The reaction of methyl vinyl ketone showed full conversion within 3 h (Table 4.10, entry 2) whereas geminal methyl substitution significantly reduced the reactivity and even after 16 h only a conversion of 72 % was observed by ^{1}H NMR (Table 4.10, entry 3). Contrarily, a *cis*-disubstitution was well tolerated and excellent conversion was achieved after 16 h (Table 4.10, entry 4). Methyl acrylate led to a lower conversion of 51 % after 3 and 91 % after 16 h. This result might be explained by the lesser electron withdrawing ability of the ester group. The use of acrolein in this context led to its polymerisation in the reaction mixture (Table 4.10, entry 6).

Table 4.10: Screening of different Michael acceptor and morpholine with [Cu(NCMe)$_4$](BF$_4$).

entry	R^1	R^2	R^3	conv. (%)^a 3 h	conv. (%)^a 16 h
1	CN	H	H	>95	–
2	C(O)CH$_3$	H	H	>95^b	–
3	C(O)CH$_3$	CH$_3$	H	16	72
4	C(O)CH$_3$	H	CH$_3$	85	93
5	C(O)OCH$_3$	H	H	51	91
6	C(O)H	H	H	–^{c}	–^{c}

^{a} ^{1}H NMR conversions were calculated with respect to 1,3,5-trimethoxybenzene as an internal standard.
^{b} Full conversion observed after 1 h.
^{c} Polymerisation of substrate.

4.5 Acetylenic Deuteration by [Cu(DAB)]

As previously mentioned in the Section 4.3, partially deuterated pyrroline **52** was observed in the ^{1}H NMR spectrum in the reaction of pentynamine **8a** and [CuCl(DAB^{Anis})] in acetone-d6 (Scheme 4.36).
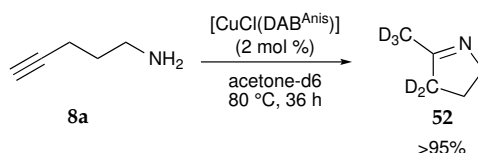
Scheme 4.36: Formation of pyrroline-d5.

The reaction was monitored every two hours for 8 h by ^{1}H NMR (Figure 4.4). Right after the addition of amine **51a** the acetylenic signal at 2.31 ppm decreased by about 50% and within the first two hours this signal disappeared completely. Furthermore, the coupling pattern on the propargylic hydrogen changed as the coupling with the acetylenic hydrogen disappeared. All other signals remained unchanged. After four hours a triplet at 3.67 ppm was observed, which steadily increased over the course of the reaction and after 36 h only triplets at 3.67 and 1.79 ppm with a ratio of 1:1 remained. Additionally, after 36 h the mass spectrum showed no $^m/z$ signals for the starting amine **8a** or pyrroline **51a** ($^m/z$ = 84) and no signals were observed

Figure 4.4: ^{1}H NMR spectra for the reaction of pent-4-yneamine **8a** in acetone-d6.

for a possible Glaser coupling between two alkyne molecules, which could have been a possible since the reaction was run in air.[186]

However, signals with $^m/_z$ ratios of 87, 88, and 89 were observed pointing towards partial deuteration of the pyrroline product. Indeed, the ^{13}C NMR spectrum after 36 h revealed five signals that matched pyrroline **51a** and the ^{2}H NMR spectrum displayed two signals with a ratio of two to three at 2.37 and 1.93 ppm, which were attributed to the methyl and methylene hydrogens on pyrroline **52**.

Additionally, no deuteration of the pyrroline was evident in absence of the copper catalyst. Therefore, it was concluded that [CuCl(DAB^{Anis})] enabled acetone-d6 to be used as deuteron source in this reaction and that prior to the hydroamination reaction, the acetylenic position was deuterated with acetone-d6 as most probable deuteron source.

Due to the enol tautomerism of acetone, the question remained, whether this acetylenic deuteration could be reproduced in absence of a base. Hence, this was further investigated with 1-hexyne as substrate (Table 4.11).

1-Hexyne was dissolved in acetone-d6 and heated with [CuCl(DAB^{Anis})] at 80 °C. The signal for the acetylenic hydrogen declined after two hours by 63%, after six hours by 79% and reached completion within sixteen hours (Table 4.11, entries 1,3, and 4). A reaction with one equivalent of triethylamine was run to investigate a possible effect of a base in this deuteration reaction but no significant change was observed for the conversion into 1-deuterohex-1-yne (Table 4.11, entry 2). Furthermore, no deuteration was observed with [Cu(NCMe)$_4$](BF$_4$) (Table 4.11, entry 5). The deuteration of acetylenic posi-

Table 4.11: Deuteration of 1-hexyne in acetone-d6 with [CuCl(DAB^{Anis})].
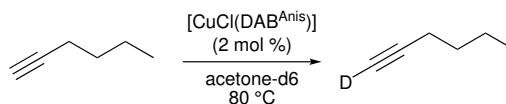
	time (h)	conv. (%)[a]
1	2	63
2[b]	2	65
3	6	79
4	16	>95
5[c]	16	0

[a] ^{1}H NMR conversions were calculated with respect to 1,3,5-trime-thoxybenzene as an internal standard.
[b] Reaction carried out with 1 equiv of NEt$_3$.
[c] Reaction with 2 mol % [Cu(NCMe)$_4$](BF$_4$).

tions had been reported with bases such as *n*-buthyl lithium, NaCO$_3$, and NEt$_3$ and deuteron sources such as D$_2$O and methanol-d4.[187–190] Therefore, our catalytic system presents an alternative for base sensitive compounds targeted for acetylenic deuteration.

4.6 Conclusions

With pent-4-ynamine **51a** as model substrate, an optimised catalytic system was established for the copper(I)-catalysed addition of primary and secondary amines to carbon–carbon unsaturated bonds. Different solvents and copper(I) salts and complexes were tested and [Cu(NCMe)$_4$](BF$_4$) in MeCN was identified as a privileged system. [Cu(DAB)] complexes were discarded as catalysts due to the displacement and decomposition of the DAB ligands in the presence of primary amines. Additionally, deuteration of pyrroline was observed in deuterated, protic solvents such as D$_2$O and methanol-d4.

Using these optimised reaction conditions, the scope of our system was then investigated, while performing all reactions in technical acetonitrile and in air without any precautions to avoid moisture.

In the intramolecular hydroamination of primary amines linear, terminal alkynes showed excellent isolated yields within short reaction times of 2–3 h. Linear, internal alkynes with substituents such as Ph, TMS, or Me showed good yields with increased catalyst loading and reaction time. Furthermore, tetrahydropyridines required longer reaction times and/or catalyst loading than pyrrolines. The only side-products formed in the reaction of linear alkynes were acetyl- and benzoyl-pyrrolines **58** and **59**. In the case of ben-

zylpyrroline, the pure product readily oxidised when stored neat and after 2 d a conversion of 30 % into **59** was observed.

Moreover, ethynylanilines and ethynylbenzylamines decomposed during the reaction and lower reaction temperatures did not prevent the decomposition. The only exception was hexynylbenzylamine **26c** that led to 3-butyl isoquinoline **63c** in moderate yields at 80 °C. The isoquinoline is presumable formed through the aromatisation of the hydroamination product, which was not observed or isolated.

Simultaneously, no reactivity was observed for a variety of secondary amines. On the other hand, tosyl substituted ethynylaniline **34a** in the presence of TBAB in water gave access within minutes to the corresponding tosyl indole **64** in excellent yields. Different solvent mixtures were tested to replace the water/TBAB system, however none was found. Additionally, TFA protected ethynylaniline **34b** reacted in the presence of K_3PO_4 to give phenylindole in excellent yields. Since TFA groups are easily removed in the presence of K_2CO_3 and water, it was not surprising to find unprotected phenylindole **62b** as the only product.

Interestingly, a tandem hydration/dehydration of 2-ethynylbenzamide **36a** to 2-cyanoacetophenone **65** was observed and isolated in moderate yields. It was suggested that the reaction might proceed *via* copper(I)-catalysed intramolecular water shift between the amide and ethynyl group, since no reaction was observed for 4-ethynylbenzamide or between benzamide and phenylacetylene.

Alternatively, the intermolecular addition of morpholine to phenylacetylene was investigated and the Markovnikov addition led to the major product **66**, along with anti-Markovnikov adduct **68** and dieneamine **69**. Under moisture and oxygen free conditions, the dieneamine was obtained as major product as it had been previously reported.[179]

However, in the intermolecular addition of *p*-toluidine to ethynylbenzene only the Markovnikov product was observed in very low yield, and with ethynylpyridine no reaction was observed at all.

On the other hand, terminal allene **40a** led to excellent conversion into vinylpiperidine **73a**, while moderate conversions were observed for the formation of vinylpiperidine **73b** or 2-methylvinylpyrrolidine **74**. Unfortunately, neither of these products could be isolated due to their volatility and/or instability.

Finally, no reactivity was achieved with 1,3-dienes or unactivated alkenes whereas our catalytic system showed a moderate reactivity in the intermolecular addition of morpholine to a variety of different Michael acceptors. Full conversions were achieved within several hours for acrylonitrile, methyl vinyl ketone and methyl acrylate.

Overall, our readily prepared and commercially available catalyst has shown a remarkable reactivity in technical MeCN and in the absence of any precautions towards oxygen or moisture.

Chapter 5

General Conclusions and Future Work

Three distinct families of [Cu(DAB)] complexes were prepared and fully characterised: homoleptic $[Cu(DAB^R)_2](BF_4)$, heteroleptic $[Cu(DAB^R)(NCMe)_2](BF_4)$ and neutral $[CuCl(DAB^R)]$ complexes (Figure 5.1). The ratio between copper and DAB ligand is dictated by the copper source and the type of ligand rather than by the stoichiometry of the reaction. The prepared complexes showed to be indefinitely stable in the solid state and did not require any particular precautions to exclude oxygen or moisture except for $[Cu(DAB^R)(NCMe)_2](BF_4)$. Additionally, all complexes displayed a tetracoordinated copper centre in the solid state with different degrees of distortion from the ideal tetrahedral geometry.
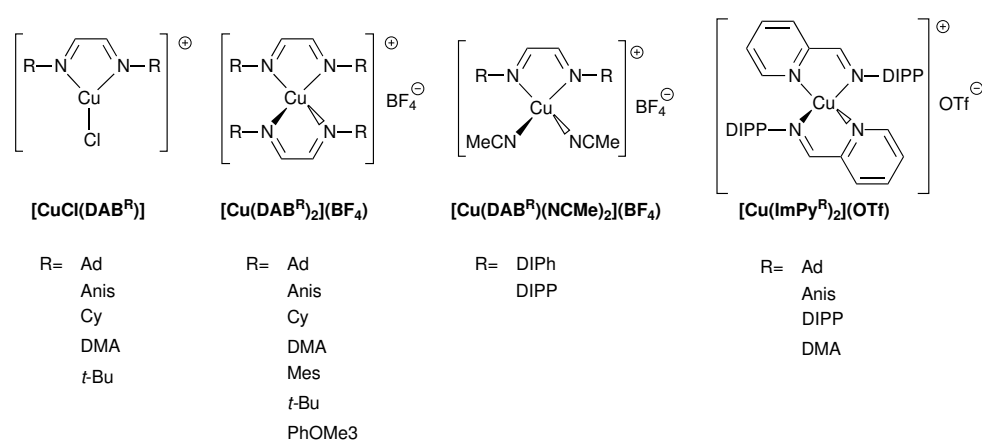
Figure 5.1: Different families of prepared [Cu(DAB)] and [Cu(ImPy)] complexes.

Furthermore, a series of novel copper(I) iminopyridine complexes was prepared and fully characterised (Figure 5.1). Once more, the obtained structures in the solid state for $[Cu(ImPy^{Ad})_2](OTf)$ and $[Cu(ImPy^{DIPP})_2](OTf)$ showed a tetrahedral coordinated copper centres. Also, all isolated complexes showed to be moisture and oxygen insensitive in the solid state. However, in solution the oxidation to a copper(II) complex was observed and $[Cu(ImPy^{DIPP})_2(OH)_2](OTf)_2$ could be characterised by X-ray diffraction.

Next, the solution behaviour of [Cu(DAB)] complexes was investigated by UV/Vis and NMR spectroscopy. The obtained results evidenced that heteroleptic $[Cu(DAB^R)(NCMe)_2]^+$ can be formed in solution. Even though they might be only stable under dilute conditions, they appear to be intermediates in the formation of the isolated homoleptic $[Cu(DAB^R)_2](BF_4)$ complexes (Scheme 5.1).

Furthermore, the initial homoleptic complex might rearrange into a dinuclear species, which is in agreement with the known lability of copper diimine complexes in solution (Scheme 5.2).[13]
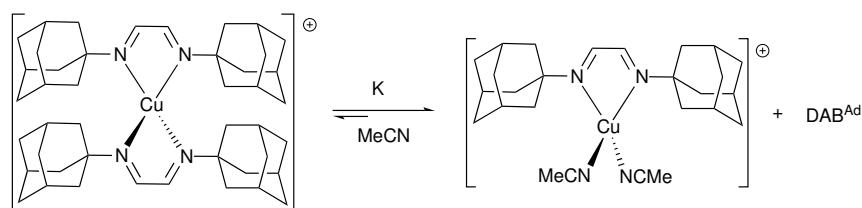
Scheme 5.1: Equilibrium between homo- and heteroleptic [Cu(DAB^{Ad})]) complexes.
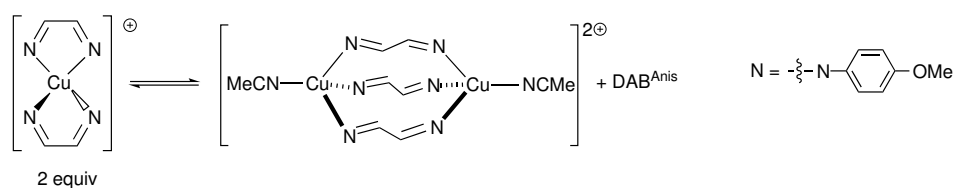
Scheme 5.2: Proposed dinuclear structure originated from [Cu(DAB^{Anis})$_2$](BF$_4$).

Even if this structural lability can be regarded as drawback for the application in photochemical processes, it certainly allows for an easy activation mode for catalytic applications.

Next, the [Cu(DAB)]-catalysed reduction reaction of aryl azides was optimised and privileged reaction conditions were found with [Cu(DAB^{DMA})$_2$] (BF$_4$) as catalyst in a mixture of toluene/H$_2$O (1:2) at 100 °C.

Different aryl- and heteroaryl azides were prepared and average to excellent yields were obtained, however electron neutral or rich compounds showed no reactivity under these reaction conditions (Scheme 5.3). The lower yield for some substrates was attributed to their thermal decomposition under the reaction conditions.
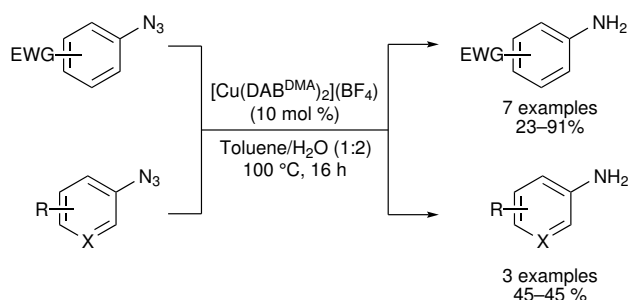
Scheme 5.3: Optimised reaction conditions for the aryl azide reduction.

With the help of DFT methods several oxidation products based on water and toluene were identified and benzyl alcohol was chosen as the most

probable one. Next, a reaction mechanism was calculated at the BP86 level in the gas phase. Following key intermediates and transition states were located. The extrusion of dinitrogen would appear to take place while the aryl azide is coordinated to the copper(I) centre and its activation energy was established to be $28.7\,\mathrm{kcal\,mol^{-1}}$ (Scheme 5.4). Next, the resulting sin-
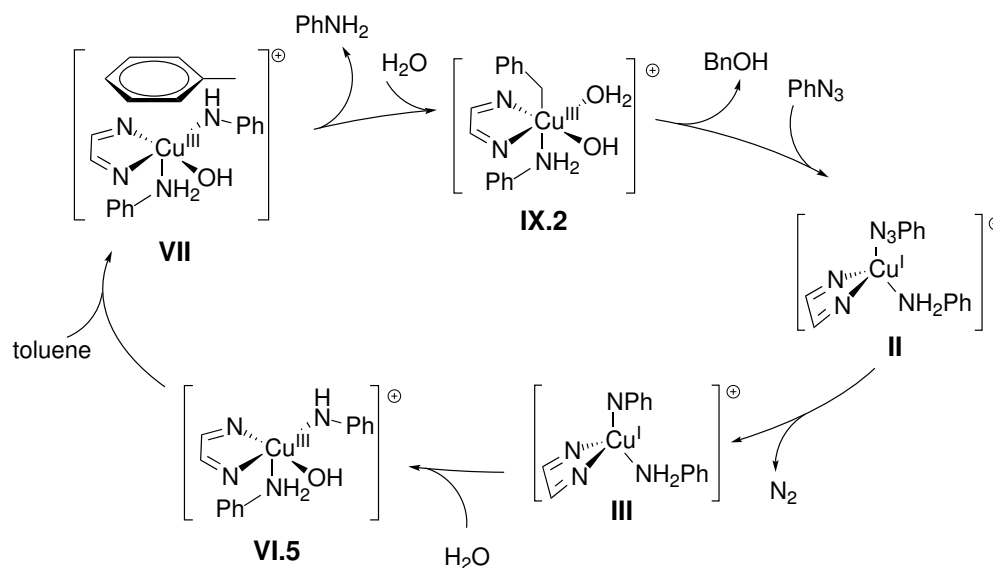
Scheme 5.4: Summary of the proposed reaction cycle for the [Cu(DAB)]-catalysed aryl azide reduction.

glet copper nitrene would undergo a spin-crossover to give rise to a triplet nitrene species. This would be followed by the oxidative addition of water resulting in a copper(III) amido hydroxyl species. Coordination of toluene through dispersion effects would lead to an intermediate from which a hydrogen would be abstracted by the amido moiety. In a final step, benzyl alcohol would be reductively eliminated, the active species regenerated, and the reaction cycle would be closed.

Furthermore, the kinetic study showed that the order of the catalyst is 1 as the amount of product was halved when the catalyst loading was reduced from 10 to 5 mol %.

[Cu(DAB)], as well as different copper(I) salts, were also tested in the intra- and intermolecular hydroamination of different carbon–carbon unsaturated bonds with primary amines and $[Cu(NCMe)_4](BF_4)$ was identified as the best performing catalyst. Different solvents, temperatures, and catalyst loading were screened and technical MeCN at 80 °C with a catalyst loading between 2 and 20 % proved to be optimal.

A substrate library for the intramolecular hydroamination was prepared and

investigated with our catalytic system. Good to excellent yields were obtained for the intramolecular addition of primary amines to alkynes and allenes with reaction times between 2–16 h, and no reactivity was observed for 1,3-dienes or alkenes (Scheme 5.5).
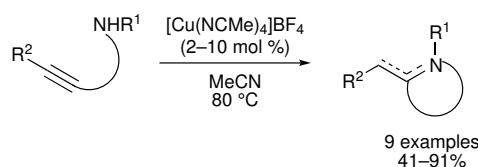
Scheme 5.5: Optimised reaction conditions for the [Cu(NCMe)$_4$](BF$_4$) mediated hydroamination reactions.

Ethynylaniline and ethynylbenzylamine based substrate showed signs of polymerisation and decomposition with the exception of hexynylbenzylamine **26c**, which was transformed into 3-butylisoquinoline **63c**. On the other, no reactivity was observed for a variety of linear, secondary amines while tosyl and trifluoroacetamide protected ethynylaniline **34a,b** gave their corresponding indoles in the presence of TBAB or K$_3$PO$_4$.

A variety of different copper(I)-catalysed intermolecular hydroamination reaction disclosed in literature were also studied. These reported hydroamination products were obtained under varying reaction conditions and our developed catalytic system was able to reproduce all of them with comparable yields. Therefore, our catalytic system is not only simple to use but also very versatile.

It is noteworthy that all reactions were performed in technical solvent without any particular precaution to exclude air or moisture.

For future work, the fate of the proposed oxidation product benzylalcohol needs to be investigated in the [Cu(DAB)]-catalysed aryl azide reduction. The possibility exists that the work-up procedure removes the benzylalcohol and thus it was not observed by ^{1}H NMR spectroscopy or, more likely, benzylalcohol decomposes in the presence of [Cu(DAB)].

Furthermore, the catalyst design needs to be optimised to allow for other hydride sources such as diphenylmethane or 2-methylpyridine. Ultimately, formic acid should be investigated as reducing agent as well, which eventually would allow to extend the substrate scope to the biologically important aminoglycosides.

Our developed catalytic system for the hydroamination reaction needs to be further exploited with a focus on 1,3-dienes and alkenes. As those substrate classes did not show any reactivity, different copper(I) catalyst with stable ligands in the presence of primary amines should be investigated.

Additionally, it appears sensible to examine [Cu(DAB)] and [Cu(ImPy)] complexes as catalysts for the hydroamination with secondary amines, since these complexes were shown to be stable in the presence of those amines.

Chapter 6

Experimental Section

6.1 Methods and Materials

All chemicals were obtained from commercial sources (Aldrich, Fisher, Fluorochem, and VWR) and used without further purification. Air and moisture sensitive manipulations were performed using standard Schlenk line techniques. Anhydrous solvents were dried passing them through columns of molecular sieves in a solvent purification system. Column chromatography and TLC were performed on silica gel (Kieselgel 60), using UV light and phosphomolybdic acid, $KMnO_4$, $Ce(SO_4)_2$, ninhydrin, or vanillin dip to visualise the products. NMR spectra were measured on Bruker AVANCE 400 spectrometers (^{1}H: 400 MHz, ^{13}C: 101 MHz, ^{19}F: 377 MHz, ^{31}P: 101 MHz) at 20 °C unless stated otherwise. The chemical shifts (δ) are given in ppm relatively to a tetramethylsilane standard or the residual solvent signal. The multiplicity is given in br., s, d, t, q, sept, and m for broad, singlet, doublet, triplet, quartet, septet, and multiplet. Assignments of some ^{1}H and ^{13}C NMR signals rely on COSY, HSQC and/or HMBC experiments. Mass spectra (MS) were recorded on a Micromass Autospec Premier, Micromass LCT Premier or a VG Platform II spectrometer using EI or ESI techniques at the Mass Spectroscopy Service of Imperial College London. Elemental analysis was performed at the London Metropolitan University (UK). UV/Vis spectra were recorded using a Perkin-Elmer Lambda 20 spectrometer. The solutions had a concentration between 0.04 and 0.17 mM in acetonitrile and DCM. Infrared spectra were recorded using a Perkin Elmer 100 series FT-IR spectrometer, equipped with a beam-condensing accessory (samples were sandwiched between diamond compressor cells). Melting points (uncorrected) were determined on an Electrothermal Gallenhamp apparatus. Single crystal X-ray diffraction were collected using Oxford Diffraction Xcalibur PX Ultra and Xcalibur 3 diffractometers, and the structures were refined using the SHELXTL, SHELX-97, and SHELX-2013 program systems. Elemental analyses were carried out by the Science Technical Support Unit at London Metropolitan University.

6.2 Preparation of Diazabutadiene (DAB) Ligands

General procedure for DAB^R preparation

To a solution of aniline (2 equiv) in methanol (0.2 M) glyoxal (40% in H_2O, 1 equiv) was slowly added followed by a few drops of formic acid. The reaction was stirred at room temperature for 16 h, then the formed precipitate was collected, washed with cold methanol, and dried under reduced pressure to give the expected, pure diazabutadiene as a solid.

N,N'-Bis(4-methoxyphenyl)-1,4-diaza-1,3-butadiene (DAB^{Anis})
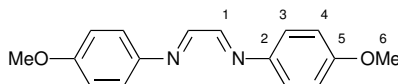
Following the general procedure from *p*-anisidine (10.74 g, 87 mmol), methanol (180 mL), and glyoxal (5 mL, 40% in H_2O, 44 mmol), DAB^{Anis} was isolated as a brown solid (6.8 g, 58%). Spectroscopic data were consistent with previously reported data for this compound.[48]

^{1}H NMR (400 MHz, CDCl$_3$): δ 8.45 (s, 2H, H^1), 7.39–7.35 (m, 4H, H^3), 7.00–6.96 (m, 4H, H^4), 3.88 (s, 6H, H^6).

^{1}H NMR (400 MHz, CD$_2$Cl$_2$): δ 8.43 (s, 2H, H^1), 7.37 (d, J = 9.0 Hz, 4H, H^3), 7.00 (d, J = 9.0 Hz, 4H, H^4), 3.88 (s, 6H, H^6).

^{13}C{^{1}H} NMR (101 MHz, CDCl$_3$): δ 159.9 (C^1), 157.7 (C^5), 143.1 (C^3), 123.2 (C^4), 114.7 (C^2), 55.7 (C^6).

IR: 2836 (C–H st, OCH$_3$), 1604, 1583 (C=N sym st), 1495, 1456, 1434, 1301, 1284, 1246, 1164, 1110, 1026, 923, 824, 805, 750, 714, 637, 600, 514, 404 cm^{-1}.

UV/Vis [λ_{max}/nm (ε/M^{-1} cm^{-1})]: 376 (26270 ± 110) (CH$_2$Cl$_2$).

N,N'-Dicyclohexyl-1,4-diazabuta-1,3-diene (DAB^{Cy})
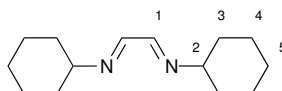
Following the general procedure from cyclohexylamine (17.4 g, 175 mmol, 2 equiv), methanol (80 mL), and glyoxal (10 mL, 40% in H_2O, 87 mmol, 1 equiv), DAB^{Cy} was isolated as a white solid (18.0 g, 94%). Spectroscopic data were consistent with previously reported data for this compound.[49]

^{1}H NMR (400 MHz, CDCl$_3$): δ 7.95 (s, 2H, H^1), 3.17 (tt, J = 11.8; 4.1 Hz, 2H, H^2), 1.82 (dt, J = 11.8; 3.3 Hz, 4H, H^3), 1.75–1.66 (m, 6H, H^{3,5}), 1.54–1.48 (m, 4H, H^4), 1.37–1.35 (m, 4H, H^4) 1.19–1.29 (m, 2H, H^5).

^{13}C{^{1}H} NMR (101 MHz, CDCl$_3$): δ 160.1 (C^1), 69.5 (C^2), 33.9 (C^3), 25.5 (C^4), 24.6 (C^5).

IR: 2923 (C–H st), 2853 (C–H st), 1621 (C=N sym st), 1449 (CH$_2$ δ), 1371, 1347, 1296, 1252, 1151, 1063, 962, 952, 886, 844, 801, 600, 530, 463 cm^{-1}.

UV/Vis: λ_{max} = 228 nm (CH$_2$Cl$_2$).

N,N'-Bis(2,6-diisopropylphenyl)-1,4-diaza-1,3-butadiene (DAB^{DIPP})
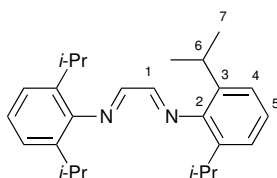
Following the general procedure from 2,6-diisopropylaniline (21.3 mL, 113 mmol), methanol (100 mL), and glyoxal (6.5 mL, 40% in H$_2$O, 56.4 mmol), DAB^{DIPP} was isolated as a bright yellow solid (14.9 g, 70%). Spectroscopic data were consistent with previously reported data for this compound.[50]

^{1}H NMR (400 MHz, CDCl$_3$): δ 8.12 (s, 2H, H^1), 7.24–7.14 (m, 6H, H^{4,5}), 2.96 (sept, J = 6.9 Hz, 4H, H^6), 1.22 (d, J = 6.9 Hz, 24H, H^7).

^{13}C{^{1}H} NMR (101 MHz, CDCl$_3$): δ 163.1 (C^1), 148.0 (C^2), 136.7 (C^3), 125.1 (C^5), 123.2 (C^4), 28.1 (C^6), 23.4 (C^7).

IR: 2962 (C–H st), 1625 (C=N sym st), 1465, 1436, 1382 (CH$_3$ δ sym), 1365 (CH$_3$ δ sym), 1329, 1290, 1255, 1241, 1176, 1109, 1060, 1047, 924, 821, 805, 790, 760, 679, 607, 515, 471, 430 cm^{-1}.

UV/Vis: λ_{max} = 352, 228 nm (CH$_2$Cl$_2$).

N,N'-Bis(4-N,N-dimethylaminophenyl)-1,4-diaza-1,3-butadiene (DAB^{DMA})
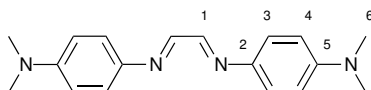
Following the general procedure from 4-(*N,N*-dimethylamino)aniline (0.5 g, 3.67 mmol), methanol (30 mL), and glyoxal (0.2 mL, 40% in H$_2$O, 1.84 mmol), DAB^{DMA} was isolated as an orange solid (0.43 g, 79 %). Spectroscopic data were consistent with previously reported data for this compound.[15]

^{1}H NMR (400 MHz, CDCl$_3$): δ 8.50 (s, 2H, H^1), 7.39 (d, J = 9.0 Hz, 4H, H^3), 6.76 (d, J = 9.0 Hz, 4H, H^4), 3.04 (s, 12H, H^6).

^{13}C{^{1}H} NMR (101 MHz, CDCl$_3$): δ 154.9 (C^1), 150.5 (C^5), 138.9 (C^2), 123.2 (C^3), 112.5 (C^4), 40.5 (C^6).

IR: 2850 (C–H st), 1603, 1565 (C=N sym st), 1512, 1444, 1357, 1289, 1228, 1122, 1066, 945, 816, 706 cm^{-1}.

UV/Vis: λ_{max} = 444, 228 nm (CH$_2$Cl$_2$).

N,N'-Bis(2,4,6-trimethylphenyl)-1,4-diazabuta-1,3-diene (DAB^{Mes})
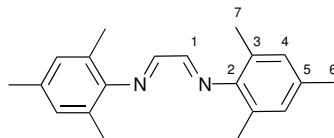
Following the general procedure from 2,4,6-trimethylaniline (5.0 g, 37.0 mmol), methanol (50 mL), and glyoxal (2.14 mL, 40% in H_2O, 18.5 mmol), DAB^{Mes} was isolated as a bright yellow solid (4.91 g, 90 %). Spectroscopic data were consistent with previously reported data for this compound.[191]
^{1}H NMR (400 MHz, CDCl$_3$): δ 8.14 (s, 2H, H^1), 6.95 (s, 4H, H^4), 2.33 (s, 3H, H^6), 2.20 (s, 6H, H^7).
^{13}C{^{1}H} NMR (101 MHz, CDCl$_3$): δ 163.5 (C^1), 147.5 (C^2), 134.3 (C^3), 129.0 (C^5), 126.6 (C^4), 20.8 (C^7), 18.8 (C^6).
IR: 2914 (C–H st), 1724, 1615 (C=N sym st), 1475 (CH$_3$ δ), 1374 (CH$_3$ δ), 1201, 1140, 850, 780, 725, 609, 524, 501 cm^{-1}.

N,N'-Bis(1,1-dimethylethyl)-1,4-diaza-1,3-butadiene (DAB^{tBu})
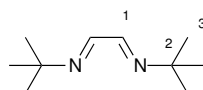
Following the general procedure from *tert*-butyl amine (4 mL, 38.1 mmol), methanol (30 mL), and glyoxal (2.1 mL, 40% in H_2O, 19.0 mmol), DAB^{tBu} was isolated as a white solid (1.21 g, 75 %). Spectroscopic data were consistent with previously reported data for this compound.[15]
^{1}H NMR (400 MHz, CDCl$_3$): δ 7.97 (s, 2H, H^1), 1.28 (s, 18H, H^3).
^{13}C{^{1}H} NMR (101 MHz, CDCl$_3$): δ 157.8 (C^1), 58.1 (C^2), 29.4 (C^3).
IR: 2965 (C–H st), 1678, 1629 (C=N sym st), 1477 (CH$_3$ δ), 1357 (CH$_3$ δ), 1209, 1077, 933, 879, 746, 595, 482, 430 cm^{-1}.
UV/Vis: λ_{max} = 228 nm (CH$_2$Cl$_2$).

N,N'-Diadamantyl-1,4-diazabuta-1,3-diene (DAB^{Ad})
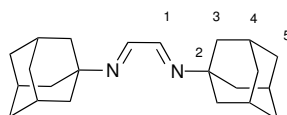
Following the general procedure from adamantylamine (550 mg, 9.5 mmol) and glyoxal (0.22 mL, 40% in H_2O, 4.75 mmol) but using a 1:1 mixture of wa-

ter and acetone (21 mL) instead of methanol, DAB^{Ad} was isolated as a white solid (287 mg, 76 %). Spectroscopic data were consistent with previously reported data for this compound.[192]

^{1}H NMR (400 MHz, CDCl$_3$): δ 7.95 (s, 2H, H^1), 2.17 (br. s, 6H, H^4), 1.78–1.58 (m, 24H, H^{3,5}).

^{1}H NMR (400 MHz, CD$_2$Cl$_2$): δ 7.89 (s, 2H, H^1), 2.16 (br. s, 6H, H^4), 1.80–1.69 (m, 24H, H^{3,5}).

^{1}H NMR (400 MHz, CD$_3$CN): δ 7.82 (s, 2H H^1), 2.11 (br. s, 6H, H^4), 1.77–1.67 (m, 24H, H^{3,5}).

^{13}C{^{1}H} NMR (101 MHz, CDCl$_3$): δ 157.9 (C^1), 58.5 (C^2), 42.8 (C^3), 36.4 (C^5), 29.4 (C^4).

IR: 2902 (C–H st), 2844 (C–H st), 1629 (C=N sym st), 1450 (CH$_2$ δ), 1343, 1313, 1091, 982, 907, 811, 721, 646, 471, 421 cm^{-1}.

UV/Vis: λ_{max} = 228 nm (CH$_2$Cl$_2$).

N,N'-Bis(2,6-bis(diphenylmethyl)-4-methylphenyl)-1,4-diaza-1,3-butadiene (DAB^{DIPh})
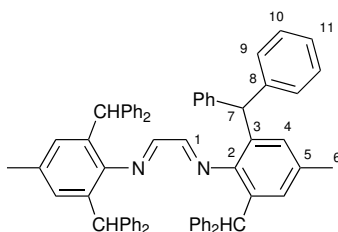
2,6-Bis(diphenylmethyl)-p-toluidine (3.9 g, 8.87 mmol) was added to DCM (90 mL) followed by glyoxal (0.5 mL, 40% in H$_2$O, 4.44 mmol), MgSO$_4$ (2.14 g, 17.74 mmol), and a few drops of formic acid at room temperature. After 4 days of stirring, the formed precipitate was filtered off and the filtrate was concentrated under reduced pressure. The resulting residue was washed with hot EtOAc (40 mL) and dried under reduced pressure to afford DAB^{DIPh} as a white solid (3.5 g, 88%). Spectroscopic data were consistent with previously reported data for this compound.[51]

^{1}H NMR (400 MHz, CDCl$_3$): δ 7.21–7.13 (m, 26H, H^{1,10,11}), 6.98–6.96 (m, 16H, H^9), 6.65 (s, 4H, H^4), 5.22 (s, 4H, H^7), 2.11 (s, 6H, H^6).

^{13}C{^{1}H} NMR (101 MHz, CDCl$_3$): δ 163.9 (C^1), 146.8 (C^2), 143.8 (C^8), 133.5 (C^3), 131.9 (C^5), 129.5 (C^4), 129.1 (C^{10}), 128.2 (C^9), 126.3 (C^{11}), 51.0 (C^7), 21.3 (C^6).

IR: 3082 (C–H st), 3056 (C–H st), 3021(C–H st), 1738, 1622 (C=N sym st), 1596, 1493, 1451, 1372, 1294, 1241, 1121, 1031, 931, 912, 856, 802, 761, 745, 733, 699, 677, 622, 606, 552, 531, 462 cm^{-1}.

N,N'-Bis(2,4,6-tris(1,1-dimethylethyl)phenyl)-1,4-diazabuta-1,3-diene (DAB^{tBu3Ph})
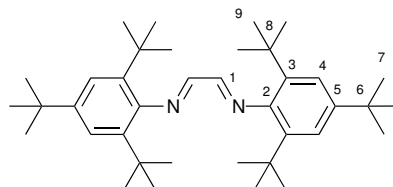
2,4,6-Tris(*t*-butyl)aniline (2.0 g, 7.7 mmol), glyoxal (0.44 mL, 40% in H_2O, 3.8 mmol), and a few drops of formic acid were dissolved in ethanol (14 mL) and refluxed for 16 h. The reaction mixture was then cooled and the resulting precipitate was collected and dried under reduced pressure to afford DAB^{tBuPh3} as a bright yellow solid (0.96 g, 46%). Spectroscopic data were consistent with previously reported data for this compound.[193]

^{1}H NMR (400 MHz, CDCl$_3$): δ 8.15 (s, 2H, H^1), 7.36 (s, 4H, H^4), 1.35 (s, 36H, H^9), 1.34 (s, 18H, H^7).

^{13}C{^{1}H} NMR (101 MHz, CDCl$_3$): δ 163.3 (C^1), 149.3 (C^2), 145.0 (C^5), 137.4 (C^3), 121.8 (C^4), 36.0 (C^8), 34.7 (C^6), 31.6 (C^9), 31.5 (C^7).

IR: 3004, 2959, 2905, 2869, 1774, 1638 (C=N sym st), 1485, 1475 (CH$_3$ δ), 1464, 1423, 1394, 1361 (CH$_3$ δ), 1283, 1271, 1243, 1216, 1199, 1115, 1028, 970, 881, 811, 786, 713, 652 cm^{-1}.

N,N'-Bis(4-N,N-dimethylaminophenyl)-1,4-diaza-2,3-dimethyl-1,3-butadiene (^{Me}DAB^{DMA})
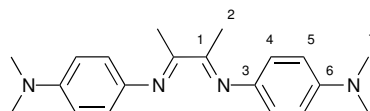
Following the general procedure from 4-(*N*,*N*-dimethylamino)aniline (5.44 g, 6.6 mmol), glyoxal (1.32 mL, 40% in H_2O, 15 mmol) but using refluxing DCM (80 mL), instead of MeOH. ^{Me}DAB^{DMA} was isolated as a greenish solid (1.25 g, 26%). Spectroscopic data were consistent with previously reported data for this compound.[194]

Mp: 160 °C.

^{1}H NMR (400 MHz, CDCl$_3$): δ 6.88–6.79 (m, 8H, H^{4,5}), 2.98 (s, 12H, H^7), 2.26 (s, 6H, H^2).

^{13}C{^{1}H} NMR (101 MHz, CDCl$_3$): δ 167.7 (C^1), 147.8 (C^6), 140.7 (C^3), 121.3 (C^4), 113.2 (C^5), 41.1 (C^7), 15.6 (C^2).

IR: 2802 (C–H st), 1680 (C=N sym st), 1601, 1509, 1444 (CH$_3$ δ), 1343 (CH$_3$

δ), 1219, 1116, 1061, 945, 829, 701 cm^{-1}.

HRMS calcd for $C_{20}H_{27}N_4$ 323.2236, found 323.2247 ([M + H]$^+$).

Preparation of N,N'-bis(3,4,5-trimethoxyphenyl)-1,4-diazabuta-1,3-diene (DAB^{PhOMe3})
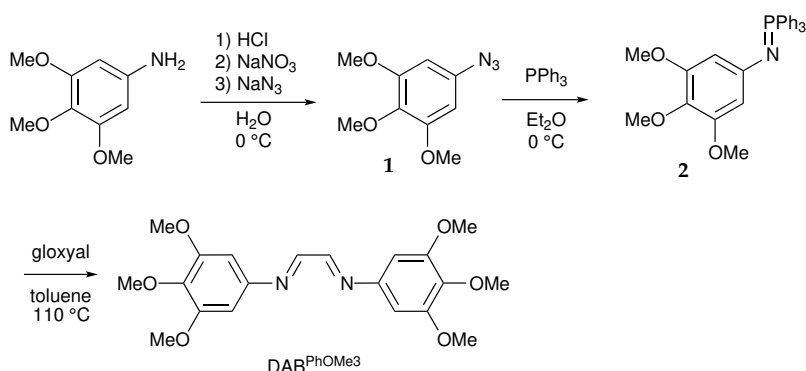
5-Azido-1,2,3-trimethoxybenzene (1)
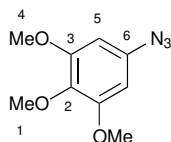
To an ice/water bath cooled suspension of 3,4,5-trimethoxyaniline (1.85 g, 10.0 mmol) in water (30 mL), HCl (12 M, 3.5 mL, 42 mmol) was added aqueous followed by a solution of NaNO$_2$ (0.69 g, 10 mmol) in water (10 mL). The reaction mixture was stirred for 10 min and a solution of NaN$_3$ (0.66 g, 10 mmol) in water (15 mL) was added before allowing the reaction mixture to warm to room temperature over 2 h. The resulting mixture was extracted with EtOAc (3×45 mL), the combined organic phases were dried over MgSO$_4$, filtered, and concentrated under reduced pressure to obtain **1** as a brown solid (1.45 g, 56%). Spectroscopic data were consistent with previously reported data for this compound.[52]

^{1}H NMR (400 MHz, CDCl$_3$): δ 6.18 (s, 2H, H^5), 3.75 (s, 9H, H^{1,4}).

^{13}C{^{1}H} NMR (101 MHz, CDCl$_3$): δ 154.2 (C^3), 135.8 (C^2), 135.0 (C^6), 96.3 (C^5), 60.3 (C^1), 56.1 (C^4).

1,1,1-Triphenyl-N-(3,4,5-trimethoxyphenyl)-λ_5-phosphanimine (2)
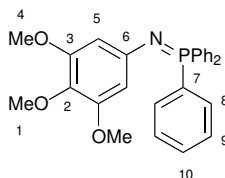
To an ice/water bath cooled suspension of azide **1** (0.293 g, 1.6 mmol) in Et_2O (30 mL) PPh_3 (0.42 g, 1.6 mmol) in Et_2O (20 mL) was added. The reaction was stirred for 30 min and then allowed to warm to room temperature over 2 h. The solvent was removed under reduced pressure to isolate **2** as a dark yellow solid (0.71 g, 67%). Spectroscopic data were consistent with previously reported data for this compound.[195]

Mp: 149 °C.

^{1}H NMR (400 MHz, CDCl$_3$): δ 7.79–7.69 (m, 6H, H^8), 7.49–7.38 (m, 9H, H^{9,10}), 6.00 (s, 2H, H^5), 3.72 (s, 3H, H^1), 3.56 (s, 6H, H^4).

^{13}C$\{^1$H$\}$ NMR (101 MHz, CDCl$_3$): δ 153.0 (C^3), 147.6 (C^6), 133.7 (C^2), 131.8 (C^7), 131.5 (C^{10}), 130.5 (C^8), 128.6 (C^9), 100.2 (C^5), 61.0 (C^1), 55.5 (C^4).

^{31}P$\{^1$H$\}$ NMR (101 MHz, CDCl$_3$): δ 3.60 (s).

IR: 2918 (C–H st), 1570, 1501, 1380, 1230, 1103, 1007, 823, 755, 714 cm^{-1}.

HRMS calcd for $C_{27}H_{27}NO_3P$ 444.1729, found 444.1730 ([M + H]$^+$).

N,N'-Bis(3,4,5-trimethoxyphenyl)-1,4-diazabuta-1,3-diene (DAB^{PhOMe3})
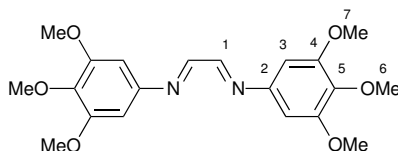
Triphenylphosphonamine **2** (250 mg, 0.58 mmol), glyoxal trimer dihydrate (38 mg, 0.15 mmol), and 4 Å molecular sieves (2 g) were heated under reflux in dry THF (10 mL) under a nitrogen atmosphere for 16 h. Volatiles were removed under reduced pressure and the resulting residue was washed with Et_2O (30 mL) to obtain DAB^{PhOMe3} as a yellow solid (52 mg, 45%). Spectroscopic data were consistent with previously reported data for this compound.[195]

Mp: 182 °C.

^{1}H NMR (400 MHz, CDCl$_3$): δ 8.43 (s, 2H, H^1), 6.63 (s, 4H, H^3), 3.90 (br. s, 18H, H^{6,7}).

^{13}C$\{^1$H$\}$ NMR (101 MHz, CDCl$_3$): δ 158.5 (C^1), 153.7 (C^2), 145.4, (C^4), 98.9

(C^5), 92.6 (C^3), 61.1 (C^6), 56.1 (C^7).
IR: 2948 (C–H st), 2839 (C–H st), 1972, 1587 (C=N asym st), 1501, 1415, 1329, 1230, 1126, 991, 828 cm^{-1}.
HRMS calcd for $C_{20}H_{25}N_2O_6$ 389.1707, found 389.1710 ([M + H]$^+$).

6.3 Preparation of Iminomethylpyridine Ligands

2-(Adamantyliminomethyl)pyridine (ImPy^{Ad})
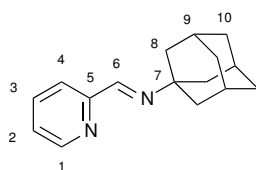
1-Adamantylamine (2.82 g, 18.7 mmol) and picolinaldehyde (1.8 mL, 18.7 mmol) in ethanol (50 mL) were heated under reflux for 16 h. Volatiles were removed and the residue was purified by Kugelrohr distillation (250 °C, 1 mbar) to give ImPy^{DMA} as a brown solid (2.85 g, 65%). Spectroscopic data were consistent with previously reported data for this compound.[55]
^{1}H NMR (400 MHz, CDCl$_3$): δ 8.63 (d, J = 4.5 Hz, 1H, H^1), 8.36 (s, 1H, H^6), 8.03 (d, J = 7.8 Hz, 1H, H^4), 7.72 (td, J = 7.8; 1.4 Hz, 1H, H^2), 7.27–7.30 (m, 1H, H^3), 2.18 (br. s, 4H, H^8) 1.69–1.84 (m, 14H, H^{9,10}).
^{13}C{^{1}H} NMR (101 MHz, CDCl$_3$): δ 156.2 (C^6), 155.7 (C^5), 149.3 (C^1), 136.5 (C^4), 124.3 (C^2), 120.9 (C^3), 58.1 (C^7), 43.0 (C^8), 36.5 (C^{10}), 29.5 (C^9).
IR: 3051, 2900, 2847, 2646, 1715 (C=N asym st), 1642 (C=N sym st), 1588, 1566, 1467, 1433, 1383, 1308, 1230, 1187, 1085, 1042, 993, 927, 883, 864, 815, 778, 745 cm^{-1}.

2-(iminomethyl)pyridine (ImPy^{Anis})
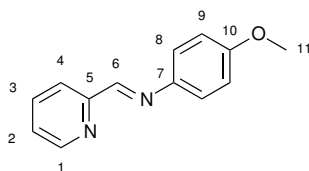
p-Anisidine (1.15 g, 9.33 mmol) and picolinaldehyde (1.0 g, 9.33 mmol) were dissolved in dry toluene (5 mL) under a nitrogen atmosphere and 4 Å molecular sieves (10 g) were added. The reaction was stirred at room temperature for 16 h before the volatiles were removed under reduced pressure to give ImPy^{Anis} as a dark red oil (1.43 g, 66 %). Spectroscopic data were consistent

with previously reported data for this compound.[55]

^{1}H NMR (400 MHz, CDCl$_3$): δ 8.72 (d, J = 4.8 Hz, 1H, H^1), 8.66 (s, 1H, H^6), 8.21 (d, J = 7.9 Hz, 1H, H^4), 7.84–7.78 (m, 1H, H^3), 7.38–7.35 (m, 3H, H^{2,8}), 6.97 (d, J = 8.6 Hz, 2H, H^9), 3.86 (s, 3H, H^{11}).

^{13}C{^{1}H} NMR (101 MHz, CDCl$_3$): δ 159.0 (C^6), 158.3 (C^5), 154.9 (C^1), 149.6 (C^7), 143.7 (C^{10}), 136.6 (C^4), 124.8 (C^9), 122.7 (C^2), 121.6 (C^3), 114.5 (C^8), 55.5 (C^{11}).

IR: 3049, 3007, 2962, 2930, 2898, 2836, 2546, 2058, 2006, 1947, 1885, 1647 (C=N asym st), 1626 (C=N st), 1601, 1584, 1564, 1506, 1467, 1439, 1344, 1300, 1288, 1242, 1203, 1185, 1174, 1157, 1114, 1036, 990, 974, 960, 880, 829, 776, 761, 745, 719 cm^{-1}.

2-(2,6-Diisopropylphenyliminomethyl)pyridine (ImPy$^{\text{DIPP}}$)
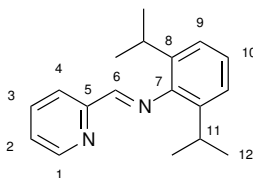
2,6-Diisopropylaniline (1.09 g, 5.64 mmol) and picolinaldehyde (0.60 g, 5.64 mmol) were dissolved in dry toluene (5 mL) under a nitrogen atmosphere and 4 Å molecular sieves (10 g) were added. The reaction was stirred at room temperature for 16 h before the volatiles were removed under reduced pressure and the resulting residue was recrystallised from petroleum ether to give ImPy$^{\text{DIPP}}$ as a yellow solid (0.70 g, 47 %). Spectroscopic data were consistent with previously reported data for this compound.[56]

^{1}H NMR (400 MHz, CDCl$_3$): δ 8.79–8.71 (m, 1H, H^1), 8.34 (s, 1H, H^6), 8.30 (ddd, J = 7.5; 1.0; 1.0 Hz, 1H, H^4), 7.90–7.86 (m, 1H, H^3), 7.44 (m, 1H, H^2), 7.22–7.14 (m, 3H, H^{9,10}), 3.00 (sept, J = 6.9 Hz, 2H, H^{11}), 1.21 (d, J = 6.9 Hz, 12H, H^{12}).

^{1}H NMR (400 MHz, acetone–d$_6$): δ 8.72 (ddd, J = 5.0; 1.0; 1.0 Hz, 1H, H^1), 8.30–8.28 (m, 2H, H^{4,6}), 7.99–7.95 (m, 1H, H^3), 7.54–7.51 (m, 1H, H^2), 7.20–7.18 (m, 2H, H^{10}), 7.11 (dd, J = 8.5; 6.7 Hz, 1H, H^9), 2.98 (d, J = 6.9 Hz, 2H, H^{11}), 1.16 (d, J = 6.9 Hz, 12H, H^{12}).

^{13}C{^{1}H} NMR (101 MHz, CDCl$_3$): δ 163.0 (C^6), 154.4 (C^5), 149.7 (C^1), 148.4 (C^7), 137.3 (C^4), 136.7 (C^8), 125.3 (C^{10}), 124.5 (C^2), 123.1 (C^9), 121.3 (C^3), 28.0 (C^{11}), 23.5 (C^{12}).

^{13}C{^{1}H} NMR (101 MHz, acetone–d$_6$): δ 168.8 (C^6), 159.6 (C^5), 155.0 (C^1), 153.9 (C^7), 142.09 (C^4), 142.04 (C^8), 130.8 (C^{10}), 129.6 (C^2), 128.2 (C^9), 125.9 (C^3), 33.0 (C^{11}), 28.0 (C^{12}).

IR: 3058, 2959, 2926, 2868, 2006, 1969, 1916, 1745 (C=N asym st), 1632 (C=N

st), 1587, 1567, 1471, 1441, 1385, 1364, 1325, 1295, 1254, 1227, 1180, 1107, 1092, 1045, 996, 934, 879, 796, 779, 754, 701 cm^{-1}.

2-(4-(N,N-dimethylamino)phenyliminomethyl)pyridine (ImPy$^{\text{DMA}}$)
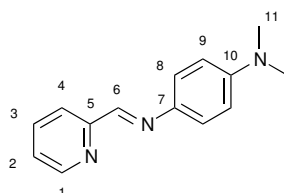
4-(N,N-Dimethylamino)aniline (2.54 g, 18.7 mmol) and picolinaldehyde (1.8 mL, 18.7 mmol) in ethanol (50 mL) were heated under reflux for 45 min. The volatiles were removed under reduced pressure and the resulting residue was purified by Kugelrohr distillation (230 °C, 0.02 mbar) to give ImPy$^{\text{DMA}}$ as an orange solid (3.7 g, 89%). Spectroscopic data were consistent with previously reported data for this compound.[57]

^{1}H NMR (400 MHz, CDCl$_3$): δ 8.71–8.64 (m, 2H, H^{1,6}); 8.18 (d, J = 7.8 Hz, 1H, H^4), 7.76 (td, J = 7.8; 1.4 Hz, 1H, H^3), 7.37 (d, J = 9.0 Hz, 2H, H^8), 7.29 (ddd, J = 7.5; 4.9; 1.4 Hz, 1H, H^2), 6.75 (d, J = 9.0 Hz, 2H, H^9), 2.99 (s, 6H, H^{11}).

^{13}C{^{1}H} NMR (101 MHz, CDCl$_3$): δ 155.3 (C^6), 155.2 (C^5), 150.1 (C^1), 149.5 (C^7), 139.4 (C^4), 136.5 (C^{10}), 124.3 (C^9), 122.9 (C^8), 121.3 (C^2), 112.6 (C^3), 40.6 (C^{11}).

IR: 3055, 2959, 2867, 2005, 1631 (C=N st), 1588, 1567, 1519, 1468, 1441, 1364, 1325, 1295, 1228, 1150, 1091, 1045, 996, 948, 934, 879, 808, 796, 778, 754, 746 cm^{-1}.

2-(2,4,6-Trimethylphenyliminomethyl)pyridine (ImPy$^{\text{Mes}}$)
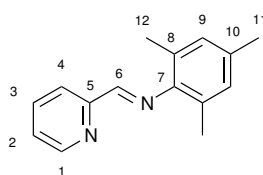
1,3,5-Trimethylaniline (5.2 mL, 37.3 mmol) and picolinaldehyde (3.6 mL, 37.3 mmol) in ethanol were heated under reflux for 90 min. The volatiles were removed under reduced pressure and the resulting residue was purified by Kugelrohr distillation (185 °C, 0.02 mbar) to give ImPy$^{\text{Mes}}$ as a yellow oil (3.51 g, 84%). Spectroscopic data were consistent with previously reported data for this compound.[196]

¹H NMR (400 MHz, CDCl₃): δ 8.71 (ddd, J = 4.9; 1.3; 1.0 Hz, 1H, H^1), 8.33 (s, 1H, H^6), 8.27 (ddd, J = 7.7; 1.3; 1.0 Hz, 1H, H^4), 7.81–7.85 (m, 1H, H^3), 7.39 (ddd, J = 7.7; 4.9; 1.2 Hz, 1H, H^2), 6.90 (s, 2H, H^9), 2.29 (s, 3H, H^{12}), 2.14 (s, 6H, H^{11}).

¹H NMR (400 MHz, acetone–d₆): δ 8.70 (ddd, J = 4.8; 1.7; 1.0 Hz, 1H, H^1), 8.30–8.27 (m, 2H, H^{4,6}), 7.95 (tdd, J = 7.6; 1.7; 0.6 Hz, 1H, H^3), 7.50 (ddd, J = 7.6; 4.8; 1.2 Hz, 1H, H^2), 6.89 (s, 2H, H^9), 2.25 (s, 3H, H^{12}), 2.09 (s, 6H, H^{11}).

¹³C{¹H} NMR (101 MHz, CDCl₃): δ 163.4 (C^6), 154.6 (C^5), 149.6 (C^1), 147.9 (C^7), 136.7 (C^4), 133.4 (C^8), 128.8 (C^2), 126.9 (C^{10}), 125.2 (C^9), 121.2 (C^3), 20.8 (C^{12}), 18.2 (C^{11}).

¹³C{¹H} NMR (101 MHz, acetone–d₆): δ 169.0 (C^6), 159.8 (C^5), 154.9 (C^1), 153.3 (C^7), 141.9 (C^4), 138.2 (C^8), 133.9 (C^2), 131.6 (C^{6}10), 130.6 (C^9), 125.7 (C^3), 25.1 (C^{12}), 22.7 (C^{11}).

IR: 2912, 1978, 1754 (C=N asym st), 1639 (C=N st), 1586, 1567, 1481, 1468, 1435, 1386, 1347, 1289, 1202, 1144, 1089, 1040, 1017, 993, 981, 936, 875, 862, 791, 768, 738 cm^{-1}.

2-(Phenyliminomethyl)pyridine (ImPy^{Ph})
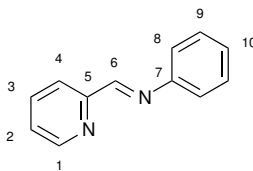
Aniline (0.87 g, 9.33 mmol) and picolinaldehyde (1.0 g, 9.33 mmol) were dissolved in dry toluene (5 mL) under a nitrogen atmosphere and 4 Å molecular sieves (10 g) were added. The reaction was stirred at room temperature for 16 h before the volatiles were removed under reduced pressure to give ImPy^{Ph} as a dark red oil (1.14 g, 61 %). Spectroscopic data were consistent with previously reported data for this compound.[197]

¹H NMR (400 MHz, CDCl₃): δ 8.74 (d, J = 4.3 Hz, 1H, H^1), 8.64 (s, 1H, H^6), 8.24 (d, J = 7.9 Hz, 1H, H^4), 7.88–7.81 (m, 1H, H^3), 7.46–7.39 (m, 3H, H^{2,8}), 7.33–7.23 (m, 3H, H^{9,10}).

¹³C{¹H} NMR (101 MHz, CDCl₃): δ 160.6 (C^6), 154.6 (C^5), 151.0 (C^1), 149.7 (C^7), 136.7 (C^4), 129.2 (C^{10}), 126.7 (C^8), 125.1 (C^9), 121.9 (C^2), 121.1 (C^3).

IR: 3305, 1954, 1623 (C=N st), 1589, 1579, 1563, 1488, 1451, 1433, 1348, 1198, 1148, 1075, 980, 912, 876, 779, 739, 687 cm^{-1}.

6.4 Preparation of Copper DAB Complexes

General procedure for [Cu(DAB)] preparation

CuCl or [Cu(NCMe)$_4$](BF$_4$) (1 equiv) and DAB^R (1 for [CuCl(DAB)] or 2 equiv for [Cu(DAB)$_2$](BF$_4$)) were suspended in dry, degassed DCM (~0.1 M) under N$_2$ atmosphere and stirred at room temperature for 16 h. The reaction mixture was then filtered through celite and concentrated to a volume of ~15 mL under reduced pressure followed by the addition of petroleum ether (40 mL). The formed precipitate was collected, washed with petroleum ether and dried under reduced pressure to give the expected [Cu(DAB^R)] complex as a strongly coloured solid.

Bis(N,N'-diadamantyl-1,4-diazabuta-1,3-diene)copper(I) tetrafluoroborate [Cu(DAB^{Ad})$_2$](BF$_4$)
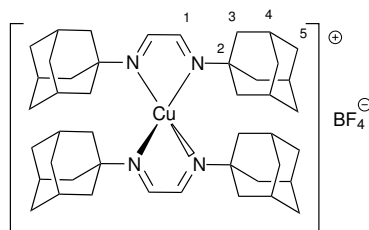
Following the general procedure from [Cu(NCMe)$_4$](BF$_4$) (150 mg, 0.48 mmol), DAB^{Ad} (308 mg, 0.96 mmol), and DCM (10 mL), [Cu(DAB^{Ad})$_2$](BF$_4$) was isolated as a red solid (225 mg, 59 %). Single crystals suitable for X-ray diffraction were grown from acetone/pentane (CCDC 1409955).

Mp: 325 °C.

^{1}H NMR (400 MHz, CDCl$_3$): δ 8.51 (s, 4H, H^1), 2.18 (s, 12H, H^4), 1.90–1.53 (m, 48H, H^{3,5}).

^{13}C{^{1}H} NMR (101 MHz, CDCl$_3$): δ 155.6 (C^1), 59.9 (C^2), 44.3 (C^3), 35.9 (C^5), 29.5 (C^4).

^{19}F NMR (377 MHz, CDCl$_3$): δ -151.6 (s).

IR: 2908 (C–H st), 2847 (C–H st), 1634 (C=N asym st), 1557 (C=N sym st), 1531 (C=N sym st), 1453 (CH$_2$ δ), 1345, 1304, 1187, 1090, 1048 (BF$_4^-$), 891, 813, 733, 519 cm^{-1}.

UV/Vis [λ_{max}/nm (ε/M^{-1} cm^{-1})]: 230 (7100 ± 160), 252 (8900 ± 1500), 532 (9560 ± 60) (CH$_2$Cl$_2$).

HRMS calcd for C$_{44}$H$_{64}$N$_4$Cu 711.4427, found 711.4431 ([Cu(DAB^{Ad})$_2$]$^+$).

Elem. anal. calcd for C$_{45}$H$_{68}$N$_4$BCuF$_4$: C, 66.28; H, 8.41; N, 6.87; found: C, 66.18; H, 8.62; N, 6.73.

Bis(N,N'-bis(4-methoxyphenyl)-1,4-diaza-1,3-butadiene)copper(I) tetrafluoroborate [Cu(DAB^{Anis})$_2$](BF$_4$)
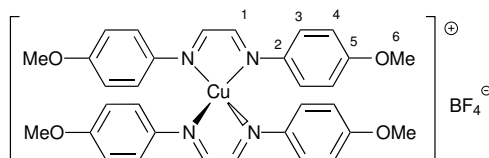
Following the general procedure from [Cu(NCMe)$_4$](BF$_4$) (206 mg, 0.65 mmol), DAB^{Anis} (354 mg, 1.30 mmol), and DCM (30 mL), [Cu(DAB^{Anis})$_2$] (BF$_4$) was isolated as a black solid (367 mg, 82 %). Single crystals suitable for X-ray diffraction were grown from DCM/hexane (CCDC 1409953).

Mp: 205 °C.

^{1}H NMR (400 MHz, CDCl$_3$): δ 8.99 (s, 4H, H^1), 7.50 (d, J = 9.0 Hz, 8H, H^3), 6.85 (d, J = 9.0 Hz, 8H, H^4), 3.79 (s, 12H, H^6).

^{1}H NMR (400 MHz, CD$_2$Cl$_2$): δ 8.91 (s, 4H, H^1), 7.53 (d, J = 9.0 Hz, 8H, H^3), 6.91 (d, J = 9.0 Hz, 8H, H^4), 3.83 (s, 12H, H^6).

^{13}C{^{1}H} NMR (101 MHz, CDCl$_3$): δ 161.5 (C^1), 150.8 (C^2), 139.1 (C^5), 124.6 (C^4), 115.2 (C^3), 55.6 (C^6).

^{19}F NMR (377 MHz, CDCl$_3$): δ -152.5 (s).

IR: 2836 (C–H st, OCH$_3$), 1599, 1562 (C=N asym st), 1503, 1455, 1438, 1392 (C=N sym st), 1253, 1164, 1096, 1058 (BF$_4^-$), 1021, 939, 885, 841, 826, 799, 658, 639, 550, 519, 426, 389 cm^{-1}.

UV/Vis [λ_{max}/nm (ε/M^{-1} cm^{-1})]: 251 (22100 ± 500), 451 (36100 ± 500), 593 (5100 ± 70) (CH$_2$Cl$_2$).

LRMS m/z = 599(100) [Cu(DAB^{Anisol})$_2$]$^+$, 372(20) [Cu(DAB^{Anis})(NCMe)]$^+$, 269 (31)

[DAB^{Anis} + H]$^+$.

Elem. anal. calcd for C$_{32}$H$_{32}$N$_4$BCuF$_4$O$_4$: C, 55.95; H 4.70; N, 8.16; found: C, 55.85; H, 4.60; N, 8.05.

Bis(N,N'-dicyclohexyl-1,4-diazabuta-1,3-diene)copper(I) tetrafluoroborate [Cu(DAB^{Cy})$_2$](BF$_4$)
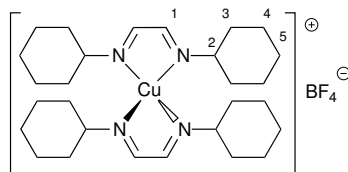
Following the general procedure from [Cu(NCMe)$_4$](BF$_4$) (174 mg, 0.55 mmol), DAB^{Cy} (240 mg, 1.10 mmol), and DCM (30 mL), [Cu(DAB^{Cy})$_2$](BF$_4$)

was isolated as a red solid (208 mg, 64 %). Single crystals suitable for X-ray diffraction were grown from DCM/hexane (CCDC 1409954).
Mp: 152 °C.
^{1}H NMR (400 MHz, CDCl$_3$): δ 8.41 (br. s, 4H, H^1), 3.60 (br. s, 4H, H^2), 1.88–1.68 (m, 20H, H^{3,4,5}), 1.41–1.08 (m, 20H, H^{3,4,5}).
^{13}C{^{1}H} NMR (101 MHz, CDCl$_3$): δ 157.2 (C^1), 67.1 (C^2), 34.9 (C^3), 25.0 (C^5), 24.7 (C^4).
^{19}F NMR (377 MHz, CDCl$_3$): δ -153.3 (s).
IR: 2928 (C–H st), 2854 (C–H st), 1627 (C=N asym st), 1541 (C=N sym st), 1450 (CH$_2$ δ), 1348, 1257, 1063 (BF$_4^-$), 1026, 873, 855, 520, 465, 412 cm^{-1}.
UV/Vis [$\lambda_{\max}$/nm (ε/M^{-1} cm^{-1})]: 241 (7250 ± 130), 516 (4360 ± 10) (CH$_2$Cl$_2$).
HRMS calcd for C$_{28}$H$_{48}$N$_4$Cu 503.3175, found 503.3180 ([Cu(DAB^{Cy})$_2$]$^+$).
Elem. anal. calcd for C$_{28}$H$_{48}$N$_4$BCuF$_4$: C, 56.90; H, 8.19; N, 9.48; found: C, 56.86; H, 8.17; N, 9.39.

Bis(N,N'-bis(4-N,N-dimethylaminophenyl)-1,4-diaza-1,3-butadien) copper(I) tetrafluoroborate [Cu(DAB^{DMA})$_2$](BF$_4$)
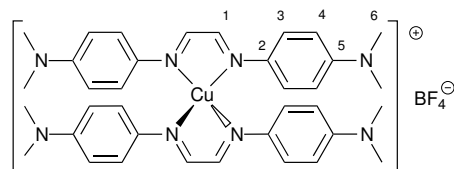
Following the general procedure from [Cu(NCMe)$_4$](BF$_4$) (78.9 mg, 0.25 mmol), DAB^{DMA} (159 mg, 0.50 mmol), and DCM (15 mL), [Cu(DAB^{DMA})$_2$] (BF$_4$) was isolated as a green solid (145 mg, 79 %).
Mp: 293 °C.
^{1}H NMR (400 MHz, CDCl$_3$): δ 8.95 (s, 4H, H^1), 7.51 (d, J = 9.0 Hz, 8H, H^4), 6.66 (d, J = 9.0 Hz, 8H, H^3), 2.92 (s, 24H, H^6).
^{13}C{^{1}H} NMR (101 MHz, CDCl$_3$): δ 151.7 (C^1), 147.3 (C^2), 135.5 (C^5), 124.9 (C^4), 112.8 C^3), 40.2 (C^6).
^{19}F NMR (377 MHz, CDCl$_3$): δ -148.3 (s).
IR: 2857 (C–H st), 2803 (C–H st), 1600, 1554 (C=N asym st), 1515, 1439, 1358 (C=N sym st), 1297, 1165, 1047 (BF$_4^-$), 945, 812, 635 cm^{-1}.
UV/Vis [$\lambda_{\max}$/nm] = 532, 262, 228 (CH$_2$Cl$_2$).
HRMS calcd for C$_{36}$H$_{44}$N$_8$Cu 651.2985, found 651.2984 ([Cu(DAB^{DMA})$_2$]$^+$).

Bis(N,N'-bis(2,4,6-trimethylphenyl)-1,4-diazabuta-1,3-diene)copper(I) tetrafluoroborate [Cu(DAB^{Mes})$_2$](BF$_4$)
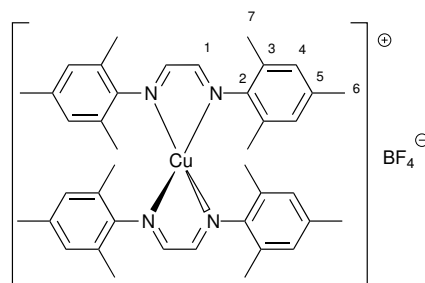
Following the general procedure from [Cu(NCMe)$_4$](BF$_4$) (108 mg, 0.34 mmol), DAB^{Mes} (209 mg, 0.68 mmol), and DCM (20 mL), [Cu(DAB^{Mes})$_2$](BF$_4$) was isolated as a black solid (179 mg, 71 %). Single crystals suitable for X-ray diffraction were grown from DCM/hexane (CCDC 1409952). Spectroscopic data were consistent with previously reported data for this compound.[58]

Mp: 297 °C.

^{1}H NMR (400 MHz, CDCl$_3$): δ 8.30 (s, 4H, H^1), 6.61 (s, 8H, H^4), 2.28 (s, 12H, H^6), 1.97 (s, 24H, H^7).

^{13}C{^{1}H} NMR (101 MHz, CDCl$_3$): δ 159.3 (C^1), 144.3 (C^2), 136.7 (C^3), 129.3 (C^4), 129.1 (C^5), 20.8 (C^6), 18.8 (C^7).

^{19}F NMR (377 MHz, CDCl$_3$): δ -153.4 (s).

IR: 2947 (C–H st), 2910 (C–H st), 1610, 1571 (C=N asym st), 1475 (C=N sym st), 1455 (CH$_3$ δ), 1439 (C=N sym st), 1379 (CH$_3$ δ), 1299, 1206, 1087, 1048 (BF$_4^-$), 886, 850, 723, 650, 587, 519, 418, 336 cm^{-1}.

UV/Vis [λ_{max}/nm (ε/M^{-1} cm^{-1})]: 228 (31170 ± 150), 398 (13600 ± 20), 727 (3150 ± 60) (CH$_2$Cl$_2$).

HRMS calcd for C$_{40}$H$_{48}$N$_4$Cu 647.3175, found 647.3150 ([Cu(DAB^{Mes})$_2$]$^+$).

Elem. anal. calcd for C$_{40}$H$_{48}$N$_4$F$_4$BCu: C, 74.10; H, 7.46; N, 8.64, found: C, 74.03; H, 7.51; N, 8.59.

Bis(N,N'-bis(1,1-dimethylethyl)-1,4-diaza-1,3-butadiene)copper(I) tetrafluoroborate [Cu(DAB^{tBu})$_2$](BF$_4$)
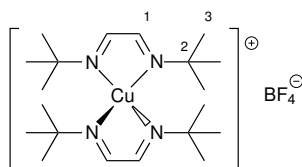
Following the general procedure from [Cu(NCMe)$_4$](BF$_4$) (140 mg, 0.45 mmol), DAB^{tBu} (159 mg, 0.90 mmol), and DCM (15 mL), [Cu(DAB^{tBu})$_2$](BF$_4$)

was isolated as a red solid (163 mg, 56 %). Single crystals suitable for X-ray diffraction were grown from DCM/hexane.

Mp: 330 °C.

^{1}H NMR (400 MHz, CDCl$_3$): δ 8.48 (s, 4H, H^1), 1.31 (s, 36H, H^3).

^{13}C{^{1}H} NMR (101 MHz, CDCl$_3$): δ 157.2 (C^1), 59.7 (C^2), 30.9 (C^3).

^{19}F NMR (377 MHz, CDCl$_3$): δ -152.9 (s).

IR: 2968 (C–H st), 1627 (C=N asym st) 1542 (C=N sym st), 1472 (CH$_3$ δ), 1380 (CH$_3$ δ), 1199, 1099, 1059 (BF$_4^-$), 984, 903, 523 cm^{-1}.

UV/Vis [λ_{max}/nm] = 524, 228 (CH$_2$Cl$_2$).

HRMS calcd for C$_{20}$H$_{40}$N$_4$Cu 399.2549, found 399.2560 ([Cu(DAB^{tBu})$_2$]$^+$).

Bis(N,N'-bis(3,4,5-trimethoxyphenyl)-1,4-diazabuta-1,3-diene)copper(I) tetrafluoroborate [Cu(DAB^{PhOMe3})$_2$](BF$_4$)
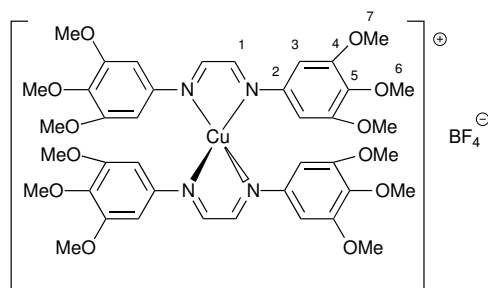
Following the general procedure from [Cu(NCMe)$_4$](BF$_4$) (41 mg, 0.13 mmol), DAB^{PhOMe3} (100 mg, 0.26 mmol), and DCM (50 mL), [Cu(DAB^{PhOMe3})$_2$](BF$_4$) was isolated as a black solid (102 mg, 75%).

Mp: 166 °C.

^{1}H NMR (400 MHz, CDCl$_3$): δ 9.03 (s, 4H, H^1), 6.82 (s, 8H, H^3), 3.86–3.78 (m, 36H, H^{6,7}).

^{13}C{^{1}H} NMR could not be measured due to low solubility of the title compound in acetone-d6, CDCl$_3$, CD$_3$CN, or DMSO–d$_6$.

^{19}F NMR (377 MHz, CDCl$_3$): δ -153.4 (s).

IR: 2943 (C–H st), 1588 (C=N sym st), 1499 1604, 1459, 1420, 1337 (C=N sym st), 1232, 1225, 999, 826 cm^{-1}.

LRMS calcd for C$_{40}$H$_{48}$N$_4$CuO$_{12}$ 839, found 839 ([Cu(DAB^{PhOMe3})$_2$]$^+$).

Bis(N,N'-bis(4-N,N-dimethylaminophenyl)-1,4-diaza-2,3-dimethyl-1,3-butadiene)copper(I) tetrafluoroborate [Cu(^{Me}DAB^{DMA})$_2$](BF$_4$)
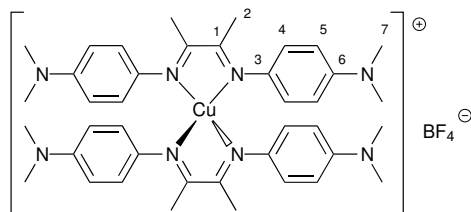
Following the general procedure from [Cu(NCMe)$_4$](BF$_4$) (97 mg, 0.31 mmol), ^{Me}DAB^{DMA} (200 mg, 0.62 mmol), and DCM (50 mL), [Cu(^{Me}DAB^{DMA})$_2$](BF$_4$) was isolated as a black solid (150 mg, 61%).

Mp: 146 °C.

^{1}H NMR (400 MHz, CDCl$_3$): δ 6.65 (s, 16H, H^{4,5}) 3.00 (s, 24H, H^7), 2.20 (s, 12H, H^2).

^{13}C{^{1}H} NMR could not be measured due to low solubility of the title compound in acetone-d6, CDCl$_3$, CD$_3$CN, or DMSO–d$_6$.

^{19}F NMR (377 MHz, CDCl$_3$): δ -153.1 (s).

IR: 2803 (C–H st), 1604, 1511 (C=N asym st), 1442, 1352 (C=N sym st), 1225, 1122, 1050 (BF$_4^-$), 944, 826 cm^{-1}.

HRMS calcd for C$_{40}$H$_{52}$N$_8$Cu 707.3605, found 707.3578 ([Cu(^{Me}DAB^{DMA})$_2$]$^+$).

Bis(acetonitrile)(N,N'-bis(2,6-diisopropylphenyl)-1,4-diaza-1,3-butadiene)copper(I) tetrafluoroborate [Cu(DAB^{DIPP})(NCMe)$_2$](BF$_4$)
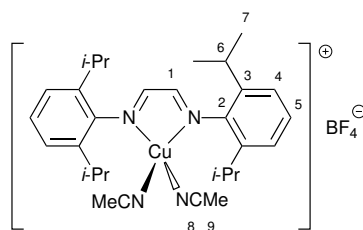
Following the general procedure from [Cu(NCMe)$_4$](BF$_4$) (0.5 mg, 1.59 mmol), DAB^{DIPP} (0.598 g, 1.59 mmol), and DCM (60 mL), [Cu(DAB^{DIPP})(NCMe)$_2$] (BF$_4$) was isolated as a black solid (714 mg, 65 %). Single crystals suitable for X-ray diffraction were grown from DCM/hexane (CCDC 1409956).

Mp: 123 °C.

^{1}H NMR (400 MHz, CDCl$_3$): δ 8.33 (s, 2H, H^1), 7.34–7.26 (m, 6H, H^{4,5}), 2.95 (sept, 4H, J = 6.8 Hz, H^6), 2.20 (s, 6H, H^9), 1.26 (d, J = 6.8 Hz, 24H, H^7).

^{1}H NMR (400 MHz, CD$_3$CN): δ 8.15 (s, 2H, H^1), 7.28–7.21 (m, 6H, H^{4,5}), 2.96 (sept, J = 6.8 Hz, 4H, H^6), 1.99 (s, 6H, H^9), 1.22 (d, J = 6.8 Hz, 24H, H^7).

^{13}C{^{1}H} NMR (101 MHz, CDCl$_3$): δ 160.0 (C^1), 144.9 (C^2), 138.4 (C^3), 127.1 (C^5), 123.8 (C^4), 111.3 (C^8), 28.2 (C^6), 23.8 (C^7) 2.2 (C^9).

^{19}F NMR (377 MHz, CDCl$_3$): δ -153.1 (s).

IR: 2965 (C–H st, aliph), 2871 (C–H st, aliph), 2277 (C≡N st), 1634 (C=N sym st), 1591, 1529 (C=N asym st), 1466, 1435, 1365 (CH$_3$ δ sym), 1334, 1256, 1186, 1050 (BF$_4^-$), 797, 753, 699 cm^{-1}.

UV/vis [λ_{max}/nm (ε/M^{-1} cm^{-1})]: 342 (2630 ± 70), 565 (256 ± 5) (CH$_2$Cl$_2$) 353 (1709 ± 4), 464 (357 ± 22), 524 (256 ± 19) (MeCN).

LRMS m/z = 480 (100) [Cu(DAB^{DIPP})(NCMe)]$^+$, 377(42) [DAB^{DIPP} + H]$^+$.

Elem. anal. calcd for C$_{30}$H$_{42}$N$_4$BCuF$_4$: C, 59.16; H, 6.95; N, 9.20; found: C, 59.07; H, 6.67; N, 9.38.

Bis(acetonitrile)(N,N'-Bis(2,6-bis(diphenylmethyl)-4-methylphenyl)-1,4-diaza-1,3-butadiene)copper(I) tetrafluoroborate [Cu(DAB^{DIPh})(NCMe)$_2$](BF$_4$)
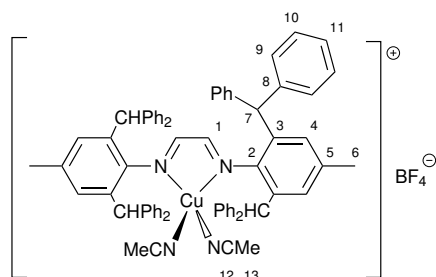
Following the general procedure from [Cu(NCMe)$_4$](BF$_4$) (50 mg, 0.15 mmol), DAB^{DIPh} (139 mg, 0.15 mmol), and DCM (5 mL), [Cu(DAB^{DIPh})(NCMe)$_2$](BF$_4$) was isolated as a brown solid (135 mg, 86 %). Single crystals suitable for X-ray diffraction were grown from DCM/hexane.

Mp: 204 °C.

^{1}H NMR (400 MHz, CDCl$_3$): δ 7.20 (m, 24H, H^{10,11}), 6.89 (m, 16H, H^9), 6.75 (s, 4H, H^4), 6.66 (s, 2H, H^1), 5.47 (s, 4H, H^7), 2.19 (s, 6H, H^6), 2.06 (s, 6H H^{13})

^{13}C{^{1}H} NMR (101 MHz, CDCl$_3$): δ 143.0 (C^1), 130.0 (C^2), 129.9 (C^5), 129.5 (C^3), 129.2 (C^8), 128.7 (C^{10}), 128.5 (C^4), 126.8 (C^9), 126.7 (C^{11}), 110.0 (C^{12}), 51.2 (C^7), 21.4 (C^6), 2.3 (C^{13}).

^{19}F NMR (377 MHz, CDCl$_3$): δ -153.1 (s).

IR: 3059, 3024, 1970, 1623 (C=N asym st), 1598, 1553 (C=N sym st), 1494, 1446, 1365, 1202, 1075 (BF$_4^-$), 1031, 851, 760, 747 cm^{-1}.

HRMS calcd for C$_{68}$H$_{56}$N$_4$Cu 963.3740, found 963.3828 ([Cu(DAB^{DIPh})]$^+$).

N,N'-Diadamantyl-1,4-diazabuta-1,3-diene copper(I) chloride [CuCl(DAB^{Ad})]
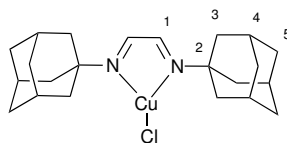
Following the general procedure from copper(I) chloride (75.3 mg, 0.76 mmol), DAB^{Ad} (241 mg, 0.76 mmol), and DCM (20 mL), [CuCl(DAB^{Ad})] was isolated as a red solid (176 mg, 56 %).

Mp: 237 °C.

^{1}H NMR (400 MHz, CDCl$_3$): δ 8.56 (br. s, 2H, H^1), 2.26 (br. s, 12H, H^3), 1.80–1.62 (m, 12H, H^5), 1.62–1.53 (m, 6H, H^4).

^{13}C{^{1}H} NMR could not be measured due to low solubility of the title compound in acetone-d6, CDCl$_3$, CD$_3$CN, or DMSO–d$_6$.

IR: 2901 (C–H st), 2848 (C–H st), 1624 (C=N asym st), 1581, 1538 (C=N sym st), 1451 (CH$_2$ δ), 1343, 1306, 1090, 981, 890, 813 cm^{-1}.

UV/Vis [λ_{max}/nm (ε/M^{-1} cm^{-1})]: 232 (6900 ± 200), 384 (900 ± 10), 530 (1290 ± 50) (CH$_2$Cl$_2$).

HRMS calcd for C$_{24}$H$_{35}$N$_3$Cu 428.2127, found 428.2132 ([Cu(DAB^{Ad})(NCMe)]$^+$).

Elem. anal. calcd for C$_{22}$H$_{32}$N$_2$ClCu: C, 62.39; H, 7.62; N, 6.61; found: C, 62.23; H, 7.65; N, 6.59.

N,N'-Bis(4-methoxyphenyl)-1,4-diaza-1,3-butadiene copper(I) chloride [CuCl(DAB^{Anis})]
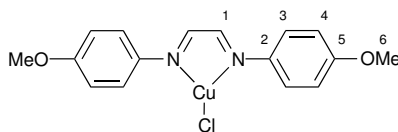
Following the general procedure from copper(I) chloride (0.5 g, 1.56 mmol), DAB^{Anis} (0.184 g, 1.56 mmole), and DCM (40 mL), [CuCl(DAB^{Anis})] was isolated as a black solid (217 mg, 32 %). Single crystals suitable for X-ray diffraction were grown from DCM/hexane (CCDC 1409957).

Mp: 220 °C.

^{1}H NMR (400 MHz, CDCl$_3$): δ 8.79 (s, 2H, H^1), 7.48–7.46 (m, 4H, H^4), 6.98–6.96 (m, 4H, H^3), 3.87 (s, 6H, H^6).

^{13}C{^{1}H} NMR could not be measured due to low solubility of the title compound in acetone-d6, CDCl$_3$, CD$_3$CN, or DMSO–d$_6$.

IR: 2835 (C–H st, OCH$_3$), 1611, 1586 (C=N asym st), 1503, 1436 (C=N sym st), 1297, 1253, 1165, 1111, 1026, 825, 798, 636, 528, 406 cm^{-1}.

UV/Vis [λ_{max}/nm (ε/M^{-1} cm^{-1})]: 232 (12900 ± 360), 393 (14300 ± 300), 589 (1250 ± 90) (CH$_2$Cl$_2$).

HRMS calcd for C$_{18}$H$_{19}$N$_3$CuO$_2$ 372.0773, found 372.0788 ([Cu(DAB^{Anisol})(NCMe)]$^+$)

Elem. anal. calcd for C$_{16}$H$_{16}$N$_2$ClCuO$_2$: C, 52.32; H, 4.39; N, 7.63; found: C, 52.55; H, 4.60; N, 7.85.

N,N'-Dicyclohexyl-1,4-diazabuta-1,3-diene copper(I) chloride [CuCl(DAB^{Cy})]
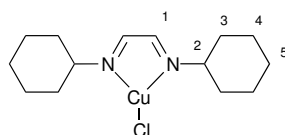
Following the general procedure from copper(I) chloride (133 mg, 1.34 mmol), DAB^{Cy} (296 mg, 1.34 mmol), and DCM (30 mL), [CuCl(DAB^{Cy})] was isolated as a red solid (220 mg, 86 %). Single crystals suitable for X-ray diffraction were grown from DCM/hexane (CCDC 1409958).

Mp: 166 °C.

^{1}H NMR (400 MHz, CDCl$_3$): δ 8.36 (br. s, 2H, H^1), 3.63 (m, 2H, H^2), 2.20–1.51 (m, 12H, H^{3,4,5}), 1.51–1.00 (m, 8H, H^{3,4}).

^{13}C{^{1}H} NMR could not be measured due to low solubility of the title compound in acetone-d6, CDCl$_3$, CD$_3$CN, or DMSO–d$_6$.

IR: 2926 (C–H st), 2852 (C–H st), 1644 (C=N asym st), 1569 (C=N sym st), 1456 (CH$_2$ δ), 1441 (CH$_2$ δ), 1393, 1379, 1155, 1102, 956, 869, 854, 584, 464, 406 cm^{-1}.

UV/Vis [λ_{max}/nm (ε/M^{-1} cm^{-1})]: 230 (7060 ± 50), 382 (856 ± 9), 515 (1830 ± 20) (CH$_2$Cl$_2$).

HRMS calcd for C$_{16}$H$_{27}$N$_3$Cu 324.1501, found 324.1494 ([Cu(DAB^{Cy})(NCMe)]$^+$).

Elem. anal. calcd for C$_{14}$H$_{24}$N$_2$ClCu: C, 52.99; H, 6.99; N, 8.83; found: C, 52.88; H, 6.78; N, 8.73.

N,N'-Bis(4-N,N-dimethylaminophenyl)-1,4-diaza-1,3-butadien copper(I) chloride [CuCl(DAB^{DMA})]
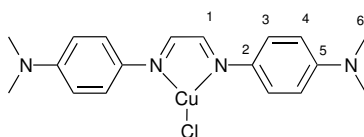
Following the general procedure from copper(I) chloride (50 mg, 0.51 mmol), DAB^{DMA} (150 mg, 0.51 mmol), and acetone (13 mL), [CuCl(DAB^{DMA})] was isolated as a black solid (100 mg, 50 %).

Mp: 198 °C.

^{1}H NMR (400 MHz, CDCl$_3$): δ 8.82 (s, 2H, H^1), 7.47 (d, J = 8.8 Hz, 4H, H^4), 6.59–6.58 (m, 4H, H^3), 2.97 (s, 12H, H^6).

^{13}C\{^{1}H\} NMR could not be measured due to low solubility of the title compound in acetone-d6, CDCl$_3$, CD$_3$CN, or DMSO–d$_6$.

IR: 2891 (C–H st), 1666, 1601, 1557 (C=N asym st), 1512, 1436, 1358 (C=N sym st), 1299, 1168, 1117, 996, 944, 816, 512 cm^{-1}.

UV/Vis [λ_{max}/nm] = 566, 444, 256 (CH$_2$Cl$_2$).

HRMS calcd for C$_{20}$H$_{25}$N$_5$Cu 398.1406, found 398.1395 ([Cu(DAB^{DMA})(NCMe)]$^+$).

N,N'-Bis(1,1-dimethylethyl)-1,4-diaza-1,3-butadiene copper(I) chloride [CuCl(DAB^{tBu})]
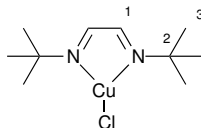
Following the general procedure from copper(I) chloride (300 mg, 3.0 mmol), DAB^{tBu} (340 mg, 3.0 mmol), but in refluxing acetone (12 mL), [CuCl(DAB^{tBu})] was isolated 3 h as a red solid (135 mg, 32 %). Spectroscopic data were consistent with previously reported data for this compound.[15]

Mp: 188 °C.

^{1}H NMR (400 MHz, CDCl$_3$): δ 8.57 (br. s, 2H, H^1), 1.55 (s, 18H, H^3).

^{13}C\{^{1}H\} NMR could not be measured due to low solubility of the title compound in acetone-d6, CDCl$_3$, CD$_3$CN, or DMSO–d$_6$.

IR: 2968 (C–H st), 1644 (C=N asym st), 1569 (C=N sym st), 1536, 1468 (CH$_3$ δ), 1371, 1196, 986, 893, 814, 482, 450, 407 cm^{-1}.

UV/Vis [λ_{max}/nm] = 524, 368, 228 (CH$_2$Cl$_2$).

HRMS calcd for C$_{12}$H$_{23}$N$_3$Cu 272.1188, found 272.1201 ([Cu(DAB^{tBu})(NCMe)]$^+$).

6.5 Percent Buried Volume Calculations

Percent buried volume ($\%V_B$) values were calculated using the on-line tool SambVca.[65] Input xyz coordinates were prepared from the cif files obtained for complexes [Cu(DAB^{Ad})$_2$] (BF$_4$), [Cu(DAB^{Anis})$_2$](BF$_4$), [Cu(DAB^{Cy})$_2$](BF$_4$), [Cu(DAB^{Mes})$_2$](BF$_4$), [Cu(DAB^{DIPP}) (NCMe)$_2$](BF$_4$), and [Cu(DAB^{DIPh})

(NCMe)$_2$](BF$_4$) by removing any solvent in the crystal lattice, all ligands except one of the diimines, and by replacing the copper centre by a hydrogen atom. The atom "coordinated at the centre of the sphere" was the hydrogen atom that replaced the copper centre and the axis was defined by the two nitrogen atoms. The considered sphere radius was 3.5 Å, the distance from the centre of the sphere was set to 0 Å, so that the sphere is centred on the metal atom, and the mesh spacing was set to 0.05. Hydrogen atoms were not included in the calculations. The calculated $\%V_B$ for the studied ligands are:

ImPy^{Ad}:	39.0%
ImPy^{DIPP}:	41.2%
DAB^{Cy}:	41.4%
DAB^{Anis}:	41.5%
DAB^{Ad}:	43.6%
DAB^{DIPP}:	44.5%
DAB^{Mes}:	47.5%
DAB^{DIPh}:	50.1%.

Since [Cu(DAB^{Mes})$_2$](BF$_4$) was considerably distorted compared to the other homoleptic copper complexes due to $\pi-\pi$ contacts between adjacent mesityl groups, we also calculated the $\%V_B$ for DAB^{Mes} using the published crystallographic data for [IrCl(DAB^{Mes})(NCt–Bu)], CCDC 916389.[198] From this structure we obtained a slightly smaller $\%V_B$ for DAB^{Mes} of 45.6%. However, this value confirms the observed steric trend for the reported DAB^R ligands.

6.6 UV/Vis Experimental Procedures

6.6.1 Experiments with DAB^{Anis}

Procedure for the titration experiments

[Cu(NCMe)$_4$](BF$_4$) (23.6 mg, 75 µmol) was dissolved in a volumetric flask in degassed DCM (25 mL) from which 0.25 mL was further diluted in another 25 mL of degassed DCM to obtain a 30 µM solution of [Cu(NCMe)$_4$](BF$_4$). DAB^{Anis} (20.1 mg, 75 µM) was dissolved in a volumetric flask in degassed DCM (25 mL), from which solutions 30, 60, and 90 µM were prepared by dissolving 0.25, 0.5, and 0.75 mL in 25 mL of DCM, respectively. Appropriate DAB^{Anis} concentrations were prepared by further dilution with DCM directly in the UV/Vis cuvette. To the final solution of DAB^{Anis} the exact same volume of the [Cu(NCMe)$_4$](BF$_4$) solution was added (Table 6.2) The absorptions at 454 and 593 nm were then plotted against the equivalents of DAB^{Anis} (Figure 1.19).

Table 6.2: Absorbances for the titration experiments with $[Cu(NCMe)_4](BF_4)/$ DAB^{Anis} in DCM.

	equiv DAB^{Anis}	Absorbance at given wavelength	
		454 nm	**593 nm**
1	0.2	0.08147	0.010690
2	0.4	0.15760	0.025540
3	0.6	0.22853	0.035100
4	0.8	0.30998	0.046680
5	1.0	0.36628	0.053820
6	1.2	0.37261	0.055400
7	1.4	0.45027	0.065850
8	1.6	0.45817	0.066960
9	1.8	0.46259	0.066600
10	2.0	0.47974	0.069550
11	2.2	0.43386	0.063500
12	2.4	0.44563	0.065480
13	2.6	0.45481	0.066620
14	2.8	0.44499	0.065070
15	3.0	0.44653	0.065129

Procedure for the Job experiments

$[Cu(NCMe)_4](BF_4)$ (23.6 mg, 75 µmol) and DAB^{Anis} (20.1 mg, 75 µmol) were separately dissolved in degassed DCM (25 mL) in a volumetric flask. From these solutions 0.5 mL were further diluted in 25 mL to give 60 µM solutions of $[Cu(NCMe)_4](BF_4)$ and DAB^{Anis}. These solutions were mixed in the required ratios in a UV/Vis cuvette before measurement and the different concentrations are shown in Figure 6.1 and the data in Table 6.3. Absorptions at 593 and 454 nm nm were used for the Job plots shown in Figure 1.19.

6.6.2 Experiments with DAB^{Ad}

Procedure for the titration experiments in DCM

$[Cu(NCMe)_4](BF_4)$ (23.6 mg, 75 µmol) was dissolved in a volumetric flask in degassed DCM (10 mL) from which 2.0 mL were further diluted in additional 25 mL of degassed DCM to give a 600 µM solution of $[Cu(NCMe)_4](BF_4)$. DAB^{Ad} (40.6 mg, 0.125 mmol) was dissolved in a volumetric flask in degassed DCM (25 mL), from which solutions of 3.0, 1.2, and 0.6 mM were prepared by dissolving 6.0, 2.4, and 1.0 mL in 10 mL of degassed DCM. Appropriate DAB^{Ad} concentrations were prepared by further dilution with degassed DCM directly in the UV/Vis cuvette. To the final solution of DAB^{Ad} was added the exact same volume of the $[Cu(NCMe)_4](BF_4)$ solution to give
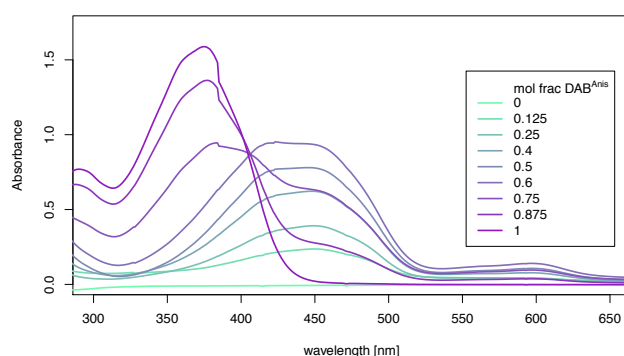
Figure 6.1: Measured spectra for the Job plots for DAB^{Anis} and [Cu(NCMe)$_4$] (BF$_4$) with a total concentration of 60 µM at room temperature in DCM.

Table 6.3: Absorbances for the Job plots with [Cu(NCMe)$_4$](BF$_4$) and DAB ^{Anis} in DCM.

		Absorbance at given wavelength	
entry	**DAB^{Anis}**	**454 nm**	**593 nm**
1	0	-0.00676	-0.00456
2	0.125	0.23626	0.03802
3	0.25	0.39057	0.04201
4	0.4	0.61970	0.07609
5	0.5	0.77421	0.10467
6	0.6	0.92939	0.13803
7	0.75	0.62694	0.09386
8	0.875	0.27345	0.03603
9	1	0.01787	0.00249

absorption spectra shown in Figure 1.23 and Table 6.4. The absorptions at 326, 430, and 530 nm were then plotted against the equivalents of DAB^{Ad} (Figure 1.24).

Procedure for the Job experiments in DCM

[Cu(NCMe)$_4$](BF$_4$) (23.6 mg, 75 µmol) and DAB^{Ad} (20.1 mg, 75 µmol) were separately dissolved in degassed DCM (25 mL) in two volumetric flasks. From these solutions, 0.5 mL were further diluted in 25 mL of DCM to give 600 µM solutions of [Cu(NCMe)$_4$](BF$_4$) and DAB^{Ad}. These solutions were mixed in the required ratios in a UV/Vis cuvette before measurement and shown in Figure 6.2. Absorptions at 326 and 530 nm (Table 6.5) were used for the Job plots shown in Figure 1.24.

Table 6.4: Absorbances for the titration experiments with $[Cu(NCMe)_4](BF_4)/$ DAB^{Ad} in DCM.

entry	equiv DAB^{Ad}	Absorbance at given wavelength		
		326 nm	430 nm	530 nm
1	0.2	0.141900	0.00646	0.00462
2	0.4	0.284870	0.01782	0.01690
3	0.6	0.410920	0.02494	0.04131
4	0.8	0.518110	0.05265	0.15991
5	1.0	0.495570	0.10810	0.49197
6	1.2	0.396810	0.21908	1.14559
7	1.4	0.272700	0.30221	1.68037
8	1.6	0.124930	0.41729	2.40312
9	1.8	0.039500	0.50343	2.93555
10	2.0	0.048510	0.49453	2.88249
11	2.2	0.050470	0.49440	2.86725
12	2.4	0.061130	0.48844	2.83119
13	2.6	0.050950	0.48098	2.80826
14	2.8	0.057900	0.48250	2.80884
15	3.0	0.074570	0.48880	2.80692
16	5.0	0.068669	0.48365	2.79767

Table 6.5: Absorbances for the Job plots with $[Cu(NCMe)_4](BF_4)$ and DAB^{Ad} in DCM.

entry	DAB^{Ad}	Absorbance at given wavelength	
		326 nm	530 nm
1	0	0.01733	0.00136
2	0.1	0.169950	0.00445
3	0.2	0.27664	0.01235
4	0.3	0.40504	0.03815
5	0.4	0.53199	0.13002
6	0.5	0.36959	0.89752
7	0.6	0.04097	1.93810
8	0.7	0.03490	1.52397
9	0.8	0.04184	0.88383
10	0.9	0.04543	0.38931
11	1.0	0.04548	0.00100
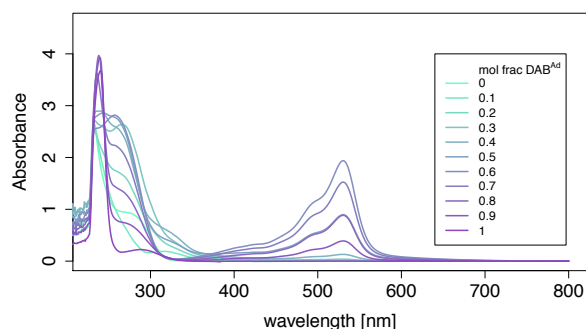
Figure 6.2: Measured spectra for the Job plots for DAB^{Ad} and [Cu(NCMe)$_4$] (BF$_4$) with a total concentration of 600 μм at room temperature in DCM.

Procedure for the titration experiments in MeCN

[Cu(NCMe)$_4$](BF$_4$) (23.6 mg, 75 μmol) was dissolved in a volumetric flask in degassed MeCN (10 mL) from which 1.33 mL were further diluted in 25 mL of degassed MeCN to give a 400 μм solution in [Cu(NCMe)$_4$](BF$_4$). DAB^{Ad} (38.9 mg, 0.12 mmol) was dissolved in a volumetric flask in degassed MeCN (10 mL), from which solutions 1.2, 0.8, and 0.4 mм were prepared by dissolving 1.00, 0.66, and 0.33 mL in 10 mL MeCN, respectively. Appropriate DAB^{Ad} concentrations were prepared by further dilution with degassed MeCN directly in the UV/Vis cuvette. To the final solution of DAB^{Ad} the exact same volume of the [Cu(NCMe)$_4$](BF$_4$) solution was added. The absorptions at 398 and 525 nm (Table 6.6) were then plotted against the equivalents of DAB^{Ad} (Figure 1.27 and Figure 1.28).

Procedure for the Job experiments in MeCN

[Cu(NCMe)$_4$](BF$_4$) (23.6 mg, 75 μmol) and DAB^{Ad} (24.3 mg, 75 μmol) were dissolved separately in degassed MeCN (10 mL) in two volumetric flasks. From these solutions, 1.33 mL were further diluted in 25 mL of degassed MeCN to obtain 400 μм solutions of [Cu(NCMe)$_4$](BF$_4$) and DAB^{Ad}. These solutions were mixed in the required ratios in a UV/Vis cuvette before measurement and shown in Figure 6.3 and Table 6.7. Absorptions at 398 and 525 nm were used for the Job plots (Figure 1.28).

6.6.3 Calculation of Extinction Coefficients

To obtain the extinction coefficient for the heteroleptic [Cu(DAB^{Ad})(NCMe)$_2$] (BF$_4$) complex, solutions with different concentrations (0.06–0.6 mм) were measured by UV/ Vis. Such solutions were prepared by mixing solutions of DAB^{Ad} and [Cu(NCMe)$_4$] (BF$_4$) in degassed MeCN. A large excess of copper source (60 mм, 100–1000 equiv) was used to prevent the formation of the homoleptic complex and indeed no band at 525 nm was observed,

Table 6.6: Absorbances for the titration experiments with [Cu(NCMe)$_4$](BF$_4$)/ DAB^{Ad} in MeCN.

| entry | equiv DAB^{Ad} | Absorbance at given wavelength | |
		398 nm	525 nm
1	0.1	0.02936	0.00191
2	0.13	0.04288	0.00287
3	0.2	0.06636	0.00501
4	0.4	0.13699	0.01621
5	0.6	0.19792	0.03607
6	0.8	0.25121	0.06740
7	1.0	0.28850	0.10877
8	1.2	0.31525	0.14276
9	1.4	0.33254	0.19726
10	1.6	0.34386	0.25269
11	1.8	0.35417	0.30750
12	2.0	0.35581	0.35789
13	2.2	0.36624	0.40524
14	2.4	0.35788	0.45388
15	2.6	0.36361	0.49848
16	2.8	0.36259	0.53762
17	3.0	0.36722	0.58133

Table 6.7: Absorbances for the Job plots with [Cu(NCMe)$_4$](BF$_4$) and DAB^{Ad} in MeCN.

| entry | equiv DAB^{Ad} | Absorbance at given wavelength | |
		398 nm	525 nm
1	0	0.00254	0.001280
2	0.1	0.07557	0.005180
3	0.2	0.15769	0.015920
4	0.3	0.21985	0.029010
5	0.4	0.26507	0.055120
6	0.5	0.28334	0.096449
7	0.6	0.26151	0.147430
8	0.7	0.20967	0.172770
9	0.8	0.14508	0.164260
10	0.9	0.07746	0.106240
11	1.0	0.00529	0.003200

indicating an absence of [Cu(DAB^{Ad})$_2$]$^+$ (Figure 1.29 and Table 6.8). As it was assumed that the initial DAB^{Ad} concentration corresponded to the concentration of the heteroleptic complex, an extinction coefficient for the band at 398 nm of 2191±22 M^{-1} cm^{-1} was calculated (Figure 6.4, R^2 = 0.99)

The extinction coefficient for the homoleptic 2:1 species was obtained by
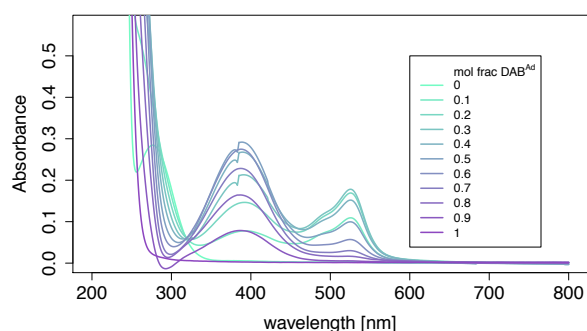
Figure 6.3: Measured spectra for the Job plots for DAB^{Ad} and [Cu(NCMe)$_4$] (BF$_4$) with a total concentration of 400 μм at room temperature in MeCN.

Table 6.8: Absorbance at 398 nm of [Cu(DAB^{Ad})(NCMe)$_2$]$^+$ at different concentrations in MeCN.

entry	conc. (mм)	Absorbance (398 nm)
1	0.06	0.1399635
2	0.12	0.2642659
3	0.18	0.4097864
4	0.30	0.6517899
5	0.36	0.7846707
6	0.60	1.3263407
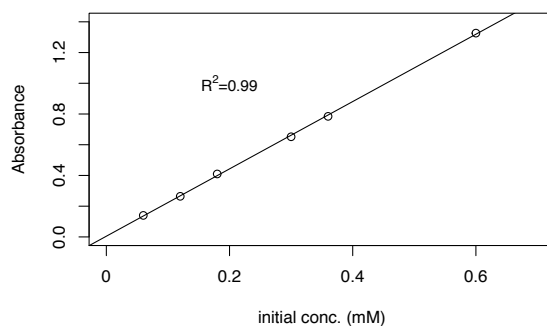
Figure 6.4: Absorbance at 398 nm plotted against total concentration of [Cu (DAB^{Ad})(NCMe)$_2$]$^+$.

preparing different concentrations of the isolated complex ([Cu(DAB^{Ad})$_2$] (BF$_4$) (0.06–0.6 mм) in degassed MeCN. To prevent the formation of the 1:1 species, DAB^{Ad} was added in excess (150–1500 equiv). Since DAB^{Ad} had a low solubility in acetonitrile, DAB^{Ad} was added as solid to each individually prepared solution. The resulting suspensions were stirred at 70 °C for 30 min to increase the solubility of DAB^{Ad}. The prepared solutions were

153

then cooled to room temperature before measurement. The obtained spectra did not show any band at 398 nm, which indicated that no 1:1 species was present (Figure 1.30 and Table 6.9).

Table 6.9: Absorbance at 525 nm of $[Cu(DAB^{Ad})\,(NCMe)_2]^+$ at different concentrations in MeCN.

entry	conc. (mм)	Absorbance (525 nm)
1	0.06	0.4166266
2	0.12	0.7448498
3	0.18	1.1049199
4	0.30	2.0093341
5	0.36	2.4101517
6	0.60	4.4122004

As no 1:1 species was present, it was assumed the concentration of $[Cu(DAB^{Ad})_2](BF_4)$ remained constant. The extinction coefficient for the band at 525 nm was then calculated to be $7448\pm255\,M^{-1}\,cm^{-1}$ (Figure 6.5).
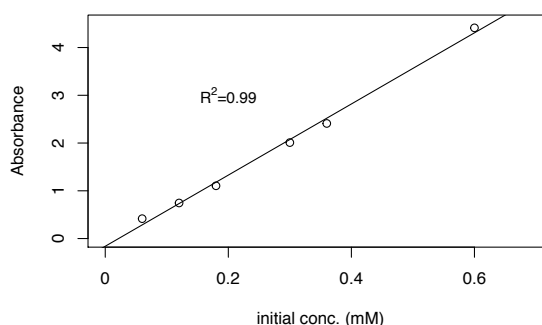
Figure 6.5: Absorbance at 525 nm plotted against total concentration of $[Cu(DAB^{Ad})(NCMe)]^+$.

6.6.4 Calculation of the Equilibrium Constant

With the obtained extinction coefficients for the hetero- and homoleptic species, it was possible to calculate the actual concentration of each species from the dilution experiments of $[Cu(DAB^{Ad})_2](BF_4)$ (Figure 6.6 and Table 6.10). These concentrations made it possible to calculate the binding constant k. The equilibrium was described as:

$$[Cu(DAB)] + [DAB] \overset{k}{\rightleftharpoons} [Cu(DAB)_2] + 2\,[MeCN] \tag{6.1}$$
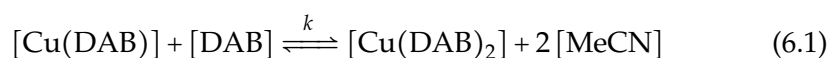
where [Cu(DAB)] represents [Cu(DAB^{Ad})(NCMe)$_2$]$^+$, [Cu(DAB)$_2$] [Cu(DAB^{Ad})$_2$]$^+$, [DAB] the free ligand, and [MeCN] the free solvent. The equilibrium constant was therefore described as

$$k = \frac{[Cu(DAB)_2][MeCN]^2}{[Cu(DAB)][DAB]} \tag{6.2}$$

The concentration of [Cu(DAB)] and [Cu(DAB)$_2$] were known experimentally whereas [DAB] was calculated with the following term:

$$[DAB] = 2([Cu(DAB)_2]_{initial} - [Cu(DAB)_2] - [Cu(DAB)]) + [Cu(DAB)] \tag{6.3}$$

Using these terms, the equilibrium constant k could be calculated to be 502427 ± 23361.
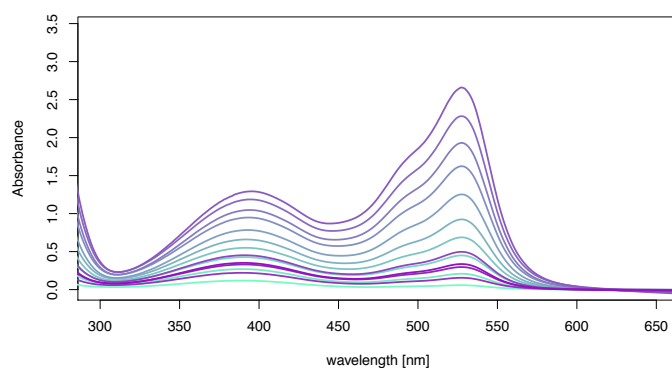
Figure 6.6: Absorbance of [Cu(DAB^{Ad})$_2$](BF$_4$) at different concentrations in MeCN.

Table 6.10: Calculated concentrations for 1:2 and 1:1 complexes, free ligand, and the equilibrium constant k.

	[Cu(DAB)$_2$]$_{initial}$	Abs 398 nm	[Cu(DAB)]	Abs 525 nm	[Cu(DAB)$_2$]	[DAB]	k
1	0.087	0.1153321	0.053	0.0580811	0.008	0.106	512865
2	0.145	0.2152029	0.098	0.1545429	0.021	0.151	514591
3	0.174	0.2638298	0.120	0.2071598	0.028	0.172	491691
4	0.203	0.3244156	0.148	0.2947056	0.040	0.179	546983
5	0.232	0.3446856	0.157	0.3339556	0.045	0.217	480714
6	0.261	0.4201880	0.192	0.4462680	0.060	0.211	543387
7	0.290	0.4445413	0.203	0.4934713	0.066	0.245	488554
8	0.348	0.5426857	0.248	0.6824657	0.092	0.266	510655
9	0.435	0.6522409	0.298	0.9165209	0.123	0.327	463621
10	0.522	0.7774151	0.355	1.2426151	0.167	0.356	483794
11	0.609	0.9424713	0.430	1.6106513	0.216	0.356	517298
12	0.697	1.0424690	0.478	1.9157090	0.257	0.403	491941
13	0.784	1.1824847	0.540	2.2668247	0.304	0.419	493639
14	0.871	1.2899500	0.589	2.6334200	0.354	0.445	494249

6.7 Preparation of Copper ImPy Complexes

General procedure for [Cu(ImPy)] preparation

$Cu(OTf) \cdot (C_7H_8)_{0.5}$ (1 equiv) and $ImPy^R$ (2 equiv) were suspended in dry, degassed toluene (~0.1 M) under N_2 atmosphere and stirred at room temperature for 16 h. The reaction mixture was then filtered and the precipitate was washed with toluene and dried under reduced pressure to obtain $[Cu(ImPy^R)_2](OTf)$ as a brown solid.

Bis(2-(adamantyliminomethyl)pyridine)copper(I) trifluoromethanesulfonate [Cu(ImPy^{Ad})$_2$](OTf)
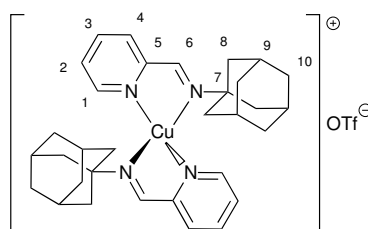
From $Cu(OTf) \cdot (C_7H_8)_{0.5}$ (126 mg, 0.5 mmol), $ImPy^{Ad}$ (241 mg, 1.0 mmol), and toluene (5 mL) and following the general procedure, $[Cu(ImPy^{Ad})_2](OTf)$ was isolated as a brown solid (290 mg, 84%). Single crystals suitable for X-ray diffraction were grown from DCM/petroleum ether.

Mp: 211 °C.

^{1}H NMR (400 MHz, CDCl$_3$): δ 8.70 (s, 2H, H^6), 8.39 (d, J = 4.2 Hz, 2H, H^1), 8.04–8.08 (m, 2H, H^3), 7.96–7.98 (m, 2H, H^4), 7.60 (dd, J = 6.2; 5.7 Hz, 2H, H^2), 2.14 (s, 6H, H^9), 1.84–1.64 (m, 24H, H^{8,10}).

^{13}C{^{1}H} NMR (101 MHz, CDCl$_3$): δ 156.2 (C^6), 151.4 (C^5), 148.5 (C^1), 138.4 (C^3), 127.9 (C^2), 127.7 (C^4), 60.1 (C^7), 43.8 (C^9), 35.9 (C^{10}), 29.3 (C^9).

^{19}F NMR (377 MHz, CDCl$_3$): δ -77.9 (s).

IR: 2905, 2851, 1647 (C=N st), 1593, 1519, 1474, 1441, 1372, 1263, 1222, 1138, 1102, 1087, 1030, 984, 1050, 771, 743, 697 cm^{-1}.

HRMS calcd for $C_{32}H_{40}N_4Cu$ 543.2549, found 543.2545 ([Cu(ImPy^{Ad})$_2$]$^+$.

Bis(2-(4-methoxyphenyliminomethyl)pyridine)copper(I) trifluoromethanesulfonate [Cu(ImPy^{Anis})$_2$](OTf)
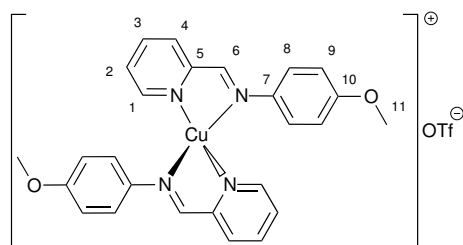
From Cu(OTf)·(C$_7$H$_8$)$_{0.5}$ (126 mg, 0.5 mmol), ImPy^{Anis} (213 mg, 1.0 mmol), and toluene (5 mL) and following the general procedure, [Cu(ImPy^{Anis})$_2$] (OTf) was isolated as a black solid (142 mg, 45%).

Mp: 120 °C.

^{1}H NMR (400 MHz, CDCl$_3$): δ 9.46 (s, 2H, H^6), 8.76–8.75 (m, 2H, H^1), 8.33–8.27 (m, 4H, H^{3,4}), 7.85–7.82 (m, 2H, H^2), 7.65 (d, J = 8.4 Hz, 4H, H^8), 6.94 (d, J = 8.4 Hz, 4H, H^9), 3.80 (s, 6H, H^{11}).

^{13}C{^{1}H} NMR could not be measured due to low solubility of the title compound in acetone-d6, CDCl$_3$, CD$_3$CN, or DMSO–d$_6$.

^{19}F NMR (377 MHz, CDCl$_3$): δ -77.8 (s).

IR: 2937, 2841, 2015, 1596 (C=N st), 1506, 1466, 1444, 1363, 1246, 1223, 1152, 1112, 1055, 1026, 833, 772, 744, 718 cm^{-1}.

HRMS calcd for C$_{28}$H$_{24}$N$_4$CuO$_2$ 487.1195, found 487.1193 ([Cu(ImPy^{Anis})$_2$]$^+$).

Bis(2-(2,6-bis(1-methylethyl)phenyliminomethyl)pyridine)copper(I) trifluoromethanesulfonate [Cu(ImPy^{DIPP})$_2$](OTf)
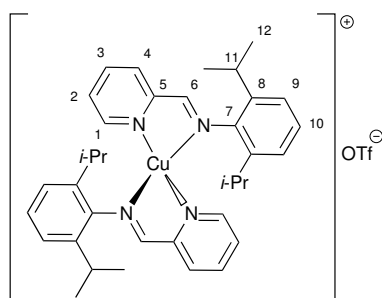
From Cu(OTf)·(C$_7$H$_8$)$_{0.5}$ (126 mg, 0.5 mmol), ImPy^{DIPP} (266 mg, 1.0 mmol), and toluene (5 mL) and following the general procedure, [Cu(ImPy^{DIPP})$_2$] (OTf) was isolated as a brown solid (356 mg, 96%). Single crystals suitable for X-ray diffraction were grown from DCM/petroleum ether.

Mp: 239 °C.

¹H NMR (400 MHz, CDCl₃): δ 8.58–8.49 (m, 2H, H^1), 8.47–8.42 (m, 2H, H^6), 8.23 (s, 2H, H^3), 8.15–7.98 (m, 2H, H^4), 7.87 (br. s, 2H, H^2), 7.22–7.03 (m, 6H, H^{9,10}), 2.87 (br. s, 4H, H^{11}), 1.11 (br. s, 12H, H^{12}), 0.53 (br. s, 12H, H$^{12'}$).

¹H NMR (400 MHz, acetone–d₆): 8.90 (s, 2H, H^1), 8.80 (t, J = 1.7 Hz, 2H, H^6), 8.39–8.30 (m, 4H, H^{2,3}), 7.99–7.96 (m, 2H, H$^4$), 7.17 (s, 6H, H^{9,10}), 3.09–3.03 (m, 4H, H^{11}), 1.11 (d, J = 0.7 Hz, 12H, H^{12}), 0.59 (d, J = 0.7 Hz, 12H, H$^{12'}$).

¹³C{¹H} NMR (101 MHz, acetone–d₆): δ 164.6 (C^6), 150.1 (C^5), 149.2 (C^1), 145.6 (C^7), 139.2 (C^8), 138.8 (C^3), 129.5 (C^2), 128.5 (C^4), 126.6 (C^9), 123.6 (C^{10}), 68.3 (C^{11}), 27.7 (C^{12}).

¹⁹F NMR (377 MHz, acetone–d₆): δ -77.9 (s).

IR: 2960, 2868, 1637, 1616, 1602, 1590, 1564, 1463, 1446, 1387, 1365, 1310, 1271, 1254, 1223, 1209, 1156, 1101, 1029, 1015, 935, 910, 779, 759, 752, 708 cm^{-1}.

HRMS calcd for C$_{36}$H$_{44}$N$_4$Cu 595.2862, found 595.2834 ([Cu(ImPy^{DIPP})$_2$]$^+$).

Bis(2-(2,4,6-trimethylphenyliminomethyl)pyridine)copper(I) trifluoromethanesulfonate [Cu(ImPy^{Mes})₂](OTf)
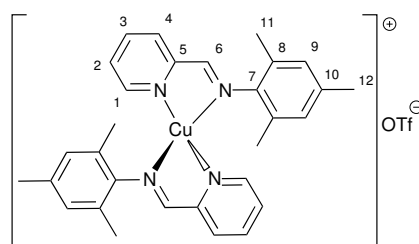
From Cu(OTf)·(C₇H₈)$_{0.5}$ (126 mg, 0.5 mmol), ImPy^{Mes} (264 mg, 1.0 mmol), and toluene (5 mL) and following the general procedure, [Cu(ImPy^{Mes})$_2$](OTf) was isolated as a brown solid (220 mg, 67%).

Mp: 219 °C.

¹H NMR (400 MHz, CDCl₃): δ 8.69–8.68 (m, 2H, H^1), 8.40 (s, 2H, H^6), 8.18–8.14 (m, 2H, H^3), 7.96–7.95 (m, 2H, H^4), 7.86–7.83 (m, 2H, H^2), 6.78 (s, 4H, H^9), 2.25 (s, 6H, H^{12}), 1.75 (s, 12H, H^{11}).

¹H NMR (400 MHz, acetone–d₆): δ 8.91 (d, J = 5.0 Hz, 2H, H^1), 8.81 (s, 2H, H^6), 8.35 (t, J = 7.3 Hz, 2H, H^3), 8.21 (d, J = 7.7 Hz, 2H, H^4), 7.97 (t, J = 5.0 Hz, 2H, H^2), 6.87 (s, 4H, H^9), 2.26 (s, 6H, H^{12}), 1.83 (s, 12H, H^{11}).

¹³C{¹H} NMR (101 MHz, acetone–d₆): δ 164.2 (C^6), 150.5 (C^5), 149.5 (C^1), 145.4 (C^7), 138.8 (C^3), 135.2 (C^8), 129.4 (C^{10}), 128.8 (C^9), 128.0 (C^2), 118.7 (C^4), 19.9 (C^{12}), 17.0 (C^{11}).

¹⁹F NMR (377 MHz, acetone–d₆): δ -78.1 (s).

IR: 2916, 1622, 1592, 1565, 1482, 1442, 1377, 1301, 1256, 1222, 1202, 1161, 1143, 1028, 958, 934, 905, 848, 793, 766 cm^{-1}.

HRMS calcd for C$_{30}$H$_{32}$N$_4$Cu 511.1917, found 511.1936 ([Cu(ImPy^{Mes})$_2$]$^+$).

6.8 Preparation of Azide Substrates

General procedure for the preparation of aryl azides

To an ice/water bath cooled solution of aniline (1 equiv) in water (0.3 M) concentrated hydrochloric acid was added followed by a slow addition of a solution of sodium nitrite (1.5 equiv) in water (0.2 M). The reaction mixture was stirred at 0 °C for 30 min before adding dropwise a solution of NaN_3 (1.5 equiv) in H_2O (0.2 M). After stirring at room temperature for 1 h, the reaction mixture was extracted with Et_2O (3×50 mL). The combined organic phases were dried over $MgSO_4$, filtered, and concentrated under reduced pressure to give the corresponding, pure azide.

1-Azido-4-nitrobenzene (3a)
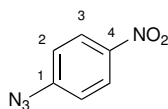
Following the general procedure 4-nitroaniline (2.49 g, 18.3 mmol), hydrochloric acid (3.5 mL) in water (13 mL), $NaNO_2$ (1.39 g, 20.0 mmol) in H_2O (20 mL), and NaN_3 (1.2 g, 18.5 mmol) in H_2O (10 mL), **3a** was obtained as a yellow solid (2.29 g, 74%). Spectroscopic data were consistent with previously reported data for this compound.[199]

^{1}H NMR (400 MHz, CDCl$_3$): δ 8.27 (d, J = 9.2 Hz, 2H, H^3), 7.16 (d, J = 9.2 Hz, 2H, H^2).

^{13}C\{^{1}H\} NMR (101 MHz, CDCl$_3$): δ 146.9 (C^1), 144.6 (C^4), 125.6 (C^3), 119.4 (C^2).

1-Azido-3-nitrobenzene (3b)
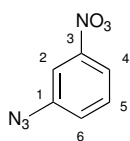
Following the general procedure 3-nitroaniline (0.69 g, 5.0 mmol), hydrochloric acid (0.4 mL) in water (50 mL), $NaNO_2$ (0.35 g, 5.0 mmol) in H_2O (10 mL), and NaN_3 (0.39 g, 18.5 mmol) in H_2O (10 mL), **3b** was obtained as a brown solid (0.57 g, 69%). Spectroscopic data were consistent with previously reported data for this compound.[199]

^{1}H NMR (400 MHz, CDCl$_3$): δ 8.04–8.01 (m, 1H, H^4), 7.92 (t, J = 2.1 Hz, 1H, H^2), 7.56 (dd, J = 8.1; 8.1 Hz, 1H, H^5), 7.37 (dd, J = 8.1; 2.1 Hz, 1H, H^6).

^{13}C{^{1}H} NMR (101 MHz, CDCl$_3$): δ 149.3 (C^3), 142.1 (C^1), 130.7 (C^5), 125.0 (C^2), 119.8 (C^4), 114.2 (C^6).

1-Azido-2-nitrobenzene (3c)
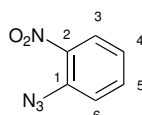
Following the general procedure 2-nitroaniline (2.76 g, 20.0 mmol), hydrochloric acid (2.5 mL) in water (100 mL), NaNO$_2$ (2.07 g, 30.0 mmol) in H$_2$O (20 mL), and NaN$_3$ (1.95 g, 30.0 mmol) in H$_2$O (20 mL), **3c** was obtained as a brown solid (2.99 g, 91%). Spectroscopic data were consistent with previously reported data for this compound.[200]
^{1}H NMR (400 MHz, CDCl$_3$): δ 7.95 (d, J = 8.0 Hz, 1H, H^3) 7.67–6.63 (m, 1H, H^4), 7.36 (d, J = 8.0 Hz, 1H, H^6), 7.30–7.25 (m, 1H, H^5).
^{13}C{^{1}H} NMR (101 MHz, CDCl$_3$): δ 140.9 (C^1), 134.8 (C^2), 134.1 (C^3), 126.2 (C^5), 125.0 (C^6), 120.9 (C^4).

4-Azidobenzonitrile (3d)
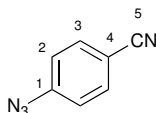
Following the general procedure 4-aminobenzonitrile (3.5 g, 30.0 mmol), hydrochloric acid (5 mL) in water (120 mL), NaNO$_2$ (3.11 g, 45.0 mmol) in H$_2$O (30 mL), and NaN$_3$ (2.93 g, 45.0 mmol) in H$_2$O (30 mL), **3d** was obtained as a grey solid (3.03 g, 71%). Spectroscopic data were consistent with previously reported data for this compound.[201]
^{1}H NMR (400 MHz, CDCl$_3$): δ 7.66 (d, J = 8.0 Hz, 2H, H^3), 7.12 (d, J = 8.0 Hz, 2H, H^2).
^{13}C{^{1}H} NMR (101 MHz, CDCl$_3$): δ 144.9 (C^1), 133.9 (C^3), 119.4 (C^2), 118.4 (C^5), 108.3 (C^4).

4-Azidoacetophenone (3e)
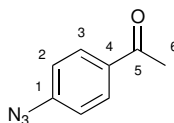
Following the general procedure 4-aminoacetophenone (3.0 g, 22.2 mmol), hydrochloric acid (3.7 mL) in water (80 mL), $NaNO_2$ (2.30 g, 33.3 mmol) in H_2O (15 mL), and NaN_3 (2.16 g, 33.3 mmol) in H_2O (15 mL), **3e** was obtained as an orange solid (3.42 g, 96%). Spectroscopic data were consistent with previously reported data for this compound.[202]

^{1}H NMR (400 MHz, CDCl$_3$): δ 7.95 (d, J = 10.0 Hz, 2H, H^2), 7.08 (d, J = 10.0 Hz, 2H, H^3), 2.58 (s, 3H, H^6).

^{13}C{^{1}H} NMR (101 MHz, CDCl$_3$): δ 196.5 (C^5), 144.9 (C^1), 133.8 (C^4), 130.3 (C^3), 119.0 (C^2), 26.5 (C^6).

Methyl 4-azidobenzoate (3f)
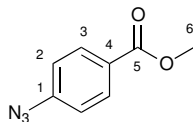
Following the general procedure methyl 4-aminobenzoate (0.64 g, 4.2 mmol), hydrochloric acid (0.8 mL) in water (7 mL), $NaNO_2$ (0.35 g, 5.0 mmol) in H_2O (2 mL), and NaN_3 (0.3 g, 4.6 mmol) in H_2O (2 mL), **3f** was obtained as a pale pink solid (0.70 g, 94%). Spectroscopic data were consistent with previously reported data for this compound.[203]

^{1}H NMR (400 MHz, CDCl$_3$): δ 8.03 (d, J = 8.6 Hz, 2H, H^3), 7.07 (d, J = 8.6 Hz, 2H, H^2), 3.94 (s, 3H, H^6).

^{13}C{^{1}H} NMR (101 MHz, CDCl$_3$): δ 166.4 (C^5), 144.9 (C^1), 131.5 (C^4), 126.8 (C^3), 119.0 (C^2), 52.3 (C^6).

1-Azido-3,5-bis(trifluoromethyl)benzene (3g)
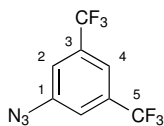
Following the general procedure 3,5-bis(trifluoromethyl)aniline (4.58 g, 20 mmol), hydrochloric acid (5 mL) in water (31 mL), $NaNO_2$ (2.07 g, 30.0 mmol) in H_2O (10 mL), and NaN_3 (1.95 g, 30.0 mmol) in H_2O (10 mL), **3g** was obtained as a yellow solid (3.73 g, 73%). Spectroscopic data were consistent with previously reported data for this compound.[204]

^{1}H NMR (400 MHz, CDCl$_3$): δ 7.64 (s, 1H, H^4), 7.44 (s, 2H, H^2).

^{13}C{^{1}H} NMR (101 MHz, CDCl$_3$): δ 142.4 (C^1), 133.6 (q, J = 31.8 Hz, C^3), 124.1 (q, J = 271.3 Hz, C^2), 119.1 (q, J = 4.5 Hz, C^5), 118.2 (dt, J = 8.1; 4.4 Hz, C^4).

^{19}F NMR (377 MHz, CDCl$_3$): δ -63.4 (s).

1-Azido-4-(trifluoromethyl)benzene (3h)
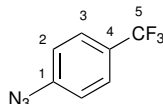
Following the general procedure 4-(trifluoromethyl)aniline (2.0 g, 12.4 mmol), hydrochloric acid (3.3 mL) in water (75 mL), $NaNO_2$ (1.28 g, 18.6 mmol) in H_2O (15 mL), and NaN_3 (1.21 g, 18.6 mmol) in H_2O (15 mL), **3h** was obtained as a green oil (2.98 g, 79%). Spectroscopic data were consistent with previously reported data for this compound.[205]

^{1}H NMR (400 MHz, CDCl$_3$): δ 7.59 (d, J = 8.0 Hz, 2H, H^2), 7.06 (d, J = 8.0 Hz, 2H, H^3).

^{13}C{^{1}H} NMR (101 MHz, CDCl$_3$): δ 143.7 (C^1), 127.0 (q, J = 3.7 Hz, C^4), 126.9 (q, J = 272.1 Hz, C^2), 122.6 (q, J = 35.2 Hz, C^3), 119.2 (C^5).

^{19}F NMR (377 MHz, CDCl$_3$): δ -62.3 (s).

1-Azido-4-chlorobenzene (3i)
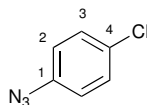
Following the general procedure 4-chloroaniline (3.83 g, 30.0 mmol), hydrochloric acid (5.0 mL) in water (50 mL), $NaNO_2$ (3.11 g, 45 mmol) in H_2O (10 mL), and NaN_3 (2.93 g, 45 mmol) in H_2O (10 mL), **3i** was obtained as a yellow oil (2.46 g, 68%). Spectroscopic data were consistent with previously reported data for this compound.[206]

^{1}H NMR (400 MHz, CDCl$_3$): δ 7.30 (ddd, J = 8.0; 4.0; 4.0 Hz, 2H, H^2), 6.96 (ddd, J = 8.0; 4.0; 4.0 Hz, 2H, H^3).

^{13}C{^{1}H} NMR (101 MHz, CDCl$_3$): δ 138.7 (C^1), 130.2 (C^4), 129.8 (C^2), 120.3 (C^3).

1-Azido-4-bromobenzene (3j)
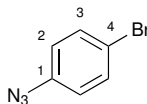
Following the general procedure 4-bromoaniline (3.0 g, 17.4 mmol), hydrochloric acid (2.9 mL) in water (100 mL), $NaNO_2$ (1.80 g, 26.1 mmol) in H_2O

(25 mL), and NaN_3 (1.70 g, 26.1 mmol) in H_2O (25 mL), **3j** was obtained as a yellow solid (2.48 g, 72%). Spectroscopic data were consistent with previously reported data for this compound.[207]

^{1}H NMR (400 MHz, CDCl$_3$): δ 7.43 (ddd, J = 10.0; 4.0; 4.0 Hz, 2H, H^2), 6.86 (ddd, J = 10.0; 4.0; 4.0 Hz, 2H, H^3).

^{13}C{^{1}H} NMR (101 MHz, CDCl$_3$): δ 139.1 (C^1), 132.7 (C^3), 120.6 (C^2), 117.7 (C^4).

1-Azido-4-iodobenzene (3k)
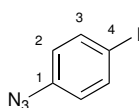
Following the general procedure 4-iodoaniline (3.65 g, 16.7 mmol), hydrochloric acid (2.7 mL) in water (37 mL), $NaNO_2$ (1.73 g, 25.1 mmol) in H_2O (15 mL), and NaN_3 (1.63 g, 25.1 mmol) in H_2O (15 mL), **3k** was obtained as an orange solid (1.97 g, 49%). Spectroscopic data were consistent with previously reported data for this compound.[208]

^{1}H NMR (400 MHz, CDCl$_3$): δ 7.63 (ddd, J = 8.0; 4.0; 4.0 Hz, 2H, H^2), 6.80 (ddd, J = 8.0; 4.0; 4.0 Hz, 2H, H^3).

^{13}C{^{1}H} NMR (101 MHz, CDCl$_3$): δ 140.0 (C^1), 138.7 (C^3), 121.1 (C^2), 88.2 (C^4).

1-Azido toluene (3l)
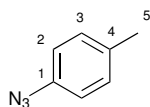
Following the general procedure *p*-toluidine (3.0 g, 28.0 mmol), hydrochloric acid (2.4 mL) in water (25 mL), $NaNO_2$ (2.90 g, 42.0 mmol) in H_2O (10 mL), and NaN_3 (2.73 g, 42.0 mmol) in H_2O (10 mL), **3l** was obtained as a yellow solid (2.98 g, 79%). Spectroscopic data were consistent with previously reported data for this compound.[209]

^{1}H NMR (400 MHz, CDCl$_3$): δ 7.14 (d, J = 8.0 Hz, 2H, H^2), 6.91 (d, J = 8.0 Hz, 2H, H^3), 2.31 (s, 3H, H^5).

^{13}C{^{1}H} NMR (101 MHz, CDCl$_3$): δ 137.2 (C^1), 134.6 (C^4), 130.4 (C^2), 118.9 (C^3), 20.9 (C^5).

1-Azido-4-methoxybenzene (3m)
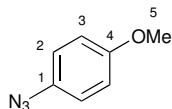
Following the general procedure 4-methoxyaniline (2.48 g, 20.1 mmol), hydrochloric acid (3.5 mL) in water (30 mL), $NaNO_2$ (1.39 g, 20.1 mmol) in H_2O (10 mL), and NaN_3 (1.31 g, 20.1 mmol) in H_2O (10 mL), **3m** was obtained as a yellow solid (2.21 g, 74%). Spectroscopic data were consistent with previously reported data for this compound.[210]

^{1}H NMR (400 MHz, CDCl$_3$): δ 6.98 (d, J = 9.2 Hz, 2H, H^2), 6.91 (d, J = 9.2 Hz, 2H, H^3), 3.82 (s, 3H, H^5).

^{13}C{^{1}H} NMR (101 MHz, CDCl$_3$): δ 157.0 (C^4), 132.3 (C^1), 120.0 (C^2), 115.1 (C^3), 55.5 (C^5).

Methyl 3-azidothiophene-2-carboxylate (3n)
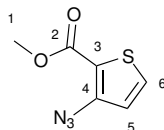
Following the general procedure methyl-3-aminoothiophene-2-carboxylate (3.15 g, 20.0 mmol), hydrochloric acid (3.3 mL) in water (30 mL), $NaNO_2$ (2.07 g, 30.0 mmol) in H_2O (10 mL), and NaN_3 (1.95 g, 30.0 mmol) in H_2O (10 mL), **3n** was obtained as a yellow solid (3.63 g, 99%). Spectroscopic data were consistent with previously reported data for this compound.[211]

^{1}H NMR (400 MHz, CDCl$_3$): δ 7.49 (d, J = 4.0 Hz, 1H, H^6), 6.93 (d, J = 4.0 Hz, 1H, H^5), 3.88 (s, 3H, H^1).

^{13}C{^{1}H} NMR (101 MHz, CDCl$_3$): δ 161.3 (C^2), 142.2 (C^4), 131.2 (C^3), 122.1 (C^6), 117.1 (C^5), 52.1 (C^1).

4-Azidopyridine (3o)
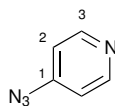
The pH of a solution of 4-chloropyridine hydrochloride (1.00 g, 6.7 mmol) in H_2O (5 mL) was adjusted with aqueous NaOH (0.1 M) to pH 7 before

adding EtOH (5 mL) and NaN$_3$ (0.870 g, 13.3 mmol). The reaction mixture was heated under reflux for 4 h, cooled to room temperature and concentrated under reduced pressure. The resulting mixture was extracted with Et$_2$O (2×20 mL) and the combined organic phases were dried over MgSO$_4$, filtered, and concentrated under reduced pressure to give **3o** as an orange oil (0.67 g, 83%). Spectroscopic data were consistent with previously reported data for this compound.[212]

^{1}H NMR (400 MHz, CDCl$_3$): δ 8.47 (d, J = 5.6 Hz, 2H, H^3), 6.92 (d, J = 5.6 Hz, 2H, H^2).

^{13}C{^{1}H} NMR (101 MHz, CDCl$_3$): δ 150.7 (C^3), 148.8 (C^1), 114.1 (C^2).

4-Azido-7-nitrobenzo[c][1,2,5]oxadiazole (3p)
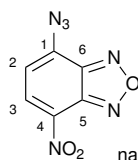
To a solution of NaN$_3$ (584 mg, 9.04 mmol) in a mixture of H$_2$O (28 mL) and acetone (28 mL) a solution of nitrobenzoxadaizole (600 mg, 3.0 mmol) in acetone (28 mL) was added dropwise. The resulting mixture was stirred for 15 min at room temperature before removing acetone under reduced pressure The formed brown precipitate was collected, washed with H$_2$O (3×20 mL) and dried under reduced pressure to give **3p** as a brown solid (260 mg, 42%). Spectroscopic data were consistent with previously reported data for this compound.[96]

^{1}H NMR (400 MHz, CDCl$_3$): δ 8.51 (d, J = 8.1 Hz, 1H, H^3) 7.06 (d, J = 8.1 Hz, 1H, H^2).

^{13}C{^{1}H} NMR (101 MHz, CDCl$_3$): δ 145.8 (C^4), 143.5 (C^5), 138.1 (C^6), 132.4 (C^1), 132.2 (C^3), 114.9 (C^2).

6.9 Aniline Formation by [Cu(DAB)] Reduction

General procedure for the reduction of aryl azides

In a microwave vial azide (0.5 mmol) and [Cu(DAB^{DMA})$_2$](BF$_4$) (10 mol %) were suspended in a microwave vial in a solution of toluene/water (1:2, 0.33 and 0.66 mL) and sealed using a crimped cap. This mixture was heated to 100 °C for 18 h before being cooled and filtered through celite and washed with EtOAc. The organic phase was washed with saturated, aqueous EDTA (3×10 mL), dried over MgSO$_4$, filtered, and concentrated under reduced pressure. Reported yields are isolated yields and are the average of at least two independent runs

4-Nitroaniline (4a)
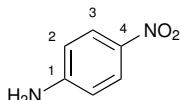
Following the general procedure, from azide **3a** (82 mg, 0.5 mmol) **4a** was isolated after purification by column chromatography (silica, PE/EtOAc = 1:2, R_f = 0.3) as a brown solid (60 mg, 89%). Spectroscopic data were consistent with previously reported data for this compound.[213]
^{1}H NMR (400 MHz, CDCl$_3$): δ 8.10 (d, J = 9.0 Hz, 2H, H^3), 6.65 (d, J = 9.0 Hz, 2H, H^2), 4.41 (s, 2H, NH$_2$).
^{13}C{^{1}H} NMR (101 MHz, CDCl$_3$): δ 152.5 (C^1), 139.8 (C^4), 126.4 (C^3), 113.4 (C^2).

3-Nitroaniline (4b)
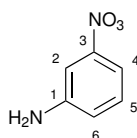
Following the general procedure azide, **3d** (72 mg, 0.5 mmol) **4d** was isolated as a brown solid (39 mg, 65%). Spectroscopic data were consistent with previously reported data for this compound.[214]
^{1}H NMR (400 MHz, CDCl$_3$): δ 7.59–7.56 (m, 1H, H^6), 7.49 (t, J = 8.8 Hz, 1H, H^2), 7.30–7.26 (m, 1H, H^4) 6.96–6.93 (m, 1H, H^5), 4.00 (br. s, 2H, NH$_2$).
^{13}C{^{1}H} NMR (101 MHz, CDCl$_3$): δ 149.3 (C^3), 141.4 (C^1), 129.9 (C^5), 120.6 (C^2), 113.2 (C^4), 109.1 (C^6).

4-Aminobenzonitrile (4d)
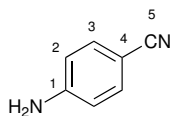
Following the general procedure, azide **3b** (82 mg, 0.5 mmol) **4b** was isolated after purification by column chromatography (silica, PE/EtOAc = 1:2, R_f = 0.2) as a brown solid (63 mg, 91%). Spectroscopic data were consistent with previously reported data for this compound.[215]
^{1}H NMR (400 MHz, CDCl$_3$): δ 7.37 (d, J = 8.1 Hz, 1H, H^2), 6.64 (d, J = 8.1 ,

1H H^3), 3.91 (br. s, 2H, NH$_2$).
^{13}C{^{1}H} NMR (101 MHz, CDCl$_3$): δ 150.6 (C^1), 133.8 (C^2), 120.2 (C^3), 114.4 (C^4), 99.9 (C^5).

4-Aminoacetophenone (4e)
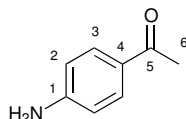
Following the general procedure, from azide **3e** (81 mg, 0.5 mmol **4q** was isolated after purification by column chromatography (silica, PE/EtOAc = 1:1, R$_f$ = 0.3) as an orange solid (25 mg, 16%). Spectroscopic data were consistent with previously reported data for this compound.[213]
^{1}H NMR (400 MHz, CDCl$_3$): δ 7.80 (d, J = 10.0 Hz, 2H, H^2), 6.65 (d, J = 10.0 Hz, 2Hl H^3), 4.17 (br. s, 2H, NH$_2$), 2.51 (s, 3H, H^6).
^{13}C{^{1}H} NMR (101 MHz, CDCl$_3$): δ 196.6 (C^5), 151.3 (C^1), 130.8 (C^3), 127.7 (C^4), 113.7 (C^2), 26.1 (C^6).

Ethyl 4-aminobenzoate (4f)
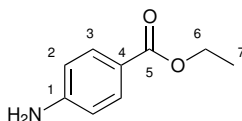
Following the general procedure, from azide **3f** (89 mg, 0.5 mmol) **4r** was isolated after purification by column chromatography (silica, PE/EtOAc = 1:2, R$_f$ = 0.5) as a yellow solid (65 mg, 85%). Spectroscopic data were consistent with previously reported data for this compound.[213]
^{1}H NMR (400 MHz, CDCl$_3$): δ 7.89–7.87 (m, 2H, H^3), 6.67–6.64 (m, 2H, H^2), 4.34 (q, J = 7.1 Hz, 2H, H^6), 4.12 (br. s, 2H, NH$_2$), 1.38 (t, J = 7,1, 3H, H^7).
^{13}C{^{1}H} NMR (101 MHz, CDCl$_3$): δ 166.7 (C^5), 150.8 (C^1), 131.5 (C^3), 120.0 (C^4), 113.8 (C^2), 60.3 (C^6), 14.4 (C^7).

3,5-Bis(trifluoromethyl)aniline (4g)
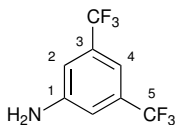
Following the general procedure, from azide **3g** (128 mg, 0.5 mmol) **4g** was isolated after purification by column chromatography (silica, PE/EtOAc = 1:2, R_f = 0.5) as a black oil (26 mg, 23%). Spectroscopic data were consistent with previously reported data for this compound.[216]

¹H NMR (400 MHz, CDCl₃): δ 7.24 (s, 1H, H⁴), 7.06 (s, 2H, H²), 4.10 (s, 2H, NH₂).

¹³C{¹H} NMR (101 MHz, CDCl₃): δ 147.3 (C¹), 132.5 (q, J = 32.9 Hz, C³), 123.4 (q, J = 272.6 Hz, C⁵), 114.1 (q, J = 3.6 Hz, C²), 111.5 (dt, J = 7.9; 4.0 Hz, C⁴).

¹⁹F NMR (377 MHz, CDCl₃): δ -63.3 (s).

4-(Trifluoromethyl)aniline (4h)
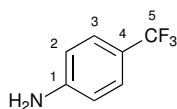
Following the general procedure, from azide **3h** (94 mg, 0.5 mmol) **4h** was isolated after purification by column chromatography (silica, PE/EtOAc = 1:2, R_f = 0.6) as a black oil (54 mg, 64%). Spectroscopic data were consistent with previously reported data for this compound.[213]

¹H NMR (400 MHz, CDCl₃): δ 7.43 (d, J = 8.4 Hz, 2H, H³), 6.71 (d, J = 8.4 Hz, 2H, H²).

¹³C{¹H} NMR (101 MHz, CDCl₃): δ 149.4 (C¹), 126.7 (q, J = 3.9 Hz, C³), 124.9 (q, J = 270.4 Hz, C⁵), 120.1 (q, J = 32.4 Hz, C⁴), 114.2 (C²).

¹⁹F NMR (377 MHz, CDCl₃): δ -61.1 (s).

4-Aminopyridine (4o)
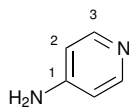
Following the general procedure, from azide **3o** (60 mg, 0.5 mmol) **4o** was isolated after purification by column chromatography (silica, PE/EtOAc/NEt₃ = 1:2:0.02, R_f = 0.3) as a red oil (22 mg, 45%). Spectroscopic data were consistent with previously reported data for this compound.[217]

¹H NMR (400 MHz, DMSO–d₆): δ 7.97 (dd, J = 4.8; 1.5 Hz, 2H, H³), 6.46 (dd, J = 4.8; 1.5 Hz, 2H, H²), 5.99 (s, 2H, NH₂).

¹³C{¹H} NMR (101 MHz, DMSO–d₆): δ 154.6 (C¹), 149.9 (C³), 109.3 (C²).

Methyl-3-azidothiophene-2-carboxylate (4n)
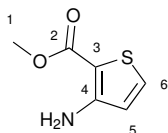
Following the general procedure, from azide **3n** (81 mg, 0.5 mmol) **4n** was isolated after purification by column chromatography (silica, PE/EtOAc = 5:1 R_f = 0.4) as a yellow solid (20 mg, 45%). Spectroscopic data were consistent with previously reported data for this compound.[218]
^{1}H NMR (400 MHz, CDCl$_3$): δ 7.26 (d, J = 8.0 Hz, 1H, H^6), 6.54 (d, J = 8.0 Hz, 1H, H^5) 5.47 (br. s, NH$_2$), 3.83 (s, 3H, H^1).
^{13}C\{^{1}H\} NMR (101 MHz, CDCl$_3$): δ 165.0 (C^2), 154.0 (C^4), 131.5 (C^6), 119.8 (C^5), 101.2 (C^3), 51.2 (C^1).

7-Nitrobenzo[c][1,2,5]oxadiazol-4-amine (4p)
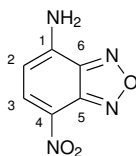
Following the general procedure, from azide **3p** (103 mg, 0.5 mmol) **4p** was isolated as a brown solid (50 mg, 55%). Spectroscopic data were consistent with previously reported data for this compound.[96]
^{1}H NMR (400 MHz, DMSO–d$_6$): δ 8.89 (br. s, 2H, NH$_2$), 8.51 (d, J = 8.8 Hz, 1H, H^3), 6.40 (d, J = 8.8 Hz, 1H, H^1).
^{13}C\{^{1}H\} NMR (101 MHz, DMSO–d$_6$): δ 147.4 (C^4), 144.3 (C^6), 144.1(C^5), 138.0 (C^3), 120.5 (C^1), 102.7 (C^2).

6.10 Preparation of Hydroamination Substrates

2-(Pent-4-yn-1-yl)isoindoline-1,3-dione (7a)
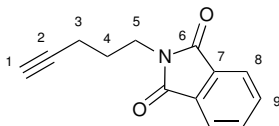
A solution of pent-1-ynyl-5-chloride (5.13 g, 50.0 mmol), phthalimide (8.83 g, 60 mmol), K$_2$CO$_3$ (6.91 g, 50 mmol), and KI (0.100 g, 0.5 mmol) in DMF (50 mL)

was stirred at 70 °C for 16 h. After cooling to room temperature, the reaction mixture was poured onto H_2O (50 mL), and extracted with Et_2O (3×200 mL). The combined organic phases were dried over $MgSO_4$, filtered, and concentrated under reduced pressure. The obtained crude was purified by column chromatography (silica, DCM, R_f = 0.4) to isolate **7a** as a white solid (6.78 g, 64%). Spectroscopic data were consistent with previously reported data for this compound.[158]

^{1}H NMR (400 MHz, CDCl$_3$): δ 7.85–7.89 (m, 2H, H^9), 7.72–7.76 (m, 2H, H^8), 3.82 (t, J = 7.0 Hz, 2H, H^5), 2.30 (td, J = 7.0; 2.7 Hz, 2H, H^3), 1.92–1.99 (m, 3H, H^{1,4}).

^{13}C{^{1}H} NMR (101 MHz, CDCl$_3$): δ 168.3 (C^6), 133.9 (C^9), 132.1 (C^7), 123.2 (C^8), 83.0 (C^2), 69.0 (C^1), 37.1 (C^5), 27.3 (C^3), 16.2 (C^4).

2-(Hex-5-yn-1-yl)isoindoline-1,3-dione (7b)
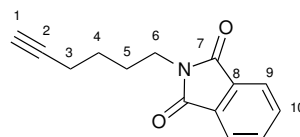
A suspension of 6-chlorohex-1-yne (2.41 g, 20.7 mmol), phthalimide (3.65 g, 24.8 mmole), K_2CO_3 (2.86 g, 20.7 mmol) and KI (41 mg, 0.25 mmol) in DMF (25 mL) was stirred at 70 °C for 17 h. After cooling to room temperature, the reaction was poured onto H_2O (50 mL), extracted with Et_2O (3×100 mL) and The combined organic phases were dried over $MgSO_4$, filtered and concentrated under reduced pressure. The obtained crude was purified by column chromatography (silica, DCM, R_f = 0.5) to obtain **7b** as a white solid (3.16 g, 72%). Spectroscopic data were consistent with previously reported data for this compound.[219]

^{1}H NMR (400 MHz, CDCl$_3$): δ 7.88–7.86 (m, 2H, H^{10}), 7.75–7.73 (m, 2H, H^9), 3.74 (t, J = 7.0 Hz, 2H, H^6), 2.28 (td, J = 7.0; 2.7 Hz, 2H, H^3), 1.97 (t, J = 2.7 Hz, 1H, H^1), 1.88–1.80 (m, 2H, H^5), 1.64–1.59 (m, 2H, H^5).

^{13}C{^{1}H} NMR (101 MHz, CDCl$_3$): δ 168.4 (C^7), 133.9 (C^{10}), 132.1 (C^8), 123.2 (C^9), 83.7 (C^2), 68.8 (C^1), 37.4 (C^6), 27.6 (C^3), 25.6 (C^5), 18.0 (C^4).

Pent-4-yn-1-yl methanesulfonate (10)
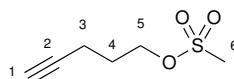
To an ice/water bath cooled solution of 4-pentynol (1 mL, 10.8 mmol) and NEt$_3$ (0.867 mL, 11.8 mmol) in Et_2O (20 mL) methansulfonyl chloride (0.92

mL, 11.8 mmol) was slowly added and the resulting mixture was stirred at room temperature for 1 h. The formed white precipitate was then filtered off and the filtrate was concentrated under reduced pressure to give **10** as a yellow oil (1.60 g, 91 %). The crude product was used without further purification. Spectroscopic data were consistent with previously reported data for this compound.[220]

^{1}H NMR (400 MHz, CDCl$_3$): δ 4.38 (t, J = 6.1 Hz, 2H, H^5), 3.05 (s, 3H, H^6), 2.39 (td, J = 6.8; 2.7 Hz, 2H, H^3), 2.03 (t, J = 2.7 Hz, 1H, H^1), 1.99 (tt, J = 6.8; 6.1 Hz, 2H, H^4).

^{13}C{^{1}H} NMR (101 MHz, CDCl$_3$): δ 69.8 (C^2), 68.3 (C^1), 52.6 (C^5), 37.2 (C^6), 27.8 (C^3), 14.7 (C^4).

5-Azidopent-1-yne (11)
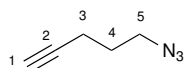
To a solution of sodium azide (0.71 g, 10.9 mmol) in DMF (55 mL) heated at 70 °C pent-4-yn-1-yl methanesulfonate **10** (1.60 g, 9.86 mmol) was added and the resulting mixture was stirred for 3 h. The reaction mixture was cooled to room temperature and water (150 mL) was carefully added (caution, exothermic). This mixture was then extracted with Et$_2$O (4×80 mL), the combined organic phases were washed with water (250 mL) and brine (200 mL), dried over MgSO$_4$, filtered, and concentrated under reduced pressure to obtain **11** as a yellow oil (0.755 g, 70 %). The crude product was used without further purification. Spectroscopic data were consistent with previously reported data for this compound.[159]

^{1}H NMR (400 MHz, CDCl$_3$): δ 3.51 (t, J = 7.0 Hz, 2H, H^5), 2.34 (td, J = 6.9; 2.7 Hz, 2H, H^3), 2.02 (t, J = 2.7 Hz, 1H, H^1), 1.82 (tt, J = 7.0; 6.9 Hz, 2H, H^4).

^{13}C{^{1}H} NMR (101 MHz, CDCl$_3$): δ 82.6 (C^2), 69.3 (C^1), 50.0 (C^5), 27.6 (C^3), 15.7 (C^4).

Hex-5-ynenitrile (12)
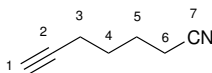
6-Chlorohex-1-yne (3.00 g, 25.7 mmol) and NaCN (1.51 g, 30.9 mmol) were dissolved in DMSO (50 mL) and heated to 80 °C for 16 h. The resulting solution was allowed to cool to room temperature and poured onto H$_2$O (100 mL). The aqueous phase was extracted with EtOAc (3×50 mL) and the combined organic phases were washed with H$_2$O (50 mL), dried over

MgSO$_4$, filtered, and concentrated under reduced pressure to obtain **12** as a colourless oil (2.61 g, 96 %). The crude product was used without further purification. Spectroscopic data were consistent with previously reported data for this compound.[160]

^{1}H NMR (400 MHz, CDCl$_3$): δ 2.41 (t, J = 7.0 Hz, 2H, H^6), 2.28 (td, J = 6.7; 2.7 Hz, 2H, H^3), 2.00 (t, J = 2.7 Hz, 1H, H^1), 1.85–1.79 (m, 1H, H^5), 1.74–1.68 (m, 1H, H^4).

^{13}C{^{1}H} NMR (101 MHz, CDCl$_3$): δ 119.4 (C^7), 83.0 (C^1), 69.3 (C^2), 27.1 (C^6), 24.3 (C^3), 17.7 (C^5), 16.8 (C^4).

Pent-4-yn-1-amine (8a)
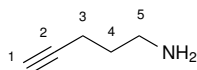
Method 1: Pentynylisoindolinedione **7a** (3.33 g, 15.6 mmol) was suspended in EtOH (70 mL) and N$_2$H$_4$·H$_2$O (2.71 mL, 55.6 mmol) was added to give a clear solution. The reaction mixture was heated at 70 °C for 2 h with vigorous stirring a white precipitate formed over this period. After cooling to room temperature, H$_2$O (50 mL) was added and the pH was adjusted to ~3.5 by addition of aqueous HCl 2 M. The resulting precipitate was filtered off and the aqueous filtrate was concentrated under reduced pressure to give a yellow oil. This oil was cooled down to 0 °C, treated with aqueous NaOH (10 M, 50 mL), and extracted with DCM (3×100 mL). The combined organic phases were dried over MgSO$_4$, filtered and concentrated under reduced pressure. The crude product was purified by *Kugelrohr* distillation (60 °C, 400 mbar) to obtain **8a** as colourless oil (412 mg, 62%). Spectroscopic data were consistent with previously reported data for this compound.[158,159]

Method 2: A solution of 5-azidopent-1-yne **11** (0.76 g, 6.92 mmol) in Et$_2$O (10 mL) was added slowly to a solution of triphenylphosphine (1.82 g, 6.92 mmol) in Et$_2$O (20 mL) at 0 °C. The resulting solution was stirred at room temperature for 2.5 h and concentrated under reduced pressure before adding H$_2$O (50 mL), followed by aqueous HCl (2 M, 3 mL). The resulting mixture was stirred at room temperature for 16 h. The formed white precipitate was filtered off and the filtrate was acidified to pH 1.5 with aqueous HCl 2 M. Water was removed under reduced pressure and the resulting yellow oil was cooled down to 0 °C for the addition of aqueous NaOH (10 M, 20 mL). The mixture was then extracted with DCM (4×30 mL) and the combined organic phases were dried over MgSO$_4$, filtered and concentrated under reduced pressure to give **8a** as a yellow oil (0.344 g, 60 %). Spectroscopic data were consistent with previously reported data for this compound.[158,159]

^{1}H NMR (400 MHz, CDCl$_3$): δ 2.84 (t, J = 6.9 Hz, 2H, H^5), 2.29 (td, J = 7.0;

2.7 Hz, 2H, H^3), 1.98 (t, J = 2.7 Hz, 1H, H^1), 1.69 (tt, J = 7.0; 6.9 Hz, 2H, H^4), 1.35 (br. s, 2H, NH$_2$).

^{1}H NMR (400 MHz, acetone-d6): δ 3.25 (t, J = 6.6 Hz, 2H, H^5), 2.31 (t, J = 2.7 Hz, 1H, H^1), 2.26 (td, J = 7.1; 2.7 Hz, 2H, H^3), 1.77 (tt, J = 7.1; 6.6 Hz, 2H, H^4).

^{1}H NMR (400 MHz, CD$_3$CN): δ 2.69 (t, J = 6.8 Hz, 2H, H^5), 2.24 (td, J = 7.2; 2.7 Hz, 2H, H^3), 2.17 (t, J = 2.7 Hz, 1H, H^1), 1.65 (br. s, 2H, NH$_2$), 1.59 (tt, J = 7.2; 6.8 Hz, 2H, H^4).

^{1}H NMR (400 MHz, C$_6$D$_6$): δ 2.44 (t, J = 6.7 Hz, 2H, H^5), 1.97 (td, J = 7.1; 2.7 Hz, 2H, H^3), 1.75 (t, J = 2.7 Hz, 1H, H^1), 1.31 (tt, J = 7.1, 6.7 Hz, 2H,H^4), 0.71 (br. s, 2H, NH$_2$).

^{1}H NMR (400 MHz, CD$_3$OD-d4): δ 2.75 (t, J = 7.1 Hz, 2H, H^5), 2.28–2.24 (m, 3H, H^{1,3}), 1.68 (t, J = 7.1 MHz, 2H, H^4).

^{1}H NMR (400 MHz, toluene-d8): δ 2.50 (t, J = 6.7 Hz, 2H, H^5), 2.02 (td, J = 7.1; 2.7 Hz, 2H, H^3), 1.78 (t, J = 2.7 Hz, 1H, H^1), 1.36 (tt, J = 7.1; 6.7 Hz, 2H, H^4), 0.50 (br. s, 2H, NH$_2$).

^{13}C{^{1}H} NMR (101 MHz, CDCl$_3$): δ 83.9 (C^2), 68.5 (C^1), 41.0 (C^5), 32.0 (C^3), 15.8 (C^4).

Hex-5-yn-1-amine (8b)
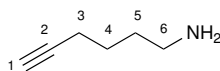
Isoindoline-1,3-dione **7b** (3.93 g, 14.9 mmol) was suspended in EtOH (50 mL), before adding N$_2$H$_4$·H$_2$O (0.80 mL, 16.4 mmol) to give a clear solution. The reaction mixture was heated at 70 °C and stirred for 2 h, a white precipitate formed over this period. After cooling to room temperature and the addition of H$_2$O (25 mL), the pH was adjusted to ~3.5 by addition of aqueous HCl (2 M). The precipitate was filtered off and the aqueous filtrate was concentrated under reduced pressure to give a yellow oil. This oil was cooled down to 0 °C, treated with aqueous NaOH (10 M, 15 mL), and extracted with DCM (3×50 mL). The combined organic phases were dried over MgSO$_4$, filtered, and concentrated under reduced pressure. The crude product was purified by *Kugelrohr* distillation (60 °C, 2 mbar) to obtain **8b** as colourless oil (218 mg, 20%). Spectroscopic data were consistent with previously reported data for this compound.[219]

^{1}H NMR (400 MHz, CDCl$_3$): δ 2.77–2.71 (m, 2H, H^6), 2.28–2.21 (m, 2H, H^3), 1.97 (t, J = 2.7 Hz, 1H, H^1), 1.66–1.55 (m, 4H, H^{4,5}), 1.42–1.26 (br. s, 2H, NH$_2$).

^{13}C{^{1}H} NMR (101 MHz, CDCl$_3$): δ 84.3 (C^2), 68.3 (C^1), 41.7 (C^6), 32.8 (C^3), 25.8 (C^5), 18.2 (C^4).

Hept-6-ynamine (8c)
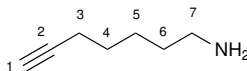
To an ice/water bath cooled suspension of LiAlH$_4$ (1.02 g, 26.8 mmol) in Et$_2$O (200 mL) a solution of nitrile **12** (2.61 g, 24.4 mmol) in Et$_2$O (10 mL) was slowly added. The bath was then removed and the reaction was stirred at room temperature for 3 h before being quenched by addition of aqueous NaOH (10 w/w%, 10 mL) (caution, H$_2$ formation!) until gas stopped evolving. The formed precipitate was filtered off and washed with Et$_2$O (10 mL). The aqueous layer was separated and extracted with Et$_2$O (3×15 mL). The combined organic phases were dried over MgSO$_4$, filtered, and concentrated under reduced pressure to obtain **8c** as a yellow oil (2.54 g, 94 %). Spectroscopic data were consistent with previously reported data for this compound.[221]

^{1}H NMR (400 MHz, CDCl$_3$): δ 2.67 (t, J = 6.8 Hz, 2H, H^7), 2.17 (td, J = 7.0; 2.7 Hz, 2H, H^3), 1.92 (t, J = 2.7 Hz, 1H, H^1), 1.54–1.49 (m, 2H, H^6), 1.45–1.40 (m, 4H, H^{4,5}), 1.31 (s, 2H, NH$_2$).

^{1}H NMR (400 MHz, CD$_3$CN): δ 2.60 (t, J = 6.7 Hz, 2H, H^7), 2.22–2.16 (m, 3H, H^{1,3}), 1.54–1.38 (m, 8H, H$^{2,4-6}$, NH$_2$).

^{13}C{^{1}H} NMR (101 MHz, CDCl$_3$): δ 84.5 (C^2), 68.2 (C^1), 42.0 (C^7), 33.3 (C^3), 28.3 (C^6), 26.0 (C^4), 18.3 (C^5).

1-Chlorohex-4-yne (13a)
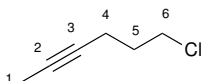
To a solution of 5-chlorohex-1-yne (2.41 mL, 23.5 mmol) in THF (80 mL), *n*-buthyllithium (2.5 M in hexane, 9.8 mL, 24.5 mmol) was slowly added at −78 °C and the resulting mixture was stirred for 1 h. Methyl iodide (1.65 mL, 26.5 mmol) was then added and the reaction was stirred at room temperature for 1 h, before being quenched by addition of H$_2$O (40 mL). The aqueous phase was extracted with Et$_2$O (3×50 mL) and the combined organic phases were washed with brine (50 mL), dried over MgSO$_4$, filtered, and concentrated under reduced pressure to obtain **13a** as a pale yellow oil (1.92 g, 70 %). The crude product was used without further purification. Spectroscopic data were consistent with previously reported data for this compound.[119]

^{1}H NMR (400 MHz, CDCl$_3$): δ 3.67 (t, J = 6.5 Hz, 2H, H^6), 2.34 (tq, J = 6.9; 2.5 Hz, 2H H^4), 1.94 (tt, J = 6.9; 6.5 Hz, 2H, H^5), 1.80 (t, J = 2.5 Hz, 3H, H^1).

^{13}C{^{1}H} NMR (101 MHz, CDCl$_3$): δ 77.2 (C^3), 76.5 (C^2), 43.8 (C^6), 31.7 (C^4), 16.2 (C^5), 3.4 (C^1).

1-Chlorohept-5-yne (13b)
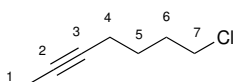
To a solution of 6-chlorohex-1-yne (3.00 g, 25.7 mmol) in Et$_2$O (50 mL), *n*-buthyllithium (2.5 M in hexane, 11.3 mL, 28.2 mmol) was slowly added at –78 °C and the resulting mixture was stirred for 1 h. Methyl iodide (1.80 mL, 29.0 mmol) was then added and the reaction was stirred at room temperature for 1 h, before being quenched by addition of H$_2$O (20 mL). The aqueous phase was extracted with Et$_2$O (3×25 mL) and the combined organic phases were washed with brine (25 mL), dried over MgSO$_4$, filtered, and concentrated under reduced pressure to obtain **13b** as a pale yellow oil (3.07 g, 91 %). The crude product was used without further purification. Spectroscopic data were consistent with previously reported data for this compound.[222]

^{1}**H NMR (400 MHz, CDCl$_3$):** δ 3.31 (t, *J* = 6.8 Hz, 2H, H^7), 2.19 (tq, *J* = 7.0; 2.5 Hz, 2H), 1.79 (t, *J* = 2.5 Hz, 3H, H^1), 1.74–1.68 (m, 2H, H^6), 1.60–1.55 (m, 2H, H^5).

^{13}**C{^{1}H} NMR (101 MHz, CDCl$_3$):** δ 78.3 (C^3), 76.2 (C^2), 51.0 (C^7), 28.0 (C^4), 26.0 (C^6), 18.3 (C^5), 3.4 (C^1).

Hex-4-ynazide (14a)
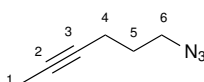
A solution of 6-chlorohex-4-yne **13a** (1.92 g, 16.6 mmol) and NaN$_3$ (1.30 g, 20.0 mmol) in DMSO (45 mL) was heated to 80 °C for 16 h, before being cooled to room temperature and quenched by the addition of H$_2$O (100 mL). The aqueous phase was extracted with Et$_2$O (3×50 mL) and the combined organic phases were washed with H$_2$O (100 mL), dried over MgSO$_4$, filtered, and concentrated under reduced pressure to a volume of 15 mL. Crude azide **14a** was directly used without further purification.

^{1}**H NMR (400 MHz, CDCl$_3$):** δ 3.42 (t, *J* = 6.7 Hz, 2H, H^6), 2.27 (tq, *J* = 6.9; 2.4 Hz, 2H, H^4), 1.81–1.73 (m, 5H, H^{1,5}).

^{13}**C{^{1}H} NMR (101 MHz, CDCl$_3$):** δ 80.1 (C^3), 73.4 (C^2), 50.2 (C^6), 32.4 (C^4), 15.9 (C^5), 3.7 (C^1).

Hept-5-ynazide (14b)
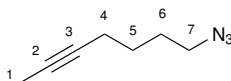
A solution of 7-chlorohept-5-yne **13b** (2.70 g, 20.7 mmol) and NaN_3 (1.61 g, 24.8 mmol) in DMSO (40 mL) was heated to 80 °C for 16 h, before being cooled to room temperature and quenched by the addition of H_2O (100 mL). The aqueous phase was extracted with Et_2O (3×50 mL) and the combined organic phases were washed with H_2O (100 mL), dried over $MgSO_4$, filtered, and concentrated under reduced pressure to a volume of 15 mL. Crude azide **14b** was directly used without further purification. Spectroscopic data were consistent with previously reported data for this compound.[222]

^{1}H NMR (400 MHz, CDCl$_3$): δ 3.31 (t, J = 6.8 Hz, 2H, H^7), 2.18 (tq, J = 7.0; 2.4 Hz, 2H, H^4), 1.79 (t, J = 2.6 Hz, 3H, H^1), 1.76–1.68 (m, 2H, H^6), 1.60–1.53 (m, 2H, H^6).

^{13}C{^{1}H} NMR (101 MHz, CDCl$_3$): δ 79.4 (C^3), 74.9 (C^2), 52.3 (C^7), 32.1 (C^4), 26.8 (C^6), 18.2 (C^5), 3.7 (C^1).

Hept-5-ynnitrile (14c)
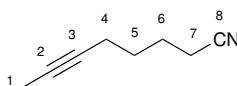
1-Chlorohept-5-yne **13b** (3.06 g, 23.4 mmol) and NaCN (1.38 g, 28.1 mmol) were dissolved in DMSO (45 mL) and heated to 80 °C for 16 h. The resulting mixture was allowed to cool to room temperature before being poured onto H_2O (100 mL). The aqueous phase was extracted with EtOAc (3×50 mL) and the combined organic phases were washed with H_2O (50 mL), dried over $MgSO_4$, filtered, and concentrated under reduced pressure to obtain **14c** as a colourless oil (2.21 g, 78 %). The product crude was used without further purification. Spectroscopic data were consistent with previously reported data for this compound.[223]

^{1}H NMR (400 MHz, CDCl$_3$): δ 2.37 (t, J = 7.1 Hz, 2H, H^8), 2.18 (tq, J = 6.9; 2.4 Hz, 2H, H^4), 1.81–1.74 (m, 5H, H^{1,6}), 1.65–1.57 (m, 2H, H^5).

^{13}C{^{1}H} NMR (101 MHz, CDCl$_3$): δ 119.6 (C^8), 77.7 (C^3), 77.4 (C^2), 27.7 (C^7), 24.4 (C^4), 17.9 (C^6), 16.7 (C^5), 3.4 (C^1).

Hex-4-ynamine (15a)
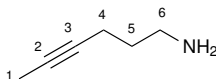
To an ice/water bath cooled solution of crude azide **14a** in Et_2O (50 mL) triphenylphospine (4.79 g, 18.26 mmol) was slowly added and the resulting solution was stirred at room temperature for 1 h before being concentrated under reduced pressure. H_2O (50 mL) was then added and the suspension mixture was stirred at room temperature for 16 h. The formed white precipitate was filtered off and pH was adjusted to 2 before evaporating the solvent. The obtained residue was cooled with an ice/water bath and treated with aqueous NaOH (10 M, 20 mL). The aqueous phase was extracted with Et_2O (3×50 mL) and combined organic phases were dried over $MgSO_4$, filtered, and concentrated under reduced pressure. The crude product was purified by distillation (70 °C, 800 mbar) to give **15a** as a colourless oil (1.16 g, 72 %). Spectroscopic data were consistent with previously reported data for this compound.[119]

^{1}H NMR (400 MHz, CDCl$_3$): δ 2.78 (t, J = 6.9 Hz, 2H, H^6), 2.19 (tq, J = 7.0; 2.5 Hz, 2H, H^4), 1.77 (t, J = 2.5 Hz, 3H, H^1), 1.60 (tt, J = 7.0; 6.9 Hz, 2H, H^5), 1.14 (s, 2H, NH$_2$).

^{13}C{^{1}H} NMR (101 MHz, CDCl$_3$): δ 78.6 (C^3), 75.8 (C^2), 41.3 (C^6), 32.8 (C^4), 16.2 (C^5), 3.5 (C^1).

Hept-5-ynamine (15b)
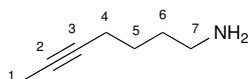
To an ice/water bath cooled suspension of LiAlH$_4$ (0.55 g, 19.5 mmol) in Et_2O (200 mL) a solution of azide **14b** (1.8 g, 13.2 mmol) in Et_2O (20 mL) was slowly added. The reaction mixture was stirred at room temperature for 3 h before being quenched by addition of aqueous KOH (20 w/w%) (caution, H_2 formation!) until gas stopped evolving. The formed grey precipitate was filtered off and washed with Et_2O (15 mL). The aqueous phase was extracted with Et_2O (3×50 mL) and the combined organic phases were washed with brine (50 mL), dried over $MgSO_4$, filtered, and concentrated under reduced pressure to give **15b** as a pale yellow oil (1.23 g, 54%). Spectroscopic data were consistent with previously reported data for this compound.[222]

**^{1}H NMR (400 MHz, CDCl$_3$):** δ 2.71 (br. s, 2H, H^7), 2.14 (tq, J = 6.8; 2.5 Hz, 2H, H^4), 1.77 (t, J = 2.5 Hz, 3H, H^1), 1.56–1.48 (m, 4H, H^{5,6}), 1.08 (s, 2H, NH$_2$).

^{13}C$\{^1$H$\}$ **NMR (101 MHz, CDCl$_3$):** δ 79.0 (C^3), 75.6 (C^2), 41.8 (C^7), 33.1 (C^4), 26.4 (C^6), 18.6 (C^5), 3.4 (C^1).

Oct-6-ynamine (15c)
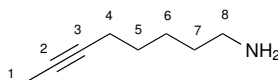
To an ice/water bath cooled suspension of LiAlH$_4$ (1.38 g, 36.3 mmol) in Et$_2$O (100 mL) a solution of nitrile **14c** (2.61 g, 24.4 mmol) in Et$_2$O (10 mL) was slowly added. The reaction mixture was stirred at room temperature for 3 h before being quenched by addition of aqueous NaOH (10 w/w%, 5 mL) (caution, H$_2$ formation!) until gas stopped evolving. The formed precipitate was filtered off and washed with Et$_2$O (10 mL). The aqueous layer was separated and extracted with Et$_2$O (3×15 mL). The combined organic phases were dried over MgSO$_4$, filtered, and concentrated under reduced pressure to obtain **15c** as a yellow oil (1.68 g, 74 %).
^{1}**H NMR (400 MHz, CDCl$_3$):** δ 2.68 (t, J = 6.7 Hz, 2H, H^8), 2.12 (tq, J = 7.0; 2.6 Hz, 2H, H^4), 1.76 (t, J = 2.6 Hz, 3H, H^1), 1.51–1.35 (m, 6H, H^{5,6,7}), 1.16 (s, 2H, NH$_2$).
^{13}C$\{^1$H$\}$ **NMR (101 MHz, CDCl$_3$):** δ 79.1 (C^3), 75.4 (C^2), 42.1 (C^8), 33.4 (C^4), 28.9 (C^7), 26.1 (C^5), 18.7 (C^6), 3.4 (C^1).
IR: 3371 (NH$_2$ st), 2928, 2857, 2150 (C≡C st), 1593, 1460, 1436, 1331, 1072, 819 cm^{-1}.
HRMS calcd for C$_8$H$_{16}$N 126.1283, found 126.1283 ([M + H]$^+$).

6-Trimethylsilylhex-5-yne-1-chloride (16b)
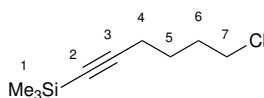
To a solution of 6-chlorohex-1-yne (2.5 g, 21.4 mmol) in Et$_2$O (40 mL) n-buthyllithium (2.5 M in hexane, 9.4 mL, 22.5 mmol) was added at −78 °C. After 35 min TMSCl (3.3 mL, 25.7 mmol) was introduced and the resulting mixture was stirred at room temperature for 1 h before being poured onto aqueous, saturated NaHCO$_3$ (20 mL) and extracted with Et$_2$O (3×30 mL). The combined organic phases were dried over MgSO$_4$, filtered, and concentrated under reduced pressure to obtain **16b** as a pale yellow oil (3.61 g, 89%). The crude product was used without further purification. Spectroscopic data were consistent with previously reported data for this compound.[224]
^{1}**H NMR (400 MHz, CDCl$_3$):** δ 3.59 (t, J = 6.6 Hz, 2H, H^7), 2.29 (t, J = 7.0 Hz,

2H, H^4), 1.96–1.87 (m, 2H, H^6), 1.78–1.61 (m, 2H, H^5), 0.17 (s, 12H, H^1).
^{13}C{^{1}H} **NMR (101 MHz, CDCl$_3$):** δ 85.1 (C^3), 68.9 (C^2), 44.5 (C^7), 31.5 (C^4), 25.7 (C^6), 19.1 (C^5), 0.1 (C^1).

5-Trimethylsilylpent-4-yn-1-amine (18a)
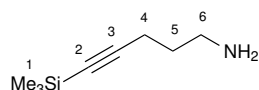
A suspension of 5-TMS-pent-5-ynchloride (3.50 g, 20.0 mmol), phthalamide (3.54 g, 24.0 mmol), K$_2$CO$_3$ (2.77 g, 20.0 mmol), and KI (33 mg, 0.2 mmol) in DMF (30 mL) was stirred at 80 °C for 16 h. The reaction mixture was cooled to room temperature and poured onto H$_2$O (50 mL), before being extracted with Et$_2$O (3×40 mL). The combined organic phases were washed with H$_2$O (2×50 mL), dried over MgSO$_4$, filtered, and concentrated under reduced pressure. The obtained residue was dissolved in ethanol (110 mL) and N$_2$H$_4 \cdot$H$_2$O (1.6 mL, 18.8 mmol) was added. The reaction mixture was heated at 70 °C for 3 h before being cooled to room temperature, filtered, and concentrated under reduced pressure. The oily residue was treated with pentane and the formed precipitate was filtered off. The filtrate was concentrated under reduced pressure and the crude product was purified by distillation (1 mbar, 90 °C) to give **18a** as a colourless oil (0.48 g, 20%). Spectroscopic data were consistent with previously reported data for this compound.[225]
^{1}**H NMR (400 MHz, CDCl$_3$):** δ 2.82 (t, J = 6.9 Hz, 2H, H^6), 2.31 (t, J = 7.0 Hz, 2H, H^4), 1.66 (tt, J = 7.0; 6.9 Hz, 2H, H^5), 0.16 (s, 9H, H^1).
^{1}**H NMR (400 MHz, CD$_3$CN):** δ 2.69 (t, J = 6.7 Hz, 2H, H^6), 2.27 (t, J = 7.2 Hz, 2H, H^4), 1.84 (s, 2H, NH$_2$), 1.57 (tt, J = 7.2; 6.7 Hz, 2H, H^5), 0.14 (s, 9H, H^1).
^{13}C{^{1}H} **NMR (101 MHz, CDCl$_3$):** δ 106.8 (C^3), 84.9 (C^2), 41.3 (C^6), 32.4 (C^4), 17.4 (C^5), 0.2 (C^1).

6-Trimethylsilylhex-5-yn-1-amine (18b)
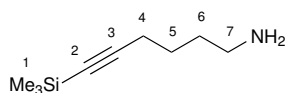
A suspension of TMS-alkynechloride **16b** (3.61 g, 19.1 mmol), phthalamide (3.38 g, 23.0 mmol), K$_2$CO$_3$ (3.17 g, 23.0 mmol), and KI (32 mg, 0.2 mmol) in DMF (30 mL) was stirred at 80 °C for 16 h. The reaction was cooled to room temperature and poured onto H$_2$O (50 mL) before being extracted with Et$_2$O (3×40 mL). The combined organic phases were washed with H$_2$O (2×50 mL),

dried over MgSO$_4$, filtered, and concentrated under reduced pressure. The obtained residue was dissolved in ethanol (150 mL) and N$_2$H$_4$·H$_2$O (2.0 mL, 23.2 mmol) was added. The reaction mixture was heated at 70 °C for 3 h before being cooled to room temperature, filtered, and concentrated under reduced pressure. The oily residue was treated with pentane and the formed precipitate was filtered off. The filtrate was concentrated under reduced pressure and the crude product was purified by distillation (1 mbar, 90 °C) to give **18b** as a colourless oil (1.07 g, 33%). Spectroscopic data were consistent with previously reported data for this compound.[225]

^{1}H NMR (400 MHz, CDCl$_3$): δ 2.71 (t, J = 6.2 Hz, 2H, H^7), 2.27–2.23 (m, 2H, H^4), 1.60–1.51 (m, 4H, H^{5,6}), 0.14 (s, 12H).

^{13}C{^{1}H} NMR (101 MHz, CDCl$_3$): δ 107.2 (C^3), 84.6 (C^2), 41.7 (C^7), 33.0 (C^4), 26.0 (C^6), 19.7 (C^5), 0.1 (C^1).

(5-Chloropent-1-yn-1-yl)benzene (19a)
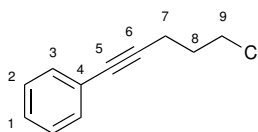
Phenylacetylene (5.37 mL, 48.9 mmol) was dissolved in THF (120 mL), cooled to –78 °C, and *n*-butyllithium (1.6 M in hexane, 32.2 mL, 51.4 mmol) was added. The resulting mixture was stirred at 0 °C for 30 min and transferred into a solution of 3-bromo-1-chloropropane (4.8 mL, 49.0 mmol) in THF (40 mL). The reaction mixture was stirred at 0 °C for 3 h and then at 80 °C for 16 h before being quenched by addition of H$_2$O (50 mL). The resulting mixture was extracted with Et$_2$O (3×30 mL). The combined organic phases were dried over MgSO$_4$, filtered, and concentrated under reduced pressure. The crude product was purified by distillation (2.5 mbar, 110 °C) to obtain **19a** as a colourless oil (6.67 g, 76 %). Spectroscopic data were consistent with previously reported data for this compound.[226]

^{1}H NMR (400 MHz, CDCl$_3$): δ 7.44–7.42 (m, 2H, H^3), 7.33–7.29 (m, 3H, H^{1,2}), 3.75 (t, J = 6.4 Hz, 2H, H^9), 2.64 (t, J = 6.8 Hz, 2H, H^7), 2.09 (tt, J = 6.8; 6.4 Hz, 2H, H^8).

^{13}C{^{1}H} NMR (101 MHz, CDCl$_3$): δ 131.6 (C^4), 128.3 (C^2), 127.8 (C^3), 123.6 (C^1), 88.1 (C^6), 81.6 (C^5), 43.8 (C^9), 31.5 (C^7), 16.9 (C^8).

(6-Chlorohex-1-yn-1-yl)benzene (19b)
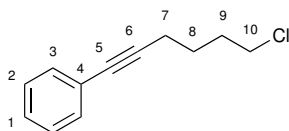
Phenylacetylene (5.37 mL, 48.9 mmol) was dissolved in THF (150 mL), cooled to −78 °C, and *n*-butyllithium (2.5 M in hexane, 20.6 mL, 51.4 mmol) was added. The resulting mixture was stirred at 0 °C for 30 min and transferred into a solution of 4-bromo-1-chlorobutane (5.6 mL, 49.0 mmol) in THF (50 mL). The reaction mixture was stirred at 0 °C for 3 h and then at 80 °C for 16 h before being quenched by addition of H_2O (50 mL). The resulting mixture was extracted with Et_2O (3×30 mL). The combined organic phases were dried over $MgSO_4$, filtered, and concentrated under reduced pressure. The crude product was purified by distillation (7.44 g, 79 %) to obtain **19b** as a colourless oil (6.67 g, 76 %). Spectroscopic data were consistent with previously reported data for this compound.[119]

^{1}H NMR (400 MHz, CDCl$_3$): δ 7.45–7.44 (m, 2H, H^3), 7.32–7.29 (m, 3H, H^{1,2}), 3.64 (t, J = 6.6 Hz, 2H, H^{10}), 2.51 (t, J = 6.9 Hz, 2H, H^7), 2.01 (tt, J = 7.1; 6.9 Hz, 2H, H^8), 1.81 (tt, J = 7.1; 6.6 Hz, 2H H^9).

^{13}C{^{1}H} NMR (101 MHz, CDCl$_3$): δ 131.6 (C^4), 128.3 (C^2), 127.7 (C^3), 123.8 (C^1), 89.3 (C^6), 81.2 (C^5), 44.6 (C^{10}), 31.7 (C^7), 26.0 (C^8), 18.8 (C^9).

(5-Azidopent-1-yn-1-yl)benzene (20a)
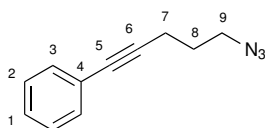
Sodium azide (2.39 g, 36.7 mmol) was dissolved in DMSO (80 mL) at 70 °C and chloropentynylbenzene **19a** (5.47 g, 30.6 mmol) was then added. The reaction mixture was heated to 80 °C for 16 h before being quenched by addition of H_2O (150 mL). The aqueous phase was extracted with Et_2O (3×100 mL) and the combined organic phases were washed with H_2O (60 mL), dried over $MgSO_4$, filtered, and concentrated under reduced pressure to obtain **20a** as a yellow oil (5.46 g, 96 %). The crude product was used without further purification. Spectroscopic data were consistent with previously reported data for this compound.[227]

^{1}H NMR (400 MHz, CDCl$_3$): δ 7.45–7.42 (m, 2H, H^3), 7.34–7.30 (m, 3H, H^{1,2}), 3.52 (t, J = 6.7 Hz, 2H, H^9), 2.57 (t, J = 6.9 Hz, 2H, H^7), 1.91 (tt, J = 6.9; 6.7 Hz, 2H, H^8).

^{13}C{^{1}H} NMR (101 MHz, CDCl$_3$): δ 131.6 (C^4), 128.2 (C^2), 127.8 (C^3), 123.5 (C^1), 88.2 (C^6), 81.7 (C^5), 50.3 (C^9), 27.9 (C^7), 16.7 (C^8).

(6-Azidohex-1-yn-1-yl)benzene (20b)
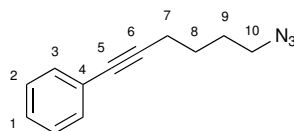
Sodium azide (0.72 g, 11.1 mmol) was dissolved in DMSO (25 mL) at 70 °C and 6-chlorohexynylbenzene **19b** (1.65 g, 9.2 mmol) was then added. The reaction mixture was heated to 80 °C for 16 h before being quenched by addition of H$_2$O (80 mL). The aqueous phase was extracted with Et$_2$O (3×30 mL) and the combined organic phases were washed with H$_2$O (40 mL), dried over MgSO$_4$, filtered, and concentrated under reduced pressure to obtain **20b** as a yellow oil (1.57 g, 92 %). The crude product was used without further purification. Spectroscopic data were consistent with previously reported data for this compound.[228]

^{1}**H NMR (400 MHz, CDCl$_3$):** δ 7.44–7.40 (m, 2H, H^3), 7.33–7.29 (m, 3H, H^{1,2}), 3.38 (t, J = 6.7 Hz, 2H, H^7), 2.50 (t, J = 6.8 Hz, 2H, H^{10}), 1.83 (tt, J = 7.2; 6.7 Hz, 2H, H^8), 1.73 (tt, J = 7.2; 6.8 Hz, 2H, H^9).

^{13}**C{^{1}H} NMR (101 MHz, CDCl$_3$):** δ 131.6 (C^4), 128.3 (C^2), 127.7 (C^3), 123.8 (C^1), 89.3 (C^6), 81.3 (C^5), 51.1 (C^{10}), 28.1 (C^7), 25.9 (C^8), 19.0 (C^9).

6-Phenylhex-5-ynenitrile (20c)
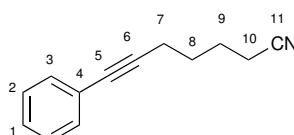
Chlorohexyne **19b** (3.76 g, 19.5 mmol) and NaCN (1.15 g, 23.4 g) were dissolved in DMSO (40 mL) and heated to 80 °C for 16 h. The reaction mixture was allowed to cool to room temperature and poured onto H$_2$O (80 mL). The aqueous phase was extracted with EtOAc (3×50 mL) and the combined organic phases were washed with H$_2$O (50 mL), dried over MgSO$_4$, filtered, and concentrated under reduced pressure to obtain **20c** as a pale yellow oil (3.22 g, 90 %). The crude product was used without further purification. Spectroscopic data were consistent with previously reported data for this compound.[229]

^{1}**H NMR (400 MHz, CDCl$_3$):** δ 7.43–7.41 (m, 2H, H^3), 7.33–7.28 (m, 3H, H^{1,2}),

2.51 (t, J = 6.7 Hz, 2H, H^{10}), 2.44 (t, J = 7.0 Hz, 2H, H^7), 1.91–1.85 (m, 2H, H^9), 1.82–1.77 (m, 2H, H^8).
^{13}C{^{1}H} NMR (101 MHz, CDCl$_3$): δ 131.5 (C^4), 128.3 (C^2), 127.8 (C^3), 123.6 (C^1), 119.5 (C^{11}), 88.6 (C^6), 81.6 (C^5), 27.4 (C^{10}), 24.5 (C^7), 18.7 (C^8), 16.8 (C^9).

5-Phenylpent-4-yn-1-amine (21a)
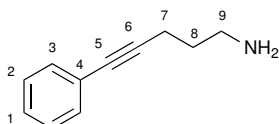
To an ice/water bath cooled suspension of LiAlH$_4$ (1.23 g, 32.4 mmol) in Et$_2$O (240 mL) a solution of azide **20a** (5.46 g, 29.5 mmol) in Et$_2$O (40 mL) was slowly added. The reaction mixture was stirred at room temperature for 3 h before being quenched by addition of aqueous KOH (20 w/w%) (caution, H$_2$ formation!) until gas stopped evolving. The formed grey precipitate was filtered off and washed with Et$_2$O (15 mL). The aqueous phase was extracted with Et$_2$O (3×100 mL), and the combined organic phases were washed with brine (100 mL), dried over MgSO$_4$, filtered and concentrated under reduced pressure. The crude product was purified by distillation (125 °C, 2 mbar) to give **21a** as a colourless oil (3.22 g, 69 %). Spectroscopic data were consistent with previously reported data for this compound.[119]
^{1}H NMR (400 MHz, CDCl$_3$): δ 7.42–7.40 (m, 2H, H^7), 7.31–7.28 (m, 3H, H^{1,2}), 2.89 (t, J = 6.9 Hz, 2H, H^9), 2.50 (t, J = 7.0 Hz, 2H, H^7), 1.76 (tt, J = 7.0; 6.9 Hz, 2H, H^8), 1.38 (s, 2H, NH$_2$).
^{13}C{^{1}H} NMR (101 MHz, CDCl$_3$): δ 131.6 (C^4), 128.2 (C^2), 127.6 (C^3), 123.9 (C^1), 89.6 (C^6), 81.0 (C^5), 41.3 (C^9), 32.4 (C^7), 16.9 (C^8).

6-Phenylhex-5-yn-1-amine (21b)
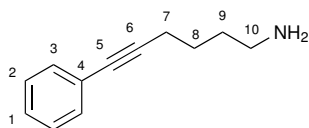
To an ice/water bath cooled suspension of LiAlH$_4$ (335 mg, 8.8 mmol) in Et$_2$O (65 mL) a solution of azide **20b** (1.60 g, 8.0 mmol) in Et$_2$O (4 mL) was slowly added. The reaction mixture was stirred at room temperature for 3 h before being quenched by addition of aqueous KOH (20 w/w%) (caution, H$_2$ formation!) until gas stopped evolving. The formed grey precipitate was filtered off and washed with Et$_2$O (15 mL). The aqueous phase was extracted with Et$_2$O (3×100 mL), and the combined organic phases were washed with

brine (100 mL), dried over $MgSO_4$, filtered and concentrated under reduced pressure to give **21b** as a colourless oil (0.99 g, 71 %). Spectroscopic data were consistent with previously reported data for this compound.[119]

[1H] NMR (400 MHz, CDCl3): δ 7.40–7.37 (m, 2H, H[3]), 7.27–7.24 (m, 3H, H[1,2]), 2.71 (t, J = 6.6 Hz, 2H, H[10]), 2.41 (t, J = 6.7 Hz, 2H, H[7]), 1.63–1.58 (m, 4H, H[8,9]), 1.31 (s, 2H, NH_2).

[13C{1H}] NMR (101 MHz, CDCl3): δ 131.5 (C[4]), 128.2 (C[2]), 127.5 (C[3]), 123.9 (C[1]), 90.0 (C[6]), 80.8 (C[5]), 41.8 (C[10]), 33.1 (C[7]), 26.1 (C[8]), 19.3 (C[9]).

7-Phenylhept-6-ynamine (21c)
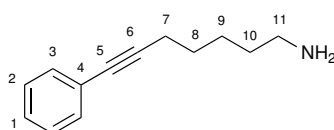
To an ice/water bath cooled suspension of $LiAlH_4$ (0.73 g, 19.3 mmol) in Et_2O (150 mL) a solution of nitrile **20c** (3.22 g, 17.5 mmol) in Et_2O (30 mL) was slowly added. The reaction was stirred at room temperature for 3 h, before being quenched by addition of aqueous NaOH (10 w/w%, 10 mL) (caution, H_2 formation!) until gas stopped evolving. The formed precipitate was filtered off and washed with Et_2O (20 mL). The aqueous layer was separated and extracted with Et_2O (3×15 mL). The combined organic phases were dried over $MgSO_4$, filtered, and concentrated under reduced pressure. **21c** was obtained as a colourless oil after distillation at 180 °C under 0.1 bar (2.62 g, 80 %). Spectroscopic data were consistent with previously reported data for this compound.[119]

[1H] NMR (400 MHz, CDCl3): δ 7.41–7.38 (m, 2H, H[3]), 7.31–7.26 (m, 3H, H[1,2]), 2.72 (t, J = 6.8 Hz, 2H, H[11]), 2.43 (t, J = 7.0 Hz, 2H, H[7]), 1.65–1.61 (m, 2H, C[10]), 1.56 (s, 2H, NH_2), 1.52–1.48 (m, 4H, H[8,9]).

[13C{1H}] NMR (101 MHz, CDCl3): δ 131.5 (C[4]), 128.2 (C[2]), 127.5 (C[3]), 124.0 (C[1]), 90.2 (C[6]), 80.7 (C[5]), 42.1 (C[11]), 33.4 (C[7]), 28.6 (C[10]), 26.2 (C[8]), 19.4 (C[9]).

2-(Phenylethynyl)aniline (23b)
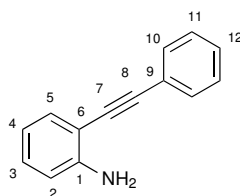
A solution of 2-iodoaniline (5.0 g, 22.8 mmol), phenylacetylene (3.1 mL, 27.8 mmol), and NEt_3 (27 mL, 0.19 mmol) in dry THF (80 mL) was degassed

three times by freeze-thaw cycles. After addition of $[PdCl_2(PPh_3)_2]$ (160 mg, 1 mol %) and CuI (130 mg, 6 mol %), the reaction mixture was stirred at room temperature for 16 h. H_2O (100 mL) was then added, the organic layer was separated and the aqueous phase was extracted with Et_2O (3×50 mL). The combined organic phases were washed with H_2O (2×50 mL) and brine (50 mL), dried over $MgSO_4$, filtered and concentrated under reduced pressure. The crude product was purified by column chromatography (silica, PE/EtOAc = 10:1, R_f = 0.3) to give **23b** as a yellow solid (3.97 g, 74%). Spectroscopic data were consistent with previously reported data for this compound.[230]

^{1}H NMR (400 MHz, CDCl$_3$): δ 7.53–7.50 (m, 2H, H^{10}), 7.37–7.30 (m, 4H, H^{5,11,12}), 7.14–7.10 (m, 1H, H^3), 6.72–6.68 (m, 2H, H^{2,4}), 4.24 (s, 2H, NH$_2$).

^{13}C{^{1}H} NMR (101 MHz, CDCl$_3$): δ 147.9 (C^6), 132.2 (C^3), 131.5 (C^{5,11}), 129.8 (C^4), 128.5 (C^{12}), 128.3 (C^{13}), 123.4 (C^{10}), 118.0 (C^7), 114.4 (C^2), 107.9 (C^1), 94.8 (C^8), 86.0 (C^9).

2-Cyano-1-ethynylbenzene (25a)
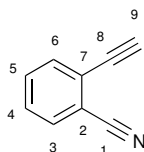
A solution of 2-iodobenzonitrile (1.71 g, 7.47 mmol), (trimethylsilyl)ethylene (1.5 mL, 11.2 mmol), and NEt$_3$ (4.0 mL, 28.6 mmol) in dry THF (12 mL) was degassed three times by freeze-thaw cycles. After addition of $[PdCl_2(PPh_3)_2]$ (160 mg, 3 mol %) and CuI (130 mg, 6 mol %), the reaction mixture was stirred at room temperature for 16 h and then filtered through a silica pad (Et$_2$O). After removal of the solvent under reduced pressure, the obtained residue was dissolved in a mixture of MeOH (4.8 mL), H_2O (1.2 mL), and KOH (837 mg, 14.9 mmol) and stirred for 30 min. EtOAc (20 mL) was added and the organic phase was separated. The aqueous layer was extracted with EtOAc (2×20 mL), and the combined organic phases were dried over $MgSO_4$, filtered, and dried under reduced pressure to give **25a** as a brown solid (0.94 g, 99%). Spectroscopic data were consistent with previously reported data for this compound.[231]

^{1}H NMR (400 MHz, CDCl$_3$): δ 7.71–7.68 (m, 1H, H^6), 7.65–7.63 (m, 1H, H^3), 7.59 (td, J = 7.7; 1.4 Hz, 1H, H^5), 7.48 (td, J = 7.6; 1.4 Hz, 1H, H^4), 3.50 (s, 1H, H^9).

^{13}C{^{1}H} NMR (101 MHz, CDCl$_3$): δ 133.0 (C^6), 132.7 (C^5), 132.4 (C^3), 129.0 (C^4), 125.9 (C^7), 117.2 (C^2), 115.9 (C^1), 83.8 (C^8), 77.3 (C^9).

2-(Phenylethynyl)benzonitrile (25b)
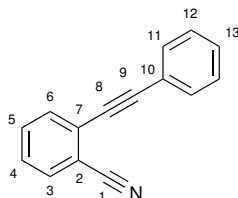
A solution of 2-iodobenzonitrile (2.5 g, 10.9 mmol), phenylacetylene (1.9 mL, 16.4 mmol), and NEt_3 (27 mL, 0.19 mol) in dry THF (80 mL) was degassed three times by freeze-thaw cycles. After addition of $[PdCl_2(PPh_3)_2]$ (77 mg, 1 mol %) and CuI (62 mg, 3 mol %), the reaction mixture was stirred at room temperature for 16 h. H_2O (100 mL) was added, the organic phase was separated and the aqueous layer was extracted with Et_2O (3×50 mL). The combined organic phases were washed with H_2O (2×50 mL) and brine (50 mL), dried over $MgSO_4$, filtered, and concentrated under reduced pressure. The crude product was purified by column chromatography (silica, PE/EtOAc = 10:1, R_f = 0.3) to obtain **25b** as a yellow oil (1.88 g, 85%). Spectroscopic data were consistent with previously reported data for this compound.[232]
^{1}H NMR (400 MHz, CDCl$_3$): δ 7.67 (dt, J = 7.8; 0.6 Hz, 1H, H^6), 7.64–7.60 (m, 3H, H^{11}), 7.57 (td, J = 7.7; 1.3 Hz, 1H, H^3), 7.43–7.35 (m, 4H, $H^{4,12,13}$).
^{13}C{^{1}H} NMR (101 MHz, CDCl$_3$): δ 132.7 (C^6), 132.4 (C^5), 132.1 (C^{11}), 132.0 (C^3), 129.3 (C^4), 128.5 (C^{13}), 128.2 (C^{12}), 127.3 (C^{10}), 122.0 (C^7), 117.6 (C^2), 115.3 (C^1), 96.0 (C^8), 85.6 (C^9).

2-(Hex-1-yn-1-yl)benzonitrile (25c)
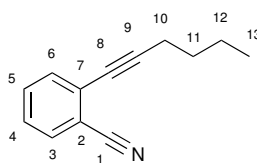
A solution of 2-iodobenzonitrile (2.5 g, 10.9 mmol), 1-hexyne (1.9 mL, 16.4 mmol), and NEt_3 (27 mL, 0.19 mmol) in dry THF (80 mL) was degassed three times by freeze-thaw cycles. After addition of $[PdCl_2(PPh_3)_2]$ (77 mg, 1 mol %) and CuI (62 mg, 3 mol %), the reaction mixture was stirred at room temperature for 16 h. H_2O (100 mL) was added, the organic phase was separated and the aqueous layer was extracted with Et_2O (3×50 mL). The combined organic phases were washed with H_2O (2×50 mL) and brine (50 mL), dried over $MgSO_4$, filtered and concentrated under reduced pressure. The crude product was purified by column chromatography (silica, PE/EtOAc

= 10:1, R_f = 0.4) to give **25c** as a yellow oil (1.80 g, 90%). Spectroscopic data were consistent with previously reported data for this compound.[233]

^{1}H NMR (400 MHz, CDCl$_3$): δ 7.61 (dt, J = 7.8; 1.0 Hz, 1H, H^3), 7.50–7.48 (m, 2H, H^{4,6}), 7.34 (ddd, J = 7.8; 5.9; 3.0 Hz, 1H, H^5), 2.49 (t, J = 7.0 Hz, 2H, H^{10}), 1.68–1.61 (m, 2H, H^{11}), 1.56–1.47 (m, 2H, H^{12}), 0.96 (t, J = 7.3 Hz, 3H, H^{13}).

^{13}C{^{1}H} NMR (101 MHz, CDCl$_3$): δ 132.5 (C^6), 132.2 (C^{3,5}), 128.1 (C^4), 127.5 (C^7), 117.8 (C^2), 115.3 (C^1), 97.9(C^9), 77.2(C^8), 30.4 (C^{10}), 22.0 (C^{11}), 19.2 (C^{12}), 13.6 (C^{13}).

2-(Ethynyl)benzylamine (26a)
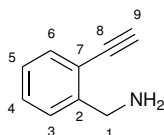
To an ice/water bath cooled suspension of LiAlH$_4$ (239 mg, 6.29 mmol) in Et$_2$O (8 mL) a solution of nitrile **25a** (400 mg, 3.15 mmol) in Et$_2$O (2 mL) was slowly added. The bath was then removed and the reaction mixture was stirred at room temperature for 3 h before being quenched by addition of aqueous NaOH (10 w/w%, 0.5 mL) (caution, H$_2$ formation!) until gas stopped evolving. The formed precipitate was filtered off and washed with Et$_2$O (5 mL). The aqueous layer was separated and extracted with Et$_2$O (3×2 mL). The combined organic phases were dried over MgSO$_4$, filtered, and concentrated under reduced pressure to obtain **26a** as a red oil (351 mg, 83%). Spectroscopic data were consistent with previously reported data for this compound.[120]

^{1}H NMR (400 MHz, CD$_3$CN): δ 7.51–7.47 (m, 2H, H^{4,5}), 7.41 (td, J = 7.5; 1.4 Hz, 1H, H^6), 7.26 (td, J = 7.5; 1.4 Hz, 1H, H^3), 3.93 (s, 2H, H^1), 3.65 (s, 1H, H^9).

^{13}C{^{1}H} NMR (101 MHz, CD$_3$CN): δ 146.6 (C^2), 132.6 (C^6), 129.2 (C^4), 127.2 (C^3), 126.4 (C^5), 125.9 (C^7), 82.2 (C^8), 81.3 (C^9), 44.5 (C^1).

2-(Phenylethynyl)benzylamine (26b)

187

To an ice/water bath cooled suspension of LiAlH$_4$ (560 mg, 14.8 mmol) in Et$_2$O (30 mL) a solution of nitrile **25b** (1.50 g, 7.38 mmol) in Et$_2$O (10 mL) was slowly added. The bath was then removed and the reaction mixture was stirred at room temperature for 3 h, before being quenched by addition of aqueous NaOH (10 w/w%, 2 mL) (caution, H$_2$ formation!) until gas stopped evolving. The formed precipitate was filtered off and washed with Et$_2$O (10 mL). The aqueous layer was separated and extracted with Et$_2$O (3×10 mL). The combined organic phases were dried over MgSO$_4$, filtered, and concentrated under reduced pressure to obtain **26b** as a red oil (1.43 g, 94%). Spectroscopic data were consistent with previously reported data for this compound.[234]

^{1}H NMR (400 MHz, CDCl$_3$): δ 7.56–7.52 (m, 3H, H^{6,11}), 7.38–7.33 (m, 4H, H^{5,12,13}), 7.31 (dd, J = 7.6; 1.4 Hz, 1H, H$_3$), 7.26–7.22 (m, 1H, H^4), 4.05 (s, 2H, H^1), 1.71 (s, 2H, NH$_2$).

^{1}H NMR (400 MHz, CD$_3$CN): δ 7.57–7.54 (m, 2H, H^{11}), 7.51 (dd, J = 7.6; 1.3 Hz, 1H, H^6), 7.48–7.46 (m, 1H, H^5), 7.42–7.35 (m, 4H, H^{3,12,13}), 7.25 (ddd, J = 7.5; 7.5; 1.3 Hz, 1H, H^4), 3.99 (s, 2H, H^1), 1.91 (s, 2H, NH$_2$).

^{13}C{^{1}H} NMR (101 MHz, CDCl$_3$): δ 145.4 (C^2), 132.4 (C^6), 131.5 (C^{11}), 128.8 (C^{13}), 128.4 (C^{12}), 127.3 (C^4), 126.8 (C^{10}), 123.1 (C^5), 121.8 (C^7), 93.9 (C^9), 87.3 (C^8), 45.7 (C^1).

2-(Hex-1-yn-1-yl)benzylamine (26c)
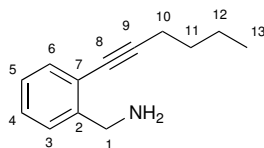
To an ice/water bath cooled suspension of LiAlH$_4$ (629 mg, 16.38 mmol) in Et$_2$O (130 mL) a solution of nitrile **25c** (1.50 g, 8.19 mmol) in Et$_2$O (10 mL) was slowly added. The bath was then removed and the reaction mixture was stirred at room temperature for 3 h, before being quenched by addition of aqueous NaOH (10 w/w%, 2 mL) (caution, H$_2$ formation!) until gas stopped evolving. The formed precipitate was filtered off and washed with Et$_2$O (10 mL). The aqueous layer was separated and extracted with Et$_2$O (3×10 mL). The combined organic phases were dried over MgSO$_4$, filtered, and concentrated under reduced pressure to obtain **26c** as a red oil (1.43 g, 94%).

^{1}H NMR (400 MHz, CDCl$_3$): δ 7.39 (dd, J = 7.4; 1.3 Hz, 1H, H^5), 7.29–7.26 (m, 1H, H^4), 7.24 (td, J = 7.4; 1.3 Hz, 1H, H^6), 7.17 (td, J = 7.4; 1.8 Hz, 1H, H^3), 3.93 (s, 2H, H^1), 2.46 (t, J = 7.0 Hz, 2H, H^{19}), 1.65–1.57 (m, 4H, H^{11} + NH$_2$), 1.55–1.45 (m, 2H, H^{12}), 0.96 (t, J = 7.3 Hz, 3H, H^{13}).

^{1}H NMR (400 MHz, CD$_3$CN): δ 7.40–7.37 (m, 1H, H^5), 7.34 (dd, J = 7.6;

1.2 Hz, 1H, H^4), 7.29 (td, J = 7.5; 1.4 Hz, 1H, H^6), 7.18 (td, J = 7.5; 1.4 Hz, 1H, H^3), 3.86 (s, 2H, H^1), 2.46 (t, J = 6.9 Hz, 2H, H^{10}), 1.78 (s, 2H, NH$_2$), 1.63–1.54 (m, 2H, H^{11}), 1.54–1.45 (m, 2H, H^{12}), 0.95 (t, J = 7.3 Hz, 3H, H^{13}).

^{13}C{^{1}H} NMR (101 MHz, CDCl$_3$): δ 145.2 (C^2), 132.4 (C^6), 127.9 (C^4), 127.2 (C^3), 126.6 (C^5), 122.6 (C^7), 95.0 (C^9), 78.5 (C^8), 45.7 (C^1), 30.9 (C^{10}), 22.1 (C^{11}), 19.2 (C^{12}), 13.6 (C^{13}).

IR: 3373 (NH$_2$ st), 2957, 2930, 2861, 2231 (C≡C st), 1598, 1482, 1448, 1430, 1379, 1327, 1993, 1105, 1061, 945, 863, 755 cm^{-1}.

HRMS calcd for C$_{13}$H$_{17}$N 188.1439, found 188.1445 ([M + H]$^+$).

Pent-4-yntosylamide (27a)
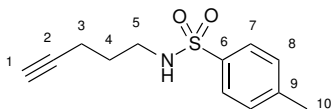
A suspension of mesylate **10** (1.92 g, 12.0 mmol), K$_2$CO$_3$ (3.48 g, 25.2 mmol), and tosylamide (2.15 g, 12.6 mmol) in MeCN (45 mL) was heated to 80 °C for 16 h. The reaction mixture was quenched by addition of H$_2$O (50 mL), the organic phase was separated and the aqueous one was extracted with Et$_2$O (3×40 mL). The combined organic phases were dried over MgSO$_4$, filtered, and concentrated under reduced pressure. The crude product was purified by column chromatography (silica, PE/EtOAc = 4:1, R$_f$ = 0.5) to give **27a** as a white solid (1.52 g, 41 %). Spectroscopic data were consistent with previously reported data for this compound.[162]

^{1}H NMR (400 MHz, CDCl$_3$): δ 7.76 (d, J = 8.1 Hz, 2H, H^7), 7.29 (d, J = 8.1 Hz, 2H, H^8), 5.32 (d, J = 6.4 Hz, 1H, NH), 3.02 (td, J = 6.8; 6.4 Hz, 2H, H^5), 2.41 (s, 3H, H^{10}), 2.19 (td, J = 6.9; 2.7 Hz, 2H, H^3), 1.93 (t, J = 2.7 Hz, 1H, H^1), 1.67 (tt, J = 6.9; 6.8 Hz, 2H, H^4).

^{13}C{^{1}H} NMR (101 MHz, CDCl$_3$): δ 143.4 (C^6), 136.8 (C^8), 129.8 (C^7), 127.1 (C^9), 83.0 (C^2), 69.4 (C^1), 42.1 (C^5), 28.2 (C^3), 21.5 (C^{10}), 15.7 (C^4).

4-Methyl-N-(5-phenylpent-4-yn-1-yl)benzenesulfonamide (27b)
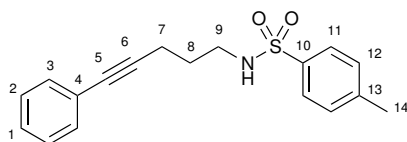
To an ice/water bath cooled solution of amine **21a** (1.5 g, 9.4 mmol) and pyridine (1.5 mL, 18.8 mmol) in DCM (80 mL) tosyl chloride (2.16 g, 11.9 mmol)

was slowly added. The reaction mixture was allowed to warm to room temperature and stirred for 16 h before adding H_2O (80 mL). The organic phase was separated and the aqueous layer was extracted with DCM (3×40 mL). The combined organic phases were dried over $MgSO_4$, filtered, and concentrated under reduced pressure. The crude was purified by column chromatography (silica, PE/EtOAc = 10:1, R_f = 0.4) to give **27b** as a white solid (1.56 g, 54%). Spectroscopic data were consistent with previously reported data for this compound.[235]

^{1}H NMR (400 MHz, CDCl$_3$): δ 7.78 (d, J = 8.3 Hz, 2H, H^{11}), 7.37–7.28 (m, 7H, H^{1,2,3,12}), 3.17 (dd, J = 6.6; 6.6 Hz, 2H, H^9), 2.47 (t, J = 6.8 Hz, 2H, H^7), 2.43 (s, 3H, H^{14}), 1.79 (tt, J = 6.8; 6.6 Hz, 2H, H^8).

^{13}C{^{1}H} NMR (101 MHz, CDCl$_3$): δ 143.5 (C^{10}), 136.9 (C^{13}), 131.6 (C^{11}), 129.8 (C^{12}), 128.3 (C^3), 127.8 (C^1), 127.2 (C^2), 123.5 (C^4), 88.4 (C^5), 81.7 (C^6), 42.3 (C^9), 28.3 (C^7), 21.5 (C^{14}), 16.7 (C^8).

N-(Pent-4-yn-1-yl)acetamide (28a)
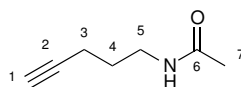
To an ice/water bath cooled solution of pentynamine **8a** (607 mg, 7.30 mmol) and NEt$_3$ (1.0 mL, 7.30 mmol) acetyl chloride (0.52 mL, 7.30 mmol) was added. The reaction was allowed to warm to room temperature and stirred for 2 h before the formed precipitate was filtered off. The solvent was then removed under reduced pressure to give **28a** as a yellow oil (696 mg, 76 %). Spectroscopic data were consistent with previously reported data for this compound.[236]

^{1}H NMR (400 MHz, CDCl$_3$): δ 5.85 (br. s, 1H, NH), 3.38 (td, J = 6.4; 6.4 Hz, 2H, H^5), 2.27 (td, J = 6.9; 2.7 Hz, 2H, H^3), 2.01–1.98 (m, 4H, H^{1,7}), 1.76 (tt, J = 6.9; 6.4 Hz, 2H, H^4).

^{1}H NMR (400 MHz, acetone-d6): δ 7.16 (s, 1H, NH), 3.25 (td, J = 6.5; 6.5 Hz, 2H, H^5), 2.35 (t, J = 2.6 Hz, 1H, H^1), 2.22 (td, J = 7.2; 2.6 Hz, 2H, H^3), 1.86 (s, 3H, H^7), 1.68 (tt, J = 7.2; 6.5 Hz, 2H, H^4).

^{1}H NMR (400 MHz, CD$_3$CN): δ 6.49 (s, 1H NH), 3.21 (td, J = 7.0; 6.4 Hz, 2H, H^5), 2.25–2.20 (m, 3H, H^{1,3}), 1.86 (s, 3H, H^7), 1.66 (tt, J = 7.0; 7.0 Hz, 2H, H^4).

^{13}C{^{1}H} NMR (101 MHz, CDCl$_3$): δ 170.4 (C^6), 83.5 (C^2), 69.1 (C^1), 38.7 (C^5), 28.0 (C^3), 23.2 (C^7), 16.1 (C^4).

N-(5-Phenylpent-4-yn-1-yl)acetamide (28b)
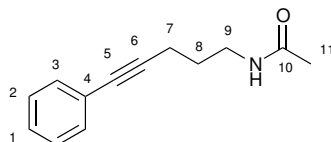
To an ice/water bath cooled solution of amine **21a** (1.0 g, 6.3 mmol) and NEt$_3$ (0.96 mL, 6.9 mmol) in Et$_2$O (10 mL) acetyl chloride (493 mg, 6.3 mmol) was slowly added and the resulting mixture was stirred at room temperature for 16 h. The formed precipitate was filtered off and the filtrate was poured onto saturated, aqueous NaHCO$_3$ (5 mL). The organic layer was separated and the aqueous phase was extracted with Et$_2$O (3×10 mL). The combined organic phases were dried over Na$_2$SO$_4$, filtered, and concentrated under reduced pressure to give **28b** as a yellow oil (0.91 g, 72%).

^{1}H NMR (400 MHz, CDCl$_3$): δ 7.38–7.36 (m, 2H, H^3), 7.27–7.24 (m, 3H, H^{1,2}), 6.60 (br. s, 1H, NH), 3.36 (td, J = 7.4; 7.4 Hz, 2H, H^9), 2.43 (t, J = 7.4 Hz, 2H, H^7), 1.95 (s, 3H, H^{11}), 1.78 (tt, J = 7.4; 7.4 Hz, 2H, H^8).

^{13}C{^{1}H} NMR (101 MHz, CDCl$_3$): δ 170.8 (C^{10}), 131.49 (C^3), 128.3 (C^1), 127.8 (C^2), 123.6 (C^4), 89.1 (C^6), 81.3 (C^5), 38.9 (C^9), 28.3 (C^7), 23.1 (C^{11}), 17.1 (C^8).

IR: 3287, 3082, 2934, 1709 (C≡C st), 1648 (C=O st), 1550, 1490, 1441, 1368, 1293, 1070, 914, 755, 691 cm^{-1}.

HRMS calcd for C$_{13}$H$_{16}$NO 202.1232, found 202.1236 ([M + H]$^+$).

N-Benzylpent-4-yn-1-amine (29a)
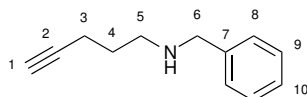
Mesylpentynamine **10** (1.61 g, 10.0 mmol) and benzylamine (6.6 mL, 60.0 mmol) were stirred neat at room temperature for 16 h. The reaction mixture was then quenched by addition of aqueous NaOH (1 M, 80 mL) and extracted with Et$_2$O (2×40 mL). The combined organic phases were dried over MgSO$_4$, filtered, and concentrated under reduced pressure. The crude product was purified by column chromatography (silica, EtOAc, R$_f$ = 0.3) to give **29a** as a pale yellow oil (1.20 g, 70 %). Spectroscopic data were consistent with previously reported data for this compound.[220]

^{1}H NMR (400 MHz, CDCl$_3$): δ 7.55–7.14 (m, 5H, H^{8,9,10}), 3.82 (s, 2H, H^6), 2.78 (t, J = 7.0 Hz, 2H, H^5), 2.31 (td, J = 7.1; 2.7 Hz, 2H, H^3), 1.99 (t, J = 2.7 Hz, 1H, H^1), 1.76 (tt, J = 7.1; 7.0 Hz, 2H, H^4), 1.40 (s, 1H, NH).

^{13}C{^{1}H} NMR (101 MHz, CDCl$_3$): δ 140.5 (C^7), 128.4 (C^9), 128.1(C^8), 126.9 (C^{10}), 84.2 (C^2), 68.6 (C^1), 53.9 (C^6), 48.2 (C^5), 28.8 (C^3), 16.4 (C^4).

N-Benzyl-5-phenylpent-4-yn-1-amine (29b)
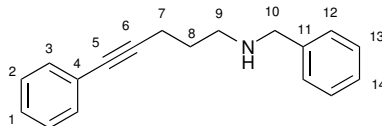
5-Phenylpent-4-yn-1-chloride **19a** (1.62 g, 10.0 mmol) was dissolved in benzylamine (6.55 mL, 60.0 mmol) and stirred at 80 °C for 16 h. The reaction mixture was then poured onto a mixture of EtOAc (40 mL) and aqueous NaOH (1 M, 80 mL). The organic phase was separated while the aqueous phase was extracted with EtOAc (2×40 mL). The combined organic phases were dried over $MgSO_4$, filtered, and concentrated under reduced pressure. The crude product was purified by column chromatography (silica, PE/EtOAc = 11:1, R_f = 0.4) to obtain **29b** as a white solid (1.04 g, 74 %). Spectroscopic data were consistent with previously reported data for this compound.[237]

^{1}H NMR (400 MHz, CDCl$_3$): δ 7.41–7.28 (m, 10H, H^{1,2,3,12,13,14}), 3.85 (s, 2H, H^{10}), 2.84 (t, J = 7.0 Hz, 2H, H^9), 2.53 (t, J = 7.0 Hz, 2H, H^7), 1.85 (tt, J = 7.0; 7.0 Hz, 2H, H^8), 1.46 (s, 1H, NH).

^{13}C{^{1}H} NMR (101 MHz, CDCl$_3$): δ 140.5 (C^{11}), 131.6 (C^{13}), 128.4 (C^3), 128.2 (C^1), 128.1 (C^{12}), 127.6 (C^{14}), 126.9 (C^2), 123.9 (C^4), 89.8 (C^6), 81.0 (C^5), 54.0 (C^{10}), 48.4 (C^9), 29.0 (C^7), 17.4 (C^8).

N-(1,1-Dimethylethyl)pent-4-yn-1-amine (30)
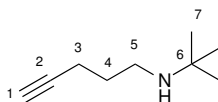
Mesylpentynamine **10** (1.92 g, 11.9 mmol) and *tert*-butylamine (5.2 mL, 71.3 mmol) were stirred neat at room temperature for 16 h. The reaction was quenched by addition of aqueous NaHCO$_3$ (1 M, 80 mL) and extracted with Et$_2$O (3×40 mL). The combined organic phases were dried over MgSO$_4$, filtered, and concentrated under reduced pressure to give **30** as a yellow oil (1.23 g, 75 %). Spectroscopic data were consistent with previously reported data for this compound.[238]

^{1}H NMR (400 MHz, CDCl$_3$): δ 2.67 (t, J = 7.1 Hz, 2H, H^5), 2.29 (td, J = 7.0; 2.7 Hz, 2H, H^3), 1.96 (t, J = 2.7 Hz, 1H, H^1), 1.68 (tt, J = 7.1; 7.0 Hz, 2H, H^4), 1.12 (s, 9H, H^7), 0.68 (s, 1H, NH).

^{13}C{^{1}H} NMR (101 MHz, CDCl$_3$): δ 84.1 (C^2), 68.4 (C^1), 50.3 (C^6), 41.4 (C^5), 29.7 (C^3), 29.1 (C^7), 16.4 (C^4).

N-(1,1-Dimethylethoxy)carbonyl pent-4-y-1-amine (33)
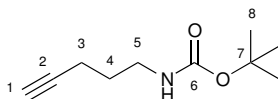
To an ice/water bath cooled solution of **8a** (500 mg, 6.02 mmol) in DCM (4 mL) NEt$_3$ (1.26 mL, 9.03 mmol) was added followed by a dropwise addition of di-*tert*-butyl dicarbonate (1.31 g, 6.02 mmol) in DCM (2 mL). The resulting solution was warmed to room temperature and stirred for 16 h. The reaction mixture was quenched by addition of H$_2$O (20 mL) and extracted with DCM (3×10 mL). The combined organic phases were dried over MgSO$_4$, filtered, and concentrated under reduced pressure. The crude product was purified by column chromatography (silica, PE/EtOAc = 5:1, R$_f$ = 0.5) to give **33** as a yellow oil (0.481 g, 44 %). Spectroscopic data were consistent with previously reported data for this compound.[239]

^{1}H NMR (400 MHz, CDCl$_3$): δ 4.65 (s, 1H, NH), 3.25 (td, J = 6.9; 6.8 Hz, 2H, H^5), 2.26 (td, J = 7.0; 2.7 Hz, 2H, H^3), 1.99 (t, J = 2.7 Hz, 1H, H^1), 1.74 (tt, J = 7.0; 7.0 Hz, 2H, H^4), 1.46 (s, 9H, H^8).

^{13}C\{^{1}H\} NMR (101 MHz, CDCl$_3$): δ 155.9 (C^6), 83.4 (C^2), 79.2 (C^7), 68.9 (C^1), 39.6 (C^5), 28.6 (C^3), 28.4 (C^8), 15.9 (C^4).

Pent-4-ynal (31)
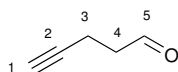
To a solution of oxalyl chloride (2.25 mL, 26.2 mmol) in DCM (60 mL) cooled at −78 °C a solution of DMSO (3.7 mL, 52.3 mmol) in DCM (10 mL) was added. After 30 min of stirring a solution of pent-4-yn-1-ol (2.20 mL, 23.8 mmol) in DCM (25 mL) was slowly added. The reaction mixture was stirred at −78 °C for 1 h and at 10 °C for 1 h, before being quenched by addition of 1% HCl in brine (20 mL). The layers were separated and the aqueous phase was extracted with DCM (3×20 mL). The combined organic phases were dried over MgSO$_4$, filtered, and concentrated under reduced pressure to obtain **31** as a yellow oil (2.1 g, 57 %, caution, strong odour!). The crude product was used without further purification. Spectroscopic data were consistent with previously reported data for this compound.[240]

^{1}H NMR (400 MHz, CDCl$_3$): δ 9.81 (t, J = 1.0 Hz, 1H, H^5), 2.71 (td, J = 7.1; 1.0 Hz, 2H, H^4), 2.52 (td, J = 7.1; 2.7 Hz, 2H, H^3), 2.00 (t, J = 2.7 Hz, 1H, H^1).

^{13}C\{^{1}H\} NMR (101 MHz, CDCl$_3$): δ 201.2 (C^5), 83.1 (C^2), 68.4 (C^1), 42.6 (C^4), 11.9 (C^3).

N-Propylpent-4-yn-1-amine (32)
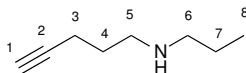
A solution of aldehyde **31** (1.21 g, 14.7 mmol) and *n*-propylamine (2.4 mL, 29.4 mmol) in MeOH (40 mL) were stirred at room temperature for 16 h before being cooled to 0 °C and slowly adding $NaBH_4$ (280 mg, 7.4 mmol). The reaction mixture was allowed to warm to room temperature over 30 min before H_2O (30 mL) was added and the resulting mixture was extracted with Et_2O (3×30 mL). The combined organic phases were dried over $MgSO_4$, filtered, and concentrated under reduced pressure. The obtained crude was purified by column chromatography (basic alumina, PE/EtOAc = 1:1, R_f = 0.5) to give **32** as a yellow oil (263 mg, 15 %).

^{1}H NMR (400 MHz, CDCl$_3$): δ 2.72 (t, J = 7.1 Hz, 2H, H^5), 2.58 (t, J = 7.3 Hz, 2H, H^6), 2.26 (td, J = 7.1; 2.7 Hz, 2H, H^3), 1.95 (t, J = 2.7 Hz, 1H, H^1), 1.72 (tt, J = 7.1; 7.1 Hz, 2H, H^4), 1.56–1.47 (m, 2H, H^7), 0.92 (t, J = 7.4 Hz, 3H, H^8).

^{13}C{^{1}H} NMR (101 MHz, CDCl$_3$): δ 84.0 (C^2), 68.5 (C^1), 51.7 (C^6), 48.6 (C^5), 28.5 (C^3), 23.0 (C^7), 16.3 (C^4), 11.7 (C^8).

IR: 3308 (NH st), 2958, 2993, 2874, 2815, 2115 (C≡C st), 1636, 1560, 1459, 1378, 1301, 1245, 1125, 1062, 896, 723 cm^{-1}.

HRMS calcd for $C_8H_{15}N$ 126.1283, found 126.1228 ([M + H]$^+$).

4-Methyl-N-2-(phenylethynyl)phenylbenzenesulfonamide (34a)
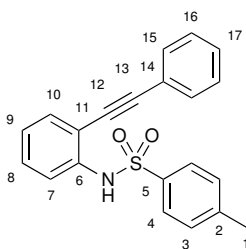
To an ice/water bath cooled solution of amine **23b** (1.2 g, 6.2 mmol) and pyridine (1.0 mL, 12.4 mmol) in DCM (40 mL) tosyl chloride (0.88 mL, 6.2 mmol) was slowly added and the resulting mixture was stirred at room temperature for 16 h before being poured onto H_2O (40 mL). The layers were separated and the aqueous phase was extracted with DCM (3×20 mL). The combined organic phases were dried over $MgSO_4$, filtered, and concentrated under reduced pressure. The crude product was purified by column chromatography (silica, PE/EtOAc = 2:1, R_f = 0.4) to obtain **34a** as a white solid (1.93 g, 90%). Spectroscopic data were consistent with previously reported data for

this compound.[241]

^{1}H NMR (400 MHz, CDCl$_3$): δ 7.69–7.66 (m, 2H, H^4), 7.63 (dd, J = 8.1; 0.8 Hz, 1H, H^7), 7.48–7.45 (m, 2H, H^{15}), 7.41–7.36 (m, 4H, H^{10,16,17}), 7.29 (td, J = 8.1; 1.3 Hz, 1H, H^8), 7.21 (s, 1H, NH), 7.18–7.15 (m, 2H, H^3), 7.06 (td, J = 7.6; 1.3 Hz, 1H, H^9), 2.33 (s, 3H, H^1).

^{13}C{^{1}H} NMR (101 MHz, CDCl$_3$): δ 144.0 (C^6), 137.5 (C^2), 136.1 (C^5), 132.0 (C^{10}), 131.6 (C^{15}), 129.6 (C^3), 129.1 (C^8), 128.5 (C^4), 127.3 (C^{16}), 124.6 (C^{17}), 122.0 (C^{14}), 120.3 (C^9), 114.6 (C^7), 110.0 (C^{11}), 96.1 (C^{13}), 83.7 (C^{12}), 21.5 (C^1).

2-(Phenylethynyl)trifluoroacetanilide (34b)
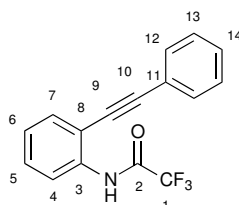
To an ice/water bath cooled solution of amine **23b** (1.0 g, 5.2 mmol) and pyridine (0.83 mL, 10.4 mmol) in DCM (50 mL) trifluoroacetic anhydride (0.88 mL, 6.2 mmol) was slowly added and the resulting mixture stirred at room temperature for 16 h before being poured onto H$_2$O (50 mL). The layers were separated and the aqueous phase was extracted with DCM (3×30 mL). The combined organic phases were washed with saturated, aqueous NaHCO$_3$ (30 mL), brine (30 mL), dried over MgSO$_4$, filtered, and concentrated under reduced pressure. The crude product was purified by column chromatography (silica, PE/EtOAc = 10:1, R$_f$ = 0.5) to obtain **34b** as a white solid (1.39 g, 94%). Spectroscopic data were consistent with previously reported data for this compound.[241]

^{1}H NMR (400 MHz, CDCl$_3$): δ 8.90 (s, 1H, NH), 8.38 (dd, J = 8.4; 1.3 Hz, 1H, H^4), 7.57 (dd, J = 7.7; 1.3 Hz, 1H, H^5), 7.55–7.52 (m, 2H, H^{12}), 7.45–7.39 (m, 4H, H^{7,13,14}), 7.22 (ddd, J = 7.7; 7.7; 7.7 Hz, 1H, H^6).

^{13}C{^{1}H} NMR (101 MHz, CDCl$_3$): δ 154.6 (C^2), 136.1 (C^3), 131.7 (C^7), 131.5 (C^{12}), 129.9 (C^5), 129.3 (C^{14}), 128.7 (C^{13}), 125.5 (C^{11}), 121.7 (C^6), 119.6 (C^4), 117.2 (C^1), 113.5 (C^8), 98.1 (C^{10}), 82.9 (C^9).

^{19}F NMR (377 MHz, CDCl$_3$): δ -75.8 (s).

2-Ethynylbenzamide (36a)
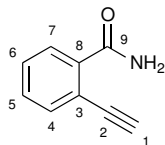
A suspension of 2-bromobenzamide (2.0 g, 10.0 mmol), (trimethylsilyl)ethyl-ene (2.1 mmol, 15.0 mmol), and PPh_3 (0.26 g, 2.0 mmol) in NEt_3 (80 mL, 0.57 mol) was degassed three times by freeze-thaw cycles under a N_2 atmosphere before $[PdCl_2(PPh_3)_2]$ (110 mg, 0.5 mol %) and CuI (95 mg, 0.5 mol %) were added. The reaction mixture was stirred at 90 °C for 24 h, and once at room temperature it was filtered through celite (Et_2O), and concentrated under reduced pressure. The resulting residue was then dissolved in a mixture of MeOH (7.5 mL), THF (18 mL), H_2O (18 mL) and KOH (1.12 g, 20.0 mmol) and stirred at room temperature for 15 min before being poured onto H_2O (50 mL) and extracted with Et_2O (3×30 mL). The combined organic phases were dried over $MgSO_4$, filtered, and concentrated under reduced pressure. The crude product was purified by column chromatography (silica, PE/E-tOAc = 1:1, R_f = 0.3) to give **36a** as a yellow solid (0.94 g, 65%). Spectroscopic data were consistent with previously reported data for this compound.[120]
^{1}H NMR (400 MHz, CDCl$_3$): δ 8.10–8.07 (m, 1H, H^7), 7.61–7.59 (m, 1H, H^4), 7.49–7.46 (m, 2H, H^{5,6}), 7.35 (s, 1H, NH), 6.21 (s, 1H, NH), 3.53 (s, 1H, H^1).
^{13}C{^{1}H} NMR (101 MHz, CD$_3$CN): δ 173.9 (C^9), 143.3 (C^8), 139.1 (C^4), 135.6 (C^5), 134.4 (C^3), 133.8 (C^6), 124.4 (C^7), 88.4 (C^2), 86.8 (C^1).

4-Ethynylbenzamide (36b)
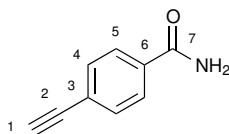
A solution of 4-bromobenzamide (1.5 g, 7.5 mmol), (trimethylsilyl)ethylene (3.2 mL, 22.5 mmol) in diethylamine (60 mL) was degassed three times by freeze-thaw cycles under a N_2 atmosphere before $[PdCl_2(PPh_3)_2]$ (210 mg, 4 mol %) and CuI (30 mg, 2 mol %) were added and the reaction mixture was stirred at room temperature for 3 days. The solvent was then evaporated and the resulting residue dissolved in EtOAc, filtered through celite, and concentrated under reduced pressure. The obtain residue was then dissolved in a mixture of MeOH (5.5 mL), THF (15 mL), H_2O (1.5 mL) and KOH (0.81 g, 14.5 mmol) and stirred at room temperature for 15 min. The solvent

was evaporated and pure **36b** was recrystallised from *i*-PrOH (0.76 g, 71%). Spectroscopic data were consistent with previously reported data for this compound.[164]

^{1}H NMR (400 MHz, DMSO–d$_6$): δ 8.05 (s, 1H, NH), 7.87 (d, *J* = 8.5 Hz, 2H, H^5), 7.56 (d, *J* = 8.5 Hz, 2H, H^4), 7.48 (s, 1H, NH), 4.37 (s, 1H, H^1).

^{13}C{^{1}H} NMR (101 MHz, DMSO–d$_6$): δ 172.2 (C^7), 139.6 (C^6), 136.8 (C^4), 132.9 (C^5), 129.6 (C^3), 88.13 (C^2), 88.00 (C^1).

Penta-3,4-dienoic acid ethyl ester (37)
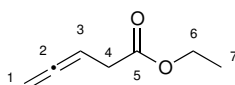
A solution of propargylic alcohol (5.0 g, 89 mmol) and propionic acid (a few drops) in triethyl orthoacetate (42.8 g, 268 mmol) was heated to 100 °C for 2 h, then to 130 °C for 4 h while ethanol was continuously removed by distillation. The reaction mixture was cooled down, poured onto aqueous HCl (0.1 M, 100 mL) and extracted with Et$_2$O (3×50 mL). The combined organic phases were washed with H$_2$O (50 mL) and brine (50 mL), dried over MgSO$_4$, filtered, and concentrated under reduced pressure. The crude product was purified by column chromatography (silica, PE/EtOAc = 10:1, R$_f$ = 0.4) to give **37** as a yellow oil (6.37 g, 57%). Spectroscopic data were consistent with previously reported data for this compound.[166]

^{1}H NMR (400 MHz, CDCl$_3$): δ 5.29 (tt, *J* = 7.4; 6.5 Hz, 1H, H^3), 4.79 (ddd, *J* = 6.5; 3.0; 3.0 Hz, 2H, H^1), 4.18 (q, *J* = 7.1 Hz, 2H, H^6), 3.07 (ddd, *J* = 7.4; 3.0; 3.0 Hz, 2H, H^4), 1.29 (t, *J* = 7.1 Hz, 3H, H^7).

^{13}C{^{1}H} NMR (101 MHz, CDCl$_3$): δ 209.3 (C^2), 171.4 (C^5), 83.5 (C^3), 75.7 (C^1), 60.8 (C^6), 34.2 (C^4), 14.2 (C^7).

Penta-3,4-dien-1-ol (38)
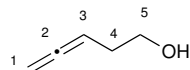
To an ice/water bath cooled suspension of LiAlH$_4$ (2.67 g, 71.1 mmol) in Et$_2$O (100 mL) ester **37** (3.91 g, 30.1 mmol) in Et$_2$O (75 mL) was slowly added. The reaction mixture was stirred at room temperature for 1 h before being quenched by addition of aqueous KOH (20 w/w%) (caution, H$_2$ formation!) until gas stopped evolving. After stirring for another 30 min, the formed white precipitate was filtered off and the filtrate was carefully concentrated under reduced pressure. The resulting oily residue was purified by column

chromatography (silica, PE/Et$_2$O = 10:1, R$_f$ = 0.4) to give **38** as a yellow oil (1.89 g, 73%). Spectroscopic data were consistent with previously reported data for this compound.[166]

^{1}H NMR (400 MHz, CDCl$_3$): δ 5.15 (tt, J = 6.8; 6.6 Hz, 1H, H^3), 4.75 (ddd, J = 6.6; 3.2; 3.2 Hz, 2H, H^1), 3.74 (t, J = 6.2 Hz, 2H, H^5), 2.30 (dtdd, J = 6.8; 6.2; 3.2; 3.2 Hz, 2H, H^4).

^{13}C{^{1}H} NMR (101 MHz, CDCl$_3$): δ 209.1 (C^2), 86.5 (C^3), 75.2 (C^1), 61.9 (C^5), 31.6 (C^4).

Penta-3,4-dien-1-nitrile (39)
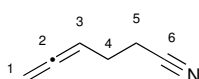
To an ice/water bath cooled solution of penta-3,4-dien-1-ol **38** (1.07 g, 12.8 mmol) and NEt$_3$ (1.90 mL, 13.4 mmol) in Et$_2$O (40 mL) mesyl chloride (1.0 mL, 12.8 mmol) was slowly added. The reaction mixture was allowed to warm to room temperature and stirred for 1 h before the precipitate was filtered off and the solvent was removed under reduced pressure. The residual oil was dissolved in DMSO (40 mL), NaCN (0.63 g, 12.8 mmol) was added and the reaction mixture was stirred at room temperature for 4 days before being poured onto H$_2$O (10 mL) and extracted with Et$_2$O (3×30 mL). The combined organic phases were washed with H$_2$O (50 mL), brine (50 mL), dried over MgSO$_4$, filtered, and carefully concentrated under reduced pressure to give **39** as a yellow oil (0.68 g, 57%). The crude product was used without further purification. Spectroscopic data were consistent with previously reported data for this compound.[165]

^{1}H NMR (400 MHz, CDCl$_3$): δ 5.12 (tt, J = 6.7; 6.6 Hz, 1H, H^3), 4.68 (dt, J = 6.6; 3.3 Hz, 2H, H^1), 2.72 (t, J = 6.7 Hz, 2H, H^5), 2.08–2.00 (m, J = 3.5 Hz, 3H, H^4).

^{13}C{^{1}H} NMR (101 MHz, CDCl$_3$): δ 208.4 (C^2), 119.3 (C^6), 87.2 (C^3), 77.4 (C^1), 23.9 (C^5), 16.6 (C^4).

2-(Hept-5,6-dienyl)isoindoline-1,3-dione (45)
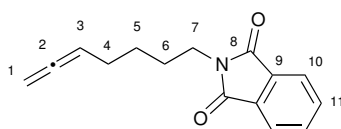
A suspension of **7a** (2.0 g, 8.9 mmol), formaldehyde (531 mg, 17.7 mmol), CuBr (444 mg, 45.0 mmol), and diisopropylamine (2.5 mL, 17.7 mmol) in dioxane (20 mL) was heated to 120 °C for 5 h. The resulting mixture was then

cooled, filtered through celite, washed with EtOAc (15 mL), and the filtrate was poured onto H_2O (50 mL). The aqueous phase was extracted with EtOAc (3×30 mL), and the combined organic phases were washed with aqueous HCl (1 M, 30 mL), aqueous saturated $NaCO_3$ (30 mL), and brine (30 mL), dried over $MgSO_4$, filtered, and concentrated under reduced pressure. The crude product was purified by column chromatography (silica, PE/EtOAc = 10:11, R_f = 0.4) to give **45** as a white solid (0.90 g, 42%). Spectroscopic data were consistent with previously reported data for this compound.[242]

^{1}H NMR (400 MHz, CDCl$_3$): δ 7.87–7.82 (m, 2H, H^{11}), 7.74–7.69 (m, 2H, H^{10}), 5.08 (tt, J = 6.7; 6.6 Hz, 1H, H^3), 4.65 (dt, J = 6.6; 3.4 Hz, 2H, H^1), 3.70 (t, J = 7.3 Hz, 2H, H^7), 2.05 (tdt, J = 7.1; 7.0; 3.4 Hz, 2H, H^5), 1.77–1.69 (m, 2H, H^6), 1.52–1.44 (m, 2H, H^5).

^{13}C{^{1}H} NMR (101 MHz, CDCl$_3$): δ 208.5 (C^2), 168.4 (C^8), 133.8 (C^9), 132.2 (C^{11}), 123.1 (C^{10}), 89.4 (C^3), 74.9 (C^1), 37.8 (C^7), 28.0 (C^4), 27.7 (C^6), 26.2 (C^5).
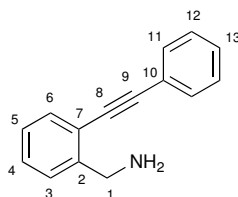
Hexa-4,5-dien-1-amine (40a)
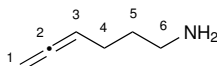
To an ice/water bath cooled suspension of LiAlH$_4$ (0.50 g, 13.2 mmol) in Et$_2$O (10 mL) a solution of nitrile **39** (0.61 g, 6.6 mmol) in Et$_2$O (10 mL) was slowly added. The bath was then removed and the reaction mixture was stirred at room temperature for 3 h, before being quenched by addition of aqueous NaOH (10 w/w%, 0.5 mL) (caution, H$_2$ formation!) until gas stopped evolving. The formed precipitate was filtered off and washed with Et$_2$O (10 mL). The aqueous layer was separated and extracted with Et$_2$O (3×10 mL). The combined organic phases were dried over MgSO$_4$, filtered, and concentrated under reduced pressure to obtain **40a** as a colourless oil after distillation at 80 °C under 80 mbar (0.42 g, 66%). Spectroscopic data were consistent with previously reported data for this compound.[165]

^{1}H NMR (400 MHz, CDCl$_3$): δ 5.11 (tt, J = 6.7; 6.7 Hz, 1H, H^3), 4.68 (dt, J = 6.6; 3.3 Hz, 2H, H^1), 2.74 (t, J = 7.0 Hz, 2H, H^6), 2.06 (tdt, J = 7.0; 6.7; 3.3 Hz, 2H, H^4), 1.58 (tt, J = 7.2; 7.0 Hz, 2H, H^5), 1.40 (s, 2H, NH$_2$).

^{13}C{^{1}H} NMR (101 MHz, CDCl$_3$): δ 208.5 (C^2), 89.5 (C^3), 74.9 (C^4), 41.5 (C^6), 32.9 (C^4), 25.5 (C^5).

Hepta-5,6-diene-1-amine (40b)
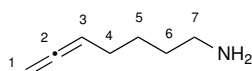
A solution of phthalamine allene **45** (0.90 g, 3.73 mmol) and hydrazine mono-hydrate (374 mg, 7.46 mmol) in MeOH (10 mL) was heated at 70 °C for 2 h. The reaction mixture was cooled to room temperature, aqueous KOH (20 w/w %, 5 mL) was added, and the aqueous layer was extracted with DCM (3×15 mL). The combined organic phases were dried over $MgSO_4$, filtered, and concentrated under reduced pressure to give **40b** as a yellow oil (393 mg, 95%). Spectroscopic data were consistent with previously reported data for this compound.[242]

^{1}H NMR (400 MHz, CDCl$_3$): δ 5.12 (tt, J = 6.8; 6.7 Hz, 1H, H^3), 4.68 (dt, J = 6.7; 3.3 Hz, 2H, H^1), 2.72 (t, J = 6.6 Hz, 2H, H^7), 2.04 (tdt, J = 6.9; 6.8; 3.3 Hz, 2H, H^4), 1.67–1.43 (m, 4H, H^{5,6}).

^{13}C{^{1}H} NMR (101 MHz, CDCl$_3$): δ 208.5 (C^2), 89.7 (C^3), 74.8 (C^1), 41.6 (C^7), 28.0 (C^4), 26.2 (C^6), 12.7 (C^5).

Penta-3,4-dienoic acid ethyl ester (41)
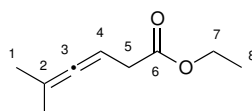
A solution of 2-methyl-butyn-2-ol (6.0 g, 71 mmol) and propionic acid (a few drops) in triethyl orthoacetate (34.7 g, 210 mmol) was heated to 100 °C for 2 h, then to 130 °C for 4 h while ethanol was continuously removed by distillation. The reaction mixture was cooled down, poured onto aqueous HCl (0.1 M, 100 mL), and extracted with Et$_2$O (3×50 mL). The combined organic phases were washed with H$_2$O (50 mL) and brine (50 mL), dried over $MgSO_4$, filtered, and concentrated under reduced pressure. The obtained oil was purified by column chromatography (silica, PE/EtOAc = 20:1, R$_f$ = 0.4) to give **41** as a yellow oil (6.37 g, 57%). Spectroscopic data were consistent with previously reported data for this compound.[242]

^{1}H NMR (400 MHz, CDCl$_3$): δ 5.10 (dsept, J = 7.1; 2.8 Hz, 1H, H^4), 4.17 (q, J = 7.2 Hz, 2H, H^7), 2.99 (d, J = 7.1 Hz, 2H, H^5), 1.70 (d, J = 2.8 Hz, 6H, H^1), 1.28 (t, J = 7.2 Hz, 3H, H^8).

^{13}C{^{1}H} NMR (101 MHz, CDCl$_3$): δ 202.9 (C^3), 171.9 (C^6), 96.3 (C^2), 81.9 (C^4), 60.5 (C^7), 35.3 (C^5), 20.3 (C^1), 14.1 (C^8).

5-Methylhexa-3,4-dion-1-ol (42)
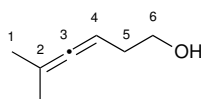
To an ice/water bath cooled suspension of $LiAlH_4$ (2.76 g, 72.6 mmol) in Et_2O (70 mL) ester **41** (5.50 g, 31.6 mmol) in Et_2O (55 mL) was slowly added. The reaction mixture was stirred at room temperature for 1 h before being quenched by addition of aqueous KOH (20 w/w%) (caution, H_2 formation!) until gas stopped evolving. After stirring for further 30 min, the formed white precipitate was filtered off and the filtrate was carefully concentrated under reduced pressure to give **42** as a yellow oil (3.76 g, 95%). The crude product was used without further purification. Spectroscopic data were consistent with previously reported data for this compound.[165]

^{1}H NMR (400 MHz, CDCl$_3$): δ 4.97 (dsept, J = 6.2; 2.9 Hz, 1H, H^4), 3.70 (t, J = 6.2 Hz, 2H, H^6), 2.23 (td, J = 6.2; 6.2 Hz, 2H, H^5), 1.71 (d, J = 2.9 Hz, 6H, H^1).

^{13}C{^{1}H} NMR (101 MHz, CDCl$_3$): δ 202.5 (C^3), 95.6 (C^2), 85.0 (C^4), 62.1 (C^6), 32.5 (C^5), 20.6 (C^1).

6-Methylhepta-4,5-dien-1-amine (44)
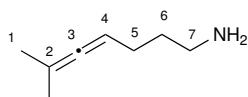
To an ice/water bath cooled solution of dienol **42** (2.66 g, 23.7 mmol) and NEt$_3$ (3.4 mL, 24.9 mmol) in Et_2O (40 mL) mesyl chloride (1.8 mL, 23.7 mmol) was slowly added. The reaction mixture was allowed to warm to room temperature and stirred for 1 h before the formed precipitate was filtered off and the solvent was removed under reduced pressure. The residual oil was dissolved in DMSO (60 mL) and NaCN (1.16 g, 23.7 mmol) was added. The resulting mixture was stirred at room temperature for 4 days before being poured onto H_2O (150 mL) and extracted with Et_2O (3×50 mL). The combined organic phases were washed with H_2O (50 mL) and brine (50 mL), dried over MgSO$_4$, filtered, and carefully concentrated under reduced pressure to ~ 10 mL under reduced pressure. The obtained solution was then slowly added to an ice/water bath cooled suspension of $LiAlH_4$ (1.67 g, 44.0 mmol) in Et_2O (100 mL). The bath was then removed and the reaction was stirred at room temperature for 3 h, before being quenched by addition of aqueous NaOH (10 w/w%, 5 mL) (caution, H_2 formation!) until gas stopped evolving. The formed precipitate was filtered off and washed with Et_2O (20 mL). The aqueous layer was separated and extracted with Et_2O (3×20 mL). The combined organic phases were dried over MgSO$_4$, filtered, and concentrated under reduced pressure to obtain **44** as a colourless oil after distillation at 90 °C under 10 mbar (2.04 g, 74%). Spectroscopic data were consistent with previously reported data for this compound.[165]

^{1}H NMR (400 MHz, CDCl$_3$): δ 4.95 (tsept, J = 6.6; 3.0 Hz, 1H, H^4), 2.73 (t, J

= 7.0 Hz, 2H, H^7), 1.99 (td, J = 7.0; 6.6 Hz, 2H, H^5), 1.68 (d, J = 3.0 Hz, 6H, H^1), 1.58–1.51 (m, 2H, H^6), 1.44 (s, 2H, NH$_2$).

^{13}C{^{1}H} NMR (101 MHz, CDCl$_3$): δ 201.7 (C^3), 95.1 (C^2), 88.2 (C^4), 41.6 (C^7), 33.1 (C^6), 26.5 (C^5), 20.7 (C^1).

Ethyl (E)-hepta-4,6-dienoate (46)
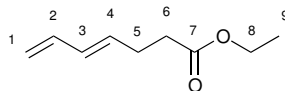
A solution of pent-1,4-dien-3-ol (5.0 g, 60.0 mmol), propionic acid (a few drops) in triethyl orthoacetate (70 mL) was heated to 150 °C for 1 h. The reaction mixture was cooled down and the formed EtOH was distilled off (b.p. = 95 °C) before the solution was heated to 150 °C for further 2 h. The remaining triethylorthoacetate was distilled off (b.p. = 160 °C) and the resulting residue was purified by column chromatography (silica, PE/EtOAc = 5:1, R$_f$ = 0.4) to obtain **46** as a colourless oil (6.0 g, 71 %). Spectroscopic data were consistent with previously reported data for this compound.[243]

^{1}H NMR (400 MHz, CDCl$_3$): δ 6.29 (dt, J = 16.9; 10.3 Hz, 1H, H^2), 6.09 (ddd, J = 15.2; 10.3; 0.5 Hz, 1H, H^3), 5.73–5.67 (m, 1H, H^4), 5.11 (d, J = 16.9 Hz, 1H, *trans*-H^1), 4.99 (d, J = 10.1 Hz, 1H, *cis*-H^1), 4.13 (q, J = 7.1 Hz, 2H, H^8), 2.41–2.40 (m, 4H, H^{5,6}), 1.25 (t, J = 7.1 Hz, 3H, H^9).

^{13}C{^{1}H} NMR (101 MHz, CDCl$_3$): δ 172.9 (C^7), 136.8 (C^4), 132.6 (C^2), 131.9 (C^3), 115.7 (C^1), 60.3 (C^8), 33.8 (C^6), 27.8 (C^5), 14.2 (C^9).

(E)-Hepta-4,6-dienamide (47)
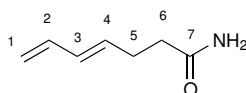
To an ice/water bath cooled suspension of NH$_4$Cl (2.14 g, 40 mmol) in dry and degassed toluene (20 mL) a solution of AlMe$_3$ in toluene (20 mL, 2 M) under N$_2$ atmosphere was added. The reaction mixture was stirred at room temperature until no further gas evolution was observed, then a solution of **46** (2.20 g, 14.6 mmol) in toluene (20 mmol) was slowly added over the course of 30 min. After heating at 55 °C for 2 days, the resulting mixture was quenched by addition of aqueous HCl (2 M, 50 mL) (caution, CH$_4$ and NH$_3$ formation!). The organic phase was separated and the aqueous layer was extracted with EtOAc (3×50 mL). The combined organic phases were dried over MgSO$_4$, filtered, and concentrated under reduced pressure. The obtained residue was purified by column chromatography (silica, EtOAc, R$_f$

= 0.5) to obtain **47** as a white solid (1.38 g, 95 %). Spectroscopic data were consistent with previously reported data for this compound.[169]

¹H NMR (400 MHz, CDCl₃): δ 6.30 (dt, J = 16.9; 10.3 Hz, 1H, H²), 6.14–6.08 (m, 1H, H³), 5.79 (s, 1H, NH), 5.75–5.68 (m, 1H, H⁴), 5.54 (s, 1H, NH), 5.15–5.10 (m, 1H, *trans*-H¹), 5.01 (ddd, J = 10.2; 1.5; 0.7 Hz, 1H, *cis*-H¹), 2.46–2.41 (m, 2H, H⁶), 2.33 (ddd, J = 8.0; 6.8; 1.2 Hz, 2H, H⁵).

¹³C{¹H} NMR (101 MHz, CDCl₃): δ 174.9 (C⁷), 136.8 (C⁴), 132.8 (C²), 132.1 (C³), 116.0 (C¹), 35.5 (C⁶), 28.5 (C⁵).

(E)-Hepta-4,6-dien-1-amine (48)
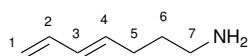
To an ice/water bath cooled suspension of LiAlH₄ (0.40 g, 10.6 mmol) in THF (15 mL) a solution of **47** (1.05 g, 7.6 mmol) in THF (15 mL) was added. The resulting mixture was stirred at room temperature for 4 h before aqueous KOH (20 w/w%) (caution, H₂ formation!) was added until no further gas evolution was observed. After stirring for 30 min, the formed precipitate was filtered off, and the filtrate was washed with H₂O (20 mL). The aqueous layer was extracted with Et₂O (3×15 mL) and the combined organic phases were dried over MgSO₄, filtered, and concentrated under reduced pressure to obtain **48** as a colourless oil (0.30 g, 35 %). Spectroscopic data were consistent with previously reported data for this compound.[169]

¹H NMR (400 MHz, CDCl₃): δ 6.31 (dt, J = 17.0; 10.1 Hz, 1H, H²), 6.10–6.04 (m, 1H, H³), 5.71 (dt, J = 14.9; 7.3 Hz, 1H, H⁴), 5.10 (dd, J = 17.0; 0.7 Hz, 1H, *trans*-H¹), 4.97 (dd, J = 10.1; 0.7 Hz, 1H, *cis*-H¹), 2.71 (t, J = 7.1 Hz, 2H, H⁷), 2.14 (dt, J = 7.3; 7.3 Hz, 2H, H⁵), 1.55 (tt, J = 7.3; 7.1 Hz, 2H, H⁶), 1.09 (br. s, 2H, NH₂).

¹³C{¹H} NMR (101 MHz, CDCl₃): δ 137.1 (C²), 134.7 (C³), 131.2 (C⁴), 114.9 (C¹), 41.7 (C⁷), 33.2 (C⁶), 29.9 (C⁵).

1,1-Diphenylbut-3-en-1-nitrile (77)
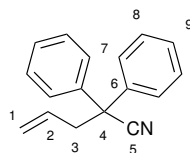
To a solution of diisopropylamine (4.55 g, 45.0 mmol) in THF (50 mL *n*-butyl-lithium (2.5 м in hexane, 17.6 mL, 44.1 mmol) was slowly added at –78 °C. After stirring at 0 °C for 5 min, the reaction mixture was cooled again to

−78 °C and a solution of diphenylacetonitrile (8.12 g, 42.0 mmol) in THF (20 mL) was slowly added. After 3 h of stirring, allylbromide (5.08 g, 42.0 mmol) was added and the reaction was stirred at room temperature for 16 h. The reaction was quenched by addition of aqueous NH_4Cl (10 w/w%, 40 mL) and extracted with Et_2O (3×40 mL). The combined organic phases were dried over $MgSO_4$, filtered, and concentrated under reduced pressure to give **77** as a pale yellow oil (7.64 g, 78 %). The crude product was used without further purification. Spectroscopic data were consistent with previously reported data for this compound.[172]

¹H NMR (400 MHz, CDCl₃): δ 7.47–7.32 (m, 10H, H$^{7-9}$), 5.77 (ddt, J = 17.0; 10.2; 7.0 Hz, 1H, H^2), 5.27 (ddt, J = 17.0; 1.5; 1.4 Hz, 1H, *trans*-H^1), 5.22 (ddt, J = 10.2; 1.5; 0.7 Hz, 1H, *cis*-H^1), 3.20 (ddd, J = 7.0; 1.4; 0.7 Hz, 2H, H^3).

¹³C{¹H} NMR (101 MHz, CDCl₃): δ 139.8 (C^6), 131.8 (C^2), 128.9 (C^9), 128.0 (C^8), 127.1 (C^7), 122.0 (C^1), 120.5 (C^5), 51.8 (C^4), 44.0 (C^3).

1,1-Diphenylpent-4-en-1-amine (50)
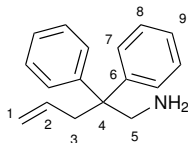
To an ice/water bath cooled suspension of $LiAlH_4$ (2.51 g, 66.1 mmol) in Et_2O (225 mL) a solution of nitrile **77** (4.00 g, 17.2 mmol) in Et_2O (10 mL) was slowly added. The bath was then removed and the reaction was stirred at room temperature for 3 h, before being quenched by addition of aqueous NaOH (10 w/w%, 7.5 mL) (caution, H_2 formation!) until gas stopped evolving. The formed precipitate was filtered off and washed with Et_2O (20 mL). The aqueous layer was separated and extracted with Et_2O (3×20 mL). The combined organic phases were dried over $MgSO_4$, filtered, and concentrated under reduced pressure to obtain **50** as a yellow oil (3.31 g, 81 %). Spectroscopic data were consistent with previously reported data for this compound.[170]

¹H NMR (400 MHz, CDCl₃): δ 7.35–7.31 (m, 4H, H^7), 7.25–7.21 (m, 6H, H^{8,9}), 5.45 (ddt, J = 17.1; 10.1; 7.0 Hz, 1H, H^2), 5.09 (d, J = 17.1 Hz, 1H, *trans*-H^1), 5.02 (dt, J = 10.1; 1.0 Hz, 1H, *cis*-H^1), 3.36 (s, 2H, H^5), 3.08-2.88 (m, 2H, H^3).

¹H NMR (400 MHz, CD₃CN): δ 7.33–7.29 (m, 4H, H^7), 7.23–7.19 (m, 6H, H^{8,9}), 5.44 (ddt, J = 17.2; 10.1; 7.1 Hz, 1H, H^2), 5.06 (ddt, J = 17.1; 2.4; 1.3 Hz, 1H, *trans*-H^1), 4.95 (ddt, J = 10.2; 2.4; 1.1 Hz, 1H, *cis*-H^1), 3.32 (s, 2H, H^5), 3.00 (ddt, J = 7.1; 1.3; 1.1 Hz, 2H, H^3).

¹³C{¹H} NMR (101 MHz, CDCl₃): δ 146.3 (C^6), 134.6 (C^2), 128.2 (C^9), 128.1 (C^8), 126.1 (C^7), 117.7 (C^1), 51.4 (C^4), 48.6 (C^3), 41.2 (C^5).

6.11 Isolated Hydroamination Products

General procedure for hydroamination reactions:

A solution of unsaturated amine (2.2 mmol, 1 equiv) and $[Cu(NCMe)_4](BF_4)$ (2–10 mol%) was heated in MeCN (5 mL, 0.4 M) at 80 °C for 2–16 h before being cooled to room temperature and poured onto aqueous EDTA (5 mL, 0.2 M). The resulting mixture was extracted with Et_2O (3×3 mL) and the combined organic phases were dried over Na_2SO_4, filtered and concentrated under reduced pressure.

N-Methyl-2-methylpyrrolinium iodide (51a)
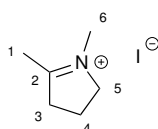
Following the general procedure a solution of pentynylamine **8a** (1.5 g, 18.0 mmol), [Cu $(NCMe)_4](BF_4)$ (113 g, 2 mol%) in MeCN (45 mL) was heated at 80 °C for 2 h before being cooled to room temperature and MeI (1.1 mL, 18.0 mmol) being added. The resulting reaction mixture was stirred at room temperature for 2 h before evaporating the solvent under reduced pressure to give **51a** as yellow, crystalline solid (3.68 g, 91%). Spectroscopic data were consistent with previously reported data for this compound.[244]

^{1}H NMR (400 MHz, CDCl$_3$): δ 4.33 (t, J = 7.6 Hz, 2H, H^5), 3.57 (s, 3H, H^6), 3.45–3.41 (m, 2H, H^3), 2.62 (s, 3H, H^1), 2.35 (tt, J = 8.0; 7.6 Hz, 2H, H^4).

^{13}C{^{1}H} NMR (101 MHz, CDCl$_3$): δ 191.1 (C^2), 63.1 (C^5), 41.7 (C^6), 38.8 (C^3), 19.3 (C^4), 18.0 (C^1).

2-Methyltetrahydropyridine (51b)
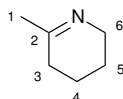
Following the general procedure alkynylamine **8b** (0.11 g, 1.1 mmol), [Cu $(NCMe)_4](BF_4)$ (7 mg, 2 mol%), and MeCN (2.5 mL) and stirring for 4 h, **51b** was isolated after purification by column chromatography (silica, EtOAc/MeOH/aq. NH_4OH = 10:1:1, R_f = 0.3) as a red oil (0.09 g, 83%). Spectroscopic data were consistent with previously reported data for this compound.[245]

^{1}H NMR (400 MHz, CD$_3$CN): δ 3.45 (br. s, 2H, H^6), 2.13 (tt, J = 6.6; 1.8 Hz,

2H, H^3), 1.85 (t, J = 1.8 Hz, 3H, H^1), 1.68–1.62 (m, 2H, H^5), 1.55–1.49 (m, 2H, H^4).
^{13}C{^{1}H} NMR (101 MHz, CDCl$_3$): δ 167.8 (C^2), 30.6 (C^6), 26.9 (C^1), 21.4 (C^{3,5}), 19.3 (C^4).

N-ethyl-2-ethylpyrrolinium iodide (54a)
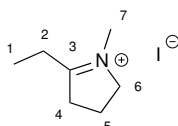
Following the general procedure a solution of pentynylamine **15a** (0.24 mL, 2.2 mmol), [Cu(NCMe)$_4$](BF$_4$) (35 mg, 5 mol %) in MeCN (5 mL) was heated at 80 °C for 16 h before being cooled to room temperature and MeI (0.14 mL, 2.2 mmol) being added. The resulting solution was stirred at room temperature for 2 h before evaporating the solvent under reduced pressure to give **54a** as a mixture with benzoylpyrroline **58** as a red oil (39 mg, 68%).
^{1}H NMR (400 MHz, CDCl$_3$): δ 4.12 (t, J = 7.9 Hz, 2H, H^6), 3.33 (s, 3H, H^7), 3.19–3.14 (m, 2H, H^4), 2.66 (q, J = 7.5 Hz, 2H, H^2), 2.11 (tt, J = 8.0; 7.9 Hz, 2H, H^5), 1.14 (t, J = 7.5 Hz, 3H, H^1).
^{13}C{^{1}H} NMR (101 MHz, CDCl$_3$): δ 194.8 (C^3), 63.1 (C^6), 38.8, 38.4 (C^7), 25.3 , 17.9 (C^2), 9.8 (C^1).

2-Ethyltetrahydropyridine (54b)
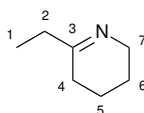
Following the general procedure alkynylamine **15b** (0.27 mL, 2.2 mmol), [Cu (NCMe)$_4$](BF$_4$) (139 mg, 20 mol %), and MeCN (5 mL) and stirring for 16 h, **54b** was isolated after purification by column chromatography (silica, EtOAc/ MeOH/ aq. NH$_4$OH = 10:1:1, R$_f$ = 0.6) as a red oil (0.10 g, 41%). Spectroscopic data were consistent with previously reported data for this compound.[119]
^{1}H NMR (400 MHz, CDCl$_3$): δ 3.56 (br. s, 2H, H^7), 2.25–2.11 (m, 4H, H^{2,4}), 1.69–1.64 (m, 2H, H^5), 1.60–1.55 (m, 2H, H^6), 1.08 (t, J = 7.5 Hz, 3H, H^1).
^{13}C{^{1}H} NMR (101 MHz, CDCl$_3$): δ 172.3 (C^3), 49.0 (C^7), 33.7 (C^2), 28.7(C^4), 21.9 (C^6), 19.5 (C^5), 10.6 (C^1).

5-Benzyl-3,4-dihydro-2H-pyrrole (57a)
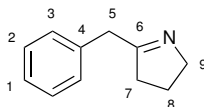
Following the general procedure alkynylamine **21a** (0.34 mg, 2.2 mmol), [Cu
(NCMe)$_4$](BF$_4$) (13.8 mg, 2 mol%), and MeCN (5 mL) and stirring for 16 h,
57a was isolated after purification by column chromatography (silica, PE/
EtOAc = 2:1, R$_f$ = 0.2) as a yellow oil (0.28 g, 68%). Spectroscopic data were
consistent with previously reported data for this compound.[119]
^{1}H NMR (400 MHz, CDCl$_3$): δ 7.35–7.31 (m, 2H, H^3), 7.28–7.25 (m, 3H, H^{1,2}),
3.86 (tddd, J = 7.3; 2.3; 1.6; 1.6 Hz, 2H, H^9), 3.70 (s, 2H, H^5), 2.44–2.40 (m, 2H,
H^7), 1.89–1.82 (m, 2H, H^8).
^{13}C{^{1}H} NMR (101 MHz, CDCl$_3$): δ 176.8 (C^6), 137.0 (C^4), 129.0 (C^3), 128.6
(C^2), 126.6 (C^1), 61.0 (C^9), 40.7 (C^5), 36.5 (C^7), 22.6 (C^8).

6-Benzyl-2,3,4,5-tetrahydropyridine (57b)
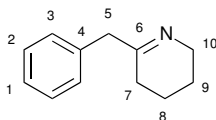
Following the general procedure alkynylamine **21b** (0.35 mg, 2.2 mmol), [Cu
(NCMe)$_4$](BF$_4$) (35 g, 5 mol%), and MeCN (5 mL) and stirring for 16 h, **57b**
was isolated after purification by column chromatography (silica, EtOAc/
MeOH = 10:1, R$_f$ = 0.5) as a red oil (0.25 g, 74%). Spectroscopic data were
consistent with previously reported data for this compound.[119]
^{1}H NMR (400 MHz, CDCl$_3$): δ 7.35–7.23 (m, 5H, H^{1,2,3}), 3.65–3.62 (m, 2H,
H^{10}), 3.51 (s, 2H, H^5), 2.08 (ddt, J = 6.5; 4.4; 2.1 Hz, 2H, H^7), 1.65–1.53 (m, 4H,
H^{8,9}).
^{13}C{^{1}H} NMR (101 MHz, CDCl$_3$): δ 170.1 (C^6), 137.8 (C^4), 129.0 (C^3), 128.5
(C^2), 126.5 (C^1), 49.5 (C^{10}), 48.3 (C^5), 28.2 (C^7), 21.8 (C^9), 19.5 (C^8).

5-Benzoyl-3,4-dihydro-2H-pyrrole (59)
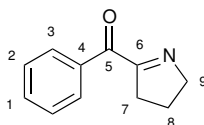
Following the general procedure alkynylamine **21a** (0.34 mg, 2.2 mmol), [Cu (NCMe)$_4$](BF$_4$) (13.8 g, 2 mol %), and MeCN (5 mL) and stirring for 16 h, **59** was isolated after purification by column chromatography (silica, PE/EtOAc = 2:1, R$_f$ = 0.7) as a yellow oil (0.06 g, 16%). Spectroscopic data were consistent with previously reported data for this compound.[244]

^{1}H NMR (400 MHz, CDCl$_3$): δ 8.21–8.19 (m, 2H, H^3), 7.60 (dddd, J = 7.8; 6.8; 1.3; 1.3 Hz, 1H, H^1), 7.51–7.46 (m, 2H, H^2), 4.25 (tt, J = 7.5; 2.4 Hz, 2H, H^9), 3.01–2.96 (m, 2H, H^7), 2.07–1.99 (m, 2H, H^8).

^{13}C{^{1}H} NMR (101 MHz, CDCl$_3$): δ 191.0 (C^5), 174.2 (C^6), 135.6 (C^4), 133.4 (C^3), 130.5 (C^1), 128.3 (C^2), 63.3 (C^9), 35.7 (C^7), 21.7 (C^8).

2-Phenyl-1-H-Indole (62a)
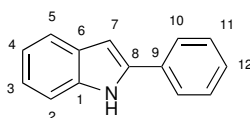
A suspension of ethynyl amide **34b** (116 mg, 0.4 mmol), K$_3$PO$_4$ (117 mg, 0.8 mmol), and [Cu(NCMe)$_4$](BF$_4$) (6.3 mg, 5 mol %) in MeCN (1 mL) was stirred for at 80 °C for 2.5 h. The reaction mixture was washed with saturated, aqueous Na$_4$EDTA after cooling to room temperature and the aqueous layer was extracted with Et$_2$O (3×3 mL). The combined organic phases were dried over MgSO$_4$, filtered and concentrated under reduced pressure to give **62a** as a white solid without any further purification (76 mg, 99%). Spectroscopic data were consistent with previously reported data for this compound.[246]

^{1}H NMR (400 MHz, CDCl$_3$): δ 8.27 (s, 1H, NH), 7.64–7.61 (m, 3H, H^{11,12}), 7.44–7.39 (m, 2H, H^{10}), 7.37 (ddd, J = 8.1; 0.9; 0.9 Hz, 1H, H^5), 7.31 (dddd, J = 7.4; 7.4; 1.5; 1.5 Hz, 1H, H^2), 7.19 (ddd, J = 8.1; 7.0; 1.2 Hz, 1H, H^3), 7.12 (ddd, J = 7.4; 7.4; 0.9 Hz, 1H, H^4), 6.81 (dd, J = 2.1; 0.9 Hz, 1H, H^7).

^{13}C{^{1}H} NMR (101 MHz, CDCl$_3$): δ 137.9 (C^8), 136.9 (C^1), 132.4 (C^9), 129.3 (C^6), 129.1 (C^{11}), 127.7 (C^{12}), 125.2 (C^{10}), 122.4 (C^3), 120.7 (C^5), 120.3 (C^4), 111.0 (C^2), 100.0 (C^7).

2-Phenyl-1-tosyl-1-H indole (64)
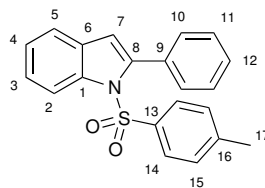
A suspension of ethynyl tosylamide **34a** (139 mg, 0.4 mmol), TBAB (13 mg, 0.04 mmol), and [Cu(NCMe)$_4$](BF$_4$) (6.3 mg, 5 mol %) in H$_2$O (6 mL) was stirred for at 80 °C for 30 min. The reaction mixture was washed with saturated, aqueous Na$_4$EDTA after cooling to room temperature and the aqueous layer was extracted with Et$_2$O (3×3 mL). The combined organic phases were dried over MgSO$_4$, filtered and concentrated under reduced pressure to give **64** as a white solid without any further purification (135 mg, 99%). Spectroscopic data were consistent with previously reported data for this compound.[176]

^{1}H NMR (400 MHz, CDCl$_3$): δ 8.30 (dd, J = 8.4; 0.6 Hz, 1H, H^2), 7.50–7.47 (m, 2H, H^{10}), 7.48–7.39 (m, 4H, H^{5,11,12}), 7.33 (ddd, J = 8.4; 7.2; 1.2 Hz, 1H, H^3), 7.26–7.23 (m, 3H, H^{4,14}), 6.99 (d, J = 8.1 Hz, 2H, H^{15}), 6.51 (s, 1H, H^7), 2.22 (s, 3H, H^{17}).

^{13}C{^{1}H} NMR (101 MHz, CDCl$_3$): δ 144.5 (C^{16}), 142.1 (C^1), 138.3 (C^{13}), 134.7 (C^9), 132.4 (C^8), 130.5 (C^{12}), 130.3 (C^6), 129.2 (C^{15}), 128.6 (C^{11}), 127.5 (C^{14}), 126.8 (C^{10}), 124.8 (C^3), 124.3 (C^5), 120.7 (C^4), 116.7 (C^2), 113.6 (C^7), 21.5 (C^{17}).

3-Butylisoquinoline (63c)
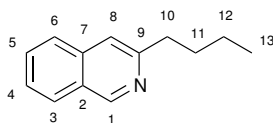
Following the general hydroamination procedure alkynylamine **26c** (0.19 mg, 1.1 mmol), [Cu(NCMe)$_4$](BF$_4$) (16 mg, 5 mol %), and MeCN (2.5 mL) and stirring for 16 h, **63c** was isolated after purification by column chromatography (silica, PE/EtOAc = 2:1, R$_f$ = 0.4) as a red oil (0.10 g, 49%). Spectroscopic data were consistent with previously reported data for this compound.[247]

^{1}H NMR (400 MHz, CDCl$_3$): δ 9.19 (s, 1H, H^1), 7.91 (dd, J = 8.1; 1.2 Hz, 1H, H^3), 7.73 (d, J = 8.2 Hz, 1H, H^6), 7.63 (ddd, J = 8.2; 6.9; 1.2 Hz, 1H, H^5), 7.51 (dd, J = 8.1; 6.9 Hz, 1H, H^4), 7.46 (s, 1H, H^8), 2.94 (t, J = 7.8 Hz, 2H, H^{10}), 1.84–1.76 (m, 2H, H^{11}), 1.47–1.38 (m, 2H, H^{12}), 0.96 (t, J = 7.4 Hz, 3H, H^{13}).

^{13}C{^{1}H} NMR (101 MHz, CDCl$_3$): δ 155.8 (C^9), 152.0 (C^1), 136.5 (C^7), 130.2 (C^5), 127.5 (C^3), 127.0 (C^2), 126.2 (C^6), 126.1 (C^4), 117.9 (C^8), 37.8 (C^{10}), 32.1 (C^{11}), 22.5 (C^{12}), 14.0 (C^{13}).

2-Acetylbenzonitrile (65)
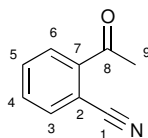
Following the general hydroamination procedure alkynylamine **36a** (0.16 mg, 1.1 mmol), [Cu(NCMe)$_4$](BF$_4$) (18 mg, 5 mol %), and MeCN (2.5 mL) and stirring for 16 h, **65** was isolated after purification by column chromatography (silica, PE/EtOAc = 1:1, R$_f$ = 0.5) as a yellow solid (0.07 g, 41%). Spectroscopic data were consistent with previously reported data for this compound.[248]

^{1}H NMR (400 MHz, CDCl$_3$): δ 7.97–7.95 (m, 1H, H^6), 7.84–7.82 (m, 1H, H^3), 7.73 (ddd, J = 7.6; 7.6; 1.5 Hz, 1H, H^4), 7.67 (ddd, J = 7.6; 7.6; 1.5 Hz, 1H, H^5), 2.71 (s, 3H, H^9).

^{13}C{^{1}H} NMR (101 MHz, CDCl$_3$): δ 196.1 (C^8), 139.8 (C^7), 135.3 (C^4), 132.64 (C^5), 132.51 (C^3), 129.9 (C^6), 118.1 (C^1), 111.0 (C^2), 27.8 (C^9).

6.12 NMR Scale Hydroamination Reactions

General procedure for NMR scale reactions:

A solution of unsaturated amine (0.22 mmol, 1 equiv) and [Cu(NCMe)$_4$](BF$_4$) (2–20 mol %) was heated in MeCN-d3 (0.5 mL, 0.44 M) at 80 °C for 16 h before the reaction mixture was cooled down and its ^{1}H NMR spectrum was measured. Reported ^{1}H NMR yields were calculated with respect to 1,3,5-trimethoxybenzene (0.04 M) as an internal standard.

2-(Trimethylsilylmethyl)pyrroline (56a)
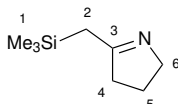
Following the general procedure silylamine **18a** (42 µL, 0.22 mmol) and [Cu(NCMe)$_4$](BF$_4$) (2.1 mg, 3 mol %) in CD$_3$CN (0.5 mL) and stirring for 16 h, the formation of **56a** was observed in 83% yield. The obtained ^{1}H NMR spectrum was consistent with previously reported data for this compound.[249]

^{1}H NMR (400 MHz, CD$_3$CN): δ 3.74–3.68 (m, 2H, H^6), 2.50–2.45 (m, 2H, H^4), 1.98 (s, 2H, H^2), 1.89–1.81 (m, 2H, H^5), 0.09 (s, 9H, H^1).

6-((Trimethylsilyl)methyl)-2,3,4,5-tetrahydropyridine (56b)
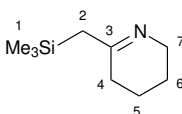
Following the general procedure silylamine **18b** (42 μL, 0.22 mmol) and [Cu(NCMe)$_4$](BF$_4$) (2.1 mg, 20 mol %) in CD$_3$CN (0.5 mL) and stirring for 16 h, the formation of **56b** was observed in 75% yield.

^{1}H NMR (400 MHz, CD$_3$CN): δ 3.48 (dd, J = 3.6; 1.9 Hz, 2H, H^7), 2.20–2.17 (m, 2H, H^4), 1.93 (t, J = 1.7 Hz, 2H, H^2), 1.68–1.63 (m, 2H, H^6), 1.58–1.53 (m, 2H, H^5), 0.09 (s, 9H, H^1).

2-Vinylpyrrolidine (73a)
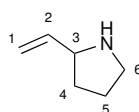
Following the general procedure alleneamine **40a** (22 mg, 0.22 mmol) and [Cu(NCMe)$_4$](BF$_4$) (3.2 mg, 5 mol %) in CD$_3$CN (0.5 mL) and stirring for 16 h, the formation of **73a** was observed in >95% yield.

^{1}H NMR (400 MHz, CD$_3$CN): δ 5.84 (ddd, J = 17.2; 10.3; 6.8 Hz, 1H, H^2), 5.14 (ddd, J = 17.2; 2.0; 1.3 Hz, 1H, *trans*-H^1), 4.98 (ddd, J = 10.3; 2.0; 1.1 Hz, 1H, *cis*-H^1), 3.49–3.44 (m, 1H, H^3), 2.94 (ddd, J = 10.1; 7.6; 5.3 Hz, 1H, H^6), 2.80 (ddd, J = 10.1; 8.2; 6.7 Hz, 1H, H^6), 1.89 (dddd, J = 12.1; 8.2; 7.1; 5.3 Hz, 1H, H^4), 1.77–1.67 (m, 2H, H^{4,5}), 1.44–1.35 (m, 1H, H^5).

6-Vinyl-2,3,4,5-tetrahydropyridine (73b)
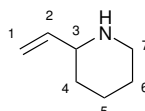
Following the general procedure alleneamine **40a** (25 mg, 0.22 mmol) and [Cu(NCMe)$_4$](BF$_4$) (3.2 mg, 5 mol %) in CD$_3$CN (0.5 mL) and stirring for 16 h, the formation of **73b** was observed in 45% yield.

^{1}H NMR (400 MHz, CDCl$_3$): δ 5.84 (ddd, J = 17.2; 10.5; 6.4 Hz, 1H, H^2), 5.15 (dt, J = 17.2; 1.4 Hz, 1H, *cis*-H^1), 5.02 (dt, J = 10.5; 1.4 Hz, 1H, *cis*-H^1), 3.22–3.16 (m, 1H, H^3), 3.12–3.05 (m, 2H, H^7), 2.08–2.01 (m, 2H, H^4), 1.84–1.80 (m, 2H, H^6), 1.31–1.23 (m, 2H, H^5).

2-(2-Methylprop-1-en-1-yl)pyrrolidine (74)
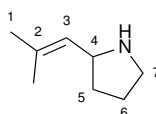
Following the general procedure alleneamine **44** (22 mg, 0.22 mmol) and [Cu (NCMe)$_4$](BF$_4$) (3.2 mg, 5 mol %) in CD$_3$CN (0.5 mL) and stirring for 16 h, the formation of **74** in 62% yield was observed.

^{1}H NMR (400 MHz, CD$_3$CN): δ 5.12 (ddt, J = 8.1; 2.8; 1.4 Hz, 1H, H^3), 3.73 (dt, J = 8.1; 7.6 Hz, 1H, H^4), 3.05 (ddd, J = 10.3; 7.6; 5.6 Hz, 1H, H^7), 2.88–2.81 (m, 1H, H^7), 1.83–1.74 (m, 3H, H^{5,6}), 1.69 (d, J = 2.8 Hz, 6H, H^1), 1.39–1.29 (m, 1H, H^6).

6.13 Computational Methodology

All calculations were carried out with the Gaussian09 program package[250] using the DFT method. The selected functional was BP86 with empirical dispersion correction of Grimme (BP86-D3).[251] The selected basis set was 6-31G(d) for C, N, O and H,[252] and sdd for Cu.[253] Additionally, calculations were carried out in the gas phase. All geometry optimisations were computed in the gas phase without symmetry restrictions. We confirmed the nature of all computed stationary points as minima or transition states through vibrational frequency calculations. Free energy corrections were calculated at 298.15 K and 105 Pa pressure, including zero point energy corrections (ZPE).

The reaction intermediates for the [Cu(DAB)] catalysed aryl azide reduction were all carried out with following Gaussian 09 syntax:

```
1  #p opt freq nosymm bp86/genecp empiricaldispersion=gd
      3 scf=xqc
```

and following tail to introduce the basis set for the elements:

```
1  -H -C -N -O 0
2  6-31g(d)
3  ****
4  -Cu 0
5  sdd
6  ****
7
8  Cu 0
9  sdd
```

Summaries for the calculations, including the obtained potential and free energies are given in Table 6.11. The relative energies were calculated with respect to [Cu(DAB^{Me})]$^+$ and PhN$_3$. The input coordinates are shown in Section A.1.

Table 6.11: Calculated energies for reaction intermediates.

label	formulea	pot. energ. (E_h)	free energ. (E_h)	rel. pot. energ. (kcal mol⁻¹)	rel. free energ. (kcal mol⁻¹)
I.1	$C_8H_{16}CuN_4$	-730.7816918	-730.591066	0	0
I.2	$C_4H_{12}CuN_2O_2$	-616.8758564	-616.751570	21.4	20.4
I.3	$C_{10}H_{17}CuN_3O$	-828.0850630	-827.874508	5.0	11.0
I.4	$C_{10}H_{15}CuN_3$	-751.6487299	-751.457863	18.7	18.4
II	$C_{16}H_{20}CuN_6$	-1147.532911	-1147.252752	-1.3	11.4
III	$C_{16}H_{20}CuN_4$	-1038.003877	-1037.730930	2.4	2.3
	$C_{16}H_{20}CuN_4$	-1038.009809	-1037.741876	-1.4	-4.6
IV	$C_{16}H_{22}CuN_4O$	-1114.445765	-1114.154607	-14.8	-9.5
V	$C_{16}H_{22}CuN_4O$	-1114.456828	-1114.166539	-21.7	-17.0
VI.1	$C_{16}H_{22}CuN_4O$	-1114.447787	-1114.154216	-16.1	-9.3
VI.2	$C_{18}H_{24}CuN_4O_2$	-1190.892531	-1190.575472	-35.0	-19.6
VI.3	$C_{18}H_{24}CuN_4O_2$	-1190.884731	-1190.569077	-30.1	-15.6
VI.4	$C_{16}H_{22}CuN_4O$	-1114.456448	-1114.162023	-21.5	-14.2
VI.5	$C_{23}H_{30}CuN_4O$	-1114.455847	-1114.161429	-21.1	-13.8
VII	$C_{23}H_{30}CuN_4O$	-1386.039054	-1385.628181	-37.4	-16.2
VII	$C_{23}H_{30}CuN_4O$	-1386.057390	-1385.640327	-48.9	-23.8
	$C_{23}H_{30}CuN_4O$	-1386.036871	-1385.621854	-36.0	-12.2
IX.1	$C_{17}H_{23}CuN_4O$	-1098.420409	-1098.110462	-24.2	-13.1
IX.2	$C_{17}H_{25}CuN_4O_2$	-1174.862748	-1174.531498	-41.7	-23.3

Transition states were obtained through the same procedure as the reaction intermediates. However, following Gaussion 09 header was used instead:

```
1  #p opt=(ts,calcfc,noeigentest) freq nosymm bp86/
      genecp empiricaldispersion=gd3 scf=xqc
```

The obtained potential and free energies for the transition states are shown in Table 6.12. The relative energies were calculated with respect to [Cu(DAB^Me)]⁺ and PhN_3. For all transition states only one imaginary frequency was observed and is given in Table 6.12 as well. The input coordinates are shown in Section A.2.

Table 6.12: Calculated energies for transition states.

label	formulea	pot. energ. (E_h)	free energ. (E_h)	rel. pot. energ. (kcal mol^{-1})	rel. free energ. (kcal mol^{-1})	imag. Freq. (cm^{-1})
TS(II)	$C_{16}H_{20}CuN_6$	-1147.500788	-1147.225252	18.9	28.7	-548.3
T(IV)	$C_{16}H_{22}CuN_4O$	-1114.432208	-1114.145692	-6.3	-3.9	-1195.0
T(V)	$C_{16}H_{22}CuN_4O$	-1114.442728	-1114.153032	-12.9	-8.6	-283.3
T(VI.2)	$C_{18}H_{24}CuN_4O_2$	-1190.876170	-1190.563843	-24.7	-12.3	-938.5
TS(VII)	$C_{23}H_{30}CuN_4O$	-1386.015050	-1385.606082	-22.3	-2.3	-1515.8
T(IX)	$C_{17}H_{25}CuN_4O_2$	-1174.840288	-1174.507444	-27.6	-8.2	-259.2

Appendix A

Appendix

A.1 Crystallographic Data

A.1 [Cu(DAB^{Ad})$_2$](BF$_4$)
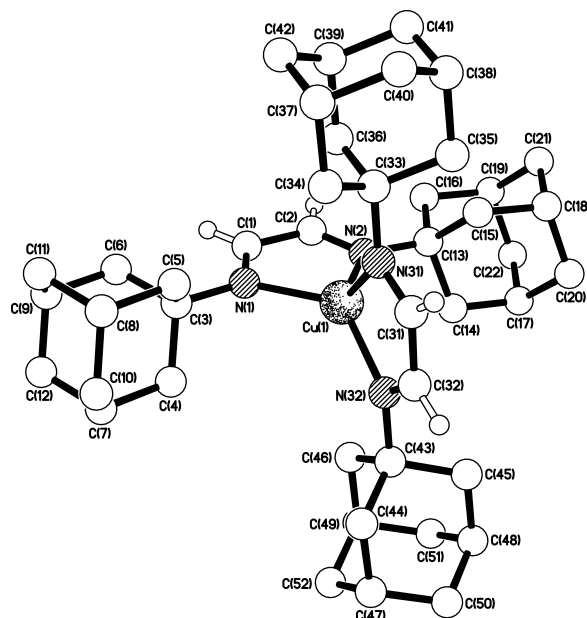
Formula	[C$_{44}$H$_{64}$CuN$_4$](BF$_4$)
Formula weight	828.38
Temperature	173 K
Diffractometer, wavelength	OD Xcalibur 3, 0.71073 Å
Crystal system, space group	Triclinic, P -1
Unit cell dimensions	a = 11.1511(3) Å α = 83.625(3) °
	b = 11.2689(3) Å β = 81.121(3) °
	c = 18.2683(7) Å γ = 70.353(3) °
Volume, Z	2131.73(12) Å^3, 2
Density (calculated)	1.291 g cm^{-3}
Absorption coefficient	0.568 mm^{-1}
F(000)	884
Crystal colour / morphology	Orange-red plates
Crystal size	0.44 x 0.33 x 0.04 mm^3
θ range for data collection	2.921 to 32.700°
Index ranges	-16<=h<=15, -17<=k<=15, -27<=l<=27
Reflns collected / unique	23910 / 13887 [R(int) = 0.0206]
Reflns observed [F>4σ(F)]	11121
Absorption correction	Analytical
Max. and min. transmission	0.977 and 0.833
Refinement method	Full-matrix least-squares on F2

217

Data / restraints / parameters	13887 / 1128 / 582
Goodness-of-fit on F^2	1.022
Final R indices [F>4σ(F)]	R1 = 0.0413, wR2 = 0.0990
R indices (all data)	R1 = 0.0581, wR2 = 0.1083
Largest diff. peak, hole	0.633, -0.382 eÅ^{-3}
Mean and maximum shift/error	0.000 and 0.001

Bond lengths [angstrom] and angles [degree] for [Cu(DAB^{Ad})$_2$](BF$_4$):

Cu(1)–N(1)	2.037(1)	C(13)–C(15)	1.538(2)	C(37)–C(4)0	1.529(3)
Cu(1)–N(2)	2.039(1)	C(13)–C(16)	1.531(2)	C(37)–C(42)	1.532(2)
Cu(1)–N(31)	2.056(1)	C(14)–C(17)	1.537(3)	C(38)–C(4)0	1.532(3)
Cu(1)–N(32)	2.027(1)	C(15)–C(18)	1.535(3)	C(38)–C(41)	1.531(2)
N(1)–C(1)	1.278(2)	C(16)–C(19)	1.538(3)	C(39)–C(41)	1.532(3)
N(1)–C(3)	1.482(2)	C(17)–C(20)	1.533(2)	C(39)–C(42)	1.534(3)
C(1)–C(2)	1.465(3)	C(17)–C(22)	1.533(3)	C(43)–C(44)	1.529(6)
C(2)–N(2)	1.282(2)	C(18)–C(20)	1.525(2)	C(43)–C(45)	1.533(7)
N(2)–C(13)	1.480(2)	C(18)–C(21)	1.531(2)	C(43)–C(46)	1.538(6)
C(3)–C(4)	1.533(2)	C(19)–C(21)	1.536(2)	C(44)–C(47)	1.543(4)
C(3)–C(5)	1.529(2)	C(19)–C(22)	1.517(3)	C(45)–C(48)	1.527(4)
C(3)–C(6)	1.532(2)	N(31)–C(31)	1.279(2)	C(46)–C(49)	1.542(5)
C(4)–C(7)	1.536(3)	N(31)–C(33)	1.490(2)	C(47)–C(50)	1.514(6)
C(5)–C(8)	1.538(3)	C(31)–C(32)	1.462(2)	C(47)–C(52)	1.542(5)
C(6)–C(9)	1.538(3)	C(32)–N(32)	1.285(2)	C(48)–C(50)	1.514(6)
C(7)–C(10)	1.531(3)	N(32)–C(43)	1.485(4)	C(48)–C(51)	1.532(4)
C(7)–C(12)	1.533(3)	C(33)–C(34)	1.539(2)	C(49)–C(51)	1.532(7)
C(8)–C(10)	1.524(3)	C(33)–C(35)	1.539(2)	C(49)–C(52)	1.511(6)
C(8)–C(11)	1.533(3)	C(33)–C(36)	1.536(2)	B(1)–F(1)	1.374(4)
C(9)–C(11)	1.528(3)	C(34)–C(37)	1.533(2)	B(1)–F(2)	1.389(5)
C(9)–C(12)	1.522(3)	C(35)–C(38)	1.535(2)	B(1)–F(3)	1.369(4)
C(13)–C(14)	1.534(2)	C(36)–C(39)	1.537(2)	B(1)–F(4)	1.394(4)

N(1)–Cu(1)–N(2)	81.95(5)	Cu(1)–N(31)–C(31)	110.6(1)
N(1)–Cu(1)–N(31)	120.12(5)	Cu(1)–N(31)–C(33)	131.90(9)
N(1)–Cu(1)–N(32)	129.81(5)	C(31)–N(31)–C(33)	117.5(1)
N(2)–Cu(1)–N(31)	119.50(5)	N(31)–C(31)–C(32)	117.9(1)
N(2)–Cu(1)–N(32)	128.66(5)	C(31)–C(32)–N(32)	118.6(1)
N(31)–Cu(1)–N(32)	81.90(5)	Cu(1)–N(32)–C(32)	111.0(1)
Cu(1)–N(1)–C(1)	110.7(1)	Cu(1)–N(32)–C(43)	131.0(2)
Cu(1)–N(1)–C(3)	129.13(9)	C(32)–N(32)–C(43)	118.0(2)
C(1)–N(1)–C(3)	120.0(1)	N(31)–C(33)–C(34)	109.7(1)
N(1)–C(1)–C(2)	118.1(1)	N(31)–C(33)–C(35)	110.8(1)

C(1)–C(2)–N(2)	118.2(1)	N(31)–C(33)–C(36)	108.4(1)
Cu(1)–N(2)–C(2)	110.5(1)	C(34)–C(33)–C(35)	109.3(1)
Cu(1)–N(2)–C(13)	129.37(9)	C(34)–C(33)–C(36)	109.3(1)
C(2)–N(2)–C(13)	120.1(1)	C(35)–C(33)–C(36)	109.3(1)
N(1)–C(3)–C(4)	107.2(1)	C(33)–C(34)–C(37)	109.4(1)
N(1)–C(3)–C(5)	107.9(1)	C(33)–C(35)–C(38)	109.2(1)
N(1)–C(3)–C(6)	114.2(1)	C(33)–C(36)–C(39)	109.7(1)
C(4)–C(3)–C(5)	108.8(1)	C(34)–C(37)–C(4)0	109.1(1)
C(4)–C(3)–C(6)	109.0(1)	C(34)–C(37)–C(42)	109.8(1)
C(5)–C(3)–C(6)	109.6(1)	C(4)0–C(37)–C(42)	109.9(1)
C(3)–C(4)–C(7)	109.8(1)	C(35)–C(38)–C(4)0	109.5(1)
C(3)–C(5)–C(8)	110.1(1)	C(35)–C(38)–C(41)	109.5(1)
C(3)–C(6)–C(9)	109.5(1)	C(4)0–C(38)–C(41)	109.9(1)
C(4)–C(7)–C(10)	109.1(2)	C(36)–C(39)–C(41)	109.4(1)
C(4)–C(7)–C(12)	109.7(2)	C(36)–C(39)–C(42)	109.1(1)
C(10)–C(7)–C(12)	109.3(2)	C(41)–C(39)–C(42)	109.8(1)
C(5)–C(8)–C(10)	109.3(1)	C(37)–C(4)0–C(38)	109.4(1)
C(5)–C(8)–C(11)	108.8(1)	C(38)–C(41)–C(39)	109.4(1)
C(10)–C(8)–C(11)	110.2(2)	C(37)–C(42)–C(39)	109.4(1)
C(6)–C(9)–C(11)	109.7(2)	N(32)–C(43)–C(44)	112.7(3)
C(6)–C(9)–C(12)	109.3(2)	N(32)–C(43)–C(45)	108.2(3)
C(11)–C(9)–C(12)	110.1(2)	N(32)–C(43)–C(46)	108.8(4)
C(7)–C(10)–C(8)	109.6(1)	C(44)–C(43)–C(45)	109.3(3)
C(8)–C(11)–C(9)	109.1(2)	C(44)–C(43)–C(46)	108.7(4)
C(7)–C(12)–C(9)	109.5(2)	C(45)–C(43)–C(46)	109.1(4)
N(2)–C(13)–C(14)	106.6(1)	C(43)–C(44)–C(47)	109.8(3)
N(2)–C(13)–C(15)	108.1(1)	C(43)–C(45)–C(48)	109.7(3)
N(2)–C(13)–C(16)	114.6(1)	C(43)–C(46)–C(49)	109.8(4)
C(14)–C(13)–C(15)	108.7(1)	C(44)–C(47)–C(50)	109.4(3)
C(14)–C(13)–C(16)	109.2(1)	C(44)–C(47)–C(52)	108.8(3)
C(15)–C(13)–C(16)	109.5(1)	C(50)–C(47)–C(52)	109.5(3)
C(13)–C(14)–C(17)	110.0(1)	C(45)–C(48)–C(50)	109.4(3)
C(13)–C(15)–C(18)	109.7(1)	C(45)–C(48)–C(51)	110.0(3)
C(13)–C(16)–C(19)	109.4(1)	C(50)–C(48)–C(51)	109.2(3)
C(14)–C(17)–C(20)	109.0(2)	C(46)–C(49)–C(51)	108.8(3)
C(14)–C(17)–C(22)	109.6(2)	C(46)–C(49)–C(52)	110.0(3)
C(20)–C(17)–C(22)	109.3(2)	C(51)–C(49)–C(52)	110.1(3)
C(15)–C(18)–C(20)	109.9(1)	C(47)–C(50)–C(48)	110.4(3)
C(15)–C(18)–C(21)	109.0(1)	C(48)–C(51)–C(49)	109.1(3)
C(20)–C(18)–C(21)	109.9(1)	C(47)–C(52)–C(49)	109.1(3)
C(16)–C(19)–C(21)	109.5(1)	F(1)–B(1)–F(2)	109.6(3)
C(16)–C(19)–C(22)	109.9(2)	F(1)–B(1)–F(3)	111.8(3)
C(21)–C(19)–C(22)	109.8(2)	F(1)–B(1)–F(4)	106.8(3)
C(17)–C(20)–C(18)	109.5(1)	F(2)–B(1)–F(3)	109.4(3)

C(18)–C(21)–C(19)	109.0(1)	F(2)–B(1)–F(4)	110.1(3)
C(17)–C(22)–C(19)	109.6(2)	F(3)–B(1)–F(4)	109.0(3)

A.2 [Cu(DAB^{tBu})$_2$](BF$_4$)
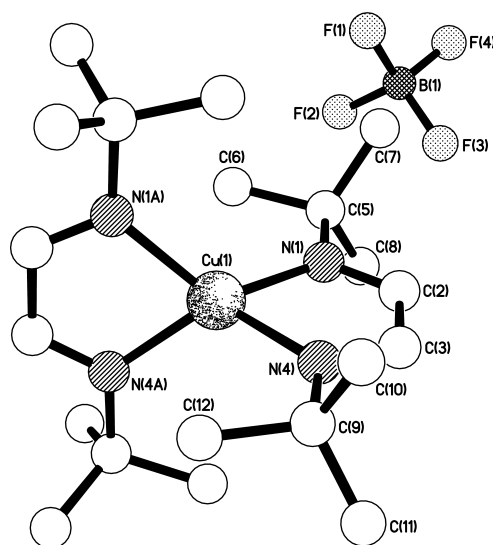
Formula	[C$_{20}$H$_{40}$CuN$_4$](BF$_4$)
Formula weight	486.91
Temperature	173 K
Diffractometer, wavelength	Agilent Xcalibur PX Ultra A, 1.54184Å
Crystal system, space group	Tetragonal, I 41/a c d
Unit cell dimensions	a = 28.7257(3) Å α = 90 °
	b = 28.7257(3) Å β = 90 °
	c = 13.0053(2) Å γ = 90 °
Volume, Z	10731.5(3) Å^3, 16
Density (calculated)	1.205 g cm^{-3}
Absorption coefficient	1.494 mm^{-1}
F(000)	4128
Crystal colour / morphology	Colourless blocky needles
Crystal size	0.37 x 0.17 x 0.11 mm^3
θ range for data collection	3.077 to 73.693°
Index ranges	-35<=h<=21, -33<=k<=33, -15<=l<=9
Reflns collected / unique	9026 / 2658 [R(int) = 0.0175]
Reflns observed [F>4σ(F)]	2302
Absorption correction	Analytical
Max. and min. transmission	0.882 and 0.736
Refinement method	Full-matrix least-squares on F2
Data / restraints / parameters	2658 / 69 / 172

Goodness-of-fit on F^2	1.065
Final R indices [F>4σ(F)]	R1 = 0.0393, wR2 = 0.1126
R indices (all data)	R1 = 0.0440, wR2 = 0.1187
Largest diff. peak, hole	0.257, -0.218 eÅ^{-3}
Mean and maximum shift/error	0.000 and 0.002

Bond lengths [Å] and angles [°] for [Cu(DAB$^{t\text{-Bu}}$)$_2$](BF$_4$):

Cu(1)–N(1A)	2.0097(14)	N(4)–C(9)	1.499(2)	C(9)–C(12)	1.522(4)
Cu(1)–N(1)	2.0098(13)	C(5)–C(7)	1.514(3)	C(9)–C(11′)	1.531(9)
Cu(1)–N(4)	2.0263(14)	C(5)–C(6)	1.523(3)	C(9)–C(12′)	1.539(8)
Cu(1)–N(4A)	2.0263(14)	C(5)–C(8)	1.523(3)	B(1)–F(3)	1.374(11)
N(1)–C(2)	1.275(2)	C(9)–C(10′)	1.459(8)	B(1)–F(4)	1.378(10)
N(1)–C(5)	1.499(2)	C(9)–C(11)	1.494(4)	B(1)–F(2)	1.385(7)
C(2)–C(3)	1.469(3)	C(9)–C(10)	1.514(4)	B(1)–F(1)	1.396(8)
C(3)–N(4)	1.265(2)				

N(1A)–Cu(1)–N(1)	126.49(8)	C(6)–C(5)–C(8)	109.7(2)
N(1A)–Cu(1)–N(4)	124.77(5)	C(10′)–C(9)–N(4)	109.2(5)
N(1)–Cu(1)–N(4)	82.15(6)	C(11)–C(9)–N(4)	111.0(2)
N(1A)–Cu(1)–N(4A)	82.15(6)	C(11)–C(9)–C(10)	111.9(3)
N(1)–Cu(1)–N(4A)	124.77(5)	N(4)–C(9)–C(10)	107.3(2)
N(4)–Cu(1)–N(4A)	122.41(8)	C(11)–C(9)–C(12)	111.0(3)
C(2)–N(1)–C(5)	118.39(15)	N(4)–C(9)–C(12)	106.65(18)
C(2)–N(1)–Cu(1)	111.26(11)	C(10)–C(9)–C(12)	108.8(3)
C(5)–N(1)–Cu(1)	130.34(12)	C(10′)–C(9)–C(11′)	110.1(6)
N(1)–C(2)–C(3)	117.73(15)	N(4)–C(9)–C(11′)	113.2(6)
N(4)–C(3)–C(2)	117.80(15)	C(10′)–C(9)–C(12′)	111.2(6)
C(3)–N(4)–C(9)	119.81(15)	N(4)–C(9)–C(12′)	106.3(4)
C(3)–N(4)–Cu(1)	111.05(12)	C(11′)–C(9)–C(12′)	106.8(6)
C(9)–N(4)–Cu(1)	129.15(12)	F(3)–B(1)–F(4)	109.0(8)
N(1)–C(5)–C(7)	109.41(16)	F(3)–B(1)–F(2)	111.2(7)
N(1)–C(5)–C(6)	106.69(16)	F(4)–B(1)–F(2)	109.5(5)
C(7)–C(5)–C(6)	110.4(2)	F(3)–B(1)–F(1)	110.6(5)
N(1)–C(5)–C(8)	108.95(15)	F(4)–B(1)–F(1)	108.8(7)
C(7)–C(5)–C(8)	111.5(2)	F(2)–B(1)–F(1)	107.8(8)

A.3 [Cu(DAB^{Cy})$_2$](BF$_4$)

Formula	[C$_{28}$H$_{48}$CuN$_4$](BF$_4$)
Formula weight	591.05
Temperature	173 K
Diffractometer, wavelength	OD Xcalibur PX Ultra, 1.54184Å
Crystal system, space group	Triclinic, P-1
Unit cell dimensions	a = 14.4357(4) Å α = 116.132(3) °
	b = 21.4133(7) Å β = 95.076(2) °
	c = 21.8614(7) Å γ = 93.921(2) °
Volume, Z	5999.5(4) Å^3, 8
Density (calculated)	1.257 309 g cm^{-3}
Absorption coefficient	1.433 mm^{-1}
F(000)	2512
Crystal colour / morphology	Orange plates
Crystal size	0.24 x 0.18 x 0.03 mm^3
θ range for data collection	2.27 to 72.54°
Index ranges	-17<=h<=17, -26<=k<=24, -26<=l<=17
Reflns collected / unique	42715 / 22886 [R(int) = 0.0433]
Reflns observed [F>4σ(F)]	18132
Absorption correction	Analytical
Max. and min. transmission	0.952 and 0.764
Refinement method	Full-matrix least-squares on F2
Data / restraints / parameters	22886 / 647 / 1478
Goodness-of-fit on F^2	1.070
Final R indices [F>4σ(F)]	R1 = 0.1160, wR2 = 0.3597
R indices (all data)	R1 = 0.1305, wR2 = 0.03666
Largest diff. peak, hole	2.809, -0.557 eÅ^{-3}
Mean and maximum shift/error	0.000 and 0.001

Structure A
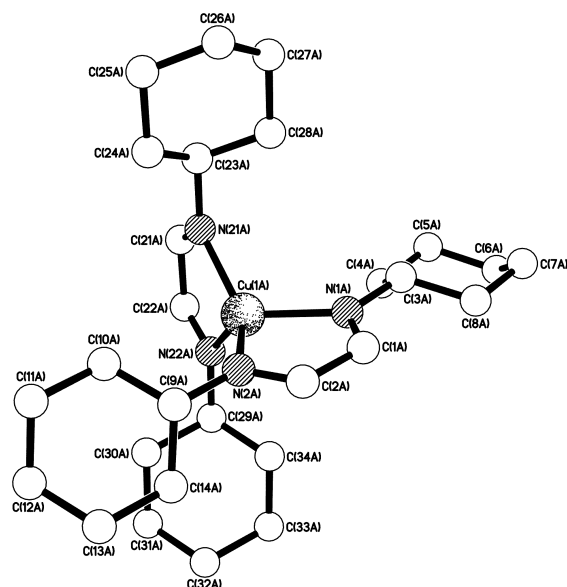
Bond lengths [Å] and angles [°] for Structure A:

Cu(1A)–N(2A)	2.009(6)	N(21A)–C(23A)	1.465(8)
Cu(1A)–N(21A)	2.015(5)	C(22A)–N(22A)	1.274(9)
Cu(1A)–N(1A)	2.034(5)	N(22A)–C(29A)	1.468(8)
Cu(1A)–N(22A)	2.035(6)	C(23A)–C(24A)	1.504(10)
C(1A)–N(1A)	1.266(9)	C(23A)–C(28A)	1.526(11)
C(1A)–C(2A)	1.465(11)	C(24A)–C(25A)	1.529(12)
N(1A)–C(3A)	1.475(9)	C(25A)–C(26A)	1.515(12)
C(2A)–N(2A)	1.260(10)	C(26A)–C(27A)	1.486(12)
N(2A)–C(9A)	1.474(9)	C(27A)–C(28A)	1.528(10)
C(3A)–C(8A)	1.522(10)	C(29A)–C(34A)	1.515(10)
C(3A)–C(4A)	1.525(10)	C(29A)–C(30A)	1.528(10)
C(4A)–C(5A)	1.529(10)	C(30A)–C(31A)	1.541(11)
C(5A)–C(6A)	1.499(12)	C(31A)–C(32A)	1.508(13)
C(6A)–C(7A)	1.517(12)	C(32A)–C(33A)	1.522(12)
C(7A)–C(8A)	1.529(11)	C(33A)–C(34A)	1.531(10)
C(9A)–C(10A)	1.516(11)	B(1)–F(14)	1.382(10)
C(9A)–C(14A)	1.523(11)	B(1)–F(12)	1.386(10)
C(10A)–C(11A)	1.529(12)	B(1)–F(11)	1.388(10)
C(11A)–C(12A)	1.517(15)	B(1)–F(13)	1.397(11)
C(12A)–C(13A)	1.523(15)	B(1′)–F(14′)	1.385(14)
C(13A)–C(14A)	1.534(12)	B(1′)–F(12′)	1.386(13)
C(21A)–N(21A)	1.266(9)	B(1′)–F(11′)	1.387(13)
C(21A)–C(22A)	1.473(9)	B(1′)–F(13′)	1.389(13)

N(2A)–Cu(1A)–N(21A)	135.5(2)	C(23A)–N(21A)–Cu(1A)	128.6(5)
N(2A)–Cu(1A)–N(1A)	82.0(2)	N(22A)–C(22A)–C(21A)	117.6(6)
N(21A)–Cu(1A)–N(1A)	117.8(2)	C(22A)–N(22A)–C(29A)	118.5(6)
N(2A)–Cu(1A)–N(22A)	124.2(2)	C(22A)–N(22A)–Cu(1A)	111.2(5)
N(21A)–Cu(1A)–N(22A)	81.4(2)	C(29A)–N(22A)–Cu(1A)	130.3(5)
N(1A)–Cu(1A)–N(22A)	121.1(2)	N(21A)–C(23A)–C(24A)	110.6(6)
N(1A)–C(1A)–C(2A)	118.0(6)	N(21A)–C(23A)–C(28A)	110.7(5)
C(1A)–N(1A)–C(3A)	120.7(6)	C(24A)–C(23A)–C(28A)	109.2(6)
C(1A)–N(1A)–Cu(1A)	110.4(5)	C(23A)–C(24A)–C(25A)	111.6(7)
C(3A)–N(1A)–Cu(1A)	128.9(4)	C(26A)–C(25A)–C(24A)	110.4(7)
N(2A)–C(2A)–C(1A)	118.1(6)	C(27A)–C(26A)–C(25A)	112.3(8)
C(2A)–N(2A)–C(9A)	117.7(6)	C(26A)–C(27A)–C(28A)	112.0(7)
C(2A)–N(2A)–Cu(1A)	111.3(5)	C(23A)–C(28A)–C(27A)	111.1(7)
C(9A)–N(2A)–Cu(1A)	130.8(5)	N(22A)–C(29A)–C(34A)	109.6(6)
N(1A)–C(3A)–C(8A)	116.0(6)	N(22A)–C(29A)–C(30A)	109.1(5)
N(1A)–C(3A)–C(4A)	108.9(5)	C(34A)–C(29A)–C(30A)	111.6(6)
C(8A)–C(3A)–C(4A)	111.4(6)	C(29A)–C(30A)–C(31A)	111.6(6)
C(3A)–C(4A)–C(5A)	111.8(6)	C(32A)–C(31A)–C(30A)	111.3(7)
C(6A)–C(5A)–C(4A)	110.7(7)	C(31A)–C(32A)–C(33A)	111.1(8)
C(5A)–C(6A)–C(7A)	111.9(7)	C(32A)–C(33A)–C(34A)	110.8(7)
C(6A)–C(7A)–C(8A)	112.3(7)	C(29A)–C(34A)–C(33A)	111.5(6)
C(3A)–C(8A)–C(7A)	111.3(7)	F(14)–B(1)–F(12)	110.4(8)
N(2A)–C(9A)–C(10A)	110.0(6)	F(14)–B(1)–F(11)	109.3(8)
N(2A)–C(9A)–C(14A)	109.0(6)	F(12)–B(1)–F(11)	110.4(8)
C(10A)–C(9A)–C(14A)	111.2(7)	F(14)–B(1)–F(13)	107.9(9)
C(9A)–C(10A)–C(11A)	112.0(7)	F(12)–B(1)–F(13)	108.4(8)
C(12A)–C(11A)–C(10A)	109.8(8)	F(11)–B(1)–F(13)	110.4(8)
C(11A)–C(12A)–C(13A)	111.1(8)	F(14′)–B(1′)–F(12′)	109.8(13)
C(12A)–C(13A)–C(14A)	111.1(8)	F(14′)–B(1′)–F(11′)	109.0(12)
C(9A)–C(14A)–C(13A)	110.6(8)	F(12′)–B(1′)–F(11′)	109.8(13)
N(21A)–C(21A)–C(22A)	117.2(6)	F(14′)–B(1′)–F(13′)	109.2(12)
C(21A)–N(21A)–C(23A)	118.7(6)	F(12′)–B(1′)–F(13′)	109.5(12)
C(21A)–N(21A)–Cu(1A)	112.4(4)	F(11′)–B(1′)–F(13′)	109.6(12)

Structure B
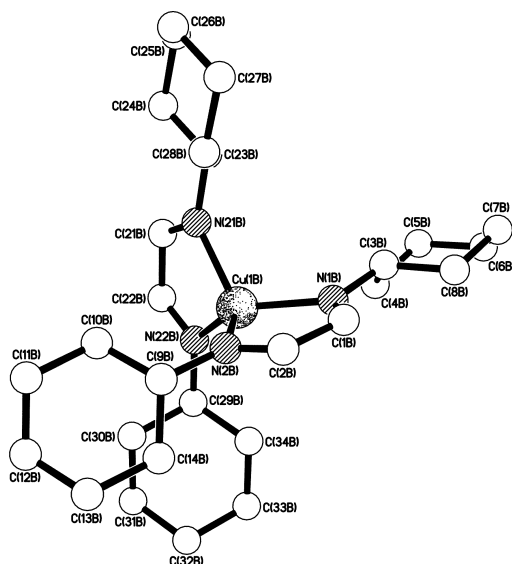
Bond lengths [Å] and angles [°] for Structure B:

Cu(1B)–N(1B)	2.014(6)	C(9B)–C(14B)	1.517(10)
Cu(1B)–N(22B)	2.015(6)	C(10B)–C(11B)	1.540(12)
Cu(1B)–N(2B)	2.016(6)	C(11B)–C(12B)	1.469(15)
Cu(1B)–N(21B)	2.038(6)	C(12B)–C(13B)	1.478(15)
C(1B)–N(1B)	1.264(10)	C(13B)–C(14B)	1.545(12)
C(1B)–C(2B)	1.469(10)	C(21B)–N(21B)	1.278(10)
N(1B)–C(3B)	1.489(10)	C(21B)–C(22B)	1.476(11)
C(2B)–N(2B)	1.266(9)	N(21B)–C(23B)	1.487(10)
N(2B)–C(9B)	1.487(9)	C(22B)–N(22B)	1.273(9)
C(3B)–C(8B)	1.481(12)	N(22B)–C(29B)	1.481(9)
C(3B)–C(4B)	1.507(13)	C(23B)–C(24B)	1.481(12)
C(4B)–C(5B)	1.567(14)	C(23B)–C(28B)	1.514(12)
C(5B)–C(6B)	1.445(16)	C(24B)–C(25B)	1.541(12)
C(6B)–C(7B)	1.467(15)	C(25B)–C(26B)	1.503(14)
C(7B)–C(8B)	1.544(13)	C(26B)–C(27B)	1.464(15)
C(9B)–C(10B)	1.516(12)	C(27B)–C(28B)	1.536(11)
C(9B)–C(14B)	1.517(10)	C(29B)–C(30B)	1.512(11)
C(10B)–C(11B)	1.540(12)	C(29B)–C(34B)	1.515(11)
C(11B)–C(12B)	1.469(15)	C(30B)–C(31B)	1.544(12)
C(12B)–C(13B)	1.478(15)	C(31B)–C(32B)	1.496(14)
C(13B)–C(14B)	1.545(12)	C(32B)–C(33B)	1.501(15)
C(21B)–N(21B)	1.278(10)	C(33B)–C(34B)	1.539(12)
C(21B)–C(22B)	1.476(11)	B(2)–F(24)	1.369(11)

N(21B)–C(23B)	1.487(10)	B(2)–F(21)	1.371(10)
C(22B)–N(22B)	1.273(9)	B(2)–F(23)	1.374(11)
N(22B)–C(29B)	1.481(9)	B(2)–F(22)	1.382(10)
C(23B)–C(24B)	1.481(12)	B(2′)–F(21′)	1.373(13)
C(23B)–C(28B)	1.514(12)	B(2′)–F(23′)	1.374(13)
C(24B)–C(25B)	1.541(12)	B(2′)–F(24′)	1.376(13)
C(25B)–C(26B)	1.503(14)	B(2′)–F(22′)	1.378(13)
C(26B)–C(27B)	1.464(15)		

N(1B)–Cu(1B)–N(22B)	135.0(3)	C(23B)–N(21B)–Cu(1B)	127.5(5)
N(1B)–Cu(1B)–N(2B)	81.1(3)	N(22B)–C(22B)–C(21B)	118.0(6)
N(22B)–Cu(1B)–N(2B)	125.1(2)	C(22B)–N(22B)–C(29B)	117.2(6)
N(1B)–Cu(1B)–N(21B)	115.1(3)	C(22B)–N(22B)–Cu(1B)	111.5(5)
N(22B)–Cu(1B)–N(21B)	81.9(2)	C(29B)–N(22B)–Cu(1B)	131.1(5)
N(2B)–Cu(1B)–N(21B)	124.3(3)	C(24B)–C(23B)–N(21B)	114.5(7)
N(1B)–C(1B)–C(2B)	117.6(6)	C(24B)–C(23B)–C(28B)	113.1(8)
C(1B)–N(1B)–C(3B)	121.7(6)	N(21B)–C(23B)–C(28B)	108.1(6)
C(1B)–N(1B)–Cu(1B)	112.1(5)	C(23B)–C(24B)–C(25B)	110.7(7)
C(3B)–N(1B)–Cu(1B)	125.0(5)	C(26B)–C(25B)–C(24B)	111.9(8)
N(2B)–C(2B)–C(1B)	116.5(6)	C(27B)–C(26B)–C(25B)	113.3(9)
C(2B)–N(2B)–C(9B)	117.2(6)	C(26B)–C(27B)–C(28B)	111.3(8)
C(2B)–N(2B)–Cu(1B)	112.6(5)	C(23B)–C(28B)–C(27B)	110.5(7)
C(9B)–N(2B)–Cu(1B)	130.2(5)	N(22B)–C(29B)–C(30B)	110.7(6)
C(8B)–C(3B)–N(1B)	116.4(8)	N(22B)–C(29B)–C(34B)	109.6(6)
C(8B)–C(3B)–C(4B)	113.1(8)	C(30B)–C(29B)–C(34B)	111.5(7)
N(1B)–C(3B)–C(4B)	108.2(7)	C(29B)–C(30B)–C(31B)	110.6(8)
C(3B)–C(4B)–C(5B)	108.5(9)	C(32B)–C(31B)–C(30B)	111.8(8)
C(6B)–C(5B)–C(4B)	110.9(10)	C(31B)–C(32B)–C(33B)	110.9(8)
C(5B)–C(6B)–C(7B)	114.9(9)	C(32B)–C(33B)–C(34B)	111.7(8)
C(6B)–C(7B)–C(8B)	111.8(8)	C(29B)–C(34B)–C(33B)	111.1(7)
C(3B)–C(8B)–C(7B)	110.2(8)	F(24)–B(2)–F(21)	110.6(8)
N(2B)–C(9B)–C(10B)	109.9(6)	F(24)–B(2)–F(23)	109.5(9)
N(2B)–C(9B)–C(14B)	109.3(6)	F(21)–B(2)–F(23)	110.8(9)
C(10B)–C(9B)–C(14B)	110.0(7)	F(24)–B(2)–F(22)	108.3(9)
C(9B)–C(10B)–C(11B)	110.6(8)	F(21)–B(2)–F(22)	109.4(8)
C(12B)–C(11B)–C(10B)	111.2(8)	F(23)–B(2)–F(22)	108.2(8)
C(11B)–C(12B)–C(13B)	112.4(9)	F(21′)–B(2′)–F(23′)	109.7(12)
C(12B)–C(13B)–C(14B)	111.7(8)	F(21′)–B(2′)–F(24′)	109.6(12)
C(9B)–C(14B)–C(13B)	111.1(7)	F(23′)–B(2′)–F(24′)	109.8(12)
N(21B)–C(21B)–C(22B)	117.1(6)	F(21′)–B(2′)–F(22′)	109.6(12)
C(21B)–N(21B)–C(23B)	121.3(6)	F(23′)–B(2′)–F(22′)	109.3(12)
C(21B)–N(21B)–Cu(1B)	111.1(5)	F(24′)–B(2′)–F(22′)	108.9(12)

Structure C
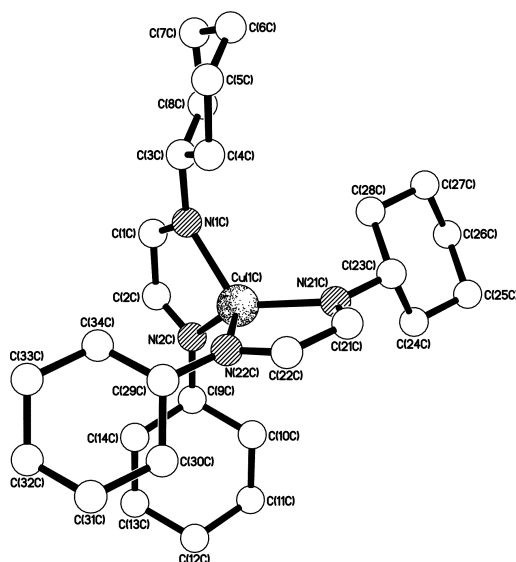
Bond lengths [Å] and angles [°] for Structure C:

Cu(1C)–N(2C)	2.000(6)	N(21C)–C(23C)	1.481(9)
Cu(1C)–N(21C)	2.022(6)	C(22C)–N(22C)	1.286(9)
Cu(1C)–N(1C)	2.034(6)	N(22C)–C(29C)	1.474(8)
Cu(1C)–N(22C)	2.034(5)	C(23C)–C(24C)	1.505(11)
C(1C)–N(1C)	1.264(10)	C(23C)–C(28C)	1.508(10)
C(1C)–C(2C)	1.459(11)	C(24C)–C(25C)	1.529(11)
N(1C)–C(3C)	1.499(10)	C(25C)–C(26C)	1.509(12)
C(2C)–N(2C)	1.258(10)	C(26C)–C(27C)	1.511(11)
N(2C)–C(9C)	1.479(9)	C(27C)–C(28C)	1.543(10)
C(3C)–C(8C)	1.385(15)	C(29C)–C(30C)	1.517(9)
C(3C)–C(4C)	1.504(12)	C(29C)–C(34C)	1.522(10)
C(4C)–C(5C)	1.534(11)	C(30C)–C(31C)	1.541(10)
C(5C)–C(6C)	1.408(15)	C(31C)–C(32C)	1.515(12)
C(6C)–C(7C)	1.536(15)	C(32C)–C(33C)	1.519(11)
C(7C)–C(8C)	1.551(13)	C(33C)–C(34C)	1.527(10)
C(9C)–C(10C)	1.508(12)	B(3)–F(32)	1.361(10)
C(9C)–C(14C)	1.525(11)	B(3)–F(34)	1.364(11)
C(10C)–C(11C)	1.532(12)	B(3)–F(33)	1.374(11)
C(11C)–C(12C)	1.519(15)	B(3)–F(31)	1.374(10)
C(12C)–C(13C)	1.498(17)	B(3′)–F(32′)	1.366(14)
C(13C)–C(14C)	1.519(12)	B(3′)–F(34′)	1.368(14)
C(21C)–N(21C)	1.266(9)	B(3′)–F(31′)	1.369(14)
C(21C)–C(22C)	1.472(9)	B(3′)–F(33′)	1.369(14)

N(2C)–Cu(1C)–N(21C)	134.8(2)	C(23C)–N(21C)–Cu(1C)	129.6(5)
N(2C)–Cu(1C)–N(1C)	81.7(2)	N(22C)–C(22C)–C(21C)	117.8(6)
N(21C)–Cu(1C)–N(1C)	121.3(2)	C(22C)–N(22C)–C(29C)	118.0(6)
N(2C)–Cu(1C)–N(22C)	122.9(2)	C(22C)–N(22C)–Cu(1C)	110.6(4)
N(21C)–Cu(1C)–N(22C)	82.0(2)	C(29C)–N(22C)–Cu(1C)	131.4(4)
N(1C)–Cu(1C)–N(22C)	119.0(2)	N(21C)–C(23C)–C(24C)	110.9(6)
N(1C)–C(1C)–C(2C)	117.9(7)	N(21C)–C(23C)–C(28C)	110.4(6)
C(1C)–N(1C)–C(3C)	117.7(7)	C(24C)–C(23C)–C(28C)	110.9(6)
C(1C)–N(1C)–Cu(1C)	110.6(5)	C(23C)–C(24C)–C(25C)	110.9(7)
C(3C)–N(1C)–Cu(1C)	131.6(5)	C(26C)–C(25C)–C(24C)	110.9(7)
N(2C)–C(2C)–C(1C)	117.8(7)	C(25C)–C(26C)–C(27C)	111.8(7)
C(2C)–N(2C)–C(9C)	118.1(6)	C(26C)–C(27C)–C(28C)	111.1(6)
C(2C)–N(2C)–Cu(1C)	111.9(5)	C(23C)–C(28C)–C(27C)	111.2(6)
C(9C)–N(2C)–Cu(1C)	129.7(5)	N(22C)–C(29C)–C(30C)	109.7(5)
C(8C)–C(3C)–N(1C)	115.1(9)	N(22C)–C(29C)–C(34C)	109.7(5)
C(8C)–C(3C)–C(4C)	116.5(10)	C(30C)–C(29C)–C(34C)	111.7(6)
N(1C)–C(3C)–C(4C)	109.5(6)	C(29C)–C(30C)–C(31C)	111.1(6)
C(3C)–C(4C)–C(5C)	111.7(7)	C(32C)–C(31C)–C(30C)	111.1(7)
C(6C)–C(5C)–C(4C)	114.9(9)	C(31C)–C(32C)–C(33C)	110.5(7)
C(5C)–C(6C)–C(7C)	112.5(10)	C(32C)–C(33C)–C(34C)	111.2(6)
C(6C)–C(7C)–C(8C)	109.2(9)	C(29C)–C(34C)–C(33C)	111.8(6)
C(3C)–C(8C)–C(7C)	112.6(10)	F(32)–B(3)–F(34)	109.7(9)
N(2C)–C(9C)–C(10C)	110.6(6)	F(32)–B(3)–F(33)	108.6(9)
N(2C)–C(9C)–C(14C)	108.4(6)	F(34)–B(3)–F(33)	108.4(9)
C(10C)–C(9C)–C(14C)	110.6(7)	F(32)–B(3)–F(31)	111.0(9)
C(9C)–C(10C)–C(11C)	111.7(8)	F(34)–B(3)–F(31)	110.6(9)
C(12C)–C(11C)–C(10C)	110.4(8)	F(33)–B(3)–F(31)	108.5(9)
C(13C)–C(12C)–C(11C)	111.4(8)	F(32′)–B(3′)–F(34′)	109.7(13)
C(12C)–C(13C)–C(14C)	112.0(9)	F(32′)–B(3′)–F(31′)	110.0(13)
C(13C)–C(14C)–C(9C)	112.0(8)	F(34′)–B(3′)–F(31′)	109.9(13)
N(21C)–C(21C)–C(22C)	117.6(6)	F(32′)–B(3′)–F(33′)	109.0(13)
C(21C)–N(21C)–C(23C)	118.3(6)	F(34′)–B(3′)–F(33′)	109.0(13)
C(21C)–N(21C)–Cu(1C)	111.8(5)	F(31′)–B(3′)–F(33′)	109.3(13)

Structure D
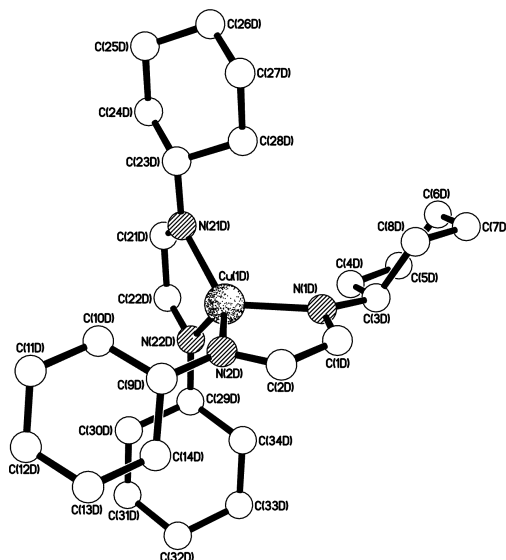
Bond lengths [Å] and angles [°] for Structure D:

Cu(1D)–N(2D)	2.002(6)	C(13D)–C(14D)	1.536(11)
Cu(1D)–N(22D)	2.021(5)	C(21D)–N(21D)	1.264(9)
Cu(1D)–N(21D)	2.024(5)	C(21D)–C(22D)	1.475(10)
Cu(1D)–N(1D)	2.047(6)	N(21D)–C(23D)	1.484(9)
C(1D)–N(1D)	1.268(10)	C(22D)–N(22D)	1.287(9)
C(1D)–C(2D)	1.461(11)	N(22D)–C(29D)	1.471(8)
N(1D)–C(3H)	1.500(12)	C(23D)–C(28D)	1.521(11)
N(1D)–C(3D)	1.528(11)	C(23D)–C(24D)	1.523(10)
C(2D)–N(2D)	1.268(9)	C(24D)–C(25D)	1.513(11)
N(2D)–C(9D)	1.478(9)	C(25D)–C(26D)	1.507(13)
C(3D)–C(4D)	1.505(11)	C(26D)–C(27D)	1.528(12)
C(3D)–C(8D)	1.526(11)	C(27D)–C(28D)	1.523(10)
C(4D)–C(5D)	1.519(12)	C(29D)–C(30D)	1.512(10)
C(5D)–C(6D)	1.514(12)	C(29D)–C(34D)	1.540(10)
C(6D)–C(7D)	1.513(12)	C(30D)–C(31D)	1.524(11)
C(7D)–C(8D)	1.523(12)	C(31D)–C(32D)	1.534(14)
C(3H)–C(8H)	1.508(12)	C(32D)–C(33D)	1.520(12)
C(3H)–C(4H)	1.509(13)	C(33D)–C(34D)	1.519(10)
C(4H)–C(5H)	1.527(13)	B(4)–F(43)	1.365(12)
C(5H)–C(6H)	1.512(12)	B(4)–F(42)	1.365(12)
C(6H)–C(7H)	1.507(12)	B(4)–F(41)	1.373(12)
C(7H)–C(8H)	1.530(12)	B(4)–F(44)	1.379(12)
C(9D)–C(14D)	1.518(11)	B(4′)–F(42′)	1.363(14)

C(9D)–C(10D)	1.520(10)	B(4′)–F(44′)	1.367(13)	
C(10D)–C(11D)	1.525(11)	B(4′)–F(43′)	1.370(14)	
C(11D)–C(12D)	1.494(14)	B(4′)–F(41′)	1.375(14	
C(12D)–C(13D)	1.515(14)			

N(2D)–Cu(1D)–N(22D)	123.9(2)	C(12D)–C(13D)–C(14D)	110.6(7)
N(2D)–Cu(1D)–N(21D)	132.9(2)	C(9D)–C(14D)–C(13D)	110.7(7)
N(22D)–Cu(1D)–N(21D)	81.8(2)	N(21D)–C(21D)–C(22D)	117.6(6)
N(2D)–Cu(1D)–N(1D)	81.4(2)	C(21D)–N(21D)–C(23D)	121.4(6)
N(22D)–Cu(1D)–N(1D)	119.1(2)	C(21D)–N(21D)–Cu(1D)	111.6(5)
N(21D)–Cu(1D)–N(1D)	123.0(2)	C(23D)–N(21D)–Cu(1D)	126.8(4)
N(1D)–C(1D)–C(2D)	116.7(6)	N(22D)–C(22D)–C(21D)	117.2(6)
C(1D)–N(1D)–C(3H)	120.9(7)	C(22D)–N(22D)–C(29D)	117.5(6)
C(1D)–N(1D)–C(3D)	115.4(7)	C(22D)–N(22D)–Cu(1D)	111.1(5)
C(1D)–N(1D)–Cu(1D)	111.4(5)	C(29D)–N(22D)–Cu(1D)	131.3(4)
C(3H)–N(1D)–Cu(1D)	125.6(6)	N(21D)–C(23D)–C(28D)	108.6(6)
C(3D)–N(1D)–Cu(1D)	131.5(5)	N(21D)–C(23D)–C(24D)	115.8(6)
N(2D)–C(2D)–C(1D)	118.7(6)	C(28D)–C(23D)–C(24D)	112.0(6)
C(2D)–N(2D)–C(9D)	118.9(6)	C(25D)–C(24D)–C(23D)	110.3(6)
C(2D)–N(2D)–Cu(1D)	111.7(5)	C(26D)–C(25D)–C(24D)	111.5(6)
C(9D)–N(2D)–Cu(1D)	129.2(4)	C(25D)–C(26D)–C(27D)	111.1(7)
C(4D)–C(3D)–C(8D)	111.4(9)	C(28D)–C(27D)–C(26D)	110.1(7)
C(4D)–C(3D)–N(1D)	111.3(8)	C(23D)–C(28D)–C(27D)	110.9(7)
C(8D)–C(3D)–N(1D)	106.1(8)	N(22D)–C(29D)–C(30D)	108.5(5)
C(3D)–C(4D)–C(5D)	112.3(9)	N(22D)–C(29D)–C(34D)	110.0(5)
C(6D)–C(5D)–C(4D)	112.4(9)	C(30D)–C(29D)–C(34D)	111.5(6)
C(7D)–C(6D)–C(5D)	111.5(9)	C(29D)–C(30D)–C(31D)	111.1(6)
C(6D)–C(7D)–C(8D)	111.3(9)	C(30D)–C(31D)–C(32D)	111.9(7)
C(7D)–C(8D)–C(3D)	110.2(9)	C(33D)–C(32D)–C(31D)	109.9(8)
N(1D)–C(3H)–C(8H)	111.3(10)	C(34D)–C(33D)–C(32D)	112.2(6)
N(1D)–C(3H)–C(4H)	105.5(10)	C(33D)–C(34D)–C(29D)	110.9(6)
C(8H)–C(3H)–C(4H)	112.2(10)	F(43)–B(4)–F(42)	109.5(11)
C(3H)–C(4H)–C(5H)	110.8(10)	F(43)–B(4)–F(41)	112.0(9)
C(6H)–C(5H)–C(4H)	111.4(10)	F(42)–B(4)–F(41)	109.6(10)
C(7H)–C(6H)–C(5H)	112.4(10)	F(43)–B(4)–F(44)	107.9(11)
C(6H)–C(7H)–C(8H)	111.1(10)	F(42)–B(4)–F(44)	106.5(10)
C(3H)–C(8H)–C(7H)	111.4(9)	F(41)–B(4)–F(44)	111.1(11)
N(2D)–C(9D)–C(14D)	109.5(6)	F(42′)–B(4′)–F(44′)	110.9(12)
N(2D)–C(9D)–C(10D)	110.1(6)	F(42′)–B(4′)–F(43′)	109.0(12)
C(14D)–C(9D)–C(10D)	110.8(6)	F(44′)–B(4′)–F(43′)	109.2(12)
C(9D)–C(10D)–C(11D)	112.1(7)	F(42′)–B(4′)–F(41′)	110.2(12)
C(12D)–C(11D)–C(10D)	111.1(7)	F(44′)–B(4′)–F(41′)	108.5(12)
C(11D)–C(12D)–C(13D)	111.4(8)	F(43′)–B(4′)–F(41′)	109.0(12)

A.4 [Cu(DAB^{Anis})$_2$](BF$_4$)
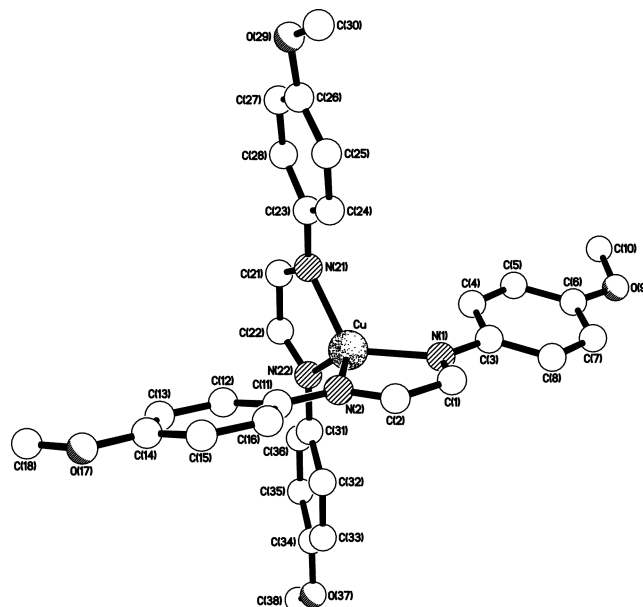
Formula	[C$_{32}$H$_{32}$CuN$_4$O$_4$](BF$_4$)
Formula weight	694.04
Temperature	173 K
Diffractometer, wavelength	OD Xcalibur PX Ultra, 1.54184Å
Crystal system, space group	Trigonal, P-3c1
Unit cell dimensions	a = 20.91645(12) Å α = 90 °
	b = 20.91645(12) Å β = 90 °
	c = 25.50567(18) Å γ = 12 °
Volume, Z	9663.70(10) Å^3, 12
Density (calculated)	1.431 g cm^{-3}
Absorption coefficient	1.659 mm^{-1}
F(000)	4290
Crystal colour / morphology	Black plates
Crystal size	0.22 x 0.14 x 0.02 mm^3
θ range for data collection	3.47 to 72.51°
Index ranges	-25<=h<=19, -24<=k<=25 -30<=l<=31
Reflns collected / unique	64828 / 6387 [R(int) = 0.0290]
Reflns observed [F>4σ(F)]	5737
Absorption correction	Analytical
Max. and min. transmission	0.963 and 0.782
Refinement method	Full-matrix least-squares on F2
Data / restraints / parameters	6387 / 232 / 502
Goodness-of-fit on F^2	1.084

Final R indices [F>4σ(F)]	R1 = 0.0417, wR2 = 0.1167
R indices (all data)	R1 = 0.0459, wR2 = 0.1204
Extinction coefficient	0.00011(3)
Largest diff. peak, hole	0.465, -0.388 eÅ^{-3}
Mean and maximum shift/error	0.000 and 0.001

Bond lengths [Å] and angles [°] for Structure [Cu(DAB$^{\text{Anis}}$)$_2$](BF$_4$):

Cu–N(22)	2.0027(17)		C(26)–C(27)	1.391(4)
Cu–N(2)	2.0095(17)		C(27)–C(28)	1.371(4)
Cu–N(1)	2.0099(17)		O(29)–C(30)	1.419(3)
Cu–N(21)	2.0292(18)		C(31)–C(36)	1.394(3)
C(1)–N(1)	1.291(3)		C(31)–C(32)	1.397(3)
C(1)–C(2)	1.448(3)		C(32)–C(33)	1.373(3)
N(1)–C(3)	1.419(3)		C(33)–C(34)	1.394(3)
C(2)–N(2)	1.286(3)		C(34)–O(37)	1.358(3)
N(2)–C(11)	1.414(3)		C(34)–C(35)	1.385(3)
C(3)–C(4)	1.381(3)		C(35)–C(36)	1.382(3)
C(3)–C(8)	1.404(3)		O(37)–C(38)	1.426(4)
C(4)–C(5)	1.392(3)		B(40)–F(43)	1.376(10)
C(5)–C(6)	1.387(3)		B(40)–F(41)	1.379(12)
C(6)–O(9)	1.358(3)		B(40)–F(44)	1.383(13)
C(6)–C(7)	1.394(3)		B(40)–F(42)	1.390(12)
C(7)–C(8)	1.372(3)		B(40′)–F(41′)	1.350(12)
O(9)–C(10)	1.421(3)		B(40′)–F(44′)	1.384(12)
C(11)–C(12)	1.389(3)		B(40′)–F(43′)	1.386(12)
C(11)–C(16)	1.401(3)		B(40′)–F(42′)	1.398(13)
C(12)–C(13)	1.380(3)		B(50)–F(53)	1.385(12)
C(13)–C(14)	1.386(3)		B(50)–F(52)	1.387(13)
C(14)–O(17)	1.362(3)		B(50)–F(54)	1.387(14)
C(14)–C(15)	1.392(3)		B(50)–F(51)	1.405(11)
C(15)–C(16)	1.373(3)		B(50′)–F(54′)	1.382(14)
O(17)–C(18)	1.427(3)		B(50′)–F(51′)	1.383(13)
C(21)–N(21)	1.296(3)		B(50′)–F(53′)	1.395(14)
C(21)–C(22)	1.438(4)		B(50′)–F(52′)	1.396(13)
N(21)–C(23)	1.414(3)		B(60)–F(63)	1.398(14)
C(22)–N(22)	1.292(3)		B(60)–F(62)	1.401(14)
N(22)–C(31)	1.410(3)		B(60)–F(64)	1.402(14)
C(23)–C(24)	1.390(3)		B(60)–F(61)	1.408(13)
C(23)–C(28)	1.400(3)		C(70)–Cl(1)	1.747(11)
C(24)–C(25)	1.388(3)		C(70)–Cl(2)	1.750(11)
C(25)–C(26)	1.385(3)		C(70′)–Cl(1′)	1.749(11)
C(26)–O(29)	1.359(3)		C(70′)–Cl(2′)	1.750(11)

N(22)–Cu–N(2)	128.18(7)	O(29)–C(26)–C(25)	124.8(2)
N(22)–Cu–N(1)	126.91(7)	O(29)–C(26)–C(27)	115.3(2)
N(2)–Cu–N(1)	82.35(7)	C(25)–C(26)–C(27)	119.9(2)
N(22)–Cu–N(21)	82.53(7)	C(28)–C(27)–C(26)	120.8(2)
N(2)–Cu–N(21)	120.85(7)	C(27)–C(28)–C(23)	120.2(2)
N(1)–Cu–N(21)	121.46(7)	C(26)–O(29)–C(30)	118.5(2)
N(1)–C(1)–C(2)	117.64(19)	C(36)–C(31)–C(32)	118.7(2)
C(1)–N(1)–C(3)	122.53(18)	C(36)–C(31)–N(22)	123.7(2)
C(1)–N(1)–Cu	111.04(15)	C(32)–C(31)–N(22)	117.61(18)
C(3)–N(1)–Cu	126.43(13)	C(33)–C(32)–C(31)	120.6(2)
N(2)–C(2)–C(1)	117.74(19)	C(32)–C(33)–C(34)	120.0(2)
C(2)–N(2)–C(11)	123.53(17)	O(37)–C(34)–C(35)	124.6(2)
C(2)–N(2)–Cu	111.16(14)	O(37)–C(34)–C(33)	115.2(2)
C(11)–N(2)–Cu	125.16(13)	C(35)–C(34)–C(33)	120.2(2)
C(4)–C(3)–C(8)	119.0(2)	C(36)–C(35)–C(34)	119.4(2)
C(4)–C(3)–N(1)	116.93(19)	C(35)–C(36)–C(31)	121.1(2)
C(8)–C(3)–N(1)	124.04(19)	C(34)–O(37)–C(38)	117.9(2)
C(3)–C(4)–C(5)	121.4(2)	F(43)–B(40)–F(41)	112.2(10)
C(6)–C(5)–C(4)	119.0(2)	F(43)–B(40)–F(44)	109.0(8)
O(9)–C(6)–C(5)	124.7(2)	F(41)–B(40)–F(44)	111.4(9)
O(9)–C(6)–C(7)	115.3(2)	F(43)–B(40)–F(42)	106.0(9)
C(5)–C(6)–C(7)	120.0(2)	F(41)–B(40)–F(42)	108.3(7)
C(8)–C(7)–C(6)	120.7(2)	F(44)–B(40)–F(42)	109.8(10)
C(7)–C(8)–C(3)	119.9(2)	F(41′)–B(40′)–F(44′)	111.3(10)
C(6)–O(9)–C(10)	117.2(2)	F(41′)–B(40′)–F(43′)	113.5(10)
C(12)–C(11)–C(16)	118.7(2)	F(44′)–B(40′)–F(43′)	103.6(9)
C(12)–C(11)–N(2)	116.81(17)	F(41′)–B(40′)–F(42′)	113.8(11)
C(16)–C(11)–N(2)	124.45(18)	F(44′)–B(40′)–F(42′)	108.0(10)
C(13)–C(12)–C(11)	121.51(19)	F(43′)–B(40′)–F(42′)	106.0(10)
C(12)–C(13)–C(14)	119.3(2)	F(53)–B(50)–F(52)	116.5(10)
O(17)–C(14)–C(13)	124.42(19)	F(53)–B(50)–F(54)	104.2(11)
O(17)–C(14)–C(15)	115.82(19)	F(52)–B(50)–F(54)	109.7(11)
C(13)–C(14)–C(15)	119.8(2)	F(53)–B(50)–F(51)	112.1(11)
C(16)–C(15)–C(14)	120.87(19)	F(52)–B(50)–F(51)	107.7(10)
C(15)–C(16)–C(11)	119.8(2)	F(54)–B(50)–F(51)	106.2(10)
C(14)–O(17)–C(18)	117.81(18)	F(54′)–B(50′)–F(51′)	109.8(10)
N(21)–C(21)–C(22)	117.8(2)	F(54′)–B(50′)–F(53′)	111.3(12)
C(21)–N(21)–C(23)	121.67(19)	F(51′)–B(50′)–F(53′)	111.3(12)
C(21)–N(21)–Cu	110.26(16)	F(54′)–B(50′)–F(52′)	109.6(12)
C(23)–N(21)–Cu	127.92(13)	F(51′)–B(50′)–F(52′)	109.3(12)
N(22)–C(22)–C(21)	118.5(2)	F(53′)–B(50′)–F(52′)	105.4(11)
C(22)–N(22)–C(31)	121.48(18)	F(63)–B(60)–F(62)	107.8(12)
C(22)–N(22)–Cu	110.89(15)	F(63)–B(60)–F(64)	108.1(12)
C(31)–N(22)–Cu	127.63(14)	F(62)–B(60)–F(64)	110.4(12)

C(24)–C(23)–C(28)	118.5(2)	F(63)–B(60)–F(61)	108.6(11)
C(24)–C(23)–N(21)	117.39(19)	F(62)–B(60)–F(61)	109.9(12)
C(28)–C(23)–N(21)	124.1(2)	F(64)–B(60)–F(61)	112.0(12)
C(25)–C(24)–C(23)	121.5(2)	Cl(1)–C(70)–Cl(2)	111.4(12)
C(26)–C(25)–C(24)	119.1(2)	Cl(1′)–C(70′)–Cl(2′)	112.9(12)

A.5 [Cu(DAB^{Mes})$_2$](BF$_4$)
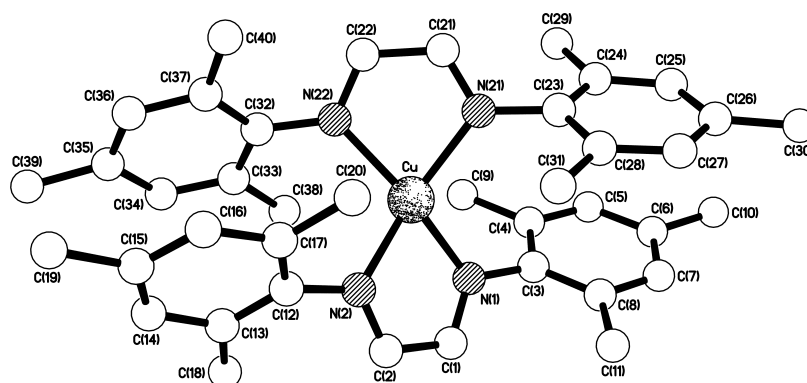
Formula	[C$_{40}$H$_{48}$CuN$_4$](BF$_4$)
Formula weight	735.17
Temperature	173 K
Diffractometer, wavelength	Agilent Xcalibur PX Ultra A, 1.54184Å
Crystal system, space group	Orthorhombic, P2(1)2(1)2(1)
Unit cell dimensions	a = 14.12849(8) Å α = 90 °
	b = 15.61579(8) Å β = 90 °
	c = 16.64347(9) Å γ = 90 °
Volume, Z	3672.01(3) Å^3, 4
Density (calculated)	1.330 g cm^{-3}
Absorption coefficient	1.288 mm^{-1}
F(000)	1544
Crystal colour / morphology	Dark green blocks
Crystal size	0.20 x 0.19 x 0.08 mm^3
θ range for data collection	3.88 to 72.53°
Index ranges	-17<=h<=17, -14<=k<=19, -20<=l<=18
Reflns collected / unique	30142 / 7215 [R(int) = 0.0296]
Reflns observed [F>4σ(F)]	6773
Absorption correction	Analytical
Max. and min. transmission	0.904 and 0.807
Refinement method	Full-matrix least-squares on F2
Data / restraints / parameters	7215 / 112 / 484
Goodness-of-fit on F^2	1.039

Final R indices [F>4σ(F)]	R1 = 0.0315, wR2 = 0.0796
	R1+ = 0.0315, wR2+ = 0.0796
	R1- = 0.0393, wR2- = 0.0998
R indices (all data)	R1 = 0.0349, wR2 = 0.0823
Absolute structure parameter	x+ = 0.000(17), x- = 1.030(17)
Largest diff. peak, hole	0.433, -0.269 eÅ^{-3}
Mean and maximum shift/error	0.000 and 0.001

Bond lengths [Å] and angles [°] for [Cu(DAB^{Mes})$_2$](BF$_4$):

Cu–N(1)	2.0239(16)	C(26)–C(30)	1.513(3)	C(27)–C(28)	1.391(3)
Cu–N(2)	2.0256(17)	C(13)–C(14)	1.400(3)	C(28)–C(31)	1.499(3)
Cu–N(21)	2.0268(15)	C(13)–C(18)	1.503(3)	C(32)–C(37)	1.405(3)
Cu–N(22)	2.0334(17)	C(14)–C(15)	1.386(3)	C(32)–C(33)	1.407(3)
N(1)–C(1)	1.294(3)	C(15)–C(16)	1.387(3)	C(33)–C(34)	1.385(3)
N(1)–C(3)	1.426(2)	C(15)–C(19)	1.510(3)	C(33)–C(38)	1.505(3)
C(1)–C(2)	1.450(3)	C(16)–C(17)	1.389(3)	C(34)–C(35)	1.386(4)
C(2)–N(2)	1.295(3)	C(17)–C(20)	1.500(3)	C(35)–C(36)	1.381(4)
N(2)–C(12)	1.422(2)	N(21)–C(21)	1.288(3)	C(35)–C(39)	1.518(3)
C(3)–C(4)	1.401(3)	N(21)–C(23)	1.435(2)	C(36)–C(37)	1.400(3)
C(3)–C(8)	1.408(3)	C(21)–C(22)	1.456(3)	C(37)–C(40)	1.509(3)
C(4)–C(5)	1.392(3)	C(22)–N(22)	1.294(3)	B(1)–F(4)	1.340(6)
C(4)–C(9)	1.503(3)	N(22)–C(32)	1.423(2)	B(1)–F(1)	1.364(7)
C(5)–C(6)	1.387(3)	C(23)–C(28)	1.401(3)	B(1)–F(3)	1.368(6)
C(6)–C(7)	1.393(3)	C(23)–C(24)	1.406(3)	B(1)–F(2)	1.414(6)
C(6)–C(10)	1.502(3)	C(24)–C(25)	1.396(3)	B(1′)–F(4′)	1.348(8)
C(7)–C(8)	1.391(3)	C(24)–C(29)	1.516(3)	B(1′)–F(3′)	1.374(8)
C(8)–C(11)	1.514(3)	C(25)–C(26)	1.379(3)	B(1′)–F(1′)	1.384(8)
C(12)–C(17)	1.400(3)	C(26)–C(27)	1.391(3)	B(1′)–F(2′)	1.423(9)
C(12)–C(13)	1.409(3)				

N(1)–Cu–N(2)	82.24(7)	N(21)–C(21)–C(22)	118.17(18)
N(1)–Cu–N(21)	108.44(7)	N(22)–C(22)–C(21)	117.53(19)
N(2)–Cu–N(21)	145.49(7)	C(22)–N(22)–C(32)	120.85(17)
N(1)–Cu–N(22)	145.46(7)	C(22)–N(22)–Cu	110.33(13)
N(2)–Cu–N(22)	107.64(7)	C(32)–N(22)–Cu	126.42(13)
N(21)–Cu–N(22)	82.41(6)	C(28)–C(23)–C(24)	121.04(18)
C(1)–N(1)–C(3)	121.35(17)	C(28)–C(23)–N(21)	117.43(17)
C(1)–N(1)–Cu	110.59(13)	C(24)–C(23)–N(21)	121.37(18)
C(3)–N(1)–Cu	125.21(13)	C(25)–C(24)–C(23)	117.40(19)
N(1)–C(1)–C(2)	117.85(19)	C(25)–C(24)–C(29)	118.88(19)
N(2)–C(2)–C(1)	117.44(19)	C(23)–C(24)–C(29)	123.70(18)
C(2)–N(2)–C(12)	122.03(17)	C(26)–C(25)–C(24)	123.0(2)

C(2)–N(2)–Cu	110.81(14)	C(25)–C(26)–C(27)	118.15(19)
C(12)–N(2)–Cu	125.21(13)	C(25)–C(26)–C(30)	121.0(2)
C(4)–C(3)–C(8)	120.30(19)	C(27)–C(26)–C(30)	120.8(2)
C(4)–C(3)–N(1)	117.44(18)	C(26)–C(27)–C(28)	121.6(2)
C(8)–C(3)–N(1)	122.00(18)	C(27)–C(28)–C(23)	118.76(19)
C(5)–C(4)–C(3)	119.01(19)	C(27)–C(28)–C(31)	120.3(2)
C(5)–C(4)–C(9)	119.7(2)	C(23)–C(28)–C(31)	120.93(18)
C(3)–C(4)–C(9)	121.25(18)	C(37)–C(32)–C(33)	120.35(19)
C(6)–C(5)–C(4)	122.1(2)	C(37)–C(32)–N(22)	122.41(18)
C(5)–C(6)–C(7)	117.8(2)	C(33)–C(32)–N(22)	117.01(18)
C(5)–C(6)–C(10)	121.5(2)	C(34)–C(33)–C(32)	119.0(2)
C(7)–C(6)–C(10)	120.7(2)	C(34)–C(33)–C(38)	119.9(2)
C(8)–C(7)–C(6)	122.4(2)	C(32)–C(33)–C(38)	121.11(19)
C(7)–C(8)–C(3)	118.4(2)	C(33)–C(34)–C(35)	121.8(2)
C(7)–C(8)–C(11)	117.8(2)	C(36)–C(35)–C(34)	118.4(2)
C(3)–C(8)–C(11)	123.7(2)	C(36)–C(35)–C(39)	120.8(2)
C(17)–C(12)–C(13)	121.02(18)	C(34)–C(35)–C(39)	120.8(2)
C(17)–C(12)–N(2)	116.55(17)	C(35)–C(36)–C(37)	122.3(2)
C(13)–C(12)–N(2)	122.14(18)	C(36)–C(37)–C(32)	118.1(2)
C(14)–C(13)–C(12)	117.33(19)	C(36)–C(37)–C(40)	117.2(2)
C(14)–C(13)–C(18)	117.52(19)	C(32)–C(37)–C(40)	124.7(2)
C(12)–C(13)–C(18)	125.1(2)	F(4)–B(1)–F(1)	115.8(6)
C(15)–C(14)–C(13)	122.51(19)	F(4)–B(1)–F(3)	111.3(4)
C(14)–C(15)–C(16)	118.5(2)	F(1)–B(1)–F(3)	107.5(4)
C(14)–C(15)–C(19)	120.8(2)	F(4)–B(1)–F(2)	108.8(4)
C(16)–C(15)–C(19)	120.6(2)	F(1)–B(1)–F(2)	106.6(4)
C(15)–C(16)–C(17)	121.5(2)	F(3)–B(1)–F(2)	106.3(5)
C(16)–C(17)–C(12)	119.10(19)	F(4′)–B(1′)–F(3′)	111.6(6)
C(16)–C(17)–C(20)	119.57(19)	F(4′)–B(1′)–F(1′)	108.5(6)
C(12)–C(17)–C(20)	121.33(18)	F(3′)–B(1′)–F(1′)	110.8(6)
C(21)–N(21)–C(23)	119.59(16)	F(4′)–B(1′)–F(2′)	110.4(6)
C(21)–N(21)–Cu	110.42(13)	F(3′)–B(1′)–F(2′)	108.0(7)
C(23)–N(21)–Cu	127.64(13)	F(1′)–B(1′)–F(2′)	107.5(7)

A.6 [Cu(DAB^{DIPP})$_2$](BF$_4$)
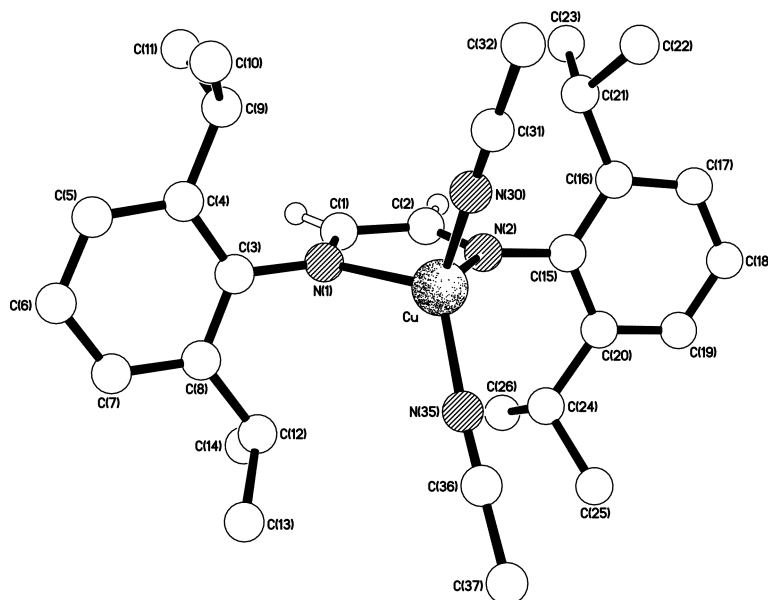
Formula	[C$_{30}$H$_{42}$CuN$_4$](BF$_4$)
Formula weight	693.95
Temperature	173 K
Diffractometer, wavelength	OD Xcalibur 3, 0.71073Å
Crystal system, space group	Monoclinic, P2(1)/c
Unit cell dimensions	a = 12.10209(18) Å α = 90 °
	b = 16.7871(2) Å β = 107.9455(17) °
	c = 18.9558(3) Å γ = 90 °
Volume, Z	3663.69(10) Å^3, 4
Density (calculated)	1.258 g cm^{-3}
Absorption coefficient	0.787 mm^{-1}
F(000)	1448
Crystal colour / morphology	Dark brown blocks
Crystal size	0.30 x 0.27 x 0.19 mm^3
θ range for data collection	3.00 to 32.07°
Index ranges	-17<=h<=16, -16<=k<=23, -26<=l<=28
Reflns collected / unique	40061 / 11585 [R(int) = 0.0218]
Reflns observed [F>4σ(F)]	9073
Absorption correction	Analytical
Max. and min. transmission	0.892 and 0.840
Refinement method	Full-matrix least-squares on F2
Data / restraints / parameters	11585 / 295 / 446
Goodness-of-fit on F^2	1.062

Final R indices [F>4σ(F)]   R1 = 0.0412, wR2 = 0.1069
R indices (all data)   R1 = 0.0412, wR2 = 0.1069
Largest diff. peak, hole   0.579, -0.429 eÅ^{-3}
Mean and maximum shift/error   0.000 and 0.002

Bond lengths [Å] and angles [°] for [Cu(DAB^{DIPP})(NCMe)$_2$](BF$_4$):

Cu–N(35)	1.9391(14)	C(5)–C(6)	1.384(3)	C(17)–C(18)	1.381(3)
Cu–N(30)	1.9424(15)	C(6)–C(7)	1.380(3)	C(18)–C(19)	1.382(3)
Cu–N(2)	2.0798(12)	C(7)–C(8)	1.389(2)	C(19)–C(20)	1.394(2)
Cu–N(1)	2.0821(12)	C(8)–C(12)	1.517(2)	C(20)–C(24)	1.519(2)
C(1)–N(1)	1.2733(19)	C(9)–C(11)	1.522(3)	C(21)–C(22)	1.527(3)
C(1)–C(2)	1.473(2)	C(9)–C(10)	1.526(3)	C(21)–C(23)	1.531(3)
N(1)–C(3)	1.4345(18)	C(12)–C(14)	1.528(3)	C(24)–C(26)	1.525(3)
C(2)–N(2)	1.2700(19)	C(12)–C(13)	1.535(3)	C(24)–C(25)	1.528(2)
N(2)–C(15)	1.4347(18)	C(15)–C(16)	1.401(2)	N(30)–C(31)	1.130(2)
C(3)–C(4)	1.398(2)	C(15)–C(20)	1.405(2)	C(31)–C(32)	1.460(3)
C(3)–C(8)	1.4105(19)	C(16)–C(17)	1.397(2)	N(35)–C(36)	1.131(2)
C(4)–C(5)	1.396(2)	C(16)–C(21)	1.522(2)	C(36)–C(37)	1.457(2)
C(4)–C(9)	1.523(2)				

N(35)–Cu–N(30)	114.52(6)	C(11)–C(9)–C(10)	110.55(17)
N(35)–Cu–N(2)	117.88(5)	C(4)–C(9)–C(10)	111.62(15)
N(30)–Cu–N(2)	110.21(6)	C(8)–C(12)–C(14)	111.27(15)
N(35)–Cu–N(1)	117.91(5)	C(8)–C(12)–C(13)	112.77(16)
N(30)–Cu–N(1)	112.60(6)	C(14)–C(12)–C(13)	110.92(15)
N(2)–Cu–N(1)	78.82(5)	C(16)–C(15)–C(20)	122.66(13)
N(1)–C(1)–C(2)	117.38(13)	C(16)–C(15)–N(2)	120.16(12)
C(1)–N(1)–C(3)	119.14(12)	C(20)–C(15)–N(2)	117.06(13)
C(1)–N(1)–Cu	112.73(10)	C(17)–C(16)–C(15)	117.08(14)
C(3)–N(1)–Cu	128.07(9)	C(17)–C(16)–C(21)	120.13(14)
N(2)–C(2)–C(1)	117.35(13)	C(15)–C(16)–C(21)	122.79(13)
C(2)–N(2)–C(15)	119.99(12)	C(18)–C(17)–C(16)	121.36(16)
C(2)–N(2)–Cu	112.90(10)	C(17)–C(18)–C(19)	120.40(15)
C(15)–N(2)–Cu	127.00(9)	C(18)–C(19)–C(20)	120.89(15)
C(4)–C(3)–C(8)	122.56(14)	C(19)–C(20)–C(15)	117.58(15)
C(4)–C(3)–N(1)	120.11(12)	C(19)–C(20)–C(24)	122.16(14)
C(8)–C(3)–N(1)	117.23(13)	C(15)–C(20)–C(24)	120.22(14)
C(5)–C(4)–C(3)	117.16(14)	C(16)–C(21)–C(22)	112.04(15)
C(5)–C(4)–C(9)	119.88(15)	C(16)–C(21)–C(23)	110.44(15)
C(3)–C(4)–C(9)	122.94(13)	C(22)–C(21)–C(23)	111.06(17)
C(6)–C(5)–C(4)	121.37(17)	C(20)–C(24)–C(26)	111.12(15)
C(7)–C(6)–C(5)	120.15(16)	C(20)–C(24)–C(25)	113.24(16)

C(6)–C(7)–C(8)	121.25(16)	C(26)–C(24)–C(25)	109.86(16)
C(7)–C(8)–C(3)	117.42(15)	C(31)–N(30)–Cu	176.42(16)
C(7)–C(8)–C(12)	121.38(14)	N(30)–C(31)–C(32)	179.1(2)
C(3)–C(8)–C(12)	121.19(14)	C(36)–N(35)–Cu	175.18(15)
C(11)–C(9)–C(4)	111.48(15)	N(35)–C(36)–C(37)	179.4(2)

A.7 [Cu(DAB^DIPh)₂](BF₄)

A.7 [Cu(DAB^{DIPh})₂](BF₄)
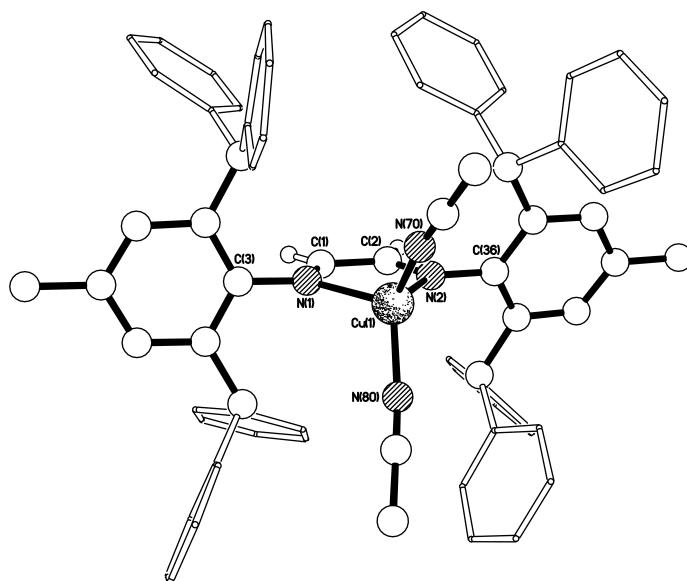
Formula	[$C_{72}H_{62}CuN_4$](BF₄)
Formula weight	1137.85
Temperature	173(2) K
Diffractometer, wavelength	Agilent Xcalibur 3 E, 0.71073Å
Crystal system, space group	Orthorhombic, Pbca
Unit cell dimensions	a = 22.0831(6) Å α = 90 °
	b = 22.3064(5) Å β = 90 °
	c = 24.4072(6) Å γ = 90 °
Volume, Z	12022.8(5) Å^3, 8
Density (calculated)	1.257 g cm^{-3}
Absorption coefficient	0.426 mm^{-1}
F(000)	4753
Crystal colour / morphology	Brown blocks
Crystal size	0.48 x 0.44 x 0.16 mm^3
θ range for data collection	2.596 to 28.381°
Index ranges	-28<=h<=17, -28<=k<=19, -32<=l<=19
Reflns collected / unique	28949 / 12099 [R(int) = 0.0253]
Reflns observed [F>4σ(F)]	8480

Absorption correction	Analytical
Max. and min. transmission	0.934 and 0.837
Refinement method	Full-matrix least-squares on F2
Data / restraints / parameters	12099 / 219 / 777
Goodness-of-fit on F^2	1.021
Final R indices [F>4σ(F)]	R1 = 0.0513, wR2 = 0.1266
R indices (all data)	R1 = 0.0854, wR2 = 0.1494
Largest diff. peak, hole	0.544, -0.557 eÅ^{-3}
Mean and maximum shift/error	0.000 and 0.002

Bond lengths [Å] and angles [°] for [Cu(DAB^{DIPh})(NCMe)$_2$](BF$_4$):

Cu(1)–N(80)	1.949(3)		C(37)–C(42)	1.523(3)
Cu(1)–N(70)	1.951(3)		C(38)–C(39)	1.386(4)
Cu(1)–N(2)	2.086(2)		C(39)–C(40)	1.383(3)
Cu(1)–N(1)	2.100(2)		C(39)–C(55)	1.505(3)
N(1)–C(1)	1.269(3)		C(40)–C(41)	1.392(3)
N(1)–C(3)	1.443(3)		C(41)–C(56)	1.530(3)
C(1)–C(2)	1.477(4)		C(42)–C(43)	1.518(4)
C(2)–N(2)	1.270(3)		C(42)–C(49)	1.526(4)
N(2)–C(36)	1.438(3)		C(43)–C(48)	1.381(5)
C(3)–C(4)	1.396(3)		C(43)–C(44)	1.385(4)
C(3)–C(8)	1.399(3)		C(44)–C(45)	1.400(6)
C(4)–C(5)	1.393(3)		C(45)–C(46)	1.375(7)
C(4)–C(9)	1.525(3)		C(46)–C(47)	1.371(6)
C(5)–C(6)	1.390(3)		C(47)–C(48)	1.394(5)
C(6)–C(7)	1.384(3)		C(49)–C(50)	1.387(4)
C(6)–C(22)	1.508(3)		C(49)–C(54)	1.390(5)
C(7)–C(8)	1.396(3)		C(50)–C(51)	1.396(5)
C(8)–C(23)	1.532(3)		C(51)–C(52)	1.370(5)
C(9)–C(10)	1.519(4)		C(52)–C(53)	1.380(6)
C(9)–C(16)	1.530(3)		C(53)–C(54)	1.385(5)
C(10)–C(11)	1.383(4)		C(56)–C(63)	1.515(4)
C(10)–C(15)	1.386(4)		C(56)–C(57)	1.531(4)
C(11)–C(12)	1.383(4)		C(57)–C(58)	1.385(4)
C(12)–C(13)	1.373(5)		C(57)–C(62)	1.393(4)
C(13)–C(14)	1.382(5)		C(58)–C(59)	1.388(4)
C(14)–C(15)	1.380(4)		C(59)–C(60)	1.374(5)
C(16)–C(21)	1.383(4)		C(60)–C(61)	1.384(5)
C(16)–C(17)	1.385(4)		C(61)–C(62)	1.382(4)
C(17)–C(18)	1.399(4)		C(63)–C(64)	1.386(4)
C(18)–C(19)	1.359(5)		C(63)–C(68)	1.394(4)
C(19)–C(20)	1.374(5)		C(64)–C(65)	1.389(5)

C(20)–C(21)	1.390(4)	C(65)–C(66)	1.376(5)
C(23)–C(30)	1.524(3)	C(66)–C(67)	1.366(5)
C(23)–C(24)	1.525(3)	C(67)–C(68)	1.389(4)
C(24)–C(29)	1.366(4)	N(70)–C(71)	1.137(4)
C(24)–C(25)	1.374(4)	C(71)–C(72)	1.454(5)
C(25)–C(26)	1.390(5)	N(80)–C(81)	1.126(4)
C(26)–C(27)	1.371(5)	C(81)–C(82)	1.470(5)
C(27)–C(28)	1.349(5)	B(1)–F(2)	1.324(5)
C(28)–C(29)	1.380(4)	B(1)–F(4)	1.367(5)
C(30)–C(35)	1.388(4)	B(1)–F(3)	1.371(5)
C(30)–C(31)	1.395(4)	B(1)–F(1)	1.380(5)
C(31)–C(32)	1.389(4)	B(1′)–F(2′)	1.349(13)
C(32)–C(33)	1.373(5)	B(1′)–F(3′)	1.355(13)
C(33)–C(34)	1.375(5)	B(1′)–F(1′)	1.355(13)
C(34)–C(35)	1.387(4)	B(1′)–F(4′)	1.358(13)
C(36)–C(41)	1.396(3)	C(90)–Cl(2)	1.70(5)
C(36)–C(37)	1.401(3)	C(90)–Cl(1)	1.71(5)
C(37)–C(38)	1.394(3)		

N(80)–Cu(1)–N(70)	105.38(12)	C(37)–C(36)–N(2)	118.5(2)
N(80)–Cu(1)–N(2)	122.20(10)	C(38)–C(37)–C(36)	118.5(2)
N(70)–Cu(1)–N(2)	115.46(10)	C(38)–C(37)–C(42)	121.1(2)
N(80)–Cu(1)–N(1)	114.33(9)	C(36)–C(37)–C(42)	120.3(2)
N(70)–Cu(1)–N(1)	118.78(10)	C(39)–C(38)–C(37)	121.8(2)
N(2)–Cu(1)–N(1)	79.91(8)	C(40)–C(39)–C(38)	118.1(2)
C(1)–N(1)–C(3)	116.9(2)	C(40)–C(39)–C(55)	121.4(2)
C(1)–N(1)–Cu(1)	111.31(16)	C(38)–C(39)–C(55)	120.6(2)
C(3)–N(1)–Cu(1)	131.84(16)	C(39)–C(40)–C(41)	122.6(2)
N(1)–C(1)–C(2)	118.5(2)	C(40)–C(41)–C(36)	118.1(2)
N(2)–C(2)–C(1)	118.5(2)	C(40)–C(41)–C(56)	119.7(2)
C(2)–N(2)–C(36)	116.5(2)	C(36)–C(41)–C(56)	122.0(2)
C(2)–N(2)–Cu(1)	111.74(16)	C(43)–C(42)–C(37)	112.4(2)
C(36)–N(2)–Cu(1)	131.76(16)	C(43)–C(42)–C(49)	114.3(2)
C(4)–C(3)–C(8)	121.5(2)	C(37)–C(42)–C(49)	111.5(2)
C(4)–C(3)–N(1)	118.4(2)	C(48)–C(43)–C(44)	118.5(3)
C(8)–C(3)–N(1)	120.1(2)	C(48)–C(43)–C(42)	122.3(2)
C(5)–C(4)–C(3)	118.6(2)	C(44)–C(43)–C(42)	119.1(3)
C(5)–C(4)–C(9)	120.7(2)	C(43)–C(44)–C(45)	119.4(4)
C(3)–C(4)–C(9)	120.7(2)	C(46)–C(45)–C(44)	121.5(4)
C(6)–C(5)–C(4)	121.6(2)	C(47)–C(46)–C(45)	119.1(4)
C(7)–C(6)–C(5)	118.0(2)	C(46)–C(47)–C(48)	119.8(4)
C(7)–C(6)–C(22)	121.5(2)	C(43)–C(48)–C(47)	121.6(3)
C(5)–C(6)–C(22)	120.5(2)	C(50)–C(49)–C(54)	117.7(3)

C(6)–C(7)–C(8)	123.0(2)	C(50)–C(49)–C(42)	122.1(3)
C(7)–C(8)–C(3)	117.2(2)	C(54)–C(49)–C(42)	120.2(3)
C(7)–C(8)–C(23)	120.1(2)	C(49)–C(50)–C(51)	120.5(3)
C(3)–C(8)–C(23)	122.6(2)	C(52)–C(51)–C(50)	120.8(3)
C(10)–C(9)–C(4)	112.4(2)	C(51)–C(52)–C(53)	119.3(4)
C(10)–C(9)–C(16)	114.2(2)	C(52)–C(53)–C(54)	120.0(4)
C(4)–C(9)–C(16)	111.7(2)	C(53)–C(54)–C(49)	121.6(3)
C(11)–C(10)–C(15)	117.9(3)	C(63)–C(56)–C(41)	110.9(2)
C(11)–C(10)–C(9)	122.7(2)	C(63)–C(56)–C(57)	115.3(2)
C(15)–C(10)–C(9)	119.4(2)	C(41)–C(56)–C(57)	111.4(2)
C(12)–C(11)–C(10)	121.2(3)	C(58)–C(57)–C(62)	117.9(3)
C(13)–C(12)–C(11)	120.4(3)	C(58)–C(57)–C(56)	123.0(2)
C(12)–C(13)–C(14)	119.1(3)	C(62)–C(57)–C(56)	119.2(2)
C(15)–C(14)–C(13)	120.4(3)	C(57)–C(58)–C(59)	121.2(3)
C(14)–C(15)–C(10)	121.1(3)	C(60)–C(59)–C(58)	120.5(3)
C(21)–C(16)–C(17)	117.9(3)	C(59)–C(60)–C(61)	118.8(3)
C(21)–C(16)–C(9)	118.8(2)	C(62)–C(61)–C(60)	121.0(3)
C(17)–C(16)–C(9)	123.2(3)	C(61)–C(62)–C(57)	120.6(3)
C(16)–C(17)–C(18)	120.4(3)	C(64)–C(63)–C(68)	118.1(3)
C(19)–C(18)–C(17)	120.9(3)	C(64)–C(63)–C(56)	119.5(2)
C(18)–C(19)–C(20)	119.3(3)	C(68)–C(63)–C(56)	122.3(2)
C(19)–C(20)–C(21)	120.4(3)	C(63)–C(64)–C(65)	120.5(3)
C(16)–C(21)–C(20)	121.1(3)	C(66)–C(65)–C(64)	120.6(3)
C(30)–C(23)–C(24)	114.7(2)	C(67)–C(66)–C(65)	119.6(3)
C(30)–C(23)–C(8)	110.0(2)	C(66)–C(67)–C(68)	120.3(3)
C(24)–C(23)–C(8)	113.1(2)	C(67)–C(68)–C(63)	120.8(3)
C(29)–C(24)–C(25)	116.7(3)	C(71)–N(70)–Cu(1)	173.3(3)
C(29)–C(24)–C(23)	121.3(2)	N(70)–C(71)–C(72)	179.0(4)
C(25)–C(24)–C(23)	121.4(2)	C(81)–N(80)–Cu(1)	171.4(3)
C(24)–C(25)–C(26)	121.3(3)	N(80)–C(81)–C(82)	179.3(4)
C(27)–C(26)–C(25)	120.2(3)	F(2)–B(1)–F(4)	108.8(4)
C(28)–C(27)–C(26)	118.7(3)	F(2)–B(1)–F(3)	112.3(4)
C(27)–C(28)–C(29)	120.7(3)	F(4)–B(1)–F(3)	105.9(4)
C(24)–C(29)–C(28)	122.1(3)	F(2)–B(1)–F(1)	110.5(4)
C(35)–C(30)–C(31)	118.0(2)	F(4)–B(1)–F(1)	108.0(4)
C(35)–C(30)–C(23)	118.7(2)	F(3)–B(1)–F(1)	111.3(4)
C(31)–C(30)–C(23)	123.3(2)	F(2′)–B(1′)–F(3′)	108.9(11)
C(32)–C(31)–C(30)	120.4(3)	F(2′)–B(1′)–F(1′)	112.1(12)
C(33)–C(32)–C(31)	120.5(3)	F(3′)–B(1′)–F(1′)	109.4(12)
C(32)–C(33)–C(34)	120.0(3)	F(2′)–B(1′)–F(4′)	107.6(11)
C(33)–C(34)–C(35)	119.8(3)	F(3′)–B(1′)–F(4′)	106.9(11)
C(34)–C(35)–C(30)	121.4(3)	F(1′)–B(1′)–F(4′)	111.8(12)
C(41)–C(36)–C(37)	120.9(2)	Cl(2)–C(90)–Cl(1)	116(5)
C(41)–C(36)–N(2)	120.6(2)		

A.8 [CuCl(DAB^{Cy})]
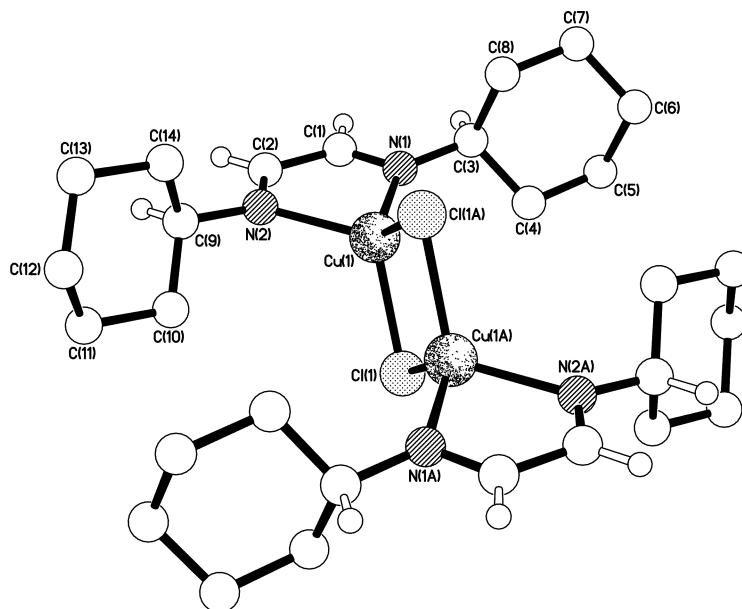
Formula	[C$_{28}$H$_{48}$Cl$_2$CuN$_4$]
Formula weight	638.68
Temperature	173 K
Diffractometer, wavelength	OD Xcalibur PX Ultra, 1.54184Å
Crystal system, space group	Monoclinic, P2(1)/c
Unit cell dimensions	a = 13.8128(4) Å α = 90 °
	b = 13.1498(2) Å β = 102.693(2) °
	c = 8.32834(18) Å γ = 90 °
Volume, Z	1475.75(6) Å^3, 2
Density (calculated)	1.437 g cm^{-3}
Absorption coefficient	3.613 mm^{-1}
F(000)	672
Crystal colour / morphology	Dark brown platy needles
Crystal size	0.27 x 0.11 x 0.05 mm^3
θ range for data collection	3.28 to 72.48°
Index ranges	-16<=h<=17, -16<=k<=16, -10<=l<=10
Reflns collected / unique	5365 / 5365 [R(int) = 0.0000]
Reflns observed [F>4σ(F)]	4647
Absorption correction	Analytical
Max. and min. transmission	0.841 and 0.474
Refinement method	Full-matrix least-squares on F2
Data / restraints / parameters	5365 / 0 / 164
Goodness-of-fit on F^2	1.038

Final R indices [F>4σ(F)]   R1 = 0.0405, wR2 = 0.1143
R indices (all data)   R1 = 0.0480, wR2 = 0.1189
Largest diff. peak, hole   0.617, -0.627 eÅ^{-3}
Mean and maximum shift/error   0.000 and 0.000

Bond lengths [Å] and angles [°] for [CuCl(DAB^{Cy})]:

Cu(1)–N(1)	2.0875(15)		C(3)–C(8)	1.531(2)
Cu(1)–N(2)	2.1025(15)		C(4)–C(5)	1.532(3)
Cu(1)–Cl(1)#1	2.2909(5)		C(5)–C(6)	1.521(3)
Cu(1)–Cl(1)	2.3625(5)		C(6)–C(7)	1.520(3)
Cu(1)–Cu(1)#1	2.9338(5)		C(7)–C(8)	1.526(3)
Cl(1)–Cu(1)#1	2.2909(5)		C(9)–C(10)	1.523(2)
C(1)–N(1)	1.280(2)		C(9)–C(14)	1.530(2)
C(1)–C(2)	1.460(2)		C(10)–C(11)	1.529(3)
N(1)–C(3)	1.457(2)		C(11)–C(12)	1.525(3)
C(2)–N(2)	1.280(2)		C(12)–C(13)	1.520(3)
N(2)–C(9)	1.455(2)		C(13)–C(14)	1.523(3)
C(3)–C(4)	1.523(3)			

N(1)–Cu(1)–N(2)	79.94(6)		C(9)–N(2)–Cu(1)	130.95(11)
N(1)–Cu(1)–Cl(1)#1	125.28(5)		N(1)–C(3)–C(4)	111.37(14)
N(2)–Cu(1)–Cl(1)#1	122.07(5)		N(1)–C(3)–C(8)	108.92(14)
N(1)–Cu(1)–Cl(1)	114.93(4)		C(4)–C(3)–C(8)	110.34(16)
N(2)–Cu(1)–Cl(1)	112.57(4)		C(3)–C(4)–C(5)	110.41(16)
Cl(1)#1–Cu(1)–Cl(1)	101.846(17)		C(6)–C(5)–C(4)	111.46(17)
N(1)–Cu(1)–Cu(1)#1	142.23(5)		C(7)–C(6)–C(5)	111.39(18)
N(2)–Cu(1)–Cu(1)#1	136.36(4)		C(6)–C(7)–C(8)	111.66(18)
Cl(1)#1–Cu(1)–Cu(1)#1	52.008(13)		C(7)–C(8)–C(3)	110.81(16)
Cl(1)–Cu(1)–Cu(1)#1	49.838(14)		N(2)–C(9)–C(10)	110.85(14)
Cu(1)#1–Cl(1)–Cu(1)	78.154(17)		N(2)–C(9)–C(14)	108.41(14)
N(1)–C(1)–C(2)	119.01(17)		C(10)–C(9)–C(14)	110.63(15)
C(1)–N(1)–C(3)	117.50(15)		C(9)–C(10)–C(11)	110.55(15)
C(1)–N(1)–Cu(1)	111.17(12)		C(12)–C(11)–C(10)	111.39(16)
C(3)–N(1)–Cu(1)	131.28(12)		C(13)–C(12)–C(11)	110.76(17)
N(2)–C(2)–C(1)	118.52(17)		C(12)–C(13)–C(14)	111.10(17)
C(2)–N(2)–C(9)	118.07(15)		C(13)–C(14)–C(9)	111.36(15)
C(2)–N(2)–Cu(1)	110.95(12)			

A.9 [CuCl(DAB^{Anis})]

Formula	[C$_{32}$H$_{32}$Cl$_2$CuN$_4$O$_4$]
Formula weight	734.60
Temperature	173 K
Diffractometer, wavelength	OD Xcalibur PX Ultra, 1.54184Å
Crystal system, space group	Monoclinic, P2(1)/c
Unit cell dimensions	a = 31.6929(5) Å α = 90 °
	b = 11.59389(16) Å β = 95.2904(13) °
	c = 34.2062(4) Å γ = 90 °
Volume, Z	12515.3(3) Å^3, 16
Density (calculated)	1.559 g cm^{-3}
Absorption coefficient	3.608 mm^{-1}
F(000)	6016
Crystal colour / morphology	Dark brown needles
Crystal size	0.24 x 0.04 x 0.03 mm^3
θ range for data collection	2.59 to 72.52°
Index ranges	-38<=h<=37, -10<=k<=14 -41<=l<=41
Reflns collected / unique	86883 / 24208 [R(int) = 0.0369]
Reflns observed [F>4σ(F)]	16663
Absorption correction	Analytical
Max. and min. transmission	0.891 and 0.572
Refinement method	Full-matrix least-squares on F2
Data / restraints / parameters	24208 / 0 / 1602
Goodness-of-fit on F^2	1.024
Final R indices [F>4σ(F)]	R1 = 0.0370, wR2 = 0.0982
R indices (all data)	R1 = 0.0623, wR2 = 0.1118
Extinction coefficient	0.000018(3)
Largest diff. peak, hole	0.624, -0.420 eÅ^{-3}
Mean and maximum shift/error	0.000 and 0.003

Structure A
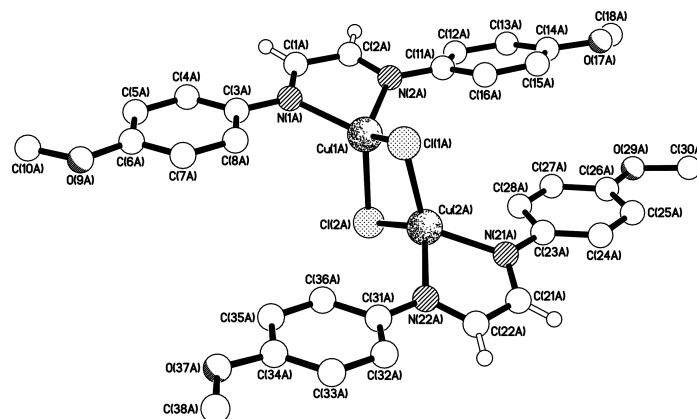
Bond lengths [Å] and angles [°] for Structure A:

Cu(1A)–N(2A)	2.0641(19)	C(14A)–C(15A)	1.381(4)
Cu(1A)–N(1A)	2.073(2)	C(14A)–O(17A)	1.389(3)
Cu(1A)–Cl(1A)	2.2773(7)	C(15A)–C(16A)	1.368(4)
Cu(1A)–Cl(2A)	2.3534(7)	O(17A)–C(18A)	1.400(4)
Cu(1A)–Cu(2A)	2.7654(5)	C(21A)–N(21A)	1.291(3)
Cu(2A)–N(21A)	2.0522(19)	C(21A)–C(22A)	1.451(3)
Cu(2A)–N(22A)	2.0772(19)	N(21A)–C(23A)	1.415(3)
Cu(2A)–Cl(2A)	2.2913(7)	C(22A)–N(22A)	1.286(3)
Cu(2A)–Cl(1A)	2.3396(7)	N(22A)–C(31A)	1.416(3)
C(1A)–N(1A)	1.287(3)	C(23A)–C(24A)	1.386(3)
C(1A)–C(2A)	1.456(4)	C(23A)–C(28A)	1.396(3)
N(1A)–C(3A)	1.415(3)	C(24A)–C(25A)	1.390(4)
C(2A)–N(2A)	1.288(3)	C(25A)–C(26A)	1.387(4)
N(2A)–C(11A)	1.412(3)	C(26A)–O(29A)	1.366(3)
C(3A)–C(4A)	1.389(3)	C(26A)–C(27A)	1.392(4)
C(3A)–C(8A)	1.398(3)	C(27A)–C(28A)	1.377(4)
C(4A)–C(5A)	1.387(4)	O(29A)–C(30A)	1.424(4)
C(5A)–C(6A)	1.387(4)	C(31A)–C(32A)	1.389(3)
C(6A)–O(9A)	1.359(3)	C(31A)–C(36A)	1.389(4)
C(6A)–C(7A)	1.391(4)	C(32A)–C(33A)	1.390(4)
C(7A)–C(8A)	1.374(4)	C(33A)–C(34A)	1.385(4)
O(9A)–C(10A)	1.430(4)	C(34A)–O(37A)	1.363(3)
C(11A)–C(12A)	1.388(3)	C(34A)–C(35A)	1.391(4)
C(11A)–C(16A)	1.395(4)	C(35A)–C(36A)	1.380(4)
C(12A)–C(13A)	1.403(4)	O(37A)–C(38A)	1.429(3)
C(13A)–C(14A)	1.376(4)		

N(2A)–Cu(1A)–N(1A)	80.53(8)	C(12A)–C(11A)–C(16A)	118.6(2)
N(2A)–Cu(1A)–Cl(1A)	123.56(6)	C(12A)–C(11A)–N(2A)	124.7(2)
N(1A)–Cu(1A)–Cl(1A)	125.29(6)	C(16A)–C(11A)–N(2A)	116.6(2)
N(2A)–Cu(1A)–Cl(2A)	110.54(6)	C(11A)–C(12A)–C(13A)	120.2(2)
N(1A)–Cu(1A)–Cl(2A)	109.85(6)	C(14A)–C(13A)–C(12A)	119.8(2)
Cl(1A)–Cu(1A)–Cl(2A)	105.29(2)	C(13A)–C(14A)–C(15A)	119.9(3)
N(2A)–Cu(1A)–Cu(2A)	127.92(6)	C(13A)–C(14A)–O(17A)	125.6(3)
N(1A)–Cu(1A)–Cu(2A)	148.71(6)	C(15A)–C(14A)–O(17A)	114.5(2)
Cl(1A)–Cu(1A)–Cu(2A)	54.243(18)	C(16A)–C(15A)–C(14A)	120.5(3)
Cl(2A)–Cu(1A)–Cu(2A)	52.433(17)	C(15A)–C(16A)–C(11A)	120.8(2)
N(21A)–Cu(2A)–N(22A)	80.37(8)	C(14A)–O(17A)–C(18A)	116.3(2)
N(21A)–Cu(2A)–Cl(2A)	117.49(6)	N(21A)–C(21A)–C(22A)	118.5(2)
N(22A)–Cu(2A)–Cl(2A)	122.74(6)	C(21A)–N(21A)–C(23A)	120.9(2)
N(21A)–Cu(2A)–Cl(1A)	121.77(6)	C(21A)–N(21A)–Cu(2A)	111.77(16)
N(22A)–Cu(2A)–Cl(1A)	108.41(6)	C(23A)–N(21A)–Cu(2A)	127.11(15)
Cl(2A)–Cu(2A)–Cl(1A)	105.30(2)	N(22A)–C(22A)–C(21A)	117.6(2)
N(21A)–Cu(2A)–Cu(1A)	134.38(6)	C(22A)–N(22A)–C(31A)	122.4(2)
N(22A)–Cu(2A)–Cu(1A)	144.57(6)	C(22A)–N(22A)–Cu(2A)	111.59(16)
Cl(2A)–Cu(2A)–Cu(1A)	54.499(18)	C(31A)–N(22A)–Cu(2A)	125.93(15)
Cl(1A)–Cu(2A)–Cu(1A)	52.178(17)	C(24A)–C(23A)–C(28A)	119.2(2)
Cu(1A)–Cl(1A)–Cu(2A)	73.58(2)	C(24A)–C(23A)–N(21A)	123.7(2)
Cu(2A)–Cl(2A)–Cu(1A)	73.07(2)	C(28A)–C(23A)–N(21A)	117.1(2)
N(1A)–C(1A)–C(2A)	118.2(2)	C(23A)–C(24A)–C(25A)	121.0(2)
C(1A)–N(1A)–C(3A)	122.1(2)	C(26A)–C(25A)–C(24A)	119.3(2)
C(1A)–N(1A)–Cu(1A)	111.17(16)	O(29A)–C(26A)–C(25A)	124.2(2)
C(3A)–N(1A)–Cu(1A)	126.67(15)	O(29A)–C(26A)–C(27A)	115.9(2)
N(2A)–C(2A)–C(1A)	118.2(2)	C(25A)–C(26A)–C(27A)	119.9(2)
C(2A)–N(2A)–C(11A)	122.0(2)	C(28A)–C(27A)–C(26A)	120.5(2)
C(2A)–N(2A)–Cu(1A)	111.35(16)	C(27A)–C(28A)–C(23A)	120.0(2)
C(11A)–N(2A)–Cu(1A)	126.57(16)	C(26A)–O(29A)–C(30A)	116.2(2)
C(4A)–C(3A)–C(8A)	118.6(2)	C(32A)–C(31A)–C(36A)	119.2(2)
C(4A)–C(3A)–N(1A)	125.3(2)	C(32A)–C(31A)–N(22A)	124.6(2)
C(8A)–C(3A)–N(1A)	116.1(2)	C(36A)–C(31A)–N(22A)	116.2(2)
C(5A)–C(4A)–C(3A)	120.9(2)	C(31A)–C(32A)–C(33A)	120.2(2)
C(4A)–C(5A)–C(6A)	120.0(2)	C(34A)–C(33A)–C(32A)	120.2(2)
O(9A)–C(6A)–C(5A)	124.9(2)	O(37A)–C(34A)–C(33A)	124.8(2)
O(9A)–C(6A)–C(7A)	115.8(2)	O(37A)–C(34A)–C(35A)	115.4(2)
C(5A)–C(6A)–C(7A)	119.3(2)	C(33A)–C(34A)–C(35A)	119.8(2)
C(8A)–C(7A)–C(6A)	120.7(2)	C(36A)–C(35A)–C(34A)	119.8(2)
C(7A)–C(8A)–C(3A)	120.6(2)	C(35A)–C(36A)–C(31A)	120.9(2)
C(6A)–O(9A)–C(10A)	118.0(2)	C(34A)–O(37A)–C(38A)	118.2(2)

Structure B
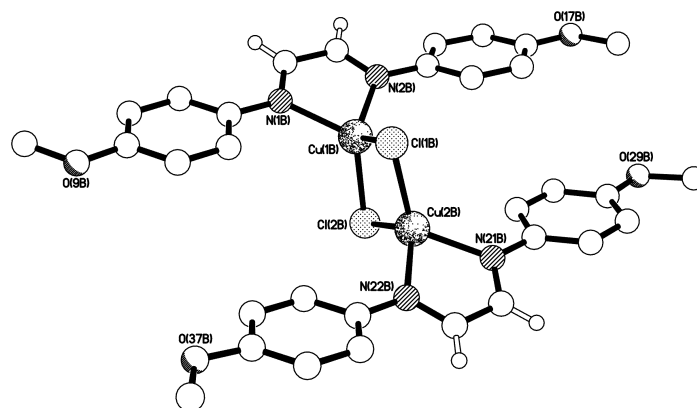
Bond lengths [Å] and angles [°] for Structure B:

Cu(1B)–N(2B)	2.0576(19)	C(14B)–O(17B)	1.368(3)
Cu(1B)–N(1B)	2.0853(19)	C(14B)–C(15B)	1.387(4)
Cu(1B)–Cl(1B)	2.2884(7)	C(15B)–C(16B)	1.383(4)
Cu(1B)–Cl(2B)	2.3339(7)	O(17B)–C(18B)	1.413(3)
Cu(1B)–Cu(2B)	2.8323(5)	C(21B)–N(21B)	1.293(3)
Cu(2B)–N(21B)	2.0564(19)	C(21B)–C(22B)	1.442(3)
Cu(2B)–N(22B)	2.0793(18)	N(21B)–C(23B)	1.411(3)
Cu(2B)–Cl(2B)	2.2906(6)	C(22B)–N(22B)	1.291(3)
Cu(2B)–Cl(1B)	2.3338(7)	N(22B)–C(31B)	1.414(3)
C(1B)–N(1B)	1.281(3)	C(23B)–C(24B)	1.393(3)
C(1B)–C(2B)	1.447(3)	C(23B)–C(28B)	1.400(3)
N(1B)–C(3B)	1.413(3)	C(24B)–C(25B)	1.386(3)
C(2B)–N(2B)	1.295(3)	C(25B)–C(26B)	1.384(3)
N(2B)–C(11B)	1.413(3)	C(26B)–O(29B)	1.364(3)
C(3B)–C(8B)	1.391(3)	C(26B)–C(27B)	1.392(4)
C(3B)–C(4B)	1.396(4)	C(27B)–C(28B)	1.380(4)
C(4B)–C(5B)	1.384(4)	O(29B)–C(30B)	1.428(3)
C(5B)–C(6B)	1.391(4)	C(31B)–C(36B)	1.391(3)
C(6B)–O(9B)	1.364(3)	C(31B)–C(32B)	1.394(3)
C(6B)–C(7B)	1.387(4)	C(32B)–C(33B)	1.383(4)
C(7B)–C(8B)	1.376(4)	C(33B)–C(34B)	1.390(4)
O(9B)–C(10B)	1.426(4)	C(34B)–O(37B)	1.363(3)
C(11B)–C(16B)	1.392(3)	C(34B)–C(35B)	1.390(3)
C(11B)–C(12B)	1.396(3)	C(35B)–C(36B)	1.375(3)
C(12B)–C(13B)	1.373(4)	O(37B)–C(38B)	1.436(3)
C(13B)–C(14B)	1.382(4)		

N(2B)–Cu(1B)–N(1B)	80.49(8)	C(16B)–C(11B)–C(12B)	118.5(2)
N(2B)–Cu(1B)–Cl(1B)	121.50(6)	C(16B)–C(11B)–N(2B)	117.5(2)
N(1B)–Cu(1B)–Cl(1B)	119.67(6)	C(12B)–C(11B)–N(2B)	124.0(2)
N(2B)–Cu(1B)–Cl(2B)	115.43(6)	C(13B)–C(12B)–C(11B)	120.6(2)
N(1B)–Cu(1B)–Cl(2B)	115.47(6)	C(12B)–C(13B)–C(14B)	120.6(2)
Cl(1B)–Cu(1B)–Cl(2B)	103.92(2)	O(17B)–C(14B)–C(13B)	114.6(2)
N(2B)–Cu(1B)–Cu(2B)	134.08(6)	O(17B)–C(14B)–C(15B)	125.7(2)
N(1B)–Cu(1B)–Cu(2B)	145.03(6)	C(13B)–C(14B)–C(15B)	119.7(2)
Cl(1B)–Cu(1B)–Cu(2B)	52.940(17)	C(16B)–C(15B)–C(14B)	119.8(2)
Cl(2B)–Cu(1B)–Cu(2B)	51.545(17)	C(15B)–C(16B)–C(11B)	120.8(2)
N(21B)–Cu(2B)–N(22B)	80.31(7)	C(14B)–O(17B)–C(18B)	117.3(2)
N(21B)–Cu(2B)–Cl(2B)	117.72(6)	N(21B)–C(21B)–C(22B)	118.1(2)
N(22B)–Cu(2B)–Cl(2B)	123.77(6)	C(21B)–N(21B)–C(23B)	120.30(19)
N(21B)–Cu(2B)–Cl(1B)	120.62(6)	C(21B)–N(21B)–Cu(2B)	111.93(15)
N(22B)–Cu(2B)–Cl(1B)	110.46(6)	C(23B)–N(21B)–Cu(2B)	127.64(15)
Cl(2B)–Cu(2B)–Cl(1B)	103.85(2)	N(22B)–C(22B)–C(21B)	118.5(2)
N(21B)–Cu(2B)–Cu(1B)	135.77(5)	C(22B)–N(22B)–C(31B)	121.41(19)
N(22B)–Cu(2B)–Cu(1B)	143.38(6)	C(22B)–N(22B)–Cu(2B)	111.06(15)
Cl(2B)–Cu(2B)–Cu(1B)	52.928(17)	C(31B)–N(22B)–Cu(2B)	127.50(15)
Cl(1B)–Cu(2B)–Cu(1B)	51.489(17)	C(24B)–C(23B)–C(28B)	118.7(2)
Cu(1B)–Cl(1B)–Cu(2B)	75.57(2)	C(24B)–C(23B)–N(21B)	124.0(2)
Cu(2B)–Cl(2B)–Cu(1B)	75.53(2)	C(28B)–C(23B)–N(21B)	117.2(2)
N(1B)–C(1B)–C(2B)	118.8(2)	C(25B)–C(24B)–C(23B)	121.2(2)
C(1B)–N(1B)–C(3B)	121.8(2)	C(26B)–C(25B)–C(24B)	119.4(2)
C(1B)–N(1B)–Cu(1B)	110.84(16)	O(29B)–C(26B)–C(25B)	124.2(2)
C(3B)–N(1B)–Cu(1B)	127.32(15)	O(29B)–C(26B)–C(27B)	115.7(2)
N(2B)–C(2B)–C(1B)	118.1(2)	C(25B)–C(26B)–C(27B)	120.0(2)
C(2B)–N(2B)–C(11B)	120.53(19)	C(28B)–C(27B)–C(26B)	120.5(2)
C(2B)–N(2B)–Cu(1B)	111.54(16)	C(27B)–C(28B)–C(23B)	120.1(2)
C(11B)–N(2B)–Cu(1B)	127.86(15)	C(26B)–O(29B)–C(30B)	117.1(2)
C(8B)–C(3B)–C(4B)	118.4(2)	C(36B)–C(31B)–C(32B)	118.7(2)
C(8B)–C(3B)–N(1B)	117.3(2)	C(36B)–C(31B)–N(22B)	117.3(2)
C(4B)–C(3B)–N(1B)	124.3(2)	C(32B)–C(31B)–N(22B)	124.0(2)
C(5B)–C(4B)–C(3B)	120.8(2)	C(33B)–C(32B)–C(31B)	121.0(2)
C(4B)–C(5B)–C(6B)	119.9(2)	C(32B)–C(33B)–C(34B)	119.7(2)
O(9B)–C(6B)–C(7B)	116.1(2)	O(37B)–C(34B)–C(35B)	115.8(2)
O(9B)–C(6B)–C(5B)	124.4(2)	O(37B)–C(34B)–C(33B)	124.6(2)
C(7B)–C(6B)–C(5B)	119.5(2)	C(35B)–C(34B)–C(33B)	119.5(2)
C(8B)–C(7B)–C(6B)	120.3(2)	C(36B)–C(35B)–C(34B)	120.5(2)
C(7B)–C(8B)–C(3B)	121.0(2)	C(35B)–C(36B)–C(31B)	120.6(2)
C(6B)–O(9B)–C(10B)	117.1(2)	C(34B)–O(37B)–C(38B)	117.8(2)

Structure C
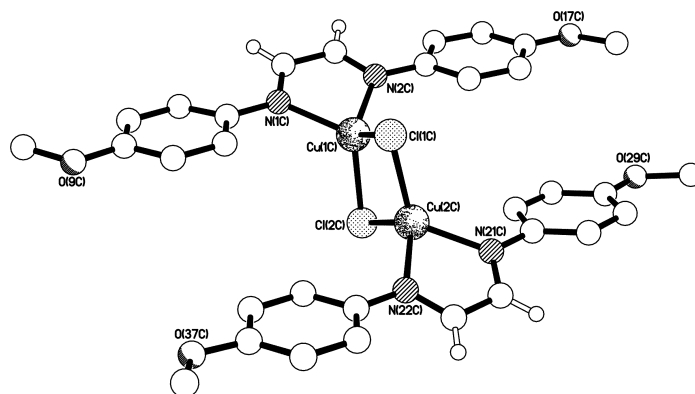
Bond lengths [Å] and angles [°] for Structure C:

Cu(1C)–N(2C)	2.0670(18)	C(14C)–O(17C)	1.374(3)
Cu(1C)–N(1C)	2.0788(19)	C(14C)–C(15C)	1.385(3)
Cu(1C)–Cl(1C)	2.3042(6)	C(15C)–C(16C)	1.386(4)
Cu(1C)–Cl(2C)	2.3317(7)	O(17C)–C(18C)	1.410(3)
Cu(1C)–Cu(2C)	2.8209(5)	C(21C)–N(21C)	1.288(3)
Cu(2C)–N(21C)	2.0447(19)	C(21C)–C(22C)	1.454(3)
Cu(2C)–N(22C)	2.0788(19)	N(21C)–C(23C)	1.415(3)
Cu(2C)–Cl(2C)	2.2726(6)	C(22C)–N(22C)	1.289(3)
Cu(2C)–Cl(1C)	2.3363(6)	N(22C)–C(31C)	1.412(3)
C(1C)–N(1C)	1.286(3)	C(23C)–C(24C)	1.391(3)
C(1C)–C(2C)	1.449(3)	C(23C)–C(28C)	1.395(3)
N(1C)–C(3C)	1.412(3)	C(24C)–C(25C)	1.389(3)
C(2C)–N(2C)	1.293(3)	C(25C)–C(26C)	1.388(3)
N(2C)–C(11C)	1.411(3)	C(26C)–O(29C)	1.364(3)
C(3C)–C(4C)	1.390(3)	C(26C)–C(27C)	1.389(3)
C(3C)–C(8C)	1.398(3)	C(27C)–C(28C)	1.376(3)
C(4C)–C(5C)	1.385(4)	O(29C)–C(30C)	1.429(3)
C(5C)–C(6C)	1.384(4)	C(31C)–C(32C)	1.386(3)
C(6C)–O(9C)	1.365(3)	C(31C)–C(36C)	1.399(3)
C(6C)–C(7C)	1.385(4)	C(32C)–C(33C)	1.387(4)
C(7C)–C(8C)	1.376(4)	C(33C)–C(34C)	1.392(4)
O(9C)–C(10C)	1.424(3)	C(34C)–O(37C)	1.361(3)
C(11C)–C(16C)	1.391(3)	C(34C)–C(35C)	1.393(3)
C(11C)–C(12C)	1.407(3)	C(35C)–C(36C)	1.382(3)
C(12C)–C(13C)	1.368(3)	O(37C)–C(38C)	1.433(3)
C(13C)–C(14C)	1.387(4)		

N(2C)–Cu(1C)–N(1C)	80.60(7)	C(16C)–C(11C)–C(12C)	118.6(2)
N(2C)–Cu(1C)–Cl(1C)	119.52(6)	C(16C)–C(11C)–N(2C)	117.5(2)
N(1C)–Cu(1C)–Cl(1C)	121.52(6)	C(12C)–C(11C)–N(2C)	123.9(2)
N(2C)–Cu(1C)–Cl(2C)	118.03(6)	C(13C)–C(12C)–C(11C)	120.4(2)
N(1C)–Cu(1C)–Cl(2C)	113.47(6)	C(12C)–C(13C)–C(14C)	120.6(2)
Cl(1C)–Cu(1C)–Cl(2C)	103.54(2)	O(17C)–C(14C)–C(15C)	125.3(2)
N(2C)–Cu(1C)–Cu(2C)	133.30(6)	O(17C)–C(14C)–C(13C)	114.7(2)
N(1C)–Cu(1C)–Cu(2C)	145.63(5)	C(15C)–C(14C)–C(13C)	120.0(2)
Cl(1C)–Cu(1C)–Cu(2C)	53.084(17)	C(14C)–C(15C)–C(16C)	119.6(2)
Cl(2C)–Cu(1C)–Cu(2C)	51.276(17)	C(15C)–C(16C)–C(11C)	120.8(2)
N(21C)–Cu(2C)–N(22C)	80.67(8)	C(14C)–O(17C)–C(18C)	117.4(2)
N(21C)–Cu(2C)–Cl(2C)	118.15(6)	N(21C)–C(21C)–C(22C)	118.0(2)
N(22C)–Cu(2C)–Cl(2C)	119.96(6)	C(21C)–N(21C)–C(23C)	120.44(19)
N(21C)–Cu(2C)–Cl(1C)	121.38(5)	C(21C)–N(21C)–Cu(2C)	112.14(15)
N(22C)–Cu(2C)–Cl(1C)	111.78(6)	C(23C)–N(21C)–Cu(2C)	127.33(15)
Cl(2C)–Cu(2C)–Cl(1C)	104.39(2)	N(22C)–C(22C)–C(21C)	118.2(2)
N(21C)–Cu(2C)–Cu(1C)	136.22(6)	C(22C)–N(22C)–C(31C)	121.6(2)
N(22C)–Cu(2C)–Cu(1C)	142.95(6)	C(22C)–N(22C)–Cu(2C)	110.87(16)
Cl(2C)–Cu(2C)–Cu(1C)	53.172(18)	C(31C)–N(22C)–Cu(2C)	127.49(15)
Cl(1C)–Cu(2C)–Cu(1C)	52.047(16)	C(24C)–C(23C)–C(28C)	118.9(2)
Cu(1C)–Cl(1C)–Cu(2C)	74.87(2)	C(24C)–C(23C)–N(21C)	123.4(2)
Cu(2C)–Cl(2C)–Cu(1C)	75.55(2)	C(28C)–C(23C)–N(21C)	117.7(2)
N(1C)–C(1C)–C(2C)	119.0(2)	C(25C)–C(24C)–C(23C)	121.0(2)
C(1C)–N(1C)–C(3C)	121.3(2)	C(26C)–C(25C)–C(24C)	119.2(2)
C(1C)–N(1C)–Cu(1C)	110.79(15)	O(29C)–C(26C)–C(25C)	124.1(2)
C(3C)–N(1C)–Cu(1C)	127.90(15)	O(29C)–C(26C)–C(27C)	115.8(2)
N(2C)–C(2C)–C(1C)	118.0(2)	C(25C)–C(26C)–C(27C)	120.1(2)
C(2C)–N(2C)–C(11C)	121.05(19)	C(28C)–C(27C)–C(26C)	120.4(2)
C(2C)–N(2C)–Cu(1C)	111.43(15)	C(27C)–C(28C)–C(23C)	120.3(2)
C(11C)–N(2C)–Cu(1C)	127.44(15)	C(26C)–O(29C)–C(30C)	116.97(19)
C(4C)–C(3C)–C(8C)	118.5(2)	C(32C)–C(31C)–C(36C)	119.0(2)
C(4C)–C(3C)–N(1C)	124.5(2)	C(32C)–C(31C)–N(22C)	124.4(2)
C(8C)–C(3C)–N(1C)	117.0(2)	C(36C)–C(31C)–N(22C)	116.6(2)
C(5C)–C(4C)–C(3C)	120.9(2)	C(31C)–C(32C)–C(33C)	121.2(2)
C(6C)–C(5C)–C(4C)	120.0(2)	C(32C)–C(33C)–C(34C)	119.5(2)
O(9C)–C(6C)–C(5C)	124.4(2)	O(37C)–C(34C)–C(33C)	124.6(2)
O(9C)–C(6C)–C(7C)	116.0(2)	O(37C)–C(34C)–C(35C)	115.5(2)
C(5C)–C(6C)–C(7C)	119.5(2)	C(33C)–C(34C)–C(35C)	119.8(2)
C(8C)–C(7C)–C(6C)	120.7(2)	C(36C)–C(35C)–C(34C)	120.3(2)
C(7C)–C(8C)–C(3C)	120.4(2)	C(35C)–C(36C)–C(31C)	120.3(2)
C(6C)–O(9C)–C(10C)	117.3(2)	C(34C)–O(37C)–C(38C)	117.9(2)

Structure D
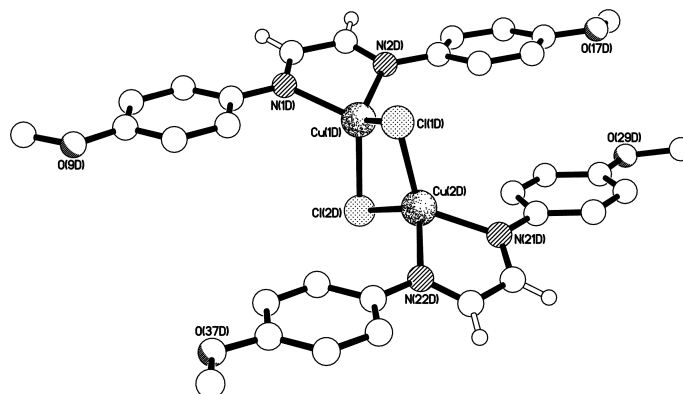
Bond lengths [Å] and angles [°] for Structure D:

Cu(1D)–N(2D)	2.0648(19)	C(14D)–O(17D)	1.372(3)
Cu(1D)–N(1D)	2.074(2)	C(14D)–C(15D)	1.391(4)
Cu(1D)–Cl(1D)	2.2984(6)	C(15D)–C(16D)	1.364(4)
Cu(1D)–Cl(2D)	2.3408(7)	O(17D)–C(18D)	1.413(3)
Cu(1D)–Cu(2D)	2.7430(5)	C(21D)–N(21D)	1.288(3)
Cu(2D)–N(21D)	2.038(2)	C(21D)–C(22D)	1.456(4)
Cu(2D)–N(22D)	2.0793(19)	N(21D)–C(23D)	1.418(3)
Cu(2D)–Cl(2D)	2.2711(7)	C(22D)–N(22D)	1.282(3)
Cu(2D)–Cl(1D)	2.3342(7)	N(22D)–C(31D)	1.411(3)
C(1D)–N(1D)	1.282(3)	C(23D)–C(24D)	1.387(3)
C(1D)–C(2D)	1.454(3)	C(23D)–C(28D)	1.392(3)
N(1D)–C(3D)	1.414(3)	C(24D)–C(25D)	1.387(4)
C(2D)–N(2D)	1.294(3)	C(25D)–C(26D)	1.384(4)
N(2D)–C(11D)	1.415(3)	C(26D)–O(29D)	1.371(3)
C(3D)–C(4D)	1.392(3)	C(26D)–C(27D)	1.387(4)
C(3D)–C(8D)	1.396(3)	C(27D)–C(28D)	1.387(4)
C(4D)–C(5D)	1.391(4)	O(29D)–C(30D)	1.425(4)
C(5D)–C(6D)	1.387(4)	C(31D)–C(36D)	1.396(4)
C(6D)–O(9D)	1.367(3)	C(31D)–C(32D)	1.398(3)
C(6D)–C(7D)	1.390(4)	C(32D)–C(33D)	1.384(4)
C(7D)–C(8D)	1.381(4)	C(33D)–C(34D)	1.384(4)
O(9D)–C(10D)	1.422(3)	C(34D)–O(37D)	1.359(3)
C(11D)–C(12D)	1.391(3)	C(34D)–C(35D)	1.398(4)
C(11D)–C(16D)	1.394(3)	C(35D)–C(36D)	1.374(4)
C(12D)–C(13D)	1.387(4)	O(37D)–C(38D)	1.434(3)
C(13D)–C(14D)	1.389(4)		

N(2D)–Cu(1D)–N(1D)	80.65(8)	C(12D)–C(11D)–C(16D)	118.5(2)
N(2D)–Cu(1D)–Cl(1D)	120.53(6)	C(12D)–C(11D)–N(2D)	125.0(2)
N(1D)–Cu(1D)–Cl(1D)	125.99(6)	C(16D)–C(11D)–N(2D)	116.5(2)
N(2D)–Cu(1D)–Cl(2D)	115.76(6)	C(13D)–C(12D)–C(11D)	120.6(2)
N(1D)–Cu(1D)–Cl(2D)	108.72(6)	C(12D)–C(13D)–C(14D)	120.0(2)
Cl(1D)–Cu(1D)–Cl(2D)	104.35(2)	O(17D)–C(14D)–C(13D)	125.4(2)
N(2D)–Cu(1D)–Cu(2D)	127.12(6)	O(17D)–C(14D)–C(15D)	115.4(2)
N(1D)–Cu(1D)–Cu(2D)	149.96(6)	C(13D)–C(14D)–C(15D)	119.2(2)
Cl(1D)–Cu(1D)–Cu(2D)	54.297(17)	C(16D)–C(15D)–C(14D)	120.7(2)
Cl(2D)–Cu(1D)–Cu(2D)	52.342(17)	C(15D)–C(16D)–C(11D)	121.0(2)
N(21D)–Cu(2D)–N(22D)	80.72(8)	C(14D)–O(17D)–C(18D)	117.3(2)
N(21D)–Cu(2D)–Cl(2D)	118.41(6)	N(21D)–C(21D)–C(22D)	118.6(2)
N(22D)–Cu(2D)–Cl(2D)	118.01(6)	C(21D)–N(21D)–C(23D)	120.6(2)
N(21D)–Cu(2D)–Cl(1D)	122.61(6)	C(21D)–N(21D)–Cu(2D)	111.80(16)
N(22D)–Cu(2D)–Cl(1D)	110.30(6)	C(23D)–N(21D)–Cu(2D)	127.47(15)
Cl(2D)–Cu(2D)–Cl(1D)	105.44(2)	N(22D)–C(22D)–C(21D)	117.5(2)
N(21D)–Cu(2D)–Cu(1D)	133.61(6)	C(22D)–N(22D)–C(31D)	122.9(2)
N(22D)–Cu(2D)–Cu(1D)	145.51(6)	C(22D)–N(22D)–Cu(2D)	111.25(16)
Cl(2D)–Cu(2D)–Cu(1D)	54.684(18)	C(31D)–N(22D)–Cu(2D)	125.87(15)
Cl(1D)–Cu(2D)–Cu(1D)	53.092(17)	C(24D)–C(23D)–C(28D)	119.2(2)
Cu(1D)–Cl(1D)–Cu(2D)	72.61(2)	C(24D)–C(23D)–N(21D)	123.3(2)
Cu(2D)–Cl(2D)–Cu(1D)	72.97(2)	C(28D)–C(23D)–N(21D)	117.5(2)
N(1D)–C(1D)–C(2D)	118.6(2)	C(23D)–C(24D)–C(25D)	121.0(2)
C(1D)–N(1D)–C(3D)	122.5(2)	C(26D)–C(25D)–C(24D)	119.3(2)
C(1D)–N(1D)–Cu(1D)	111.06(16)	O(29D)–C(26D)–C(25D)	124.2(2)
C(3D)–N(1D)–Cu(1D)	126.38(15)	O(29D)–C(26D)–C(27D)	115.4(2)
N(2D)–C(2D)–C(1D)	118.1(2)	C(25D)–C(26D)–C(27D)	120.4(2)
C(2D)–N(2D)–C(11D)	121.9(2)	C(26D)–C(27D)–C(28D)	120.0(2)
C(2D)–N(2D)–Cu(1D)	111.12(16)	C(27D)–C(28D)–C(23D)	120.0(2)
C(11D)–N(2D)–Cu(1D)	126.86(15)	C(26D)–O(29D)–C(30D)	116.3(2)
C(4D)–C(3D)–C(8D)	118.7(2)	C(36D)–C(31D)–C(32D)	118.9(2)
C(4D)–C(3D)–N(1D)	124.7(2)	C(36D)–C(31D)–N(22D)	116.8(2)
C(8D)–C(3D)–N(1D)	116.6(2)	C(32D)–C(31D)–N(22D)	124.3(2)
C(5D)–C(4D)–C(3D)	120.7(2)	C(33D)–C(32D)–C(31D)	120.2(2)
C(6D)–C(5D)–C(4D)	119.9(2)	C(34D)–C(33D)–C(32D)	120.6(2)
O(9D)–C(6D)–C(5D)	124.8(2)	O(37D)–C(34D)–C(33D)	125.3(2)
O(9D)–C(6D)–C(7D)	115.4(2)	O(37D)–C(34D)–C(35D)	115.4(3)
C(5D)–C(6D)–C(7D)	119.8(2)	C(33D)–C(34D)–C(35D)	119.3(2)
C(8D)–C(7D)–C(6D)	120.1(2)	C(36D)–C(35D)–C(34D)	120.3(3)
C(7D)–C(8D)–C(3D)	120.7(2)	C(35D)–C(36D)–C(31D)	120.7(2)
C(6D)–O(9D)–C(10D)	117.8(2)	C(34D)–O(37D)–C(38D)	117.3(2)

A.10 [Cu(ImPy^{Ad})$_2$](OTf)
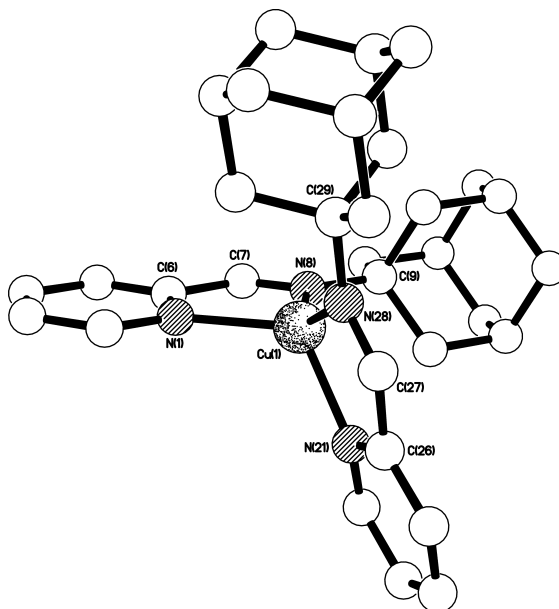
Formula	[C$_{32}$H$_{40}$CuN$_4$](CF$_3$O$_3$S)
Formula weight	735.75
Temperature	173(2) K
Diffractometer, wavelength	Agilent Xcalibur PX Ultra A, 1.54184Å
Crystal system, space group	Monoclinic, P2$_1$/n
Unit cell dimensions	a = 12.3905(3) Å α = 90 °
	b = 19.0233(5) Å β = 102.996(2) °
	c = 14.4810(3) Å γ = 90 °
Volume, Z	3325.85(14) Å^3, 4
Density (calculated)	1.469 g cm^{-3}
Absorption coefficient	2.744 mm^{-1}
F(000)	1532
Crystal colour / morphology	Red-platy needles
Crystal size	0.43 x 0.15 x 0.02 mm^3
θ range for data collection	3.901 to 73.783°
Index ranges	-14<=h<=15, -21<=k<=23, -7<=l<=17
Reflns collected / unique	10945 / 6376 [R(int) = 0.0316]
Reflns observed [F>4σ(F)]	4921
Absorption correction	Analytical
Max. and min. transmission	0.957 and 0.604
Refinement method	Full-matrix least-squares on F2
Data / restraints / parameters	6376 / 134 / 479
Goodness-of-fit on F^2	1.039

Final R indices [F>4σ(F)]   R1 = 0.504, wR2 = 0.0984
R indices (all data)   R1 = 0.0549, wR2 = 0.1092
Largest diff. peak, hole   0.438, -0.280 eÅ^{-3}
Mean and maximum shift/error   0.000 and 0.001

Bond lengths [Å] and angles [°] for [Cu(ImPy^{Ad})$_2$](OTf):

Cu(1)–N(28)	2.0204(17)	C(27)–N(28)	1.284(3)
Cu(1)–N(8)	2.0258(17)	N(28)–C(29)	1.484(3)
Cu(1)–N(1)	2.0772(18)	C(29)–C(30)	1.529(3)
Cu(1)–N(21)	2.0805(18)	C(29)–C(31)	1.534(3)
N(1)–C(2)	1.345(3)	C(29)–C(32)	1.538(3)
N(1)–C(6)	1.351(3)	C(30)–C(33)	1.538(3)
C(2)–C(3)	1.389(3)	C(31)–C(34)	1.537(3)
C(3)–C(4)	1.390(4)	C(32)–C(35)	1.540(3)
C(4)–C(5)	1.386(3)	C(33)–C(36)	1.521(4)
C(5)–C(6)	1.391(3)	C(33)–C(38)	1.532(4)
C(6)–C(7)	1.468(3)	C(34)–C(37)	1.525(4)
C(7)–N(8)	1.275(3)	C(34)–C(36)	1.529(4)
N(8)–C(9)	1.484(3)	C(35)–C(37)	1.526(4)
C(9)–C(10)	1.528(3)	C(35)–C(38)	1.527(3)
C(9)–C(11)	1.531(3)	S(40)–O(41)	1.440(2)
C(9)–C(12)	1.541(3)	S(40)–O(43)	1.451(3)
C(10)–C(13)	1.541(3)	S(40)–O(42)	1.454(3)
C(11)–C(14)	1.541(3)	S(40)–C(40)	1.820(3)
C(12)–C(15)	1.547(3)	C(40)–F(41)	1.336(4)
C(13)–C(16)	1.523(4)	C(40)–F(42)	1.336(4)
C(13)–C(18)	1.527(3)	C(40)–F(43)	1.337(4)
C(14)–C(17)	1.529(4)	S(40')–O(43')	1.445(15)
C(14)–C(16)	1.536(3)	S(40')–O(41')	1.454(13)
C(15)–C(17)	1.517(4)	S(40')–O(42')	1.455(15)
C(15)–C(18)	1.528(3)	S(40')–C(40')	1.807(14)
N(21)–C(22)	1.336(3)	C(40')–F(42')	1.333(15)
N(21)–C(26)	1.350(3)	C(40')–F(41')	1.336(14)
C(22)–C(23)	1.388(3)	C(40')–F(43')	1.339(14)
C(23)–C(24)	1.379(4)	C(50)–Cl(1)	1.730(11)
C(24)–C(25)	1.390(4)	C(50)–Cl(2)	1.764(9)
C(25)–C(26)	1.391(3)	C(50')–Cl(2')	1.735(18)
C(26)–C(27)	1.459(3)	C(50')–Cl(1')	1.744(18)

N(28)–Cu(1)–N(8)	142.27(8)	N(28)–C(27)–C(26)	118.92(18)
N(28)–Cu(1)–N(1)	119.99(7)	C(27)–N(28)–C(29)	119.88(17)
N(8)–Cu(1)–N(1)	81.25(7)	C(27)–N(28)–Cu(1)	113.10(15)

N(28)–Cu(1)–N(21)	81.42(7)	C(29)–N(28)–Cu(1)	126.78(12)
N(8)–Cu(1)–N(21)	116.67(7)	N(28)–C(29)–C(30)	114.97(17)
N(1)–Cu(1)–N(21)	119.79(8)	N(28)–C(29)–C(31)	108.11(16)
C(2)–N(1)–C(6)	117.88(18)	C(30)–C(29)–C(31)	109.36(19)
C(2)–N(1)–Cu(1)	131.35(15)	N(28)–C(29)–C(32)	106.66(17)
C(6)–N(1)–Cu(1)	110.75(14)	C(30)–C(29)–C(32)	109.08(18)
N(1)–C(2)–C(3)	122.9(2)	C(31)–C(29)–C(32)	108.46(18)
C(2)–C(3)–C(4)	118.8(2)	C(29)–C(30)–C(33)	109.74(18)
C(5)–C(4)–C(3)	119.0(2)	C(29)–C(31)–C(34)	110.10(18)
C(4)–C(5)–C(6)	118.9(2)	C(29)–C(32)–C(35)	109.81(19)
N(1)–C(6)–C(5)	122.6(2)	C(36)–C(33)–C(38)	109.9(2)
N(1)–C(6)–C(7)	115.50(18)	C(36)–C(33)–C(30)	109.4(2)
C(5)–C(6)–C(7)	121.89(19)	C(38)–C(33)–C(30)	109.6(2)
N(8)–C(7)–C(6)	119.11(18)	C(37)–C(34)–C(36)	109.2(2)
C(7)–N(8)–C(9)	120.07(17)	C(37)–C(34)–C(31)	109.8(2)
C(7)–N(8)–Cu(1)	113.32(15)	C(36)–C(34)–C(31)	109.1(2)
C(9)–N(8)–Cu(1)	126.51(13)	C(37)–C(35)–C(38)	109.2(2)
N(8)–C(9)–C(10)	114.80(16)	C(37)–C(35)–C(32)	109.8(2)
N(8)–C(9)–C(11)	107.42(16)	C(38)–C(35)–C(32)	109.6(2)
C(10)–C(9)–C(11)	109.51(18)	C(33)–C(36)–C(34)	109.6(2)
N(8)–C(9)–C(12)	107.62(17)	C(34)–C(37)–C(35)	109.6(2)
C(10)–C(9)–C(12)	108.93(17)	C(35)–C(38)–C(33)	109.01(19)
C(11)–C(9)–C(12)	108.39(18)	O(41)–S(40)–O(43)	115.50(18)
C(9)–C(10)–C(13)	110.17(18)	O(41)–S(40)–O(42)	115.58(17)
C(9)–C(11)–C(14)	110.22(18)	O(43)–S(40)–O(42)	115.6(2)
C(9)–C(12)–C(15)	109.93(18)	O(41)–S(40)–C(40)	102.19(15)
C(16)–C(13)–C(18)	109.9(2)	O(43)–S(40)–C(40)	102.54(18)
C(16)–C(13)–C(10)	108.56(19)	O(42)–S(40)–C(40)	102.27(18)
C(18)–C(13)–C(10)	109.6(2)	F(41)–C(40)–F(42)	106.5(3)
C(17)–C(14)–C(16)	109.1(2)	F(41)–C(40)–F(43)	107.0(3)
C(17)–C(14)–C(11)	108.7(2)	F(42)–C(40)–F(43)	106.6(3)
C(16)–C(14)–C(11)	109.27(19)	F(41)–C(40)–S(40)	111.8(2)
C(17)–C(15)–C(18)	110.1(2)	F(42)–C(40)–S(40)	112.2(2)
C(17)–C(15)–C(12)	109.36(19)	F(43)–C(40)–S(40)	112.3(2)
C(18)–C(15)–C(12)	108.6(2)	O(43′)–S(40′)–O(41′)	121.9(19)
C(13)–C(16)–C(14)	110.1(2)	O(43′)–S(40′)–O(42′)	102(2)
C(15)–C(17)–C(14)	110.30(19)	O(41′)–S(40′)–O(42′)	121.3(19)
C(13)–C(18)–C(15)	109.63(19)	O(43′)–S(40′)–C(40′)	103.3(11)
C(22)–N(21)–C(26)	117.97(19)	O(41′)–S(40′)–C(40′)	102.7(9)
C(22)–N(21)–Cu(1)	131.56(15)	O(42′)–S(40′)–C(40′)	102.3(11)
C(26)–N(21)–Cu(1)	110.28(14)	F(42′)–C(40′)–F(41′)	104(2)
N(21)–C(22)–C(23)	123.0(2)	F(42′)–C(40′)–F(43′)	109(2)
C(24)–C(23)–C(22)	118.8(2)	F(41′)–C(40′)–F(43′)	103.8(18)
C(23)–C(24)–C(25)	119.2(2)	F(42′)–C(40′)–S(40′)	113.7(13)

C(24)–C(25)–C(26)	118.4(2)	F(41′)–C(40′)–S(40′)	112.3(12)
N(21)–C(26)–C(25)	122.6(2)	F(43′)–C(40′)–S(40′)	113.3(12)
N(21)–C(26)–C(27)	116.04(18)	Cl(1)–C(50)–Cl(2)	109.8(6)
C(25)–C(26)–C(27)	121.3(2)	Cl(2′)–C(50′)–Cl(1′)	111.3(18)

A.11 [Cu(ImPy$^{\text{DIPP}}$)$_2$](OTf)
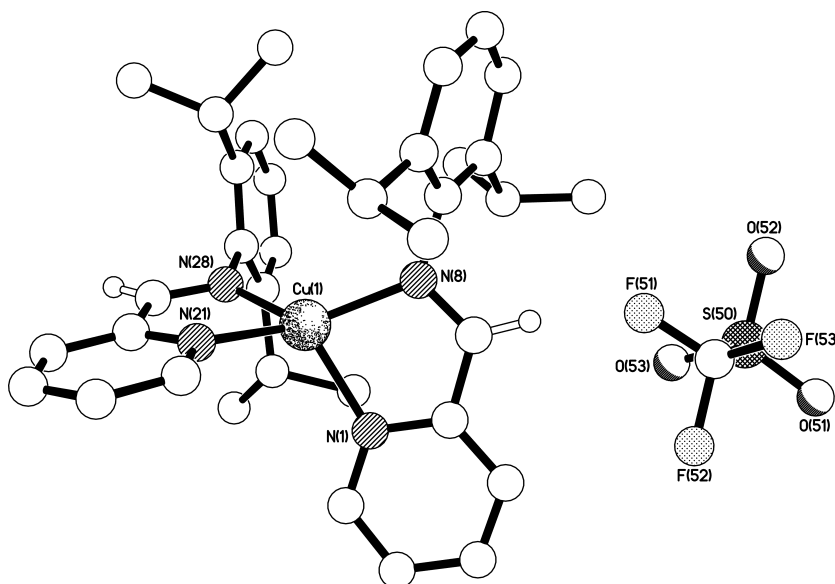
Formula	[C$_{36}$H$_{46}$CuN$_4$O]$_2$(CF$_3$O$_3$S)
Formula weight	745.36
Temperature	233(2) K
Diffractometer, wavelength	Agilent Xcalibur 3 E, 0.71073Å
Crystal system, space group	Triclinic, P-1
Unit cell dimensions	a = 9.1002(5) Å α = 89.693(4) °
	b = 10.9858(6) Å β = 79.192(4) °
	c = 19.3481(7) Å γ = 82.793(4) °
Volume, Z	1884.64(16) Å^3, 2
Density (calculated)	1.313 g cm^{-3}
Absorption coefficient	0.689 mm^{-1}
F(000)	780
Crystal colour / morphology	Red-brown blocks
Crystal size	0.63 x 0.23 x 0.15 mm^3
θ range for data collection	2.721 to 28.199°
Index ranges	-11<=h<=8, -11<=k<=13, -25<=l<=22
Reflns collected / unique	10872 / 7408 [R(int) = 0.0215]
Reflns observed [F>4σ(F)]	5713
Absorption correction	Analytical

Max. and min. transmission	0.912 and 0.794
Refinement method	Full-matrix least-squares on F2
Data / restraints / parameters	7408 / 139 / 483
Goodness-of-fit on F^2	1.021
Final R indices [F>4σ(F)]	R1 = 0.504, wR2 = 0.1138
R indices (all data)	R1 = 0.0703, wR2 = 0.1271
Largest diff. peak, hole	0.639, -0.411 eÅ^{-3}
Mean and maximum shift/error	0.000 and 0.002

Bond lengths [Å] and angles [°] for [Cu(ImPy^{DIPP})$_2$](OTf):

Cu(1)–N(28)	2.021(2)		C(25)–C(26)	1.380(4)
Cu(1)–N(8)	2.026(2)		C(26)–C(27)	1.455(4)
Cu(1)–N(1)	2.051(2)		C(27)–N(28)	1.272(3)
Cu(1)–N(21)	2.058(2)		N(28)–C(29)	1.438(3)
N(1)–C(2)	1.336(4)		C(29)–C(30)	1.394(4)
N(1)–C(6)	1.342(3)		C(29)–C(34)	1.395(4)
C(2)–C(3)	1.370(4)		C(30)–C(31)	1.388(4)
C(3)–C(4)	1.368(4)		C(30)–C(35)	1.525(4)
C(4)–C(5)	1.379(4)		C(31)–C(32)	1.365(5)
C(5)–C(6)	1.378(4)		C(32)–C(33)	1.368(5)
C(6)–C(7)	1.463(4)		C(33)–C(34)	1.387(4)
C(7)–N(8)	1.274(3)		C(34)–C(38)	1.505(4)
N(8)–C(9)	1.430(3)		C(35)–C(37)	1.505(5)
C(9)–C(10)	1.389(4)		C(35)–C(36)	1.526(6)
C(9)–C(14)	1.401(4)		C(38)–C(40)	1.525(5)
C(10)–C(11)	1.400(4)		C(38)–C(39)	1.525(5)
C(10)–C(15)	1.524(4)		S(50)–O(51)	1.432(4)
C(11)–C(12)	1.359(5)		S(50)–O(53)	1.438(3)
C(12)–C(13)	1.362(5)		S(50)–O(52)	1.465(4)
C(13)–C(14)	1.385(4)		S(50)–C(50)	1.794(7)
C(14)–C(18)	1.513(4)		C(50)–F(53)	1.323(6)
C(15)–C(17)	1.511(5)		C(50)–F(51)	1.328(7)
C(15)–C(16)	1.519(5)		C(50)–F(52)	1.375(7)
C(18)–C(19)	1.513(5)		S(50′)–O(53′)	1.359(10)
C(18)–C(20)	1.514(5)		S(50′)–O(51′)	1.371(11)
N(21)–C(22)	1.325(4)		S(50′)–O(52′)	1.586(11)
N(21)–C(26)	1.345(3)		S(50′)–C(50′)	1.830(11)
C(22)–C(23)	1.375(5)		C(50′)–F(53′)	1.315(12)
C(23)–C(24)	1.365(5)		C(50′)–F(52′)	1.324(12)
C(24)–C(25)	1.370(5)		C(50′)–F(51′)	1.356(12)

N(28)–Cu(1)–N(8)	128.58(8)		C(25)–C(26)–C(27)	122.7(3)

N(28)–Cu(1)–N(1)	127.33(9)	N(28)–C(27)–C(26)	119.3(2)
N(8)–Cu(1)–N(1)	80.98(9)	C(27)–N(28)–C(29)	118.7(2)
N(28)–Cu(1)–N(21)	80.75(9)	C(27)–N(28)–Cu(1)	112.68(18)
N(8)–Cu(1)–N(21)	134.02(9)	C(29)–N(28)–Cu(1)	128.60(17)
N(1)–Cu(1)–N(21)	110.44(9)	C(30)–C(29)–C(34)	122.5(2)
C(2)–N(1)–C(6)	117.1(2)	C(30)–C(29)–N(28)	118.6(2)
C(2)–N(1)–Cu(1)	130.7(2)	C(34)–C(29)–N(28)	118.9(2)
C(6)–N(1)–Cu(1)	112.06(18)	C(31)–C(30)–C(29)	117.4(3)
N(1)–C(2)–C(3)	123.1(3)	C(31)–C(30)–C(35)	120.2(3)
C(4)–C(3)–C(2)	119.4(3)	C(29)–C(30)–C(35)	122.4(3)
C(3)–C(4)–C(5)	118.7(3)	C(32)–C(31)–C(30)	121.3(3)
C(6)–C(5)–C(4)	118.7(3)	C(31)–C(32)–C(33)	120.1(3)
N(1)–C(6)–C(5)	123.0(3)	C(32)–C(33)–C(34)	121.7(3)
N(1)–C(6)–C(7)	114.6(2)	C(33)–C(34)–C(29)	116.9(3)
C(5)–C(6)–C(7)	122.4(3)	C(33)–C(34)–C(38)	121.1(3)
N(8)–C(7)–C(6)	119.2(2)	C(29)–C(34)–C(38)	122.0(3)
C(7)–N(8)–C(9)	118.6(2)	C(37)–C(35)–C(30)	110.8(3)
C(7)–N(8)–Cu(1)	112.99(18)	C(37)–C(35)–C(36)	110.0(3)
C(9)–N(8)–Cu(1)	128.37(17)	C(30)–C(35)–C(36)	112.6(3)
C(10)–C(9)–C(14)	122.2(3)	C(34)–C(38)–C(40)	110.5(3)
C(10)–C(9)–N(8)	120.6(2)	C(34)–C(38)–C(39)	112.9(3)
C(14)–C(9)–N(8)	117.2(2)	C(40)–C(38)–C(39)	109.6(3)
C(9)–C(10)–C(11)	117.0(3)	O(51)–S(50)–O(53)	116.8(3)
C(9)–C(10)–C(15)	123.2(3)	O(51)–S(50)–O(52)	113.7(3)
C(11)–C(10)–C(15)	119.8(3)	O(53)–S(50)–O(52)	113.5(3)
C(12)–C(11)–C(10)	121.2(3)	O(51)–S(50)–C(50)	106.0(4)
C(11)–C(12)–C(13)	120.9(3)	O(53)–S(50)–C(50)	104.4(3)
C(12)–C(13)–C(14)	120.9(3)	O(52)–S(50)–C(50)	100.2(3)
C(13)–C(14)–C(9)	117.7(3)	F(53)–C(50)–F(51)	107.6(6)
C(13)–C(14)–C(18)	121.6(3)	F(53)–C(50)–F(52)	107.6(6)
C(9)–C(14)–C(18)	120.7(3)	F(51)–C(50)–F(52)	106.8(6)
C(17)–C(15)–C(16)	110.4(3)	F(53)–C(50)–S(50)	111.4(5)
C(17)–C(15)–C(10)	111.0(3)	F(51)–C(50)–S(50)	114.7(5)
C(16)–C(15)–C(10)	111.1(3)	F(52)–C(50)–S(50)	108.5(5)
C(19)–C(18)–C(14)	112.0(3)	O(53′)–S(50′)–O(51′)	128.5(10)
C(19)–C(18)–C(20)	110.3(3)	O(53′)–S(50′)–O(52′)	108.6(9)
C(14)–C(18)–C(20)	112.6(3)	O(51′)–S(50′)–O(52′)	108.6(9)
C(22)–N(21)–C(26)	117.5(3)	O(53′)–S(50′)–C(50′)	104.6(8)
C(22)–N(21)–Cu(1)	130.5(2)	O(51′)–S(50′)–C(50′)	107.4(8)
C(26)–N(21)–Cu(1)	110.98(17)	O(52′)–S(50′)–C(50′)	93.4(7)
N(21)–C(22)–C(23)	123.0(3)	F(53′)–C(50′)–F(52′)	110.2(11)
C(24)–C(23)–C(22)	119.2(3)	F(53′)–C(50′)–F(51′)	109.7(12)
C(23)–C(24)–C(25)	119.1(3)	F(52′)–C(50′)–F(51′)	110.9(11)
C(24)–C(25)–C(26)	118.7(3)	F(53′)–C(50′)–S(50′)	112.4(10)

N(21)–C(26)–C(25)	122.6(3)		F(52')–C(50')–S(50')	106.1(9)
N(21)–C(26)–C(27)	114.6(2)		F(51')–C(50')–S(50')	107.4(9)

A.12 [Cu(ImPy$^{\text{DIPP}}$)$_2$(OH$_2$)](OTf)$_2$
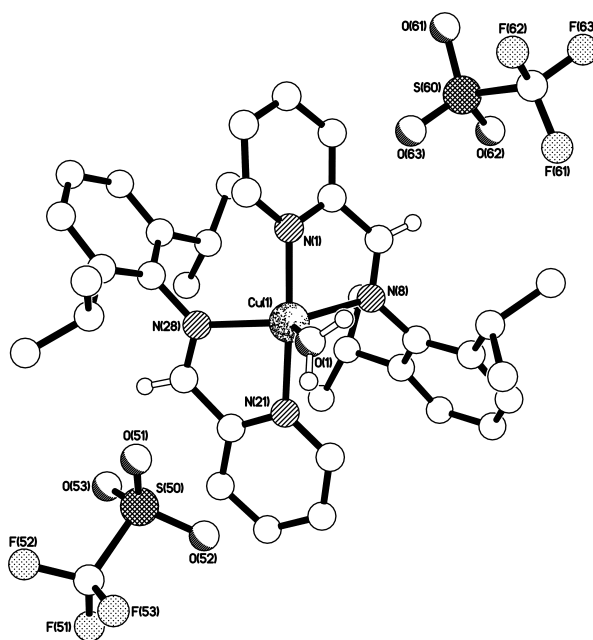
Formula	[C$_{36}$H$_{44}$CuN$_4$](CF$_3$O$_3$S)
Formula weight	966.49
Temperature	173(2) K
Diffractometer, wavelength	Agilent Xcalibur 3 E, 0.71073Å
Crystal system, space group	Orthorhombic, Fdd2
Unit cell dimensions	a = 21.033(3) Å α = 90°
	b = 21.3226(13) Å β = 90°
	c = 39.427(2) Å γ = 90°
Volume, Z	17682(3) Å^3, 16
Density (calculated)	1.452 g cm^{-3}
Absorption coefficient	0.672 mm^{-1}
F(000)	8048
Crystal colour / morphology	Green needles
Crystal size	0.87 x 0.08 x 0.02 mm^3
θ range for data collection	2.721 to 28.205°
Index ranges	-16<=h<=20, -28<=k<=17, -28<=l<=50
Reflns collected / unique	7563 / 4983 [R(int) = 0.0388]
Reflns observed [F>4σ(F)]	4177
Absorption correction	Analytical

Max. and min. transmission	0.985 and 0.772
Refinement method	Full-matrix least-squares on F2
Data / restraints / parameters	4983 / 3 / 568
Goodness-of-fit on F^2	1.064
Final R indices [$F>4\sigma(F)$]	R1 = 0.0391, wR2 = 0.0837
R indices (all data)	R1 = 0.0543, wR2 = 0.0905
Absolute structure parameter	0.302(19)
Largest diff. peak, hole	0.342, -0.373 e$\mathring{A}^{-3}$
Mean and maximum shift/error	0.000 and 0.001

Bond lengths [Å] and angles [°] for [Cu(ImPy^{DIPP})$_2$(OH$_2$)](OTf)$_2$:

Cu(1)–N(1)	1.976(5)	C(25)–C(26)	1.397(9)
Cu(1)–N(21)	2.000(5)	C(26)–C(27)	1.467(8)
Cu(1)–O(1)	2.015(4)	C(27)–N(28)	1.278(8)
Cu(1)–N(28)	2.091(5)	N(28)–C(29)	1.440(7)
Cu(1)–N(8)	2.100(5)	C(29)–C(30)	1.404(8)
N(1)–C(2)	1.331(7)	C(29)–C(34)	1.417(9)
N(1)–C(6)	1.353(8)	C(30)–C(31)	1.376(8)
C(2)–C(3)	1.380(9)	C(30)–C(35)	1.518(9)
C(3)–C(4)	1.347(10)	C(31)–C(32)	1.387(10)
C(4)–C(5)	1.402(9)	C(32)–C(33)	1.370(9)
C(5)–C(6)	1.379(9)	C(33)–C(34)	1.388(8)
C(6)–C(7)	1.475(8)	C(34)–C(38)	1.502(8)
C(7)–N(8)	1.279(8)	C(35)–C(36)	1.521(9)
N(8)–C(9)	1.440(8)	C(35)–C(37)	1.549(10)
C(9)–C(14)	1.397(9)	C(38)–C(40)	1.502(10)
C(9)–C(10)	1.408(8)	C(38)–C(39)	1.535(9)
C(10)–C(11)	1.380(9)	S(50)–O(51)	1.434(4)
C(10)–C(15)	1.509(9)	S(50)–O(53)	1.438(4)
C(11)–C(12)	1.384(10)	S(50)–O(52)	1.442(5)
C(12)–C(13)	1.354(10)	S(50)–C(50)	1.816(8)
C(13)–C(14)	1.394(9)	C(50)–F(52)	1.310(9)
C(14)–C(18)	1.515(9)	C(50)–F(53)	1.329(7)
C(15)–C(17)	1.532(10)	C(50)–F(51)	1.335(8)
C(15)–C(16)	1.540(10)	S(60)–O(61)	1.424(5)
C(18)–C(19)	1.517(10)	S(60)–O(62)	1.433(5)
C(18)–C(20)	1.526(12)	S(60)–O(63)	1.440(6)
N(21)–C(22)	1.339(7)	S(60)–C(60)	1.818(9)
N(21)–C(26)	1.340(8)	C(60)–F(63)	1.315(10)
C(22)–C(23)	1.374(9)	C(60)–F(62)	1.319(10)
C(23)–C(24)	1.360(10)	C(60)–F(61)	1.321(10)
C(24)–C(25)	1.389(9)		

N(1)–Cu(1)–N(21)	172.04(18)	N(21)–C(26)–C(25)	122.8(6)
N(1)–Cu(1)–O(1)	93.1(2)	N(21)–C(26)–C(27)	115.4(5)
N(21)–Cu(1)–O(1)	94.80(19)	C(25)–C(26)–C(27)	121.8(6)
N(1)–Cu(1)–N(28)	94.3(2)	N(28)–C(27)–C(26)	118.3(6)
N(21)–Cu(1)–N(28)	80.7(2)	C(27)–N(28)–C(29)	119.5(6)
O(1)–Cu(1)–N(28)	121.2(2)	C(27)–N(28)–Cu(1)	111.6(4)
N(1)–Cu(1)–N(8)	80.1(2)	C(29)–N(28)–Cu(1)	128.9(4)
N(21)–Cu(1)–N(8)	98.1(2)	C(30)–C(29)–C(34)	122.0(5)
O(1)–Cu(1)–N(8)	110.1(2)	C(30)–C(29)–N(28)	118.2(6)
N(28)–Cu(1)–N(8)	128.58(16)	C(34)–C(29)–N(28)	119.5(5)
C(2)–N(1)–C(6)	118.5(5)	C(31)–C(30)–C(29)	118.4(6)
C(2)–N(1)–Cu(1)	126.6(5)	C(31)–C(30)–C(35)	120.8(5)
C(6)–N(1)–Cu(1)	114.6(4)	C(29)–C(30)–C(35)	120.7(5)
N(1)–C(2)–C(3)	122.7(7)	C(30)–C(31)–C(32)	121.3(6)
C(4)–C(3)–C(2)	118.8(6)	C(33)–C(32)–C(31)	119.1(6)
C(3)–C(4)–C(5)	120.3(6)	C(32)–C(33)–C(34)	123.5(6)
C(6)–C(5)–C(4)	117.7(7)	C(33)–C(34)–C(29)	115.8(5)
N(1)–C(6)–C(5)	122.0(6)	C(33)–C(34)–C(38)	120.4(6)
N(1)–C(6)–C(7)	114.4(5)	C(29)–C(34)–C(38)	123.8(5)
C(5)–C(6)–C(7)	123.4(7)	C(30)–C(35)–C(36)	111.5(6)
N(8)–C(7)–C(6)	117.0(6)	C(30)–C(35)–C(37)	113.7(6)
C(7)–N(8)–C(9)	120.3(6)	C(36)–C(35)–C(37)	109.7(5)
C(7)–N(8)–Cu(1)	112.4(4)	C(40)–C(38)–C(34)	111.3(6)
C(9)–N(8)–Cu(1)	127.1(4)	C(40)–C(38)–C(39)	108.9(6)
C(14)–C(9)–C(10)	122.3(6)	C(34)–C(38)–C(39)	111.7(6)
C(14)–C(9)–N(8)	120.0(5)	O(51)–S(50)–O(53)	116.0(3)
C(10)–C(9)–N(8)	117.3(6)	O(51)–S(50)–O(52)	114.7(3)
C(11)–C(10)–C(9)	117.5(6)	O(53)–S(50)–O(52)	114.3(3)
C(11)–C(10)–C(15)	121.2(6)	O(51)–S(50)–C(50)	104.3(3)
C(9)–C(10)–C(15)	121.3(5)	O(53)–S(50)–C(50)	102.9(3)
C(10)–C(11)–C(12)	121.3(6)	O(52)–S(50)–C(50)	102.2(3)
C(13)–C(12)–C(11)	119.7(7)	F(52)–C(50)–F(53)	107.1(6)
C(12)–C(13)–C(14)	122.5(7)	F(52)–C(50)–F(51)	107.9(7)
C(13)–C(14)–C(9)	116.6(6)	F(53)–C(50)–F(51)	107.1(6)
C(13)–C(14)–C(18)	120.5(6)	F(52)–C(50)–S(50)	112.3(5)
C(9)–C(14)–C(18)	122.9(6)	F(53)–C(50)–S(50)	111.4(6)
C(10)–C(15)–C(17)	114.0(6)	F(51)–C(50)–S(50)	110.8(5)
C(10)–C(15)–C(16)	110.6(6)	O(61)–S(60)–O(62)	115.1(3)
C(17)–C(15)–C(16)	110.0(5)	O(61)–S(60)–O(63)	113.4(3)
C(14)–C(18)–C(19)	112.0(7)	O(62)–S(60)–O(63)	115.7(4)
C(14)–C(18)–C(20)	111.3(6)	O(61)–S(60)–C(60)	103.8(4)
C(19)–C(18)–C(20)	109.2(7)	O(62)–S(60)–C(60)	104.7(4)
C(22)–N(21)–C(26)	118.5(5)	O(63)–S(60)–C(60)	102.0(4)
C(22)–N(21)–Cu(1)	127.6(5)	F(63)–C(60)–F(62)	107.2(9)

C(26)–N(21)–Cu(1)	113.9(4)	F(63)–C(60)–F(61)	107.6(7)
N(21)–C(22)–C(23)	122.2(7)	F(62)–C(60)–F(61)	108.4(7)
C(24)–C(23)–C(22)	119.1(6)	F(63)–C(60)–S(60)	110.8(6)
C(23)–C(24)–C(25)	120.5(6)	F(62)–C(60)–S(60)	111.5(6)
C(24)–C(25)–C(26)	116.8(7)	F(61)–C(60)–S(60)	111.3(7)

A.2 Computational Data

A.1 Input Coordinates for Reaction Intermediates

Intermediate I.1

```
1 1
Cu   5.890721    2.131651    4.891941
 N   5.68408     0.116098    4.677587
 C   6.803423   -0.42349     4.377132
 H   6.859215   -1.347928    4.16458
 C   7.998104    0.424737    4.369567
 H   8.851155    0.06513     4.155574
 N   7.862058    1.665428    4.660295
 C   4.455417   -0.709846    4.740092
 C   9.049255    2.545447    4.731986
 N   4.98882     3.409017    3.557185
 C   4.359852    4.335315    4.175568
 H   3.886549    5.008225    3.699848
 C   4.391499    4.326842    5.637314
 H   3.944685    5.001061    6.136992
 N   5.035895    3.388374    6.23264
 C   4.92918     3.412679    2.06824
 C   5.091214    3.413163    7.716722
 H   4.59333653  -1.72597979  4.43455914
 H   4.11541913  -0.69427639  5.75451747
 H   3.71580643  -0.24564574  4.12171159
 H   3.91956663   3.26330858  1.74688454
 H   5.53799444   2.61166685  1.70406351
 H   5.29260438   4.33909298  1.67507355
 H   8.86092227   3.40683236  4.12581272
 H   9.96473627   2.08543077  4.4234749
 H   9.13725213   2.8571053   5.75180246
 H   5.60821666   2.54059089  8.05764157
 H   4.12062214   3.4343898   8.16661183
 H   5.63853322   4.2825784   8.01581819
```

Intermediate I.2

```
            1 1
  C   -0.974425    0.884145   -0.734388
  H   -1.574487    1.629677   -1.279937
  C    0.341566    1.259704   -0.202545
  H    0.724975    2.279094   -0.368407
  C   -2.69457    -0.74064    -1.04583
  H   -3.305381   -1.096796   -0.197552
  H   -3.232525    0.07098    -1.570537
  H   -2.554215   -1.592578   -1.734355
  C    2.32824     0.695768    0.993225
  H    2.63355     1.738759    0.787016
  H    2.314438    0.526144    2.084305
  H    3.072448    0.004588    0.559305
  N   -1.387633   -0.333379   -0.537082
  N    1.01337     0.360241    0.453911
  Cu  -0.01919    -1.397867    0.524736
  H   -1.309075   -2.813885    2.460038
  H    0.073784   -2.394404    3.056909
  H    1.707678   -3.443393    0.066932
  H    0.336205   -3.86553    -0.553709
  O   -0.611621   -2.12736     2.409493
  O    0.890305   -3.086225   -0.33893
```

Intermediate I.3

```
            1 1
  C   -1.023356    0.91058    -0.674854
  H   -1.669314    1.68157    -1.122106
  C    0.324584    1.261365   -0.211086
  H    0.740128    2.254034   -0.449678
  C   -2.758734   -0.707928   -0.975951
  H   -3.294417   -1.128495   -0.10656
  H   -3.338267    0.139338   -1.386489
  H   -2.67958    -1.50612    -1.733665
  C    2.354619    0.624672    0.878466
  H    2.731587    1.617058    0.567155
  H    2.412913    0.534853    1.977887
  H    2.998167   -0.166503    0.454532
  N   -1.41094    -0.328678   -0.551373
  N    0.98263     0.363895    0.459122
  Cu  -0.088785   -1.443001    0.396786
  H    1.100174   -3.700098    0.660674
```

H	1.260334	-3.378929	-0.864495
O	1.280077	-2.970311	0.026947
N	-0.14913514	-2.4382595	1.99946572
H	-0.82866169	-3.05887447	1.60821041
H	0.59470353	-2.97047934	2.40375036
C	-0.78091527	-1.61168795	3.03799032
C	-0.79606615	-0.22245772	2.9103923
C	-1.36533152	-2.2162017	4.15090043
C	-1.39492589	0.56203999	3.89586279
H	-0.33456045	0.25386561	2.03325471
C	-1.96528311	-1.43166136	5.13627571
H	-1.35363679	-3.31112824	4.25153898
C	-1.98005091	-0.04273294	5.00900921
H	-1.40635437	1.65708641	3.79566673
H	-2.42635294	-1.90859374	6.01344407
H	-2.45222276	0.57601823	5.78585995

Intermediate I.4

1 1

C	-0.979917	0.827822	-0.660905
H	-1.613748	1.578252	-1.15757
C	0.336648	1.23044	-0.120591
H	0.674961	2.269738	-0.268015
C	-2.653859	-0.841342	-1.059541
H	-3.238249	-1.264242	-0.224289
H	-3.218725	-0.018702	-1.533309
H	-2.483825	-1.649998	-1.790723
C	2.351665	0.68558	1.032468
H	2.641948	1.736745	0.848051
H	2.352364	0.487863	2.119506
H	3.098498	0.011144	0.57615
N	-1.355452	-0.408589	-0.539887
N	1.039	0.341933	0.500991
Cu	-0.084875	-1.535752	0.38982
N	0.725856	-3.172423	1.109052
H	1.05770157	-2.70155084	1.92646128
H	1.06068696	-2.70049539	0.29347088
C	1.21583918	-4.55835824	1.109052
C	0.30916067	-5.61873516	1.10654322
C	2.5871593	-4.81335532	1.11144881
C	0.77378567	-6.9337808	1.10711334
H	-0.77189976	-5.41736763	1.10543122
C	3.05209148	-6.12874415	1.11102351

H	3.30190309	-3.97773154	1.1132464
C	2.14568885	-7.18891734	1.10899445
H	0.05919133	-7.76963343	1.10577001
H	4.13337378	-6.32949438	1.11249827
H	2.5117933	-8.22586657	1.10938439

Intermediate II

1 1

C	-0.48826	0.618702	0.443166
H	-1.232819	1.405498	0.645181
C	0.93419	0.885058	0.684488
H	1.275679	1.913173	0.882096
C	-2.219297	-0.933803	-0.113811
H	-2.418909	-1.748526	0.606941
H	-2.913283	-0.09524	0.081768
H	-2.392019	-1.336521	-1.126618
C	3.183346	0.094083	0.88812
H	3.437949	1.156363	1.058971
H	3.511026	-0.511739	1.750375
H	3.729799	-0.271779	0.000699
N	-0.814803	-0.565428	0.017103
N	1.754014	-0.128949	0.676451
N	0.134726	-3.414375	1.198287
N	0.23025	-4.568368	0.695883
N	0.419984	-5.556336	0.133661
C	-0.799279	-3.233754	2.285574
C	-0.651001	-2.058743	3.043991
C	-1.832355	-4.149227	2.55608
C	-1.552145	-1.799038	4.085748
H	0.170413	-1.371297	2.814252
C	-2.72196	-3.876775	3.606155
H	-1.94563	-5.05961	1.957154
C	-2.588355	-2.704788	4.369892
H	-1.436467	-0.889291	4.683777
H	-3.52624	-4.58694	3.822935
H	-3.287813	-2.500285	5.186208
Cu	0.829846	-1.824199	0.131622
N	1.73654749	-2.95904183	-1.22386891
H	1.36194959	-3.79272852	-1.62963105
H	2.69913403	-3.10335403	-0.99451951
C	1.62233658	-1.85235408	-2.18464885
C	2.48706571	-0.76096755	-2.09752579
C	0.64957689	-1.89337273	-3.18345022

C	2.37854764	0.2894336	-3.00862567
H	3.25336246	-0.72857076	-1.30950198
C	0.54153596	-0.84319225	-4.09551272
H	-0.03193069	-2.75356245	-3.25237112
C	1.40571384	0.24818609	-4.00818037
H	3.05969196	1.15000241	-2.93963126
H	-0.22527074	-0.87599909	-4.88317091
H	1.32037945	1.07647929	-4.72647331

Intermediate III (singlet)

1 1

C	-0.329131	0.754852	0.411159
H	-0.718576	1.780195	0.329392
C	0.899725	0.464722	1.14543
H	1.407539	1.240642	1.7376
C	-2.109871	-0.12708	-0.96656
H	-2.942426	-0.672358	-0.488939
H	-2.394462	0.928433	-1.126639
H	-1.903152	-0.619865	-1.932215
C	2.547726	-1.182354	1.777636
H	2.996242	-0.370121	2.378108
H	2.281808	-2.02796	2.435451
H	3.284009	-1.55357	1.043644
N	-0.920758	-0.270153	-0.137129
N	1.348677	-0.759124	1.063048
N	-0.083606	-3.732022	0.482983
C	-0.188337	-4.49298	1.573286
C	-0.456224	-3.951559	2.892314
C	-0.037491	-5.928358	1.448475
C	-0.543427	-4.784814	3.998548
H	-0.586543	-2.865246	2.969467
C	-0.152878	-6.754367	2.561572
H	0.162349	-6.329945	0.449878
C	-0.39832	-6.184845	3.831658
H	-0.739513	-4.374532	4.994471
H	-0.047432	-7.839389	2.463243
H	-0.482449	-6.83924	4.706288
Cu	0.016382	-1.971303	0.207047
N	0.37326331	-2.39995237	-1.77436631
H	-0.47161338	-2.71590866	-2.20605484
H	1.02610398	-3.15593969	-1.72659364
C	0.94908919	-1.30467905	-2.56790327
C	0.11075402	-0.39003652	-3.20594293

C	2.33354053	-1.17972283	-2.68291886
C	0.65682396	0.64889986	-3.95936217
H	-0.98069012	-0.4892757	-3.11570394
C	2.87995174	-0.13994673	-3.43572051
H	2.99442864	-1.90041118	-2.17996337
C	2.04187274	0.77423515	-4.0740246
H	-0.00390671	1.36950064	-4.46281626
H	3.97157377	-0.04143235	-3.52588968
H	2.47220007	1.59351498	-4.66807451

Intermediate III (triplet)

1 3

C	-0.329131	0.754852	0.411159
H	-0.718576	1.780195	0.329392
C	0.899725	0.464722	1.14543
H	1.407539	1.240642	1.7376
C	-2.109871	-0.12708	-0.96656
H	-2.942426	-0.672358	-0.488939
H	-2.394462	0.928433	-1.126639
H	-1.903152	-0.619865	-1.932215
C	2.547726	-1.182354	1.777636
H	2.996242	-0.370121	2.378108
H	2.281808	-2.02796	2.435451
H	3.284009	-1.55357	1.043644
N	-0.920758	-0.270153	-0.137129
N	1.348677	-0.759124	1.063048
N	-0.083606	-3.732022	0.482983
C	-0.188337	-4.49298	1.573286
C	-0.456224	-3.951559	2.892314
C	-0.037491	-5.928358	1.448475
C	-0.543427	-4.784814	3.998548
H	-0.586543	-2.865246	2.969467
C	-0.152878	-6.754367	2.561572
H	0.162349	-6.329945	0.449878
C	-0.39832	-6.184845	3.831658
H	-0.739513	-4.374532	4.994471
H	-0.047432	-7.839389	2.463243
H	-0.482449	-6.83924	4.706288
Cu	0.016382	-1.971303	0.207047
N	0.37326331	-2.39995237	-1.77436631
H	-0.47161338	-2.71590866	-2.20605484
H	1.02610398	-3.15593969	-1.72659364
C	0.94908919	-1.30467905	-2.56790327

C	0.11075402	-0.39003652	-3.20594293
C	2.33354053	-1.17972283	-2.68291886
C	0.65682396	0.64889986	-3.95936217
H	-0.98069012	-0.4892757	-3.11570394
C	2.87995174	-0.13994673	-3.43572051
H	2.99442864	-1.90041118	-2.17996337
C	2.04187274	0.77423515	-4.0740246
H	-0.00390671	1.36950064	-4.46281626
H	3.97157377	-0.04143235	-3.52588968
H	2.47220007	1.59351498	-4.66807451

Intermediate IV

1 3			
C	-1.173435	0.723236	0.08528
H	-1.529256	1.763466	0.161212
C	0.145032	0.362207	0.635249
H	0.753184	1.129303	1.142522
C	-3.205394	0.082163	-1.007528
H	-3.945775	-0.538775	-0.473298
H	-3.482503	1.149057	-0.921357
H	-3.229075	-0.222401	-2.068624
C	1.807853	-1.330758	1.012604
H	2.380629	-0.542759	1.536117
H	1.611622	-2.176719	1.696797
H	2.393546	-1.729423	0.165236
N	-1.883211	-0.213678	-0.465546
N	0.533031	-0.864807	0.499536
N	-1.137154	-3.561463	0.480146
C	-0.453024	-4.286579	1.373123
C	-0.27066	-3.799276	2.718889
C	0.119308	-5.561372	1.015493
C	0.466049	-4.543619	3.635953
H	-0.722692	-2.837958	2.983288
C	0.8444	-6.284955	1.957777
H	-0.037444	-5.934843	-0.001588
C	1.027231	-5.786311	3.266334
H	0.603881	-4.164403	4.654196
H	1.27471	-7.252631	1.678725
H	1.598747	-6.366292	3.997526
Cu	-0.924008	-2.028996	-0.457107
N	-0.251068	-2.364584	-2.402909
H	-0.40162236	-3.32308032	-2.74134876
H	0.77350649	-2.17571115	-2.332493

C	-0.91377306	-1.39199353	-3.24277333
C	-2.09054777	-1.73525912	-3.93140929
C	-0.41537388	-0.07674989	-3.2913164
C	-2.76641458	-0.75782103	-4.67853043
H	-2.4745018	-2.76160126	-3.88406494
C	-1.10009214	0.89220123	-4.04025099
H	0.50373116	0.16979681	-2.7497618
C	-2.27657852	0.55869001	-4.7344203
H	-3.67653395	-1.0298108	-5.22325559
H	-0.70661813	1.91307619	-4.08454881
H	-2.80445392	1.31731218	-5.32055641
O	-1.268314	-4.969979	-2.049481
H	-1.544634	-4.626323	-1.16217
H	-2.017017	-5.512953	-2.369795

Intermediate V

1 3

C	-0.520325	0.731073	0.719192
H	-0.735229	1.802284	0.86154
C	0.387417	0.024795	1.630983
H	0.897471	0.572212	2.438484
C	-1.923229	0.582941	-1.243669
H	-2.81008	-0.070301	-1.301743
H	-2.215708	1.628681	-1.037345
H	-1.415298	0.520717	-2.223247
C	1.465016	-1.996239	2.31073
H	2.066059	-1.336957	2.963164
H	0.86415	-2.684704	2.930482
H	2.126573	-2.620821	1.688615
N	-1.027671	0.030063	-0.244236
N	0.564368	-1.251311	1.43667
C	-0.172178	-4.655722	1.352103
C	-1.112129	-4.381337	2.38802
C	1.005345	-5.389634	1.667158
C	-0.870877	-4.820541	3.691022
H	-2.019585	-3.819542	2.14073
C	1.232331	-5.827373	2.974372
H	1.730587	-5.606211	0.873775
C	0.303414	-5.541779	3.994272
H	-1.601377	-4.608722	4.478725
H	2.13904	-6.396555	3.204614
H	0.487474	-5.885661	5.016757
Cu	-0.454293	-1.937746	-0.190135

```
N     0.157018    -2.121156    -2.079284
H    -0.495001    -2.657067    -2.673624
C     0.914459    -1.25405     -2.792
C     0.821174    -1.131954    -4.222397
C     1.846415    -0.412564    -2.090506
C     1.613025    -0.210336    -4.89996
H     0.115238    -1.77111     -4.765816
C     2.62779      0.503882    -2.78311
H     1.916358    -0.5271      -1.002775
C     2.517503     0.612474    -4.189659
H     1.535223    -0.120913    -5.988205
H     3.337318     1.139526    -2.243352
H     3.138447     1.333133    -4.731011
N    -0.416087    -4.161631     0.08327
H     0.227154    -4.513895    -0.636518
O    -2.28623     -2.779047    -0.633088
H    -1.558518    -3.711591    -0.277521
H    -2.976455    -2.627407     0.047722
```

Intermediate VI.1

```
1 3
C    -0.520325     0.731073     0.719192
H    -0.736229     1.802284     0.86154
C     0.387417     0.024795     1.630983
H     0.896471     0.572212     2.439484
C    -1.923229     0.581941    -1.243669
H    -2.80908     -0.072301    -1.301743
H    -2.215708     1.627681    -1.036345
H    -1.415298     0.520717    -2.223247
C     1.465016    -1.996239     2.31073
H     2.066059    -1.336957     2.963164
H     0.86415     -2.684704     2.930482
H     2.126573    -2.620821     1.688615
N    -1.027671     0.030063    -0.244236
N     0.565368    -1.251311     1.43567
C    -0.173178    -4.656722     1.355103
C    -1.112129    -4.381337     2.38802
C     1.004345    -5.388634     1.666158
C    -0.870877    -4.820541     3.691022
H    -2.019585    -3.819542     2.14073
C     1.232331    -5.827373     2.974372
H     1.729587    -5.606211     0.872775
C     0.303414    -5.541779     3.994272
```

H	-1.601377	-4.608722	4.478725
H	2.13904	-6.396555	3.203614
H	0.487474	-5.885661	5.016757
Cu	-0.455293	-1.937746	-0.190135
N	0.158018	-2.121156	-2.079284
H	-0.498001	-2.655067	-2.672624
C	0.914459	-1.25405	-2.792
C	0.821174	-1.131954	-4.222397
C	1.846415	-0.412564	-2.090506
C	1.613025	-0.210336	-4.89996
H	0.115238	-1.77111	-4.765816
C	2.62779	0.503882	-2.78311
H	1.916358	-0.5271	-1.002775
C	2.517503	0.612474	-4.189659
H	1.535223	-0.120913	-5.988205
H	3.337318	1.139526	-2.243352
H	3.138447	1.333133	-4.731011
N	-0.415087	-4.160631	0.08227
H	0.216154	-4.515895	-0.645518
O	-2.28623	-2.774047	-0.634088
H	-1.489518	-3.775591	-0.251521
H	-2.974455	-2.613407	0.046722

Intermediate VI.2

1 3			
C	-0.280661	0.647977	0.310215
H	-0.262618	1.745439	0.219858
C	0.604695	-0.031264	1.260996
H	1.233957	0.556603	1.947082
C	-1.898511	0.45865	-1.452603
H	-2.942623	0.152037	-1.271897
H	-1.836751	1.56081	-1.504043
H	-1.584509	0.021604	-2.416793
C	1.486064	-2.055487	2.167228
H	2.135904	-1.381856	2.754687
H	0.853299	-2.654063	2.845641
H	2.100191	-2.768429	1.592603
N	-1.050068	-0.101815	-0.414092
N	0.62276	-1.330736	1.242621
C	-0.228835	-4.721926	1.534901
C	-1.179574	-4.453454	2.542527
C	0.970979	-5.390214	1.849477
C	-0.921986	-4.852292	3.860148

H	-2.102387	-3.921662	2.282926
C	1.219447	-5.783148	3.172559
H	1.702951	-5.60287	1.060871
C	0.279436	-5.512498	4.181832
H	-1.66157	-4.647067	4.640937
H	2.14909	-6.308799	3.413492
H	0.476857	-5.820972	5.213112
Cu	-0.631527	-2.106949	-0.182461
N	0.374875	-2.32096	-2.027555
H	-0.372592	-2.726673	-2.619356
C	0.97066	-1.279447	-2.661751
C	0.600763	-0.846022	-3.983692
C	2.020375	-0.568816	-1.982308
C	1.246477	0.233831	-4.579605
H	-0.194033	-1.385654	-4.513008
C	2.654842	0.508316	-2.590709
H	2.307922	-0.918217	-0.985356
C	2.272602	0.918741	-3.88971
H	0.960939	0.5529	-5.587301
H	3.461984	1.035637	-2.071208
H	2.778655	1.764764	-4.36545
N	-0.458196	-4.221908	0.221051
H	0.20775	-4.573597	-0.478497
O	-2.20909	-2.77311	-1.040391
H	-1.428195	-4.32647	-0.133096
H	-2.968655	-2.16813	-0.904679
O	1.18444513	-4.17523395	-1.72149274
H	1.66525833	-4.85862738	-2.19413646
H	1.26317995	-3.34310583	-2.19368297

Intermediate VI.3

1 3

C	-0.011378	0.554191	-0.037342
H	0.037855	1.644623	-0.189865
C	1.125685	-0.147704	0.578562
H	1.99743	0.42615	0.926878
C	-2.18355	0.441928	-1.034391
H	-3.085713	0.204965	-0.44288
H	-2.094405	1.537836	-1.150339
H	-2.301456	-0.022995	-2.028822
C	2.174401	-2.178385	1.272153
H	3.017714	-1.519773	1.547538
H	1.80492	-2.710588	2.165902

H	2.487997	-2.947385	0.536568
N	-1.029841	-0.159815	-0.386116
N	1.063353	-1.43842	0.693807
C	-0.294589	-4.743263	1.537135
C	-1.573425	-4.74201	2.172954
C	0.865742	-5.063104	2.302624
C	-1.676818	-5.032765	3.532314
H	-2.454796	-4.483979	1.57449
C	0.74352	-5.361355	3.66049
H	1.832865	-5.115979	1.792038
C	-0.522479	-5.339762	4.284392
H	-2.658344	-5.024574	4.017827
H	1.632822	-5.630262	4.239871
H	-0.610376	-5.572669	5.350256
Cu	-0.522188	-2.237965	-0.254116
N	0.538363	-2.516739	-2.165321
H	-0.284095	-2.896089	-2.65613
C	1.009739	-1.30776	-2.668491
C	0.212532	-0.501971	-3.524538
C	2.289672	-0.844686	-2.258931
C	0.682513	0.74334	-3.948241
H	-0.766973	-0.872352	-3.849675
C	2.749367	0.401194	-2.694055
H	2.905194	-1.492887	-1.626436
C	1.948199	1.204834	-3.531335
H	0.068722	1.357492	-4.615237
H	3.743913	0.747339	-2.393688
H	2.315484	2.178203	-3.871345
N	-0.162628	-4.426739	0.196403
H	0.95493	-4.499085	-0.402966
O	-2.05053	-2.965426	-1.048357
H	-1.028918	-4.594047	-0.339922
H	-2.791504	-2.32253	-1.036922
O	2.012518	-4.235658	-1.013594
H	2.343298	-5.010081	-1.512765
H	1.279811	-3.296144	-1.801334

Intermediate VI.4

1 3			
C	-0.974209	0.624088	-0.300932
H	-1.126604	1.695013	-0.505968
C	0.350691	0.129878	0.112806
H	1.218169	0.807372	0.108206

C	-3.256481	0.076889	-0.838967
H	-3.96688	-0.439754	-0.175941
H	-3.436988	1.166744	-0.861624
H	-3.415525	-0.351279	-1.846883
C	1.7209	-1.709887	0.798612
H	2.545656	-0.974879	0.805726
H	1.632773	-2.195768	1.785475
H	1.941302	-2.503323	0.063556
N	-1.91341	-0.259392	-0.40914
N	0.439191	-1.118854	0.447885
N	-0.34493383	-3.88562448	0.25922985
C	0.03465117	-4.46732848	1.42408585
C	-0.14372083	-3.75058548	2.65651385
C	0.60984917	-5.78475848	1.46828385
C	0.25236617	-4.32033348	3.86115485
H	-0.61818583	-2.76288148	2.62207585
C	0.99925617	-6.33820548	2.68323485
H	0.74252117	-6.34339048	0.53401385
C	0.82789917	-5.61246648	3.88497885
H	0.10649817	-3.77148148	4.79689785
H	1.43792117	-7.34069148	2.70894485
H	1.13263617	-6.05608048	4.83790485
Cu	-1.41120375	-2.16960883	-0.27948703
N	-0.587766	-2.064286	-2.418015
H	-1.541847	-1.92835	-2.770794
H	-0.275531	-3.004402	-2.677402
C	0.330943	-1.047025	-2.789846
C	-0.130072	0.241911	-3.138863
C	1.71853	-1.280892	-2.686062
C	0.789822	1.274452	-3.390682
H	-1.206097	0.423156	-3.24388
C	2.626646	-0.2448	-2.939431
H	2.08183	-2.280101	-2.4166
C	2.169032	1.039571	-3.287732
H	0.419135	2.263774	-3.679091
H	3.701397	-0.443849	-2.871095
H	2.883451	1.842902	-3.4915
O	-3.02935775	-2.8737386	-0.18961513
H	-0.24339883	-4.52058448	-0.54453515
H	-3.02523175	-3.8358046	-0.01812313

Intermediate VI.5

13

C	-0.093091	0.298629	-0.348534
H	-0.081261	1.39588	-0.402593
C	1.153447	-0.440694	-0.100518
H	2.082961	0.108231	0.109826
C	-2.429501	0.187081	-0.88973
H	-2.790286	-0.32468	-1.797835
H	-3.153655	-0.036129	-0.090089
H	-2.359079	1.278903	-1.044421
C	2.318985	-2.527592	0.007887
H	2.183684	-3.215413	0.861187
H	2.479598	-3.140824	-0.897222
H	3.216352	-1.907227	0.188897
N	-1.157876	-0.410722	-0.532432
N	1.111536	-1.735315	-0.169955
N	-0.720549	-4.116398	0.168111
C	-1.699974	-4.624901	0.960266
C	-1.464959	-5.761364	1.808566
C	-2.99138	-3.991383	0.993478
C	-2.466074	-6.224373	2.655012
H	-0.483036	-6.249322	1.787192
C	-3.980563	-4.475491	1.843189
H	-3.166102	-3.143604	0.320264
C	-3.727769	-5.585515	2.681454
H	-2.276583	-7.085589	3.303583
H	-4.962805	-3.992271	1.863127
H	-4.510861	-5.954576	3.351225
Cu	-0.735894	-2.399948	-0.770343
N	0.142637	-1.91146	-2.969458
H	-0.822133	-2.16387	-3.239078
H	0.817381	-2.63587	-3.227942
C	0.542512	-0.58784	-3.239842
C	-0.411826	0.382769	-3.620028
C	1.882469	-0.191724	-3.018567
C	-0.027718	1.720153	-3.776552
H	-1.448042	0.076266	-3.799229
C	2.258628	1.1498	-3.19185
H	2.62679	-0.943244	-2.728686
C	1.30682	2.11313	-3.562689
H	-0.774348	2.459881	-4.084443
H	3.303674	1.439464	-3.038252
H	1.603037	3.157749	-3.699037

O	-2.309519	-2.660436	-1.820628
H	0.155988	-4.65283	0.247609
H	-2.488428	-3.623849	-1.887107

Intermediate VII

1 3

C	-0.375414	0.732638	-0.652982
H	-0.401806	1.747584	-1.076758
C	0.880933	0.182532	-0.130591
H	1.782667	0.808714	-0.07937
C	-2.701481	0.348625	-1.128173
H	-3.098523	-0.51426	-1.690619
H	-3.384959	0.51341	-0.274432
H	-2.652708	1.258706	-1.753703
C	2.086987	-1.702007	0.719723
H	1.886303	-2.192149	1.687159
H	2.378645	-2.484049	-0.005889
H	2.926449	-0.993862	0.844587
N	-1.408751	-0.045305	-0.605336
N	0.87095	-1.059442	0.249305
N	-0.6124	-3.583235	1.035315
C	-1.62377	-4.56465	1.164848
C	-1.339289	-5.948162	1.080739
C	-2.954978	-4.136291	1.399281
C	-2.374475	-6.882498	1.202425
H	-0.308432	-6.283063	0.911955
C	-3.979668	-5.078928	1.532519
H	-3.159719	-3.061255	1.453322
C	-3.695422	-6.453861	1.43061
H	-2.150485	-7.951096	1.123587
H	-5.005891	-4.7421	1.711375
H	-4.500213	-7.188775	1.530648
Cu	-0.880986	-1.983488	-0.209068
N	0.136506	-2.191228	-2.411515
H	-0.807192	-2.597054	-2.554885
H	0.881448	-2.891125	-2.401885
C	0.429842	-0.986056	-3.066426
C	-0.593958	-0.263828	-3.724214
C	1.725283	-0.421675	-2.973662
C	-0.317122	0.98763	-4.286139
H	-1.597135	-0.698643	-3.790329
C	1.992368	0.829975	-3.551364
H	2.520953	-0.978773	-2.463949

C	0.974766	1.542991	-4.204842
H	-1.113966	1.529452	-4.806809
H	3.004268	1.244843	-3.49159
H	1.186453	2.516171	-4.658367
O	-2.322407	-2.638912	-1.256702
H	0.304325	-4.037969	0.89431
H	-2.614917	-3.520085	-0.938609
C	0.826319	-0.297913	3.434111
C	0.914589	1.063916	3.141564
C	-0.205548	1.753312	2.627745
C	-1.417363	1.066143	2.422592
C	-1.504517	-0.30015	2.698347
C	-0.385803	-1.015127	3.218669
H	1.689075	-0.8264	3.856233
H	1.848397	1.604352	3.330763
H	-0.138905	2.825517	2.415114
H	-2.291951	1.601758	2.038137
H	-2.444933	-0.837588	2.52726
C	-0.471832	-2.448457	3.444735
H	-1.462605	-2.847901	3.719332
H	-0.453673	-2.985549	2.227957
H	0.351977	-2.91704	4.003048

Intermediate VIII (triplet)

1 3

C	0.160357	1.763343	0.89436
H	0.019273	2.637746	1.546621
C	1.498239	1.215608	0.676321
H	2.36757	1.658075	1.184055
C	-2.195903	1.622835	0.435976
H	-2.761366	0.898951	1.050589
H	-2.264982	2.619683	0.909393
H	-2.653644	1.643384	-0.567309
C	2.910496	-0.375794	-0.410568
H	3.686	-0.036992	0.300589
H	2.819537	-1.474297	-0.350455
H	3.217381	-0.104015	-1.435595
N	-0.827499	1.155808	0.31341
N	1.608949	0.216291	-0.149364
Cu	-0.19338	-0.398971	-0.830316
N	0.450274	-2.06973	-1.975348
H	-0.481358	-2.514291	-1.902253
H	1.159084	-2.655271	-1.517209

C	0.806307	-1.736406	-3.321811
C	-0.208527	-1.371067	-4.229187
C	2.160366	-1.674814	-3.701616
C	0.147442	-0.910786	-5.506081
H	-1.251457	-1.408646	-3.893822
C	2.503675	-1.204341	-4.979402
H	2.940556	-1.996358	-3.00194
C	1.50055	-0.80359	-5.877953
H	-0.637359	-0.617264	-6.211458
H	3.557403	-1.161597	-5.273936
H	1.765962	-0.419576	-6.867687
O	-1.882801	-1.080641	-1.389526
H	-2.544864	-0.886937	-0.69274
C	-0.348425	-1.138331	2.288187
C	0.702376	-0.479443	3.006483
C	0.414397	0.395228	4.05921
C	-0.921695	0.645779	4.428367
C	-1.973122	-0.005427	3.745102
C	-1.697667	-0.881669	2.696983
H	1.742066	-0.69842	2.73797
H	1.231716	0.877015	4.606835
H	-1.144347	1.328325	5.254684
H	-3.010525	0.169306	4.050299
H	-2.513088	-1.392183	2.170557
C	-0.066418	-1.96299	1.168329
H	0.968775	-2.260693	0.968178
H	-0.861165	-2.540985	0.685773
C	0.947823	2.291792	-2.365519
C	2.255493	2.080555	-2.849318
C	3.274307	2.988055	-2.529563
C	3.010217	4.118933	-1.734194
C	1.702357	4.345255	-1.276305
C	0.675115	3.437098	-1.582333
H	2.457249	1.211566	-3.488015
H	4.283906	2.817525	-2.91939
H	3.811156	4.824217	-1.492396
H	1.473027	5.238257	-0.684603
H	-0.3514	3.628813	-1.246633
N	-0.052948	1.310576	-2.568434
H	-1.01251	1.655738	-2.509132
H	0.068283	0.734797	-3.406701

Intermediate VIII (singlet)

1 1			
C	0.061703	1.670207	0.66604
H	-0.050536	2.595392	1.250711
C	1.387395	1.128549	0.381187
H	2.288583	1.631494	0.760609
C	-2.322084	1.441918	0.440277
H	-2.812452	0.701506	1.098234
H	-2.372818	2.435076	0.922365
H	-2.859741	1.46546	-0.522642
C	2.726875	-0.556683	-0.677599
H	3.581593	-0.00195	-0.250185
H	2.74338	-1.595116	-0.300415
H	2.821611	-0.603178	-1.776498
N	-0.955746	1.007156	0.20394
N	1.44451	0.045843	-0.345421
Cu	-0.370346	-0.765689	-0.636799
N	0.216166	-2.339922	-1.970893
H	-0.75726	-2.690304	-2.011682
H	0.830351	-3.064652	-1.580679
C	0.683815	-1.830121	-3.230032
C	-0.164895	-0.978738	-3.967536
C	1.981409	-2.124367	-3.689697
C	0.294709	-0.427295	-5.169695
H	-1.167775	-0.765211	-3.579023
C	2.431019	-1.561363	-4.894401
H	2.626924	-2.806952	-3.122983
C	1.592409	-0.711335	-5.634808
H	-0.364452	0.227537	-5.748754
H	3.435387	-1.799259	-5.259247
H	1.945538	-0.276824	-6.575137
O	-2.047089	-1.434531	-1.139462
H	-2.792659	-0.977567	-0.697004
C	-0.238385	-1.173131	2.351698
C	0.864298	-0.449623	2.908664
C	0.665249	0.486956	3.927318
C	-0.632499	0.73644	4.417234
C	-1.734457	0.027465	3.888631
C	-1.546238	-0.909613	2.874687
H	1.875792	-0.667018	2.547728
H	1.522276	1.017325	4.35608
H	-0.784639	1.466247	5.218837
H	-2.738815	0.207153	4.2865

H	-2.397123	-1.466489	2.464939
C	-0.053886	-2.091006	1.276491
H	0.960681	-2.435714	1.041758
H	-0.875369	-2.754959	0.983682
C	1.15172325	2.48166106	-2.5312447
C	2.54024274	2.34640265	-2.54503713
C	3.3429876	3.33400272	-1.97453862
C	2.75729446	4.4580981	-1.39093803
C	1.36911943	4.59348421	-1.37760688
C	0.56623343	3.60501793	-1.94744754
H	3.0014941	1.46028097	-3.00468626
H	4.43741676	3.22715828	-1.9848149
H	3.39043623	5.23668296	-0.9412343
H	0.9072225	5.47929016	-0.91774466
H	-0.52811358	3.71186837	-1.93664755
N	0.30586189	1.44031027	-3.13208335
H	-0.53886287	1.85272641	-3.47318891
H	0.79576743	1.0089305	-3.88964791

Intermediate IX.1

1 1

C	-0.386083	0.444893	-0.306906
H	-0.639437	1.480731	-0.566049
C	0.974928	0.068798	0.078928
H	1.774662	0.820197	0.124394
C	-2.609729	-0.343149	-0.802536
H	-3.25991	-1.030393	-0.243473
H	-2.940278	0.70349	-0.688436
H	-2.656074	-0.636592	-1.866341
C	2.486713	-1.681448	0.74034
H	3.301008	-1.101992	0.268384
H	2.599001	-1.61767	1.838921
H	2.541137	-2.744591	0.45327
N	-1.245597	-0.523769	-0.345896
N	1.173166	-1.184254	0.363197
Cu	-0.414383	-2.309612	-0.054553
N	0.357582	-2.190072	-2.392402
H	-0.431072	-2.719726	-2.778145
H	1.201658	-2.768438	-2.356147
C	0.542634	-0.907431	-2.952778
C	-0.512614	-0.262293	-3.634992
C	1.755596	-0.210427	-2.740272
C	-0.356265	1.054459	-4.086369

281

H	-1.442668	-0.80778	-3.83391
C	1.905923	1.104626	-3.21216
H	2.588345	-0.716679	-2.237843
C	0.85002	1.747955	-3.874746
H	-1.178298	1.536653	-4.625859
H	2.859414	1.622421	-3.062526
H	0.969555	2.771743	-4.241981
O	-1.976085	-3.17919	-0.488929
H	-2.094863	-3.960812	0.095941
C	-0.18757714	-1.06050802	2.32732724
C	1.17478286	-0.93375802	2.66929724
C	1.82835386	0.30574698	2.60163224
C	1.12868386	1.45019998	2.17941224
C	-0.24320414	1.34811598	1.87164524
C	-0.89021214	0.10852998	1.95150524
H	1.71921386	-1.82319202	3.00214524
H	2.88467786	0.38208098	2.88496724
H	1.63320186	2.42153598	2.13361524
H	-0.80756914	2.24158398	1.58222524
H	-1.95888914	0.03649398	1.71664924
C	-0.87414414	-2.40691502	2.33399224
H	-0.30689114	-3.15340602	2.91560424
H	-1.89600514	-2.34304202	2.74687024

Intermediate IX.2

1 1

C	-1.030884	0.933806	-1.518682
H	-1.68015	1.478244	-2.215057
C	0.415848	1.109643	-1.509093
H	0.930235	1.74287	-2.24202
C	-2.904985	-0.217021	-0.485649
H	-3.179319	-0.106549	0.575322
H	-3.530732	0.433905	-1.120879
H	-3.060938	-1.277066	-0.746844
C	2.501788	0.437517	-0.488243
H	2.968165	0.485666	-1.487995
H	2.808553	1.310383	0.113916
H	2.796867	-0.479256	0.047279
N	-1.498035	0.102886	-0.632445
N	1.05387	0.432582	-0.598842
Cu	-0.111231	-0.775952	0.37148
H	-0.777502	-2.46965	1.696037
H	1.243922	-1.29126	2.152142

O	-1.325779	-1.773349	1.26245
O	1.258528	-1.621559	1.223814
N	0.187259	-2.207171	-1.681668
H	-0.687611	-2.729246	-1.583373
H	0.980195	-2.745855	-1.320909
C	0.388808	-1.556472	-2.909443
C	1.698295	-1.292647	-3.377482
C	-0.718166	-1.047517	-3.634046
C	1.887927	-0.552923	-4.551067
H	2.559287	-1.69349	-2.829706
C	-0.512489	-0.315916	-4.816817
H	-1.735632	-1.269155	-3.290427
C	0.786679	-0.057549	-5.276632
H	2.906199	-0.374827	-4.912579
H	-1.379087	0.044565	-5.381053
H	0.944431	0.508822	-6.199321
C	-0.159866	1.7817	2.369114
C	-1.358443	2.189551	1.740738
C	-1.351221	3.166651	0.73575
C	-0.138139	3.756441	0.330653
C	1.060393	3.378221	0.963484
C	1.046478	2.398152	1.967637
H	-2.305348	1.739136	2.061395
H	-2.294226	3.479938	0.273252
H	-0.133178	4.534338	-0.44058
H	2.00435	3.858921	0.68261
H	1.981589	2.113526	2.465194
C	-0.191338	0.743531	3.469737
H	-0.693256	1.13863	4.372278
H	-1.10615635	-1.14676026	1.99223846
H	0.826501	0.439198	3.772569

A.2 Input Coordinates for Transition states

Transition State TS(II)

1 1			
C	0.539058	0.9413	1.28529
H	-0.106516	1.821794	1.43936
C	1.822623	0.850896	1.997247
H	2.138766	1.670665	2.661884
C	-1.073626	-0.065159	-0.16909
H	-1.628529	-0.957782	0.173642
H	-1.679084	0.843443	0.009971

H	-0.888752	-0.193484	-1.249685
C	3.807741	-0.3681	2.546446
H	4.029904	0.482327	3.21779
H	3.766902	-1.303207	3.131879
H	4.621595	-0.47895	1.808937
N	0.207951	-0.048573	0.516529
N	2.544362	-0.219683	1.828192
N	0.764612	-3.202683	1.246819
N	1.17017374	-4.91772095	0.34428673
N	1.57853074	-5.82391595	-0.24986127
C	-0.57038	-2.999107	1.758957
C	-0.69898	-2.055841	2.791689
C	-1.693406	-3.637999	1.205481
C	-1.977282	-1.745378	3.275205
H	0.200646	-1.576636	3.190207
C	-2.966084	-3.322097	1.705701
H	-1.577765	-4.362757	0.392058
C	-3.111974	-2.375266	2.73442
H	-2.086264	-1.014719	4.083182
H	-3.846694	-3.816612	1.283393
H	-4.108285	-2.132627	3.116653
Cu	1.741303	-1.488387	0.49897
N	2.35794	-2.178477	-1.323538
H	2.558998	-3.190535	-1.320885
H	3.227966	-1.714475	-1.61963
C	1.275249	-1.877884	-2.252377
C	1.263208	-0.649291	-2.933555
C	0.215306	-2.788252	-2.40022
C	0.180384	-0.334056	-3.769925
H	2.091069	0.058283	-2.805855
C	-0.863755	-2.461701	-3.235982
H	0.241488	-3.752539	-1.880567
C	-0.887315	-1.235674	-3.921461
H	0.176501	0.619783	-4.307224
H	-1.683889	-3.17651	-3.358679
H	-1.727993	-0.987315	-4.576386

Transition State TS(IV)

1 3			
C	-0.884451	0.643227	0.107571
H	-1.195777	1.697931	0.143789
C	0.408273	0.22456	0.645841
H	1.083149	0.960098	1.112051

C	-2.956545	0.039669	-0.96006
H	-3.731401	-0.480173	-0.370766
H	-3.159553	1.125866	-0.966635
H	-3.010139	-0.352661	-1.99074
C	1.978725	-1.559244	0.99725
H	2.576813	-0.815945	1.556842
H	1.78918	-2.442718	1.632025
H	2.540613	-1.905944	0.110556
N	-1.647504	-0.286932	-0.401237
N	0.704679	-1.037108	0.538333
N	-1.027358	-3.824177	0.240133
C	-0.505323	-4.405343	1.329576
C	-0.346555	-3.717223	2.593912
C	-0.099301	-5.792896	1.259111
C	0.188854	-4.370486	3.69676
H	-0.681986	-2.674429	2.64238
C	0.437939	-6.43369	2.371268
H	-0.214449	-6.304364	0.296955
C	0.58015	-5.727434	3.586699
H	0.297542	-3.850598	4.654334
H	0.748356	-7.48179	2.311351
H	0.993143	-6.239573	4.462564
Cu	-0.903015	-2.096974	-0.265779
N	-0.332831	-2.451896	-2.323946
H	-0.813643	-1.783005	-2.937034
H	-0.654132	-3.439145	-2.514043
C	1.09097	-2.322445	-2.388041
C	1.68291	-1.059834	-2.595916
C	1.897308	-3.45673	-2.156817
C	3.079368	-0.935628	-2.58682
H	1.046425	-0.181737	-2.76015
C	3.292718	-3.319654	-2.152767
H	1.418621	-4.429737	-2.002513
C	3.890516	-2.063001	-2.365185
H	3.53602	0.044579	-2.75965
H	3.918576	-4.203242	-1.989037
H	4.980538	-1.964231	-2.363391
O	-1.12421899	-4.91859006	-2.32193017
H	-1.1082476	-5.02878752	-0.61935188
H	-1.60956701	-5.76288194	-2.22299383

Transition State TS(V)

1 3			
C	-0.557037	1.171853	0.489636
H	-0.766124	2.25359	0.442435
C	0.606268	0.745906	1.284491
H	1.295893	1.547267	1.615675
C	-2.489809	0.868753	-0.865087
H	-3.401612	0.463993	-0.393434
H	-2.520234	1.972694	-0.848712
H	-2.471298	0.483713	-1.895558
C	1.946751	-0.868354	2.354924
H	1.60615	-1.224376	3.345778
H	2.437398	-1.724554	1.859239
H	2.677039	-0.047362	2.498195
N	-1.328913	0.33803	-0.139385
N	0.78026	-0.496188	1.574416
N	-1.224754	-3.396398	0.188901
C	-0.354577	-4.203996	0.861982
C	0.26838	-3.72518	2.056433
C	-0.025439	-5.517866	0.389316
C	1.192748	-4.515945	2.73496
H	-0.024107	-2.733646	2.4106
C	0.895468	-6.299598	1.082664
H	-0.487827	-5.876514	-0.537512
C	1.511432	-5.802968	2.253836
H	1.663057	-4.14446	3.651255
H	1.145875	-7.300873	0.717518
H	2.230745	-6.425786	2.795441
Cu	-1.012722	-1.593323	-0.216312
N	0.471073	-1.623441	-1.609747
H	0.14409637	-2.70272077	-2.48975701
O	-0.886133	-3.730168	-2.70368
H	-1.588116	-3.896804	-0.6397
H	-0.69816	-3.938498	-3.641191
C	1.744991	-1.819168	-1.104776
C	2.692458	-0.759482	-0.952696
C	2.148572	-3.146102	-0.761933
C	3.974661	-1.020553	-0.473766
H	2.392177	0.262436	-1.214305
C	3.425835	-3.391179	-0.25359
H	1.454944	-3.965698	-0.958122
C	4.343857	-2.334099	-0.102888
H	4.696633	-0.203323	-0.373691

H	3.714078	-4.414578	0.007682
H	5.348752	-2.529074	0.28499
H	0.396152	-0.662191	-1.981716
O	-2.666285	-1.865679	-1.963226
H	-2.01438903	-2.93787285	-2.66558387
H	-3.465327	-2.291189	-1.590931

Transition State TS(VI.2)

1 3

C	0.029805	0.451861	0.054038
H	0.033996	1.548842	-0.045349
C	1.157883	-0.232987	0.700966
H	1.995703	0.352486	1.109046
C	-2.087233	0.297289	-1.055606
H	-3.002711	0.000148	-0.514301
H	-2.034611	1.399605	-1.114607
H	-2.14075	-0.118952	-2.076548
C	2.20758	-2.270002	1.383158
H	3.010138	-1.609311	1.757976
H	1.79231	-2.868718	2.212872
H	2.600302	-2.980492	0.630174
N	-0.93713	-0.286896	-0.383485
N	1.117901	-1.52729	0.769935
C	-0.316888	-4.690623	1.60563
C	-1.567583	-4.472711	2.224466
C	0.772532	-5.188475	2.351466
C	-1.721518	-4.755362	3.586403
H	-2.393965	-4.077917	1.621901
C	0.605841	-5.463869	3.716294
H	1.729761	-5.378149	1.852978
C	-0.636685	-5.246483	4.337964
H	-2.691951	-4.592303	4.066399
H	1.446536	-5.863011	4.2931
H	-0.762176	-5.465591	5.40295
Cu	-0.455637	-2.317565	-0.24845
N	0.55102	-2.471403	-2.247089
H	-0.31432	-2.805472	-2.707113
C	0.935645	-1.255031	-2.733562
C	0.160587	-0.497142	-3.674458
C	2.169356	-0.6948	-2.259721
C	0.589043	0.761145	-4.091907
H	-0.770497	-0.929753	-4.06038
C	2.587544	0.56248	-2.689837

H	2.776645	-1.299747	-1.578308
C	1.797479	1.302822	-3.598402
H	-0.007565	1.329586	-4.813068
H	3.539113	0.973518	-2.336183
H	2.131004	2.289534	-3.935077
N	-0.155664	-4.361639	0.227966
H	1.06129427	-4.89721074	-0.34385502
O	-2.011416	-3.012809	-1.060706
H	-0.948946	-4.666952	-0.357271
H	-2.708048	-2.33049	-1.163465
O	2.289523	-4.236846	-1.078367
H	2.732765	-4.841964	-1.706027
H	1.55954	-3.38870066	-2.11649314

Transition State TS(VII)

1 3			
C	-0.392053	0.423401	-0.508895
H	-0.435191	1.506652	-0.694364
C	0.86289	-0.199888	-0.074635
H	1.738365	0.42473	0.149132
C	-2.688055	0.116396	-1.14685
H	-3.049396	-0.593294	-1.910244
H	-3.404648	0.07236	-0.306016
H	-2.639037	1.146939	-1.543882
C	2.13382	-2.16116	0.378837
H	2.494009	-1.801486	1.358945
H	1.969748	-3.246972	0.438923
H	2.913023	-1.970803	-0.382457
N	-1.403726	-0.364842	-0.677752
N	0.886294	-1.496189	0.010548
N	-0.773501	-4.015612	0.347234
C	-1.77063	-4.673187	0.990904
C	-1.506752	-5.841767	1.787326
C	-3.120744	-4.181298	0.912643
C	-2.539643	-6.475022	2.46909
H	-0.479821	-6.220584	1.853161
C	-4.139125	-4.832176	1.600512
H	-3.312912	-3.302693	0.285939
C	-3.86048	-5.976267	2.383088
H	-2.329456	-7.362028	3.075134
H	-5.164532	-4.454046	1.537056
H	-4.668287	-6.47815	2.924861
Cu	-0.864059	-2.332502	-0.634284

N	0.181395	-1.945421	-2.855782
H	-0.762676	-2.265894	-3.126328
H	0.897301	-2.664478	-2.977106
C	0.549676	-0.638108	-3.199519
C	-0.416152	0.27368	-3.688875
C	1.866372	-0.179908	-2.950619
C	-0.063409	1.606339	-3.932223
H	-1.435618	-0.078316	-3.881515
C	2.209593	1.156766	-3.206533
H	2.62084	-0.884054	-2.579488
C	1.248443	2.057852	-3.692224
H	-0.816604	2.296618	-4.326991
H	3.237066	1.491455	-3.028128
H	1.519758	3.098306	-3.895449
O	-2.305242	-2.776477	-1.808668
H	0.142886	-4.451721	0.522422
H	-2.415381	-3.751994	-1.831276
C	0.74975563	-0.08878445	3.19991238
C	0.43285963	1.25105055	2.92360238
C	-0.85875137	1.59370255	2.47853838
C	-1.81858437	0.58448655	2.30357838
C	-1.48664237	-0.75631045	2.54897038
C	-0.20078037	-1.11326745	3.00860438
H	1.74352063	-0.34267445	3.59009338
H	1.18193463	2.03362055	3.08856138
H	-1.11788437	2.64227555	2.29547638
H	-2.83108537	0.84036855	1.97260038
H	-2.24100437	-1.53825245	2.40267238
C	0.15495563	-2.55518545	3.29801538
H	-0.53417929	-3.00722161	4.03072044
H	-0.2274607	-3.36752764	1.83520074
H	1.18229922	-2.64561852	3.69240468

Transition State TS(IX)

1 1			
C	-0.906331	1.015013	-2.053068
H	-1.481223	1.202863	-2.972345
C	0.433784	1.614065	-1.901521
H	0.792273	2.294109	-2.694998
C	-2.711715	-0.336783	-1.210132
H	-3.352648	0.039292	-0.393775
H	-3.188845	-0.134382	-2.184527
H	-2.597126	-1.424088	-1.067248

289

C	2.409606	1.911387	-0.606651
H	2.77454	2.553594	-1.432385
H	2.341706	2.503852	0.324626
H	3.133293	1.100009	-0.409113
N	-1.393994	0.28209	-1.101512
N	1.10867	1.321501	-0.844215
Cu	-0.190526	-0.28314	0.306605
H	-0.121052	-2.724456	1.334333
H	0.26793222	-0.39466313	2.50912196
O	-0.613389	-3.371171	0.740134
O	0.34680022	-0.76595513	1.60660096
N	0.698435	-1.753907	-1.061848
H	0.314881	-2.591302	-0.549894
H	1.690659	-1.626413	-0.829069
C	0.418836	-1.746186	-2.453494
C	1.202327	-0.981984	-3.345969
C	-0.712253	-2.440907	-2.934014
C	0.849595	-0.910486	-4.703396
H	2.093977	-0.463079	-2.976674
C	-1.058336	-2.357405	-4.288771
H	-1.294541	-3.060503	-2.242633
C	-0.286384	-1.586204	-5.177925
H	1.472501	-0.329998	-5.392067
H	-1.928592	-2.910813	-4.657059
H	-0.558392	-1.530149	-6.236504
C	0.05789378	1.58645213	1.81196104
C	-0.27105522	2.71149613	1.00781204
C	0.45882478	3.89868513	1.10576404
C	1.53741978	3.98989813	2.00830204
C	1.88106678	2.88418013	2.81102704
C	1.15355978	1.69406113	2.71061604
H	-1.11105622	2.63362913	0.30771904
H	0.18597978	4.76215313	0.49020504
H	2.10502678	4.92257113	2.09042304
H	2.71347578	2.95746213	3.51832404
H	1.42226278	0.83566513	3.33675004
C	-0.70989822	0.35015913	1.70292004
H	-1.72319522	0.45645613	1.29049004
H	-0.355413	-4.264706	1.043974
H	-0.69580722	-0.31955887	2.57451604

Bibliography

[1]   K. Gupta and A. K. Sutar, *Coord. Chem. Rev.*, 2008, **252**, 1420–1450, doi: 10.1016/j.ccr.2007.09.005.

[2]   I. Kostova and L. Saso, *Curr. Med. Chem.*, 2013, **20**, 4609–4632, doi: 10.2174/09298673113209990149.

[3]   S. R. Collinson and D. E. Fenton, *Coord. Chem. Rev.*, 1996, **148**, 19–40, doi: 10.1016/0010-8545(95)01156-0.

[4]   B. Champin, P. Mobian, J.-P. Sauvage, Y. Luo, K. Beverly, J. Sampaio, F. M. Raymo, J. F. Stoddart, J. R. Heath, N. Spencer, J. F. Stoddart, M. Venturi, S. Wenger, A. J. P. White and D. J. Williams, *Chem. Soc. Rev.*, 2007, **36**, 358–366, doi: 10.1039/B604484K.

[5]   Z. Gonda, S. Kovács, C. Wéber, T. Gáti, A. Mészáros, A. Kotschy and Z. Novák, *Org. Lett.*, 2014, **16**, 4268–4271, doi: 10.1021/ol501967c.

[6]   B. L. Tran, B. Li, M. Driess and J. F. Hartwig, *J. Am. Chem. Soc.*, 2014, **136**, 2555–2563, doi: 10.1021/ja411912p.

[7]   D.-L. Mo and L. L. Anderson, *Angew. Chem., Int. Ed.*, 2013, **52**, 6722–6725, doi: 10.1002/anie.201301963.

[8]   J. E. Steves and S. S. Stahl, *J. Am. Chem. Soc.*, 2013, **135**, 15742–15745, doi: 10.1021/ja409241h.

[9]   Y.-F. Wang, H. Chen, X. Zhu and S. Chiba, *J. Am. Chem. Soc.*, 2012, **134**, 11980–11983, doi: 10.1021/ja305833a.

[10]   A. Lavie-Cambot, M. Cantuel, Y. Leydet, G. Jonusauskas, D. M. Bassani and N. D. McClenaghan, *Coord. Chem. Rev.*, 2008, **252**, 2572–2584, doi: 10.1016/j.ccr.2008.03.013.

[11]   N. Armaroli, V. Balzani, J.-P. Collin, P. Gaviña, J.-P. Sauvage, B. Ventura, L. Hammarström, J.-F. Nierengarten, V. Vicinelli and V. Balzani, *Chem. Soc. Rev.*, 2001, **30**, 113–124, doi: 10.1039/b000703j.

[12] O. Horváth, *Coord. Chem. Rev.*, 1994, **135-136**, 303–324, doi: 10.1016/0010-8545(94)80071-5.

[13] A. Kaeser, M. Mohankumar, J. Mohanraj, F. Monti, M. Holler, J.-J. Cid, O. Moudam, I. Nierengarten, L. Karmazin-Brelot, C. Duhayon, B. Delavaux-Nicot, N. Armaroli and J.-F. Nierengarten, *Inorg. Chem.*, 2013, **52**, 12140–12151, doi: 10.1021/ic4020042.

[14] I. Andrés-Tomé, J. Fyson, F. Baiao Dias, A. P. Monkman, G. Iacobellis and P. Coppo, *Dalton Trans.*, 2012, **41**, 8669–8674, doi: 10.1039/c2dt30698k.

[15] H. tom Dieck and I. W. Renk, *Chem. Ber.*, 1971, **104**, 92–109, doi: 10.1002/cber.19711040115.

[16] H. Ayranci, C. Daul, M. Zobrist and A. V. Zelewsky, *Helv. Chim. Acta*, 1975, **58**, 1732–1735, doi: 10.1002/Hlca.19750580626.

[17] H. tom Dieck and L. Stamp, *Z. Naturforsch. B.*, 1990, **45**, 1369–1382, doi: 10.1515/znb-1990-1005.

[18] L. Stamp and H. tom Dieck, *Inorg. Chim. Acta*, 1987, **129**, 107–114, doi: 10.1016/S0020-1693(00)85911-3.

[19] P. Krumholz, *J. Am. Chem. Soc.*, 1953, **75**, 2163–2166, doi: 10.1021/ja01105a043.

[20] A. Vlček, *Coord. Chem. Rev.*, 2002, **230**, 225–242, doi: 10.1016/S0010-8545(02)00047-4.

[21] G. van Koten and K. Vrieze, *Adv. Organomet. Chem.*, 1982, **21**, 151–239, doi: 10.1016/S0065-3055(08)60380-9.

[22] H. van der Poel, G. van Koten and K. Vrieze, *Inorg. Chem.*, 1980, **19**, 1145–1151, doi: 10.1021/ic50207a008.

[23] H. van der Poel, G. van Koten, K. Vrieze, M. Kokkes and C. H. Stam, *Inorg. Chim. Acta*, 1980, **39**, 197–205, doi: 10.1016/S0020-1693(00)93655-7.

[24] H. Staal, J. Keijsper, G. van Koten, K. Vrieze, J. A. Cras and W. P. Bosman, *Inorg. Chem.*, 1981, **56**, 555–562, doi: 10.1021/ic50216a048.

[25] H. W. Frühauf, A. Landers, R. Goddard and C. Krüger, *Angew. Chem.*, 1978, **90**, 56–57, doi: 10.1017/CBO9781107415324.004.

[26] M. Lersch and M. Tilset, *Chem. Rev.*, 2005, **105**, 2471–2526, doi: 10.1021/cr030710y.

[27] G. Gerdes and P. Chen, *Organometallics*, 2004, **23**, 3031–3036, doi: 10.1021/om030685m.

[28]   S. D. Ittel, L. K. Johnson and M. Brookhart, *Chem. Rev.*, 2000, **100**, 1169–1203, doi: 10.1021/cr9804644.

[29]   L. K. Johnson, C. M. Killian and M. Brookhart, *J. Am. Chem. Soc.*, 1995, **117**, 6414–6415, doi: 10.1021/ja00128a054.

[30]   C. M. Killian, L. K. Johnson and M. Brookhart, *Organometallics*, 1997, **16**, 2005–2007, doi: 10.1021/om961057q.

[31]   G. J. P. Britovsek, V. C. Gibson, S. K. Spitzmesser, K. P. Tellmann, A. J. P. White, D. J. Williams, O. Müller, R. Herbst-Irmer, L. N. Markovskii, Y. G. Shermolovich, A. J. P. White and D. J. Williams, *Dalton Trans.*, 2002, **38**, 1159, doi: 10.1039/b106614p.

[32]   G. A. Grasa, A. C. Hillier and S. P. Nolan, *Org. Lett.*, 2001, **3**, 1077–1080, doi: 10.1021/ol015676t.

[33]   M. W. van Laren and C. J. Elsevier, *Angew. Chem., Int. Ed.*, 1999, **38**, 3715–3717, doi: 10.1002/(SICI)1521-3773(19991216)38:24<3715::AID-ANIE3715>3.0.CO;2-O.

[34]   S. Anga, K. Naktode, H. Adimulam, T. K. Panda, G. A. Molander, K. Takehira, P. G. Jones, M. Tamm, M. Hummert and H. Schumann, *Dalton Trans.*, 2014, **43**, 14876–14888, doi: 10.1039/C4DT02013H.

[35]   S. Anga, R. K. Kottalanka, T. Pal and T. K. Panda, *J. Mol. Struct.*, 2013, **1040**, 129–138, doi: 10.1016/j.molstruc.2013.02.037.

[36]   Y. Liu and L. Yang, *Chin. J. Chem.*, 2015, **33**, 473–478, doi: 10.1002/cjoc.201400787.

[37]   C. C. Lu, E. Bill, T. Weyhermüller, E. Bothe and K. Wieghardt, *J. Am. Chem. Soc.*, 2008, **130**, 3181–3197, doi: 10.1021/ja710663n.

[38]   P. Shejwalkar, N. P. Rath, E. B. Bauer, S. J. Hong, S. K. Kimb, C. Kim, P. Monne-Loccoz, D. P. Goldberg and J. L. Que, *Dalton Trans.*, 2011, **40**, 7617–7631, doi: 10.1039/c1dt10387c.

[39]   B. Moreau, J. Y. Wu and T. Ritter, *Org. Lett.*, 2009, **11**, 337–339, doi: 10.1021/ol802524r.

[40]   M. Wang, L. Chen, L. Sun, T. D. Jarvi, A. J. Esswein, J. J. H. Pijpers, D. G. Nocera, L. Spiccia, V. Artero and D. L. Lichtenberger, *Energy Environ. Sci.*, 2012, **5**, 6763–6778, doi: 10.1039/c2ee03309g.

[41]   B. D. Stubbert, J. C. Peters and H. B. Gray, *J. Am. Chem. Soc.*, 2011, **133**, 18070–18073, doi: 10.1021/ja2078015.

[42]   X. Tang, W.-H. Sun, T. Gao, J. Hou, J. Chen and W. Chen, *J. Organomet. Chem.*, 2005, **690**, 1570–1580, doi: 10.1016/j.jorganchem.2004.12.027.

[43] T. Irrgang, S. Keller, H. Maisel, W. Kretschmer and R. Kempe, *Eur. J. Inorg. Chem.*, 2007, 4221–4228, doi: 10.1002/ejic.200700322.

[44] W. Massa, S. Dehghanpour and K. Jahani, *Inorg. Chim. Acta*, 2009, **362**, 2872–2878, doi: 10.1016/j.ica.2009.01.008.

[45] S. Dehghanpour, N. Bouslimani, R. Welter and F. Mojahed, *Polyhedron*, 2007, **26**, 154–162, doi: 10.1016/j.poly.2006.08.011.

[46] D. M. Haddleton, D. J. Duncalf, D. Kukulj, M. C. Crossman, S. G. Jackson, S. A. F. Bon, A. J. Clark and A. J. Shooter, *Eur. J. Inorg. Chem.*, 1998, 1799–1806, doi: 10.1002/(SICI)1099-0682(199811)1998:11<1799::AID-EJIC1799>3.0.CO;2-6.

[47] B. Zelenay, R. Frutos-Pedreño, J. Markalain-Barta, E. Vega-Isa, A. J. P. White and S. Díez-González, *Eur. J. Inorg. Chem.*, 2016, 4649–4658, doi: 10.1002/ejic.201600620.

[48] B. R. Buckley and S. P. Neary, *Tetrahedron*, 2010, **66**, 7988–7994, doi: 10.1016/j.tet.2010.08.018.

[49] N. Ledoux, B. Allaert, S. Pattyn, H. van der Mierde, C. Vercaemst and F. Verpoort, *Chem. - Eur. J.*, 2006, **12**, 4654–4661, doi: 10.1002/chem.200600064.

[50] L. Jafarpour, E. D. Stevens and S. P. Nolan, *J. Organomet. Chem.*, 2000, **606**, 49–54, doi: 10.1016/S0022-328X(00)00260-6.

[51] O. Santoro, A. Collado, A. M. Z. Slawin, S. P. Nolan and C. S. J. Cazin, *Chem. Commun.*, 2013, **49**, 10483–10485, doi: 10.1039/c3cc45488f.

[52] M. Hu, J. Li and S. Q. Yao, *Org. Lett.*, 2008, **10**, 5529–5531, doi: 10.1021/ol802286g.

[53] F. Nourmohammadian and M. D. Gholami, *Helv. Chim. Acta*, 2012, **95**, 1548–1555, doi: 10.1002/hlca.201200080.

[54] S. Sen, N. N. Nair, T. Yamada, H. Kitagawa and P. K. Bharadwaj, *J. Am. Chem. Soc.*, 2012, **134**, 19432–19437, doi: 10.1021/Ja3076378.

[55] D. C. Rogness, N. A. Markina, J. P. Waldo and R. C. Larock, *J. Org. Chem.*, 2012, **77**, 2743–2755, doi: 10.1021/jo2025543.

[56] L. Annunziata, S. Pragliola, D. Pappalardo, C. Tedesco and C. Pellecchia, *Macromolecules*, 2011, **44**, 1934–1941, doi: 10.1021/ma1028455.

[57] S. S. Hindo, A. M. Mancino, J. J. Braymer, Y. Liu, S. Vivekanandan, A. Ramamoorthy and M. H. Lim, *J. Am. Chem. Soc.*, 2009, **131**, 16663–16665, doi: 10.1021/ja907045h.

[58] C. L. Foster, C. A. Kilner, M. Thornton-Pett and M. A. Halcrow, *Acta Crystallogr., C*, 2000, **56**, 319–320, doi: 10.1107/S0108270199015863.

[59] G. M. Sheldrick, *Acta Crystallogr., A*, 2008, **64**, 112–122, doi: 10.1107/S0108767307043930.

[60] L. Yang, D. R. Powell and R. P. Houser, *Dalton Trans.*, 2007, **0**, 955–964, doi: 10.1039/b617136b.

[61] A. Bondi, *J. Phys. Chem.*, 1964, **68**, 441–451, doi: 10.1021/j100785a001.

[62] M. Burke-Laing and M. Laing, *Acta Crystallogr., B*, 1976, **32**, 3216–3224, doi: 10.1107/S0567740876009989.

[63] A. Poater, B. Cosenza, A. Correa, S. Giudice, F. Ragone, V. Scarano and L. Cavallo, *Eur. J. Inorg. Chem.*, 2009, 1759–1766, doi: 10.1002/ejic.200801160.

[64] H. Clavier and S. P. Nolan, *Chem. Commun.*, 2010, **46**, 841–861, doi: 10.1039/b922984a.

[65] *SambVca*, www.molnac.unisa.it/OMtools/sambvca.php., (last accessed March 2017).

[66] T. Kern, U. Monkowius, M. Zabel and G. Knor, *Inorg. Chim. Acta*, 2011, **374**, 632–636, doi: 10.1016/j.ica.2011.02.042.

[67] G. C. van Stein, G. van Koten, K. Vrieze, C. Brevard and A. L. Spek, *J. Am. Chem. Soc.*, 1984, **106**, 4486–4492, doi: 10.1021/ja00328a031.

[68] M. Miles, G. Doyle, R. Cooney and R. Tobias, *Spectrochim. Acta Mol. Biomol. Spectrosc.*, 1969, **25**, 1515–1526, doi: 10.1016/0584-8539(69)80135-2.

[69] A. W. Addison, T. N. Rao, J. Reedijk, J. van Rijn and G. C. Verschoor, *Dalton Trans.*, 1984, 1349–1356, doi: 10.1039/DT9840001349.

[70] L. J. Carlson, J. Welby, K. A. Zebrowski, M. M. Wilk, R. Giroux, N. Ciancio, J. M. Tanski, A. Bradley and L. A. Tyler, *Inorg. Chim. Acta*, 2011, **365**, 159–166, doi: 10.1016/j.ica.2010.09.002.

[71] R. Papadakis, E. Rivière, M. Giorgi, H. Jamet, P. Rousselot-Pailley, M. Réglier, A. J. Simaan and T. Tron, *Inorg. Chem.*, 2013, **52**, 5824–5830, doi: 10.1021/ic3027545.

[72] J. Markalain Barta and S. Díez-González, *Molecules*, 2013, **18**, 8919–8928, doi: 10.3390/molecules18088919.

[73] M. A. Andrade, S. I. O'Donoghue and B. Rost, *J. Mol. Biol.*, 1998, **276**, 517–525, doi: 10.1006/jmbi.1997.1498.

[74] D. L. Nelson and M. M. Cox, *Principles of Biochemistry*, Macmillan Higher Education, New York, 6th edn., 2009, doi: 10.1017/CBO9781107415324.004.

[75] C. Jonathan, G. Nick and W. Stuart, *Organic Chemistry*, Oxford University Press, Oxford, 2012.

[76] M. S. Gibson and R. W. Bradshaw, *Angew. Chem., Int. Ed. Engl.*, 1968, **7**, 919–930, doi: 10.1002/anie.196809191.

[77] A. M. Tafesh and J. Weiguny, *Chem. Rev.*, 1996, **96**, 2035–2052, doi: 10.1021/cr950083f.

[78] K. Nomura, *J. Mol. Catal. A: Chem.*, 1995, **95**, 203–210, doi: 10.1016/1381-1169(94)00133-2.

[79] D. Amantini, F. Fringuelli, F. Pizza and L. Vaccaro, *Org. Prep. Proc. Int.*, 2002, **34**, 109–147, doi: 10.1080/00304940209355751.

[80] E. F. V. Scriven and K. Turnbull, *Chem. Rev.*, 1988, **88**, 297–368, doi: 10.1021/cr00084a001.

[81] B. Gopalan and K. K. Balasubramanian, *Click Reactions in Organic Synthesis*, Wiley-VCH, Weinheim, Germany, 1st edn., 2016, pp. 25–76, doi: 10.1002/9783527694174.ch2.

[82] H. C. Kolb, M. G. Finn and K. B. Sharpless, *Angew. Chem., Int. Ed.*, 2001, **40**, 2004–2021, doi: 10.1002/1521-3773(20010601)40:11<2004::AID-ANIE2004>3.0.CO;2-5.

[83] H. C. Kolb and K. Sharpless, *Drug Discov. Today*, 2003, **8**, 1128–1137, doi: 10.1016/S1359-6446(03)02933-7.

[84] T. Curtius, *Ber. Dtsch. Chem. Ges.*, 1890, **23**, 3023–3033, doi: 10.1002/cber.189002302232.

[85] Z. Wang, *Schmidt Reaction*, John Wiley & Sons, Inc., Hoboken, NJ, 2010, doi: 10.1002/9780470638859.conrr566.

[86] J. Silva and I. Carvalho, *Curr. Med. Chem.*, 2007, **14**, 1101–1119, doi: 10.2174/092986707780362817.

[87] H. S. G. Beckmann and V. Wittman, *Azides in Carbohydrate Chemistry*, Wiley-VCH, Chichester, UK, 1st edn., 2010, doi: 10.1002/9780470682517.ch16.

[88] R. a. W. Johnstone, A. H. Wilby and I. D. Entwistle, *Chem. Rev.*, 1985, **85**, 129–170, doi: 10.1021/cr00066a003.

[89] H. Kotsuki, T. Ohishi and T. Araki, *Tetrahedron Lett.*, 1997, **38**, 2129–2132, doi: 10.1016/S0040-4039(97)00324-9.

[90] Y. G. Gololobov and L. F. Kasukhin, *Tetrahedron*, 1992, **48**, 1353–1406, doi: 10.1016/S0040-4020(01)92229-X.

[91] F. L. Lin, H. M. Hoyt, H. Van Halbeek, R. G. Bergman and C. R. Bertozzi, *J. Am. Chem. Soc.*, 2005, **127**, 2686–2695, doi: 10.1021/ja044461m.

[92] H. Bayley, D. N. Standring and J. R. Knowles, *Tetrahedron Lett.*, 1978, **19**, 3633–3634, doi: 10.1016/S0040-4039(01)95015-4.

[93] A. Capperucci, A. Degl'Innocenti, M. Funicello, G. Mauriello, P. Scafato and P. Spagnolo, *J. Org. Chem.*, 1995, **60**, 2254–2256, doi: 10.1021/jo00112a054.

[94] H. S. Prakash Rao and P. Siva, *Synth. Commun.*, 1994, **24**, 549–555, doi: 10.1080/00397919408011505.

[95] Y. Xia, W. Li, F. Qu, Z. Fan, X. Liu, C. Berro, E. Rauzy and L. Peng, *Org. Biomol. Chem.*, 2007, **5**, 1695–1701, doi: 10.1039/b703420b.

[96] H. Peng, K. H. Dornevil, A. B. Draganov, W. Chen, C. Dai, W. H. Nelson, A. Liu and B. Wang, *Tetrahedron*, 2013, **69**, 5079–5085, doi: 10.1016/j.tet.2013.04.091.

[97] R. N. Salvatore, C. H. Yoon and K. W. Jung, *Tetrahedron*, 2001, **57**, 7785–7811, doi: 10.1016/S0040-4020(01)00722-0.

[98] N. Menechutkin, *Z. Phys. Chem.*, 1890, **5**, 589–600, doi: 10.1515/zpch-1890-0546.

[99] S. Kobayashi, M. Ueno, R. Suzuki, H. Ishitani, H. S. Kim and Y. Wataya, *J. Org. Chem.*, 1999, **64**, 6833–6841, doi: 10.1021/jo990877k.

[100] Y. Hayashi, T. Urushima, M. Shin and M. Shoji, *Tetrahedron*, 2005, **61**, 11393–11404, doi: 10.1016/j.tet.2005.09.013.

[101] S. Bähn, S. Imm, L. Neubert, M. Zhang, H. Neumann and M. Beller, *ChemCatChem*, 2011, **3**, 1853–1864, doi: 10.1002/cctc.201100255.

[102] L. Huang, M. Arndt, K. Gooßen, H. Heydt and L. J. Gooßen, *Chem. Rev.*, 2015, **115**, 2596–2697, doi: 10.1021/cr300389u.

[103] T. E. Müller, K. C. Hultzsch, M. Yus, F. Foubelo and M. Tada, *Chem. Rev.*, 2008, **108**, 3795–3892, doi: 10.1021/cr0306788.

[104] P. L. McGrane and T. Livinghouse, *J. Org. Chem.*, 1992, **57**, 1323–1324, doi: 10.1021/jo00031a003.

[105] H.-J. Knölker and S. Agarwal, *Tetrahedron Lett.*, 2005, **46**, 1173–1175, doi: 10.1016/j.tetlet.2004.12.066.

[106] R. W. Bates and Y. Lu, *J. Org. Chem.*, 2009, **74**, 9460–9465, doi: 10.1021/jo9021925.

[107] E. Lippert, *Angew. Chem.*, 1960, **72**, 602–624, doi: 10.1002/ange.19600721618.

[108] N. Bruns and A. F. M. Kilbinger, *Bio-inspired Polymers*, Royal Society of Chemistry, Cambridge, 1st edn., 2016, doi: 10.1039/9781782626664.

[109] A. C. Lavoie, D. A. Bors and W. T. Brown, *US Pat., 5 494 975 A*, 1995.

[110] W. Reppe, K. Herrle and F. H, *Ger. Pat., 0 922 378 B*, 1943.

[111] W. Reppe, C. Schuster and A. Hartmann, *Ger. Pat., 0 737 663 A*, 1939.

[112] X. Shen and S. L. Buchwald, *Angew. Chem., Int. Ed.*, 2010, **49**, 564–567, doi: 10.1002/anie.200905402.

[113] M. Otsuka, H. Yokoyama, K. Endo and T. Shibata, *Org. Biomol. Chem.*, 2012, **10**, 3815–3818, doi: 10.1039/c2ob25457c.

[114] K. C. Nicolaou, S. A. Snyder, T. Montagnon and G. Vassilikogiannakis, *Angew. Chem., Int. Ed.*, 2002, **41**, 1668–1698, doi: 10.1002/1521-3773(20020517)41:10<1668::AID-ANIE1668>3.0.CO;2-Z.

[115] G. Desimoni and G. Tacconi, *Chem. Rev.*, 1975, **75**, 651–692, doi: 10.1021/cr60298a001.

[116] C. Gaulon, R. Dhal, T. Chapin, V. Maisonneuve and G. Dujardin, *J. Org. Chem.*, 2004, **69**, 4192–4202, doi: 10.1021/jo040102y.

[117] Y. Huang, T. Iwama, V. H. Rawal and S. E. Avenue, *J. Am. Chem. Soc.*, 2000, **122**, 7843–7844, doi: 10.1021/JA002058J.

[118] J. P. Wolfe, *Synthesis of Heterocycles via Reactions that Generate One or More Carbon- Heteroatom Bonds*, Springer, Berlin, Heidelberg, 2013, vol. 14, pp. 109–155, doi: 10.1007/978-3-642-38880-4.

[119] Y. W. Li and T. J. Marks, *J. Am. Chem. Soc.*, 1996, **118**, 9295–9306, doi: 10.1021/Ja9612413.

[120] A. Varela-Fernández, J. Varela and C. Saá, *Synthesis*, 2012, **44**, 3285–3295, doi: 10.1055/s-0032-1316539.

[121] J. K. Vandavasi, W.-P. Hu, H.-Y. Chen, G. C. Senadi, C.-Y. Chen and J.-J. Wang, *Org. Lett.*, 2012, **14**, 3134–3137, doi: 10.1021/ol301219c.

[122] Z. J. Garlets, M. Silvi and J. P. Wolfe, *Org. Lett.*, 2016, **18**, 2331–2334, doi: 10.1021/acs.orglett.6b00598.

[123] I. Ojima, *Catalytic Asymmetric Synthesis*, Wiley-VCH, Hoboken, 3rd edn., 2010, pp. 998–1014, doi: 10.1002/9780470584248.

[124] A. Behr and L. Johnen, *ChemSusChem*, 2009, **2**, 1072–1095, doi: 10.1002/cssc.200900186.

[125] S. Kozlov, N, B. Dinaburskaya and T. Rubina, *J. Gen. Chem. USSR*, 1936, **6**, 1341–1345.

[126] R. R. Vogt and G. Vol, *J. Am. Chem. Soc.*, 1939, **61**, 1462–1463, doi: 10.1021/ja01875a040.

[127] P. F. Hudrilk and A. M. Hudrlik, *J. Org. Chem*, 1973, **38**, 4254–4258, doi: 10.1021/jo00964a009.

[128] B. W. Howk, E. L. Little, S. L. Scott and G. M. Whitman, *J. Am. Chem. Soc.*, 1954, **76**, 1899–1902, doi: 10.1021/ja01636a048.

[129] D. R. Coulson, *Tetrahedron Lett.*, 1971, **12**, 429–430, doi: 10.1016/S0040-4039(01)96459-7.

[130] P. J. Walsh, A. M. Baranger and R. G. Bergman, *J. Am. Chem. Soc.*, 1992, **114**, 1708–1719, doi: 10.1021/ja00031a026.

[131] P. L. McGrane, M. Jensen and T. Livinghouse, *J. Am. Chem. Soc.*, 1992, **114**, 5459–5460, doi: 10.1021/ja00039a087.

[132] J. B. Pedley, R. D. Naylor and S. P. Kirby, *Prediction of Standard Enthalpies of Formation*, Springer, Dordrecht, 1986, pp. 7–51, doi: 10.1007/978-94-009-4099-4_3.

[133] T. E. Müller and M. Beller, *Chem. Rev.*, 1998, **98**, 675–703, doi: 10.1021/cr960433d.

[134] L. L. Anderson, J. Arnold and R. G. Bergman, *J. Am. Chem. Soc.*, 2005, **127**, 14542–14543, doi: 10.1021/ja053700i.

[135] B. D. Ward, A. Maisse-François, P. Mountford, L. H. Gade, P. Mountford, D. J. M. Trösch and D. J. M. Trösch, *Chem. Commun.*, 2004, 704–705, doi: 10.1039/B316383K.

[136] R. L. Cowan and W. C. Trogler, *J. Am. Chem. Soc.*, 1989, **111**, 4750–4761, doi: 10.1021/ja00195a031.

[137] J.-J. Brunet, D. Neibecker and K. Philippot, *Chem. Commun.*, 1992, 1215–1216, doi: 10.1039/c39920001215.

[138] C. Sievers, O. Jiménez, R. Knapp, X. Lin, T. E. Müller, A. Türler, B. Wierczinski and J. A. Lercher, *J. Mol. Catal. A: Chem.*, 2008, **279**, 187–199, doi: 10.1016/j.molcata.2007.06.016.

[139] M. Kawatsura and J. F. Hartwig, *J. Am. Chem. Soc.*, 2000, **122**, 9546–9547, doi: 10.1021/ja002284t.

[140] T. Ishikawa, T. Sonehara, M. Minakawa and M. Kawatsura, *Org. Lett.*, 2016, **18**, 1422–1425, doi: 10.1021/acs.orglett.6b00352.

[141] S.-L. Shi and S. L. Buchwald, *Nat. Chem.*, 2014, **7**, 38–44, doi: 10.1038/nchem.2131.

[142] R. Blieck, J. Bahri, M. Taillefer and F. Monnier, *Org. Lett.*, 2016, **18**, 1482–1485, doi: 10.1021/acs.orglett.6b00452.

[143] J. G. Taylor, N. Whittall and K. K. Hii, *Org. Lett.*, 2006, **8**, 3561–3564, doi: 10.1021/ol061355b.

[144] T. E. Müller and A. K. Pleier, *Dalton Trans.*, 1999, 583–587, doi: 10.1039/A808938H.

[145] M. J. Pouy, S. A. Delp, J. Uddin, V. M. Ramdeen, N. A. Cochrane, G. C. Fortman, T. B. Gunnoe, T. R. Cundari, M. Sabat and W. H. Myers, *ACS Catal.*, 2012, **2**, 2182–2193, doi: 10.1021/cs300544w.

[146] J. Penzien, C. Haeßner, A. Jentys, K. Köhler, T. E. Müller and J. A. Lercher, *J. Catal.*, 2004, **221**, 302–312, doi: 10.1016/S0021-9517(03)00283-5.

[147] A. Tsuhako, D. Oikawa, K. Sakai and S. Okamoto, *Tetrahedron Lett.*, 2008, **49**, 6529–6532, doi: 10.1016/j.tetlet.2008.09.003.

[148] H. Ohmiya, T. Moriya and M. Sawamura, *Org. Lett.*, 2009, **11**, 2145–2147, doi: 10.1021/ol9007712.

[149] *Discovery and initial Optimisation*, The discovery of aniline formation from aryl azides in the presence of [Cu(DAB)] and the initial optimisation was performed by Zaira Monasterio Peiteado.

[150] G. L'Abbé, *Chem. Rev.*, 1969, **69**, 345–363, doi: 10.1021/cr60259a004.

[151] *Database of Frequency Scale Factors for Electronic Model Chemistries*, https://comp.chem.umn.edu/freqscale/version3b2.htm., (last accessed March 2017).

[152] S. Fountoulaki, P. L. Gkizis, T. S. Symeonidis, E. Kaminioti, A. Karina, I. Tamiolakis, G. S. Armatas and I. N. Lykakis, *Adv. Synth. Catal.*, 2016, **358**, 1500–1508, doi: 10.1002/adsc.201500957.

[153] H. R. Lucas, L. Li, A. A. N. Sarjeant, M. A. Vance, E. I. Solomon and K. D. Karlin, *J. Am. Chem. Soc.*, 2009, **131**, 3230–3245, doi: 10.1021/ja807081d.

[154] P. Roy and M. Manassero, *Dalton Trans.*, 2010, **39**, 1539–1545, doi: 10.1039/B914017D.

[155] S. Y. Tee, K. Y. Win, W. S. Teo, L. D. Koh, S. Liu, C. P. Teng and M. Y. Han, *Adv. Sci.*, 2017, **4**, 1600337, doi: 10.1002/advs.201600337.

[156] S. M. Barnett, K. I. Goldberg and J. M. Mayer, *Nat. Chem.*, 2012, **4**, 498–502, doi: 10.1038/nchem.1350.

[157] A. M. Romine, N. Nebra, A. I. Konovalov, E. Martin, J. Benet-Buchholz and V. V. Grushin, *Angew. Chem., Int. Ed.*, 2015, **54**, 2745–2749, doi: 10.1002/anie.201411348.

[158] T. B. Yu, J. Z. Bai and Z. Guan, *Angew. Chem., Int. Ed.*, 2009, **48**, 1097–1101, doi: 10.1002/anie.200805009.

[159] M. Sarkis, D. N. Tran, S. Kolb, M. A. Miteva, B. O. Villoutreix, C. Garbay and E. Braud, *Bioorg. Med. Chem. Lett.*, 2012, **22**, 7345–7350, doi: 10.1016/J.Bmcl.2012.10.072.

[160] A. Mukherjee and R. S. Liu, *Org. Lett.*, 2011, **13**, 660–663, doi: 10.1021/ol1029047.

[161] T. E. Müller, M. Grosche, E. Herdtweck, A. K. Pleier, E. Walter and Y. K. Yan, *Organometallics*, 2000, **19**, 170–183, doi: 10.1021/om9906013.

[162] X. H. Wang, Z. L. Yao, S. L. Dong, F. Wei, H. Wang and Z. H. Xu, *Org. Lett.*, 2013, **15**, 2234–2237, doi: 10.1021/ol400803f.

[163] S. Cacchi, G. Fabrizi and L. M. Parisi, *Org. Lett.*, 2003, **5**, 3843–3846, doi: 10.1021/ol035378r.

[164] N. H. Nguyen, J. W. Apriletti, J. D. Baxter and T. S. Scanlan, *J. Am. Chem. Soc.*, 2005, **127**, 4599–4608, doi: 10.1021/ja0440093.

[165] C. Jonasson, A. Horvath and J. E. Bäckvall, *J. Am. Chem. Soc.*, 2000, **122**, 9600–9609, doi: 10.1021/ja001748k.

[166] W. G. Dauben and G. Shapiro, *J. Org. Chem.*, 1984, **49**, 4252–4258, doi: 10.1021/jo00196a028.

[167] T. Takahashi, H. Tanaka and T. Nakada, *US Pat., 9 073 802*, 2012.

[168] W. Roush, H. Gillis and A. Ko, *J. Am. Chem. Soc.*, 1982, **104**, 2269–2283, doi: 10.1021/ja00372a027.

[169] S. Hong, A. M. Kawaoka and T. J. Marks, *J. Am. Chem. Soc.*, 2003, **125**, 15878–15892, doi: 10.1021/ja036266y.

[170] G. Q. Liu, Z. Y. Ding, L. Zhang, T. T. Li, L. Li, L. L. Duan and Y. M. Li, *Adv. Synth. Catal.*, 2014, **356**, 2303–2310, doi: 10.1002/adsc.201301125.

[171] T. E. Müller and A.-K. Pleier, *Dalton Trans.*, 1999, 583–587, doi: 10.1039/a808938h.

[172] S. Hong, S. Tian, M. V. Metz and T. J. Marks, *J. Am. Chem. Soc.*, 2003, **125**, 14768–14783, doi: 10.1021/ja0364672.

[173] L. Ackermann, R. G. Bergman and R. N. Loy, *J. Am. Chem. Soc.*, 2003, **125**, 11956–11963, doi: 10.1021/ja0361547.

[174] F. Xu, J. Y. L. Chung, J. C. Moore, Z. Liu, N. Yoshikawa, R. S. Hoerrner, J. Lee, M. Royzen, E. Cleator, A. G. Gibson, R. Dunn, K. M. Maloney, M. Alam, A. Goodyear, J. Lynch, N. Yasuda and P. N. Devine, *Org. Lett.*, 2013, **15**, 3133–3136, doi: 10.1021/ol400252p.

[175] J. Ezquerra, C. Pedregal, C. Lamas, J. Barluenga, M. Pérez, M. A. García-Martín and J. M. González, *J. Org. Chem.*, 1996, **61**, 5804–5812, doi: 10.1021/jo952119+.

[176] S. Song, M. Huang, W. Li, X. Zhu and Y. Wan, *Tetrahedron*, 2015, **71**, 451–456, doi: 10.1016/j.tet.2014.12.007.

[177] M. Ishizaki, K.-I. Kurihara, E. Tanazawa, O. Hoshino, M. Kobayashi, S. Ishimoto, K. Kotera and Y. Iitaka, *J. Chem. Soc., Perkin Trans. 1*, 1993, **23**, 101–110, doi: 10.1039/P19930000101.

[178] H. Murayama, K. Nagao, H. Ohmiya and M. Sawamura, *Org. Lett.*, 2015, **17**, 2039–2041, doi: 10.1021/acs.orglett.5b00758.

[179] J. Bahri, B. Jamoussi, A. van Der Lee, M. Taillefer and F. Monnier, *Org. Lett.*, 2015, **17**, 1224–1227, doi: 10.1021/acs.orglett.5b00177.

[180] *Spectroscopic data for unknown compound*, ^{1}H NMR (400 MHz, CDCl$_3$): δ 7.81 (d, *J* = 8.3 Hz, 2H), 7.53 (dd, *J* = 8.3 Hz, 2H), 7.37–7.29 (m, 5H), 2.42 (s, 3H); ^{13}C NMR (101 MHz, CDCl$_3$): δ 151.0, 141.3, 132.6, 129.9, 129.4, 128.6, 122.9, 121.9, 81.7, 74.1, 21.6; IR 3051 (m), 2923 (m), 2149 (w), 1950 (w), 1807 (w), 1670 (w), 1598 cm^{-1}. Mass: 450 (main) *m/z*.

[181] J. Han, B. Xu and G. B. Hammond, *J. Am. Chem. Soc.*, 2010, **132**, 916–927, doi: 10.1021/ja908883n.

[182] I. D. Jurberg, B. Peng, E. Wöstefeld, M. Wasserloos and N. Maulide, *Angew. Chem., Int. Ed.*, 2012, **51**, 1950–1953, doi: 10.1002/anie.201108639.

[183] J. L. Stavinoha, P. S. Mariano, A. Leone-Bay, R. Swanson and C. Bracken, *J. Am. Chem. Soc.*, 1981, **103**, 3148–3160, doi: 10.1021/ja00401a037.

[184] H. Firouzabadi, N. Iranpoor and A. A. Jafari, *Adv. Synth. Catal.*, 2005, **347**, 655–661, doi: 10.1002/adsc.200404348.

[185] K. R. Reddy and N. S. Kumar, *Synlett*, 2006, 2246–2250, doi: 10.1055/s-2006-949623.

[186] K. S. Sindhu and G. Anilkumar, *RSC Adv.*, 2014, **4**, 27867–27887, doi: 10.1039/C4RA02416H.

[187] I. Shibata, T. Suwa, K. Ryu and A. Baba, *J. Am. Chem. Soc.*, 2001, **123**, 4101–4102, doi: 10.1021/ja0056973.

[188] S. P. Bew, G. D. Hiatt-Gipson, J. A. Lovell and C. Poullain, *Org. Lett.*, 2012, **14**, 456–459, doi: 10.1021/ol2029178.

[189] Y. Yabe, Y. Sawama, Y. Monguchi and H. Sajiki, *Chem. - Eur. J.*, 2013, **19**, 484–488, doi: 10.1002/chem.201203337.

[190] C. A. Townsend, A. M. Brown and L. T. Nguyen, *J. Am. Chem. Soc.*, 1983, **105**, 919–927, doi: 10.1021/ja00342a047.

[191] S. Shahane, L. Toupet, C. Fischmeister and C. Bruneau, *Eur. J. Inorg. Chem.*, 2013, 54–60, doi: 10.1002/ejic.201200966.

[192] G. A. Grasa, M. S. Viciu, J. K. Huang and S. P. Nolan, *J. Org. Chem.*, 2001, **66**, 7729–7737, doi: 10.1021/jo010613+.

[193] S. R. Stauffer, N. A. Beare, J. P. Stambuli and J. F. Hartwig, *J. Am. Chem. Soc.*, 2001, **123**, 4641–4642, doi: 10.1021/ja0157402.

[194] H. Erlenmeyer and H. Lehr, *Helv. Chim. Acta*, 1946, **29**, 69–71, doi: 10.1002/hlca.19460290113.

[195] H. A. Zhong, J. A. Labinger and J. E. Bercaw, *J. Am. Chem. Soc.*, 2002, **124**, 1378–1399, doi: 10.1021/ja011189x.

[196] C. Burstein, C. W. Lehmann and F. Glorius, *Tetrahedron*, 2005, **61**, 6207–6217, doi: 10.1016/j.tet.2005.03.115.

[197] S. J. Dickson, M. J. Paterson, C. E. Willans, K. M. Anderson and J. W. Steed, *Chem. - Eur. J.*, 2008, **14**, 7296–7305, doi: 10.1002/chem.200800772.

[198] A. Eißler, P. Kläring, F. Emmerling and T. Braun, *Eur. J. Inorg. Chem.*, 2013, 4775–4788, doi: 10.1002/ejic.201300625.

[199] K. Kutonova, M. Trusova, P. Postnikov, V. Filimonov and J. Parello, *Synthesis*, 2013, **45**, 2706–2710, doi: 10.1055/s-0033-1339648.

[200] A. Nocentini, F. Carta, M. Ceruso, G. Bartolucci and C. T. Supuran, *Bioorg. Med. Chem.*, 2015, **23**, 6955–6966, doi: 10.1016/j.bmc.2015.09.041.

[201] A. Nicolaides, T. Enyo, D. Miura and H. Tomioka, *J. Am. Chem. Soc.*, 2001, **123**, 2628–2636, doi: 10.1021/ja003709e.

[202] L. Lin, W. Yin, X. Fu, J. Zhang, X. Ma and R. Wang, *Org. Biomol. Chem.*, 2012, **10**, 83–89, doi: 10.1039/C1OB05899A.

[203] F. R. Bou-Hamdan, F. Lévesque, A. G. O'Brien and P. H. Seeberger, *Beilstein J. Org. Chem.*, 2011, **7**, 1124–1129, doi: 10.3762/bjoc.7.129.

[204] J. M. Altimari, B. Niranjan, G. P. Risbridger, S. S. Schweiker, A. E. Lohning and L. C. Henderson, *Bioorg. Med. Chem.*, 2014, **22**, 2692–2706, doi: 10.1016/j.bmc.2014.03.018.

[205] Z.-C. Dai, Y.-F. Chen, M. Zhang, S.-K. Li, T.-T. Yang, L. Shen, J.-X. Wang, S.-S. Qian, H.-L. Zhu and Y.-H. Ye, *Org. Biomol. Chem.*, 2014, **13**, 477–486, doi: 10.1039/C4OB01758G.

[206] Y.-Q. Yu, *Synthesis*, 2013, **45**, 2545–2550, doi: 10.1055/s-0033-1339377.

[207] O. Berger, A. Kaniti, C. T. van Ba, H. Vial, S. A. Ward, G. A. Biagini, P. G. Bray and P. M. O'Neill, *ChemMedChem*, 2011, **6**, 2094–2108, doi: 10.1002/cmdc.201100265.

[208] S. W. Kwok, J. R. Fotsing, R. J. Fraser, V. O. Rodionov and V. V. Fokin, *Org. Lett.*, 2010, **12**, 4217–4219, doi: 10.1021/ol101568d.

[209] S. Zhou, H. Liao, M. Liu, G. Feng, B. Fu, R. Li, M. Cheng, Y. Zhao and P. Gong, *Bioorg. Med. Chem.*, 2014, **22**, 6438–6452, doi: 10.1016/j.bmc.2014.09.037.

[210] S. K. Mamidyala and M. A. Cooper, *Chem. Commun.*, 2013, **49**, 8407–8409, doi: 10.1039/c3cc43838d.

[211] N. T. Pokhodylo, O. Y. Shyyka and M. D. Obushak, *Synth. Commun.*, 2014, **44**, 1002–1006, doi: 10.1080/00397911.2013.840729.

[212] M. Ni, F. A. Mautner, M. Scherzer, C. Berger, R. C. Fischer, R. Vicente and S. S. Massoud, *Polyhedron*, 2015, **85**, 329–336, doi: 10.1016/j.poly.2014.08.012.

[213] Y. Monguchi, T. Maejima, S. Mori, T. Maegawa and H. Sajiki, *Chem. - Eur. J.*, 2010, **16**, 7372–7375, doi: 10.1002/chem.200903511.

[214] H.-L. Qi, D.-S. Chen, J.-S. Ye and J.-M. Huang, *J. Org. Chem.*, 2013, **78**, 7482–7487, doi: 10.1021/jo400981f.

[215] S. Sharma, M. Kumar, V. Kumar, N. Kumar and H. Pradesh, *J. Org. Chem.*, 2014, **79**, 9433–9439, doi: 10.1021/jo5019415.

[216] D. Y. Lee and J. F. Hartwig, *Org. Lett.*, 2005, **7**, 1169–1172, doi: 10.1021/ol050141b.

[217] H. Xu and C. Wolf, *Chem. Commun.*, 2009, **64**, 3035–3037, doi: 10.1039/b904188e.

[218] K. W. Temburnikar, S. C. Zimmermann, N. T. Kim, C. R. Ross, C. Gelbmann, C. E. Salomon, G. M. Wilson, J. Balzarini and K. L. Seley-Radtke, *Bioorg. Med. Chem.*, 2014, **22**, 2113–2122, doi: 10.1016/j.bmc.2014.02.033.

[219] D. I. Rozkiewicz, D. Jańczewski, W. Verboom, B. J. Ravoo and D. N. Reinhoudt, *Angew. Chem., Int. Ed.*, 2006, **45**, 5292–5296, doi: 10.1002/anie.200601090.

[220] W. Hess and J. W. Burton, *Chem. - Eur. J.*, 2010, **16**, 12303–12306, doi: 10.1002/chem.201001951.

[221] J. H. Kalin, H. Zhang, S. Gaudrel-Grosay, G. Vistoli and A. P. Kozikowski, *ChemMedChem*, 2012, **7**, 425–439, doi: 10.1002/cmdc.201100522.

[222] A. F. Kyle, P. Jakubec, D. M. Cockfield, E. Cleator, J. Skidmore and D. J. Dixon, *Chem. Commun.*, 2011, **47**, 10037–10039, doi: 10.1039/c1cc13665h.

[223] P. Kraft and C. Berthold, *Synthesis*, 2008, **40**, 543–550, doi: 10.1055/s-2008-1032135.

[224] D. M. Hodgson, A. H. Labande, F. Y. T. M. Pierard and M. A. Expósito Castro, *J. Org. Chem.*, 2003, **68**, 6153–6159, doi: 10.1021/jo0343735.

[225] J. Egger, C. Weckerle, B. Cutting, O. Schwardt, S. Rabbani, K. Lemme and B. Ernst, *J. Am. Chem. Soc.*, 2013, **135**, 9820–9828, doi: 10.1021/ja4029582.

[226] Y. Ashikari, T. Nokami and J. I. Yoshida, *Org. Lett.*, 2012, **14**, 938–941, doi: 10.1021/ol203467v.

[227] N. Murakami, M. Kawanishi, S. Itagaki, T. Horii and M. Kobayashi, *Bioorg. Med. Chem. Lett.*, 2004, **14**, 3513–3516, doi: 10.1016/j.bmcl.2004.04.086.

[228] J. J. Chen, C. Chen, J. Chen, H. P. Gao and H. M. Qu, *Synlett*, 2014, 2721–2726, doi: 10.1055/s-0034-1379248.

[229] Y. Wang, C. Chen, S. Zhang, Z. B. Lou, X. Su, L. R. Wen and M. Li, *Org. Lett.*, 2013, **15**, 4794–4797, doi: 10.1021/ol402164s.

[230] Á. González-Gómez, G. Domínguez and J. Pérez-Castells, *Eur. J. Org. Chem.*, 2009, 5057–5062, doi: 10.1002/ejoc.200900745.

[231] G. Cahiez, O. Gager and J. Buendia, *Angew. Chem., Int. Ed.*, 2010, **49**, 1278–1281, doi: 10.1002/anie.200905816.

[232] Y. He, X. Zhang and X. Fan, *Chem. Commun.*, 2014, **50**, 5641–5643, doi: 10.1039/c4cc01738b.

[233] P. Y. Choy, W. K. Chow, C. M. So, C. P. Lau and F. Y. Kwong, *Chem. - Eur. J.*, 2010, **16**, 9982–9985, doi: 10.1002/chem.201001269.

[234] K. Hiroya, R. Jouka, M. Kameda, A. Yasuhara and T. Sakamoto, *Tetrahedron*, 2001, **57**, 9697–9710, doi: 10.1016/S0040-4020(01)00991-7.

[235] Y. Yin, W. Ma, Z. Chai and G. Zhao, *J. Org. Chem.*, 2007, **72**, 5731–5736, doi: 10.1021/jo070681h.

[236] K. Oh and Z. Guan, *Chem. Commun.*, 2006, **101**, 3069–3071, doi: 10.1039/B606185K.

[237] H. J. Lu, C. Q. Li, H. L. Jiang, C. L. Lizardi and X. P. Zhang, *Angew. Chem., Int. Ed.*, 2014, **53**, 7028–7032, doi: 10.1002/anie.201400557.

[238] K. S. Rao, B. M. Antonio, S. Jiandong and B. M. F., *US Pat., WO2006 105 372*, 2006.

[239] S. B. Daval, C. Valant, D. Bonnet, E. Kellenberger, M. Hibert, J. L. Galzi and B. Ilien, *J. Med. Chem.*, 2012, **55**, 2125–2143, doi: 10.1021/jm201348t.

[240] T. C. Adams, A. C. Dupont, J. P. Carter, J. F. Kachur, M. E. Guzewska, W. J. Rzeszotarski, S. G. Farmer, L. Noronha-Blob and C. Kaiser, *J. Med. Chem.*, 1991, **34**, 1585–1593, doi: 10.1021/jm00109a010.

[241] N. K. Swamy, A. Yazici and S. G. Pyne, *J. Org. Chem.*, 2010, **75**, 3412–3419, doi: 10.1021/jo1005119.

[242] B. M. Trost, A. B. Pinkerton and M. Seidel, *J. Am. Chem. Soc.*, 2001, **123**, 12466–12476, doi: 10.1021/ja011428g.

[243] C. Spino, J. Crawford and J. Bishop, *J. Org. Chem.*, 1995, **60**, 844–851, doi: 10.1021/jo00109a014.

[244] J. M. Carney, P. J. Donoghue, W. M. Wuest, O. Wiest and P. Helquist, *Org. Lett.*, 2008, **10**, 3903–3906, doi: 10.1021/ol801458g.

[245] D. H. Hua, S. W. Miao, S. N. Bharathi, T. Katsuhira and A. A. Bravo, *J. Org. Chem.*, 1990, **55**, 3682–3684, doi: 10.1021/jo00298a062.

[246] D. T. D. Tang, K. D. Collins, J. B. Ernst and F. Glorius, *Angew. Chem., Int. Ed.*, 2014, **53**, 1809–1813, doi: 10.1002/anie.201309305.

[247] L. A. Flippin and J. M. Muchowski, *J. Org. Chem.*, 1993, **58**, 2631–2632, doi: 10.1021/jo00061a046.

[248] J. Mangas-Sánchez, E. Busto and V. Gotor-Fernández, *Org. Lett.*, 2012, **14**, 1444–1447, doi: 10.1021/ol300191s.

[249] D. Aguilar, M. Contel and E. P. Urriolabeitia, *Chem. - Eur. J.*, 2010, **16**, 9287–9296, doi: 10.1002/chem.201000587.

[250] M. J. Frisch, G. W. Trucks, H. B. Schlegel, G. E. Scuseria, M. A. Robb, J. R. Cheeseman, G. Scalmani, V. Barone, B. Mennucci, G. A. Petersson, H. Nakatsuji, M. Caricato, X. Li, H. P. Hratchian, A. F. Izmaylov, J. Bloino, G. Zheng, J. L. Sonnenberg, M. Hada, M. Ehara, K. Toyota, R. Fukuda, J. Hasegawa, M. Ishida, T. Nakajima, Y. Honda, O. Kitao, H. Nakai, T. Vreven, J. A. Montgomery Jr., J. E. Peralta, F. Ogliaro, M. Bearpark, J. J. Heyd, E. Brothers, K. N. Kudin, V. N. Staroverov, R. Kobayashi, J. Normand, K. Raghavachari, A. Rendell, J. C. Burant, S. S. Iyengar, J. Tomasi, M. Cossi, N. Rega, J. M. Millam, M. Klene, J. E. Knox, J. B. Cross, V. Bakken, C. Adamo, J. Jaramillo, R. Gomperts, R. E. Stratmann, O. Yazyev, A. J. Austin, R. Cammi, C. Pomelli, J. W. Ochterski, R. L. Martin, K. Morokuma, V. G. Zakrzewski, G. A. Voth, P. Salvador, J. J. Dannenberg, S. Dapprich, A. D. Daniels, Ö. Farkas, J. B. Foresman, J. V. Ortiz, J. Cioslowski and D. J. Fox, *Gaussian 09 Revision A.01*, Gaussian, Inc., Wallingford, CT, 2009.

[251] S. Grimme, J. Antony, S. Ehrlich and H. Krieg, *J. Chem. Phys.*, 2010, **132**, 154104, doi: 10.1063/1.3382344.

[252] J. P. Perdew, *Phys. Rev. B*, 1986, **33**, 8822–8824, doi: 10.1103/PhysRevB.33.8822.

[253] H. Stoll, P. Fuentealba, P. Schwerdtfeger, J. Flad, L. v. Szentpály and H. Preuss, *J. Chem. Phys.*, 1984, **81**, 2732–2736, doi: 10.1063/1.447992.